NISTIR 8271 DRAFT SUPPLEMENT

Face Recognition Vendor Test (FRVT)

Part 2: Identification

Patrick Grother
Mei Ngan
Kayee Hanaoka
Information Access Division
Information Technology Laboratory

This document is a draft supplement of NIST Interagency Report 8271

2021/08/05

National Institute of Standards and Technology
U.S. Department of Commerce

NISTIR 8271 DRAFT SUPPLEMENT

Face Recognition Vendor Test (FRVT)

Part 2: Identification

Patrick Grother
Mei Ngan
Kayee Hanaoka
Information Access Division
Information Technology Laboratory

This document is a draft supplement of NIST Interagency Report 8271

June 2021

U.S. Department of Commerce
Wynn Coggins, Acting Secretary

National Institute of Standards and Technology
James Altoff, Under Secretary of Commerce for Standards and Technology and Director, acting

RELEASE NOTES

2021-08-02: The 1:N track of the FRVT remains open. Three news items:

- This document is the nineth draft update to NIST Interagency Report 8271. It includes results for algorithms recently submitted by eight participants: Cyberlink Corp, NEC Corp, N-Tech Lab, Realnetworks Inc., Sensetime Group, Veridas Digital, Viettel Group, and Vigilant Solutions.
- Algorithms submitted since July 24 will be included in the next update scheduled for September 9, 2021.
- A new report, NIST Interagency Report 8381 - FRVT Part 7: Identification for Paperless Travel and Immigration, has been released [PDF, webpage]. It documents the use of FRVT 1:N algorithms in positive access control and immigration status update travel applications where the enrolled population size is as low as 420 people for aircraft boarding, and $42\,000$ for an airport security line. These population sizes are much smaller than those used in the main 1:N evaluation. Going forward, we will update the report and webpage with results for new algorithms.

2021-07-07: The 1:N track of the FRVT remains open. One update:

- This document is the eighth draft update to NIST Interagency Report 8271. It include results for an algorithm from one participant: Kakao Enterprises.

2021-06-22: The 1:N track of the FRVT remains open. Three updates:

- This is the seventh draft of the update to NIST Interagency Report 8271. It includes results for algorithms from three new participants: Line Corporation, Rendip, and Samsung S1 Corp.
- We have also added results for algorithms from five returning developers: Imagus Technology, Kneron, Tevian, Visidon, and Xforward AI Technology.
- The algorithm-specific report cards (examples: 1, 2, and 3) now include figures showing how low threshold values can be used to reduce candidate list lengths for human review, while (usually) elevating miss rates (FNIR) only modestly. The reports also feature some minor additions and clarifications.

2021-03-26: The 1:N track of the FRVT remains open. Three updates:

- This is the sixth draft of the update to NIST Interagency Report 8271. It includes results for algorithms from three returning developers: Neurotechnology, Guangzhou Pixel Solutions, and Tech5 SA.
- We have added results on the webpage and in the report for a new ageing dataset in which border crossing photos are searched against a gallery of border crossing photos collected between 10 and 15 years prior to the mated search photos. See section 2 for a description of the images. Table 1 has a new entry describing the experiment.
- We will mostly discontinue running the mugshot ageing test, reserving it for algorithms that show high accuracy on the new border-crossing set.

2021-03-26: Regarding the fifth draft of the update to NIST Interagency Report 8271:

- In addition have added results for first algorithms from two new participants: Viettel Group and Veridas Digital Authentication Solutions.
- We have added results for algorithms from two returning developers: Idemia and Cognitec Systems.
- In addition to the report, the results page and its hyperlinked report cards have been updated.

2021-02-08: Regarding the fourth draft of the update to NIST Interagency Report 8271:

- We have added results for eight algorithms submitted by eight developers: Cyberlink, Dermalog, Imagus, Paravision, Sensetime, Trueface, Vigilant Solutions, and X-Forward AI. With the exception of Trueface, all of these developers have participated previously.

- ▷ We anticipate updating this report again in the first week of March 2021.
- ▷ The main results page has been revised with tabs for the investigative and lights-out identification tables, and a new tab dedicated to speed and resource consumption.
- ▷ The report cards (example here) hyperlinked from the results page have been revised to improve content and format.

2020-12-14: Regarding third draft of the update to NIST Interagency Report 8271:

- ▷ We have added results for fifteen algorithms submitted by thirteen developers. The four first-time participants are: Acer, Akurat Satu Indonesia, Canon, and Xforward AI Technology. The ten returning developers are: AllGoVision, Cyberlink Corp, Dahua Technology, Deepglint, Guangzhou Pixel Solutions, IIT Vision, Innovatrics, Rank One Computing, Scanovate, Sensetime Group, Synesis, and VisionLabs.
- ▷ We have added two new datasets to the evaluation: First a set of "visa-border" photos, representing search of an airport immigration lane photo against a database of closely ISO standard portraits; second a "visa-kiosk" set representing search of a photo collected in a registered traveller kiosk against the same ISO portrait gallery. The images are described in section 2.1.
- ▷ As in previous reports, we include results for searching mugshots against a mugshot gallery containing a single image of each of 12 million people. However we have suspending running searches against a gallery in which multiple lifetime photos per person are present, because this is computationally expensive. We retain a N = 3 million search test dedicated to ageing in which mugshots taken up to 18 years after the first photograph are searched - see Table 6.
- ▷ Tables containing computational resource information, Table 2. . ., now include duration of the finalization step, in which search algorithms can, at their option, build fast-search data structures.
- ▷ We have linked revised per-algorithm PDF report cards from the main results page.
- ▷ We have regenerated all figures and tables to drop algorithms submitted before June 2018. Results for prior algorithms appear in archived editions of this report.
- ▷ Going forward, we anticipate producing more frequent updates to this report. Developers may submit one algorithm to this evaluation every four calendar months.

2020-03-24: Regarding the second draft of the update to NIST Interagency Report 8271:

- ▷ Adds results for three algorithms from three developers, Dermalog, Innovatrics, and Synesis.
- ▷ Adds Table 6 on ageing showing the increase in false negative rates with time elapsed between two photos. Some of the results were contained in graphs in prior editions of this report, but the table adds results for some newly submitted algorithms.
- ▷ Adjusts frontal mugshot results (for recent and lifetime consolidated galleries) to include the effect of removing some images that should not have been included in image test sets. These images were mostly profile views, images of tattoos containing faces, images of faces on tee shirts, and images of photographs on walls behind the intended subject. This affects many tables and reduces false negative identification rates for all algorithms. The reduction is larger for "recent" enrollments than for "lifetime consolidated" ones with the consequence that accuracy on recent images is now superior.

2020-02-26: Regarding the first draft of the update to NIST Interagency Report 8271:

- ▷ Adds results for 38 algorithms from 31 different developers, eleven of whom are entirely new to the 1:N track of FRVT. These are Allgovision, Cyberlink, Deepsea Tencent, Farbar F8, Imperial College London, Intsys MSU, Kedacom, Kneron, Pixelall, and Scanovate.

DISCLAIMER

Specific hardware and software products identified in this report were used in order to perform the evaluations described in this document. In no case does identification of any commercial product, trade name, or vendor, imply recommendation or endorsement by the National Institute of Standards and Technology, nor does it imply that the products and equipment identified are necessarily the best available for the purpose.

INSTITUTIONAL REVIEW BOARD

The National Institute of Standards and Technology's Research Protections Office reviewed the protocol for this project and determined it is not human subjects research as defined in Department of Commerce Regulations, 15 CFR 27, also known as the Common Rule for the Protection of Human Subjects (45 CFR 46, Subpart A).

ACKNOWLEDGMENTS

The authors are grateful for the support and collaboration of the the Department of Homeland Security's Science & Technology Directorate (S&T), Office of Biometric Identity Management (OBIM), and Customs and Border Protection (CBP).

Additionally, the authors are grateful to staff in the NIST Biometrics Research Laboratory for infrastructure supporting rapid evaluation of algorithms.

Executive Summary

This document is a draft revision of the September 2019 report NIST Interagency Report 8271. That report gave extensive documentation of face recognition applied to mugshots. This report extends that by adding more two more challenging datasets containing images with serious departures from canonical frontal image standards. The report also adds results for algorithms submitted to NIST since in 2019 and 2020. The algorithms, which implement one-to-many identification of faces appearing in two-dimensional images, are prototypes from the research and development laboratories of mostly commercial suppliers, and are submitted to NIST as compiled black-box libraries implementing a NIST-specified C++ test interface. The report therefore does not describe how algorithms operate. The report lists accuracy results alongside developer names and will therefore be useful for comparison of face recognition algorithms and assessment of absolute capability. The report is accompanied by a webpage with sortable results.

The evaluation uses six datasets: frontal mugshots, profile view mugshots, desktop webcam photos, visa-like immigration application photos, immigration lane photos, and registered traveler kiosk photos. These datasets are sequestered at NIST, meaning that developers do not have access to them for training or testing. This aspect is important because face recognition algorithms are very often deployed without the developer having access to the customers image data. A possible exception to this would be in a cloud-based application where the operational image data is uploaded to a cloud operated by a face recognition developer.

The major result in NIST IR 8271 was that massive gains in accuracy have been achieved in the years 2013 to 2018 and these far exceed improvements made in the prior period, 2010 to 2013. While the industry gains were broad - at least 30 developers' algorithms outperformed the most accurate algorithm from late 2013, there remains a wide range of capability. While this report shows accuracy gains only over the period 2018-2020, the most accurate algorithm reported here is substantially more accurate than anything reported in NIST IR 8271. This is evidence that face recognition development continues apace, and that FRVT reports are but a snapshot of contemporary capability.

From discussion with developers, the accuracy gains stem from the adoption of deep convolutional neural networks. As such, face recognition has undergone an industrial revolution, with algorithms increasingly tolerant of poorly illuminated and other low quality images, and poorly posed subjects. One related result is that a few algorithms correctly match side-view photographs to galleries of frontal photos, with search accuracy approaching that of the best c. 2010 algorithms operating on purely frontal images. The capability to recognize under a 90-degree change in viewpoint - pose invariance - has been a long-sought milestone in face recognition research.

With good quality portrait photos, the most accurate algorithms will find matching entries, when present, in galleries containing 12 million individuals, with rank one miss rates of approaching 0.1%. The remaining errors are in large part attributable to long-run ageing, facial injury and poor image quality. Given this impressive achievement - close to perfect recognition - an advocate might claim that cooperative face recognition is a solved problem, a statement that can be refuted with the following context and caveats:

- **Mugshots vs. less constrained captures:** The low error rates reported here are attained using mostly excellent cooperative live-capture mugshot images collected with an attendant present. Recognition in other circumstances, particularly those without a dedicated photographic environment and human or automated quality control checks, will lead to declines in accuracy. This is documented here for side-view images, poorer quality webcam images, and, particularly, for newly introduced ATM-style kiosk photos that were not originally intended for automated face recognition. In this case, recognition error rates are much higher, often in excess of 20% even with the more accurate algorithms which variously remain intolerant of face cropping (at image edge) and of large downward head pitch.

- **Algorithm accuracy spectrum:** Recognition accuracy is very strongly dependent on the algorithm and, more

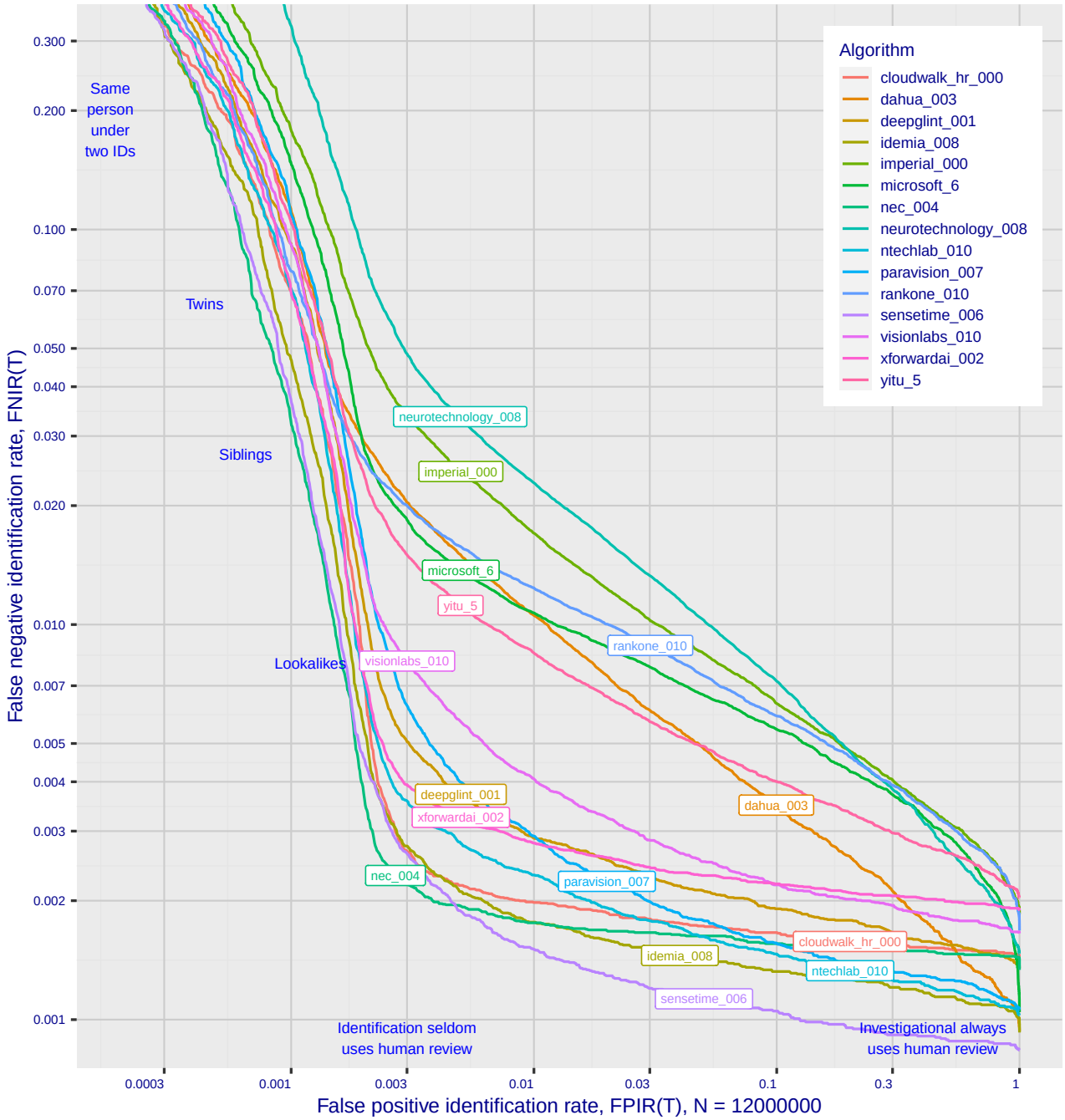

Figure 1: Identification miss rates across the false positive range. N = 12 million individuals are enrolled with one recent image.

generally, on the developer of the algorithm. False negative error rates in a particular scenario range from a few tenths of one percent to beyond fifty percent. This is tabulated exhaustively later: For example Table 9 shows accuracy across datasets. Figure 1 here compares algorithms on mugshot searches in a consolidated gallery of 12 million subjects and 12 million photos. Many algorithms do not achieve the low error rates noted above, and while many of those may still be useful and valuable to end-users, only the most accurate excel on poor quality images and those collected long after the initial enrollment sample.

▷ **Versioning:** While results for up to ten algorithms from each developer are reported here, the intra-provider

accuracy variations are usually smaller than the inter-provider variations. That said different versions give an order of magnitude fewer misses. Some developers demonstrate speed-accuracy tradeoffs[1]. See Figs. 18, 19.

- **Low similarity scores:** In thousands of mugshot cases the correct gallery image is returned at rank 1 but its similarity score is nevertheless low, below some operationally required score threshold. This is not so important when face recognition is used for "lead generation" in investigational applications because human reviewers are specifically required to review potentially long candidate lists and the threshold is effectively 0. In applications where search volumes are higher and labor is not available to review the results from searches, a higher threshold must be applied. This reduces the length of candidate lists and false positive identification rates at the expense of increased false negative miss rates. The tradeoff between the two error rates is reported extensively later.

- **Population size:** As the number of enrolled subjects grows, some mates are displaced from rank one, decreasing accuracy. As tabulated later for N up to 12 million, false negative rates generally rise slowly with population size. This enables use of face recognition in very large populations. However in most positive and negative identification applications[2], a score threshold is set to limit the rate at which non-mate searches produce false positives. This has the consequence that some mated searches will report the mate below threshold, i.e. a miss, even if it is at rank 1. The utility of this is that many non-mated searches will return no candidate identities at all. As the error-tradeoff characteristic shows, investigational miss rates on the right side are very low but then rise steadily (in the center region) as threshold is increased to support "lights-out" applications, and ultimately rise quickly (left side) as discussed below. Thus, if we demand that just one in one thousand non-mate searches produce any false positives, the most accurate algorithms there (Sensetime-004 and NEC-3) would fail on between 3 and 5% of mated searches. Even though the graph shows results for the most accurate algorithms, all but two would fail to find the mate in more than 8% of mated searches. While the two most accurate algorithms produce a relatively flat error tradeoff until the threshold is raised to limit false positives to about 1 in 400 non-mated searches[3]

  Thereafter, as the threshold is raised to further reduce false positives, miss rates rise rapidly. This means that low false positive identification rates are inaccesible with these algorithms, a result that does not apply for ten-finger identification algorithms. The rapid rise occurs because the lower mate scores are mixed with very high non-mate scores, the low scores from poor image quality and ageing, the high non-mates from the presence of lookalikes persons (doppelgangers), twins (discussed next) and, ultimately, the presence of a few unconsolidated subjects i.e. persons present under multiple IDs.

- **False negatives from ageing:** A large source of error in long-run applications where subjects are not re-enrolled on a set schedule is ageing. Changes in facial appearance increase with the time elapsed between photographs. These will depress similarity scores and eventually cause false negatives. All faces age and while this usually proceeds in a graceful and progressive manner, drug use can accelerate this [28]. Elective surgery may be effective in delaying it although this has not been formally quantified with face recognition. As ageing is essentially unavoidable, it can only be mitigated by scheduled re-capture, as in passport re-issuance. To quantify ageing effects, we used the more accurate algorithms to enroll the earliest image of 3.1 million adults and then search

[1] For example, NEC-0 prepares templates much faster than NEC-2 but gives twenty times more misses. Dermalog-5 executes a template search much more quickly than Dermalog-6 but is also much less accurate.

[2] In a positive identification application such as a registered traveler system, a user is making an implicit claim to be enrolled in the system - most users will be. In a negative application, such as with deportees, the implicit claim is that the subejct is not enrolled - most will not be.

[3] The gallery size here is 12 million people, one image per person. Given 331 201 non-mated searches, an exhaustive implementation of one-too-many search would execute almost 4 trillion comparisons. At a false positive identification rate of 0.0025 the number of false positives is, to first order, 828 corresponding to single-comparison false match rate of 828 / 4 trillion = 2.1 10^{-10} i.e. about 1 in 5 billion. Strictly this FMR computation is meaningful only for algorithms that implement 1:N search using N 1:1 comparisons, which is not always the case.

with 10.3 million newer photos taken up to 18 years after the the initial enrollment photo. Figure 2 puts ageing into context by contrasting it with the increase in false negatives that occurs when the number of individuals in an enrollment database becomes larger and the chance of a false positive increases such that higher thresholds may become necessary[4].

The Figure shows, from to bottom, increases in false negative identification rates (FNIR) with the algorithm being tested. This applies to increases due to N on the left side, and increases due to ageing on the right side. The relative spacing of the dots shows that for all algorithms the dependency of FNIR on N (up to 12 million) is considerably less than on ΔT (up to 18 years).

In the inset table, accuracy is seen to degrade progressively with time, as mate scores decline and non-mates displace mates from rank 1 position. More accurate algorithms tend to be less sensitive to ageing. The more accurate algorithms give fewer errors after 18 years of ageing than middle tier algorithms give after four. Note also we do not quantify an ageing rate - more formal methods [2] borrowed from the longitudinal analysis literature have been published for doing so (given suitable repeated measures data). See Figures 60, 80 and 90.

[4]Some algorithms implement stragegies to automatically adjust scores to account for increased population size. This relieves the system owner of having to increase thresholds as N increases.

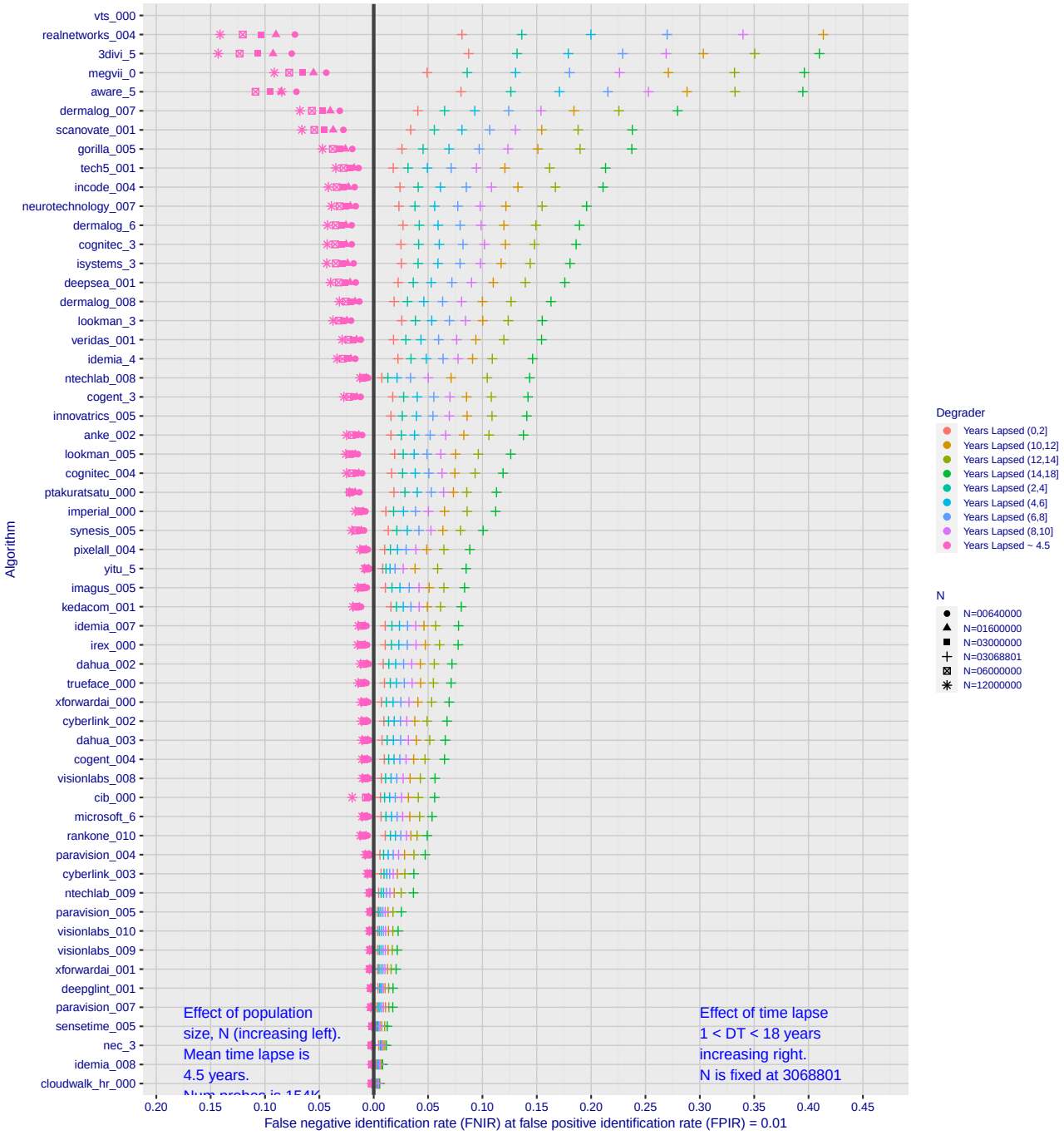

Figure 2: Identification miss rates as a function of enrolled population size, N, and time-lapse, ΔT.

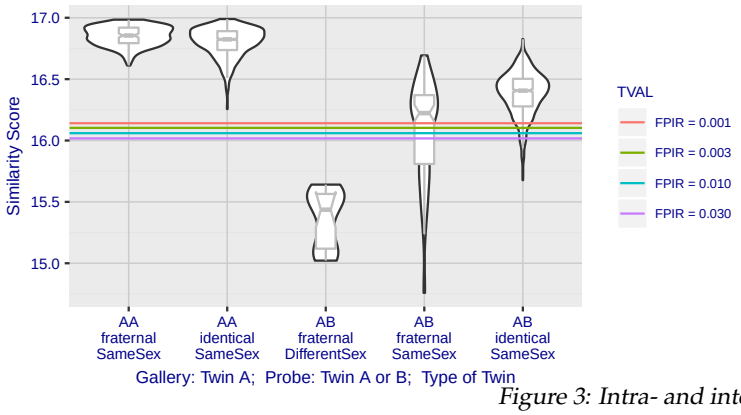

Figure 3: Intra- and inter-twin scores

- **False positives from twins:** By enrolling 640 000 mugshots, adding photos of one twin, and then searching photos of those subjects and their twin the inset figure shows, for one typical algorithm, the similarity is generally greater when searching twins against themselves (A) than when searching twins against their sibling (B) but very often still above even stringent thresholds i.e. those corresponding to one in one thousand searches producing a false positive. Thus twins will very often produce a high-scoring non-match on a candidate list and a false alarm in an online identification system. The plot of Fig. 3 shows that fraternal twins are sometimes correctly rejected at those thresholds - including most different sex twins (at center). Figure **??** shows substantially similar behavior for all algorithms tested. In an investigative search, a twin would typically appear at rank 1, or rank 2 if their sibling happened to also be the gallery. Twins (and triplets etc.) constituted 3.3% of all live births [17] in recent years[5], and because that number is higher today than when the individuals in current adult databases were born, the false positives that arise from twins are now, and will increasingly be, an operational problem. Relative to the United States, twins are born with considerable regional variation. For example they are much less common in East Asia, and much more common in Sub-Saharan Africa [21].

  The presence of twins in the mugshot database is inevitable given its size, around 12.3 million people. As this is not an insignificant sample of the domestic United States population, people with other familial ties will be present also. The data was collected over an extended period and because location information is not available, we are unable to estimate the proportion of the domestic population that is present in the dataset. However, if we assume twins are neither more or less disposed to arrest than the general population, we can estimate that hundreds of thousands of individuals in the dataset are twins. This will affect false positive rates because we randomly set aside 331 201 individuals for nonmate searches, and some proportion of those will be twins with siblings in the gallery.

- **Database integrity:** An operational error rate should be added to all false negative rates in this report reflecting the proportion of images in a real database that are un-matchable. Such anomalies arise from images that: do not contain a face; include multiple persons; cannot be decoded; are rotated by 90° or 180°; depict a face on clothing; and others introduced by a long tail of various clerical errors. While the mugshot trials in this report have been constructed to minimize such effects, they are a real problem in actual operations.

This report is being updated continuously as new algorithms are submitted to FRVT, and run on new datasets. Participation in the one-to-many identification track is independent of participation in the one-to-one verification track of FRVT.

[5]See the CDC's National Vital Statistics Report for 2017: https://www.cdc.gov/nchs/data/nvsr/nvsr67/nvsr67_08-508.pdf

Scope and Context

Audience: This report is intended for developers, integrators, end users, policy makers and others who have some familiarity with biometrics applications. The methods and metrics documented here will be of interest to organizations engaged in tests of face recognition algorithms. Some of these have been incorporated in the ISO/IEC 19795 Part 1 Biometric Testing and Reporting Framework standard, now nearing publication.

Prior benchmarks: Automated face recognition accuracy has improved massively in the two decades since initial commercialization of the various technologies. NIST has tracked that improvement through its conduct of regular independent, free, open, and public evaluations. These have fostered improvements in the state of the art. This report serves as an update to the NIST Interagency Report 8271 on performance of face identification algorithms, published in September 2019.

Demographics: In December 2019, NIST published a first report on demographic dependencies in face recognition, NIST Interagency Report 8280 that documented age, sex and race differentials in one-to-one and one-to-many false positive and false negative rates.

Scope: NIST IR 8271 documented recognition results for four databases containing in excess of 30.2 million still photographs of 14.4 million individuals. That constituted the largest public and independent evaluation of face recognition ever conducted. It includes results for accuracy, speed, investigative vs. identification applications, scalability to large populations, use of multiple images per person, images of cooperative and non-cooperative subjects.

The report also includes results for ageing, recognition of twins, and recognition of profile-view images against frontal galleries. It otherwise does not address causes of recognition failure, neither image-specific problems nor subject-specific factors including demographics. Separate reports on demographic dependencies in face recognition will be published in the future. Additionally out of scope are: performance of live human-in-the-loop transactional systems like automated border control gates; human recognition accuracy as used in forensic applications; and recognition of persons in video sequences (which NIST evaluated separately [9]). Some of those applications share core matching technologies that *are* tested in this report.

Images: Five kinds of images are employed; these are either compared with images of the same kind, or against others from different capture environments as follows. The primary dataset is a set of law enforcement mugshot images (Fig. 5) which are enrolled and then searched with three kinds of images: other mugshots (i.e. within-domain); profile-view photographs (90 degree cross-view); and lower quality webcam images (Fig. 6) collected in similar detention operations (cross-domain). Additionally we compare high quality visa-like photos collected in immigration offices, with: medium quality border crossing images collected in primary immigration lanes; poor quality images collected in ATM-like registered traveller kiosks.

Participation and industry coverage: The report includes performance figures for prototype algorithms from the research laboratories of commercial developers and a few universities. This represents a substantial majority of the face recognition industry, but only a tiny minority of the academic community. Participation was open worldwide. While there is no charge for participation, developers incur some software engineering expense in implementing their algorithms behind the NIST application programming interface (API). The test is a black-box test where the function of the algorithm, and the intellectual property associated with it, is hidden inside pre-compiled libraries.

Recent technology development: Most face recognition research with deep convolutional neural networks (CNNs) has been aimed at achieving invariance to pose, illumination and expression variations that characterize photojournalism and social media images. The initial research [18, 22] employed large numbers of images of relatively few ($\sim 10^4$) individuals to learn invariance. Inevitably much larger populations ($\sim 10^7$) were employed for training [11, 20] but the benchmark, Labeled Faces in the Wild with (essentially) an equal error rate metric [12], represents an easy task,

one-to-one verification at very high false match rates. While a larger scale identification benchmark duly followed, Megaface [15], its primary metric, rank one hit rate, contrasts with the high threshold discrimination task required in most large-population applications of face recognition, namely credential de-duplication, and background checks. There, identification in galleries containing up to 10^8 individuals must be performed using a) very few images per individual and b) stringent thresholds to afford very low false positive identification rates. This track of FRVT was launched to measure the capability of the new technologies, including in these two cases. FRVT has included open-set identification tests since 2002, reporting both false negative and positive identification rates [7].

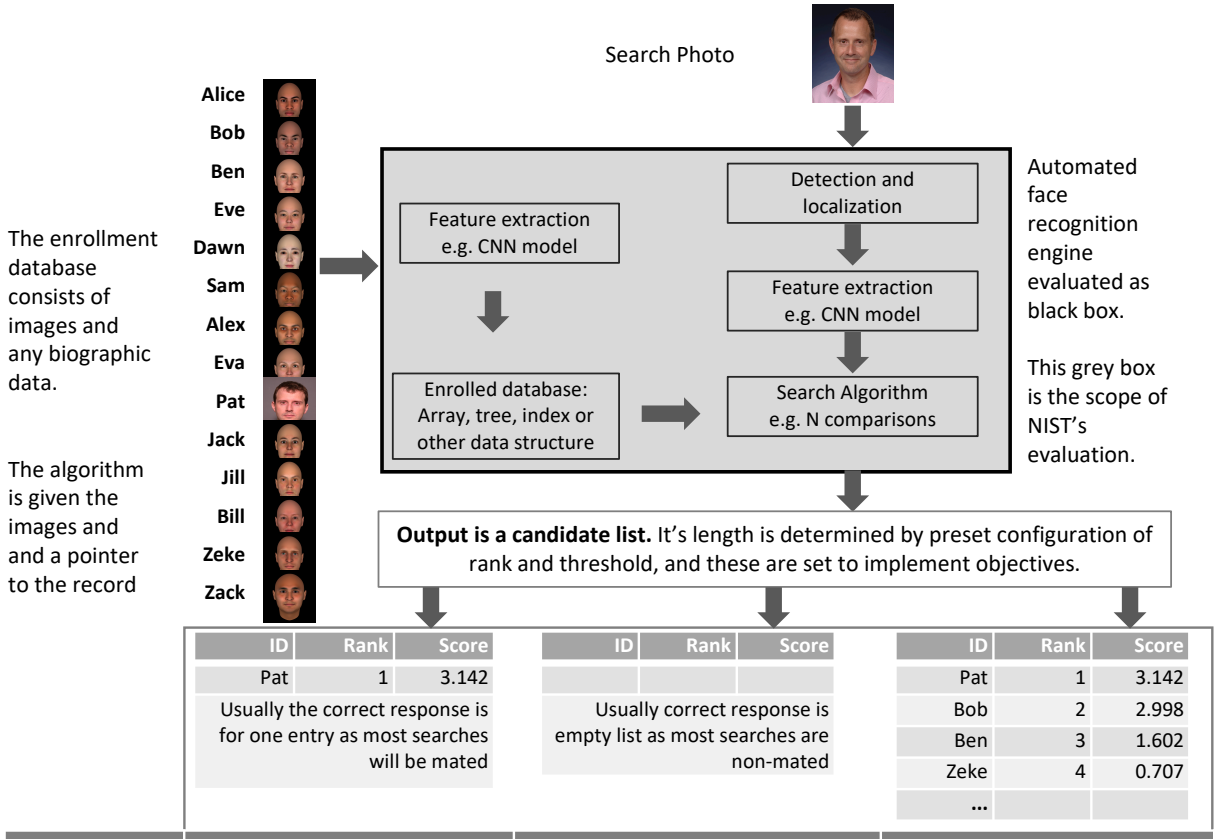

	Positive identification	Negative identification	Post-event investigation
Example	Access to a gym or cruise ship	Watchlist e.g. Detection of deportee or duplicate drivers license applications	Crime scene photos, or of detainee without ID documents.
Claim of identity	Implicit claim to be enrolled	Implicit claim to not be enrolled	No claim: Inquiry
Threshold	High, to implement security objective	High, to limit false positives	Zero
Num. candidates	1	0	L, set by request to algorithm
Human role	Review candidate to assist user in resolution of false negatives, or to detect impostor	Review candidate to determine false positive or correct hit	Review multiple candidates, refer possible hits to examiners see [26]
Intended human involvement frequency	Rare – approx. the false negative identification rate plus prior probability of impostor	Rare – approx. the false positive identification rate plus prior probability of an actual mate	Always
Performance metric of interest	**FNIR at low FPIR. See sec. 3.1, 3.2 and Tables 10, 19**	**FNIR at low FPIR. See sec. 3.1, 3.2 and Tables 10, 19**	**FNIR at ranks 1... 50, say. FPIR = 1. See sec. 3.2 and Table 12, 14, 16**

Performance metrics for applications: This report documents the performance of one-to-many face recognition algorithms. The word "performance" here refers to recognition accuracy and computational resource usage, as measured

by executing those algorithms on massive sequestered datasets.

This report includes extensive tabulation of recognition error rates germane to the main use-cases for face search technology. The Figure below, inspired by the Figure 1 in [23] differentiates different applications of the technolgy. The last row directs readers to the main tables relevant to those applications, respectively threshold-based and rank-based metrics that are special cases of the metrics given in section 3. The terms negative identification and positive identification are taken from the ISO/IEC 2382-37:2017 standardized biometrics vocabulary.

The algorithms are specifically configured for these applications by setting thresholds and candidate list lengths. Both rank-based metrics and threshold-based metrics include tradeoffs. In investigation, overall accuracy will be reduced if labor is only available to review a few candidates from the automated system. Note that when a fixed number of candidates are returned, the false positive identification rate of the automated face recognition engine will be 100%, because a probe image of anyone not enrolled will still return candidates. In identification applications where false positives must be limited to satisfy reviewer labor availability or a security objective, higher false negative rates are implied. This report includes extensive quantification of this threshold-based tradeoff. See Sec. 3

Template diversity: The FRVT is designed to evaluate black-box technologies with the consequence that the templates that hold features extracted from face images are entirely proprietary opaque binary data that embed considerable intellectual property of the developer. Despite migration to CNN-based technologies there is no consensus on the optimal feature vector dimension. This is evidenced by template sizes ranging from below 100 bytes to more than four kilobytes. This diversity of approaches, suggests there is no prospect of a standard template something that would require a common feature set to be extracted from faces. Interoperability in automated face recognition remains solidly based on images and documentary standards for those, in particular the ICAO portrait [27] specification deriving from the ISO/IEC 19794-5 Token frontal [24] standard, which are similar to certain ANSI/NIST Type 10 [26] formats.

Training: The algorithms submitted to NIST have been developed using image datasets that developers do not disclose. The development will often include application of machine learning techniques and will additionally involve iterative training and testing cycles. NIST itself does not perform any training and does not refine or alter the algorithm in any way. Thus the model, data files, and libraries that define an algorithm are fixed for the duration of the tests. This reflects typical operational reality where recognition software, once installed, is fixed and constant until upgraded. This situation persists because on-site training of algorithms on customer data is atypical essentially because training is not a turnkey process.

Automated search and human review: Virtually all applications using automated face search require human review of the outputs at some frequency: Always for investigational applications; rarely in positive identification applications, after rejection (false or otherwise); and rarely in negative identification applications, after an alarm (false or otherwise). The human role is usually to compare a reference image with the query image or the live-subject if present, to render either a definitive decision on "exclusion" (different subjects), or "identification" (same subject), or a declaration that one or both images have "no value" and that no decision can be made. Note that automated face recognition algorithms are not built to do exclusion - low scores from a face comparison arise from different faces *and* poor quality images of the same face.

Human reviewers make recognition errors [5, 19, 25] and are sensitive to image acquisition and quality. Accurate human review is supported by high resolution - as specified in the Type 50, 51 acquisition profiles of the ANSI/NIST Type 10 record [26], and by multiple non-frontal views as specified in the same standard. These often afford views of the ear. Organizations involved in image collection should consider supporting human adjudication by collecting high-resolution frontal and non-frontal views, preparing low resolution versions for automated face recognition [24], and retaining both for any subsequent resolution of candidate matches. Along these lines, the ISO/IEC Joint Technical

Committee 1 subcommittee 37 on biometrics has just initiated projects on image quality assessment and face-aware capture.

Release Notes

FRVT Activities: Since February 2017, NIST has been evaluating one-to-one verification algorithms on an ongoing basis. NIST then restarted FRVT's one-to-many track in February 2018, inviting participants to send up to prototype algorithms. Both tracks allows developers to submit updated algorithms to NIST at any time but no more frequently than four calendar months. This more closely aligns development and evaluation schedules. Results are posted to the web within a few weeks of submission. Details and full report are linked from the Ongoing FRVT site.

FRVT Reports: The results of the FRVT appear in the series NIST Interagency Reports tabulated below. The reports were developed separately and released on different schedules. In prior years NIST has mostly reported FRVT results as a single report; this had the disadvantage that results from completed sub-studies were not published until all other studies were complete.

Date	Link	Title	No.
2014-03-20	PDF	FRVT Performance of Automated Age Estimation Algorithms	7995
2015-04-20	PDF	Face Recognition Vendor Test (FRVT) Performance of Automated Gender Classification Algorithms	8052
2014-05-21	PDF	FRVT Performance of face identification algorithms	8009
2017-03-07	PDF	Face In Video Evaluation (FIVE) Face Recognition of Non-Cooperative Subjects	8173
2017-11-23	PDF	The 2017 IARPA Face Recognition Prize Challenge (FRPC)	8197
2018-11-27	PDF	Face Recognition Vendor Test - Part 2: Identification	8271
2019-09-11	PDF	Face Recognition Vendor Test - Part 2: Identification	8271
2019-12-11	PDF	Face Recognition Vendor Test - Part 3: Demographic Effects	8280
2020-01-03	WWW	Face Recognition Vendor Test (FRVT) - Part 1 Verification	Draft

Details appear on pages linked from `https://www.nist.gov/programs-projects/face-projects`.

Appendices: This report is accompanied by appendices which present exhaustive results on a per-algorithm basis. These are machine-generated and are included because the authors believe that visualization of such data is broadly informative and vital to understanding the context of the report.

Typesetting: Virtually all of the tabulated content in this report was produced automatically. This involved the use of scripting tools to generate directly type-settable LaTeX content. This improves timeliness, flexibility, maintainability, and reduces transcription errors.

Graphics: Many of the Figures in this report were produced using the ggplot2 package running under R, the capabilities of which extend beyond those evident in this document.

Contents

1 Introduction

One-to-many identification represents the largest market for face recognition technology. Algorithms are used across the world in a diverse range of biometric applications: detection of duplicates in databases, detection of fraudulent applications for credentials such as passports and driving licenses, token-less access control, surveillance, social media tagging, lookalike discovery, criminal investigation, and forensic clustering.

This report contains a breadth of performance measurements relevant to many applications. Performance here refers to accuracy and resource consumption. In most applications, the core accuracy of a facial recognition algorithm is the most important performance variable. Resource consumption will be important also as it drives the amount of hardware, power, and cooling necessary to accommodate high volume workflows. Algorithms consume processing time, they require computer memory, and their static template data requires storage space. This report documents these variables.

1.1 Open-set searches

FRVT tested open-set identification algorithms. Real-world applications are almost always "open-set", meaning that some searches have an enrolled mate, but some do not. For example, some subjects have truly not been issued a visa or drivers license before; some law enforcement searches are from first-time arrestees[6]. In an "open-set" application, algorithms make no prior assumption about whether or not to return a high-scoring result, and for a mated search, the ideal behaviour is that the search produces the correct mate at high score and first rank. For a non-mate search, the ideal behavior is that the search produces zero high-scoring candidates.

Many academic benchmarks execute only closed-set searches. The proportion of mates found in the rank one position is the default accuracy metric. This hit rate metric ignores the score with which a mate is found; weak hits count as much as strong hits. This ignores the real-world imperative that in many applications it is necessary to elevate a threshold to reduce the number of false positives.

[6]Operationally closed-set applications are rare because it is usually not the case that all searches have an enrolled mate. One counter-example, however, is a cruise ship in which all passengers are enrolled and all searches should produce exactly one identity. Another example is forensic identification of dental records from an aircraft crash.

2 Evaluation datasets

This report documents accuracy for four kinds of images - mugshots, webcam, profiles and wild - as described in the following sections.

2.1 Immigration-related images

This report includes benchmark tests sharing a common enrollment of high quality frontal portrait images collected while subject make applications for various immigration benefits. We then search that with two kinds of images, webcam images collected during in-bound immigration and also images collected from registered travelers using a ATM-style kiosk. These are described below and depicted in Figure 4.

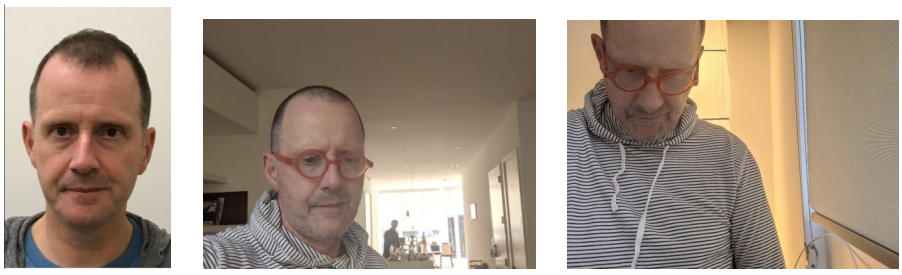

a) Application b) Immigration Lane c) Kiosk

Figure 4: Example photos.

- **Application reference photos**: The images are collected in an attended interview setting using dedicated capture equipment and lighting. The images, at size 300x300 pixels, are smaller than normally indicated by ISO. The images are all high-quality frontal portraits collected in immigration offices and with a white background. As such, potential quality related drivers of high false match rates (such as blur) can be expected to be absent. The images are encoded as ISO/IEC 10918-1 i.e. JPEG. Older images had a compression ration of about 16:1, while newer images, since 2010, are more lightly compressed at 4:1. When these images are provided as input into the algorithm, they are labeled with the type "iso". This report enrols 1 600 000 application images, one per person.

- **Border crossing photos**: Most images are have width 320 and height 240 pixels. They are JPEG compressed at 16:1 i.e. filesize just below 15KB. The images present challenges for face recognition in that subjects often exhibit non-zero yaw and pitch (associated with the rotational degrees of freedom of the camera mount), low contrast (due to varying and intense background lights), and poor spatial resolution (due to inexpensive cameras). There are often subjects standing in the background, usually at very low resolution (see Figure 4b). In such cases, algorithms should detect all faces and determine which is the largest and most centered. When these images are provided as input into the algorithm, they are labeled with the type "wild".

- **Kiosk photos**: These photos were collected from subjects whose attention was focused on interaction with an immigration kiosk. They images were not intended for use with automated face recognition. The camera is situated above a display which the user touches, and is triggered either without directing the subject to look at it, or without waiting for the subject to comply. The images are therefore characterized by pitch-down pose, sometimes exceeding 45 degrees, as in Figure 4c. Yaw-angle variation is mild, with most images close to frontal. The images

have width 320 pixels and height 240 pixels and therefore tall individuals are sometimes cropped. This is often just above the eyes and can occur at the nose or mouth. Conversely, short individuals are sometimes cropped such that only the top part of the face is visible. In a quite small number of cases, there other subjects standing just behind the primary subject such that algoriths should detect all faces and determine which is the largest and most centered. Background ceiling lighting is often visible and this sometimes leads to under-exposure of the face When these images are provided as input into the algorithm, they are labeled with the type "wild".

2.2 Law enforcement images

The main mugshot dataset used is referred to as the FRVT 2018 set. This set was collected over the period 2002 to 2017 in routine United States law enforcement operations. This set yields three subsets

- **Mugshots**: Mugshots comprise about 86% of the database. They have reasonable compliance with the ANSI/NIST ITL1-2011 Type 10 standard's subject acquisition profiles levels 10-20 for frontal images [26]. The most common departure from the standard's requirements is the presence of mild pose variations around frontal - the images of Figure 5 are typical. The images vary in size, with many being 480x600 pixels with JPEG compression applied to produce filesizes of between 18 and 36KB with many images outside this range, implying that about 0.5 bits are being encoded per pixel. When these images are provided as input into the algorithm, they are labeled with the type "mugshot". Example images appear in Fig. 5

  NIST Interagency Report 8238 includes a comparison of this set of mugshots with the smaller and easier sets of mugshots used in tests run in 2010 and 2014.

- **Profile images**: Profile-view images have been collected in law enforcement for more than 100 years, as human capability is improved with orthogonal information. The profile images used in this report were collected during the same session as the frontal mugshot photograph, in the same standardized photographic setup. These would not therefore be used with automated face recognition. A small subset, 200 000 images, were set aside for testing. When these images are provided as input into the algorithm, they are labeled with the type "wild". Example images appear in Fig. 7

- **Webcam images**: The remaining 14% of the images were collected using an inexpensive webcam attached to a flexible operator-directed mount. These images are all of size 240x240 pixels, that are in considerable violation of most quality-related clauses of all face recognition standards. As evident in the figure, the most common defects are non-frontal pose (associated with the rotational degrees of freedom of the camera mount), low contrast (due to varying and intense background lights), and poor spatial resolution (due to inexpensive camera optics) - see examples in Fig 6. The images are overly JPEG compressed, to between 4 and 7KB, implying that only 0.5 to 1 bits are being encoded per color pixel. When these images are provided as input into the algorithm, they are labeled with the type "wild". Example images appear in Fig. 6

These are drawn from NIST Special Database 32 which may be downloaded here.

These images were partitioned in galleries and probesets for the various experiment listed in Table 1.

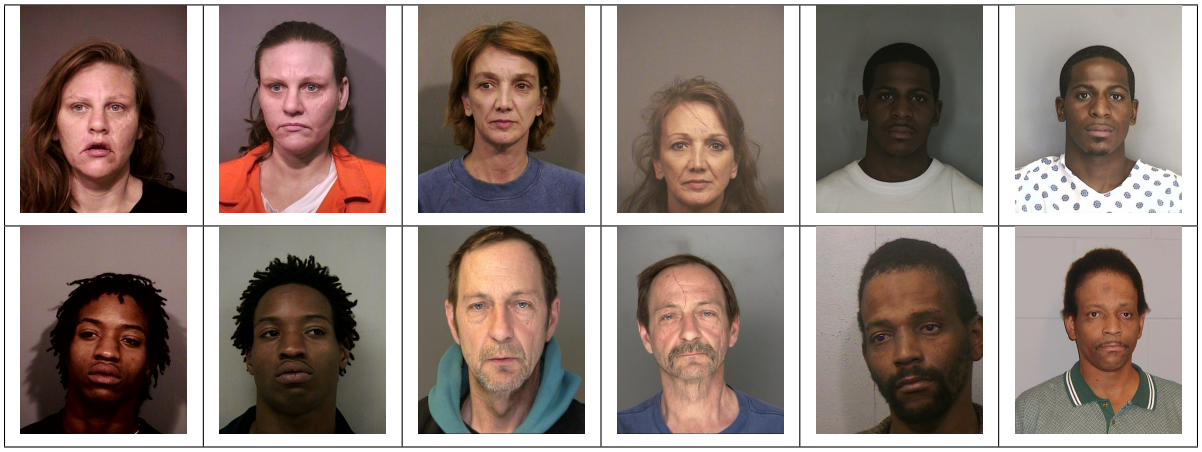

Figure 5: Six mated mugshot pairs representative of the FRVT-2014 (LEO) and FRVT-2018 datasets. The images are collected live, i.e. not scanned from paper. Image source: NIST Special Database 32 the Multiple Encounter Deceased Subjects dataset.

Figure 6: Twelve webcam images representative of probes against the FRVT-2018 mugshot gallery. The first eight images are four mated pairs. Such images present challenges to recognition including pose, non-uniform illumination, low contrast, compression, cropping, and low spatial sampling rate. Image source: NIST Special Database 32 the Multiple Encounter Deceased Subjects dataset.

Figure 7: **[Profile views]** *The three images are a frontal enrollment, subsequent frontal probe, and same-session ninety degree profile view. While collection of both frontal and profile views has been typical in law enforcement for more than a century, the recognition of profile to frontal views has essentially been impossible. However, reasonbly high accuracy results is now possible - see section E.*

Image		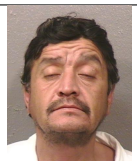		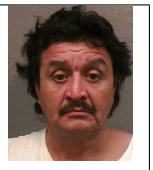
Encounter	1	...	$K_i - 1$	K_i
Capture Time	T_1	...	T_{K_i-1}	T_{K_i}
Role RECENT	Not used	Not used	Enrolled	Search
Role LIFETIME	Enrolled	Enrolled	Enrolled	Search

Figure 8: Depiction of the "recent" and "lifetime" enrollment types. Image source: NIST Special Database 32

2.3 Enrollment strategies

Many operational applications include collection and enrollment of biometric data from subjects on more than one occasion. This might be done on a regular basis, as might occur in credential (re-)issuance, or irregularly, as might happen in a criminal recidivist situation [4]. The number of images per person will depend on the application area. In civil identity credentialing (e.g. passports, driver's licenses), the images will be acquired approximately uniformly over time (e.g. ten years for a passport). While the distribution of dates for such images of a person might be assumed uniform, a number of factors might undermine this assumption[7]. In criminal applications, the number of images would depend on the number of arrests. The distribution of dates for arrest records for a person (i.e. the recidivism distribution) has been modeled using the exponential distribution but is recognized to be more complicated[8].

In any case, the 2010 NIST evaluation of face recognition showed that considerable accuracy benefits accrue with retention and use of *all* historical images [6].

To this end, the FRVT API document provides $K \geq 1$ images of an individual to the enrollment software. The software is tasked with producing a single proprietary undocumented "black-box" template[9] from the K images. This affords the algorithm an ability to generate a *model* of the individual, rather than to simply extract features from each image on a sequential basis.

As depicted in Figure 8, the i-th individual in the FRVT 2018 dataset has K_i images. These are labelled as x_k for $k = 1 \ldots K_i$ in chronological order of capture date. To measure the utility of having multiple enrollment images, this report evaluates three kinds of enrollment:

- ▷ **Recent**: Only the second most recent image, x_{K_i-1} is enrolled. This strategy of enrollment mimics the operational policy of retaining the imagery from the most recent encounter. This might be done operationally to ameliorate the effects of face ageing. Obviously retaining only the most recent image should only be done if the identity of the person is trusted to be correct. For example, in an access control situation retention of the most recent successful *authentication* image would be hazardous if it could be a false positive.
- ▷ **Lifetime-consolidated**: All but the most recent image are enrolled, $x_1 \ldots x_{K_i-1}$. This subject-centric strategy might be adopted if quality variations exist where an older image might be more suitable for matching, despite the ageing effect.

[7] For example, a person might skip applying for a passport for one cycle, letting it expire. In addition, a person might submit identical images (from the same photography session) to consecutive passport applications at five year intervals.
[8] A number of distributions have been considered to model recidivism, see for example [3].
[9] There are no formal face template standards. Template standards only exist for fingerprint minutiae - see ISO/IEC 19794-2:2011.

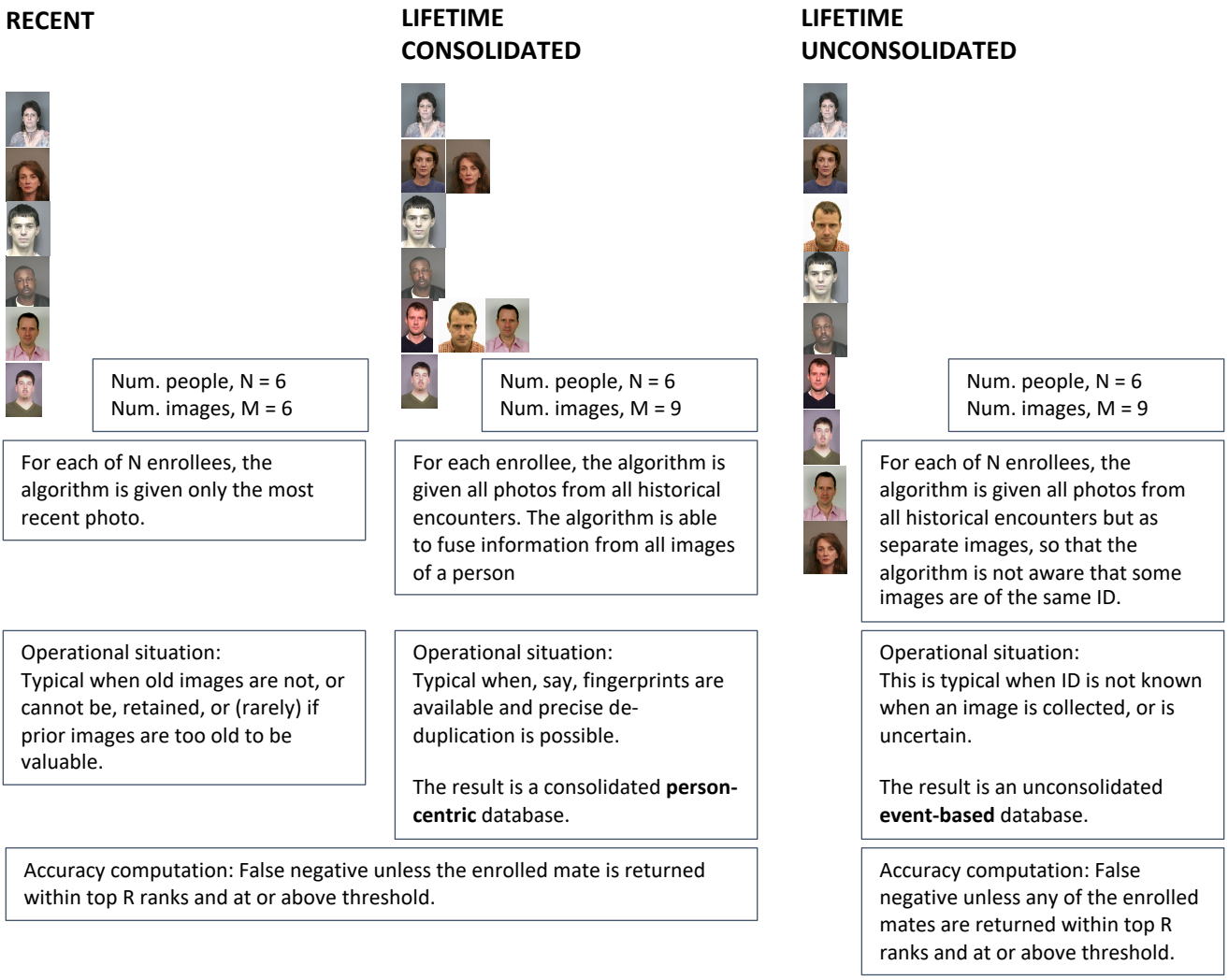

Figure 9: **Enrollment strategies**. *The figure shows the three kinds of enrollment databases examined in this report. Image source: NIST Special Database 32*

	ENROLLMENT				SEARCH			
	TYPE SEE	POPULATION			MATE		NON-MATE	
	SECTION 2.3	FILTER	N-SUBJECTS	N-IMAGES	N-SUBJECTS	N-IMAGES	N-SUBJECTS	N-IMAGES
Mugshot trials from enrollment of single images								
1	RECENT	NATURAL	640 000	640 000	154 549	154 549	331 254	331 254
2	RECENT	NATURAL	1 600 000	1 600 000				
3	RECENT	NATURAL	3 000 000	3 000 000				
4	RECENT	NATURAL	6 000 000	6 000 000				
5	RECENT	NATURAL	12 000 000	12 000 000				
Cross-domain								
13	MUGSHOTS AS ON ROW 2				82 106 WEBCAM	82 106 WEBCAM	331 254 WEBCAM	331 254 WEBCAM
Cross-view								
14	MUGSHOTS AS ON ROW 2				100 000 PROFILE	100 000 PROFILE	100 000 PROFILE	100 000 PROFILE
Mugshot ageing								
17	OLDEST	NATURAL	3 068 801	3 068 801	2 853 221	10 951 064	0	0
Border crossing ageing								
17	OLDEST	NATURAL	1 600 000	1 600 000	1 922 437	1 922 437	1 920 000	1 920 000
Visa-border								
19	PRIOR	NATURAL	1 600 000 VISA	1 600 000 VISA	80 000 BORDER	80 000 BORDER	80 000 BORDER	80 000 BORDER
20	VISA AS ON ROW 18				21 016 BORDER	21 016 BORDER	21 016 BORDER	21 016 BORDER

Table 1: **Enrollment and search sets**. *Each row summarizes one identification trial. Unless stated otherwise, all entries refer to mugshot images. The term "natural" means that subjects were selected without heed to demographics, i.e. in the distribution native to this dataset. The probe images were collected in a different calendar year to the enrollment image. Missing values in rows 2-12 are the same as in row 1.*

▷ **Lifetime-unconsolidated**: Again all but the most recent image are enrolled $x_1 \ldots x_{K_i-1}$ but now separately, with different identifiers, such that the algorithm is not aware that the images are from the same face. This kind of event- or encounter-centric enrollment is very common when operational constraints preclude reliable consolidation of the historical encounters into a single identity. This aspect also prevents the recognition algorithm from a) building a holistic model of identity (as is common in speaker recognition systems) and b) implementing fusion, for example template-level fusion of feature vectors, or post-search score-level fusion. The result is that searches will typically yield more than one image of a person in the top ranks. This has consequences for appropriate metrics, as detailed in section 3.2.1

NIST first evaluated this kind of enrollment in mid 2018, and the results tables include some comparison of accuracy available from all three enrollment styles.

In all cases, the most recent image, x_{K_i}, is reserved as the search image. For the 1.6 million subject enrollment partition of the FRVT 2018 data, $1 \leq K_i \leq 33$ with $K_i = 1$ in 80.1% of the individuals, $K_i = 2$ in 13.4%, $K_i = 3$ in 3.7%, $K_i = 4$ in 1.4%, $K_i = 5$ in 0.6%, $K_i = 6$ in 0.3%, and $K_i > 6$ is 0.2% for everyone else. This distribution is substantially dependent on United States recidivism rates.

We did not evaluate the case of retaining only the highest quality image, since automated quality assessment is out of scope for this report. We do not anticipate that such strategies will prove beneficial when the quality assessment apparatus is imperfect and unvalidated.

3 Performance metrics

This section gives specific definitions for accuracy and timing metrics. Tests of open-set biometric algorithms must quantify frequency of two error conditions:

- **False positives**: Type I errors occur when search data from a person who has never been seen before is incorrectly associated with one or more enrollees' data.
- **Misses**: Type II errors arise when a search of an enrolled person's biometric does not return the correct identity.

Many practitioners prefer to talk about "hit rates" instead of "miss rates" - the first is simply one minus the other as detailed below. Sections 3.1 and 3.2 define metrics for the Type I and Type II performance variables.

Additionally, because recognition algorithms sometimes fail to produce a template from an image, or fail to execute a one-to-many search, the occurrence of such events must be recorded. Further because algorithms might elect to not produce a template from, for example, a poor quality image, these failure rates must be combined with the recognition error rates to support algorithm comparison. This is addressed in section 3.5.

Finally, section 3.7 discusses measurement of computation duration, and section 3.8 addresses the uncertainty associated with various measurements. Template size measurement is included with the results.

3.1 Quantifying false positives

It is typical for a search to be conducted into an enrolled population of N identities, and for the algorithm to be configured to return the closest L candidate identities. These candidates are ranked by their score, in descending order, with all scores required to be greater than or equal to zero. A human analyst might examine either all L candidates, or just the top $R \leq L$ identities, or only those with score greater than threshold, T. The workload associated with such examination is discussed later, in 3.6.

False alarm performance is quantified in two related ways. These express how many searches produces false positives, and then, how many false positives are produced in a search.

False positive identification rate: The first quantity, FPIR, is the proportion of non-mate searches that produce an adverse outcome:

$$\text{FPIR}(N,T) = \frac{\text{Num. non-mate searches where one or more enrolled candidates are returned with score at or above threshold}}{\text{Num. non-mate searches attempted.}} \tag{1}$$

Under this definition, FPIR can be computed from the highest non-mate candidate produced in a search - it is not necessary to consider candidates at rank 2 and above. FPIR is the primary measure of Type I errors in this report.

Selectivity: However, note that in any given search, several non-mate may be returned above threshold. In order to quantify such events, a second quantity, selectivity (SEL), is defined as the *number* of non-mates returned on a candidate list, averaged over all searches.

$$\text{SEL}(N,T) = \frac{\text{Num. non-mate enrolled candidates returned with score at or above threshold}}{\text{Num. non-mate searches attempted.}} \tag{2}$$

where $0 \leq$ SEL(N, T) $\leq$L. Both of these metrics are useful operationally. FPIR is useful for targeting how often an

adverse false positive outcome can occur, while SEL as a number is related to workload associated with adjudicating candidate lists. The relationship between the two quantities is complicated - it depends on whether an algorithm concentrates the false alarms in the results of a few searches or whether it disburses them across many. This was detailed in FRVT 2014, NISTIR 8009. It has not yet been detailed in FRVT 2018.

3.2 Quantifying hits and misses

If L candidates are returned in a search, a shorter candidate list can be prepared by taking the top $R \leq L$ candidates for which the score is above some threshold, $T \geq 0$. This reduction of the candidate list is done because thresholds may be applied, and only short lists might be reviewed (according to policy or labor availability, for example). It is useful then to state accuracy in terms of R and T, so we define a "miss rate" with the general name **false negative identification rate** (FNIR), as follows:

$$\text{FNIR}(N, R, T) = \frac{\text{Num. mate searches with enrolled mate found outside top R ranks or score below threshold}}{\text{Num. mate searches attempted.}} \quad (3)$$

This formulation is simple for evaluation in that it does not distinguish between causes of misses. Thus a mate that is not reported on a candidate list is treated the same as a miss arising from face finding failure, algorithm intolerance of poor quality, or software crashes. Thus if the algorithm fails to produce a candidate list, either because the search failed, or because a search template was not made, the result is regarded as a miss, adding to FNIR.

Hit rates, and true positive identification rates: While FNIR states the "miss rate" as how often the correct candidate is either not above threshold or not at good rank, many communities prefer to talk of "hit rates". This is simply the **true positive identification rate**(TPIR) which is the complement of FNIR giving a positive statement of how often mated searches are successful:

$$\text{TPIR}(N, R, T) = 1 - \text{FNIR}(N, R, T) \quad (4)$$

This report does not report true positive "hit" rates, preferring false negative miss rates for two reasons. First, costs rise linearly with error rates. For example, if we double FNIR in an access control system, then we double user inconvenience and delay. If we express that as decrease of TPIR from, say 98.5% to 97%, then we mentally have to invert the scale to see a doubling in costs. More subtly, readers don't perceive differences in numbers near 100% well, becoming inured to the "high nineties" effect where numbers close to 100 are perceived indifferently.

Reliability is a corresponding term, typically being identical to TPIR, and often cited in automated (fingerprint) identification system (AFIS) evaluations.

An important special case is the **cumulative match characteristic**(CMC) which summarizes accuracy of mated-searches only. It ignores similarity scores by relaxing the threshold requirement, and just reports the fraction of mated searches returning the mate at rank R or better.

$$\text{CMC}(N, R) = 1 - \text{FNIR}(N, R, 0) \quad (5)$$

We primarily cite the complement of this quantity, $\text{FNIR}(N, R, 0)$, the fraction of mates *not* in the top R ranks.

The **rank one hit rate** is the fraction of mated searches yielding the correct candidate at best rank, i.e. CMC(N, 1). While this quantity is the most common summary indicator of an algorithm's efficacy, it is not dependent on similarity scores, so it does not distinguish between strong (high scoring) and weak hits. It also ignores that an adjudicating reviewer is often willing to look at many candidates.

3.2.1 False negative rates for unconsolidated galleries

As detailed in section 2.3 a common type of gallery, here referred to as the lifetime unconsolidate type, is populated with all images of an individual without any association between them. That is, the gallery construction algorithm is not provided with any ID labels that would support processing of a person's images jointly. This constrasts with the lifetime consolidate type where an algorithm may explicitly fuse features from multiple images of a person, or select a best image. In such cases, where the number of enrolled images is a random variable, we define two false negative rates as follows.

The first demands that the algorithm place any of the K_i mates in the top $R \geq 1$ ranks. The proportion of searches for which this does not occur forms a false negative identification rate:

$$\text{FNIR}_{\text{any}}(N, R, T) = 1 - \frac{\text{Num. mate searches where any enrolled mate is found in the top R ranks and at-or-above threshold}}{\text{Num. mate searches attempted.}} \tag{6}$$

The second demands that the algorithm place all K_i mates in the top $R \geq K_i$ ranks. The proportion of searches for which this does not occur forms a false negative identification rate:

$$\text{FNIR}_{\text{all}}(N, R, T) = 1 - \frac{\text{Num. mate searches where all enrolled mates are found in the top R ranks and at-or-above threshold}}{\text{Num. mate searches attempted.}} \tag{7}$$

Placing all mates in the top ranks is a more difficult task than correctly retrieving any image, so it holds that: $\text{FNIR}_{\text{all}} \geq \text{FNIR}_{\text{any}}$. This is evident in the results presented for November 2018 algorithms in Tables starting at **??**.

The information retrieval community might prefer to compute and plot *precision* and *recall*; this is a valid approach, but we advance the two metrics above because they relate to our normal definition of consolidated FNIR, and they cover the two extreme use-cases of wanting any hit vs. all hits.

3.3 DET interpretation

In biometrics, a false negative occurs when an algorithm fails to match two samples of one person – a Type II error. Correspondingly, a false positive occurs when samples from two persons are improperly associated – a Type I error.

Matches are declared by a biometric system when the native comparison score from the recognition algorithm meets some threshold. Comparison scores can be either similarity scores, in which case higher values indicate that the samples are more likely to come from the same person, or dissimilarity scores, in which case higher values indicate different people. Similarity scores are traditionally computed by fingerprint and face recognition algorithms, while dissimilarities are used in iris recognition. In some cases, the dissimilarity score is a distance possessing metric properties. In any case, scores can be either mate scores, coming from a comparison of one person's samples, or nonmate scores, coming from comparison of different persons' samples.

The words "genuine" or "authentic" are synonyms for mate, and the word "impostor" is used as a synonym for nonmate. The words "mate" and "nonmate" are traditionally used in identification applications (such as law enforcement search, or background checks) while genuine and impostor are used in verification applications (such as access control).

An error tradeoff characteristic represents the tradeoff between Type II and Type I classification errors. For identification this plots false negative vs. false positive identification rates i.e. FNIR vs. FPIR parametrically with T. Such plots

are often called detection error tradeoff (DET) characteristics or receiver operating characteristic (ROC). These serve the same function − to show error tradeoff − but differ, for example, in plotting the complement of an error rate (e.g. TPIR = 1 − FNIR) and in transforming the axes, most commonly using logarithms, to show multiple decades of FPIR. More rarely, the function might be the inverse of the Gaussian cumulative distribution function.

The slides of Figures 10 through 15 discuss presentation and interpretation of DETs used in this document for reporting face identification accuracy. Further detail is provided in formal biometrics testing standards, see the various parts of ISO/IEC 19795 Biometrics Testing and Reporting. More terms, including and beyond those to do with accuracy, appear in ISO/IEC 2382-37 Information technology – Vocabulary – Part 37: Harmonized biometric vocabulary.

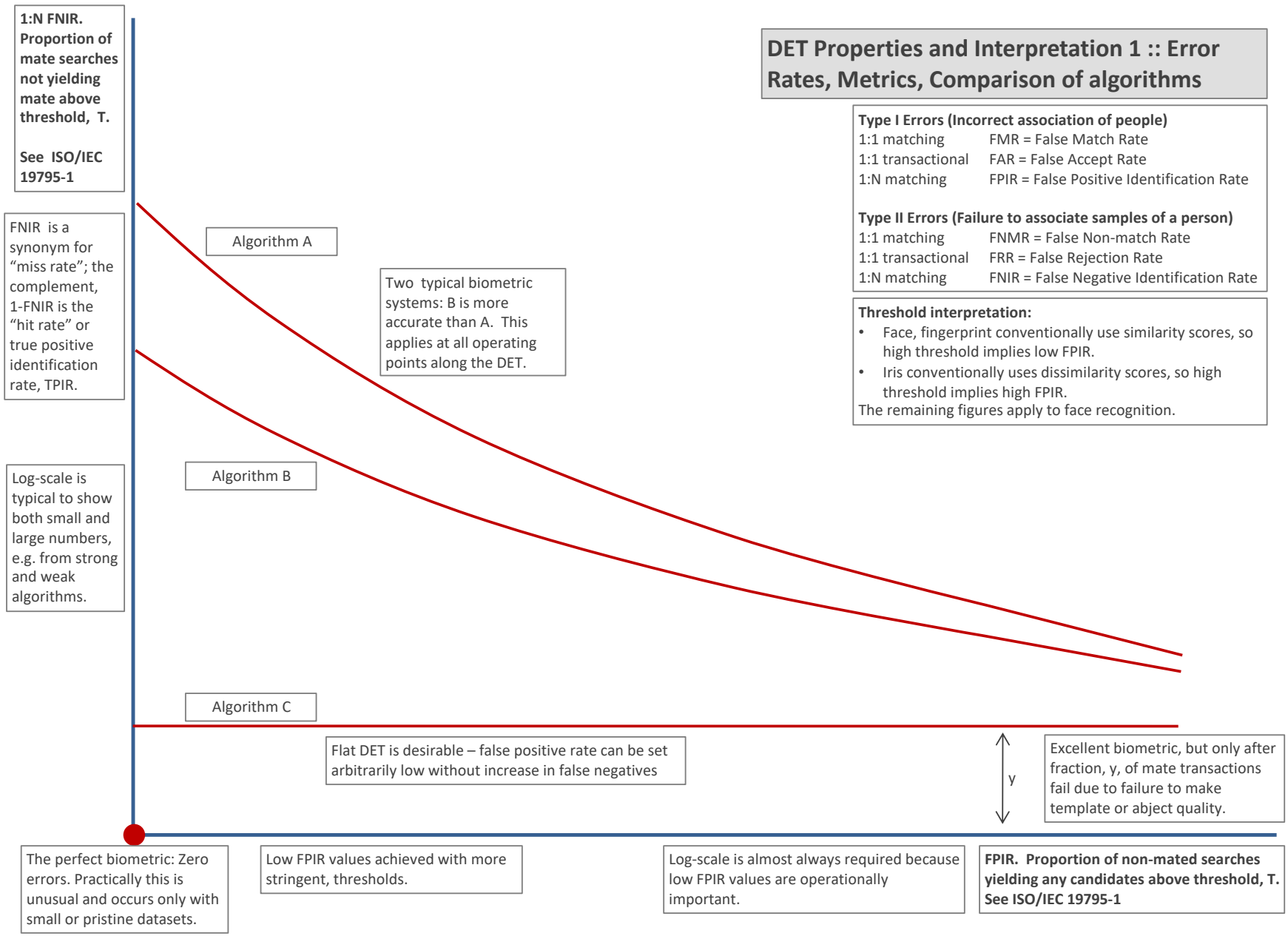

Figure 10: **DET as the primary performance reporting mechanism**.

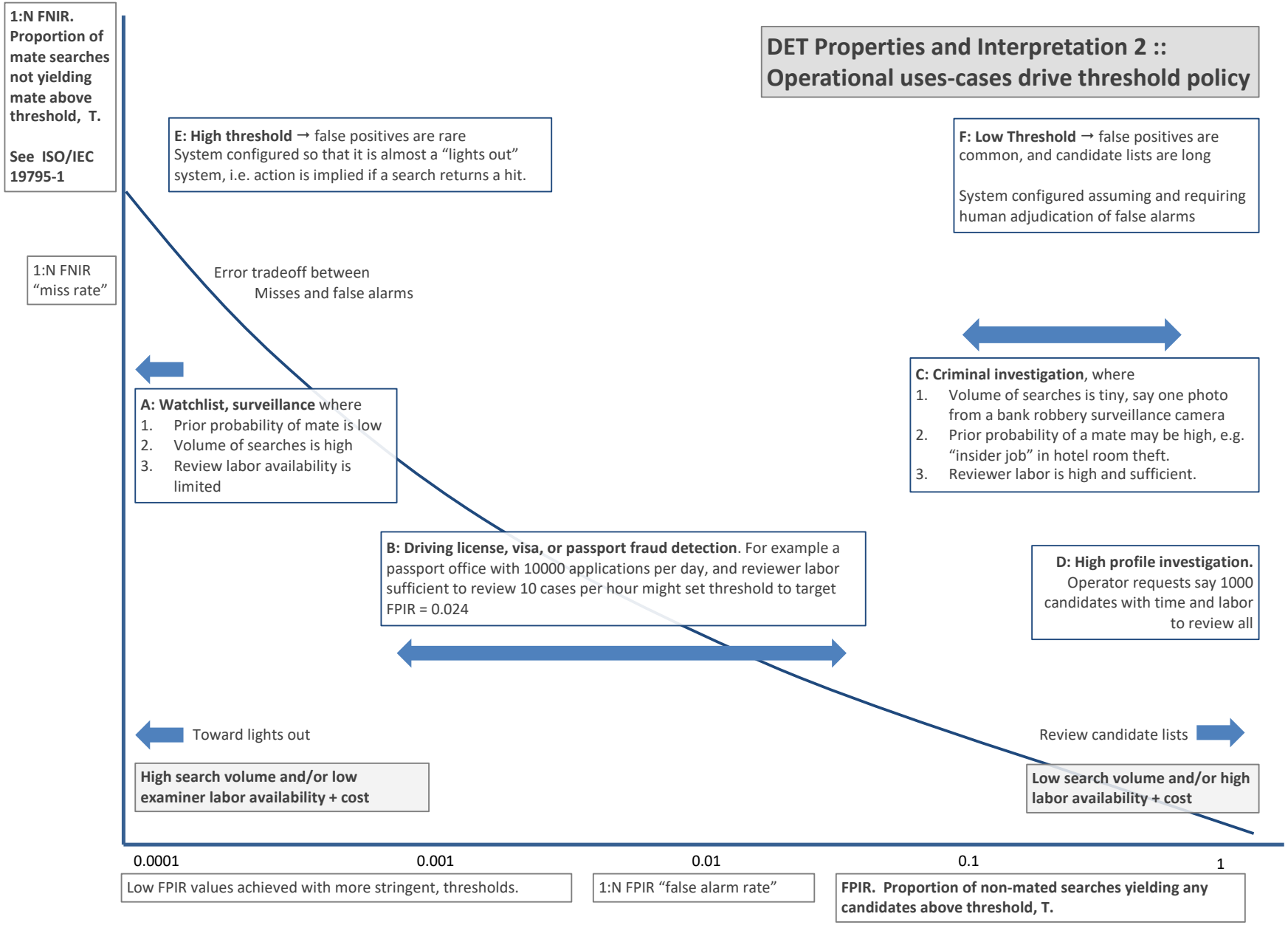

Figure 11: **DET as the primary performance reporting mechanism**.

FNIR(N, R, T) = False neg. identification rate
FPIR(N, T) = False pos. identification rate
N = Num. enrolled subjects
R = Num. candidates examined
T = Threshold
T = 0 → Investigation
T > 0 → Identification

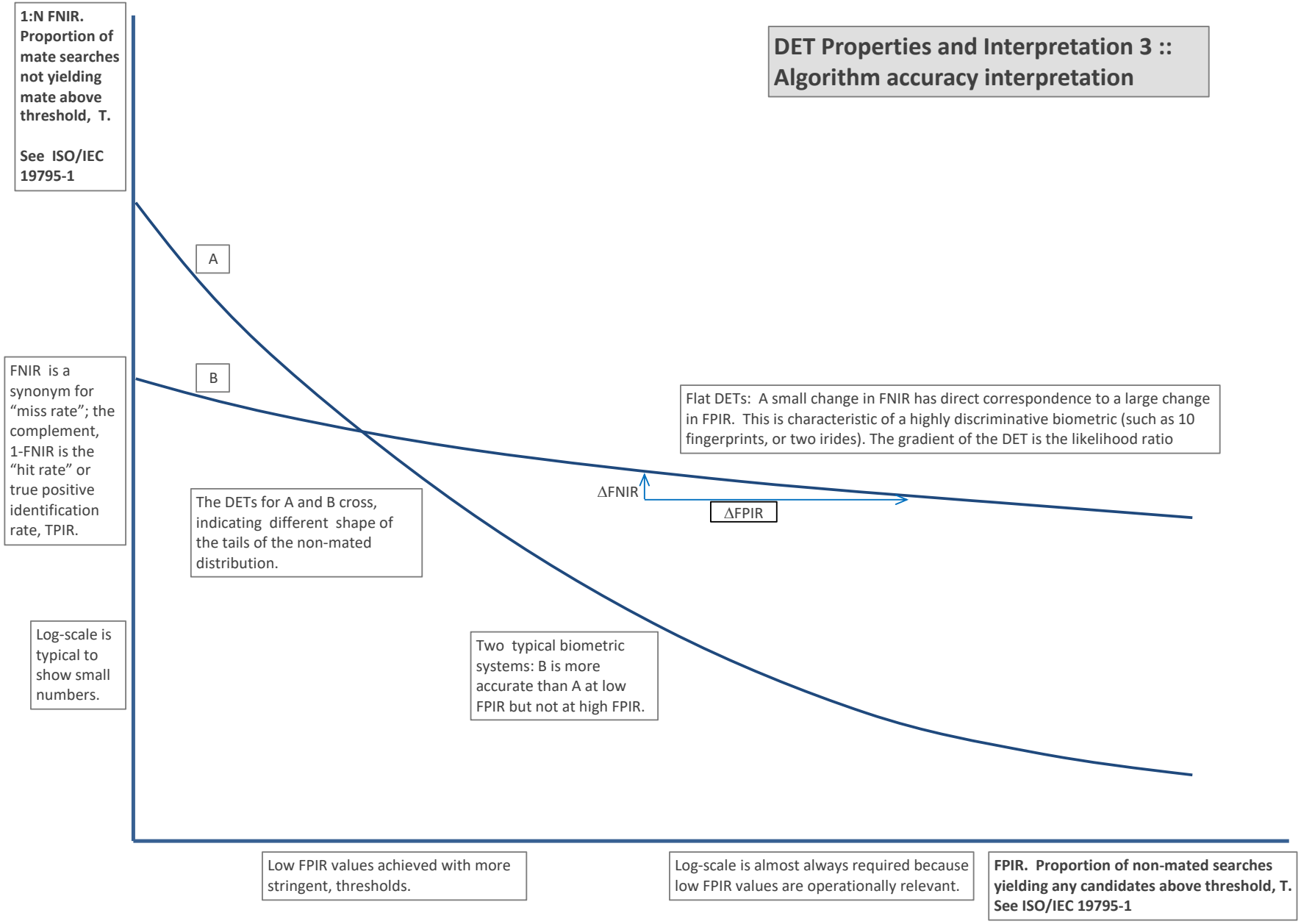

Figure 12: **DET as the primary performance reporting mechanism**.

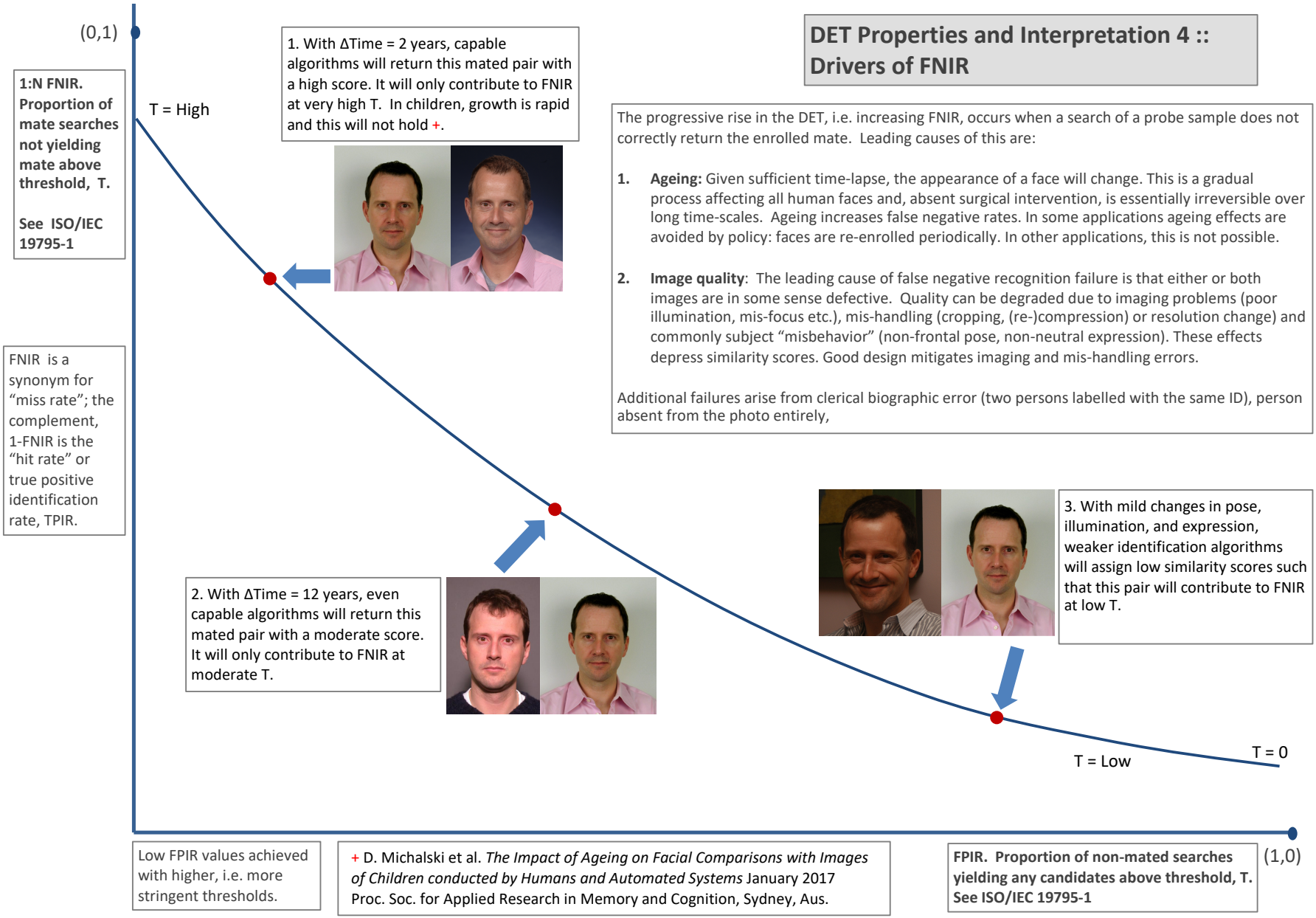

Figure 13: **DET as the primary performance reporting mechanism**.

FNIR(N, R, T) = False neg. identification rate
FPIR(N, T) = False pos. identification rate
N = Num. enrolled subjects
R = Num. candidates examined
T = Threshold
T = 0 → Investigation
T > 0 → Identification

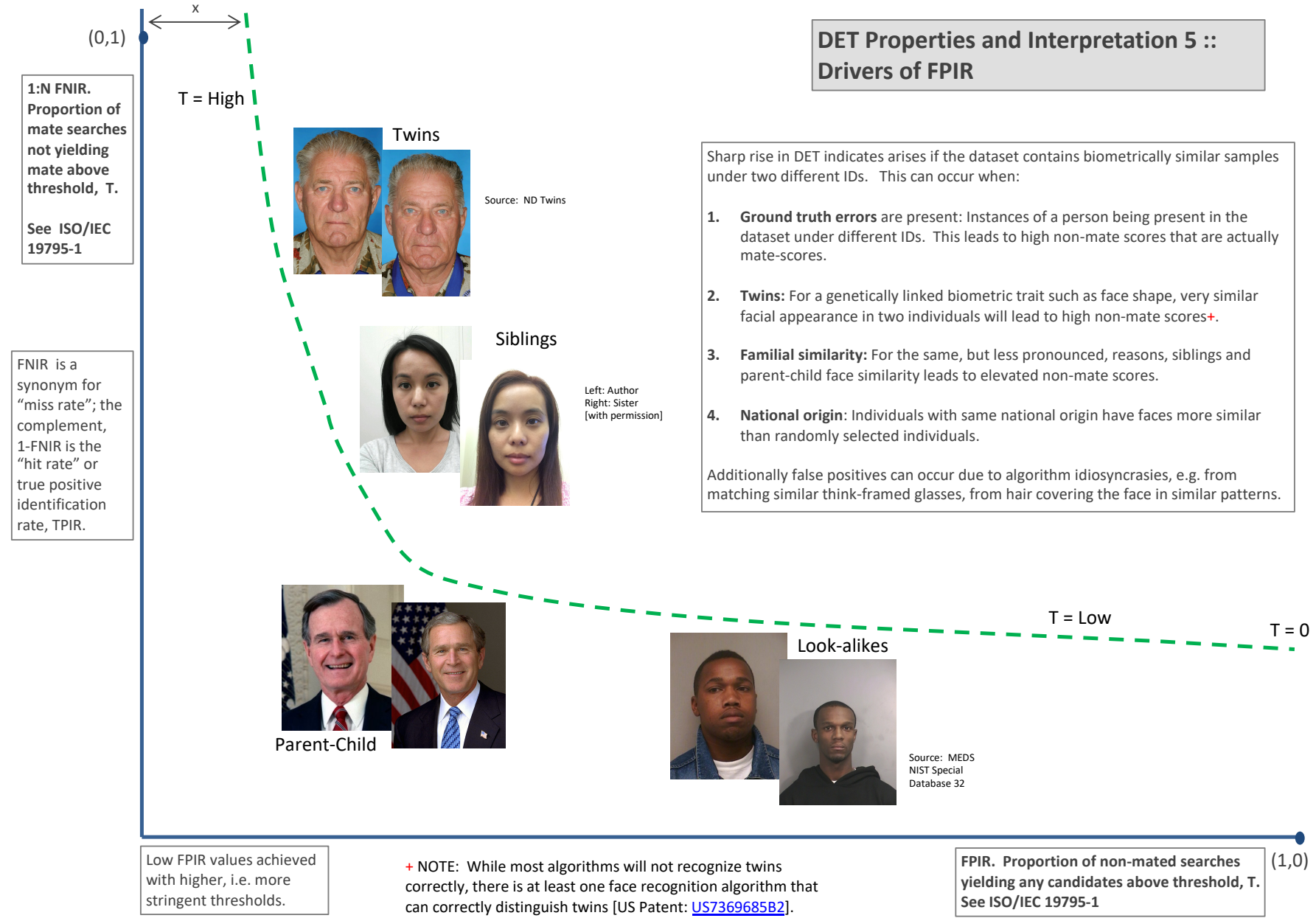

Figure 14: **DET as the primary performance reporting mechanism**.

2021/08/05 02:00:58
FNIR(N, R, T) = False neg. identification rate
FPIR(N, T) = False pos. identification rate
N = Num. enrolled subjects
R = Num. candidates examined
T = Threshold
T = 0 → Investigation
T > 0 → Identification

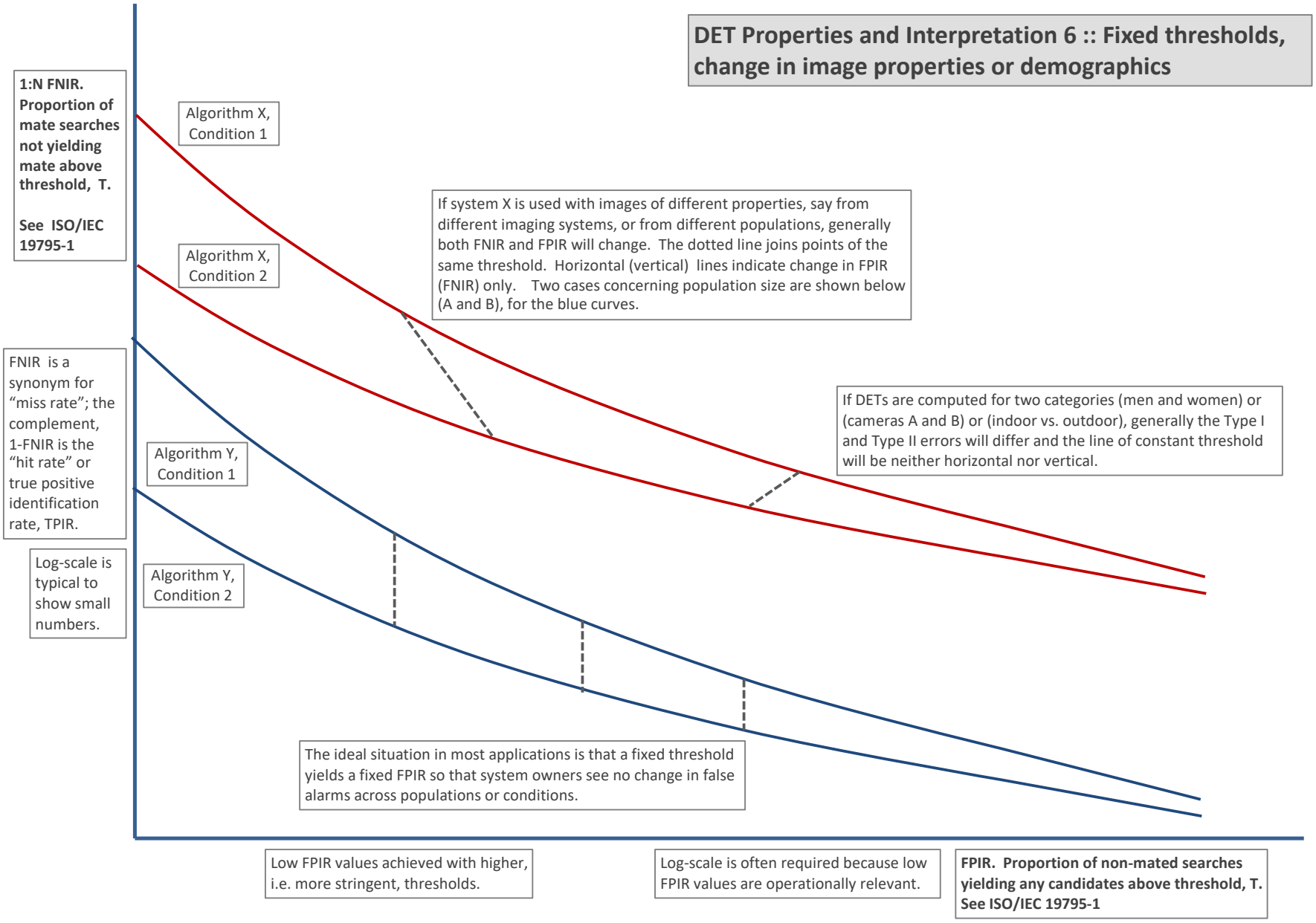

Figure 15: **DET as the primary performance reporting mechanism**.

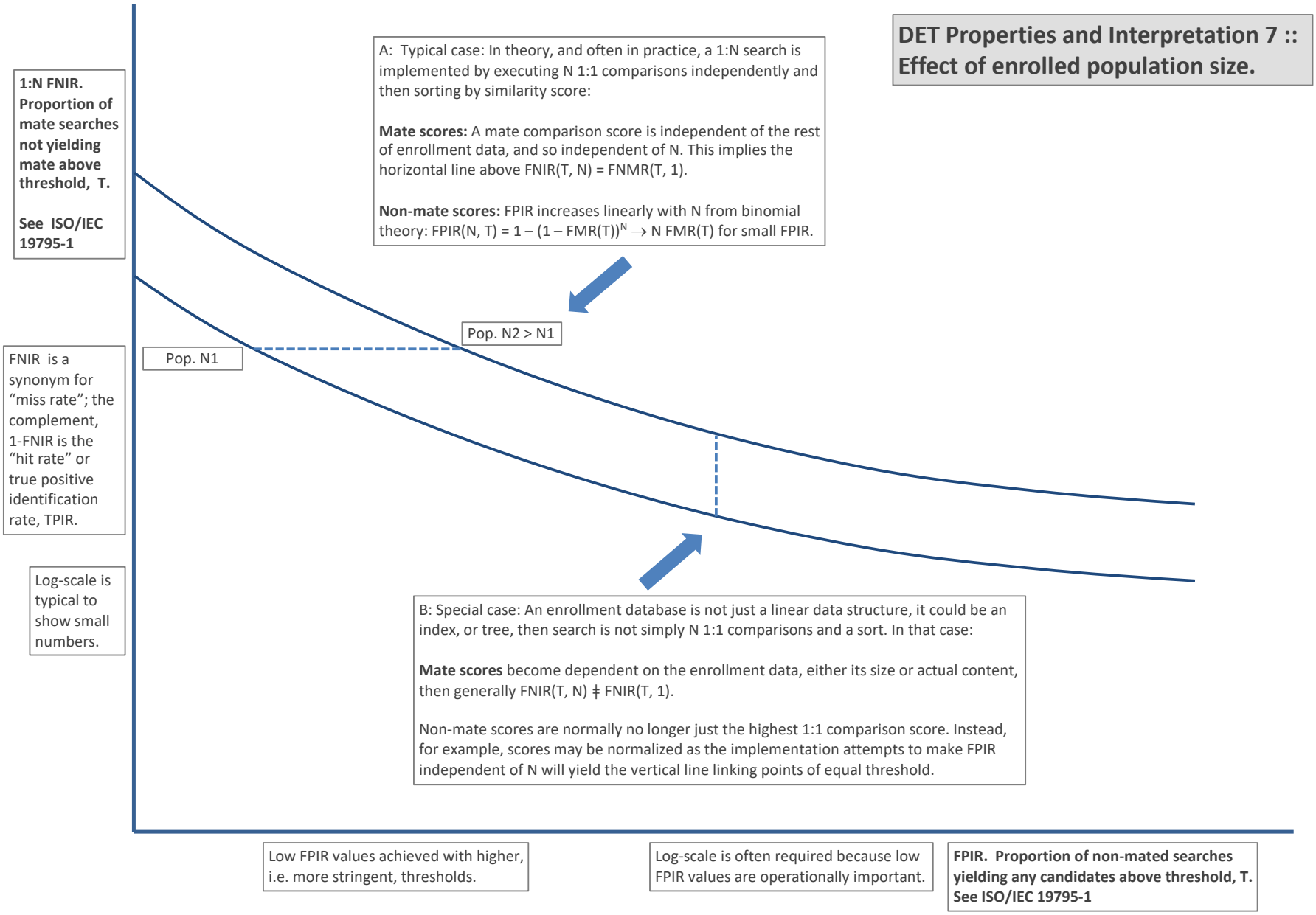

Figure 16: **DET as the primary performance reporting mechanism**.

FNIR(N, R, T) = FPIR(N, T) = False neg. identification rate / False pos. identification rate
N = Num. enrolled subjects
R = Num. candidates examined
T = Threshold
T = 0 → Investigation
T > 0 → Identification

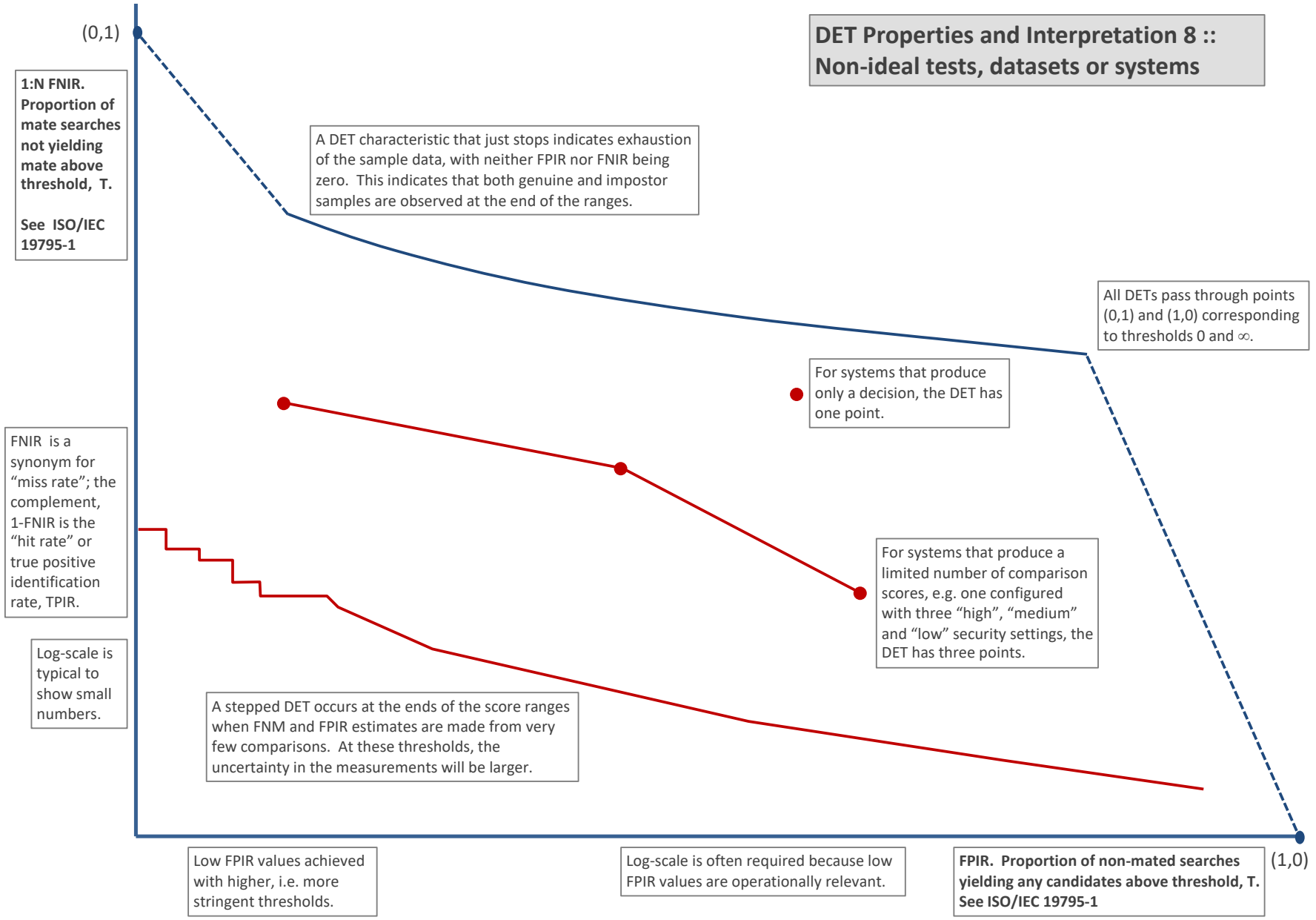

Figure 17: **DET as the primary performance reporting mechanism**.

2021/08/05 02:00:58

FNIR(N, R, T) = False neg. identification rate
FPIR(N, T) = False pos. identification rate
N = Num. enrolled subjects
R = Num. candidates examined
T = Threshold
T = 0 → Investigation
T > 0 → Identification

3.4 Best practice testing requires execution of searches with and without mates

FRVT embeds 1:N searches of two kinds: Those for which there is an enrolled mate, and those for which there is not. The respective numbers for these types of searches appear in Table 1. However, it is common to conduct only mated searches[10]. The cumulative match characteristic is computed from candidate lists produced in mated searches. Even if the CMC is the only metric of interest, the actual trials executed in a test should nevertheless include searches for which no mate exists. As detailed in Table 1 the FRVT reserved disjoint populations of subjects for executing true non-mate searches.

3.5 Failure to extract features

During enrollment some algorithms fail to convert a face image to a template. The proportion of failures is the failure-to-enroll rate, denoted by FTE. Similarly, some search images are not converted to templates. The corresponding proportion is termed failure-to-extract, denoted by FTX.

We do not report FTX because we assume that the same underlying algorithm is used for template generation for enrollment and search.

Failure to extract rates are incorporated into FNIR and FPIR measurements as follows.

- **Enrollment templates**: Any failed enrollment is regarded as producing a zero length template. Algorithms are required by the API [10] to transparently process zero length templates. The effect of template generation failure on search accuracy depends on whether subsequent searches are mated, or non-mated: Mated searches will fail giving elevated FNIR; non-mated searches will not produce false positives so, to first order, FPIR will be reduced by a factor of $1-\text{FTE}$.

- **Search templates and 1:N search**: In cases where the algorithm fails to produce a search template from input imagery, the result is taken to be a candidate list whose entries have no hypothesized identities and zero score. The effect of template generation failure on search accuracy depends on whether searches are mated, or non-mated: Mated searches will fail giving elevated FNIR; Non-mated searches will not produce false positives, so FPIR will be reduced. Thus given a measurement of false negative and positive rates made over only those where failures-to-extract did not occur, those rates - call them $\text{FNIR}^\dagger$ and $\text{FPIR}^\dagger$ - could be adjusted by an explicit measurement of FTX as follows

$$\text{FNIR} = \text{FTX} + (1 - \text{FTX})\text{FNIR}^\dagger \tag{8}$$

$$\text{FPIR} = (1 - \text{FTX})\text{FPIR}^\dagger \tag{9}$$

This approach is the correct treatment for positive-identification applications such as access control where cooperative users are enrolled and make attempts at recognition. This approach is not appropriate to negative identification applications, such as visa fraud detection, in which hostile individuals may attempt to evade detection by submitting poor quality samples. In those cases, template generation failures should be investigated as though a false alarm had occurred.

[10]For example, the Megaface benchmark. This is bad practice for several reasons: First, if a developer knows, or can reasonably assume, that a mate always exists, then unrealistic gaming of the test is possible. A second reason is that it does not put FPIR on equal footing with FNIR and that matters because in most applications, not all searches have mates - not everyone has been previously enrolled in a driving license issuance or a criminal justice system - so addressing between-class separation becomes necessary.

3.6 Fixed length candidate lists, threshold independent workload

Suppose an automated face identification algorithm returns L candidates, and a human reviewer is retained to examine up to R candidates, where $R \leq L$ might be set by policy, preference or labor availability. For now, assume also that the reviewer is not provided with, or ignores, similarity scores, and thresholds are not applied. Given the algorithm typically places mates at low (good) ranks, the number of candidates a reviewer can be expected to review can be derived as follows. Note that the reviewer will:

- ▷ Always inspect the first ranked image — Frac. reviewed = 1
- ▷ Then inspect those candidates where mate not confirmed at rank 1 — Frac. reviewed = 1-CMC(1)
- ▷ Then inspect those candidates where mate not confirmed at rank 1 or 2 — Frac. reviewed = 1-CMC(2)

etc. Thus if the reviewer will stop after a maximum of R candidates, the expected number of candidate reviews is

$$M(R) = 1 + (1 - CMC(1)) + (1 - CMC(2)) + \ldots + (1 - CMC(R-1)) \tag{10}$$

$$= R - \sum_{r=1}^{R-1} CMC(r) \tag{11}$$

A recognition algorithm that front-loads the cumulative match characteristic will offer reduced workload for the reviewer. This workload is defined only over the searches for which a mate exists. In the cases where there truly is no mate, the reviewer would review all R candidates. Thus, if the proportion of searches for which a mate does exist is β, which in the law enforcement context would be the recidivism rate [3], the full expression for workload becomes:

$$M(R) = \beta \left(R - \sum_{r=1}^{R-1} CMC(r) \right) \quad + \quad (1 - \beta)R \tag{12}$$

$$= R - \beta \sum_{r=1}^{R-1} CMC(r) \tag{13}$$

3.7 Timing measurement

Algorithms were submitted to NIST as implementations of the application programming interface(API) specified by NIST in the Evaluation Plan [10]. The API includes functions for initialization, template generation, finalization, search, gallery insert, and gallery delete. Two template generation functions are required, one for the preparation of an enrollment template, and one for a search template.

In NIST's test harness, all functions were wrapped by calls to the C++ std::chrono::high resolution clock which on the dedicated timing machine counts 1ns clock ticks. Precision is somewhat worse than that however.

3.8 Uncertainty estimation

3.8.1 Random error

This study leverages operational datasets for measurement of recognition error rates. This affords several advantages. First, large numbers of searches are conducted (see Table 1) giving precision to the measurements. Moreover, for the two mugshot datasets, these do not involve reuse of individuals so binomial statistics can be expected to apply to recognition error counts. In that case, an observed count of a particular recognition outcome (i.e. a false negative or false positive) in M trials will sustain 95% confidence that the actual error rate is no larger than some value.

As an example, the minimum number of mugshot searches conducted in this report is M =154 549, and for an observed FNIR around 0.002, the measurement supports a conclusion that the actual FNIR is no higher than 0.00228 at 99% confidence level. On the false positive side, we tabulate FNIR at FPIR values as low as 0.001. Given estimates based on 331 254 non-mate trials, the actual FPIR values will be below 0.00115 at 99% confidence. In conclusion, large scale evaluation, without reuse of subjects, supports tight uncertainty bounds on the measured error rates.

3.8.2 Systematic error

The FRVT 2018 dataset includes anomalies discovered as a result of inspecting images involved in recognition failures from the most accurate algorithms. Two kinds of failure occur: False negatives (which, for the purpose here, include failures to make templates) and false positives.

False negative errors: We reviewed 600 false negative pairs for which either or both of the leading two algorithms did not put the correct mate in the top 50 candidates. Given 154 549 searches, this number represents 0.39% of the total, resulting in FNIR ~ 0.0039. Of the 600 pairs:

- **A: Poor quality**: About 20% of the pairs included images of very low quality, often greyscale, low resolution, blurred, low contrast, partially cropped, interlaced, or noisy scans of paper images. Additionally, in a few cases, the face is injured or occluded by bandages or heavy cosmetics.
- **B: Ground truth identity label bugs**: About 15% of the pairs are not actually mated. We only assigned this outcome when a pair is clearly not mated.
- **C: Profile views**: About 35% included an image of a profile (side) view of the face, or, more rarely, an image that was rotated 90 degrees in-plane (roll).
- **D: Tattoos**: About 30% included an image of a tattoo that contained a face image. These arise from mis-labelling in the parent dataset metadata.
- **E: Ageing**: There is considerable time-lapse between the two captures.

All these estimates are approximate. Of these, the tattoo and mislabled images can never be matched. These constitute an accuracy floor in the sample implying that FNIR cannot be below 0.0018[11]. The profile-views, low-quality images, and images with considerable ageing can, in principle, be successfully matched - indeed some algorithms do so - so are not part of the accuracy floor.

[11] This value is the sum of two partial false negative rates: FNIR_B = 0.15 * 0.0039 plus FNIR_D = 0.3 * 0.0039

For the microsoft-4 algorithm the lowest miss rate from (recent entry in Table 20) is FNIR(640 000, 50, 0) = 0.0018. This is close to the value estimated from the inspection of misses. It is below the 0.0039 figure because the algorithm does match some profile and poor quality images, that the yitu-2 algorithm does not.

For many tables (e.g. Table 20), the FNIR values obtained for the FRVT-2018 mugshots could be corrected by reducing them by 0.0018. The best values would then be indistinct from zero. The results in this report *were not* adjusted to account for this systematic error.

False positive errors: As shown in Figure 1 and discussed in Figure 14 many of the DET characteristics in this report exhibit a pronounced turn upward at low false positive rates. The shape can be caused by identity labelling errors in the ground truth of a dataset, specifically persons present in the database under two IDs such that some proportion of non-mate pairs are actually mated. To look for such possibilities, we merged the highest 1000 non-mate pairs produced by three different algorithms which resulted in 1839 unique pairs. This constitutes 0.56% of all non-mate searches. We assert that it is *very* difficult for human reviewers to assign the pairs into the following three categories: twins; doppelgangers; or ground-truth errors (instances of the same person under two IDs). Given this difficulty we made no attempt to correct any possible ground truth errors except by removing 57 pairs in the following categories:

- **A: Profile views**: Thirteen pairs included one or two profile-view images. As described in Figure 165, these can cause false positives.
- **B: Same-session photographs**: For twelve pairs, the images were identical or trivially altered (e.g. cropped) versions of the same photo. These were present under a different ID likely due to some clerical or procedural mistake.
- **C: Tattoos of faces**: There were fourteen instances of tattoo photographs that contained faces causing false matches.
- **D: T-shirt faces**: There were six instances of T-shirt photographs (of Bob Marley and Che Guevara) being detected instead of the face and causing false positives.
- **E: Background faces**: There were twelve instances of one subject appearing in the background of two otherwise correct portrait photos.

Note we did not remove any images where there was a chance that the pair was actually a different person.

In any case, the results in this report have not been adjusted for this systematic error.

4 Results

This section gives extensive results for algorithms submitted to FRVT 2018. Three page "report cards" for each algorithm are contained in a separate supplement. Performance metrics were described in section 3. The main results are summarized in tabular form with more exhaustive data included as DET, CMC and related graphs in appendices as follows:

- The three tables 2-4 list algorithms alongside full developer names, acceptance date, size of the provided configuration data, template size and generation time, and search duration data.
  - The **template generation duration** is most important to applications that require fast response. For example, an eGate taking more than two seconds to produce a template might be unacceptable. Note that GPUs may be of utility in expediting this operation for some algorithms, though at additional expense. Two additional factors should be considered[12][13].
  - The **search duration** is the time taken for a search of a search template into a gallery of N enrollment templates. This performance variable, together with the volume of searches, is influential on the amount of hardware needed to sustain an operational deployment. This is measured here with the algorithm running on a single core of a contemporary CPU. Search is most simply implemented as N computations of a distance metric followed by a sort operation to find the closest enrollments. However, considerable optimization of this process is possible, up to and including fast-search algorithms that, by various means, avoid computation of all N distances.
  - The **template size** is the size of the extracted feature vector (or vectors) and any needed header information. Large template sizes may be influential on bus or network bandwidth, storage requirements, and on search duration. While the template itself is an opaque data blob, the feature dimensionality might be estimated by assuming a four-bytes-per-float encoding. There is a wide range of encodings. For the more accurate algorithm, sizes range from 256 bytes to about 2KB bytes, indicating essentially no consensus on face modeling and template design.
  - The **template size multiplier** column shows how, given k input images, the size of the template grows. Most implementations internally extract features from each image and concatenate them, and implement some score-level fusion logic during search. Other implementations, including many of the most accurate algorithms, produce templates whose size does not grow with k. This could be achieved via selection of the best quality image - but this is not optimal in handling ageing where the oldest image could be the best quality. Another mechanism would be feature-level fusion where information is fused from all k inputs. In any case, as a black-box test, the fusion scheme is proprietary and unknown.
  - The size of the **configuration data** is the total size of all files resident in a vendor-provided directory that contains arbitrary read-only files such as parameters, recognition models (e.g caffe). Generally a large value for this quantity may prohibit the use of the algorithm on a resource-constrained device.

[12] The FRVT 2018 API prohibited threading, so some gains from parallelism may be available on multiple-cores or multiple processors, if the feature extraction code could be distributed across them.

[13] Note also that factors of two or more may be realizable by exploiting modern vector processing instructions on CPUs. It is not clear in our measurements whether all developers exploited Intel's AVX2 instructions, for example. Our machine was so equipped, but we insisted that the same compiled library should also run on older machines lacking that instruction. The more sophisticated implementations may have detected AVX2 presence and branched accordingly. The less sophisticated may be defaulted to the reduced instruction set. Readers should see the FRVT 2018 API document for the specific chip details.

▷ Tables 20-21 report core rank-based accuracy for mugshot images. The population size is limited to N = 1.6 million identities because this is the largest gallery size on which all algorithms were executed. Notable observations from these tables are as follows:

- **Accuracy gains since 2018**: NIST Interagency Report 8238 documented massive gains over those reported in the FRVT 2014 report, NIST Interagency Report 8009. Further gains are documented in this report. Comparing the most accurate algorithm in November 2018, NEC-3, the value of FNIR(N, L, T) reduced from 0.0031 to 0.0024 for the Sensetime-004 algorithm with N = 12 million recent images. The tables show broader gains: many developers have made advances since 2018 with between two and five-fold reduction in errors.
- **Wide range in accuracy**: The rank-1 miss rates vary from FNIR(N, 1, 0) = 0.0012 for sensetime-004 up to about 0.5 for the very fast but inaccurate microfocus-x algorithms. Among the developers who are superior to NEC in 2013, the range is from 0.002 to 0.035 for camvi-3. This large accuracy range is consistent with the buyer-beware maxim, and indicates that face recognition software is far from being commoditized.

▷ Tables 24-25 report threshold-based error rates, FNIR(N, L, T), for N = 1.6 million for mugshot-mugshot accuracy on FRVT 2014, FRVT 2018, and also (in pink) mugshot-webcam accuracy using FRVT 2018 enrollments. Notable observations from these tables are as follows:

- **Order of magnitude accuracy gains since 2014**: As with rank-based results, the gains in accuracy are substantial, though somewhat reduced. At FPIR = 0.01, the best improvement over NEC in 2014 is a 27 fold reduction in FNIR using the NEC_2 algorithm. At FPIR = 0.001, the largest gain is a six-fold reduction in FNIR via the NEC_3 algorithm.
- **Broad gains across the industry**: About 19 companies realize accuracy better than the NEC benchmark from 2014. This is somewhat lower than the 28 developers who succeeded on the rank-1 metric. This may be due to the ubiquity of, and emphasis on, the rank-1 metric in many published algorithm development papers.
- **Webcam images**: Searches of webcam images give FNIR(N, T) values around 2 to 3 times higher than mugshot searches. Notably the leading developers with mugshots are approximately the same with poorer quality webcams. But some developers e.g. Camvi, Megvii, TongYi, and Neurotechnology do improve their relative rankings on webcams, perhaps indicating their algorithms were tailored to less constrained images.

▷ Tables 14, 17, 18 and show, respectively, high-threshold, rank 1, and rank 50 FNIR values for all algorithms performing searches into five different gallery sizes, N = 640 000, N = 1 600 000, N = 3 000 000, N = 6 000 000 and 12 000 000. The FPIR = 0.001 table is included to inform high-volume duplicate detection applications. The Rank-1 table is included as a primary accuracy indicator. The Rank-50 table is included to inform agencies who routinely produce 50 candidates for human-review. The notable results are:

- **Slow growth in rank-based miss rates:** FNIR(N, R) generally grows as a power law, aN^b. From the straight lines of many graphs of Figure 20 this is clearly a reasonable model for most, but not all, algorithms. The coefficient a can be interpreted as FNIR in a gallery of size 1. The more important coefficient b indicates scalability, and often, $b \ll 1$, implies very benign growth in FNIR. The coefficients of the models appear in the Tables 17 and 18.
- **Slow growth in threshold-based miss rates:** FNIR(N, T) also generally grows as a power law, aN^b except at the high threshold values corresponding to low FPIR values. This is visible in the plots of Figure 36 which

show straight lines except for FPIR = 0.001, which increase more rapidly with N above 3 000 000. Each trace in those figures shows FNIR(N, T) at fixed FPIR with both N and T varying. Thus at large N, it is usually necessary to elevate T to maintain fixed FPIR. This causes increased FNIR. Why that would no-longer obey a power-law is not known. However, if we expect large galleries to contain individuals with familial relations to the non-mate search images - in the most extreme case, twins - then suppression of false positives becomes more difficult. This is discussed in the Figures starting at Fig. 10

▷ Figure **??** shows false positives from twins against their enrolled siblings, broken out by type of twin: fraternal or identical. The Figure is based on the enrollment of 104 single images on one of a pair of twins, and then the search of 2354 second images. Note that the dataset is heavily skewed towards identical twins which is not representative of the true population. There is also a skew towards same sex fraternal twin pairs compared to different sex fraternal twin pairs again not representative of the true population.

The notable results are:

- For all algorithms tested, the 1087 mated searches (Twin A vs. Twin A) produce scores almost always above typical operational thresholds, with (not shown) matches at rank 1. The images are of good quality, so this is the result expected from the rest of this report.
- For the 1066 identical twin searches (AB), almost all produce the twin at rank 1, with a few producing the mate at further down the candidate lists rank and low score.
- For the 169 fraternal searches (AB) from same sex pairs, most algorithms give a large number of very high scores, implying false positives at all thresholds. However, there there are long tails containing lower scores that are correctly below threshold. In general, scores that are higher in this distribution are all rank 1 whereas the lower scores have much higher ranks.
- (Not shown) Of the 169, there are 24 fraternal searches (AB) involving different sex twins. Here most algorithms correctly report scores well below the lowest threshold, and usually not on the candidate list at all.

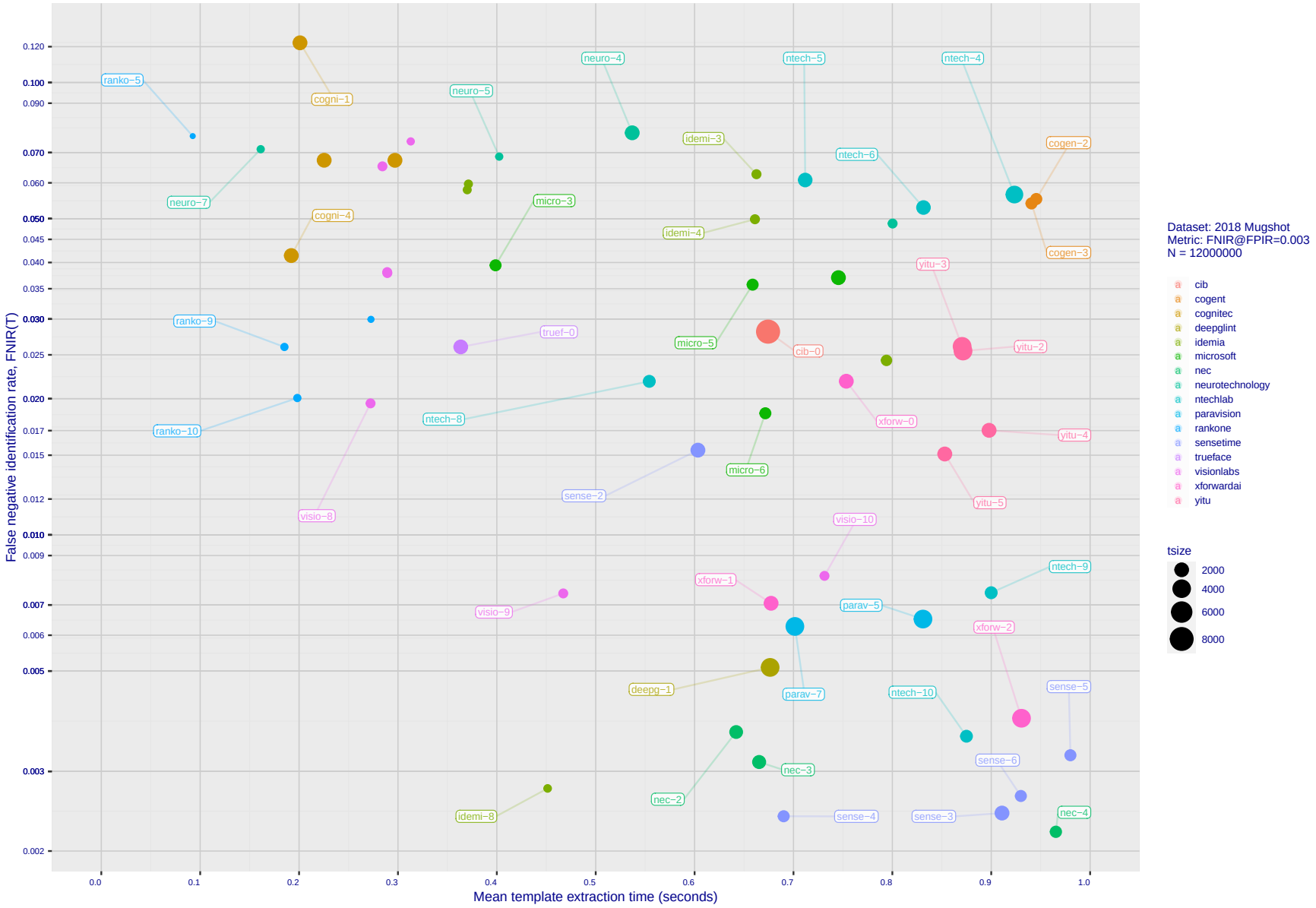

Figure 18: **[Mugshot Dataset] Speed-accuracy tradeoff**. *For developers of the more accurate algorithms the plot shows the tradeoff of high-threshold recognition miss-rates, FNIR(N, N, T) for FPIR(N, T) = 0.003, and template generation time. Developers are coded by color. Template size is encoded by the size of the circle. Some labels are quite distant from the respective point, to avoid superposing text. Without any other influences, the assumption would be that taking time to localize the face, and extract features, would lead to better accuracy. The most notable result, for NEC, is that their slower algorithms are much more accurate than the version that extract features in fewer than 90 milliseconds.*

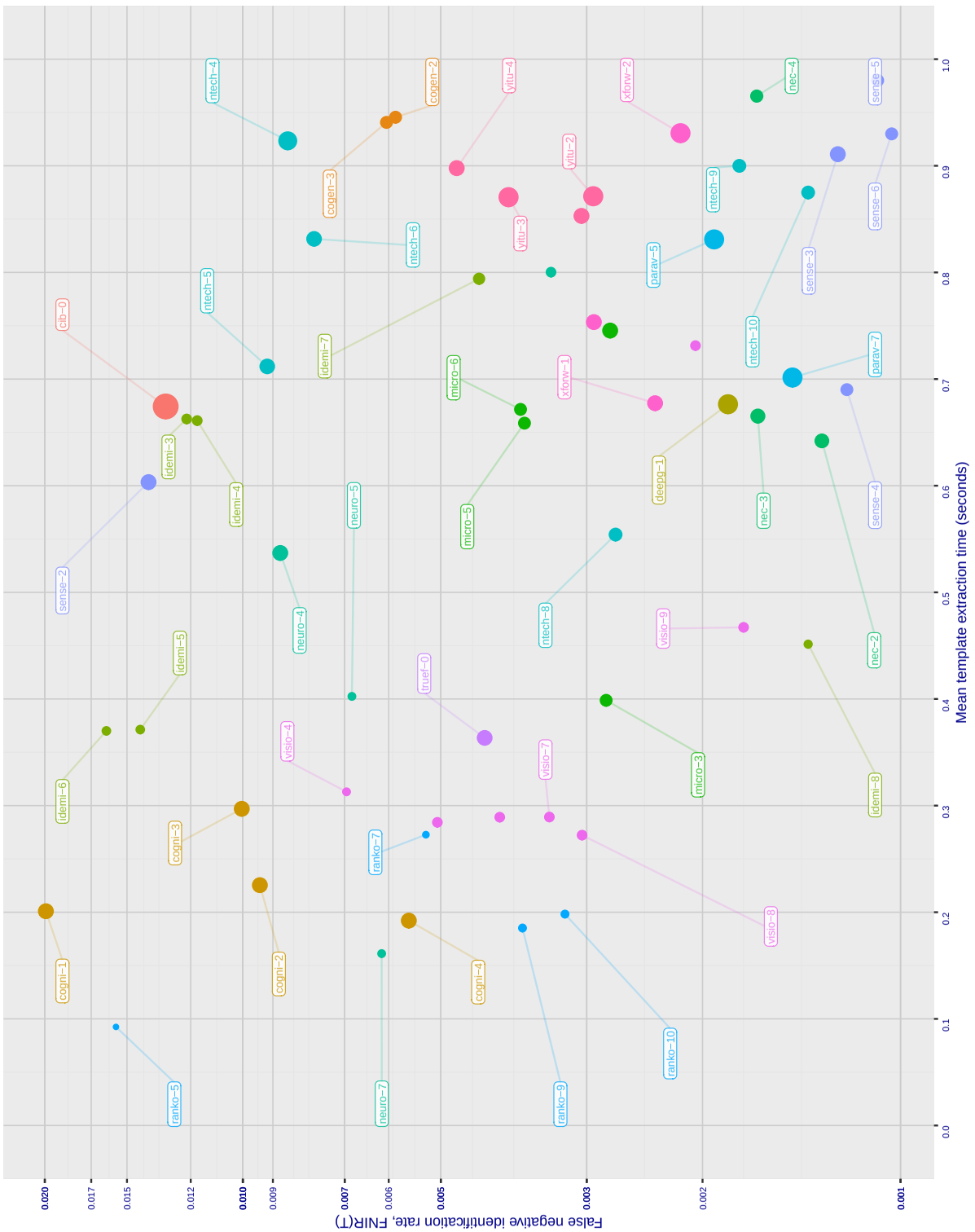

Figure 19: **[Mugshot Dataset] Speed-accuracy tradeoff**. *For developers of the more accurate algorithms the plot shows the tradeoff of rank-one recognition miss-rates, FNIR(N, 1, 0), and template generation time. Developers are coded by color. Template size is encoded by the size of the circle. Some labels are quite distant from the respective point, to avoid superposing text. Without any other influences, the assumption would be that taking time to localize the face, and extract features, would lead to better accuracy. This occurs for NEC with their slower algorithm being much accurate than the version that extract features in fewer than 90 milliseconds.*

	DEVELOPER	SHORT	SEQ.	VALIDATION	CONFIG[1]	LIB[1]	TEMPLATE GENERATION			FINALIZE[2]	SEARCH DURATION[5] MILLISEC					
	FULL NAME	NAME	NUM.	DATE	DATA (MB)	DATA (MB)	SIZE (B)	MULT[3]	TIME (MS)[4]	TIME (S)	L=1	L=50	L=50	L=50	L=50	POWER LAW
											N=1.6M	N=1.6M	N=3M	N=6M	N=12M	(μs)
1	3Divi	3divi	5	2018-10-26	186	51	[148]4096	k	[84]638	[120]28	[73]538	[73]537	[66]1377	[64]2614	[60]5530	[101]$0.07N^{1.1}$
2	3Divi	3divi	6	2018-10-26	187	51	[31]528	k	[85]640	[21]5	[11]33	[12]33	-	-	-	
3	Acer Incorporated	acer	000	2020-08-12	35	67	[22]512	-	[15]198	[13]4	[50]295	[51]295	[41]623	[58]2302	[53]4915	[128]$0.00N^{1.3}$
4	Akurat Satu Indonesia	ptakuratsatu	000	2020-10-23	0	572	[32]538	-	[154]905	[161]28633	[6]15	[6]16	[6]17	[5]17	[4]17	[3]$6827.74N^{0.1}$
5	Alchera Inc	alchera	2	2018-10-30	7	14	[81]2048	k	[6]114	[145]63	[135]2923	[138]2929	-	-	-	
6	Alchera Inc	alchera	3	2018-10-30	251	14	[80]2048	k	[69]531	[146]63	[136]2955	[139]2956	[119]6546	[120]15013	[120]35262	[123]$0.10N^{1.2}$
7	Alivia / Innovation Sys	isystems	3	2018-10-30	350	784	[94]2048	1	[133]825	[95]16	[60]385	[61]389	[53]979	[53]1822	[76]9348	[129]$0.00N^{1.3}$
8	AllGoVision	allgovision	000	2019-07-30	168	150	[72]2048	k	[45]404	[52]12	[138]3226	[141]3193	[117]6129	[117]12449	[117]25835	[55]$1.40N^{1.0}$
9	AllGoVision	allgovision	001	2020-07-14	283	126	[77]2048	-	[122]777	[58]13	[137]3174	[140]3183	[116]6073	[115]12284	[116]25701	[53]$1.42N^{1.0}$
10	Anke Investments	anke	0	2018-10-30	779	27	[134]2072	k	[50]429	[93]16	[83]675	[87]748	[71]1483	[70]2968	[64]6148	[74]$0.21N^{1.1}$
11	Anke Investments	anke	1	2018-10-30	779	27	[133]2072	k	[51]430	[87]15	[87]707	[90]769	-	-	-	
12	Anke Investments	anke	002	2019-06-27	341	401	[126]2056	k	[80]623	[67]13	[82]624	[82]682	[64]1306	[60]2403	[57]5082	[48]$0.30N^{1.0}$
13	Aware	aware	5	2018-10-30	368	27	[142]3100	k	[127]792	[129]34	[15]95	[18]98	[16]203	[15]371	[12]252	[13]$4.13N^{0.7}$
14	Aware	aware	6	2018-10-30	368	27	[2]124	k	[126]789	[2]2	[28]158	[28]162	-	-	-	
15	Ayonix	ayonix	1	2018-10-29	74	2	[46]1036	k	[2]12	[47]11	[46]279	[47]279	-	-	-	
16	Ayonix	ayonix	2	2018-10-30	74	2	[47]1036	1	[1]11	[72]14	[45]279	[46]276	[33]535	[31]1087	[31]2284	[62]$0.11N^{1.0}$
17	Camvi Technologies	camvitech	4	2018-10-30	233	220	[40]1024	1	[99]686	[127]31	[12]33	[11]32	[10]38	[9]40	[7]48	[4]$8492.66N^{0.1}$
18	Camvi Technologies	camvitech	5	2018-10-30	257	220	[41]1024	1	[118]751	[125]31	[10]31	[9]30	-	-	-	
19	Canon Inc	cib	000	2020-10-19	426	127	[163]8196	-	[94]674	[149]113	[139]3589	[143]3604	[120]6738	[118]13495	[118]27114	[23]$2.33N^{1.0}$
20	Cloudwalk - Hengrui AI Technology	hr	000	2021-02-10	501	392	[71]2048	-	[155]905	[80]15	[47]282	[45]276	[35]539	[38]1268	[44]3177	[105]$0.03N^{1.1}$
21	Cognitec Systems GmbH	cognitec	2	2018-10-30	463	26	[123]2052	k	[18]225	[115]27	[122]1733	[124]1763	[106]3660	[104]7279	[103]13895	[52]$0.83N^{1.0}$
22	Cognitec Systems GmbH	cognitec	3	2018-10-30	465	26	[115]2052	k	[28]297	[91]16	[121]1719	[125]1791	[105]3638	[103]7277	[106]14904	[68]$0.66N^{1.0}$
23	Cognitec Systems GmbH	cognitec	004	2021-03-08	384	60	[116]2052	-	[13]192	[65]13	[120]1673	[123]1727	[98]2904	[96]5801	[94]11707	[20]$1.15N^{1.0}$
24	Cyberlink Corp	cyberlink	000	2019-06-12	217	93	[122]2052	1	[88]654	[123]30	[85]696	[84]701	[67]1379	[65]2639	[66]6214	[64]$0.28N^{1.0}$
25	Cyberlink Corp	cyberlink	001	2019-10-07	459	102	[118]2052	1	[48]423	[121]28	[86]698	[83]700	[65]1350	[94]5524	[97]12031	[127]$0.00N^{1.3}$
26	Cyberlink Corp	cyberlink	002	2020-07-31	333	109	[158]4140	-	[113]724	[153]6875	[113]1353	[142]3198	[118]6138	[114]12205	[101]13106	[15]$16.71N^{0.8}$
27	Cyberlink Corp	cyberlink	003	2021-01-05	333	100	[160]6212	-	[102]691	[132]35	[68]488	[85]723	[69]1415	[68]2886	[61]5643	[87]$0.12N^{1.1}$
28	Cyberlink Corp	cyberlink	004	2021-07-16	371	100	[161]6212	-	[115]728	[112]23	[69]492	[72]504	[52]923	[43]1448	[46]3350	[18]$0.73N^{0.9}$
29	Dahua Technology Co Ltd	dahua	0	2018-10-29	276	167	[105]2048	k	[39]374	[110]22	-	[43]258	-	-	-	
30	Dahua Technology Co Ltd	dahua	1	2018-10-29	276	167	[86]2048	k	[35]369	[117]28	-	[42]257	[39]602	[36]1202	[42]3007	[112]$0.02N^{1.2}$
31	Dahua Technology Co Ltd	dahua	002	2019-12-02	607	137	[82]2048	k	[98]685	[105]19	[38]243	[44]269	[60]1189	[69]2950	[69]6732	[133]$0.00N^{1.5}$
32	Dahua Technology Co Ltd	dahua	003	2020-11-18	889	154	[84]2048	-	[112]723	[98]18	[48]283	[41]249	[30]468	[29]935	[28]1871	[24]$0.16N^{1.0}$
33	Deepglint	deepglint	001	2019-11-15	448	265	[151]4096	-	[96]676	[130]35	[84]677	[116]1495	[75]1724	[66]2747	[67]6246	[14]$25.27N^{0.8}$
34	Dermalog	dermalog	5	2018-10-26	0	440	[3]128	1	[68]528	[152]3155	[1]0	[1]0	[1]0	[1]0	[1]0	[5]$66.21N^{0.2}$
35	Dermalog	dermalog	6	2018-10-26	0	453	[13]256	1	[64]507	[3]2	[25]142	[25]144	[21]269	[20]531	[19]1294	[69]$0.05N^{1.0}$
36	Dermalog	dermalog	007	2020-02-12	0	424	[4]128	1	[47]410	[1]1	[18]98	[16]96	[18]218	[16]429	[16]1013	[94]$0.01N^{1.1}$
37	Dermalog	dermalog	008	2021-01-25	0	531	[21]512	-	[37]370	[15]4	[54]335	[38]246	[29]462	[28]924	[27]1849	[27]$0.15N^{1.0}$
38	FarBar Inc	f8	001	2019-10-03	266	19	[102]2048	k	[131]810	[70]14	-	-	-	-	-	
39	Gorilla Technology	gorilla	2	2018-10-29	91	1252	[52]1132	k	[32]338	[114]24	[26]145	[26]146	[22]293	[21]612	[23]1509	[92]$0.02N^{1.1}$
40	Gorilla Technology	gorilla	3	2018-10-26	94	1252	[135]2156	k	[71]559	[157]12020	-	[128]2047	-	-	-	
41	Gorilla Technology	gorilla	004	2020-01-06	182	1244	[136]2192	k	[41]388	[134]41	[49]286	[50]285	[61]1191	[61]2416	[56]5036	[126]$0.00N^{1.3}$
42	Gorilla Technology	gorilla	005	2021-02-22	306	1420	[162]6288	-	[61]483	[148]78	[91]802	[91]799	[72]1514	[77]4454	[72]8820	[114]$0.05N^{1.2}$
43	Guangzhou Pixel Solutions Co Ltd	pixelall	002	2019-07-01	0	165	[139]2560	k	[12]190	[84]15	[111]1296	[113]1334	[91]2526	[86]5136	[90]11045	[63]$0.52N^{1.0}$
44	Guangzhou Pixel Solutions Co Ltd	pixelall	003	2019-11-05	0	690	[137]2560	k	[106]703	[111]22	[108]1273	[110]1307	[88]2474	[87]5198	[91]11141	[70]$0.46N^{1.0}$
45	Guangzhou Pixel Solutions Co Ltd	pixelall	004	2020-07-02	0	538	[140]2560	k	[52]449	[97]17	[107]1259	[109]1300	[87]2465	[92]5492	[92]11443	[79]$0.34N^{1.1}$
46	Guangzhou Pixel Solutions Co Ltd	pixelall	005	2021-03-23	0	717	[138]2560	-	[138]840	[46]11	[117]1606	[117]1528	[93]2609	[83]4926	[95]11770	[41]$0.73N^{1.0}$
47	Hikvision Research Institute	hikvision	5	2018-10-29	593	9	[57]1408	1	[77]607	[90]16	[96]883	[97]895	[77]1908	[73]3792	[77]9387	[102]$0.10N^{1.1}$
48	Hikvision Research Institute	hikvision	6	2018-10-29	593	9	[56]1408	1	[75]598	[92]16	[94]871	[96]877	-	-	-	
49	Idemia	idemia	5	2018-10-29	417	48	[19]352	1	[38]371	[20]5	[22]137	[23]138	[27]437	[25]724	[24]1630	[120]$0.01N^{1.2}$
50	Idemia	idemia	6	2018-10-29	417	48	[20]352	1	[36]370	[19]4	[23]137	[22]138	[28]442	[27]827	[25]1646	[122]$0.01N^{1.2}$
51	Idemia	idemia	007	2020-01-17	738	113	[37]860	1	[128]794	[71]14	[27]151	[27]152	[44]683	[45]1481	[43]3022	[131]$0.00N^{1.4}$
52	Idemia	idemia	008	2021-03-15	378	65	[18]300	-	[54]451	[11]3	[21]132	[21]131	[19]247	[18]501	[17]1013	[38]$0.07N^{1.0}$

Notes	
1	Configuration size does not capture static data present in libraries. Libraries are included but the size also includes any ancillary libraries for image processing (e.g. openCV) or numerical computation (e.g. blas).
2	Finalization is the processing of converting N = 1600000 templates into a searchable data structure an operation which can be a simple copy, or the building of an index or tree, for example. The duration of the operation may be data dependent, and may not be linear in the number of input templates.
3	This multiplier expresses the increase in template size when k images are passed to the template generation function.
4	All durations are measured on Intel®Xeon®CPU E5-2630 v4 @ 2.20GHz processors. Estimates are made by wrapping the API function call in calls to std::chrono::high_resolution_clock which on the machine in (3) counts 1ns clock ticks. Precision is somewhat worse than that however.
5	Search durations are measured as in the prior note. The power-law model in the final column mostly fits the empirical results in Figure 166. However in certain cases the model is not correct and should not be used numerically.

Table 2: Summary of algorithms and properties included in this report. The blue superscripts give ranking for the quantity in that column. Missing search durations, denoted by "-", are absent because those runs were not executed, usually because we did not run on the larger galleries. Caution: The power-law model is sometimes an incorrect model. It is included here only to show broad sublinear behavior, which is flagged in green. The models should not be used for prediction.

	DEVELOPER	SHORT	SEQ.	VALIDATION	CONFIG[1]	LIB[1]	TEMPLATE GENERATION			FINALIZE[2]	SEARCH DURATION[5] MILLISEC					
	FULL NAME	NAME	NUM.	DATE	DATA (MB)	DATA (MB)	SIZE (B)	MULT[3]	TIME (MS)[4]	TIME (S) N=1.6M	L=1 N=1.6M	L=50 N=1.6M	L=50 N=3M	L=50 N=6M	L=50 N=12M	POWER LAW (μs)
53	Imagus Technology Pty Ltd	imagus	005	2021-01-15	222	311	[78]2048	-	[125]786	[69]14	[37]236	[53]313	[42]651	[41]1361	[32]2461	[100]$0.03N^{1.1}$
54	Imagus Technology Pty Ltd	imagus	006	2021-05-27	248	369	[91]2048	-	[153]904	[38]9	[52]317	[37]234	[31]499	[39]1273	[35]2727	[119]$0.01N^{1.2}$
55	Imperial College London	imperial	000	2019-08-28	461	15	[76]2048	1	[72]577	[57]13	[57]360	[60]379	[73]1626	[75]4057	[88]10291	[134]$0.00N^{1.5}$
56	Incode Technologies Inc	incode	2	2018-10-29	71	31	[103]2048	1	[27]289	[89]15	[65]411	[62]404	-	-	-	
57	Incode Technologies Inc	incode	3	2018-10-29	133	31	[106]2048	1	[104]697	[79]15	[64]408	[65]412	[49]847	[46]1608	[51]4486	[96]$0.05N^{1.1}$
58	Incode Technologies Inc	incode	004	2019-06-24	254	50	[97]2048	1	[59]475	[50]12	[58]365	[59]378	[70]1482	[48]1660	[41]2954	[77]$0.12N^{1.1}$
59	Innovatrics	innovatrics	4	2018-10-30	0	400	[50]1076	k	[42]399	[154]10902	[5]8	[4]8	[4]11	[2]9	[3]13	[9]$668.38N^{0.2}$
60	Innovatrics	innovatrics	005	2019-09-30	0	455	[33]538	1	[134]827	[156]11897	[4]8	[5]8	[3]9	[3]9	[2]9	[1]$4055.65N^{0.1}$
61	IrexAI	irex	000	2021-02-09	724	46	[141]3080	-	[139]844	[104]19	[81]616	[79]600	[57]1120	[63]2477	[62]5863	[82]$0.13N^{1.1}$
62	Kakao Enterprise	kakao	000	2021-06-23	404	124	[120]2052	-	[137]835	[31]8	[36]213	[35]215	[32]510	[30]971	[29]1955	[84]$0.05N^{1.1}$
63	Kedacom International Pte	kedacom	001	2019-09-16	239	36	[16]292	1	[65]507	[4]2	[89]764	[88]760	[78]1940	[71]2983	[68]6623	[66]$0.31N^{1.0}$
64	Kneron	kneron	000	2020-03-03	366	13	[79]2048	k	[67]523	[62]13	[132]2535	[135]2506	[114]4752	[112]9696	[115]20926	[67]$0.95N^{1.0}$
65	Kneron	kneron	001	2021-06-10	270	69	[93]2048	-	[58]472	[35]9	[133]2690	[137]2642	-	-	-	
66	Line Corporation	line	000	2021-06-02	138	397	[104]2048	-	[60]481	[32]8	[144]5433	[148]5418	[124]10144	-	-	[22]$3.65N^{1.0}$
67	Lomonosov Moscow State University	intsysmsu	000	2019-08-19	375	168	[110]2048	1	[78]614	[63]13	[66]430	[67]431	[51]860	[49]1730	[59]5353	[110]$0.03N^{1.1}$
68	Lookman Electroplast Industries	lookman	3	2018-10-28	203	24	[17]292	1	[31]336	[10]3	[88]739	[86]745	[68]1394	[67]2817	[70]8286	[90]$0.13N^{1.1}$
69	Lookman Electroplast Industries	lookman	4	2018-10-28	184	24	[35]548	1	[29]320	[18]4	[97]981	[98]998	-	-	-	
70	Lookman Electroplast Industries	lookman	005	2019-09-16	239	36	[34]548	1	[63]506	[14]4	[98]1005	[99]1008	[92]2597	[91]5446	[73]8939	[88]$0.19N^{1.1}$
71	Megvii/Face++	megvii	1	2018-10-28	1703	41	[150]4096	1	[82]631	[128]32	[74]552	[77]561	[63]1222	[59]2321	[63]5968	[95]$0.08N^{1.1}$
72	Megvii/Face++	megvii	2	2018-10-28	1735	42	[144]4096	1	[83]635	[126]31	[75]553	[75]558	-	-	-	
73	MicroFocus	microfocus	5	2018-10-29	94	26	[10]256	k	[22]262	[7]2	[33]182	[32]186	[25]354	[24]708	[21]1425	[35]$0.11N^{1.0}$
74	MicroFocus	microfocus	6	2018-10-29	94	26	[12]256	k	[21]262	[9]2	[34]183	[31]186	-	-	-	
75	Microsoft	microsoft	5	2018-10-29	381	155	[39]1024	1	[89]658	[48]11	[116]1606	[120]1673	[102]3076	[100]6302	[102]13160	[47]$0.79N^{1.0}$
76	Microsoft	microsoft	6	2018-10-29	478	155	[38]1024	1	[92]671	[83]15	[118]1642	[119]1618	[107]3710	[101]6401	[100]12892	[59]$0.68N^{1.0}$
77	N-Tech Lab	ntech	5	2018-10-30	1685	113	[68]1940	k	[110]711	[143]55	[40]243	[40]246	[34]538	[32]1100	[38]2867	[106]$0.02N^{1.1}$
78	N-Tech Lab	ntech	6	2018-10-30	1686	117	[69]1940	k	[136]831	[144]63	[39]243	[39]246	[36]546	[33]1104	[39]2873	[108]$0.02N^{1.1}$
79	N-Tech Lab	ntechlab	007	2019-06-25	2450	51	[143]3348	k	[129]795	[147]73	[61]393	[66]427	[47]780	[52]1768	[48]3499	[65]$0.16N^{1.0}$
80	N-Tech Lab	ntechlab	008	2020-01-06	1111	51	[54]1300	k	[70]554	[133]36	[32]179	[29]184	[24]341	[23]683	[20]1395	[33]$0.11N^{1.0}$
81	N-Tech Lab	ntechlab	009	2021-03-01	1208	42	[55]1300	-	[152]899	[131]35	[31]178	[30]184	[23]336	[22]676	[26]1704	[78]$0.05N^{1.1}$
82	N-Tech Lab	ntechlab	010	2021-06-24	351	213	[53]1280	-	[144]874	[22]6	[67]440	[68]435	[48]821	[47]1645	[45]3337	[42]$0.22N^{1.0}$
83	NEC	nec	2	2018-10-30	705	35	[64]1616	k	[86]642	[101]18	[62]405	[64]409	[55]1072	[50]1755	[50]4255	[97]$0.06N^{1.1}$
84	NEC	nec	3	2018-10-30	774	110	[65]1712	k	[90]665	[107]21	[3]7	[3]7	[5]14	[8]40	[9]82	[115]$0.00N^{1.2}$
85	NEC	nec	004	2021-07-19	971	63	[51]1104	-	[163]965	[24]7	[55]349	[56]351	[43]662	[40]1330	[34]2685	[36]$0.20N^{1.0}$
86	Neurotechnology	neurotech	5	2018-10-30	266	53	[9]256	k	[43]402	[8]2	[92]835	[93]839	[74]1690	[72]3219	[74]8955	[83]$0.19N^{1.1}$
87	Neurotechnology	neurotech	6	2018-10-30	564	53	[8]256	k	[114]726	[6]2	[93]839	[94]842	-	-	-	
88	Neurotechnology	neurotech	007	2019-10-03	57	51	[11]256	k	[7]161	[5]2	[101]1118	[102]1110	[81]2143	[76]4397	[75]9045	[46]$0.55N^{1.0}$
89	Neurotechnology	neurotechnology	008	2021-03-22	355	49	[30]514	-	[130]800	[17]4	[104]1167	[105]1149	[83]2266	[80]4573	[81]9586	[50]$0.55N^{1.0}$
90	Newland Computer Co Ltd	newland	2	2018-10-30	96	27	[96]2048	-	[141]855	[85]15	[154]8741	[159]8854	[135]17892	[132]39356	-	[93]$1.32N^{1.1}$
91	Noblis	noblis	1	2018-10-30	114	176	[87]2048	1	[16]206	[81]15	[109]1273	[108]1272	-	-	-	
92	Noblis	noblis	2	2018-10-30	153	176	[159]6144	1	[66]517	[136]43	[131]2513	[136]2522	[115]5649	[116]12432	[122]44262	[124]$0.04N^{1.3}$
93	Paravision (EverAI)	everai	2	2018-10-30	224	304	[109]2048	1	[34]366	[124]30	[44]278	[49]283	-	-	-	
94	Paravision (EverAI)	everai	3	2018-10-30	438	304	[95]2048	1	[111]717	[119]28	[43]278	[48]281	[37]572	[34]1146	[30]2278	[60]$0.12N^{1.0}$
95	Paravision (EverAI)	everai-paravision	004	2019-06-19	527	128	[153]4096	1	[93]672	[139]45	[76]559	[76]559	[94]2611	[102]6445	[104]14519	[132]$0.00N^{1.5}$
96	Paravision (EverAI)	paravision	005	2019-12-11	543	154	[146]4096	1	[135]830	[141]48	[77]561	[78]564	[54]1056	[56]2298	[54]4966	[75]$0.16N^{1.1}$
97	Paravision (EverAI)	paravision	007	2021-02-01	529	235	[145]4096	-	[105]701	[142]48	[78]569	[74]558	[56]1086	[54]2111	[49]4254	[17]$1.11N^{0.9}$
98	Quantasoft	quantasoft	1	2018-10-30	276	452	[90]2048	k	[40]385	[23]6	[155]15422	[160]14858	[133]14717	-	[110]18323	
99	Rank One Computing	rankone	4	2018-10-09	0	101	[1]85	k	[3]36	[25]7	[19]101	[19]101	[15]190	-	-	[21]$0.07N^{1.0}$
100	Rank One Computing	rankone	5	2018-10-24	0	101	[5]133	k	[4]92	[26]7	[24]140	[24]144	[20]266	[19]525	[18]1049	[19]$0.11N^{1.0}$
101	Rank One Computing	rankone	006	2019-06-03	0	133	[6]165	k	[20]245	[30]8	-	-	-	-	-	
102	Rank One Computing	rankone	007	2019-11-12	0	137	[7]165	k	[23]272	[28]7	[20]116	[20]115	[17]215	[17]439	[15]877	[34]$0.07N^{1.0}$
103	Rank One Computing	rankone	009	2020-06-26	0	105	[14]260	k	[11]185	[45]11	[16]95	[17]96	[14]181	[14]362	[14]727	[26]$0.06N^{1.0}$
104	Rank One Computing	rankone	010	2020-11-05	0	135	[15]261	-	[14]198	[41]10	[17]95	[15]95	[13]178	[13]357	[13]714	[25]$0.06N^{1.0}$

Notes	
1	Configuration size does not capture static data present in libraries. Libraries are included but the size also includes any ancillary libraries for image processing (e.g. openCV) or numerical computation (e.g. blas).
2	Finalization is the processing of converting N = 1600000 templates into a searchable data structure an operation which can be a simple copy, or the building of an index or tree, for example. The duration of the operation may be data dependent, and may not be linear in the number of input templates.
3	This multiplier expresses the increase in template size when k images are passed to the template generation function.
4	All durations are measured on Intel®Xeon®CPU E5-2630 v4 @ 2.20GHz processors. Estimates are made by wrapping the API function call in calls to std::chrono::high_resolution_clock which on the machine in (3) counts 1ns clock ticks. Precision is somewhat worse than that however.
5	Search durations are measured as in the prior note. The power-law model in the final column mostly fits the empirical results in Figure 166. However in certain cases the model is not correct and should not be used numerically.

Table 3: Summary of algorithms and properties included in this report. The blue superscripts give ranking for the quantity in that column. Missing search durations, denoted by "-", are absent because those runs were not executed, usually because we did not run on the larger galleries. Caution: The power-law model is sometimes an incorrect model. It is included here only to show broad sublinear behavior, which is flagged in green. The models should not be used for prediction.

2021/08/05 02:00:58

FNIR(N, R, T) = False neg. identification rate
FPIR(N, T) = False pos. identification rate

N = Num. enrolled subjects
R = Num. candidates examined

T = Threshold

T = 0 → Investigation
T > 0 → Identification

	DEVELOPER	SHORT	SEQ.	VALIDATION	CONFIG[1]	LIB[1]	TEMPLATE GENERATION			FINALIZE[2]	SEARCH DURATION[5] MILLISEC					
	FULL NAME	NAME	NUM.	DATE	DATA (MB)	DATA (MB)	SIZE (B)	MULT[3]	TIME (MS)[4]	TIME (S)	L=1	L=50	L=50	L=50	L=50	POWER LAW
										N=1.6M	N=1.6M	N=1.6M	N=3M	N=6M	N=12M	(μs)
105	Realnetworks Inc	realnetworks	2	2018-10-30	105	104	[156]4104	k	[19]241	[118]28	[124]2008	[129]2048	[109]4194	[108]8642	[107]15035	[40]$1.08N^{1.0}$
106	Realnetworks Inc	realnetworks	003	2019-06-12	93	102	[66]1848	k	[10]173	[56]13	[103]1145	[103]1132	[80]2142	[88]5241	[89]10495	[86]$0.21N^{1.1}$
107	Realnetworks Inc	realnetworks	004	2019-10-17	94	102	[67]1848	1	[9]171	[44]11	[102]1143	[104]1137	[82]2149	[82]4740	[84]9693	[73]$0.36N^{1.0}$
108	Realnetworks Inc	realnetworks	005	2021-06-23	168	209	[127]2056	-	[30]332	[34]9	[119]1654	[118]1616	[101]3030	[98]6068	[98]12134	[29]$1.01N^{1.0}$
109	Remark Holdings	remarkai	0	2018-10-30	187	847	[85]2048	k	[73]593	[74]14	[147]5685	[151]5723	-	-	-	
110	Remark Holdings	remarkai	000	2019-06-12	234	1092	[75]2048	k	[87]650	[55]12	[148]5776	[150]5703	[126]11604	[131]32133	[131]91436	[125]$0.05N^{1.3}$
111	Remark Holdings	remarkai	1	2018-10-30	187	847	[107]2048	k	[49]427	[78]14	[146]5680	[152]5761	[129]12475	[129]28726	[129]59618	[116]$0.37N^{1.2}$
112	Rendip	rendip	000	2021-05-21	0	416	[83]2048	-	[149]890	[36]9	[41]249	[57]368	[46]697	[44]1452	[40]2926	[80]$0.08N^{1.1}$
113	Samsung S1 Corp	s1	000	2021-06-03	257	196	[152]4096	-	[142]865	[106]20	[152]6715	[157]6794	[132]13032	[128]26372	[128]55723	[58]$2.82N^{1.0}$
114	Scanovate Ltd	scanovate	000	2020-01-15	250	446	[108]2048	-	[107]705	[76]14	[115]1419	[115]1412	[100]3008	[113]11616	[96]12012	[117]$0.10N^{1.2}$
115	Scanovate Ltd	scanovate	001	2020-09-10	250	446	[74]2048	-	[95]675	[61]13	[112]1321	[112]1320	[89]2502	[85]5047	[86]10163	[43]$0.65N^{1.0}$
116	Sensetime Group	sensetime	0	2018-10-30	525	6	[154]4104	k	[103]693	[135]41	[70]498	[69]501	[62]1212	[55]2281	[55]5032	[91]$0.09N^{1.1}$
117	Sensetime Group	sensetime	1	2018-10-30	525	6	[155]4104	k	[81]628	[140]48	[72]516	[70]502	[58]1146	[57]2301	[52]4765	[89]$0.09N^{1.1}$
118	Sensetime Group	sensetime	002	2019-06-03	523	6	[129]2056	k	[76]603	[99]18	[56]359	[58]370	[76]1897	[78]4508	[80]9543	[135]$0.00N^{1.5}$
119	Sensetime Group	sensetime	003	2019-12-02	769	76	[128]2056	1	[156]910	[103]19	[143]4885	[147]4989	[128]12325	[125]24712	[124]49445	[99]$0.67N^{1.1}$
120	Sensetime Group	sensetime	004	2020-08-10	456	29	[42]1032	-	[101]690	[54]12	[130]2490	[133]2477	[113]4654	[111]9402	[114]19651	[45]$1.22N^{1.0}$
121	Sensetime Group	sensetime	005	2020-12-17	631	39	[45]1032	-	[164]980	[43]11	[128]2459	[144]3939	[121]7398	[119]14768	[113]19016	[16]$14.03N^{0.9}$
122	Sensetime Group	sensetime	006	2021-07-26	526	54	[43]1032	-	[157]929	[29]7	[127]2414	[132]2422	[111]4527	[109]9128	[111]18640	[37]$1.35N^{1.0}$
123	Shaman Software	shaman	6	2018-10-26	0	200	[111]2048	k	[108]706	[75]14	[80]603	[80]612	-	-	-	
124	Shaman Software	shaman	7	2018-10-26	0	200	[88]2048	k	[109]707	[77]14	[79]602	[81]614	[59]1187	[62]2448	[58]5083	[61]$0.25N^{1.0}$
125	Shanghai Yitu Technology	yitu	4	2018-10-30	2119	136	[131]2070	1	[151]897	[138]45	[110]1288	[107]1203	[86]2440	[89]5241	[83]9671	[57]$0.52N^{1.0}$
126	Shanghai Yitu Technology	yitu	5	2018-10-30	2043	136	[132]2070	1	[140]853	[137]44	[106]1237	[106]1199	[90]2513	[84]5013	[82]9620	[54]$0.55N^{1.0}$
127	Smilart	smilart	4	2018-10-30	65	89	[25]512	k	[8]167	[16]4	[156]16137	[161]15633	-	-	-	
128	Smilart	smilart	5	2018-10-30	562	89	[89]2048	k	[53]450	[73]14	-	-	-	-	-	
129	Synesis	synesis	003	2019-07-04	143	17	[114]2048	k	[17]211	[51]12	[71]507	[71]502	[84]2297	[79]4564	[78]9452	[130]$0.00N^{1.4}$
130	Synesis	synesis	3	2018-10-30	237	150	[149]4096	k	[5]99	[122]29	[90]789	[92]801	[79]1941	[74]3888	[71]8810	[107]$0.07N^{1.1}$
131	Synesis	synesis	005	2020-09-08	494	24	[157]4104	-	[120]756	[113]24	[95]877	[95]865	[103]3182	[81]4658	[85]9750	[118]$0.06N^{1.2}$
132	Tech5 SA	tech5	001	2019-08-19	1394	116	[58]1536	k	[148]887	[40]10	[59]383	[89]766	[96]2767	[99]6149	[65]6178	[98]$0.12N^{1.1}$
133	Tech5 SA	tech5	002	2021-04-07	727	112	[29]513	-	[159]940	[12]4	[142]4682	[156]6689	[130]12541	[126]25145	[126]50239	[28]$4.18N^{1.0}$
134	Tencent Deepsea Lab	deepsea	001	2019-07-29	250	323	[73]2048	1	[117]737	[53]12	[99]1021	[100]1020	[97]2774	[95]5767	[99]12341	[121]$0.06N^{1.2}$
135	Tevian	tevian	5	2018-10-30	773	15	[99]2048	1	[46]405	[82]15	[63]405	[63]408	[50]854	[51]1757	[47]3380	[72]$0.14N^{1.0}$
136	Tevian	tevian	006	2021-04-16	769	19	[44]1032	-	[74]597	[39]10	[51]295	[52]295	[38]578	[35]1187	[37]2741	[81]$0.06N^{1.1}$
137	Thales	cogent	2	2018-10-30	681	39	[48]1043	k	[161]945	[116]27	[125]2017	[130]2144	[110]4298	[107]8472	[109]16429	[44]$1.08N^{1.0}$
138	Thales	cogent	3	2018-10-30	681	39	[49]1043	k	[160]940	[37]9	[105]1230	[111]1311	[95]2687	[90]5398	[87]10184	[51]$0.62N^{1.0}$
139	Thales	cogent	004	2021-02-10	1376	59	[125]2053	-	[162]947	[68]14	[134]2903	[126]1911	[104]3566	[105]7498	[108]16370	[71]$0.64N^{1.0}$
140	TigerIT Americas LLC	tiger	2	2018-10-29	416	518	[117]2052	k	[56]461	[86]15	[123]1816	[127]1921	[108]3833	[106]7526	[105]14820	[56]$0.83N^{1.0}$
141	TigerIT Americas LLC	tiger	3	2018-10-30	416	518	[121]2052	k	[55]461	[163]37431	[35]191	[33]189	-	-	-	
142	Toshiba	toshiba	0	2018-10-30	961	105	[63]1548	k	[146]876	[49]12	[151]6153	[153]6236	[127]12221	[127]25355	[125]49448	[113]$0.36N^{1.2}$
143	Toshiba	toshiba	1	2018-10-30	961	105	[130]2060	k	[145]875	[164]44701	[150]6007	[154]6355	-	-	-	
144	Trueface.ai	trueface	000	2021-01-27	247	119	[70]2000	-	[33]363	[59]13	[42]271	[55]327	[40]614	[37]1239	[33]2678	[49]$0.15N^{1.0}$
145	Veridas Digital Authentication Solutions S.L.	veridas	001	2021-03-05	347	875	[98]2048	-	[143]872	[60]13	[145]5493	[149]5469	[125]10350	[123]20655	[121]41264	[30]$3.40N^{1.0}$
146	Veridas Digital Authentication Solutions S.L.	veridas	002	2021-07-06	347	870	[112]2048	-	[147]877	[42]10	[53]322	[54]325	[45]685	[42]1365	[36]2730	[76]$0.09N^{1.1}$
147	Viettel Group	vts	000	2021-03-12	250	257	[101]2048	-	[62]492	[151]2295	[2]4	[2]4	[2]6	[4]11	-	[12]$0.61N^{0.6}$
148	Viettel Group	vts	001	2021-07-16	352	600	[92]2048	-	[150]891	[109]21	[129]2477	[134]2487	[112]4644	[110]9313	[112]18713	[31]$1.53N^{1.0}$
149	Vigilant Solutions	vigilant	5	2018-10-30	335	122	[59]1544	k	[121]762	[102]19	-	[122]1720	-	-	-	
150	Vigilant Solutions	vigilant	6	2018-10-30	337	122	[62]1544	k	[132]816	[108]21	-	[121]1713	-	-	-	
151	Vigilant Solutions	vigilantsolutions	007	2021-01-08	340	51	[61]1544	-	[79]616	[96]16	[114]1354	[114]1352	[99]2911	[97]5966	[93]11466	[85]$0.27N^{1.1}$
152	Vigilant Solutions	vigilantsolutions	008	2021-07-23	340	51	[60]1544	-	[44]403	[64]13	[100]1062	[101]1061	[85]2330	[93]5520	[79]9499	[103]$0.11N^{1.1}$
153	Visidon	visidon	1	2018-10-30	166	42	[124]2052	k	[91]667	[88]15	[140]4370	[146]4472	[122]8454	[121]17262	[119]34288	[39]$2.40N^{1.0}$
154	Visidon	vd	002	2021-05-18	248	42	[119]2052	-	[100]687	[33]9	[126]2089	[131]2336	-	-	-	
155	VisionLabs	visionlabs	6	2018-10-30	360	17	[27]512	1	[25]289	[160]20290	[13]36	[13]36	[11]39	[10]44	[8]53	[8]$3211.93N^{0.2}$
156	VisionLabs	visionlabs	7	2018-10-30	360	17	[28]512	1	[26]289	[162]34666	[14]63	[14]63	[12]72	[12]80	[10]115	[10]$2076.32N^{0.2}$

Notes	
1	Configuration size does not capture static data present in libraries. Libraries are included but the size also includes any ancillary libraries for image processing (e.g. openCV) or numerical computation (e.g. blas).
2	Finalization is the processing of converting N = 1600000 templates into a searchable data structure an operation which can be a simple copy, or the building of an index or tree, for example. The duration of the operation may be data dependent, and may not be linear in the number of input templates.
3	This multiplier expresses the increase in template size when k images are passed to the template generation function.
4	All durations are measured on Intel®Xeon®CPU E5-2630 v4 @ 2.20GHz processors. Estimates are made by wrapping the API function call in calls to std::chrono::high_resolution_clock which on the machine in (3) counts 1ns clock ticks. Precision is somewhat worse than that however.
5	Search durations are measured as in the prior note. The power-law model in the final column mostly fits the empirical results in Figure 166. However in certain cases the model is not correct and should not be used numerically.

Table 4: Summary of algorithms and properties included in this report. The blue superscripts give ranking for the quantity in that column. Missing search durations, denoted by "-", are absent because those runs were not executed, usually because we did not run on the larger galleries. Caution: The power-law model is sometimes an incorrect model. It is included here only to show broad sublinear behavior, which is flagged in green. The models should not be used for prediction.

FNIR(N, R, T) = False neg. identification rate
FPIR(N, T) = False pos. identification rate
N = Num. enrolled subjects
R = Num. candidates examined
T = Threshold
T = 0 → Investigation
T > 0 → Identification

	DEVELOPER	SHORT	SEQ.	VALIDATION	CONFIG[1]	LIB[1]	TEMPLATE GENERATION			FINALIZE[2]	SEARCH DURATION[5] MILLISEC					
	FULL NAME	NAME	NUM.	DATE	DATA (MB)	DATA (MB)	SIZE (B)	MULT[3]	TIME (MS)[4]	TIME (S)	L=1	L=50	L=50	L=50	L=50	POWER LAW
										N=1.6M	N=1.6M	N=1.6M	N=3M	N=6M	N=12M	(μs)
157	VisionLabs	visionlabs	008	2019-06-18	348	17	[23]512	1	[24]272	[158]12747	[8]23	[7]24	[7]26	[6]29	[5]33	[6]$2539.61N^{0.2}$
158	VisionLabs	visionlabs	009	2020-08-04	689	20	[26]512	-	[57]467	[159]13245	[9]23	[8]29	[8]34	[11]61	[11]145	[11]$8.88N^{0.6}$
159	VisionLabs	visionlabs	010	2021-02-05	1042	20	[24]512	-	[116]731	[155]11837	[7]21	[10]32	[9]36	[7]39	[6]43	[7]$3183.79N^{0.2}$
160	Vocord	vocord	5	2018-10-30	1035	185	[36]768	k	[123]780	[27]7	[29]158	[34]204	[26]383	[26]767	[22]1466	[32]$0.12N^{1.0}$
161	Vocord	vocord	6	2018-10-30	1035	185	[164]10240	k	[124]785	[150]243	[30]170	[36]216	-	-	-	
162	Xforward AI Technology	xforwardai	000	2020-07-24	236	171	[113]2048	-	[119]753	[66]13	[141]4603	[158]7647	[134]15723	[124]23900	[127]53729	[104]$0.56N^{1.1}$
163	Xforward AI Technology	xforwardai	001	2021-01-21	332	50	[100]2048	-	[97]677	[94]16	[149]5887	[145]4384	[123]8798	[122]18553	[123]48993	[111]$0.32N^{1.1}$
164	Xforward AI Technology	xforwardai	002	2021-05-24	691	50	[147]4096	-	[158]930	[100]18	[153]6957	[155]6400	[131]12659	[130]31077	[130]65158	[109]$0.52N^{1.1}$

Notes	
1	Configuration size does not capture static data present in libraries. Libraries are included but the size also includes any ancillary libraries for image processing (e.g. openCV) or numerical computation (e.g. blas).
2	Finalization is the processing of converting N = 1600000 templates into a searchable data structure an operation which can be a simple copy, or the building of an index or tree, for example. The duration of the operation may be data dependent, and may not be linear in the number of input templates.
3	This multiplier expresses the increase in template size when k images are passed to the template generation function.
4	All durations are measured on Intel®Xeon®CPU E5-2630 v4 @ 2.20GHz processors. Estimates are made by wrapping the API function call in calls to std::chrono::high_resolution_clock which on the machine in (3) counts 1ns clock ticks. Precision is somewhat worse than that however.
5	Search durations are measured as in the prior note. The power-law model in the final column mostly fits the empirical results in Figure 166. However in certain cases the model is not correct and should not be used numerically.

Table 5: Summary of algorithms and properties included in this report. The blue superscripts give ranking for the quantity in that column. Missing search durations, denoted by "-", are absent because those runs were not executed, usually because we did not run on the larger galleries. Caution: The power-law model is sometimes an incorrect model. It is included here only to show broad sublinear behavior, which is flagged in green. The models should not be used for prediction.

2021/08/05 02:00:58

FNIR(N, R, T) = False neg. identification rate
FPIR(N, T) = False pos. identification rate
N = Num. enrolled subjects
R = Num. candidates examined
T = Threshold
T = 0 → Investigation
T > 0 → Identification

MISS RATES		INVESTIGATION, FNIR(N, R = 1, T = 0)								IDENTIFICATION, FNIR(N, R = L, T $\geq$ 0) FOR FPIR = 0.001							
#	ALGORITHM	(0, 2]	(2, 4]	(4, 6]	(6, 8]	(8, 10]	(10, 12]	(12, 14]	(14, 18]	(0, 2]	(2, 4]	(4, 6]	(6, 8]	(8, 10]	(10, 12]	(12, 14]	(14, 18]
1	3DIVI-005	[93]0.0207	[92]0.0304	[92]0.0415	[92]0.0533	[92]0.0646	[92]0.0735	[92]0.0884	[93]0.1148	[96]0.1580	[93]0.2316	[93]0.3033	[93]0.3740	[93]0.4285	[93]0.4742	[94]0.5329	[92]0.5975
2	ANKE-000	[90]0.0162	[90]0.0245	[90]0.0333	[90]0.0428	[90]0.0515	[90]0.0615	[90]0.0780	[89]0.1028	[91]0.1132	[91]0.1761	[91]0.2402	[91]0.3057	[90]0.3640	[90]0.4200	[90]0.4928	[90]0.5680
3	ANKE-002	[44]0.0055	[45]0.0074	[45]0.0090	[44]0.0103	[43]0.0116	[44]0.0135	[43]0.0162	[42]0.0202	[49]0.0329	[49]0.0560	[51]0.0843	[52]0.1169	[52]0.1481	[52]0.1820	[52]0.2280	[51]0.2831
4	AWARE-005	[101]0.0328	[101]0.0519	[101]0.0712	[99]0.0910	[99]0.1078	[99]0.1235	[99]0.1457	[99]0.1831	[101]0.3605	[102]0.4949	[102]0.5948	[102]0.6783	[103]0.7393	[103]0.7905	[103]0.8408	[104]0.8831
5	AWARE-006	[105]0.0702	[105]0.1110	[105]0.1502	[105]0.1899	[105]0.2253	[106]0.2614	[105]0.3045	[105]0.3659								
6	AYONIX-002	[108]0.3360	[109]0.4389	[109]0.5144	[109]0.5814	[109]0.6340	[109]0.6818	[109]0.7297	[110]0.7774	[105]0.8288	[106]0.9013	[106]0.9375	[106]0.9603	[106]0.9744	[107]0.9837	[107]0.9893	[107]0.9927
7	CAMVI-004	[104]0.0623	[104]0.0944	[104]0.1243	[104]0.1548	[103]0.1812	[103]0.2056	[103]0.2344	[101]0.2672	[86]0.0810	[86]0.1267	[83]0.1721	[83]0.2203	[83]0.2619	[81]0.3040	[80]0.3543	[76]0.4124
8	CAMVI-005	[106]0.0849	[106]0.1255	[106]0.1631	[106]0.1989	[106]0.2298	[105]0.2585	[104]0.2915	[104]0.3246								
9	CIB-000	[11]0.0022	[11]0.0030	[12]0.0037	[12]0.0044	[13]0.0049	[13]0.0057	[13]0.0069	[13]0.0062	[20]0.0139	[21]0.0240	[22]0.0373	[23]0.0525	[23]0.0689	[21]0.0859	[21]0.1109	[21]0.1454
10	CLOUDWALK-HR-000	[3]0.0019	[4]0.0024	[3]0.0029	[4]0.0032	[3]0.0032	[3]0.0036	[1]0.0041	[1]0.0020	[1]0.0029	[1]0.0041	[1]0.0054	[1]0.0064	[1]0.0073	[1]0.0085	[1]0.0102	[1]0.0112
11	COGENT-000	[86]0.0128	[86]0.0184	[88]0.0250	[87]0.0327	[87]0.0407	[86]0.0488	[85]0.0611	[85]0.0794	[72]0.0559	[73]0.0923	[71]0.1342	[71]0.1812	[70]0.2243	[69]0.2675	[69]0.3240	[73]0.3992
12	COGENT-001	[85]0.0128	[85]0.0184	[87]0.0250	[88]0.0327	[88]0.0407	[87]0.0488	[86]0.0611	[84]0.0794	[73]0.0559	[74]0.0923	[72]0.1342	[72]0.1812	[71]0.2243	[70]0.2675	[68]0.3240	[72]0.3992
13	COGENT-002	[64]0.0081	[61]0.0105	[58]0.0123	[59]0.0137	[57]0.0157	[57]0.0175	[55]0.0215	[55]0.0280	[64]0.0499	[63]0.0827	[62]0.1207	[62]0.1639	[62]0.2037	[61]0.2432	[62]0.2972	[63]0.3638
14	COGENT-003	[66]0.0082	[62]0.0108	[60]0.0128	[62]0.0145	[61]0.0168	[63]0.0191	[64]0.0239	[61]0.0312	[75]0.0582	[75]0.0971	[75]0.1417	[75]0.1918	[75]0.2380	[76]0.2836	[78]0.3440	[79]0.4207
15	COGENT-004	[54]0.0066	[48]0.0080	[40]0.0085	[34]0.0080	[26]0.0083	[26]0.0092	[27]0.0106	[30]0.0130	[58]0.0410	[60]0.0720	[60]0.1099	[60]0.1539	[59]0.1974	[62]0.2443	[65]0.3043	[65]0.3757
16	COGNITEC-000	[100]0.0265	[98]0.0423	[98]0.0588	[98]0.0757	[97]0.0894	[97]0.1014	[97]0.1169	[96]0.1381	[95]0.1522	[94]0.2330	[94]0.3051	[94]0.3751	[94]0.4300	[94]0.4779	[93]0.5307	[91]0.5913
17	COGNITEC-001	[88]0.0149	[89]0.0228	[89]0.0312	[89]0.0399	[89]0.0479	[89]0.0546	[88]0.0656	[86]0.0806	[88]0.0963	[88]0.1562	[88]0.2157	[88]0.2771	[88]0.3287	[88]0.3771	[87]0.4343	[86]0.4959
18	COGNITEC-002	[72]0.0101	[75]0.0138	[76]0.0170	[76]0.0201	[76]0.0237	[75]0.0264	[73]0.0309	[72]0.0389	[67]0.0517	[66]0.0879	[67]0.1269	[68]0.1707	[66]0.2098	[63]0.2463	[61]0.2919	[61]0.3535
19	COGNITEC-003	[73]0.0104	[76]0.0140	[77]0.0174	[77]0.0205	[77]0.0238	[76]0.0266	[74]0.0311	[74]0.0401	[66]0.0504	[65]0.0855	[64]0.1235	[64]0.1662	[63]0.2045	[60]0.2403	[60]0.2854	[59]0.3451
20	COGNITEC-004	[59]0.0073	[58]0.0099	[57]0.0118	[54]0.0130	[54]0.0147	[56]0.0163	[52]0.0189	[51]0.0239	[48]0.0325	[48]0.0548	[47]0.0798	[46]0.1074	[45]0.1325	[46]0.1591	[43]0.1952	[42]0.2414
21	CYBERLINK-002	[45]0.0055	[40]0.0068	[36]0.0075	[30]0.0078	[27]0.0084	[27]0.0094	[28]0.0107	[26]0.0114	[27]0.0180	[28]0.0302	[28]0.0460	[27]0.0643	[28]0.0837	[28]0.1058	[27]0.1370	[27]0.1787
22	CYBERLINK-003	[30]0.0041	[29]0.0052	[22]0.0057	[20]0.0058	[20]0.0061	[20]0.0068	[16]0.0078	[19]0.0078	[15]0.0109	[15]0.0175	[16]0.0259	[16]0.0356	[16]0.0468	[16]0.0594	[16]0.0787	[17]0.1072
23	DAHUA-002	[26]0.0035	[23]0.0047	[23]0.0058	[22]0.0067	[23]0.0074	[22]0.0082	[24]0.0100	[24]0.0108	[23]0.0169	[27]0.0294	[26]0.0449	[25]0.0635	[25]0.0817	[26]0.1013	[24]0.1291	[23]0.1638
24	DAHUA-003	[16]0.0026	[16]0.0036	[16]0.0043	[16]0.0050	[16]0.0055	[15]0.0062	[18]0.0080	[16]0.0073	[24]0.0160	[25]0.0280	[24]0.0432	[24]0.0615	[24]0.0794	[24]0.0987	[23]0.1270	[22]0.1587
25	DEEPGLINT-001	[14]0.0024	[13]0.0032	[11]0.0037	[10]0.0040	[10]0.0043	[11]0.0049	[11]0.0060	[11]0.0052	[9]0.0058	[7]0.0087	[8]0.0119	[8]0.0155	[8]0.0199	[9]0.0249	[8]0.0338	[8]0.0463
26	DEEPSEA-001	[65]0.0081	[65]0.0116	[68]0.0149	[71]0.0182	[71]0.0216	[74]0.0260	[76]0.0332	[76]0.0432	[61]0.0458	[61]0.0752	[59]0.1086	[58]0.1460	[58]0.1812	[58]0.2186	[58]0.2663	[57]0.3213
27	DERMALOG-006	[77]0.0113	[77]0.0142	[73]0.0163	[72]0.0183	[69]0.0200	[68]0.0218	[66]0.0251	[64]0.0329	[70]0.0545	[68]0.0889	[68]0.1271	[67]0.1697	[65]0.2090	[65]0.2498	[64]0.3028	[64]0.3670
28	DERMALOG-007	[83]0.0125	[83]0.0170	[83]0.0214	[83]0.0264	[82]0.0309	[81]0.0356	[82]0.0432	[82]0.0579	[87]0.0910	[87]0.1453	[87]0.2009	[87]0.2602	[87]0.3134	[87]0.3649	[86]0.4289	[87]0.5007
29	DERMALOG-008	[47]0.0057	[47]0.0077	[49]0.0095	[49]0.0110	[48]0.0128	[50]0.0148	[49]0.0180	[50]0.0223	[65]0.0501	[64]0.0850	[65]0.1247	[66]0.1692	[67]0.2105	[66]0.2541	[66]0.3102	[66]0.3762
30	GORILLA-002	[95]0.0213	[95]0.0359	[96]0.0528	[97]0.0716	[98]0.0895	[98]0.1088	[98]0.1367	[98]0.1765	[98]0.1828	[99]0.2787	[99]0.3654	[99]0.4485	[99]0.5168	[97]0.5823	[97]0.6508	[97]0.7180
31	GORILLA-005	[33]0.0044	[42]0.0070	[53]0.0102	[57]0.0136	[62]0.0170	[66]0.0204	[69]0.0272	[71]0.0373	[74]0.0566	[76]0.0973	[72]0.1432	[76]0.1937	[76]0.2398	[78]0.2862	[77]0.3437	[77]0.4150
32	IDEMIA-003	[76]0.0110	[81]0.0151	[81]0.0196	[80]0.0238	[79]0.0281	[79]0.0313	[79]0.0368	[78]0.0504	[82]0.0717	[81]0.1147	[81]0.1614	[81]0.2113	[80]0.2553	[80]0.2976	[79]0.3537	[80]0.4334
33	IDEMIA-004	[75]0.0107	[79]0.0148	[80]0.0192	[79]0.0233	[78]0.0277	[78]0.0312	[78]0.0367	[79]0.0512	[53]0.0373	[50]0.0587	[49]0.0833	[48]0.1100	[47]0.1340	[45]0.1580	[42]0.1911	[43]0.2482
34	IDEMIA-005	[79]0.0118	[82]0.0167	[85]0.0218	[84]0.0270	[83]0.0317	[82]0.0357	[81]0.0425	[81]0.0579	[60]0.0440	[59]0.0689	[55]0.0964	[54]0.1254	[53]0.1513	[51]0.1762	[46]0.2113	[47]0.2698
35	IDEMIA-006	[82]0.0124	[84]0.0171	[84]0.0218	[82]0.0263	[81]0.0302	[80]0.0321	[77]0.0356	[77]0.0471	[57]0.0409	[54]0.0620	[52]0.0850	[47]0.1097	[44]0.1309	[40]0.1486	[37]0.1738	[36]0.2200
36	IDEMIA-007	[42]0.0050	[43]0.0071	[43]0.0089	[45]0.0106	[46]0.0124	[46]0.0142	[46]0.0171	[48]0.0220	[31]0.0202	[31]0.0335	[29]0.0491	[28]0.0663	[26]0.0825	[25]0.0999	[22]0.1240	[24]0.1645
37	IDEMIA-008	[3]0.0018	[3]0.0024	[3]0.0029	[3]0.0032	[5]0.0035	[4]0.0039	[4]0.0046	[6]0.0033	[2]0.0034	[2]0.0051	[3]0.0069	[4]0.0087	[4]0.0102	[3]0.0123	[2]0.0146	[2]0.0186
38	IMAGUS-005	[28]0.0039	[28]0.0052	[26]0.0061	[24]0.0067	[25]0.0077	[25]0.0088	[25]0.0103	[25]0.0109	[34]0.0212	[34]0.0357	[35]0.0539	[35]0.0755	[33]0.0967	[33]0.1183	[32]0.1485	[30]0.1893
39	IMPERIAL-000	[29]0.0040	[30]0.0054	[31]0.0067	[33]0.0079	[35]0.0093	[36]0.0112	[35]0.0139	[37]0.0178	[44]0.0286	[46]0.0503	[46]0.0779	[49]0.1116	[51]0.1455	[53]0.1844	[55]0.2341	[54]0.2951
40	INCODE-003	[89]0.0155	[91]0.0247	[91]0.0348	[91]0.0463	[91]0.0571	[91]0.0674	[91]0.0856	[92]0.1114	[97]0.1627	[97]0.2507	[97]0.3322	[95]0.4122	[95]0.4772	[96]0.5368	[96]0.6059	[96]0.6766
41	INCODE-004	[51]0.0061	[54]0.0087	[54]0.0110	[56]0.0136	[59]0.0161	[59]0.0185	[62]0.0236	[60]0.0309	[68]0.0532	[69]0.0908	[70]0.1334	[70]0.1809	[72]0.2245	[71]0.2675	[70]0.3249	[69]0.3932
42	INNOVATRICS-004	[109]0.3594	[108]0.3629	[108]0.3688	[107]0.3754	[107]0.3813	[107]0.3870	[107]0.3960	[107]0.4135	[102]0.4234	[101]0.4642	[101]0.5073	[101]0.5522	[100]0.5902	[100]0.6274	[98]0.6736	[98]0.7253
43	INNOVATRICS-005	[36]0.0046	[36]0.0063	[37]0.0078	[40]0.0092	[40]0.0106	[38]0.0124	[38]0.0149	[38]0.0178	[50]0.0343	[51]0.0590	[53]0.0886	[53]0.1222	[54]0.1544	[55]0.1881	[54]0.2321	[52]0.2874
44	IREX-000	[20]0.0031	[20]0.0042	[20]0.0051	[21]0.0060	[21]0.0068	[21]0.0080	[22]0.0095	[23]0.0107	[47]0.0313	[47]0.0539	[48]0.0815	[51]0.1137	[50]0.1442	[50]0.1755	[51]0.2181	[48]0.2718

Table 6: **Accuracy for the FRVT 2018 mugshot sets under ageing**. *The second row shows the time lapse between gallery and subsequent probe images, in years. The first two columns identify the algorithm The next 8 values give rank-based FNIR with R = 1, T = 0 and FPIR = 1. All these are relevant to investigational uses where candidates from all searches would need human review. The second 8 values give threshold-based FNIR with T $\geq$ 0, FPIR = 0.001 and no rank criterion. The shaded cells indictate indicate the three most accurate algorithms for that elapsed time. The gallery size is 3068801. The total number of searches is 10951064.*

2021/08/05 02:00:58

FNIR(N, R, T) = FPIR(N, T) = False neg. identification rate / False pos. identification rate

N = Num. enrolled subjects
R = Num. candidates examined

T = Threshold

T = 0 → Investigation
T > 0 → Identification

MISS RATES		INVESTIGATION, FNIR(N, R = 1, T = 0)								IDENTIFICATION, FNIR(N, R = L, T $\geq$ 0) FOR FPIR = 0.001							
#	ALGORITHM	(0, 2]	(2, 4]	(4, 6]	(6, 8]	(8, 10]	(10, 12]	(12, 14]	(14, 18]	(0, 2]	(2, 4]	(4, 6]	(6, 8]	(8, 10]	(10, 12]	(12, 14]	(14, 18]
45	ISYSTEMS-002	[71] 0.0101	[74] 0.0135	[75] 0.0169	[74] 0.0197	[75] 0.0228	[72] 0.0256	[72] 0.0304	[73] 0.0398	[85] 0.0779	[85] 0.1258	[86] 0.1759	[85] 0.2299	[85] 0.2758	[84] 0.3204	[84] 0.3763	[82] 0.4401
46	ISYSTEMS-003	[70] 0.0089	[64] 0.0115	[64] 0.0139	[64] 0.0158	[65] 0.0177	[65] 0.0198	[61] 0.0234	[58] 0.0303	[79] 0.0647	[79] 0.1056	[79] 0.1502	[79] 0.1986	[78] 0.2402	[74] 0.2819	[73] 0.3351	[71] 0.3976
47	KEDACOM-001	[78] 0.0116	[70] 0.0130	[62] 0.0135	[55] 0.0133	[52] 0.0135	[45] 0.0141	[39] 0.0151	[36] 0.0176	[36] 0.0241	[36] 0.0360	[34] 0.0513	[29] 0.0689	[29] 0.0866	[29] 0.1060	[25] 0.1327	[25] 0.1694
48	LOOKMAN-003	[81] 0.0123	[78] 0.0144	[72] 0.0158	[65] 0.0168	[66] 0.0178	[61] 0.0188	[54] 0.0212	[54] 0.0260	[59] 0.0438	[57] 0.0687	[56] 0.0978	[56] 0.1296	[55] 0.1581	[54] 0.1879	[53] 0.2294	[50] 0.2756
49	LOOKMAN-005	[80] 0.0118	[72] 0.0134	[65] 0.0142	[61] 0.0144	[56] 0.0150	[55] 0.0160	[47] 0.0176	[45] 0.0213	[46] 0.0310	[44] 0.0480	[41] 0.0698	[41] 0.0954	[41] 0.1216	[41] 0.1491	[41] 0.1890	[41] 0.2381
50	MICROFOCUS-005	[110] 0.4269	[110] 0.5527	[110] 0.6355	[111] 0.7024	[111] 0.7503	[111] 0.7876	[111] 0.8234	[112] 0.8601	[106] 0.8338	[107] 0.9113	[107] 0.9468	[107] 0.9667	[107] 0.9771	[106] 0.9836	[106] 0.9880	[106] 0.9924
51	MICROSOFT-003	[24] 0.0034	[27] 0.0050	[28] 0.0064	[31] 0.0078	[33] 0.0092	[33] 0.0107	[34] 0.0135	[35] 0.0166	[45] 0.0288	[45] 0.0503	[45] 0.0763	[45] 0.1067	[49] 0.1359	[48] 0.1680	[47] 0.2116	[45] 0.2644
52	MICROSOFT-004	[21] 0.0032	[22] 0.0047	[24] 0.0060	[27] 0.0075	[30] 0.0087	[30] 0.0103	[33] 0.0131	[33] 0.0159	[42] 0.0268	[43] 0.0470	[44] 0.0716	[43] 0.1007	[43] 0.1291	[47] 0.1610	[45] 0.2052	[44] 0.2590
53	MICROSOFT-005	[19] 0.0031	[24] 0.0047	[30] 0.0066	[38] 0.0084	[38] 0.0103	[42] 0.0131	[44] 0.0164	[40] 0.0185	[38] 0.0243	[39] 0.0432	[39] 0.0658	[39] 0.0913	[40] 0.1172	[38] 0.1476	[40] 0.1874	[38] 0.2272
54	MICROSOFT-006	[22] 0.0032	[26] 0.0049	[29] 0.0065	[37] 0.0081	[37] 0.0096	[37] 0.0117	[36] 0.0144	[34] 0.0160	[19] 0.0134	[19] 0.0233	[20] 0.0346	[18] 0.0462	[17] 0.0578	[18] 0.0713	[18] 0.0903	[18] 0.1156
55	NEC-000	[92] 0.0195	[94] 0.0316	[94] 0.0445	[94] 0.0581	[93] 0.0699	[94] 0.0817	[94] 0.0998	[94] 0.1237	[84] 0.0759	[84] 0.1245	[84] 0.1729	[84] 0.2240	[84] 0.2671	[83] 0.3117	[81] 0.3639	[81] 0.4348
56	NEC-001	[99] 0.0246	[97] 0.0382	[95] 0.0524	[95] 0.0672	[96] 0.0793	[96] 0.0904	[95] 0.1076	[95] 0.1317	[89] 0.1019	[89] 0.1623	[89] 0.2214	[89] 0.2834	[89] 0.3341	[89] 0.3844	[89] 0.4440	[88] 0.5183
57	NEC-002	[23] 0.0033	[19] 0.0041	[15] 0.0043	[13] 0.0044	[11] 0.0045	[10] 0.0049	[10] 0.0056	[7] 0.0041	[12] 0.0066	[8] 0.0090	[7] 0.0111	[7] 0.0131	[6] 0.0149	[6] 0.0171	[7] 0.0207	[7] 0.0267
58	NEC-003	[27] 0.0036	[21] 0.0046	[19] 0.0051	[19] 0.0055	[19] 0.0059	[16] 0.0067	[15] 0.0077	[17] 0.0073	[6] 0.0056	[6] 0.0076	[6] 0.0091	[5] 0.0105	[5] 0.0119	[5] 0.0137	[4] 0.0162	[4] 0.0209
59	NEUROTECHNOLOGY-003	[96] 0.0234	[96] 0.0379	[97] 0.0549	[96] 0.0682	[95] 0.0720	[93] 0.0747	[93] 0.0886	[91] 0.1066	[104] 0.6802	[104] 0.8187	[105] 0.8920	[105] 0.9355	[105] 0.9594	[105] 0.9738	[105] 0.9828	[105] 0.9885
60	NEUROTECHNOLOGY-004	[74] 0.0104	[73] 0.0134	[71] 0.0156	[68] 0.0173	[67] 0.0195	[67] 0.0212	[65] 0.0245	[62] 0.0320	[78] 0.0642	[77] 0.1015	[76] 0.1426	[74] 0.1881	[73] 0.2299	[72] 0.2722	[71] 0.3269	[70] 0.3943
61	NEUROTECHNOLOGY-005	[69] 0.0089	[66] 0.0116	[63] 0.0136	[63] 0.0152	[64] 0.0173	[64] 0.0196	[60] 0.0233	[59] 0.0306	[71] 0.0556	[71] 0.0913	[69] 0.1315	[69] 0.1766	[69] 0.2192	[68] 0.2617	[67] 0.3174	[67] 0.3843
62	NEUROTECHNOLOGY-007	[61] 0.0078	[60] 0.0103	[59] 0.0124	[60] 0.0140	[58] 0.0161	[58] 0.0185	[57] 0.0225	[56] 0.0290	[77] 0.0641	[80] 0.1069	[80] 0.1546	[80] 0.2075	[81] 0.2572	[82] 0.3081	[83] 0.3713	[83] 0.4421
63	NOBLIS-002	[107] 0.1520	[107] 0.2419	[107] 0.3296	[108] 0.4114	[108] 0.4856	[108] 0.5528	[108] 0.6061	[108] 0.6532	[108] 0.9984	[108] 0.9996	[108] 0.9998	[108] 0.9999	[108] 0.9999	[108] 1.0000	[108] 1.0000	[112] 1.0000
64	NTECHLAB-003	[60] 0.0078	[71] 0.0131	[82] 0.0202	[85] 0.0295	[86] 0.0405	[88] 0.0543	[89] 0.0761	[90] 0.1035	[63] 0.0491	[67] 0.0881	[74] 0.1384	[78] 0.1985	[82] 0.2594	[85] 0.3270	[85] 0.4065	[85] 0.4891
65	NTECHLAB-004	[57] 0.0068	[63] 0.0110	[74] 0.0167	[81] 0.0239	[84] 0.0330	[85] 0.0447	[87] 0.0641	[88] 0.0891	[55] 0.0379	[58] 0.0688	[61] 0.1108	[61] 0.1629	[68] 0.2192	[77] 0.2846	[82] 0.3657	[84] 0.4524
66	NTECHLAB-006	[46] 0.0056	[57] 0.0095	[67] 0.0148	[78] 0.0218	[80] 0.0301	[83] 0.0413	[84] 0.0591	[87] 0.0814	[51] 0.0349	[55] 0.0636	[58] 0.1023	[59] 0.1506	[61] 0.2024	[67] 0.2617	[74] 0.3374	[78] 0.4185
67	NTECHLAB-007	[32] 0.0044	[38] 0.0066	[44] 0.0089	[52] 0.0118	[55] 0.0150	[62] 0.0189	[67] 0.0255	[67] 0.0342	[40] 0.0256	[41] 0.0450	[43] 0.0705	[44] 0.1012	[46] 0.1334	[49] 0.1692	[48] 0.2170	[49] 0.2752
68	NTECHLAB-008	[15] 0.0025	[18] 0.0038	[21] 0.0052	[26] 0.0074	[30] 0.0104	[47] 0.0146	[63] 0.0236	[68] 0.0348	[21] 0.0143	[23] 0.0267	[27] 0.0459	[32] 0.0733	[35] 0.1062	[37] 0.1469	[44] 0.2044	[46] 0.2698
69	NTECHLAB-009	[10] 0.0022	[12] 0.0031	[13] 0.0038	[14] 0.0045	[15] 0.0055	[18] 0.0067	[20] 0.0088	[22] 0.0100	[14] 0.0073	[14] 0.0117	[14] 0.0170	[14] 0.0238	[15] 0.0319	[15] 0.0419	[15] 0.0577	[15] 0.0833
70	PARAVISION-002	[48] 0.0058	[53] 0.0083	[55] 0.0111	[58] 0.0137	[60] 0.0162	[60] 0.0187	[59] 0.0229	[57] 0.0295								
71	PARAVISION-003	[39] 0.0048	[39] 0.0067	[46] 0.0090	[47] 0.0109	[49] 0.0128	[48] 0.0148	[48] 0.0178	[46] 0.0219	[52] 0.0354	[53] 0.0618	[54] 0.0931	[55] 0.1290	[56] 0.1625	[56] 0.1964	[56] 0.2408	[53] 0.2924
72	PARAVISION-004	[13] 0.0024	[14] 0.0032	[14] 0.0040	[15] 0.0047	[14] 0.0053	[14] 0.0061	[14] 0.0073	[15] 0.0072	[16] 0.0118	[18] 0.0209	[19] 0.0327	[19] 0.0465	[19] 0.0613	[19] 0.0779	[19] 0.1008	[19] 0.1285
73	PARAVISION-005	[9] 0.0021	[10] 0.0028	[10] 0.0035	[11] 0.0041	[12] 0.0046	[12] 0.0054	[12] 0.0067	[14] 0.0070	[8] 0.0057	[9] 0.0093	[9] 0.0144	[11] 0.0207	[12] 0.0278	[12] 0.0368	[13] 0.0508	[13] 0.0715
74	PARAVISION-007	[4] 0.0019	[5] 0.0025	[4] 0.0029	[6] 0.0033	[6] 0.0036	[6] 0.0042	[6] 0.0049	[4] 0.0030	[7] 0.0057	[10] 0.0094	[11] 0.0144	[10] 0.0206	[11] 0.0275	[11] 0.0357	[11] 0.0485	[11] 0.0652
75	PIXELALL-002	[67] 0.0085	[68] 0.0119	[66] 0.0147	[67] 0.0172	[68] 0.0198	[69] 0.0225	[68] 0.0270	[69] 0.0349	[92] 0.1193	[92] 0.1900	[92] 0.2601	[92] 0.3332	[92] 0.3955	[92] 0.4565	[92] 0.5268	[93] 0.6030
76	PIXELALL-003	[41] 0.0050	[37] 0.0063	[34] 0.0072	[29] 0.0077	[28] 0.0085	[28] 0.0095	[29] 0.0113	[27] 0.0119	[39] 0.0248	[38] 0.0418	[38] 0.0622	[38] 0.0861	[38] 0.1104	[35] 0.1364	[35] 0.1723	[34] 0.2167
77	PIXELALL-004	[40] 0.0049	[35] 0.0063	[35] 0.0072	[32] 0.0079	[31] 0.0089	[32] 0.0103	[32] 0.0127	[31] 0.0146	[33] 0.0211	[35] 0.0360	[37] 0.0553	[37] 0.0792	[34] 0.1045	[34] 0.1317	[34] 0.1700	[37] 0.2246
78	PTAKURATSATU-000	[49] 0.0061	[50] 0.0082	[50] 0.0097	[48] 0.0109	[44] 0.0120	[41] 0.0131	[37] 0.0146	[39] 0.0180	[54] 0.0375	[52] 0.0596	[50] 0.0842	[50] 0.1116	[48] 0.1357	[44] 0.1553	[38] 0.1820	[40] 0.2326
79	RANKONE-002	[94] 0.0212	[93] 0.0313	[93] 0.0431	[93] 0.0562	[94] 0.0712	[95] 0.0881	[96] 0.1130	[97] 0.1543	[90] 0.1111	[90] 0.1707	[90] 0.2305	[90] 0.2968	[91] 0.3646	[91] 0.4345	[91] 0.5172	[94] 0.6110
80	RANKONE-004	[103] 0.0424	[102] 0.0643	[102] 0.0875	[102] 0.1127	[102] 0.1364	[100] 0.1579	[100] 0.1914	[100] 0.2378	[99] 0.1855	[98] 0.2681	[98] 0.3431	[96] 0.4155	[96] 0.4785	[95] 0.5350	[95] 0.5980	[95] 0.6722
81	RANKONE-005	[87] 0.0136	[88] 0.0192	[86] 0.0246	[86] 0.0303	[85] 0.0362	[84] 0.0422	[83] 0.0521	[83] 0.0694	[76] 0.0582	[70] 0.0910	[66] 0.1260	[63] 0.1645	[60] 0.2005	[59] 0.2353	[59] 0.2816	[60] 0.3522
82	RANKONE-007	[62] 0.0078	[59] 0.0099	[56] 0.0113	[53] 0.0123	[53] 0.0139	[54] 0.0156	[53] 0.0191	[52] 0.0242	[37] 0.0242	[37] 0.0376	[36] 0.0542	[33] 0.0737	[32] 0.0935	[31] 0.1130	[29] 0.1416	[29] 0.1811
83	RANKONE-009	[43] 0.0054	[44] 0.0072	[41] 0.0085	[42] 0.0098	[42] 0.0113	[40] 0.0130	[45] 0.0169	[49] 0.0220	[32] 0.0208	[33] 0.0345	[32] 0.0504	[31] 0.0706	[31] 0.0930	[32] 0.1174	[33] 0.1504	[32] 0.2002
84	RANKONE-010	[37] 0.0047	[33] 0.0061	[33] 0.0070	[28] 0.0076	[29] 0.0087	[29] 0.0098	[30] 0.0113	[28] 0.0120	[26] 0.0177	[24] 0.0269	[21] 0.0368	[21] 0.0479	[18] 0.0590	[17] 0.0688	[17] 0.0803	[16] 0.0991
85	REALNETWORKS-002	[102] 0.0381	[103] 0.0687	[103] 0.1062	[103] 0.1495	[104] 0.1963	[104] 0.2513	[106] 0.3206	[106] 0.3927	[100] 0.2153	[100] 0.3323	[100] 0.4444	[100] 0.5485	[101] 0.6355	[101] 0.7132	[102] 0.7855	[102] 0.8437
86	REALNETWORKS-003	[98] 0.0245	[100] 0.0437	[100] 0.0686	[101] 0.0975	[101] 0.1312	[102] 0.1719	[102] 0.2294	[103] 0.2907	[93] 0.1468	[95] 0.2370	[96] 0.3313	[98] 0.4269	[98] 0.5142	[99] 0.5979	[100] 0.6815	[100] 0.7567
87	REALNETWORKS-004	[97] 0.0244	[99] 0.0428	[99] 0.0663	[100] 0.0939	[100] 0.1251	[101] 0.1634	[101] 0.2170	[102] 0.2785	[94] 0.1484	[96] 0.2377	[95] 0.3303	[97] 0.4249	[97] 0.5106	[98] 0.5924	[99] 0.6758	[99] 0.7534
88	SCANOVATE-001	[63] 0.0079	[67] 0.0117	[70] 0.0151	[73] 0.0185	[73] 0.0221	[73] 0.0259	[73] 0.0321	[73] 0.0427	[83] 0.0727	[83] 0.1169	[82] 0.1650	[82] 0.2115	[79] 0.2528	[79] 0.2925	[76] 0.3437	[75] 0.4084

Table 7: **Accuracy for the FRVT 2018 mugshot sets under ageing**. *The second row shows the time lapse between gallery and subsequent probe images, in years. The first two columns identify the algorithm The next 8 values give rank-based FNIR with R = 1, T = 0 and FPIR = 1. All these are relevant to investigational uses where candidates from all searches would need human review. The second 8 values give threshold-based FNIR with T $\geq$ 0, FPIR = 0.001 and no rank criterion. The shaded cells indictate indicate the three most accurate algorithms for that elapsed time. The gallery size is 3068801. The total number of searches is 10951064.*

2021/08/05 02:00:58

FNIR(N, R, T) = FPIR(N, T) = False neg. identification rate / False pos. identification rate

N = Num. enrolled subjects
R = Num. candidates examined

T = Threshold

T = 0 → Investigation
T > 0 → Identification

MISS RATES		INVESTIGATION, FNIR(N, R = 1, T = 0)								IDENTIFICATION, FNIR(N, R = L, T $\geq$ 0) FOR FPIR = 0.001							
#	ALGORITHM	(0, 2]	(2, 4]	(4, 6]	(6, 8]	(8, 10]	(10, 12]	(12, 14]	(14, 18]	(0, 2]	(2, 4]	(4, 6]	(6, 8]	(8, 10]	(10, 12]	(12, 14]	(14, 18]
89	SENSETIME-002	[91]0.0186	[87]0.0191	[79]0.0183	[70]0.0179	[63]0.0173	[43]0.0133	[21]0.0089	[12]0.0059	[35]0.0220	[20]0.0236	[15]0.0237	[15]0.0240	[9]0.0245	[7]0.0219	[6]0.0195	[5]0.0222
90	SENSETIME-003	[8]0.0021	[9]0.0028	[8]0.0031	[5]0.0033	[4]0.0035	[5]0.0040	[5]0.0047	[5]0.0033	[5]0.0046	[5]0.0064	[4]0.0076	[3]0.0086	[3]0.0101	[2]0.0122	[3]0.0155	[3]0.0196
91	SENSETIME-004	[2]0.0016	[2]0.0022	[2]0.0025	[2]0.0028	[2]0.0030	[2]0.0035	[3]0.0043	[2]0.0025	[3]0.0036	[3]0.0052	[2]0.0066	[2]0.0081	[2]0.0099	[4]0.0126	[5]0.0169	[6]0.0230
92	SENSETIME-005	[1]0.0015	[1]0.0020	[1]0.0024	[1]0.0026	[1]0.0029	[1]0.0035	[2]0.0043	[3]0.0028	[4]0.0036	[4]0.0059	[5]0.0089	[6]0.0128	[7]0.0177	[8]0.0240	[9]0.0345	[9]0.0493
93	SIAT-002	[112]0.8309	[112]0.8310	[112]0.8311	[112]0.8306	[112]0.8296	[112]0.8302	[112]0.8300	[111]0.8301	[107]0.8340	[105]0.8368	[104]0.8404	[104]0.8445	[104]0.8480	[104]0.8532	[104]0.8595	[103]0.8691
94	SYNESIS-003	[84]0.0125	[80]0.0151	[78]0.0174	[75]0.0199	[74]0.0223	[70]0.0240	[70]0.0279	[63]0.0331	[80]0.0658	[78]0.1052	[78]0.1483	[77]0.1968	[77]0.2399	[75]0.2834	[75]0.3405	[74]0.4046
95	SYNESIS-005	[35]0.0044	[32]0.0058	[32]0.0070	[35]0.0080	[32]0.0091	[31]0.0103	[31]0.0125	[32]0.0152	[41]0.0262	[40]0.0444	[40]0.0666	[40]0.0923	[39]0.1156	[36]0.1399	[36]0.1736	[35]0.2185
96	TECH5-001	[52]0.0061	[56]0.0093	[61]0.0128	[66]0.0171	[72]0.0221	[77]0.0289	[80]0.0412	[80]0.0560	[81]0.0660	[82]0.1156	[85]0.1733	[86]0.2385	[86]0.2998	[86]0.3629	[88]0.4424	[89]0.5284
97	TOSHIBA-001	[68]0.0086	[69]0.0119	[69]0.0150	[69]0.0178	[70]0.0209	[71]0.0241	[71]0.0292	[70]0.0365								
98	TRUEFACE-000	[31]0.0043	[31]0.0057	[25]0.0061	[23]0.0067	[22]0.0073	[23]0.0084	[23]0.0097	[21]0.0099	[30]0.0200	[32]0.0338	[33]0.0504	[30]0.0705	[30]0.0904	[30]0.1112	[28]0.1401	[28]0.1792
99	VERIDAS-001	[53]0.0063	[51]0.0083	[51]0.0099	[51]0.0113	[51]0.0132	[49]0.0148	[50]0.0184	[47]0.0219	[56]0.0403	[56]0.0684	[57]0.1012	[57]0.1386	[57]0.1741	[57]0.2113	[57]0.2611	[58]0.3233
100	VISIONLABS-004	[38]0.0048	[41]0.0069	[47]0.0091	[50]0.0111	[50]0.0130	[52]0.0152	[51]0.0187	[53]0.0242	[69]0.0540	[72]0.0916	[73]0.1358	[73]0.1855	[74]0.2303	[73]0.2745	[72]0.3312	[68]0.3913
101	VISIONLABS-005	[34]0.0044	[34]0.0063	[38]0.0081	[41]0.0095	[41]0.0109	[39]0.0125	[40]0.0151	[41]0.0187	[62]0.0479	[62]0.0812	[63]0.1212	[65]0.1664	[64]0.2078	[64]0.2473	[63]0.2999	[62]0.3577
102	VISIONLABS-006	[25]0.0035	[25]0.0048	[27]0.0061	[25]0.0069	[24]0.0077	[24]0.0087	[26]0.0105	[29]0.0120	[43]0.0273	[42]0.0465	[42]0.0702	[42]0.0970	[42]0.1228	[39]0.1486	[39]0.1847	[39]0.2295
103	VISIONLABS-008	[18]0.0028	[17]0.0037	[18]0.0047	[18]0.0053	[18]0.0058	[17]0.0067	[19]0.0081	[20]0.0085	[22]0.0143	[22]0.0241	[23]0.0373	[22]0.0519	[22]0.0677	[20]0.0850	[20]0.1104	[20]0.1444
104	VISIONLABS-009	[7]0.0020	[7]0.0026	[7]0.0030	[7]0.0034	[8]0.0038	[8]0.0044	[9]0.0052	[9]0.0046	[11]0.0065	[12]0.0105	[12]0.0156	[12]0.0217	[13]0.0289	[13]0.0368	[12]0.0499	[12]0.0681
105	VISIONLABS-010	[6]0.0020	[6]0.0025	[6]0.0030	[8]0.0034	[7]0.0036	[7]0.0043	[7]0.0051	[10]0.0047	[13]0.0069	[13]0.0113	[13]0.0170	[13]0.0238	[14]0.0316	[14]0.0411	[14]0.0557	[14]0.0740
106	VTS-000	[111]0.5878	[111]0.6312	[111]0.6602	[110]0.6863	[110]0.7073	[110]0.7246	[110]0.7458	[109]0.7747	[103]0.5929	[103]0.6397	[103]0.6729	[103]0.7034	[102]0.7279	[102]0.7493	[101]0.7739	[101]0.8076
107	XFORWARDAI-000	[17]0.0027	[15]0.0034	[17]0.0044	[17]0.0052	[17]0.0058	[19]0.0067	[17]0.0079	[18]0.0076	[23]0.0157	[26]0.0281	[25]0.0443	[26]0.0635	[27]0.0834	[27]0.1050	[26]0.1330	[26]0.1714
108	XFORWARDAI-001	[12]0.0023	[8]0.0028	[9]0.0034	[9]0.0037	[9]0.0039	[9]0.0045	[8]0.0052	[8]0.0043	[10]0.0060	[11]0.0096	[10]0.0144	[9]0.0200	[10]0.0260	[10]0.0334	[10]0.0435	[10]0.0586
109	YITU-002	[55]0.0066	[52]0.0083	[48]0.0094	[43]0.0101	[45]0.0121	[51]0.0150	[56]0.0223	[63]0.0328	[28]0.0189	[29]0.0317	[30]0.0494	[34]0.0750	[36]0.1066	[42]0.1494	[49]0.2171	[55]0.2958
110	YITU-003	[58]0.0072	[55]0.0089	[52]0.0100	[46]0.0107	[47]0.0125	[53]0.0153	[58]0.0226	[66]0.0334	[29]0.0194	[30]0.0321	[31]0.0500	[36]0.0756	[37]0.1071	[43]0.1500	[50]0.2177	[56]0.2964
111	YITU-004	[50]0.0061	[46]0.0075	[39]0.0081	[36]0.0081	[34]0.0092	[34]0.0107	[42]0.0154	[44]0.0207	[18]0.0125	[17]0.0204	[18]0.0314	[20]0.0469	[21]0.0671	[23]0.0955	[31]0.1421	[33]0.2006
112	YITU-005	[56]0.0067	[49]0.0080	[42]0.0087	[39]0.0085	[36]0.0094	[35]0.0108	[41]0.0151	[43]0.0204	[17]0.0124	[16]0.0198	[17]0.0308	[17]0.0462	[20]0.0667	[22]0.0953	[30]0.1418	[31]0.1930

Table 8: **Accuracy for the FRVT 2018 mugshot sets under ageing**. *The second row shows the time lapse between gallery and subsequent probe images, in years. The first two columns identify the algorithm The next 8 values give rank-based FNIR with R = 1, T = 0 and FPIR = 1. All these are relevant to investigational uses where candidates from all searches would need human review. The second 8 values give threshold-based FNIR with T $\geq$ 0, FPIR = 0.001 and no rank criterion. The shaded cells indictate indicate the three most accurate algorithms for that elapsed time. The gallery size is 3068801. The total number of searches is 10951064.*

#	ALGORITHM	INVESTIGATION MODE						IDENTIFICATION MODE						FAILURE TO EXTRACT					
		RANK ONE MISS RATE, FNIR(N, 0, 1)						HIGH T ⟶ FPIR = 0.001, FNIR(N, T, L)						FEATURES					
		N=1.6M						N=1.6M											
	GALLERY	MUGSHOT	MUGSHOT	MUGSHOT	VISA	BORDER	VISA	MUGSHOT	MUGSHOT	MUGSHOT	VISA	BORDER	VISA	MUGSHOT	MUGSHOT	MUGSHOT	VISA	BORDER	KIOSK
	PROBE	MUGSHOT	WEBCAM	PROFILE	BORDER	BOR¿10YR	KIOSK	MUGSHOT	WEBCAM	PROFILE	BORDER	BOR¿10YR	KIOSK	MUGSHOT	WEBCAM	PROFILE	BORDER	BOR¿10YR	KIOSK
1	3DIVI-003	[200]0.083	[196]0.206		[128]0.141		[134]0.474	[196]0.400	[196]0.626		[130]0.605		[108]0.821	0.002	0.005				
2	3DIVI-004	[161]0.018	[170]0.062		[111]0.035		[115]0.279	[170]0.169	[177]0.343		[113]0.277		[88]0.607	0.002	0.005				
3	3DIVI-005	[162]0.018	[169]0.062	[138]0.930	[146]0.821		[116]0.279	[167]0.166	[175]0.339	[104]0.996	[135]0.864		[87]0.597	0.002	0.005	0.442			
4	3DIVI-006	[172]0.024	[177]0.074		[113]0.047		[124]0.312	[169]0.168	[176]0.342		[114]0.283		[91]0.615	0.002	0.005				
5	ACER-000	[141]0.011	[134]0.036	[119]0.827	[99]0.025		[100]0.209	[160]0.146	[155]0.246	[66]0.981	[108]0.201		[76]0.490	0.000	0.000	0.042			
6	ALCHERA-000	[157]0.016	[157]0.047	[126]0.870	[112]0.046		[121]0.292	[157]0.138	[143]0.216	[119]0.999	[105]0.176		[104]0.803	0.006	0.014	0.328			
7	ALCHERA-001	[226]0.987	[222]1.000		[148]1.000		[223]1.000	[223]0.999	[217]1.000		[150]1.000		[167]1.000	0.006	0.013	0.324			
8	ALCHERA-002	[201]0.095	[193]0.166	[151]0.954	[143]0.668		[132]0.446	[203]0.486	[193]0.591	[140]1.000	[134]0.827		[105]0.811	0.001	0.002	0.106			
9	ALCHERA-003	[138]0.010	[132]0.035	[96]0.741	[92]0.016		[98]0.206	[161]0.155	[152]0.239	[128]0.999	[104]0.172		[73]0.464	0.001	0.002	0.106			
10	ALLGOVISION-000	[144]0.011	[129]0.033	[129]0.894	[96]0.021		[118]0.282	[137]0.088	[132]0.166	[81]0.990	[89]0.117		[82]0.526	0.002	0.003	0.122			
11	ALLGOVISION-001	[129]0.009	[142]0.038	[86]0.661	[95]0.021		[110]0.241	[143]0.102	[146]0.221	[72]0.986	[99]0.150		[77]0.491	0.001	0.001	0.042			
12	ANKE-000	[152]0.013	[137]0.038	[141]0.931	[222]1.000		[184]1.000	[147]0.117	[145]0.220	[86]0.994	[174]1.000		[159]1.000	0.000	0.001	0.080			
13	ANKE-001	[153]0.013	[138]0.038	[140]0.946	[192]1.000		[221]1.000	[151]0.119	[144]0.220	[91]0.994	[146]1.000		[173]1.000	0.000	0.001	0.080			
14	ANKE-002	[67]0.003	[69]0.016	[66]0.522	[45]0.005		[59]0.119	[71]0.032	[60]0.079	[43]0.948	[46]0.034		[32]0.245	0.001	0.001	0.049			
15	AWARE-003	[179]0.031	[182]0.090	[163]0.966	[134]0.316		[120]0.290	[155]0.128	[169]0.298	[70]0.984	[122]0.428		[83]0.530	0.004	0.003	0.874			
16	AWARE-004	[195]0.068	[195]0.176	[170]0.976	[126]0.122		[130]0.414	[183]0.269	[189]0.509	[144]1.000	[119]0.397		[106]0.816	0.003	0.003	0.776			
17	AWARE-005	[180]0.031	[171]0.067	[171]0.978	[115]0.048		[123]0.308	[191]0.364	[156]0.253	[146]1.000	[112]0.255		[115]0.916	0.001	0.002	0.189			
18	AWARE-006	[197]0.070	[189]0.128	[173]0.983	[125]0.111		[131]0.421	[184]0.276	[180]0.398	[137]0.999	[117]0.368		[98]0.749	0.001	0.002	0.189			
19	AYONIX-000	[220]0.450	[217]0.685	[182]0.996	[142]0.607		[145]0.867	[212]0.811	[211]0.939	[109]0.998	[139]0.954		[125]0.982	0.010	0.031	0.939			
20	AYONIX-001	[216]0.341	[210]0.527	[178]0.993	[147]0.994		[143]0.778	[214]0.824	[206]0.920	[133]0.999	[143]0.999		[122]0.969	0.010	0.031	0.939			
21	AYONIX-002	[215]0.341	[211]0.527	[177]0.993	[138]0.464		[142]0.778	[213]0.824	[207]0.920	[135]0.999	[136]0.915		[123]0.969	0.010	0.031	0.939			
22	CAMVI-003	[191]0.052	[183]0.090	[131]0.911	[122]0.093		[127]0.360	[121]0.071	[110]0.132	[51]0.970	[88]0.114		[65]0.402	0.006	0.013	0.675			
23	CAMVI-004	[189]0.047	[178]0.077	[98]0.744	[120]0.072		[122]0.296	[122]0.072	[112]0.136	[132]0.999	[86]0.100		[102]0.787	0.000	0.000	0.000			
24	CAMVI-005	[194]0.065	[187]0.103	[100]0.746	[123]0.098		[126]0.341	[141]0.099	[139]0.179	[139]1.000	[100]0.156		[132]0.999	0.000	0.000	0.000			
25	CIB-000	[21]0.002	[10]0.008	[14]0.100	[8]0.002	[13]0.011	[4]0.069	[28]0.012	[28]0.045	[150]1.000	[25]0.017	[19]0.141	[113]0.894	0.000	0.000	0.000		0.000	
26	CLOUDWALK-HR-000	[18]0.001	[21]0.010	[4]0.064	[6]0.002	[3]0.006	[1]0.057	[6]0.002	[6]0.013	[1]0.133	[4]0.005	[2]0.033	[4]0.099	0.001	0.000	0.042		0.000	
27	COGENT-000	[139]0.010	[155]0.046	[161]0.965				[100]0.053	[114]0.140	[99]0.995				0.000	0.000	0.000			
28	COGENT-001	[140]0.010	[154]0.046	[162]0.965				[99]0.053	[113]0.140	[96]0.995				0.000	0.000	0.000			
29	COGENT-002	[81]0.004	[93]0.020	[136]0.925				[87]0.044	[84]0.098	[108]0.998				0.000	0.000	0.000			
30	COGENT-003	[83]0.004	[97]0.021	[145]0.939				[91]0.046	[78]0.095	[110]0.998				0.000	0.000	0.000			
31	COGENT-004	[40]0.002	[44]0.013	[135]0.922	[38]0.004	[22]0.019	[55]0.113	[72]0.033	[33]0.051	[106]0.997	[31]0.022	[17]0.126	[72]0.456	0.000	0.000	0.000		0.000	
32	COGNITEC-000	[174]0.025	[166]0.059	[159]0.964				[165]0.161	[170]0.303	[83]0.992				0.003	0.002	0.924			
33	COGNITEC-001	[145]0.012	[131]0.034	[154]0.958				[142]0.102	[150]0.230	[188]1.000				0.003	0.002	0.924			
34	COGNITEC-002	[106]0.006	[117]0.025	[148]0.949				[102]0.053	[138]0.178	[149]1.000				0.003	0.002	0.924			
35	COGNITEC-003	[110]0.006	[116]0.025	[140]0.930				[98]0.053	[130]0.162	[152]1.000				0.004	0.002	0.878			
36	COGNITEC-004	[74]0.003	[68]0.016	[116]0.813	[86]0.013	[40]0.057	[77]0.143	[70]0.031	[82]0.097	[78]0.990	[75]0.068	[37]0.316	[46]0.288	0.002	0.001	0.635		0.006	
37	CYBERLINK-000	[85]0.004	[92]0.020	[94]0.717	[69]0.007		[71]0.134	[108]0.056	[95]0.116	[99]0.995	[73]0.063		[58]0.339	0.001	0.001	0.063			
38	CYBERLINK-001	[29]0.004	[81]0.018	[95]0.731	[64]0.007		[70]0.133	[103]0.054	[92]0.109	[95]0.995	[70]0.062		[92]0.652	0.000	0.000	0.040			
39	CYBERLINK-002	[61]0.003	[35]0.012	[79]0.577	[36]0.004		[48]0.107	[35]0.015	[37]0.053	[77]0.988	[32]0.024		[47]0.288	0.001	0.000	0.042			
40	CYBERLINK-003	[24]0.002	[16]0.009	[59]0.474	[21]0.003	[14]0.012	[20]0.082	[20]0.008	[23]0.035	[54]0.972	[18]0.012	[13]0.100	[60]0.368	0.000	0.000	0.039		0.000	
41	CYBERLINK-004	[27]0.002	[32]0.011	[53]0.423	[20]0.003	[12]0.011	[42]0.104	[19]0.007	[24]0.036	[160]1.000	[20]0.013	[14]0.109	[121]0.954	0.000	0.000	0.011		0.000	
42	DAHUA-000	[133]0.009	[119]0.026					[133]0.086	[111]0.135					0.004	0.003				
43	DAHUA-001	[114]0.007	[111]0.024	[93]0.703				[124]0.073	[103]0.122	[64]0.980				0.002	0.002	0.346			
44	DAHUA-002	[34]0.002	[34]0.012	[38]0.304	[17]0.003		[21]0.084	[36]0.015	[30]0.046	[19]0.638	[24]0.017		[19]0.159	0.001	0.000	0.099			
45	DAHUA-003	[10]0.001	[7]0.007	[26]0.206	[7]0.002	[10]0.009	[8]0.073	[32]0.014	[27]0.041	[16]0.579	[19]0.013	[11]0.081	[14]0.134	0.000	0.000	0.000		0.000	
46	DEEPGLINT-001	[16]0.001	[6]0.007	[25]0.200	[14]0.002		[9]0.073	[12]0.003	[7]0.014	[138]1.000	[7]0.006		[18]0.159	0.000	0.000	0.038			

Table 9: **Miss rates by dataset:** *At left, rank 1 miss rates relevant to investigations; at right, with threshold set to target FPIR = 0.01 for higher volume, low prior, uses. Yellow indicates most accurate algorithm. Throughout blue superscripts indicate the rank of the algorithm for that column.*

2021/08/05 02:00:58

FNIR(N, R, T) = False neg. identification rate
FPIR(N, T) = False pos. identification rate

N = Num. enrolled subjects
R = Num. candidates examined

T = Threshold

T = 0 → Investigation
T > 0 → Identification

#	ALGORITHM	INVESTIGATION MODE						IDENTIFICATION MODE						FAILURE TO EXTRACT					
		RANK ONE MISS RATE, FNIR(N, 0, 1)						HIGH T → FPIR = 0.001, FNIR(N, T, L)						FEATURES					
		N=1.6M						N=1.6M											
	GALLERY	MUGSHOT	MUGSHOT	MUGSHOT	VISA	BORDER	VISA	MUGSHOT	MUGSHOT	MUGSHOT	VISA	BORDER	VISA	MUGSHOT	MUGSHOT	MUGSHOT	VISA	BORDER	KIOSK
	PROBE	MUGSHOT	WEBCAM	PROFILE	BORDER	BOR¿10YR	KIOSK	MUGSHOT	WEBCAM	PROFILE	BORDER	BOR¿10YR	KIOSK	MUGSHOT	WEBCAM	PROFILE	BORDER	BOR¿10YR	KIOSK
47	DEEPSEA-001	[90]0.004	[66]0.016	[117]0.814	[75]0.010		[76]0.140	[90]0.046	[86]0.101	[71]0.985	[79]0.077		[56]0.326	0.000	0.001	0.047			
48	DERMALOG-003	[205]0.126	[198]0.217		[133]0.296		[137]0.560	[202]0.482	[198]0.655		[133]0.677		[111]0.870	0.002	0.002	0.103			
49	DERMALOG-004	[204]0.125	[197]0.215	[139]0.930	[127]0.135		[133]0.467	[201]0.480	[199]0.657	[100]0.995	[129]0.603		[110]0.856	0.001	0.002	0.107			
50	DERMALOG-005	[156]0.015	[136]0.037	[92]0.701	[132]0.242		[129]0.384	[136]0.088	[123]0.154	[79]0.990	[115]0.300		[90]0.614	0.001	0.002	0.102			
51	DERMALOG-006	[124]0.008	[115]0.024	[84]0.619	[76]0.010		[84]0.155	[97]0.052	[88]0.105	[65]0.981	[68]0.059		[55]0.318	0.003	0.006	0.181			
52	DERMALOG-007	[132]0.009	[120]0.027	[88]0.675	[89]0.014		[87]0.170	[134]0.086	[121]0.152	[80]0.990	[85]0.099		[86]0.557	0.001	0.002	0.102			
53	DERMALOG-008	[68]0.003	[58]0.015	[65]0.516	[62]0.007	[37]0.029	[75]0.139	[89]0.045	[75]0.094	[169]1.000	[65]0.057	[40]0.382	[119]0.940	0.000	0.000	0.002		0.000	
54	EYEDEA-003	[199]0.080	[191]0.148	[157]0.960	[124]0.101		[128]0.379	[193]0.388	[191]0.543	[92]0.994	[127]0.570		[103]0.792	0.001	0.003	0.161			
55	F8-001	[149]0.012		[87]0.669	[197]1.000		[217]1.000	[166]0.166		[118]0.998				0.004	1.000	0.158			
56	GLORY-000	[209]0.178	[204]0.320	[181]0.994	[131]0.228		[139]0.678	[192]0.367	[192]0.547	[94]0.995	[124]0.453		[109]0.839	0.011	0.013	0.985			
57	GLORY-001	[206]0.127	[201]0.267	[176]0.992	[130]0.178		[138]0.594	[185]0.305	[190]0.537	[84]0.993	[121]0.408		[107]0.819	0.011	0.013	0.988			
58	GORILLA-001	[192]0.060	[184]0.095	[143]0.936	[119]0.069		[125]0.329	[197]0.406	[185]0.453	[158]1.000	[125]0.468		[140]1.000	0.001	0.001	0.069			
59	GORILLA-002	[168]0.020	[151]0.044	[101]0.753	[100]0.027		[105]0.214	[173]0.188	[163]0.268	[164]1.000	[111]0.250		[135]1.000	0.001	0.001	0.069			
60	GORILLA-003	[181]0.036	[173]0.070	[118]0.821	[114]0.048		[113]0.265	[187]0.318	[184]0.434	[193]1.000	[120]0.407		[156]1.000	0.001	0.001	0.069			
61	GORILLA-004	[111]0.006	[112]0.024	[91]0.697	[79]0.012		[85]0.162	[139]0.089	[129]0.160	[45]0.959	[94]0.135		[69]0.438	0.000	0.001	0.042			
62	GORILLA-005	[73]0.003	[82]0.018	[27]0.209	[56]0.006		[61]0.124	[112]0.058	[116]0.142	[22]0.700	[83]0.088		[54]0.315	0.000	0.000	0.040			
63	HIK-003	[146]0.012	[123]0.027	[90]0.689	[82]0.012		[81]0.151	[144]0.103	[125]0.158	[49]0.969	[97]0.142		[71]0.445	0.000	0.000	0.048			
64	HIK-004	[143]0.011	[121]0.027	[97]0.743	[80]0.012		[83]0.152	[140]0.099	[122]0.153	[56]0.976	[95]0.137		[68]0.434	0.000	0.000	0.048			
65	HIK-005	[95]0.005	[71]0.017	[70]0.535	[66]0.007		[52]0.111	[84]0.044	[59]0.077	[136]0.999	[74]0.068		[84]0.541	0.000	0.000	0.000			
66	HIK-006	[94]0.005	[70]0.017	[71]0.535				[92]0.047	[67]0.086	[154]1.000				0.000	0.000	0.000			
67	IDEMIA-003	[117]0.007	[130]0.034	[152]0.958	[93]0.018		[101]0.210	[93]0.047	[131]0.165		[91]0.123		[101]0.766	0.000	0.000	0.041			
68	IDEMIA-004	[113]0.007	[128]0.032	[147]0.947	[94]0.018		[102]0.210	[80]0.037	[99]0.118	[55]0.973	[90]0.123		[100]0.766	0.000	0.000	0.041			
69	IDEMIA-005	[123]0.008	[143]0.039	[150]0.954	[97]0.021		[106]0.217	[86]0.044	[120]0.150	[60]0.978	[92]0.130		[112]0.879	0.000	0.000	0.041			
70	IDEMIA-006	[136]0.010	[175]0.072	[165]0.969	[102]0.030		[112]0.253	[83]0.043	[148]0.226	[67]0.982	[98]0.144		[96]0.733	0.000	0.000	0.041			
71	IDEMIA-007	[60]0.003	[63]0.015	[192]1.000	[57]0.006	[38]0.036	[67]0.131	[42]0.018	[39]0.055	[209]1.000	[61]0.052	[24]0.182	[203]1.000	0.000	0.000	0.040		0.000	
72	IDEMIA-008	[6]0.001	[3]0.007	[10]0.079	[4]0.001	[5]0.007	[12]0.075	[5]0.002	[5]0.013	[3]0.204	[3]0.005	[4]0.036	[7]0.106	0.000	0.000	0.040		0.000	
73	IMAGUS-002	[212]0.220	[202]0.301	[175]0.988				[210]0.749	[203]0.816	[168]1.000				0.004	0.008	0.550			
74	IMAGUS-003	[217]0.356	[208]0.513	[179]0.993				[211]0.807	[205]0.909	[153]1.000				0.004	0.008	0.550			
75	IMAGUS-005	[37]0.002	[36]0.012	[40]0.319	[55]0.006	[24]0.022	[69]0.132	[45]0.018	[47]0.066	[32]0.838	[36]0.029	[23]0.161	[34]0.231	0.000	0.000	0.000		0.000	
76	IMAGUS-006	[41]0.002	[48]0.014	[37]0.293	[39]0.004	[23]0.019	[53]0.112	[47]0.019	[50]0.069	[39]0.897	[35]0.028	[22]0.161	[41]0.260	0.000	0.000	0.000		0.000	
77	IMPERIAL-000	[59]0.002	[60]0.015	[36]0.280	[43]0.004		[33]0.097	[58]0.026	[49]0.068	[122]0.999	[52]0.042		[38]0.245	0.000	0.000	0.000			
78	INCODE-000	[190]0.049	[186]0.100	[149]0.951				[186]0.310	[182]0.420	[114]0.998				0.001	0.004	0.173			
79	INCODE-001	[159]0.017	[156]0.046	[102]0.762				[176]0.212	[166]0.296	[167]1.000				0.001	0.004	0.173			
80	INCODE-002	[163]0.018	[158]0.048	[121]0.843				[172]0.184	[164]0.269	[85]0.993				0.000	0.001	0.066			
81	INCODE-003	[151]0.013	[145]0.040	[103]0.764				[168]0.167	[160]0.264	[134]0.999				0.000	0.001	0.066			
82	INCODE-004	[80]0.004	[79]0.017	[60]0.475	[73]0.008		[73]0.135	[105]0.054	[102]0.120	[93]0.995	[72]0.063		[52]0.313	0.000	0.001	0.066			
83	INNOVATRICS-002	[188]0.045	[176]0.074	[124]0.853				[181]0.234	[171]0.310	[156]1.000				0.000	0.001	0.046			
84	INNOVATRICS-003	[175]0.026	[161]0.055	[123]0.845				[177]0.221	[167]0.297	[142]1.000				0.000	0.001	0.046			
85	INNOVATRICS-004	[150]0.012	[147]0.040	[153]0.958				[156]0.132	[147]0.222	[63]0.980				0.000	0.001	0.046			
86	INNOVATRICS-005	[58]0.002	[55]0.014	[52]0.407	[44]0.005		[49]0.109	[73]0.034	[70]0.089	[33]0.846	[58]0.047		[39]0.251	0.000	0.001	0.041			
87	INTSYSMSU-000	[207]0.146	[110]0.023	[78]0.562	[121]0.072		[68]0.132	[221]0.998	[216]1.000	[143]1.000	[142]0.999		[133]0.999	0.000	0.000	0.050			
88	IREX-000	[91]0.004	[17]0.010	[89]0.681	[13]0.002	[15]0.012	[18]0.082	[66]0.028	[43]0.060	[44]0.957	[55]0.044	[36]0.302	[22]0.170	0.000	0.000	0.042		0.000	
89	ISYSTEMS-002	[112]0.006	[118]0.026	[122]0.844				[127]0.078	[106]0.126	[107]0.998				0.002	0.002	0.142			
90	ISYSTEMS-003	[101]0.005	[107]0.023	[106]0.791				[113]0.059	[91]0.107	[145]1.000				0.002	0.002	0.142			
91	KAKAO-000	[17]0.001	[27]0.011	[16]0.119	[15]0.002	[17]0.013	[15]0.078	[38]0.015	[40]0.056	[11]0.468	[27]0.019	[18]0.141	[17]0.158	0.000	0.000	0.041		0.000	
92	KEDACOM-001	[120]0.008	[133]0.036	[167]0.972	[107]0.034		[107]0.237	[54]0.023	[54]0.072	[73]0.986	[64]0.055		[50]0.305	0.000	0.000	0.000			

Table 10: **Miss rates by dataset:** *At left, rank 1 miss rates relevant to investigations; at right, with threshold set to target FPIR = 0.01 for higher volume, low prior, uses. Yellow indicates most accurate algorithm. Throughout blue superscripts indicate the rank of the algorithm for that column.*

2021/08/05 02:00:58

FNIR(N, R, T) = False neg. identification rate
FPIR(N, T) = False pos. identification rate

N = Num. enrolled subjects
R = Num. candidates examined

T = Threshold

T = 0 → Investigation
T > 0 → Identification

#	ALGORITHM	INVESTIGATION MODE						IDENTIFICATION MODE						FAILURE TO EXTRACT					
		RANK ONE MISS RATE, FNIR(N, 0, 1)						HIGH T → FPIR = 0.001, FNIR(N, T, L)						FEATURES					
		N=1.6M						N=1.6M											
	GALLERY	MUGSHOT	MUGSHOT	MUGSHOT	VISA	BORDER	VISA	MUGSHOT	MUGSHOT	MUGSHOT	VISA	BORDER	VISA	MUGSHOT	MUGSHOT	MUGSHOT	VISA	BORDER	KIOSK
	PROBE	MUGSHOT	WEBCAM	PROFILE	BORDER	BOR¿10YR	KIOSK	MUGSHOT	WEBCAM	PROFILE	BORDER	BOR¿10YR	KIOSK	MUGSHOT	WEBCAM	PROFILE	BORDER	BOR¿10YR	KIOSK
93	KNERON-000	[107]0.006	[122]0.027	[76]0.552	[101]0.028		[96]0.195							0.000	0.000	0.000			
94	KNERON-001	[178]0.030	[216]0.621	[32]0.237	[129]0.144	[43]0.207	[117]0.280							0.000	0.000	0.000		0.000	
95	LINE-000	[47]0.002	[50]0.014	[30]0.223	[48]0.005	[35]0.029	[46]0.107	[69]0.031	[79]0.095		[56]0.046	[34]0.278	[219]1.000	0.000	0.000	0.000		0.000	
96	LOOKMAN-003	[128]0.009	[141]0.038		[110]0.035		[109]0.239	[85]0.044	[94]0.112		[82]0.084		[59]0.355	0.000	0.000				
97	LOOKMAN-004	[130]0.009	[144]0.039	[169]0.973				[88]0.045	[90]0.105	[57]0.977				0.000	0.000	0.000			
98	LOOKMAN-005	[122]0.008	[135]0.036	[168]0.972	[109]0.035		[108]0.237	[68]0.030	[66]0.086	[59]0.978	[71]0.062		[51]0.308	0.000	0.000	0.000			
99	MEGVII-001	[147]0.012	[78]0.017		[223]1.000			[123]0.072	[83]0.097					0.002	0.000				
100	MEGVII-002	[148]0.012	[80]0.017	[56]0.450	[155]1.000			[126]0.077	[81]0.096	[117]0.998				0.002	0.000	0.033			
101	MICROFOCUS-003	[224]0.594	[220]0.781		[145]0.708		[147]0.907	[217]0.931	[215]0.979		[141]0.982		[129]0.991	0.001	0.005				
102	MICROFOCUS-004	[222]0.576	[219]0.758		[144]0.701		[146]0.904	[222]0.999	[213]0.975		[140]0.974		[127]0.989	0.001	0.005				
103	MICROFOCUS-005	[218]0.424	[214]0.601		[140]0.494		[141]0.777	[215]0.835	[209]0.928		[138]0.935		[126]0.985	0.001	0.005				
104	MICROFOCUS-006	[219]0.427	[213]0.583		[139]0.490		[144]0.782	[219]0.978	[208]0.923		[137]0.923		[124]0.971	0.001	0.005				
105	MICROSOFT-003	[25]0.002	[30]0.012		[35]0.004		[50]0.109	[64]0.028	[70]0.091		[48]0.036		[36]0.233	0.000	0.001				
106	MICROSOFT-004	[19]0.001	[38]0.012		[29]0.004		[51]0.109	[59]0.026	[68]0.087		[44]0.033		[32]0.222	0.000	0.001				
107	MICROSOFT-005	[35]0.002	[30]0.011	[20]0.144	[24]0.003		[34]0.099	[57]0.026	[52]0.070	[17]0.587	[33]0.027		[24]0.180	0.000	0.001	0.049			
108	MICROSOFT-006	[39]0.002	[33]0.011	[22]0.150	[32]0.004		[36]0.100	[25]0.012	[25]0.037	[6]0.386	[41]0.032		[23]0.178	0.000	0.001	0.049			
109	NEC-000	[160]0.017	[149]0.041	[156]0.959	[98]0.025		[111]0.243	[129]0.079	[115]0.140	[61]0.979			[75]0.474	0.001	0.002	0.890			
110	NEC-001	[169]0.021	[162]0.056	[164]0.967	[106]0.033		[114]0.277	[146]0.106	[141]0.197	[74]0.986	[93]0.133		[74]0.468	0.005	0.003	0.934			
111	NEC-002	[5]0.001	[15]0.009	[48]0.363	[28]0.003		[57]0.117	[10]0.003	[12]0.020	[131]0.999	[11]0.008		[94]0.676	0.000	0.001	0.041			
112	NEC-003	[13]0.001	[23]0.010	[47]0.352	[31]0.004	[16]0.013	[60]0.120	[8]0.002	[11]0.017	[29]0.824	[14]0.008	[5]0.036	[93]0.668	0.000	0.001	0.041		0.001	
113	NEC-004	[15]0.001	[14]0.009	[72]0.538	[23]0.003	[7]0.007	[11]0.075	[2]0.002	[4]0.013	[18]0.622	[2]0.004	[1]0.019	[5]0.100	0.000	0.001	0.041		0.001	
114	NEUROTECHNOLOGY-003	[170]0.022	[150]0.042	[158]0.961				[208]0.636	[162]0.266	[194]1.000				0.000	0.001	0.131			
115	NEUROTECHNOLOGY-004	[103]0.006	[91]0.020	[166]0.970				[117]0.063	[96]0.117	[89]0.994				0.000	0.001	0.131			
116	NEUROTECHNOLOGY-005	[89]0.004	[114]0.024	[128]0.893				[106]0.054	[108]0.130	[111]0.998				0.000	0.000	0.030			
117	NEUROTECHNOLOGY-006	[164]0.018	[153]0.045	[83]0.606				[182]0.249	[181]0.418					0.000	0.000				
118	NEUROTECHNOLOGY-007	[84]0.004	[96]0.021	[109]0.796	[74]0.009		[93]0.180	[116]0.062	[135]0.173	[147]1.000	[116]0.339		[184]1.000	0.001	0.001	0.041			
119	NEUROTECHNOLOGY-008	[46]0.002	[54]0.014	[57]0.457	[37]0.004	[26]0.023	[38]0.101	[101]0.053	[62]0.080	[165]1.000	[47]0.035	[35]0.293	[29]0.203	0.000	0.001	0.052		0.001	
120	NEWLAND-002	[198]0.079	[188]0.117	[142]0.936				[199]0.438	[186]0.466	[125]0.999				0.007	0.012	0.200			
121	NOBLIS-001	[214]0.249	[209]0.522	[180]0.993				[224]1.000	[223]1.000	[161]1.000				0.000	0.000	0.000			
122	NOBLIS-002	[210]0.179	[206]0.392	[172]0.982				[220]0.997	[224]1.000	[162]1.000				0.000	0.000	0.000			
123	NTECHLAB-003	[108]0.006	[104]0.023	[61]0.504				[104]0.054	[97]0.118	[31]0.837				0.000	0.000	0.040			
124	NTECHLAB-004	[98]0.005	[87]0.019	[62]0.506	[71]0.008		[64]0.129	[81]0.041	[89]0.105	[30]0.833	[63]0.053		[43]0.263	0.000	0.000	0.040			
125	NTECHLAB-005	[96]0.005	[83]0.018	[49]0.367	[72]0.008		[58]0.118	[82]0.042	[87]0.102	[25]0.771	[77]0.073		[48]0.294	0.000	0.000	0.040			
126	NTECHLAB-006	[88]0.004	[75]0.017	[46]0.347	[68]0.007		[56]0.113	[76]0.037	[76]0.094	[24]0.754	[66]0.057		[42]0.260	0.000	0.000	0.040			
127	NTECHLAB-007	[62]0.003	[40]0.012	[41]0.326	[42]0.004		[43]0.107	[56]0.026	[48]0.067	[23]0.750	[42]0.032		[33]0.223	0.000	0.000	0.042			
128	NTECHLAB-008	[28]0.002	[18]0.010	[23]0.157	[27]0.003		[22]0.084	[33]0.014	[29]0.045	[15]0.529	[45]0.033		[25]0.183	0.000	0.000	0.044			
129	NTECHLAB-009	[12]0.001	[8]0.008	[18]0.138	[9]0.002	[18]0.013	[10]0.074	[17]0.005	[13]0.022	[8]0.430	[21]0.015	[15]0.109	[15]0.142	0.000	0.000	0.041		0.001	
130	NTECHLAB-010	[7]0.001	[11]0.008	[11]0.085	[5]0.002	[8]0.008	[2]0.057	[9]0.003	[9]0.015	[5]0.252	[8]0.007	[9]0.059	[2]0.098	0.001	0.001	0.043		0.000	
131	PARAVISION-000	[165]0.019	[140]0.038	[69]0.534	[137]0.423		[136]0.529	[138]0.089	[133]0.170	[127]0.999	[126]0.470		[118]0.926	0.000	0.000	0.000			
132	PARAVISION-001	[82]0.004	[94]0.020	[42]0.329	[136]0.414		[135]0.484	[94]0.049	[107]0.128	[120]0.999	[123]0.444		[97]0.739	0.000	0.000	0.000			
133	PARAVISION-002	[87]0.004	[99]0.022	[44]0.335	[90]0.015		[89]0.175	[95]0.050	[100]0.119	[68]0.983	[80]0.080		[78]0.497	0.000	0.000	0.032			
134	PARAVISION-003	[72]0.003	[88]0.019	[33]0.252	[91]0.015		[86]0.167	[74]0.035	[80]0.096	[90]0.994	[67]0.058		[49]0.296	0.000	0.000	0.032			
135	PARAVISION-004	[26]0.002	[25]0.010	[15]0.104	[53]0.006		[54]0.112	[24]0.010	[26]0.038	[157]1.000	[26]0.018		[114]0.908	0.000	0.000	0.032			
136	PARAVISION-005	[20]0.002	[19]0.010	[9]0.079	[65]0.007		[44]0.106	[14]0.004	[14]0.024	[62]0.980	[17]0.011		[12]0.132	0.000	0.000	0.038			
137	PARAVISION-007	[9]0.001	[9]0.008	[5]0.066	[47]0.005	[11]0.010	[37]0.101	[13]0.004	[15]0.025	[163]1.000	[16]0.009	[16]0.113	[214]1.000	0.000	0.000	0.000		0.000	
138	PIXELALL-002	[93]0.005	[101]0.022	[114]0.810	[78]0.011		[94]0.187	[145]0.105	[179]0.388	[155]1.000	[128]0.602		[183]1.000	0.000	0.000	0.000			

Table 11: **Miss rates by dataset:** *At left, rank 1 miss rates relevant to investigations; at right, with threshold set to target FPIR = 0.01 for higher volume, low prior, uses. Yellow indicates most accurate algorithm. Throughout blue superscripts indicate the rank of the algorithm for that column.*

2021/08/05 02:00:58

FNIR(N, R, T) = False neg. identification rate
FPIR(N, T) = False pos. identification rate

N = Num. enrolled subjects
R = Num. candidates examined

T = Threshold

T = 0 → Investigation
T > 0 → Identification

#	ALGORITHM	INVESTIGATION MODE						IDENTIFICATION MODE						FAILURE TO EXTRACT					
		RANK ONE MISS RATE, FNIR(N, 0, 1)						HIGH T → FPIR = 0.001, FNIR(N, T, L)						FEATURES					
		N=1.6M						N=1.6M											
	GALLERY	MUGSHOT	MUGSHOT	MUGSHOT	VISA	BORDER	VISA	MUGSHOT	MUGSHOT	MUGSHOT	VISA	BORDER	VISA	MUGSHOT	MUGSHOT	MUGSHOT	VISA	BORDER	KIOSK
	PROBE	MUGSHOT	WEBCAM	PROFILE	BORDER	BOR¿10YR	KIOSK	MUGSHOT	WEBCAM	PROFILE	BORDER	BOR¿10YR	KIOSK	MUGSHOT	WEBCAM	PROFILE	BORDER	BOR¿10YR	KIOSK
139	PIXELALL-003	[45]0.002	[53]0.014	[64]0.515	[61]0.006		[80]0.151	[51]0.022	[55]0.073	[141]1.000	[50]0.037		[85]0.554	0.000	0.000	0.000			
140	PIXELALL-004	[43]0.002	[57]0.015	[67]0.523	[50]0.005		[82]0.152	[44]0.018	[61]0.079	[151]1.000	[60]0.051		[130]0.994	0.000	0.000	0.000			
141	PIXELALL-005	[36]0.002	[29]0.011	[35]0.264	[81]0.012	[32]0.028	[78]0.146	[27]0.012	[32]0.050	[166]1.000	[34]0.027	[27]0.203	[134]1.000	0.000	0.000	0.000		0.000	
142	PTAKURATSATU-000	[71]0.003	[74]0.017	[82]0.605	[49]0.005	[30]0.027	[43]0.105	[75]0.037	[105]0.124	[41]0.924	[57]0.046	[29]0.206	[35]0.232	0.000	0.001	0.039		0.000	
143	QUANTASOFT-001	[211]0.218	[218]0.727					[209]0.639						0.000	0.000				
144	RANKONE-002	[167]0.019	[174]0.071					[149]0.118	[158]0.261					0.000	0.000				
145	RANKONE-003	[166]0.019	[172]0.068					[150]0.118	[157]0.255					0.000	0.000				
146	RANKONE-004	[187]0.041	[190]0.141					[174]0.193	[183]0.426					0.000	0.000				
147	RANKONE-005	[134]0.009	[148]0.041	[174]0.986				[114]0.059	[136]0.173	[112]0.998				0.000	0.000	0.489			
148	RANKONE-006	[100]0.005		[111]0.797				[77]0.037		[58]0.977				0.002		0.167			
149	RANKONE-007	[76]0.003	[86]0.019	[108]0.796				[53]0.022	[77]0.095	[48]0.967				0.001	0.001	0.102			
150	RANKONE-009	[54]0.002	[42]0.013	[73]0.549	[52]0.006		[72]0.134	[41]0.018	[57]0.076	[50]0.969	[69]0.062		[57]0.328	0.000	0.000	0.000			
151	RANKONE-010	[48]0.002	[20]0.010	[50]0.374	[46]0.005	[29]0.027	[62]0.126	[31]0.014	[41]0.058	[27]0.802	[62]0.052	[30]0.208	[40]0.259	0.000	0.000	0.000		0.000	
152	REALNETWORKS-000	[186]0.040	[180]0.078					[179]0.234	[173]0.319					0.001	0.000				
153	REALNETWORKS-001	[185]0.040	[181]0.078					[180]0.234	[174]0.319					0.001	0.000				
154	REALNETWORKS-002	[182]0.039	[179]0.078					[178]0.231	[172]0.315					0.001	0.000				
155	REALNETWORKS-003	[173]0.024	[168]0.062	[105]0.771	[105]0.031		[99]0.209	[164]0.159	[161]0.266	[116]0.998	[102]0.164		[79]0.500	0.001	0.000	0.009			
156	REALNETWORKS-004	[171]0.024	[165]0.059	[110]0.797	[104]0.031		[104]0.213	[163]0.158	[159]0.263	[129]0.999	[103]0.170		[89]0.613	0.001	0.000	0.009			
157	REALNETWORKS-005	[50]0.002	[45]0.013	[55]0.433	[40]0.004	[25]0.023	[39]0.102	[63]0.028	[56]0.074	[52]0.971	[49]0.037	[31]0.223	[31]0.215	0.000	0.000	0.006		0.000	
158	REMARKAI-000	[78]0.003	[84]0.018	[88]0.660	[70]0.008		[79]0.148	[107]0.055	[101]0.120	[126]0.999	[76]0.069		[95]0.717	0.000	0.000	0.000			
159	REMARKAI-000	[127]0.009	[127]0.030					[154]0.128	[142]0.203					0.000	0.001				
160	REMARKAI-002	[125]0.008	[126]0.029	[112]0.802				[153]0.124	[140]0.196	[82]0.991				0.000	0.001	0.017			
161	RENDIP-000	[23]0.002	[59]0.015	[54]0.424	[58]0.006	[31]0.028	[23]0.084	[26]0.012	[42]0.059	[38]0.894	[29]0.022	[25]0.185	[20]0.167	0.000	0.000	0.041		0.000	
162	S1-000	[56]0.002	[73]0.017	[34]0.258	[51]0.005	[28]0.025	[26]0.090	[65]0.028	[65]0.085	[172]1.000	[59]0.047	[135]1.000	[189]1.000	0.000	0.000	0.040		0.000	
163	SCANOVATE-000	[99]0.005	[152]0.045	[77]0.560	[108]0.035		[103]0.211	[120]0.067	[154]0.240	[37]0.893	[109]0.215		[64]0.400	0.000	0.001	0.057			
164	SCANOVATE-001	[102]0.005	[146]0.040	[81]0.585	[103]0.031		[92]0.178	[130]0.081	[149]0.227	[40]0.911	[106]0.192		[67]0.404	0.000	0.001	0.044			
165	SENSETIME-000	[52]0.002	[65]0.016	[68]0.528				[49]0.021	[45]0.063	[178]1.000				0.004	0.000	0.042			
166	SENSETIME-001	[53]0.002	[64]0.016					[52]0.022	[46]0.064					0.004	0.000				
167	SENSETIME-002	[154]0.014	[89]0.020	[51]0.384	[77]0.011		[41]0.104	[34]0.015	[19]0.028	[88]0.994	[40]0.032		[81]0.523	0.009	0.000	0.040			
168	SENSETIME-003	[4]0.001	[4]0.007	[21]0.150	[18]0.003		[27]0.091	[4]0.002	[1]0.012	[12]0.477	[12]0.008		[13]0.133	0.000	0.000	0.041			
169	SENSETIME-004	[3]0.001	[5]0.007	[8]0.072	[12]0.002		[24]0.084	[1]0.002	[3]0.013	[4]0.229	[6]0.006		[10]0.113	0.000	0.000	0.041			
170	SENSETIME-005	[2]0.001	[2]0.006	[3]0.059	[11]0.002	[6]0.007	[17]0.082	[7]0.002	[8]0.014	[2]0.173	[9]0.007	[7]0.051	[6]0.104	0.000	0.000	0.041		0.000	
171	SENSETIME-006	[1]0.001	[1]0.006	[1]0.055	[1]0.001	[1]0.004	[3]0.064	[3]0.002	[2]0.012	[115]0.998	[1]0.004	[3]0.034	[1]0.093	0.000	0.000	0.025		0.000	
172	SHAMAN-003	[202]0.124	[194]0.172					[200]0.451	[194]0.597					0.020	0.011				
173	SHAMAN-004	[213]0.222	[203]0.319					[207]0.615	[201]0.754					0.020	0.011				
174	SHAMAN-006	[184]0.040	[164]0.058	[144]0.938				[158]0.141	[151]0.237	[53]0.972				0.020	0.011	0.869			
175	SHAMAN-007	[183]0.040	[163]0.057					[159]0.141	[153]0.240					0.020	0.010				
176	SIAT-001	[30]0.002	[205]0.333		[41]0.004		[35]0.099	[39]0.018	[178]0.365		[38]0.031			0.000	0.000				
177	SIAT-002	[31]0.002	[207]0.446		[135]0.348		[40]0.102	[50]0.022	[187]0.478		[118]0.372		[117]0.923	0.000	0.000				
178	SMILART-004	[225]0.965	[221]0.974					[218]0.968	[214]0.976					0.011	0.013				
179	SMILART-005													0.011	0.013				
180	SYNESIS-003	[158]0.016	[108]0.023	[120]0.827	[84]0.013		[74]0.136	[118]0.065	[104]0.123	[46]0.960	[78]0.075		[53]0.314	0.000	0.001	0.063			
181	SYNESIS-003	[208]0.170	[199]0.235					[205]0.582	[197]0.646					0.006	0.015				
182	SYNESIS-005	[126]0.009	[43]0.013	[99]0.744	[26]0.003		[28]0.092	[55]0.025	[53]0.072	[69]0.984	[43]0.032		[30]0.214	0.001	0.000	0.135			
183	TECH5-001	[86]0.004	[72]0.017	[80]0.584	[63]0.007		[47]0.107	[109]0.057	[210]0.935	[171]1.000	[110]0.244		[131]0.994	0.000	0.000	0.006			
184	TECH5-002	[63]0.003	[28]0.011	[39]0.312	[25]0.003	[36]0.029	[25]0.089	[62]0.027	[51]0.070	[28]0.805	[51]0.039	[28]0.205	[70]0.440	0.001	0.000	0.041		0.000	

Table 12: **Miss rates by dataset:** *At left, rank 1 miss rates relevant to investigations; at right, with threshold set to target FPIR = 0.01 for higher volume, low prior, uses. Yellow indicates most accurate algorithm. Throughout blue superscripts indicate the rank of the algorithm for that column.*

2021/08/05 02:00:58

FNIR(N, R, T) = False neg. identification rate
FPIR(N, T) = False pos. identification rate

N = Num. enrolled subjects
R = Num. candidates examined

T = Threshold

T = 0 → Investigation
T > 0 → Identification

#	ALGORITHM	INVESTIGATION MODE						IDENTIFICATION MODE						FAILURE TO EXTRACT					
		RANK ONE MISS RATE, FNIR(N, 0, 1)						HIGH T → FPIR = 0.001, FNIR(N, T, L)						FEATURES					
		N=1.6M						N=1.6M											
	GALLERY	MUGSHOT	MUGSHOT	MUGSHOT	VISA	BORDER	VISA	MUGSHOT	MUGSHOT	MUGSHOT	VISA	BORDER	VISA	MUGSHOT	MUGSHOT	MUGSHOT	VISA	BORDER	KIOSK
	PROBE	MUGSHOT	WEBCAM	PROFILE	BORDER	BOR¿10YR	KIOSK	MUGSHOT	WEBCAM	PROFILE	BORDER	BOR¿10YR	KIOSK	MUGSHOT	WEBCAM	PROFILE	BORDER	BOR¿10YR	KIOSK
185	TEVIAN-003	[155]0.015	[159]0.052					[171]0.177	[168]0.298					0.001	0.002				
186	TEVIAN-004	[142]0.011	[139]0.038					[148]0.117	[137]0.176					0.001	0.002				
187	TEVIAN-005	[119]0.007	[125]0.028	[58]0.467				[135]0.087	[117]0.144	[47]0.962				0.001	0.002	0.116			
188	TEVIAN-006	[57]0.002	[31]0.011	[17]0.123	[19]0.003	[19]0.013	[7]0.071	[22]0.010	[21]0.032	[7]0.425	[22]0.016	[12]0.093	[120]0.951	0.001	0.000	0.062		0.000	
189	TIGER-000	[193]0.062	[185]0.095					[195]0.390	[188]0.500					0.000	0.000				
190	TIGER-002	[105]0.006	[105]0.023	[63]0.514				[132]0.086	[127]0.158	[124]0.999				0.000	0.000	0.056			
191	TIGER-003	[104]0.006	[106]0.023					[131]0.086	[126]0.158					0.000	0.000				
192	TONGYITRANS-000	[115]0.007	[103]0.022					[125]0.074	[93]0.112					0.003	0.001				
193	TONGYITRANS-001	[116]0.007	[102]0.022					[119]0.066	[85]0.101					0.003	0.001				
194	TOSHIBA-000	[92]0.004	[98]0.022	[104]0.766				[115]0.062	[98]0.118	[98]0.995				0.000	0.000	0.070			
195	TOSHIBA-001	[97]0.005	[100]0.022					[111]0.058	[74]0.092					0.000	0.000				
196	TRUEFACE-000	[75]0.003	[46]0.014	[31]0.230	[67]0.007	[27]0.024	[29]0.092	[43]0.018	[44]0.062	[34]0.882	[37]0.030	[26]0.194	[27]0.188	0.001	0.001	0.047		0.003	
197	VD-000	[221]0.474	[213]0.551					[216]0.917	[212]0.946					0.011	0.013				
198	VD-001	[177]0.028	[160]0.053					[175]0.201	[165]0.281					0.005	0.001				
199	VD-002	[135]0.010	[124]0.027	[127]0.893	[87]0.013	[39]0.050	[90]0.176	[128]0.079	[119]0.148	[101]0.996	[84]0.095	[38]0.367	[61]0.372	0.004	0.003	0.156		0.002	
200	VERIDAS-001	[66]0.003	[51]0.014	[75]0.550	[60]0.006	[33]0.028	[65]0.131	[79]0.037	[64]0.082	[76]0.987	[54]0.044	[32]0.266	[44]0.264	0.000	0.002	0.093		0.001	
201	VERIDAS-002	[65]0.003	[52]0.014	[74]0.550	[59]0.006	[34]0.028	[66]0.131	[78]0.037	[63]0.082	[75]0.987	[53]0.044	[33]0.266	[45]0.264	0.000	0.002	0.093		0.001	
202	VIGILANTSOLUTIONS-003	[196]0.069	[192]0.151	[155]0.958				[198]0.408	[200]0.660	[121]0.999				0.000	0.001	0.127			
203	VIGILANTSOLUTIONS-004	[203]0.125	[200]0.244	[160]0.965				[204]0.549	[204]0.817	[103]0.996				0.000	0.001	0.127			
204	VIGILANTSOLUTIONS-005	[131]0.009		[133]0.920				[194]0.388		[170]1.000				0.000	0.001	0.127			
205	VIGILANTSOLUTIONS-006	[137]0.010		[134]0.921				[189]0.353		[159]1.000				0.000	0.001	0.127			
206	VIGILANTSOLUTIONS-007	[77]0.003	[76]0.017	[137]0.925	[85]0.013	[41]0.068	[88]0.175	[67]0.028	[69]0.088	[102]0.996	[81]0.081	[39]0.371	[63]0.391	0.000	0.001	0.127		0.001	
207	VIGILANTSOLUTIONS-008	[70]0.003	[77]0.017	[132]0.913	[88]0.014	[42]0.072	[91]0.178	[48]0.021	[58]0.077	[123]0.999	[87]0.104	[41]0.398	[80]0.511	0.000	0.001	0.127		0.001	
208	VISIONLABS-004	[64]0.003	[90]0.020	[45]0.343				[110]0.058	[128]0.159	[36]0.890				0.001	0.001	0.046			
209	VISIONLABS-005	[55]0.002	[85]0.019	[43]0.334				[96]0.050	[118]0.147	[35]0.888				0.001	0.001	0.046			
210	VISIONLABS-006	[32]0.002	[62]0.015	[29]0.211	[33]0.004		[32]0.096	[61]0.027	[72]0.090	[20]0.672				0.001	0.001	0.051			
211	VISIONLABS-007	[29]0.002	[61]0.015	[28]0.211	[30]0.004		[31]0.095	[60]0.027	[71]0.090	[21]0.672	[39]0.031		[26]0.185	0.001	0.001	0.051			
212	VISIONLABS-008	[42]0.002	[47]0.014	[19]0.141	[10]0.002		[16]0.081	[29]0.013	[35]0.051	[13]0.481	[23]0.017		[16]0.151	0.001	0.000	0.075			
213	VISIONLABS-009	[8]0.001	[13]0.008	[13]0.091	[3]0.001		[6]0.071	[15]0.005	[16]0.025	[26]0.799	[15]0.008		[9]0.113	0.000	0.000	0.060			
214	VISIONLABS-010	[14]0.001	[26]0.010	[7]0.069	[2]0.001	[2]0.006	[5]0.069	[18]0.005	[18]0.027		[10]0.008	[8]0.055	[8]0.109	0.000	0.000	0.040		0.000	
215	VOCORD-003	[109]0.006	[113]0.024	[113]0.804	[118]0.061		[95]0.188	[152]0.122	[124]0.155	[113]0.998	[101]0.157		[66]0.404	0.001	0.011	0.425			
216	VOCORD-004	[121]0.008	[95]0.021	[107]0.792	[83]0.012		[63]0.127	[190]0.355	[134]0.173	[148]1.000	[107]0.193		[128]0.991	0.000	0.000	0.000			
217	VOCORD-005	[118]0.007	[109]0.023	[115]0.812	[116]0.055		[97]0.206	[162]0.158	[109]0.130	[105]0.997	[96]0.138		[62]0.381	0.001	0.009	0.554			
218	VOCORD-006	[227]1.000	[226]1.000	[199]1.000	[177]1.000		[156]1.000	[228]1.000	[228]1.000	[227]1.000	[225]1.000		[191]1.000	0.001	0.009	0.554			
219	VTS-000	[223]0.594	[215]0.608	[130]0.909	[141]0.607	[44]0.724	[140]0.739	[206]0.598	[198]0.619	[130]0.999	[131]0.613	[42]0.760	[98]0.761	0.000	0.001	0.047		0.000	
220	VTS-001	[22]0.002	[22]0.010	[24]0.167	[54]0.006	[21]0.018	[14]0.077	[30]0.013	[34]0.051	[87]0.994	[30]0.022	[20]0.141	[28]0.192	0.000	0.000	0.040		0.000	
221	XFORWARDAI-000	[49]0.002	[47]0.014	[12]0.089	[34]0.004	[20]0.015	[30]0.094	[37]0.015	[38]0.053	[9]0.440	[28]0.021	[21]0.159	[21]0.169	0.000	0.000	0.000		0.000	
222	XFORWARDAI-001	[44]0.002	[41]0.013	[6]0.067	[22]0.003	[9]0.009	[19]0.082	[16]0.005	[20]0.028	[10]0.448	[13]0.008	[10]0.062	[11]0.123	0.000	0.000	0.000		0.000	
223	XFORWARDAI-002	[38]0.002	[37]0.012	[2]0.059	[16]0.002	[4]0.007	[13]0.077	[11]0.003	[10]0.016	[14]0.525	[5]0.005	[6]0.041	[3]0.099	0.000	0.000	0.000		0.000	
224	YISHENG-001	[176]0.027	[167]0.060		[117]0.058		[119]0.287	[188]0.346	[202]0.808		[132]0.666		[116]0.919	0.002	0.005				
225	YITU-002	[33]0.002	[24]0.010					[40]0.018	[31]0.049					0.000	0.000				
226	YITU-003	[69]0.003	[67]0.016					[46]0.019	[36]0.052					0.003	0.001				
227	YITU-004	[11]0.001	[12]0.008	[125]0.866				[21]0.010	[17]0.027	[42]0.936				0.000	0.000	0.000			
228	YITU-005	[51]0.002	[56]0.014					[23]0.010	[22]0.032					0.003	0.001				

Table 13: **Miss rates by dataset:** *At left, rank 1 miss rates relevant to investigations; at right, with threshold set to target FPIR = 0.01 for higher volume, low prior, uses. Yellow indicates most accurate algorithm. Throughout blue superscripts indicate the rank of the algorithm for that column.*

2021/08/05 02:00:58

FNIR(N, R, T) = False neg. identification rate
FPIR(N, T) = False pos. identification rate
N = Num. enrolled subjects
R = Num. candidates examined
T = Threshold
T = 0 → Investigation
T > 0 → Identification

MISSES BELOW THRESHOLD, T FNIR(N, T> 0, R >L)		ENROL MOST RECENT DATASET: FRVT 2018 MUGSHOTS				
#	ALGORITHM	N=0.64M	N=1.6M	N=3.0M	N=6.0M	N=12.0M
1	3DIVI-005	[167]0.1358	[162]0.1664	[146]0.1915	[138]0.2370	[133]0.3054
2	ACER-000	[161]0.1185	[160]0.1455	[141]0.1714	[132]0.2074	[126]0.2537
3	ALCHERA-003	[159]0.1176	[161]0.1553	[142]0.1853	[139]0.2409	[141]0.3553
4	ALLGOVISION-000	[136]0.0688	[137]0.0881	[124]0.1084	[117]0.1389	[106]0.2129
5	ALLGOVISION-001	[142]0.0785	[143]0.1017	[131]0.1218	[124]0.1584	[113]0.2273
6	ANKE-000	[148]0.0942	[147]0.1169	[136]0.1404	[129]0.1776	[127]0.2559
7	ANKE-002	[71]0.0229	[71]0.0318	[72]0.0406	[68]0.0605	[61]0.1466
8	AWARE-003	[156]0.1098	[155]0.1283	[137]0.1447	[127]0.1768	[118]0.2364
9	AWARE-005	[192]0.3389	[191]0.3643	[153]0.3993	[147]0.4526	[125]0.2531
10	AYONIX-002	[213]0.7862	[213]0.8242	[159]0.8508	[152]0.8704	[149]0.8939
11	CAMVI-004	[96]0.0367	[122]0.0716	[119]0.0983	[141]0.2508	[130]0.2701
12	CIB-000	[26]0.0086	[28]0.0125	[27]0.0160	[34]0.0303	[47]0.1251
13	CLOUDWALK-HR-000	[7]0.0019	[6]0.0020	[4]0.0023	[7]0.0072	[11]0.0701
14	COGENT-000	[112]0.0430	[100]0.0527	[99]0.0695	[103]0.1133	[95]0.1960
15	COGENT-001	[113]0.0430	[99]0.0527	[101]0.0695	[102]0.1133	[96]0.1960
16	COGENT-002	[83]0.0322	[87]0.0444	[87]0.0610	[100]0.1116	[108]0.2180
17	COGENT-003	[84]0.0328	[91]0.0463	[98]0.0683	[110]0.1294	[120]0.2445
18	COGENT-004	[68]0.0210	[72]0.0331	[82]0.0527	[105]0.1138	[105]0.2119
19	COGNITEC-000	[169]0.1377	[165]0.1606	[145]0.1870	[134]0.2176	[132]0.2831
20	COGNITEC-001	[144]0.0807	[142]0.1017	[130]0.1214	[120]0.1513	[111]0.2238
21	COGNITEC-002	[106]0.0406	[102]0.0531	[94]0.0666	[88]0.0935	[91]0.1874
22	COGNITEC-003	[104]0.0400	[98]0.0526	[90]0.0650	[84]0.0895	[84]0.1772
23	COGNITEC-004	[70]0.0222	[70]0.0313	[68]0.0388	[64]0.0540	[32]0.1103
24	CYBERLINK-000	[108]0.0414	[108]0.0565	[105]0.0707	[96]0.1031	[102]0.2050
25	CYBERLINK-001	[100]0.0392	[103]0.0536	[100]0.0695	[93]0.0973	[85]0.1794
26	CYBERLINK-002	[32]0.0105	[35]0.0148	[38]0.0202	[49]0.0399	[48]0.1255
27	CYBERLINK-003	[20]0.0056	[20]0.0077	[19]0.0100	[22]0.0235	[44]0.1237
28	CYBERLINK-004	[19]0.0051	[19]0.0071	[20]0.0102	[18]0.0199	[50]0.1269
29	DAHUA-001	[125]0.0569	[124]0.0727	[113]0.0878	[106]0.1148	[90]0.1867
30	DAHUA-002	[36]0.0108	[36]0.0151	[35]0.0191	[31]0.0291	[39]0.1153
31	DAHUA-003	[30]0.0100	[32]0.0139	[33]0.0180	[32]0.0296	[34]0.1130
32	DEEPGLINT-001	[12]0.0027	[12]0.0033	[12]0.0043	[12]0.0121	[21]0.0922
33	DEEPSEA-001	[92]0.0347	[90]0.0462	[86]0.0586	[82]0.0802	[82]0.1708
34	DERMALOG-005	[140]0.0700	[136]0.0880	[126]0.1144	[123]0.1578	[121]0.2451
35	DERMALOG-006	[101]0.0395	[97]0.0517	[91]0.0659	[92]0.0973	[83]0.1745
36	DERMALOG-007	[137]0.0691	[134]0.0863	[125]0.1107	[119]0.1504	[116]0.2299
37	DERMALOG-008	[88]0.0338	[89]0.0455	[89]0.0626	[97]0.1060	[114]0.2276
38	GORILLA-002	[173]0.1539	[173]0.1880	[149]0.2184	[142]0.2596	[140]0.3398
39	GORILLA-004	[139]0.0699	[139]0.0892	[122]0.1048	[115]0.1370	[99]0.1969
40	GORILLA-005	[116]0.0453	[112]0.0583	[104]0.0704	[94]0.0974	[62]0.1474
41	HIK-003	[145]0.0828	[144]0.1028	[129]0.1202	[122]0.1525	[123]0.2480
42	HIK-004	[143]0.0796	[140]0.0988	[127]0.1147	[118]0.1474	[124]0.2483
43	HIK-005	[81]0.0312	[84]0.0436	[85]0.0560	[86]0.0911	[107]0.2129
44	IDEMIA-003	[90]0.0346	[93]0.0471	[114]0.0892	[144]0.2789	[144]0.4311
45	IDEMIA-004	[80]0.0300	[80]0.0373	[74]0.0447	[69]0.0617	[80]0.1635
46	IDEMIA-005	[95]0.0360	[86]0.0440	[83]0.0537	[81]0.0764	[92]0.1915
47	IDEMIA-006	[93]0.0351	[83]0.0433	[81]0.0525	[78]0.0734	[109]0.2201
48	IDEMIA-007	[43]0.0136	[42]0.0181	[39]0.0228	[42]0.0357	[59]0.1402
49	IDEMIA-008	[5]0.0016	[5]0.0019	[6]0.0024	[4]0.0053	[6]0.0470
50	IMAGUS-005	[44]0.0137	[45]0.0185	[44]0.0237	[43]0.0368	[30]0.1067
51	IMAGUS-006	[45]0.0137	[47]0.0190	[46]0.0244	[47]0.0396	[40]0.1159
52	IMPERIAL-000	[58]0.0187	[58]0.0259	[65]0.0358	[77]0.0733	[86]0.1794
53	INCODE-003	[166]0.1324	[168]0.1672	[147]0.1961	[137]0.2345	[135]0.3123
54	INCODE-004	[105]0.0403	[105]0.0538	[93]0.0662	[87]0.0917	[77]0.1619
55	INTSYSMSU-000	[223]0.9982	[221]0.9984	[163]0.9985	[155]0.9987	[151]0.9988
56	IREX-000	[62]0.0190	[66]0.0280	[69]0.0391	[73]0.0677	[65]0.1479
57	ISYSTEMS-002	[127]0.0584	[127]0.0783	[118]0.0973	[116]0.1373	[115]0.2295
58	ISYSTEMS-003	[115]0.0438	[113]0.0590	[111]0.0807	[108]0.1259	[117]0.2357
59	KAKAO-000	[37]0.0109	[38]0.0151	[37]0.0196	[37]0.0324	[23]0.1010
60	KEDACOM-001	[55]0.0181	[54]0.0227	[48]0.0265	[52]0.0422	[56]0.1340
61	LOOKMAN-003	[91]0.0346	[85]0.0437	[79]0.0514	[76]0.0724	[78]0.1620
62	LOOKMAN-005	[72]0.0240	[68]0.0301	[64]0.0356	[58]0.0512	[55]0.1334
63	MEGVII-001	[123]0.0562	[123]0.0722	[112]0.0872	[112]0.1309	[131]0.2713
64	MICROFOCUS-005	[220]0.9732	[215]0.8354	[160]0.8555	[153]0.8755	[150]0.8954
65	MICROSOFT-003	[64]0.0198	[64]0.0278	[63]0.0356	[63]0.0538	[71]0.1539
66	MICROSOFT-004	[57]0.0185	[59]0.0259	[58]0.0333	[59]0.0517	[69]0.1510
67	MICROSOFT-005	[56]0.0181	[57]0.0256	[57]0.0320	[57]0.0512	[67]0.1491
68	MICROSOFT-006	[28]0.0091	[25]0.0120	[28]0.0162	[33]0.0301	[66]0.1482
69	NEC-000	[131]0.0637	[129]0.0789	[117]0.0933	[107]0.1163	[94]0.1941
70	NEC-001	[146]0.0863	[146]0.1055	[132]0.1249	[121]0.1519	[112]0.2253
71	NEC-002	[9]0.0020	[10]0.0026	[10]0.0033	[14]0.0135	[9]0.0653
72	NEC-003	[10]0.0021	[8]0.0024	[7]0.0028	[6]0.0059	[8]0.0540

Table 14: **Identification-mode: Effect of N on FNIR at high threshold.** *Values are threshold-based miss rates i.e.* FNIR *at* FPIR = *0.001 for five enrollment population sizes, N. The right six columns apply for enrollment of one image. Missing entries usually apply because another algorithm from the same developer was run instead. Some developers are missing because less accurate algorithms were not run on galleries with* $N \geq 3\,000\,000$. *Throughout blue superscripts indicate the rank of the algorithm for that column.*

MISSES BELOW THRESHOLD, T FNIR(N, T> 0, R >L)		ENROL MOST RECENT DATASET: FRVT 2018 MUGSHOTS				
#	ALGORITHM	N=0.64M	N=1.6M	N=3.0M	N=6.0M	N=12.0M
73	NEC-004	[6]0.0017	[2]0.0018	[1]0.0020	[1]0.0037	[1]0.0329
74	NEUROTECHNOLOGY-003	[207]0.5698	[208]0.6362	[158]0.7035	[151]0.7602	[148]0.8224
75	NEUROTECHNOLOGY-004	[118]0.0466	[117]0.0629	[106]0.0779	[104]0.1135	[104]0.2102
76	NEUROTECHNOLOGY-005	[102]0.0396	[106]0.0538	[96]0.0675	[91]0.0950	[98]0.1966
77	NEUROTECHNOLOGY-007	[114]0.0436	[116]0.0623	[108]0.0802	[113]0.1320	[119]0.2393
78	NEUROTECHNOLOGY-008	[89]0.0339	[101]0.0530	[115]0.0893	[128]0.1769	[138]0.3288
79	NTECHLAB-003	[110]0.0421	[104]0.0537	[95]0.0674	[85]0.0907	[75]0.1582
80	NTECHLAB-004	[82]0.0312	[81]0.0405	[80]0.0519	[75]0.0722	[68]0.1503
81	NTECHLAB-005	[86]0.0334	[82]0.0424	[84]0.0537	[80]0.0760	[73]0.1543
82	NTECHLAB-006	[78]0.0288	[76]0.0367	[77]0.0471	[72]0.0670	[70]0.1523
83	NTECHLAB-007	[59]0.0188	[56]0.0256	[55]0.0317	[56]0.0495	[54]0.1306
84	NTECHLAB-008	[34]0.0107	[33]0.0145	[34]0.0187	[29]0.0286	[22]0.0995
85	NTECHLAB-009	[17]0.0037	[17]0.0049	[17]0.0062	[13]0.0125	[14]0.0735
86	NTECHLAB-010	[8]0.0020	[9]0.0025	[8]0.0030	[8]0.0077	[13]0.0710
87	PARAVISION-003	[74]0.0260	[74]0.0351	[75]0.0447	[71]0.0657	[79]0.1630
88	PARAVISION-004	[22]0.0074	[24]0.0101	[24]0.0136	[27]0.0267	[49]0.1256
89	PARAVISION-005	[14]0.0032	[14]0.0041	[14]0.0057	[17]0.0174	[25]0.1037
90	PARAVISION-007	[13]0.0030	[13]0.0040	[13]0.0055	[19]0.0211	[31]0.1097
91	PIXELALL-002	[141]0.0716	[145]0.1052	[139]0.1475	[140]0.2489	[143]0.3904
92	PIXELALL-003	[51]0.0158	[51]0.0218	[54]0.0288	[53]0.0474	[37]0.1138
93	PIXELALL-004	[39]0.0129	[44]0.0183	[47]0.0245	[44]0.0378	[57]0.1375
94	PIXELALL-005	[27]0.0087	[27]0.0121	[30]0.0171	[23]0.0250	[27]0.1052
95	PTAKURATSATU-000	[75]0.0275	[75]0.0366	[76]0.0458	[61]0.0523	[7]0.0523
96	QUANTASOFT-001	[209]0.6387	[209]0.6387	[157]0.6387		[146]0.6387
97	RANKONE-002	[154]0.0973	[149]0.1175	[133]0.1359	[125]0.1718	[129]0.2613
98	RANKONE-003	[153]0.0973	[150]0.1175	[134]0.1359	[126]0.1718	[128]0.2613
99	RANKONE-005	[119]0.0473	[114]0.0592	[102]0.0700	[89]0.0944	[100]0.1998
100	RANKONE-007	[53]0.0168	[53]0.0222	[49]0.0266	[46]0.0381	[35]0.1132
101	RANKONE-009	[40]0.0132	[41]0.0177	[41]0.0230	[39]0.0344	[20]0.0921
102	RANKONE-010	[33]0.0106	[31]0.0136	[31]0.0174	[26]0.0265	[16]0.0785
103	REALNETWORKS-002	[179]0.1943	[178]0.2314	[152]0.2656	[146]0.3134	[137]0.3208
104	REALNETWORKS-003	[165]0.1300	[164]0.1594	[144]0.1858	[135]0.2246	[134]0.3076
105	REALNETWORKS-004	[164]0.1279	[163]0.1581	[143]0.1857	[136]0.2329	[136]0.3179
106	REALNETWORKS-005	[65]0.0202	[62]0.0277	[62]0.0355	[67]0.0560	[60]0.1431
107	REMARKAI-000	[107]0.0406	[109]0.0552	[97]0.0676	[95]0.1028	[101]0.2003
108	RENDIP-000	[25]0.0085	[26]0.0121	[26]0.0156	[28]0.0277	[42]0.1182
109	S1-000	[67]0.0204	[65]0.0279	[67]0.0382	[70]0.0630	[81]0.1707
110	SCANOVATE-000	[120]0.0498	[120]0.0667	[109]0.0804	[99]0.1097	[33]0.1109
111	SCANOVATE-001	[130]0.0630	[130]0.0815	[120]0.0993	[109]0.1292	[97]0.1960
112	SENSETIME-000	[50]0.0158	[49]0.0208	[51]0.0270	[48]0.0398	[43]0.1232
113	SENSETIME-001	[52]0.0161	[52]0.0219	[53]0.0277	[51]0.0420	[52]0.1304
114	SENSETIME-002	[47]0.0146	[34]0.0148	[25]0.0153	[21]0.0234	[10]0.0657
115	SENSETIME-003	[3]0.0016	[4]0.0018	[3]0.0021	[5]0.0054	[4]0.0451
116	SENSETIME-004	[2]0.0015	[1]0.0018	[2]0.0021	[2]0.0040	[2]0.0354
117	SENSETIME-005	[4]0.0016	[7]0.0022	[9]0.0031	[10]0.0089	[5]0.0454
118	SENSETIME-006	[1]0.0014	[3]0.0018	[5]0.0023	[3]0.0047	[3]0.0372
119	SHAMAN-007	[163]0.1212	[159]0.1413	[140]0.1587	[130]0.1879	[122]0.2460
120	SIAT-001	[42]0.0136	[39]0.0176	[42]0.0230	[38]0.0344	[24]0.1035
121	SIAT-002	[49]0.0154	[50]0.0216	[52]0.0273	[50]0.0404	[51]0.1283
122	SYNESIS-003	[121]0.0499	[118]0.0652	[110]0.0804	[98]0.1095	[93]0.1916
123	SYNESIS-003	[205]0.5341	[205]0.5821	[156]0.6113	[150]0.6479	[147]0.6822
124	SYNESIS-005	[54]0.0181	[55]0.0248	[56]0.0319	[60]0.0518	[74]0.1580
125	TECH5-001	[109]0.0420	[109]0.0574	[116]0.0911	[133]0.2106	[142]0.3725
126	TECH5-002	[63]0.0194	[62]0.0269	[61]0.0346	[62]0.0537	[76]0.1607
127	TEVIAN-005	[138]0.0692	[135]0.0873	[123]0.1066	[111]0.1301	[88]0.1840
128	TEVIAN-006	[24]0.0078	[22]0.0098	[22]0.0130	[25]0.0261	[53]0.1305
129	TIGER-002	[133]0.0647	[132]0.0861	[121]0.1036	[114]0.1332	[110]0.2231
130	TOSHIBA-000	[117]0.0460	[115]0.0620	[107]0.0780	[101]0.1117	[103]0.2082
131	TRUEFACE-000	[41]0.0134	[43]0.0182	[45]0.0238	[45]0.0380	[58]0.1385
132	VD-001	[175]0.1642	[175]0.2015	[151]0.2351	[143]0.2736	[139]0.3293
133	VERIDAS-001	[77]0.0278	[79]0.0373	[78]0.0491	[79]0.0753	[72]0.1541
134	VERIDAS-002	[76]0.0278	[78]0.0373	[66]0.0373	[55]0.0491	[15]0.0753
135	VIGILANTSOLUTIONS-008	[48]0.0146	[48]0.0205	[50]0.0269	[54]0.0489	[41]0.1164
136	VISIONLABS-004	[111]0.0427	[110]0.0578	[103]0.0703	[90]0.0949	[89]0.1853
137	VISIONLABS-005	[98]0.0369	[96]0.0502	[88]0.0626	[83]0.0847	[87]0.1815
138	VISIONLABS-006	[60]0.0188	[61]0.0267	[60]0.0336	[66]0.0542	[63]0.1478
139	VISIONLABS-007	[61]0.0188	[60]0.0266	[59]0.0335	[65]0.0540	[64]0.1479
140	VISIONLABS-008	[29]0.0096	[29]0.0131	[29]0.0166	[30]0.0291	[46]0.1247
141	VISIONLABS-009	[15]0.0034	[15]0.0046	[15]0.0060	[15]0.0140	[18]0.0881
142	VISIONLABS-010	[18]0.0038	[18]0.0051	[18]0.0070	[16]0.0149	[19]0.0920
143	VOCORD-005	[160]0.1179	[162]0.1577	[148]0.2183	[145]0.3122	[145]0.4490
144	VTS-001	[31]0.0102	[30]0.0133	[32]0.0175	[35]0.0322	[45]0.1243

Table 15: **Identification-mode: Effect of N on FNIR at high threshold.** *Values are threshold-based miss rates i.e.* FNIR *at* FPIR *= 0.001 for five enrollment population sizes, N. The right six columns apply for enrollment of one image. Missing entries usually apply because another algorithm from the same developer was run instead. Some developers are missing because less accurate algorithms were not run on galleries with $N \geq 3\,000\,000$. Throughout blue superscripts indicate the rank of the algorithm for that column.*

MISSES BELOW THRESHOLD, T		ENROL MOST RECENT				
FNIR(N, T> 0, R >L)		DATASET: FRVT 2018 MUGSHOTS				
#	ALGORITHM	N=0.64M	N=1.6M	N=3.0M	N=6.0M	N=12.0M
145	XFORWARDAI-000	[35]0.0107	[37]0.0151	[36]0.0195	[36]0.0324	[28]0.1057
146	XFORWARDAI-001	[16]0.0037	[16]0.0049	[16]0.0060	[11]0.0120	[17]0.0800
147	XFORWARDAI-002	[11]0.0026	[11]0.0030	[11]0.0035	[9]0.0078	[12]0.0706
148	YITU-002	[38]0.0129	[40]0.0177	[40]0.0228	[40]0.0345	[36]0.1133
149	YITU-003	[46]0.0138	[46]0.0185	[43]0.0236	[41]0.0353	[38]0.1148
150	YITU-004	[21]0.0067	[21]0.0096	[21]0.0129	[20]0.0232	[26]0.1046
151	YITU-005	[23]0.0074	[23]0.0101	[23]0.0135	[24]0.0255	[29]0.1057

Table 16: **Identification-mode: Effect of N on FNIR at high threshold.** *Values are threshold-based miss rates i.e.* FNIR *at* FPIR = *0.001 for five enrollment population sizes, N. The right six columns apply for enrollment of one image. Missing entries usually apply because another algorithm from the same developer was run instead. Some developers are missing because less accurate algorithms were not run on galleries with* $N \geq 3\,000\,000$. *Throughout blue superscripts indicate the rank of the algorithm for that column.*

MISSES AT GIVEN RANK		ENROL MOST RECENT											
FNIR(N, T= 0, R)		RANK 1						RANK 50					
#	ALGORITHM	N=0.64M	N=1.6M	N=3.0M	N=6.0M	N=12.0M	aN^b	N=0.64M	N=1.6M	N=3.0M	N=6.0M	N=12.0M	aN^b
1	3DIVI-005	[164] 0.0137	[162] 0.0176	[139] 0.0210	[134] 0.0253	[132] 0.0302	[107] 0.0004 N^0.271 [114]	[148] 0.0040	[147] 0.0049	[129] 0.0057	[126] 0.0068	[124] 0.0081	[46] 0.0002 N^0.240 [119]
2	ACER-000	[135] 0.0081	[141] 0.0106	[127] 0.0128	[126] 0.0157	[125] 0.0195	[51] 0.0001 N^0.299 [138]	[104] 0.0020	[116] 0.0026	[108] 0.0031	[109] 0.0037	[106] 0.0045	[17] 0.0000 N^0.284 [132]
3	ALCHERA-003	[132] 0.0079	[138] 0.0104	[125] 0.0123	[125] 0.0147	[123] 0.0180	[71] 0.0002 N^0.278 [125]	[130] 0.0027	[129] 0.0032	[114] 0.0035	[112] 0.0042	[107] 0.0048	[50] 0.0002 N^0.199 [109]
4	ALLGOVISION-000	[147] 0.0101	[144] 0.0114	[126] 0.0127	[124] 0.0145	[122] 0.0166	[130] 0.0010 N^0.171 [59]	[167] 0.0063	[161] 0.0067	[134] 0.0071	[129] 0.0075	[123] 0.0081	[135] 0.0020 N^0.086 [68]
5	ALLGOVISION-001	[125] 0.0069	[129] 0.0090	[120] 0.0107	[119] 0.0128	[119] 0.0157	[62] 0.0002 N^0.277 [123]	[119] 0.0023	[119] 0.0027	[109] 0.0031	[105] 0.0036	[103] 0.0043	[39] 0.0001 N^0.211 [114]
6	ANKE-000	[150] 0.0102	[152] 0.0132	[135] 0.0155	[131] 0.0188	[128] 0.0225	[93] 0.0003 N^0.270 [113]	[139] 0.0032	[140] 0.0040	[125] 0.0046	[120] 0.0056	[115] 0.0066	[38] 0.0001 N^0.247 [121]
7	ANKE-002	[68] 0.0024	[67] 0.0028	[67] 0.0032	[64] 0.0037	[60] 0.0043	[56] 0.0002 N^0.203 [70]	[80] 0.0016	[79] 0.0017	[73] 0.0017	[64] 0.0018	[59] 0.0019	[92] 0.0006 N^0.067 [59]
8	AWARE-003	[181] 0.0238	[179] 0.0306	[150] 0.0361	[145] 0.0431	[145] 0.0506	[128] 0.0008 N^0.258 [108]	[161] 0.0055	[162] 0.0075	[144] 0.0092	[140] 0.0113	[142] 0.0143	[28] 0.0001 N^0.323 [142]
9	AWARE-005	[182] 0.0245	[180] 0.0311	[151] 0.0366	[146] 0.0434	[136] 0.0312	[144] 0.0056 N^0.118 [35]	[165] 0.0062	[173] 0.0082	[146] 0.0101	[143] 0.0128	[126] 0.0089	[104] 0.0007 N^0.169 [104]
10	AYONIX-002	[215] 0.2935	[215] 0.3414	[161] 0.3736	[154] 0.4101	[151] 0.4465	[149] 0.0440 N^0.143 [44]	[214] 0.0950	[216] 0.1274	[161] 0.1524	[153] 0.1828	[150] 0.2150	[137] 0.0023 N^0.279 [130]
11	CAMVI-004	[157] 0.0124	[189] 0.0468	[155] 0.0719	[153] 0.2363	[150] 0.2367	[1] 0.0000 N^1.055 [152]	[187] 0.0117	[202] 0.0464	[157] 0.0715	[154] 0.2361	[151] 0.2364	[1] 0.0000 N^1.071 [152]
12	CIB-000	[22] 0.0014	[21] 0.0015	[20] 0.0017	[23] 0.0019	[113] 0.0131	[2] 0.0000 N^0.635 [151]	[31] 0.0012	[27] 0.0012	[25] 0.0012	[25] 0.0012	[138] 0.0122	[2] 0.0000 N^0.647 [151]
13	CLOUDWALK-HR-000	[26] 0.0015	[18] 0.0015	[17] 0.0015	[14] 0.0016	[11] 0.0017	[124] 0.0007 N^0.054 [9]	[68] 0.0014	[53] 0.0014	[45] 0.0014	[42] 0.0014	[30] 0.0014	[125] 0.0012 N^0.012 [11]
14	COGENT-000	[148] 0.0101	[139] 0.0105	[121] 0.0109	[115] 0.0115	[110] 0.0125	[142] 0.0038 N^0.071 [14]	[111] 0.0021	[111] 0.0024	[104] 0.0028	[107] 0.0036	[129] 0.0095	[6] 0.0000 N^0.466 [148]
15	COGENT-001	[149] 0.0101	[140] 0.0105	[122] 0.0109	[114] 0.0115	[111] 0.0125	[141] 0.0038 N^0.071 [13]	[112] 0.0021	[110] 0.0024	[103] 0.0028	[108] 0.0036	[130] 0.0095	[7] 0.0000 N^0.466 [147]
16	COGENT-002	[78] 0.0029	[81] 0.0036	[79] 0.0041	[78] 0.0049	[75] 0.0059	[38] 0.0001 N^0.244 [100]	[64] 0.0014	[70] 0.0015	[67] 0.0017	[68] 0.0019	[70] 0.0021	[51] 0.0002 N^0.144 [98]
17	COGENT-003	[84] 0.0031	[83] 0.0038	[83] 0.0043	[81] 0.0051	[78] 0.0060	[49] 0.0001 N^0.230 [90]	[74] 0.0015	[82] 0.0017	[83] 0.0018	[81] 0.0020	[75] 0.0022	[55] 0.0002 N^0.143 [97]
18	COGENT-004	[40] 0.0018	[40] 0.0020	[40] 0.0022	[39] 0.0025	[34] 0.0028	[77] 0.0002 N^0.159 [53]	[59] 0.0013	[51] 0.0014	[49] 0.0014	[44] 0.0015	[37] 0.0015	[95] 0.0007 N^0.050 [45]
19	COGNITEC-000	[175] 0.0195	[174] 0.0252	[147] 0.0297	[143] 0.0352	[140] 0.0417	[122] 0.0006 N^0.259 [109]	[157] 0.0050	[160] 0.0065	[141] 0.0077	[139] 0.0097	[137] 0.0122	[35] 0.0001 N^0.305 [136]
20	COGNITEC-001	[143] 0.0090	[145] 0.0117	[132] 0.0139	[129] 0.0166	[126] 0.0199	[85] 0.0002 N^0.271 [116]	[135] 0.0030	[134] 0.0034	[122] 0.0040	[119] 0.0046	[111] 0.0054	[49] 0.0002 N^0.207 [113]
21	COGNITEC-002	[108] 0.0048	[106] 0.0057	[100] 0.0067	[96] 0.0079	[97] 0.0094	[78] 0.0002 N^0.232 [92]	[121] 0.0024	[118] 0.0026	[106] 0.0028	[100] 0.0030	[93] 0.0034	[81] 0.0005 N^0.117 [84]
22	COGNITEC-003	[111] 0.0053	[110] 0.0062	[103] 0.0072	[101] 0.0085	[100] 0.0100	[91] 0.0003 N^0.222 [82]	[132] 0.0028	[126] 0.0030	[111] 0.0032	[103] 0.0035	[97] 0.0037	[108] 0.0008 N^0.097 [76]
23	COGNITEC-004	[74] 0.0027	[74] 0.0032	[74] 0.0037	[73] 0.0045	[72] 0.0056	[29] 0.0001 N^0.253 [106]	[58] 0.0013	[55] 0.0014	[55] 0.0015	[57] 0.0017	[54] 0.0019	[59] 0.0002 N^0.123 [89]
24	CYBERLINK-000	[89] 0.0034	[85] 0.0040	[86] 0.0046	[83] 0.0054	[80] 0.0063	[73] 0.0002 N^0.209 [76]	[108] 0.0021	[105] 0.0022	[97] 0.0023	[94] 0.0025	[87] 0.0027	[89] 0.0006 N^0.092 [73]
25	CYBERLINK-001	[81] 0.0030	[79] 0.0035	[81] 0.0042	[80] 0.0050	[77] 0.0060	[39] 0.0001 N^0.243 [99]	[82] 0.0016	[86] 0.0017	[79] 0.0018	[74] 0.0020	[73] 0.0022	[71] 0.0004 N^0.109 [80]
26	CYBERLINK-002	[67] 0.0024	[61] 0.0026	[59] 0.0028	[55] 0.0031	[47] 0.0035	[117] 0.0005 N^0.121 [36]	[105] 0.0020	[100] 0.0021	[93] 0.0021	[88] 0.0022	[76] 0.0022	[122] 0.0012 N^0.036 [31]
27	CYBERLINK-003	[24] 0.0015	[24] 0.0016	[21] 0.0017	[19] 0.0018	[17] 0.0020	[102] 0.0003 N^0.110 [29]	[28] 0.0011	[25] 0.0012	[24] 0.0012	[24] 0.0012	[21] 0.0013	[86] 0.0006 N^0.047 [41]
28	CYBERLINK-004	[32] 0.0016	[27] 0.0017	[26] 0.0018	[20] 0.0019	[19] 0.0021	[118] 0.0005 N^0.085 [21]	[65] 0.0014	[56] 0.0014	[46] 0.0014	[43] 0.0014	[34] 0.0015	[123] 0.0010 N^0.022 [26]
29	DAHUA-001	[112] 0.0053	[114] 0.0067	[107] 0.0079	[106] 0.0093	[104] 0.0112	[64] 0.0002 N^0.256 [107]	[129] 0.0027	[121] 0.0029	[110] 0.0031	[102] 0.0034	[99] 0.0038	[84] 0.0005 N^0.121 [87]
30	DAHUA-002	[36] 0.0017	[34] 0.0018	[34] 0.0021	[31] 0.0023	[28] 0.0027	[72] 0.0002 N^0.156 [47]	[51] 0.0013	[47] 0.0013	[42] 0.0014	[38] 0.0014	[33] 0.0015	[101] 0.0007 N^0.043 [38]
31	DAHUA-003	[7] 0.0010	[10] 0.0012	[11] 0.0014	[13] 0.0016	[15] 0.0018	[20] 0.0001 N^0.199 [69]	[12] 0.0009	[10] 0.0009	[9] 0.0009	[10] 0.0009	[9] 0.0009	[87] 0.0006 N^0.027 [28]
32	DEEPGLINT-001	[20] 0.0014	[16] 0.0014	[16] 0.0015	[15] 0.0016	[14] 0.0018	[111] 0.0004 N^0.089 [22]	[50] 0.0013	[38] 0.0013	[36] 0.0013	[31] 0.0013	[25] 0.0013	[121] 0.0010 N^0.017 [18]
33	DEEPSEA-001	[88] 0.0033	[90] 0.0043	[90] 0.0052	[90] 0.0065	[89] 0.0081	[16] 0.0001 N^0.311 [141]	[44] 0.0012	[50] 0.0014	[59] 0.0015	[59] 0.0017	[60] 0.0020	[42] 0.0001 N^0.157 [102]
34	DERMALOG-005	[156] 0.0114	[156] 0.0149	[137] 0.0201	[139] 0.0289	[143] 0.0447	[6] 0.0000 N^0.470 [150]	[181] 0.0094	[182] 0.0122	[152] 0.0171	[147] 0.0254	[146] 0.0406	[8] 0.0000 N^0.505 [149]
35	DERMALOG-006	[127] 0.0075	[124] 0.0081	[115] 0.0086	[107] 0.0093	[101] 0.0104	[136] 0.0017 N^0.109 [28]	[166] 0.0062	[159] 0.0063	[132] 0.0064	[125] 0.0065	[116] 0.0068	[142] 0.0043 N^0.028 [29]
36	DERMALOG-007	[133] 0.0080	[132] 0.0092	[119] 0.0102	[117] 0.0118	[115] 0.0140	[120] 0.0006 N^0.190 [66]	[159] 0.0051	[153] 0.0054	[128] 0.0056	[121] 0.0058	[114] 0.0063	[136] 0.0020 N^0.068 [60]
37	DERMALOG-008	[66] 0.0024	[68] 0.0029	[69] 0.0034	[68] 0.0040	[68] 0.0048	[33] 0.0001 N^0.239 [97]	[73] 0.0015	[68] 0.0015	[65] 0.0016	[60] 0.0017	[55] 0.0019	[75] 0.0004 N^0.088 [69]
38	GORILLA-002	[166] 0.0147	[168] 0.0197	[143] 0.0238	[138] 0.0288	[137] 0.0351	[95] 0.0003 N^0.295 [134]	[138] 0.0032	[142] 0.0041	[127] 0.0049	[124] 0.0062	[122] 0.0080	[18] 0.0000 N^0.315 [139]
39	GORILLA-004	[109] 0.0048	[111] 0.0063	[105] 0.0075	[105] 0.0091	[106] 0.0114	[34] 0.0001 N^0.292 [132]	[78] 0.0015	[87] 0.0018	[94] 0.0021	[92] 0.0025	[91] 0.0029	[30] 0.0001 N^0.222 [116]
40	GORILLA-005	[71] 0.0026	[73] 0.0032	[76] 0.0038	[75] 0.0046	[73] 0.0056	[18] 0.0001 N^0.271 [118]	[42] 0.0012	[40] 0.0013	[44] 0.0014	[52] 0.0016	[50] 0.0018	[57] 0.0002 N^0.127 [91]
41	HIK-003	[144] 0.0091	[146] 0.0117	[133] 0.0140	[130] 0.0169	[127] 0.0203	[81] 0.0002 N^0.274 [121]	[120] 0.0024	[125] 0.0030	[118] 0.0036	[116] 0.0044	[110] 0.0053	[23] 0.0001 N^0.278 [129]
42	HIK-004	[142] 0.0088	[143] 0.0113	[130] 0.0134	[127] 0.0163	[124] 0.0195	[83] 0.0002 N^0.271 [119]	[123] 0.0024	[122] 0.0030	[115] 0.0035	[113] 0.0042	[109] 0.0052	[29] 0.0001 N^0.259 [126]
43	HIK-005	[94] 0.0036	[95] 0.0046	[93] 0.0053	[89] 0.0065	[88] 0.0081	[31] 0.0001 N^0.274 [120]	[39] 0.0012	[64] 0.0015	[64] 0.0016	[69] 0.0019	[72] 0.0022	[33] 0.0001 N^0.202 [111]
44	IDEMIA-003	[114] 0.0054	[117] 0.0069	[112] 0.0084	[112] 0.0101	[109] 0.0122	[45] 0.0001 N^0.281 [127]	[116] 0.0023	[120] 0.0027	[107] 0.0031	[106] 0.0036	[101] 0.0041	[43] 0.0002 N^0.201 [110]
45	IDEMIA-004	[117] 0.0054	[113] 0.0066	[109] 0.0079	[111] 0.0097	[108] 0.0117	[50] 0.0001 N^0.270 [112]	[97] 0.0018	[101] 0.0021	[100] 0.0025	[99] 0.0030	[96] 0.0036	[27] 0.0001 N^0.241 [120]
46	IDEMIA-005	[121] 0.0064	[123] 0.0081	[117] 0.0097	[116] 0.0118	[116] 0.0143	[53] 0.0002 N^0.277 [124]	[115] 0.0022	[124] 0.0030	[117] 0.0036	[117] 0.0044	[112] 0.0055	[15] 0.0000 N^0.300 [135]
47	IDEMIA-006	[129] 0.0076	[136] 0.0096	[124] 0.0113	[121] 0.0135	[121] 0.0161	[84] 0.0002 N^0.259 [110]	[131] 0.0028	[137] 0.0037	[124] 0.0046	[122] 0.0059	[120] 0.0076	[13] 0.0000 N^0.341 [144]
48	IDEMIA-007	[54] 0.0021	[60] 0.0026	[62] 0.0030	[60] 0.0036	[61] 0.0044	[21] 0.0001 N^0.250 [104]	[25] 0.0011	[29] 0.0012	[30] 0.0012	[34] 0.0014	[36] 0.0015	[60] 0.0002 N^0.110 [82]
49	IDEMIA-008	[5] 0.0010	[6] 0.0011	[6] 0.0011	[6] 0.0013	[6] 0.0014	[69] 0.0002 N^0.121 [37]	[13] 0.0009	[11] 0.0009	[11] 0.0009	[11] 0.0009	[8] 0.0009	[100] 0.0007 N^0.016 [16]
50	IMAGUS-005	[39] 0.0018	[37] 0.0019	[39] 0.0022	[38] 0.0025	[32] 0.0028	[76] 0.0002 N^0.158 [52]	[45] 0.0013	[46] 0.0013	[41] 0.0014	[41] 0.0014	[39] 0.0016	[83] 0.0005 N^0.066 [58]
51	IMAGUS-006	[41] 0.0018	[41] 0.0020	[38] 0.0022	[37] 0.0025	[35] 0.0029	[79] 0.0002 N^0.156 [46]	[63] 0.0014	[59] 0.0014	[54] 0.0015	[45] 0.0015	[42] 0.0016	[99] 0.0007 N^0.049 [44]
52	IMPERIAL-000	[62] 0.0022	[59] 0.0024	[56] 0.0027	[54] 0.0030	[48] 0.0035	[90] 0.0003 N^0.157 [48]	[86] 0.0016	[81] 0.0017	[74] 0.0017	[63] 0.0018	[53] 0.0018	[115] 0.0009 N^0.041 [36]
53	INCODE-003	[146] 0.0098	[151] 0.0129	[134] 0.0154	[132] 0.0191	[129] 0.0233	[68] 0.0002 N^0.296 [135]	[122] 0.0024	[122] 0.0031	[120] 0.0036	[118] 0.0046	[113] 0.0056	[21] 0.0001 N^0.285 [133]
54	INCODE-004	[79] 0.0029	[80] 0.0035	[80] 0.0041	[79] 0.0049	[76] 0.0060	[37] 0.0001 N^0.244 [101]	[95] 0.0018	[90] 0.0019	[89] 0.0020	[84] 0.0021	[74] 0.0022	[91] 0.0006 N^0.077 [64]
55	INTSYSMSU-000	[207] 0.1395	[207] 0.1457	[157] 0.1498	[150] 0.1544	[147] 0.1591	[151] 0.0768 N^0.045 [6]	[216] 0.1098	[214] 0.1163	[160] 0.1206	[152] 0.1252	[149] 0.1296	[151] 0.0519 N^0.056 [51]
56	IREX-000	[101] 0.0043	[91] 0.0044	[84] 0.0044	[74] 0.0046	[67] 0.0048	[138] 0.0028 N^0.032 [4]	[152] 0.0043	[143] 0.0043	[123] 0.0043	[114] 0.0043	[102] 0.0043	[141] 0.0042 N^0.002 [4]
57	ISYSTEMS-002	[113] 0.0053	[112] 0.0064	[104] 0.0072	[100] 0.0083	[98] 0.0096	[105] 0.0003 N^0.204 [72]	[141] 0.0033	[135] 0.0034	[116] 0.0036	[110] 0.0038	[100] 0.0041	[128] 0.0013 N^0.071 [61]
58	ISYSTEMS-003	[104] 0.0046	[101] 0.0052	[94] 0.0057	[91] 0.0066	[86] 0.0076	[112] 0.0004 N^0.174 [61]	[137] 0.0031	[131] 0.0033	[112] 0.0034	[104] 0.0035	[98] 0.0037	[129] 0.0013 N^0.063 [56]
59	KAKAO-000	[15] 0.0013	[17] 0.0015	[19] 0.0016	[22] 0.0019	[23] 0.0022	[32] 0.0001 N^0.192 [68]	[16] 0.0009	[15] 0.0010	[14] 0.0010	[16] 0.0010	[15] 0.0011	[78] 0.0005 N^0.050 [46]
60	KEDACOM-001	[130] 0.0076	[120] 0.0077	[108] 0.0079	[99] 0.0083	[91] 0.0087	[143] 0.0040 N^0.047 [7]	[169] 0.0071	[163] 0.0072	[138] 0.0072	[127] 0.0073	[117] 0.0073	[146] 0.0063 N^0.009 [9]
61	KNERON-000	[107] 0.0048	[107] 0.0059	[101] 0.0067	[97] 0.0079	[96] 0.0093	[82] 0.0002 N^0.226 [87]	[154] 0.0048	[155] 0.0059	[133] 0.0067	[132] 0.0079	[128] 0.0093	[58] 0.0002 N^0.226 [117]
62	LOOKMAN-003	[137] 0.0083	[128] 0.0088	[116] 0.0091	[109] 0.0096	[102] 0.0104	[139] 0.0030 N^0.076 [15]	[172] 0.0072	[166] 0.0074	[140] 0.0075	[130] 0.0076	[121] 0.0077	[144] 0.0054 N^0.022 [25]
63	LOOKMAN-005	[131] 0.0078	[122] 0.0080	[111] 0.0083	[102] 0.0086	[94] 0.0092	[140] 0.0038 N^0.053 [8]	[170] 0.0072	[164] 0.0072	[139] 0.0073	[128] 0.0073	[118] 0.0074	[145] 0.0060 N^0.013 [14]
64	MEGVII-001	[152] 0.0105	[147] 0.0118	[128] 0.0128	[123] 0.0142	[120] 0.0161	[134] 0.0015 N^0.143 [45]	[174] 0.0077	[172] 0.0080	[142] 0.0082	[137] 0.0086	[127] 0.0089	[140] 0.0040 N^0.048 [43]
65	MICROFOCUS-005	[218] 0.3700	[218] 0.4242	[162] 0.4610	[155] 0.5000	[152] 0.5391	[150] 0.0674 N^0.128 [39]	[219] 0.1300	[219] 0.1724	[162] 0.2046	[155] 0.2425	[152] 0.2810	[139] 0.0040 N^0.263 [127]
66	MICROSOFT-003	[14] 0.0013	[25] 0.0016	[27] 0.0018	[30] 0.0022	[33] 0.0028	[12] 0.0000 N^0.271 [117]	[2] 0.0006	[2] 0.0006	[3] 0.0007	[6] 0.0008	[7] 0.0009	[26] 0.0001 N^0.158 [103]
67	MICROSOFT-004	[13] 0.0012	[19] 0.0015	[25] 0.0018	[28] 0.0021	[31] 0.0028	[11] 0.0000 N^0.281 [126]	[1] 0.0006	[1] 0.0006	[1] 0.0007	[1] 0.0007	[4] 0.0009	[36] 0.0001 N^0.139 [95]
68	MICROSOFT-005	[27] 0.0015	[35] 0.0019	[43] 0.0023	[52] 0.0030	[51] 0.0037	[7] 0.0000 N^0.320 [143]	[3] 0.0006	[3] 0.0006	[2] 0.0007	[2] 0.0008	[5] 0.0009	[37] 0.0001 N^0.136 [94]
69	MICROSOFT-006	[29] 0.0016	[39] 0.0020	[49] 0.0025	[53] 0.0030	[55] 0.0038	[10] 0.0000 N^0.305 [139]	[4] 0.0006	[4] 0.0007	[4] 0.0007	[7] 0.0009	[12] 0.0010	[20] 0.0000 N^0.184 [106]
70	NEC-000	[160] 0.0131	[160] 0.0170	[138] 0.0203	[133] 0.0244	[131] 0.0294	[101] 0.0003 N^0.276 [122]	[134] 0.0029	[139] 0.0038	[126] 0.0048	[123] 0.0059	[119] 0.0074	[14] 0.0000 N^0.319 [140]
71	NEC-001	[172] 0.0180	[169] 0.0209	[142] 0.0233	[137] 0.0266	[133] 0.0304	[135] 0.0016 N^0.179 [63]	[185] 0.0109	[178] 0.0113	[147] 0.0116	[141] 0.0121	[139] 0.0129	[143] 0.0051 N^0.056 [50]
72	NEC-002	[3] 0.0009	[5] 0.0010	[5] 0.0011	[5] 0.0012	[5] 0.0013	[75] 0.0002 N^0.113 [33]	[5] 0.0008	[5] 0.0008	[5] 0.0008	[4] 0.0008	[3] 0.0008	[77] 0.0005 N^0.038 [32]

Table 17: **Investigation-mode: Effect of N on FNIR on recent images** *For five enrollment population sizes, N, with T = 0 and FPIR = 1. The left five columns are rank 1 miss rates The right five columns are rank 50 miss rates Missing entries usually apply because another algorithm from the same developer was run instead. Some developers are missing because less accurate algorithms were not run on galleries with $N > 1\,600\,000$. Throughout blue superscripts indicate the rank of the algorithm for that column, and yellow highlighting indicates the most accurate value. Caution: The Power-low models are mostly intended to draw attention to the kind of behavior, not as a model to be used for prediction.*

MISSES AT GIVEN RANK FNIR(N, T= 0, R)		ENROL MOST RECENT											
		RANK 1						RANK 50					
#	ALGORITHM	N=0.64M	N=1.6M	N=3.0M	N=6.0M	N=12.0M	aN^b	N=0.64M	N=1.6M	N=3.0M	N=6.0M	N=12.0M	aN^b
73	NEC-003	[16]0.0013	[13]0.0014	[12]0.0015	[12]0.0016	[9]0.0016	[113]0.0005 $N^{0.079}$ [16]	[37]0.0012	[28]0.0012	[26]0.0012	[23]0.0012	[19]0.0012	[113]0.0009 $N^{0.019}$ [23]
74	NEC-004	[19]0.0014	[15]0.0014	[13]0.0015	[11]0.0016	[10]0.0017	[121]0.0006 $N^{0.059}$ [11]	[48]0.0013	[39]0.0013	[35]0.0013	[33]0.0013	[23]0.0013	[122]0.0010 $N^{0.016}$ [17]
75	NEUROTECHNOLOGY-003	[171]0.0179	[170]0.0225	[144]0.0263	[140]0.0306	[138]0.0361	[127]0.0007 $N^{0.239}$ [98]	[151]0.0042	[154]0.0057	[137]0.0072	[138]0.0090	[136]0.0112	[19]0.0000 $N^{0.334}$ [143]
76	NEUROTECHNOLOGY-004	[105]0.0046	[103]0.0056	[99]0.0064	[95]0.0074	[92]0.0088	[86]0.0002 $N^{0.220}$ [81]	[113]0.0022	[112]0.0025	[105]0.0028	[101]0.0031	[94]0.0034	[62]0.0003 $N^{0.154}$ [100]
77	NEUROTECHNOLOGY-005	[92]0.0035	[89]0.0043	[88]0.0049	[85]0.0057	[81]0.0068	[66]0.0002 $N^{0.223}$ [84]	[110]0.0021	[108]0.0023	[99]0.0024	[95]0.0025	[88]0.0028	[90]0.0006 $N^{0.092}$ [74]
78	NEUROTECHNOLOGY-007	[86]0.0032	[84]0.0039	[85]0.0044	[82]0.0052	[79]0.0062	[58]0.0002 $N^{0.222}$ [83]	[106]0.0020	[103]0.0022	[96]0.0023	[90]0.0024	[82]0.0026	[103]0.0007 $N^{0.076}$ [63]
79	NEUROTECHNOLOGY-008	[43]0.0019	[46]0.0022	[46]0.0025	[49]0.0029	[45]0.0034	[40]0.0001 $N^{0.205}$ [74]	[55]0.0013	[44]0.0013	[40]0.0013	[36]0.0014	[32]0.0015	[102]0.0007 $N^{0.043}$ [37]
80	NTECHLAB-003	[106]0.0046	[108]0.0062	[106]0.0076	[108]0.0094	[105]0.0114	[22]0.0001 $N^{0.310}$ [140]	[54]0.0013	[74]0.0016	[82]0.0018	[87]0.0022	[83]0.0026	[22]0.0001 $N^{0.237}$ [118]
81	NTECHLAB-004	[95]0.0037	[98]0.0048	[95]0.0058	[92]0.0071	[90]0.0085	[24]0.0001 $N^{0.291}$ [131]	[29]0.0011	[49]0.0013	[58]0.0015	[58]0.0017	[68]0.0021	[32]0.0001 $N^{0.198}$ [108]
82	NTECHLAB-005	[90]0.0035	[96]0.0047	[96]0.0058	[93]0.0073	[95]0.0092	[14]0.0000 $N^{0.334}$ [146]	[9]0.0008	[23]0.0011	[28]0.0012	[49]0.0015	[57]0.0019	[9]0.0000 $N^{0.283}$ [131]
83	NTECHLAB-006	[80]0.0030	[88]0.0041	[89]0.0050	[87]0.0062	[87]0.0078	[13]0.0000 $N^{0.326}$ [145]	[6]0.0008	[12]0.0009	[22]0.0011	[27]0.0013	[44]0.0016	[11]0.0000 $N^{0.253}$ [122]
84	NTECHLAB-007	[58]0.0022	[62]0.0027	[63]0.0031	[63]0.0037	[62]0.0044	[26]0.0001 $N^{0.245}$ [102]	[27]0.0011	[31]0.0012	[33]0.0013	[37]0.0014	[38]0.0015	[61]0.0003 $N^{0.109}$ [81]
85	NTECHLAB-008	[23]0.0014	[28]0.0017	[28]0.0020	[35]0.0024	[29]0.0027	[19]0.0001 $N^{0.224}$ [86]	[21]0.0010	[22]0.0010	[20]0.0011	[20]0.0011	[18]0.0012	[73]0.0004 $N^{0.065}$ [57]
86	NTECHLAB-009	[12]0.0012	[12]0.0013	[10]0.0014	[10]0.0015	[13]0.0018	[65]0.0002 $N^{0.140}$ [42]	[17]0.0009	[14]0.0009	[13]0.0010	[14]0.0010	[13]0.0010	[85]0.0005 $N^{0.041}$ [34]
87	NTECHLAB-010	[8]0.0011	[7]0.0011	[7]0.0012	[7]0.0013	[7]0.0014	[97]0.0003 $N^{0.091}$ [24]	[23]0.0010	[20]0.0010	[15]0.0010	[13]0.0010	[11]0.0010	[116]0.0009 $N^{0.005}$ [8]
88	PARAVISION-003	[73]0.0026	[72]0.0031	[71]0.0035	[70]0.0042	[69]0.0048	[54]0.0002 $N^{0.210}$ [77]	[85]0.0016	[85]0.0017	[81]0.0018	[78]0.0020	[69]0.0021	[79]0.0005 $N^{0.089}$ [70]
89	PARAVISION-004	[28]0.0015	[26]0.0016	[24]0.0017	[21]0.0019	[20]0.0021	[103]0.0003 $N^{0.111}$ [30]	[52]0.0013	[42]0.0013	[39]0.0013	[30]0.0013	[28]0.0014	[120]0.0010 $N^{0.020}$ [24]
90	PARAVISION-005	[25]0.0015	[20]0.0015	[18]0.0016	[18]0.0018	[16]0.0019	[110]0.0004 $N^{0.094}$ [25]	[56]0.0013	[45]0.0013	[39]0.0013	[32]0.0013	[26]0.0014	[124]0.0011 $N^{0.015}$ [15]
91	PARAVISION-007	[10]0.0011	[9]0.0012	[9]0.0012	[8]0.0013	[8]0.0015	[99]0.0003 $N^{0.091}$ [23]	[22]0.0010	[19]0.0010	[16]0.0010	[15]0.0010	[14]0.0011	[110]0.0008 $N^{0.018}$ [21]
92	PIXELALL-002	[97]0.0037	[93]0.0045	[91]0.0052	[88]0.0062	[85]0.0075	[52]0.0002 $N^{0.238}$ [96]	[90]0.0017	[96]0.0019	[92]0.0021	[91]0.0024	[85]0.0027	[54]0.0002 $N^{0.154}$ [101]
93	PIXELALL-003	[45]0.0019	[45]0.0021	[45]0.0024	[44]0.0028	[43]0.0032	[59]0.0002 $N^{0.182}$ [65]	[62]0.0014	[57]0.0014	[48]0.0014	[46]0.0015	[40]0.0016	[107]0.0007 $N^{0.045}$ [39]
94	PIXELALL-004	[37]0.0017	[43]0.0020	[42]0.0023	[41]0.0026	[38]0.0030	[47]0.0001 $N^{0.192}$ [67]	[53]0.0013	[48]0.0013	[43]0.0014	[39]0.0014	[35]0.0015	[97]0.0007 $N^{0.046}$ [40]
95	PIXELALL-005	[38]0.0018	[36]0.0019	[29]0.0020	[27]0.0021	[26]0.0024	[115]0.0005 $N^{0.098}$ [26]	[77]0.0015	[73]0.0016	[63]0.0016	[53]0.0016	[45]0.0016	[126]0.0012 $N^{0.018}$ [19]
96	PTAKURATSATU-000	[70]0.0025	[71]0.0030	[73]0.0036	[67]0.0040	[57]0.0040	[94]0.0003 $N^{0.167}$ [56]	[76]0.0015	[75]0.0016	[84]0.0018	[75]0.0020	[63]0.0020	[74]0.0004 $N^{0.096}$ [75]
97	QUANTASOFT-001	[214]0.2177	[211]0.2177	[160]0.2177		[148]0.2177	[152]0.2177 $N^{0.000}$ [1]	[217]0.1116	[213]0.1116	[159]0.1116		[148]0.1116	[152]0.1116 $N^{-0.000}$ [1]
98	RANKONE-002	[168]0.0155	[167]0.0194	[141]0.0224	[135]0.0262	[135]0.0304	[125]0.0007 $N^{0.230}$ [88]	[156]0.0048	[157]0.0060	[135]0.0071	[136]0.0085	[134]0.0102	[45]0.0002 $N^{0.254}$ [124]
99	RANKONE-003	[167]0.0155	[166]0.0194	[140]0.0224	[136]0.0262	[134]0.0304	[126]0.0007 $N^{0.230}$ [89]	[155]0.0048	[158]0.0060	[136]0.0071	[135]0.0085	[133]0.0102	[44]0.0002 $N^{0.254}$ [125]
100	RANKONE-005	[128]0.0075	[134]0.0094	[123]0.0110	[120]0.0132	[118]0.0156	[88]0.0003 $N^{0.251}$ [105]	[128]0.0026	[128]0.0032	[119]0.0036	[115]0.0043	[108]0.0050	[40]0.0001 $N^{0.221}$ [115]
101	RANKONE-007	[77]0.0028	[76]0.0034	[75]0.0038	[72]0.0045	[71]0.0053	[61]0.0002 $N^{0.211}$ [78]	[75]0.0015	[77]0.0017	[77]0.0018	[72]0.0019	[71]0.0021	[64]0.0003 $N^{0.123}$ [88]
102	RANKONE-009	[48]0.0020	[54]0.0024	[55]0.0027	[57]0.0032	[54]0.0038	[36]0.0001 $N^{0.219}$ [80]	[60]0.0013	[54]0.0014	[52]0.0015	[47]0.0015	[41]0.0016	[88]0.0006 $N^{0.059}$ [53]
103	RANKONE-010	[52]0.0020	[48]0.0022	[48]0.0025	[48]0.0029	[44]0.0032	[80]0.0002 $N^{0.164}$ [55]	[70]0.0014	[60]0.0015	[56]0.0015	[51]0.0016	[47]0.0017	[93]0.0006 $N^{0.058}$ [52]
104	REALNETWORKS-002	[186]0.0299	[182]0.0393	[153]0.0470	[148]0.0562	[146]0.0580	[132]0.0013 $N^{0.236}$ [95]	[160]0.0054	[168]0.0076	[145]0.0097	[142]0.0126	[140]0.0132	[31]0.0001 $N^{0.320}$ [141]
105	REALNETWORKS-003	[173]0.0183	[173]0.0242	[146]0.0291	[142]0.0352	[142]0.0423	[109]0.0004 $N^{0.287}$ [130]	[150]0.0041	[151]0.0054	[131]0.0064	[133]0.0080	[132]0.0101	[25]0.0001 $N^{0.307}$ [137]
106	REALNETWORKS-004	[170]0.0175	[171]0.0236	[145]0.0284	[141]0.0347	[139]0.0416	[104]0.0003 $N^{0.295}$ [133]	[147]0.0040	[148]0.0050	[130]0.0061	[131]0.0078	[131]0.0099	[24]0.0001 $N^{0.315}$ [138]
107	REALNETWORKS-005	[49]0.0020	[50]0.0023	[53]0.0026	[51]0.0030	[49]0.0037	[43]0.0001 $N^{0.207}$ [75]	[34]0.0012	[32]0.0012	[34]0.0013	[35]0.0014	[31]0.0015	[72]0.0004 $N^{0.081}$ [65]
108	REMARKAI-000	[75]0.0027	[78]0.0034	[78]0.0040	[77]0.0048	[74]0.0058	[28]0.0001 $N^{0.260}$ [111]	[71]0.0014	[72]0.0015	[66]0.0016	[62]0.0018	[61]0.0020	[66]0.0003 $N^{0.108}$ [78]
109	RENDIP-000	[21]0.0014	[23]0.0015	[23]0.0017	[24]0.0019	[22]0.0022	[60]0.0002 $N^{0.158}$ [50]	[33]0.0012	[30]0.0012	[27]0.0012	[22]0.0012	[20]0.0013	[112]0.0008 $N^{0.025}$ [27]
110	S1-000	[53]0.0021	[56]0.0024	[58]0.0028	[58]0.0032	[53]0.0037	[48]0.0001 $N^{0.203}$ [71]	[72]0.0014	[67]0.0015	[60]0.0015	[55]0.0016	[49]0.0017	[96]0.0007 $N^{0.055}$ [49]
111	SCANOVATE-000	[98]0.0038	[99]0.0050	[97]0.0059	[94]0.0073	[84]0.0073	[63]0.0002 $N^{0.235}$ [94]	[66]0.0014	[71]0.0015	[72]0.0017	[82]0.0020	[66]0.0020	[53]0.0002 $N^{0.142}$ [96]
112	SCANOVATE-001	[100]0.0041	[102]0.0053	[98]0.0064	[98]0.0079	[99]0.0098	[23]0.0001 $N^{0.299}$ [136]	[61]0.0013	[69]0.0015	[71]0.0017	[83]0.0021	[81]0.0024	[34]0.0001 $N^{0.207}$ [112]
113	SENSETIME-000	[59]0.0022	[52]0.0023	[52]0.0026	[47]0.0028	[42]0.0032	[106]0.0003 $N^{0.135}$ [40]	[87]0.0016	[83]0.0017	[78]0.0018	[66]0.0018	[64]0.0020	[105]0.0007 $N^{0.060}$ [54]
114	SENSETIME-001	[57]0.0022	[53]0.0023	[50]0.0025	[50]0.0029	[50]0.0037	[70]0.0002 $N^{0.177}$ [62]	[84]0.0016	[76]0.0016	[70]0.0017	[65]0.0018	[70]0.0024	[63]0.0003 $N^{0.125}$ [90]
115	SENSETIME-002	[163]0.0136	[154]0.0137	[131]0.0137	[122]0.0138	[114]0.0139	[147]0.0124 $N^{0.007}$ [2]	[191]0.0136	[184]0.0136	[149]0.0136	[144]0.0136	[141]0.0136	[148]0.0135 $N^{0.001}$ [3]
116	SENSETIME-003	[6]0.0010	[4]0.0010	[4]0.0010	[4]0.0011	[4]0.0012	[96]0.0003 $N^{0.085}$ [20]	[15]0.0009	[13]0.0009	[12]0.0009	[12]0.0010	[10]0.0010	[109]0.0008 $N^{0.013}$ [13]
117	SENSETIME-004	[4]0.0010	[3]0.0010	[3]0.0010	[3]0.0011	[3]0.0012	[98]0.0003 $N^{0.081}$ [17]	[10]0.0008	[8]0.0009	[8]0.0009	[8]0.0009	[6]0.0009	[94]0.0007 $N^{0.018}$ [22]
118	SENSETIME-005	[2]0.0008	[2]0.0009	[2]0.0009	[2]0.0010	[2]0.0011	[89]0.0003 $N^{0.085}$ [19]	[7]0.0008	[6]0.0008	[6]0.0008	[3]0.0008	[1]0.0008	[111]0.0008 $N^{0.002}$ [5]
119	SENSETIME-006	[1]0.0008	[1]0.0009	[1]0.0009	[1]0.0010	[1]0.0010	[100]0.0003 $N^{0.069}$ [12]	[8]0.0008	[7]0.0008	[7]0.0008	[5]0.0008	[2]0.0008	[98]0.0007 $N^{0.011}$ [10]
120	SHAMAN-007	[190]0.0371	[183]0.0396	[152]0.0416	[147]0.0443	[144]0.0473	[146]0.0122 $N^{0.083}$ [18]	[204]0.0308	[198]0.0314	[155]0.0319	[148]0.0326	[145]0.0337	[149]0.0207 $N^{0.029}$ [30]
121	SIAT-001	[35]0.0017	[30]0.0018	[31]0.0020	[33]0.0023	[30]0.0027	[55]0.0002 $N^{0.173}$ [60]	[24]0.0010	[24]0.0011	[23]0.0012	[26]0.0013	[24]0.0013	[67]0.0003 $N^{0.085}$ [67]
122	SIAT-002	[34]0.0016	[31]0.0018	[33]0.0020	[32]0.0023	[27]0.0027	[57]0.0002 $N^{0.171}$ [58]	[30]0.0011	[33]0.0012	[32]0.0013	[29]0.0013	[27]0.0014	[82]0.0005 $N^{0.062}$ [55]
123	SYNESIS-003	[169]0.0161	[158]0.0162	[136]0.0163	[128]0.0165	[130]0.0254	[137]0.0027 $N^{0.127}$ [38]	[194]0.0160	[189]0.0160	[151]0.0160	[146]0.0160	[144]0.0245	[117]0.0009 $N^{0.192}$ [107]
124	SYNESIS-003	[208]0.1456	[208]0.1700	[158]0.1876	[151]0.2088	[149]0.2317	[148]0.0177 $N^{0.158}$ [51]	[210]0.0828	[210]0.0869	[158]0.0920	[151]0.0998	[147]0.1104	[150]0.0218 $N^{0.098}$ [77]
125	SYNESIS-005	[139]0.0085	[126]0.0085	[114]0.0085	[103]0.0086	[93]0.0088	[145]0.0072 $N^{0.012}$ [3]	[178]0.0085	[174]0.0085	[143]0.0085	[134]0.0085	[125]0.0085	[147]0.0085 $N^{0.000}$ [2]
126	TECH5-001	[85]0.0032	[86]0.0040	[87]0.0047	[84]0.0057	[83]0.0071	[27]0.0001 $N^{0.271}$ [115]	[79]0.0016	[80]0.0017	[80]0.0018	[76]0.0020	[77]0.0023	[65]0.0003 $N^{0.119}$ [85]
127	TECH5-002	[51]0.0020	[63]0.0027	[65]0.0031	[62]0.0037	[66]0.0047	[15]0.0000 $N^{0.285}$ [129]	[14]0.0009	[17]0.0010	[21]0.0011	[21]0.0012	[22]0.0013	[47]0.0002 $N^{0.127}$ [92]
128	TEVIAN-005	[118]0.0056	[119]0.0073	[113]0.0084	[113]0.0105	[112]0.0130	[46]0.0001 $N^{0.283}$ [128]	[103]0.0020	[107]0.0023	[101]0.0025	[97]0.0028	[92]0.0034	[48]0.0002 $N^{0.178}$ [105]
129	TEVIAN-006	[65]0.0023	[57]0.0024	[54]0.0026	[45]0.0028	[41]0.0031	[119]0.0005 $N^{0.106}$ [27]	[81]0.0016	[78]0.0017	[65]0.0017	[61]0.0017	[51]0.0018	[114]0.0009 $N^{0.041}$ [35]
130	TIGER-002	[102]0.0044	[105]0.0056	[102]0.0068	[104]0.0086	[103]0.0105	[25]0.0001 $N^{0.299}$ [137]	[47]0.0013	[65]0.0015	[76]0.0018	[85]0.0021	[84]0.0027	[16]0.0000 $N^{0.253}$ [123]
131	TOSHIBA-000	[91]0.0035	[92]0.0045	[92]0.0052	[86]0.0061	[117]0.0154	[4]0.0000 $N^{0.449}$ [149]	[83]0.0016	[89]0.0018	[87]0.0019	[86]0.0021	[135]0.0105	[3]0.0000 $N^{0.539}$ [150]
132	TRUEFACE-000	[83]0.0031	[73]0.0033	[72]0.0035	[66]0.0039	[59]0.0043	[123]0.0006 $N^{0.115}$ [34]	[125]0.0025	[114]0.0026	[102]0.0026	[96]0.0027	[89]0.0028	[131]0.0015 $N^{0.038}$ [33]
133	VD-001	[180]0.0230	[177]0.0276	[148]0.0315	[144]0.0363	[141]0.0418	[133]0.0015 $N^{0.204}$ [73]	[188]0.0120	[183]0.0130	[150]0.0140	[145]0.0154	[143]0.0170	[138]0.0024 $N^{0.120}$ [86]
134	VERIDAS-001	[64]0.0023	[66]0.0028	[66]0.0032	[65]0.0037	[63]0.0045	[35]0.0001 $N^{0.231}$ [91]	[69]0.0014	[62]0.0015	[57]0.0015	[56]0.0016	[52]0.0018	[76]0.0005 $N^{0.083}$ [66]
135	VERIDAS-002	[63]0.0023	[65]0.0028	[57]0.0028	[56]0.0032	[52]0.0037	[92]0.0003 $N^{0.158}$ [49]	[67]0.0014	[61]0.0015	[51]0.0015	[48]0.0015	[43]0.0016	[106]0.0007 $N^{0.047}$ [42]
136	VIGILANTSOLUTIONS-008	[69]0.0025	[70]0.0029	[70]0.0034	[69]0.0040	[64]0.0047	[44]0.0001 $N^{0.224}$ [85]	[32]0.0012	[36]0.0013	[47]0.0014	[50]0.0015	[48]0.0017	[52]0.0002 $N^{0.130}$ [93]
137	VISIONLABS-004	[60]0.0022	[64]0.0027	[68]0.0032	[71]0.0044	[82]0.0070	[5]0.0000 $N^{0.387}$ [147]	[43]0.0012	[52]0.0014	[69]0.0017	[93]0.0025	[105]0.0045	[4]0.0000 $N^{0.435}$ [146]
138	VISIONLABS-005	[47]0.0020	[55]0.0024	[61]0.0029	[61]0.0037	[70]0.0051	[9]0.0000 $N^{0.322}$ [144]	[41]0.0012	[41]0.0013	[61]0.0016	[73]0.0019	[90]0.0029	[10]0.0000 $N^{0.298}$ [134]
139	VISIONLABS-006	[33]0.0016	[32]0.0018	[41]0.0022	[46]0.0028	[58]0.0041	[8]0.0000 $N^{0.314}$ [142]	[38]0.0012	[37]0.0013	[53]0.0015	[67]0.0019	[86]0.0027	[12]0.0000 $N^{0.275}$ [128]
140	VISIONLABS-007	[31]0.0016	[29]0.0018	[30]0.0020	[34]0.0023	[46]0.0034	[17]0.0001 $N^{0.248}$ [103]	[35]0.0012	[34]0.0012	[31]0.0013	[28]0.0013	[62]0.0020	[41]0.0001 $N^{0.152}$ [99]
141	VISIONLABS-008	[42]0.0019	[42]0.0020	[37]0.0021	[40]0.0025	[39]0.0030	[67]0.0002 $N^{0.169}$ [57]	[88]0.0016	[84]0.0017	[75]0.0017	[77]0.0020	[78]0.0023	[68]0.0003 $N^{0.114}$ [83]
142	VISIONLABS-009	[9]0.0011	[8]0.0011	[8]0.0012	[9]0.0014	[12]0.0017	[41]0.0001 $N^{0.160}$ [54]	[19]0.0010	[16]0.0010	[17]0.0010	[19]0.0011	[29]0.0014	[56]0.0002 $N^{0.109}$ [79]
143	VISIONLABS-010	[18]0.0014	[14]0.0014	[15]0.0015	[16]0.0017	[18]0.0021	[74]0.0002 $N^{0.137}$ [41]	[46]0.0013	[35]0.0013	[38]0.0013	[40]0.0014	[46]0.0017	[70]0.0004 $N^{0.090}$ [72]
144	VOCORD-005	[119]0.0060	[118]0.0070	[110]0.0082	[110]0.0097	[107]0.0117	[87]0.0003 $N^{0.232}$ [93]	[142]0.0033	[136]0.0035	[121]0.0037	[111]0.0040	[104]0.0043	[118]0.0010 $N^{0.090}$ [71]

Table 18: **Investigation-mode: Effect of N on FNIR on recent images** *For five enrollment population sizes, N, with T = 0 and FPIR = 1. The left five columns are rank 1 miss rates The right five columns are rank 50 miss rates Missing entries usually apply because another algorithm from the same developer was run instead. Some developers are missing because less accurate algorithms were not run on galleries with $N > 1\,600\,000$. Throughout blue superscripts indicate the rank of the algorithm for that column, and yellow highlighting indicates the most accurate value. Caution: The Power-low models are mostly intended to draw attention to the kind of behavior, not as a model to be used for prediction.*

MISSES AT GIVEN RANK		ENROL MOST RECENT											
FNIR(N, T= 0, R)		RANK 1						RANK 50					
#	ALGORITHM	N=0.64M	N=1.6M	N=3.0M	N=6.0M	N=12.0M	aN^b	N=0.64M	N=1.6M	N=3.0M	N=6.0M	N=12.0M	aN^b
145	VTS-001	[17] 0.0014	[22] 0.0015	[22] 0.0017	[25] 0.0019	[24] 0.0023	[42] 0.0001 $N^{0.179}$ [64]	[20] 0.0010	[18] 0.0010	[18] 0.0010	[17] 0.0011	[16] 0.0011	[80] 0.0005 $N^{0.051}$ [47]
146	XFORWARDAI-000	[56] 0.0021	[49] 0.0023	[44] 0.0024	[42] 0.0027	[36] 0.0029	[114] 0.0005 $N^{0.111}$ [31]	[101] 0.0019	[95] 0.0019	[88] 0.0019	[79] 0.0020	[65] 0.0020	[130] 0.0015 $N^{0.018}$ [20]
147	XFORWARDAI-001	[50] 0.0020	[44] 0.0020	[35] 0.0021	[29] 0.0022	[25] 0.0024	[129] 0.0009 $N^{0.055}$ [10]	[100] 0.0019	[94] 0.0019	[86] 0.0019	[71] 0.0019	[58] 0.0019	[134] 0.0018 $N^{0.004}$ [7]
148	XFORWARDAI-002	[46] 0.0019	[38] 0.0020	[32] 0.0020	[26] 0.0021	[21] 0.0022	[131] 0.0011 $N^{0.038}$ [5]	[99] 0.0019	[93] 0.0019	[85] 0.0019	[70] 0.0019	[56] 0.0019	[133] 0.0018 $N^{0.003}$ [6]
149	YITU-002	[30] 0.0016	[33] 0.0018	[36] 0.0021	[36] 0.0024	[37] 0.0029	[30] 0.0001 $N^{0.213}$ [79]	[18] 0.0009	[21] 0.0010	[19] 0.0010	[18] 0.0011	[17] 0.0012	[69] 0.0004 $N^{0.073}$ [62]
150	YITU-003	[72] 0.0026	[69] 0.0029	[64] 0.0031	[59] 0.0035	[56] 0.0039	[108] 0.0004 $N^{0.141}$ [43]	[107] 0.0020	[102] 0.0021	[95] 0.0022	[89] 0.0023	[80] 0.0024	[119] 0.0010 $N^{0.054}$ [48]
151	YITU-004	[11] 0.0011	[11] 0.0013	[14] 0.0015	[17] 0.0017	[65] 0.0047	[3] 0.0000 $N^{0.438}$ [148]	[11] 0.0008	[9] 0.0009	[10] 0.0009	[9] 0.0009	[95] 0.0036	[5] 0.0000 $N^{0.395}$ [145]
152	YITU-005	[61] 0.0022	[51] 0.0023	[49] 0.0025	[43] 0.0027	[40] 0.0031	[116] 0.0005 $N^{0.113}$ [32]	[102] 0.0020	[97] 0.0020	[91] 0.0020	[80] 0.0020	[62] 0.0020	[132] 0.0017 $N^{0.012}$ [12]

Table 19: **Investigation-mode: Effect of N on FNIR on recent images** *For five enrollment population sizes, N, with T = 0 and FPIR = 1. The left five columns are rank 1 miss rates The right five columns are rank 50 miss rates Missing entries usually apply because another algorithm from the same developer was run instead. Some developers are missing because less accurate algorithms were not run on galleries with $N > 1\,600\,000$. Throughout blue superscripts indicate the rank of the algorithm for that column, and yellow highlighting indicates the most accurate value. Caution: The Power-low models are mostly intended to draw attention to the kind of behavior, not as a model to be used for prediction.*

MISSES OUTSIDE RANK R		RESOURCE USAGE		ENROL MOST RECENT, N = 1.6M					
FNIR(N, T=0, R)		TEMPLATE		FRVT 2018 MUGSHOTS					
#	ALGORITHM	BYTES	MSEC	R=1	R=5	R=10	R=20	R=50	WORK-10
1	3DIVI-003	[39]512	[120]625	[200]0.0833	[195]0.0444	[195]0.0349	[191]0.0270	[191]0.0191	[196]1.447
2	3DIVI-004	[211]4096	[121]628	[161]0.0175	[154]0.0091	[152]0.0075	[150]0.0061	[146]0.0049	[158]1.092
3	3DIVI-005	[207]4096	[122]653	[162]0.0176	[155]0.0091	[150]0.0074	[149]0.0061	[147]0.0049	[159]1.092
4	3DIVI-006	[47]528	[129]653	[172]0.0240	[179]0.0171	[181]0.0160	[182]0.0154	[187]0.0148	[177]1.162
5	ACER-000	[41]512	[29]201	[141]0.0106	[126]0.0051	[123]0.0041	[122]0.0034	[116]0.0026	[127]1.053
6	ALCHERA-000	[133]2048	[42]263	[157]0.0161	[166]0.0124	[171]0.0117	[176]0.0111	[177]0.0105	[165]1.116
7	ALCHERA-001	[130]2048	[6]66	[226]0.9869	[226]0.9782	[226]0.9735	[226]0.9679	[225]0.9590	[226]9.811
8	ALCHERA-002	[148]2048	[14]115	[201]0.0949	[200]0.0555	[198]0.0443	[198]0.0354	[193]0.0254	[200]1.544
9	ALCHERA-003	[136]2048	[109]548	[138]0.0104	[128]0.0054	[128]0.0045	[128]0.0038	[129]0.0032	[130]1.055
10	ALLGOVISION-000	[112]2048	[81]425	[144]0.0114	[149]0.0084	[155]0.0078	[156]0.0073	[161]0.0067	[149]1.079
11	ALLGOVISION-001	[119]2048	[179]792	[129]0.0090	[124]0.0048	[122]0.0040	[121]0.0033	[119]0.0027	[124]1.048
12	ANKE-000	[186]2072	[83]431	[152]0.0132	[140]0.0073	[140]0.0060	[140]0.0050	[140]0.0040	[145]1.072
13	ANKE-001	[185]2072	[85]433	[153]0.0132	[141]0.0073	[142]0.0061	[141]0.0050	[141]0.0040	[146]1.073
14	ANKE-002	[179]2056	[123]641	[67]0.0028	[68]0.0020	[68]0.0018	[75]0.0018	[79]0.0017	[69]1.019
15	AWARE-003	[187]2076	[161]716	[179]0.0306	[176]0.0162	[173]0.0127	[170]0.0100	[167]0.0075	[178]1.163
16	AWARE-004	[2]92	[157]712	[195]0.0679	[192]0.0348	[189]0.0274	[189]0.0208	[186]0.0145	[192]1.354
17	AWARE-005	[198]3100	[185]827	[180]0.0311	[177]0.0167	[175]0.0134	[172]0.0107	[173]0.0082	[179]1.167
18	AWARE-006	[3]124	[182]818	[197]0.0697	[194]0.0369	[190]0.0288	[190]0.0223	[188]0.0158	[194]1.371
19	AYONIX-000	[74]1036	[1]10	[220]0.4505	[221]0.3540	[221]0.3176	[221]0.2834	[221]0.2381	[221]4.288
20	AYONIX-001	[72]1036	[3]12	[216]0.3414	[215]0.2338	[215]0.1977	[216]0.1652	[215]0.1274	[215]3.226
21	AYONIX-002	[71]1036	[2]11	[215]0.3414	[216]0.2338	[216]0.1977	[215]0.1652	[216]0.1274	[216]3.226
22	CAMVI-003	[64]1024	[154]707	[191]0.0520	[199]0.0517	[200]0.0517	[203]0.0517	[203]0.0517	[198]1.466
23	CAMVI-004	[60]1024	[163]718	[189]0.0468	[197]0.0465	[199]0.0465	[200]0.0464	[202]0.0464	[195]1.419
24	CAMVI-005	[63]1024	[173]769	[194]0.0652	[201]0.0648	[204]0.0648	[205]0.0648	[207]0.0647	[201]1.584
25	CIB-000	[227]8196	[135]674	[21]0.0015	[22]0.0013	[22]0.0012	[25]0.0012	[29]0.0012	[24]1.012
26	CLOUDWALK-HR-000	[144]2048	[213]908	[18]0.0015	[34]0.0014	[38]0.0014	[45]0.0014	[53]0.0014	[31]1.013
27	COGENT-000	[44]525	[110]551	[139]0.0105	[159]0.0096	[164]0.0095	[117]0.0032	[111]0.0024	[156]1.088
28	COGENT-001	[45]525	[111]552	[140]0.0105	[160]0.0096	[165]0.0095	[116]0.0032	[110]0.0024	[155]1.088
29	COGENT-002	[76]1043	[226]987	[81]0.0036	[77]0.0022	[76]0.0020	[73]0.0018	[70]0.0015	[78]1.021
30	COGENT-003	[75]1043	[224]960	[83]0.0038	[87]0.0024	[83]0.0021	[87]0.0019	[82]0.0017	[84]1.023
31	COGENT-004	[175]2053	[222]952	[40]0.0020	[42]0.0016	[44]0.0015	[50]0.0015	[51]0.0014	[41]1.015
32	COGNITEC-000	[169]2052	[19]176	[174]0.0252	[172]0.0136	[170]0.0107	[169]0.0085	[160]0.0065	[173]1.136
33	COGNITEC-001	[174]2052	[30]202	[145]0.0117	[134]0.0062	[134]0.0051	[136]0.0042	[134]0.0034	[134]1.062
34	COGNITEC-002	[170]2052	[35]227	[106]0.0057	[107]0.0037	[108]0.0032	[109]0.0029	[118]0.0026	[107]1.035
35	COGNITEC-003	[162]2052	[52]297	[110]0.0062	[114]0.0040	[116]0.0036	[120]0.0033	[126]0.0030	[113]1.039
36	COGNITEC-004	[171]2052	[26]192	[74]0.0032	[71]0.0020	[63]0.0018	[56]0.0015	[53]0.0014	[72]1.020
37	CYBERLINK-000	[164]2052	[148]699	[85]0.0040	[96]0.0028	[100]0.0026	[102]0.0024	[105]0.0022	[95]1.027
38	CYBERLINK-001	[163]2052	[84]433	[79]0.0035	[83]0.0023	[82]0.0021	[78]0.0018	[86]0.0017	[80]1.022
39	CYBERLINK-002	[222]4140	[169]738	[61]0.0026	[79]0.0023	[88]0.0022	[96]0.0021	[100]0.0021	[76]1.021
40	CYBERLINK-003	[224]6212	[147]696	[24]0.0016	[24]0.0013	[25]0.0013	[24]0.0012	[25]0.0012	[25]1.012
41	CYBERLINK-004	[225]6212	[170]738	[27]0.0017	[37]0.0015	[43]0.0015	[47]0.0014	[56]0.0014	[35]1.014
42	DAHUA-000	[157]2048	[69]378	[133]0.0093	[132]0.0066	[141]0.0061	[147]0.0057	[150]0.0054	[135]1.062
43	DAHUA-001	[111]2048	[65]371	[114]0.0067	[115]0.0040	[114]0.0036	[119]0.0033	[121]0.0029	[115]1.040
44	DAHUA-002	[133]2048	[149]699	[34]0.0018	[36]0.0015	[41]0.0014	[44]0.0014	[47]0.0013	[36]1.014
45	DAHUA-003	[151]2048	[166]725	[10]0.0012	[9]0.0010	[10]0.0009	[10]0.0009	[10]0.0009	[7]1.009
46	DEEPGLINT-001	[210]4096	[139]687	[16]0.0014	[27]0.0014	[29]0.0013	[33]0.0013	[38]0.0013	[27]1.012
47	DEEPSEA-001	[114]2048	[177]780	[90]0.0043	[78]0.0022	[66]0.0018	[62]0.0016	[50]0.0014	[81]1.022
48	DERMALOG-003	[6]128	[33]211	[205]0.1259	[204]0.0744	[203]0.0603	[202]0.0480	[201]0.0347	[204]1.731
49	DERMALOG-004	[4]128	[31]208	[204]0.1251	[203]0.0739	[202]0.0598	[201]0.0475	[200]0.0343	[203]1.727
50	DERMALOG-005	[5]128	[103]532	[156]0.0149	[169]0.0129	[172]0.0125	[178]0.0123	[182]0.0122	[166]1.118
51	DERMALOG-006	[16]256	[100]514	[124]0.0081	[139]0.0069	[143]0.0066	[151]0.0065	[159]0.0063	[137]1.063
52	DERMALOG-007	[7]128	[79]413	[132]0.0092	[138]0.0066	[139]0.0060	[146]0.0057	[153]0.0054	[136]1.062
53	DERMALOG-008	[37]512	[64]370	[68]0.0029	[67]0.0020	[63]0.0018	[65]0.0017	[68]0.0015	[68]1.019
54	EYEDEA-003	[73]1036	[70]385	[199]0.0800	[196]0.0451	[196]0.0362	[192]0.0289	[192]0.0211	[197]1.448
55	F8-001	[139]2048	[196]851	[149]0.0120	[161]0.0105	[168]0.0102	[171]0.0100	[175]0.0099	[161]1.096
56	GLORY-000	[29]418	[15]160	[209]0.1781	[211]0.1391	[211]0.1266	[211]0.1154	[211]0.1007	[210]2.298
57	GLORY-001	[97]1726	[76]405	[206]0.1268	[206]0.0967	[206]0.0869	[207]0.0778	[208]0.0673	[206]1.903
58	GORILLA-001	[188]2156	[17]169	[192]0.0603	[187]0.0304	[186]0.0230	[186]0.0174	[179]0.0117	[187]1.309
59	GORILLA-002	[79]1132	[61]341	[168]0.0197	[156]0.0092	[146]0.0070	[143]0.0054	[142]0.0041	[160]1.096
60	GORILLA-003	[189]2156	[113]563	[181]0.0361	[174]0.0146	[169]0.0106	[163]0.0078	[152]0.0054	[176]1.158
61	GORILLA-004	[190]2192	[72]395	[111]0.0063	[104]0.0032	[101]0.0026	[99]0.0023	[87]0.0018	[104]1.033
62	GORILLA-005	[226]6288	[95]483	[73]0.0032	[58]0.0019	[57]0.0017	[51]0.0015	[40]0.0013	[66]1.018
63	HIK-003	[84]1408	[122]633	[146]0.0117	[133]0.0060	[132]0.0048	[133]0.0039	[125]0.0030	[133]1.061
64	HIK-004	[80]1152	[99]510	[143]0.0113	[131]0.0059	[131]0.0047	[126]0.0037	[122]0.0030	[132]1.060
65	HIK-005	[86]1408	[119]619	[95]0.0046	[88]0.0025	[79]0.0020	[68]0.0017	[64]0.0015	[90]1.025
66	HIK-006	[85]1408	[116]610	[94]0.0046	[89]0.0025	[80]0.0020	[67]0.0017	[63]0.0015	[89]1.025
67	IDEMIA-003	[46]528	[141]689	[117]0.0069	[120]0.0045	[120]0.0039	[123]0.0034	[120]0.0027	[118]1.043
68	IDEMIA-004	[48]528	[133]669	[113]0.0066	[111]0.0038	[109]0.0032	[108]0.0027	[101]0.0021	[109]1.038
69	IDEMIA-005	[28]352	[67]374	[123]0.0081	[118]0.0044	[117]0.0036	[118]0.0032	[124]0.0030	[120]1.044
70	IDEMIA-006	[27]352	[66]373	[136]0.0096	[122]0.0052	[125]0.0042	[132]0.0039	[137]0.0037	[126]1.052
71	IDEMIA-007	[56]860	[181]807	[60]0.0026	[43]0.0016	[37]0.0014	[31]0.0013	[29]0.0012	[47]1.015
72	IDEMIA-008	[26]300	[88]451	[6]0.0011	[7]0.0009	[9]0.0009	[11]0.0009	[11]0.0009	[5]1.009

Table 20: **Rank-based accuracy for the FRVT 2018 mugshot sets**. *In columns 3 and 4 are template size and template generation duration. Thereafter values are rank-based FNIR with T = 0 and FPIR = 1. This is appropriate to investigational uses but not those with higher volumes where candidates from all searches would need review. The next column is a workload statistic, a small value shows an algorithm front-loads mates into the first 10 candidates. Throughout, blue superscripts indicate the rank of the algorithm for that column, and the best value is highlighted in yellow.*

MISSES OUTSIDE RANK R		RESOURCE USAGE		ENROL MOST RECENT, N = 1.6M					
FNIR(N, T=0, R)		TEMPLATE		FRVT 2018 MUGSHOTS					
#	ALGORITHM	BYTES	MSEC	R=1	R=5	R=10	R=20	R=50	WORK-10
73	IMAGUS-002	34 512	7 76	212 0.2203	210 0.1342	209 0.1090	208 0.0871	206 0.0632	211 2.308
74	IMAGUS-003	36 512	5 57	217 0.3559	217 0.2491	217 0.2132	217 0.1791	217 0.1397	217 3.363
75	IMAGUS-005	147 2048	178 788	37 0.0019	44 0.0016	45 0.0015	43 0.0014	46 0.0013	42 1.015
76	IMAGUS-006	113 2048	211 905	41 0.0020	47 0.0016	49 0.0015	52 0.0015	59 0.0014	44 1.015
77	IMPERIAL-000	150 2048	130 654	59 0.0024	60 0.0019	67 0.0018	74 0.0018	81 0.0017	59 1.018
78	INCODE-000	63 1024	24 190	190 0.0489	185 0.0261	185 0.0204	183 0.0160	180 0.0117	185 1.262
79	INCODE-001	110 2048	142 690	150 0.0166	150 0.0084	145 0.0067	144 0.0055	144 0.0043	151 1.086
80	INCODE-002	152 2048	49 291	163 0.0178	153 0.0090	147 0.0070	145 0.0056	145 0.0043	157 1.092
81	INCODE-003	135 2048	150 704	151 0.0129	136 0.0064	135 0.0051	134 0.0040	127 0.0031	139 1.066
82	INCODE-004	125 2048	98 508	80 0.0035	84 0.0024	86 0.0021	90 0.0020	90 0.0019	82 1.023
83	INNOVATRICS-002	50 530	40 255	188 0.0451	190 0.0342	192 0.0322	194 0.0308	196 0.0297	191 1.321
84	INNOVATRICS-003	49 530	39 255	175 0.0263	167 0.0126	163 0.0095	158 0.0074	149 0.0053	170 1.129
85	INNOVATRICS-004	77 1076	77 406	150 0.0123	135 0.0063	133 0.0050	135 0.0040	130 0.0032	138 1.064
86	INNOVATRICS-005	51 538	193 842	58 0.0024	54 0.0018	56 0.0017	61 0.0016	58 0.0014	54 1.017
87	INTSYSMSU-000	123 2048	136 675	207 0.1457	209 0.1320	212 0.1272	212 0.1225	214 0.1163	209 2.203
88	IREX-000	197 3080	228 2379	91 0.0044	116 0.0043	122 0.0043	137 0.0043	143 0.0043	114 1.039
89	ISYSTEMS-002	145 2048	57 316	112 0.0064	117 0.0043	121 0.0039	125 0.0037	135 0.0034	117 1.041
90	ISYSTEMS-003	143 2048	197 856	101 0.0052	112 0.0039	118 0.0036	124 0.0034	131 0.0033	108 1.037
91	KAKAO-000	167 2052	191 840	17 0.0015	16 0.0011	17 0.0011	14 0.0010	15 0.0010	16 1.010
92	KEDACOM-001	25 292	105 537	120 0.0077	142 0.0074	148 0.0073	155 0.0072	163 0.0072	140 1.067
93	KNERON-000	126 2048	102 530	107 0.0059	132 0.0059	138 0.0059	148 0.0059	155 0.0059	128 1.053
94	KNERON-001	146 2048	93 468	178 0.0295	186 0.0295	191 0.0295	193 0.0295	195 0.0295	186 1.266
95	LINE-000	116 2048	94 482	47 0.0022	40 0.0015	35 0.0014	28 0.0013	26 0.0012	40 1.015
96	LOOKMAN-003	24 292	62 342	128 0.0088	146 0.0078	154 0.0076	160 0.0075	166 0.0074	143 1.071
97	LOOKMAN-004	54 548	58 325	130 0.0091	147 0.0079	153 0.0076	159 0.0075	165 0.0073	144 1.072
98	LOOKMAN-005	53 548	101 514	122 0.0080	144 0.0075	151 0.0074	157 0.0073	164 0.0072	141 1.068
99	MEGVII-001	213 4096	126 652	149 0.0118	157 0.0093	157 0.0087	169 0.0084	172 0.0080	152 1.086
100	MEGVII-002	205 4096	131 656	148 0.0118	158 0.0093	159 0.0088	166 0.0084	171 0.0080	153 1.087
101	MICROFOCUS-003	14 256	45 269	224 0.5942	223 0.4692	223 0.4204	223 0.3724	223 0.3095	223 5.361
102	MICROFOCUS-004	17 256	46 270	222 0.5763	222 0.4519	222 0.4026	222 0.3560	222 0.2957	222 5.199
103	MICROFOCUS-005	20 256	44 266	218 0.4242	218 0.3028	218 0.2606	218 0.2209	219 0.1724	218 3.861
104	MICROFOCUS-006	13 256	43 265	219 0.4268	219 0.3049	219 0.2623	220 0.2233	220 0.1746	219 3.880
105	MICROSOFT-003	62 1024	74 404	25 0.0016	11 0.0010	6 0.0009	3 0.0008	2 0.0006	11 1.009
106	MICROSOFT-004	103 2048	175 773	19 0.0015	5 0.0009	1 0.0008	1 0.0007	1 0.0006	9 1.009
107	MICROSOFT-005	61 1024	134 673	35 0.0019	8 0.0010	4 0.0008	2 0.0008	3 0.0006	14 1.010
108	MICROSOFT-006	59 1024	145 695	39 0.0020	17 0.0011	11 0.0010	4 0.0008	4 0.0007	18 1.011
109	NEC-000	196 2592	8 82	160 0.0170	152 0.0086	144 0.0066	142 0.0052	139 0.0038	154 1.087
110	NEC-001	195 2592	9 88	169 0.0209	173 0.0141	174 0.0128	177 0.0119	178 0.0113	172 1.135
111	NEC-002	95 1616	128 653	5 0.0010	3 0.0009	5 0.0008	5 0.0008	5 0.0008	3 1.008
112	NEC-003	96 1712	143 690	13 0.0014	21 0.0012	21 0.0012	27 0.0012	28 0.0012	19 1.011
113	NEC-004	78 1104	225 967	15 0.0014	26 0.0013	30 0.0013	34 0.0013	39 0.0013	26 1.012
114	NEUROTECHNOLOGY-003	159 2048	108 547	170 0.0225	168 0.0126	166 0.0100	164 0.0078	154 0.0057	169 1.125
115	NEUROTECHNOLOGY-004	158 2048	107 543	103 0.0056	106 0.0036	112 0.0032	113 0.0029	112 0.0025	106 1.035
116	NEUROTECHNOLOGY-005	18 256	78 412	89 0.0043	98 0.0029	102 0.0027	103 0.0024	108 0.0023	98 1.028
117	NEUROTECHNOLOGY-006	21 256	171 746	164 0.0180	148 0.0079	137 0.0059	138 0.0046	132 0.0033	150 1.083
118	NEUROTECHNOLOGY-007	19 256	18 169	84 0.0039	93 0.0027	98 0.0025	100 0.0023	103 0.0022	91 1.026
119	NEUROTECHNOLOGY-008	43 514	180 804	46 0.0022	38 0.0015	40 0.0014	41 0.0014	44 0.0013	39 1.015
120	NEWLAND-002	105 2048	201 868	198 0.0786	198 0.0480	197 0.0397	197 0.0332	194 0.0263	199 1.468
121	NOBLIS-001	154 2048	32 211	214 0.2492	214 0.1772	214 0.1542	214 0.1339	212 0.1112	214 2.679
122	NOBLIS-002	223 6144	104 535	210 0.1794	207 0.1108	207 0.0903	206 0.0722	205 0.0535	207 2.077
123	NTECHLAB-003	201 3484	187 831	108 0.0062	100 0.0029	95 0.0023	88 0.0019	74 0.0016	103 1.030
124	NTECHLAB-004	200 3484	216 929	98 0.0048	81 0.0023	70 0.0019	64 0.0016	49 0.0013	87 1.024
125	NTECHLAB-005	100 1940	162 717	96 0.0047	76 0.0022	61 0.0017	36 0.0013	23 0.0011	83 1.023
126	NTECHLAB-006	101 1940	192 841	80 0.0041	59 0.0019	46 0.0015	21 0.0012	12 0.0009	71 1.019
127	NTECHLAB-007	199 3348	189 834	62 0.0027	48 0.0017	39 0.0014	39 0.0013	31 0.0012	50 1.016
128	NTECHLAB-008	82 1300	112 562	28 0.0017	19 0.0012	20 0.0012	20 0.0011	22 0.0010	20 1.012
129	NTECHLAB-009	83 1300	210 900	12 0.0013	14 0.0011	15 0.0010	13 0.0010	14 0.0009	15 1.010
130	NTECHLAB-010	81 1280	204 875	7 0.0011	12 0.0010	13 0.0010	15 0.0010	20 0.0010	10 1.009
131	PARAVISION-000	142 2048	87 438	165 0.0188	178 0.0171	183 0.0167	185 0.0165	190 0.0164	175 1.156
132	PARAVISION-001	137 2048	114 590	82 0.0038	86 0.0024	87 0.0022	93 0.0020	91 0.0019	85 1.023
133	PARAVISION-002	141 2048	68 377	87 0.0040	90 0.0025	93 0.0022	95 0.0021	92 0.0019	88 1.025
134	PARAVISION-003	122 2048	168 735	72 0.0031	75 0.0022	81 0.0020	84 0.0019	85 0.0017	75 1.021
135	PARAVISION-004	209 4096	163 720	26 0.0016	29 0.0014	33 0.0013	37 0.0013	42 0.0013	29 1.013
136	PARAVISION-005	204 4096	198 858	20 0.0015	28 0.0014	31 0.0013	38 0.0013	45 0.0013	28 1.013
137	PARAVISION-007	203 4096	153 706	9 0.0012	15 0.0011	16 0.0010	17 0.0010	19 0.0010	13 1.010
138	PIXELALL-002	194 2560	27 198	93 0.0045	99 0.0029	99 0.0025	98 0.0022	96 0.0019	99 1.028
139	PIXELALL-003	193 2560	164 719	45 0.0021	45 0.0016	48 0.0015	48 0.0014	57 0.0014	46 1.015
140	PIXELALL-004	191 2560	89 453	43 0.0020	39 0.0015	42 0.0015	46 0.0014	48 0.0013	38 1.014
141	PIXELALL-005	192 2560	195 845	36 0.0019	49 0.0017	52 0.0016	63 0.0016	73 0.0016	45 1.015
142	PTAKURATSATU-000	52 538	215 910	71 0.0030	74 0.0021	75 0.0019	71 0.0018	75 0.0016	73 1.020
143	QUANTASOFT-001	138 2048	73 396	211 0.2177	213 0.1643	213 0.1468	213 0.1312	213 0.1116	213 2.539
144	RANKONE-002	9 133	12 113	167 0.0194	163 0.0112	162 0.0093	161 0.0077	157 0.0060	162 1.111

Table 21: **Rank-based accuracy for the FRVT 2018 mugshot sets**. *In columns 3 and 4 are template size and template generation duration. Thereafter values are rank-based FNIR with T = 0 and FPIR = 1. This is appropriate to investigational uses but not those with higher volumes where candidates from all searches would need review. The next column is a workload statistic, a small value shows an algorithm front-loads mates into the first 10 candidates. Throughout, blue superscripts indicate the rank of the algorithm for that column, and the best value is highlighted in yellow.*

MISSES OUTSIDE RANK R		RESOURCE USAGE		ENROL MOST RECENT, N = 1.6M					
FNIR(N, T=0, R)		TEMPLATE		FRVT 2018 MUGSHOTS					
#	ALGORITHM	BYTES	MSEC	R=1	R=5	R=10	R=20	R=50	WORK-10
145	RANKONE-003	8 133	13 114	166 0.0194	162 0.0112	161 0.0093	162 0.0077	158 0.0060	163 1.111
146	RANKONE-004	1 85	4 36	187 0.0415	184 0.0226	184 0.0177	180 0.0141	176 0.0102	184 1.225
147	RANKONE-005	10 133	10 94	134 0.0094	129 0.0054	129 0.0046	131 0.0039	128 0.0032	129 1.054
148	RANKONE-006	11 165	41 261	100 0.0050	103 0.0030	103 0.0027	101 0.0024	99 0.0021	102 1.030
149	RANKONE-007	12 165	48 278	76 0.0034	82 0.0023	84 0.0021	80 0.0018	77 0.0017	79 1.022
150	RANKONE-009	22 260	25 191	54 0.0024	46 0.0016	50 0.0015	53 0.0015	54 0.0014	48 1.015
151	RANKONE-010	23 261	28 200	48 0.0022	52 0.0018	54 0.0016	58 0.0015	60 0.0015	51 1.016
152	REALNETWORKS-000	214 4100	37 244	186 0.0402	183 0.0195	179 0.0149	174 0.0111	169 0.0077	182 1.201
153	REALNETWORKS-001	215 4104	36 243	185 0.0402	182 0.0195	178 0.0149	175 0.0111	170 0.0077	183 1.201
154	REALNETWORKS-002	219 4104	38 245	182 0.0393	181 0.0189	177 0.0142	173 0.0108	168 0.0076	181 1.195
155	REALNETWORKS-003	98 1848	20 178	173 0.0242	165 0.0117	160 0.0090	154 0.0070	151 0.0054	167 1.120
156	REALNETWORKS-004	99 1848	21 185	171 0.0236	164 0.0112	158 0.0087	152 0.0068	148 0.0050	164 1.116
157	REALNETWORKS-005	178 2056	60 337	50 0.0023	41 0.0016	36 0.0014	40 0.0013	32 0.0012	43 1.015
158	REMARKAI-000	118 2048	144 691	78 0.0034	73 0.0021	69 0.0019	66 0.0017	72 0.0015	74 1.020
159	REMARKAI-000	153 2048	117 615	127 0.0086	119 0.0044	115 0.0036	115 0.0031	113 0.0025	121 1.045
160	REMARKAI-002	156 2048	86 434	125 0.0081	113 0.0040	107 0.0031	104 0.0026	98 0.0021	116 1.041
161	RENDIP-000	117 2048	208 894	23 0.0015	23 0.0013	23 0.0012	26 0.0012	30 0.0012	23 1.012
162	S1-000	206 4096	200 865	56 0.0024	51 0.0018	55 0.0017	60 0.0016	67 0.0015	53 1.017
163	SCANOVATE-000	124 2048	158 712	99 0.0050	92 0.0026	89 0.0022	77 0.0018	71 0.0015	94 1.026
164	SCANOVATE-001	134 2048	137 675	102 0.0053	94 0.0027	92 0.0022	79 0.0018	69 0.0015	97 1.028
165	SENSETIME-000	218 4104	160 715	52 0.0023	69 0.0020	73 0.0019	76 0.0018	83 0.0017	64 1.018
166	SENSETIME-001	216 4104	132 656	53 0.0023	66 0.0020	71 0.0019	70 0.0017	76 0.0016	62 1.018
167	SENSETIME-002	176 2056	125 650	154 0.0137	171 0.0136	176 0.0136	179 0.0136	184 0.0136	168 1.122
168	SENSETIME-003	177 2056	220 940	4 0.0010	10 0.0010	12 0.0010	12 0.0009	13 0.0009	6 1.009
169	SENSETIME-004	70 1032	156 710	3 0.0010	4 0.0009	7 0.0009	8 0.0009	8 0.0009	4 1.008
170	SENSETIME-005	69 1032	227 1007	2 0.0009	1 0.0008	2 0.0008	6 0.0008	6 0.0008	1 1.008
171	SENSETIME-006	68 1032	223 956	1 0.0009	2 0.0008	3 0.0008	7 0.0008	7 0.0008	2 1.008
172	SHAMAN-003	132 2048	151 704	202 0.1243	205 0.0823	205 0.0708	204 0.0616	204 0.0518	205 1.789
173	SHAMAN-004	127 2048	124 642	213 0.2221	212 0.1473	210 0.1241	210 0.1049	209 0.0825	212 2.411
174	SHAMAN-006	128 2048	152 706	184 0.0398	191 0.0344	194 0.0332	196 0.0323	199 0.0315	190 1.316
175	SHAMAN-007	109 2048	155 709	183 0.0396	189 0.0342	193 0.0331	195 0.0322	198 0.0314	188 1.315
176	SIAT-001	160 2052	194 842	30 0.0018	31 0.0014	26 0.0013	22 0.0012	24 0.0011	30 1.013
177	SIAT-002	172 2052	212 906	31 0.0018	30 0.0014	32 0.0013	32 0.0013	33 0.0012	33 1.013
178	SMILART-004	30 512	16 167	225 0.9648	225 0.9641	225 0.9640	225 0.9639	226 0.9638	225 9.678
179	SMILART-005	129 2048	92 464						227 10.000
180	SYNESIS-003	107 2048	34 215	158 0.0162	175 0.0160	180 0.0160	184 0.0160	189 0.0160	174 1.144
181	SYNESIS-003	212 4096	11 103	208 0.1700	208 0.1172	208 0.1047	209 0.0953	210 0.0869	208 2.120
182	SYNESIS-005	217 4104	174 772	126 0.0085	151 0.0085	156 0.0085	168 0.0085	174 0.0085	148 1.076
183	TECH5-001	87 1536	209 898	86 0.0040	85 0.0024	85 0.0021	81 0.0018	80 0.0017	86 1.024
184	TECH5-002	42 513	221 941	63 0.0027	33 0.0014	24 0.0012	21 0.0011	17 0.0010	37 1.014
185	TEVIAN-003	140 2048	54 300	153 0.0147	143 0.0074	136 0.0059	139 0.0047	138 0.0037	149 1.075
186	TEVIAN-004	121 2048	53 299	142 0.0113	130 0.0057	130 0.0047	127 0.0037	123 0.0030	131 1.058
187	TEVIAN-005	108 2048	80 416	119 0.0073	110 0.0038	106 0.0031	107 0.0027	107 0.0023	112 1.038
188	TEVIAN-006	67 1032	115 599	57 0.0024	55 0.0018	62 0.0018	69 0.0017	78 0.0017	53 1.017
189	TIGER-000	166 2052	82 428	193 0.0616	188 0.0310	182 0.0236	187 0.0178	181 0.0120	189 1.315
190	TIGER-002	165 2052	90 464	105 0.0056	101 0.0029	97 0.0024	83 0.0019	65 0.0015	100 1.030
191	TIGER-003	161 2052	91 464	104 0.0056	102 0.0029	96 0.0024	82 0.0019	66 0.0015	101 1.030
192	TONGYITRANS-000	181 2070	23 190	115 0.0069	108 0.0038	111 0.0032	112 0.0029	117 0.0026	110 1.038
193	TONGYITRANS-001	184 2070	22 189	116 0.0069	109 0.0038	110 0.0032	111 0.0029	115 0.0026	111 1.038
194	TOSHIBA-000	94 1548	217 930	92 0.0045	91 0.0026	91 0.0022	92 0.0020	89 0.0018	92 1.026
195	TOSHIBA-001	180 2060	218 931	97 0.0048	95 0.0027	94 0.0023	94 0.0020	88 0.0018	96 1.027
196	TRUEFACE-000	102 2000	63 365	75 0.0033	97 0.0028	104 0.0028	106 0.0026	114 0.0026	93 1.026
197	VD-000	66 1028	59 337	221 0.4737	220 0.3204	220 0.2695	219 0.2215	218 0.1678	220 4.058
198	VD-001	173 2052	146 695	177 0.0276	180 0.0181	182 0.0162	181 0.0146	183 0.0130	180 1.174
199	VD-002	168 2052	140 689	135 0.0095	145 0.0077	149 0.0073	153 0.0070	162 0.0068	142 1.071
200	VERIDAS-001	120 2048	205 885	66 0.0028	63 0.0019	59 0.0017	59 0.0015	62 0.0015	63 1.018
201	VERIDAS-002	106 2048	206 888	65 0.0028	62 0.0019	58 0.0017	57 0.0015	61 0.0015	61 1.018
202	VIGILANTSOLUTIONS-003	93 1544	188 832	196 0.0694	193 0.0349	188 0.0262	188 0.0201	185 0.0140	193 1.355
203	VIGILANTSOLUTIONS-004	91 1544	186 830	203 0.1249	202 0.0706	201 0.0557	199 0.0434	197 0.0305	203 1.699
204	VIGILANTSOLUTIONS-005	90 1544	176 778	131 0.0092	121 0.0045	113 0.0036	110 0.0029	104 0.0022	122 1.046
205	VIGILANTSOLUTIONS-006	92 1544	190 834	137 0.0099	123 0.0048	119 0.0038	114 0.0030	106 0.0022	125 1.049
206	VIGILANTSOLUTIONS-007	89 1544	118 618	77 0.0034	65 0.0020	60 0.0017	55 0.0015	43 0.0013	70 1.019
207	VIGILANTSOLUTIONS-008	88 1544	75 405	70 0.0029	57 0.0018	51 0.0016	49 0.0015	36 0.0013	60 1.018
208	VISIONLABS-004	15 256	56 315	64 0.0027	53 0.0018	53 0.0016	54 0.0015	52 0.0014	57 1.017
209	VISIONLABS-005	38 512	55 300	55 0.0024	50 0.0017	47 0.0015	42 0.0014	41 0.0013	49 1.016
210	VISIONLABS-006	32 512	50 292	32 0.0018	35 0.0015	34 0.0014	35 0.0013	37 0.0013	34 1.014
211	VISIONLABS-007	33 512	51 293	29 0.0018	32 0.0014	28 0.0013	29 0.0013	34 0.0012	32 1.013
212	VISIONLABS-008	35 512	47 277	42 0.0020	56 0.0018	64 0.0018	72 0.0018	84 0.0017	52 1.017
213	VISIONLABS-009	31 512	97 494	8 0.0011	13 0.0011	14 0.0010	16 0.0010	16 0.0010	12 1.010
214	VISIONLABS-010	40 512	167 732	14 0.0014	25 0.0013	27 0.0013	30 0.0013	35 0.0013	23 1.012
215	VOCORD-003	58 896	159 714	109 0.0062	105 0.0035	105 0.0030	105 0.0026	109 0.0023	105 1.035
216	VOCORD-004	57 896	106 538	121 0.0079	125 0.0049	126 0.0043	130 0.0038	133 0.0034	123 1.048

Table 22: **Rank-based accuracy for the FRVT 2018 mugshot sets**. *In columns 3 and 4 are template size and template generation duration. Thereafter values are rank-based FNIR with T = 0 and FPIR = 1. This is appropriate to investigational uses but not those with higher volumes where candidates from all searches would need review. The next column is a workload statistic, a small value shows an algorithm front-loads mates into the first 10 candidates. Throughout, blue superscripts indicate the rank of the algorithm for that column, and the best value is highlighted in yellow.*

MISSES OUTSIDE RANK R		RESOURCE USAGE		ENROL MOST RECENT, N = 1.6M					
FNIR(N, T=0, R)		TEMPLATE		FRVT 2018 MUGSHOTS					
#	ALGORITHM	BYTES	MSEC	R=1	R=5	R=10	R=20	R=50	WORK-10
217	VOCORD-005	[55] 768	[183] 822	[118] 0.0070	[122] 0.0046	[124] 0.0041	[129] 0.0038	[136] 0.0035	[119] 1.044
218	VOCORD-006	[228] 10240	[184] 825	[227] 1.0000	[227] 1.0000	[227] 1.0000	[227] 1.0000	[227] 1.0000	[228] 10.000
219	VTS-000	[149] 2048	[96] 492	[223] 0.5937	[224] 0.5936	[224] 0.5936	[224] 0.5936	[224] 0.5936	[224] 6.343
220	VTS-001	[131] 2048	[207] 891	[22] 0.0015	[18] 0.0012	[18] 0.0011	[18] 0.0011	[18] 0.0010	[17] 1.011
221	XFORWARDAI-000	[104] 2048	[172] 768	[49] 0.0023	[70] 0.0020	[77] 0.0020	[89] 0.0019	[95] 0.0019	[65] 1.018
222	XFORWARDAI-001	[115] 2048	[138] 681	[44] 0.0020	[64] 0.0019	[74] 0.0019	[86] 0.0019	[93] 0.0019	[58] 1.018
223	XFORWARDAI-002	[208] 4096	[219] 935	[38] 0.0020	[61] 0.0019	[72] 0.0019	[85] 0.0019	[93] 0.0019	[56] 1.017
224	YISHENG-001	[202] 3704	[71] 387	[126] 0.0265	[170] 0.0130	[167] 0.0102	[165] 0.0080	[156] 0.0059	[171] 1.134
225	YITU-002	[221] 4138	[202] 870	[33] 0.0018	[20] 0.0012	[19] 0.0011	[19] 0.0011	[21] 0.0010	[21] 1.012
226	YITU-003	[220] 4138	[203] 871	[69] 0.0029	[80] 0.0023	[90] 0.0022	[97] 0.0021	[102] 0.0021	[77] 1.021
227	YITU-004	[183] 2070	[214] 910	[11] 0.0013	[6] 0.0009	[8] 0.0009	[9] 0.0009	[9] 0.0009	[8] 1.009
228	YITU-005	[182] 2070	[199] 861	[51] 0.0023	[72] 0.0021	[78] 0.0020	[91] 0.0020	[92] 0.0020	[67] 1.019

Table 23: **Rank-based accuracy for the FRVT 2018 mugshot sets**. *In columns 3 and 4 are template size and template generation duration. Thereafter values are rank-based FNIR with T = 0 and FPIR = 1. This is appropriate to investigational uses but not those with higher volumes where candidates from all searches would need review. The next column is a workload statistic, a small value shows an algorithm front-loads mates into the first 10 candidates. Throughout, blue superscripts indicate the rank of the algorithm for that column, and the best value is highlighted in yellow.*

MISSES BELOW THRESHOLD, T		ENROL RECENT MUGSHOT, N = 1.6M									ENROL APPLICATION PORTRAIT, N = 1.6M				
ENROL		DATASET: MUGSHOT			DATASET: MUGSHOT			DATASET: MUGSHOT			DATASET: VISA		DATASET: BORDER		DATASET: VISA
PROBE		DATASET: MUGSHOT			DATASET: WEBCAM			DATASET: PROFILE			DATASET: BORDER		DATASET: BORDER 10+YR		DATASET: KIOSK
#	ALGORITHM	FPIR=0.0003	FPIR=0.001	FPIR=0.0003	FPIR=0.001	FPIR=0.001	FPIR=0.01	FPIR=0.001	FPIR=0.01	FPIR=0.001	FPIR=0.01	FPIR=0.001	FPIR=0.01		
1	3DIVI-003	[184]0.482	[196]0.400	[187]0.685	[196]0.626	[198]0.497			[130]0.605	[130]0.445			[108]0.821	[119]0.717	
2	3DIVI-004	[158]0.256	[170]0.169	[160]0.400	[177]0.343	[180]0.237			[113]0.277	[115]0.172			[88]0.607	[101]0.485	
3	3DIVI-005	[157]0.255	[167]0.166	[159]0.395	[175]0.339	[179]0.234	[104]0.996	[110]0.990	[135]0.864	[137]0.846			[87]0.597	[100]0.484	
4	3DIVI-006	[156]0.253	[169]0.168	[163]0.403	[176]0.342	[181]0.238			[114]0.283	[116]0.174			[91]0.615	[102]0.490	
5	ACER-000	[146]0.208	[160]0.146	[145]0.300	[155]0.246	[155]0.157	[66]0.981	[77]0.955	[108]0.201	[111]0.114			[76]0.490	[88]0.363	
6	ALCHERA-000	[151]0.231	[157]0.138	[135]0.259	[143]0.216	[149]0.146	[119]0.999	[136]0.996	[105]0.176	[109]0.111			[104]0.803	[97]0.456	
7	ALCHERA-001	[223]1.000	[223]0.999	[220]1.000	[217]1.000	[218]1.000			[150]1.000	[215]1.000			[167]1.000	[158]1.000	
8	ALCHERA-002	[203]0.807	[203]0.486	[186]0.685	[193]0.591	[193]0.442	[140]1.000	[155]0.999	[134]0.827	[134]0.770			[105]0.811	[116]0.705	
9	ALCHERA-003	[179]0.450	[161]0.155	[146]0.304	[152]0.239	[154]0.152	[128]0.999	[141]0.997	[104]0.172	[103]0.097			[73]0.464	[87]0.362	
10	ALLGOVISION-000	[113]0.138	[137]0.088	[123]0.202	[132]0.166	[138]0.106	[81]0.990	[100]0.982	[89]0.117	[93]0.066			[82]0.526	[95]0.396	
11	ALLGOVISION-001	[122]0.155	[143]0.102	[139]0.275	[146]0.221	[148]0.141	[72]0.986	[66]0.933	[99]0.150	[99]0.081			[77]0.491	[94]0.389	
12	ANKE-000	[133]0.184	[147]0.117	[133]0.256	[145]0.220	[152]0.151	[86]0.994	[108]0.990	[174]1.000	[194]1.000			[159]1.000	[164]1.000	
13	ANKE-001	[131]0.183	[151]0.119	[134]0.256	[144]0.220	[153]0.151	[91]0.994	[119]0.992	[146]1.000	[208]1.000			[173]1.000	[155]1.000	
14	ANKE-002	[66]0.062	[71]0.032	[56]0.103	[60]0.079	[62]0.050	[43]0.948	[48]0.795	[46]0.034	[48]0.018			[37]0.245	[47]0.190	
15	AWARE-003	[130]0.174	[155]0.128	[155]0.351	[169]0.298	[173]0.204	[70]0.984	[95]0.977	[122]0.428	[124]0.378			[83]0.530	[96]0.443	
16	AWARE-004	[171]0.355	[183]0.269	[180]0.619	[189]0.509	[191]0.375	[144]1.000	[157]0.999	[119]0.397	[120]0.279			[106]0.816	[111]0.631	
17	AWARE-005	[193]0.608	[191]0.364	[150]0.342	[156]0.253	[157]0.163	[146]1.000	[156]0.999	[112]0.255	[113]0.122			[115]0.916	[118]0.714	
18	AWARE-006	[183]0.475	[184]0.276	[171]0.466	[180]0.398	[184]0.283	[137]0.999	[152]0.999	[117]0.368	[118]0.254			[98]0.749	[108]0.623	
19	AYONIX-000	[206]0.846	[212]0.811	[203]0.956	[211]0.939	[213]0.892	[109]0.998	[133]0.995	[139]0.954	[139]0.891			[125]0.982	[133]0.959	
20	AYONIX-001	[207]0.875	[214]0.824	[198]0.946	[206]0.920	[209]0.845	[133]0.999	[137]0.996	[143]0.999	[143]0.998			[122]0.969	[129]0.926	
21	AYONIX-002	[208]0.876	[213]0.824	[199]0.946	[207]0.920	[208]0.845	[135]0.999	[138]0.996	[136]0.915	[135]0.821			[123]0.969	[130]0.926	
22	CAMVI-003	[86]0.094	[121]0.071	[95]0.152	[110]0.132	[139]0.108	[51]0.970	[72]0.940	[88]0.114	[104]0.100			[65]0.402	[91]0.377	
23	CAMVI-004	[95]0.107	[122]0.072	[130]0.240	[112]0.136	[128]0.100	[132]0.999	[144]0.998	[86]0.100	[98]0.081			[102]0.787	[103]0.507	
24	CAMVI-005	[114]0.139	[141]0.099	[169]0.451	[139]0.179	[144]0.132	[139]1.000	[150]0.998	[100]0.156	[110]0.112			[132]0.999	[139]0.983	
25	CIB-000	[45]0.044	[28]0.012	[37]0.077	[28]0.045	[28]0.025	[150]1.000	[163]1.000	[25]0.017	[20]0.008	[19]0.141	[18]0.068	[113]0.894	[104]0.521	
26	CLOUDWALK-HR-000	[3]0.004	[6]0.002	[4]0.015	[6]0.013	[9]0.012	[1]0.133	[2]0.095	[4]0.005	[3]0.003	[2]0.033	[3]0.018	[4]0.099	[1]0.075	
27	COGENT-000	[118]0.143	[100]0.053	[106]0.175	[114]0.140	[132]0.100	[97]0.995	[116]0.991							
28	COGENT-001	[117]0.143	[99]0.053	[105]0.175	[113]0.140	[131]0.100	[96]0.995	[114]0.991							
29	COGENT-002	[128]0.159	[87]0.044	[74]0.124	[84]0.098	[86]0.063	[108]0.998	[124]0.994							
30	COGENT-003	[144]0.203	[91]0.046	[72]0.121	[78]0.095	[84]0.061	[110]0.998	[132]0.995							
31	COGENT-004	[147]0.209	[72]0.033	[30]0.067	[33]0.051	[34]0.031	[106]0.997	[134]0.995	[31]0.022	[30]0.012	[17]0.126	[20]0.072	[72]0.456	[41]0.178	
32	COGNITEC-000	[150]0.226	[165]0.161	[167]0.439	[170]0.303	[171]0.200	[83]0.992	[85]0.971							
33	COGNITEC-001	[142]0.192	[142]0.102	[213]0.997	[150]0.230	[146]0.135	[188]1.000	[81]0.965							
34	COGNITEC-002	[102]0.122	[102]0.053	[210]0.990	[138]0.178	[135]0.101	[149]1.000	[78]0.956							
35	COGNITEC-003	[90]0.099	[98]0.053	[127]0.222	[130]0.162	[129]0.100	[152]1.000	[73]0.946							
36	COGNITEC-004	[61]0.055	[70]0.031	[77]0.127	[82]0.097	[77]0.058	[78]0.990	[62]0.919	[75]0.068	[76]0.038	[37]0.316	[39]0.196	[46]0.288	[55]0.218	
37	CYBERLINK-000	[112]0.137	[108]0.056	[100]0.162	[95]0.116	[96]0.070	[99]0.995	[99]0.981	[73]0.063	[71]0.032			[58]0.339	[61]0.232	
38	CYBERLINK-001	[87]0.096	[103]0.054	[88]0.138	[92]0.109	[91]0.067	[95]0.995	[101]0.984	[70]0.062	[67]0.031			[92]0.652	[63]0.239	
39	CYBERLINK-002	[41]0.038	[35]0.015	[33]0.068	[37]0.053	[37]0.032	[77]0.988	[79]0.957	[32]0.024	[32]0.013			[47]0.288	[32]0.157	
40	CYBERLINK-003	[48]0.045	[20]0.008	[21]0.045	[23]0.035	[20]0.021	[54]0.972	[54]0.845	[18]0.012	[19]0.007	[13]0.100	[15]0.051	[60]0.368	[19]0.120	
41	CYBERLINK-004	[140]0.188	[19]0.007	[28]0.063	[24]0.036	[22]0.022	[160]1.000	[158]0.999	[20]0.013	[18]0.007	[14]0.109	[13]0.050	[121]0.954	[76]0.291	
42	DAHUA-000	[107]0.128	[133]0.086	[108]0.179	[111]0.135	[114]0.083									
43	DAHUA-001	[94]0.106	[124]0.073	[94]0.151	[103]0.122	[105]0.075	[64]0.980	[67]0.933							
44	DAHUA-002	[27]0.026	[36]0.015	[26]0.060	[30]0.046	[31]0.029	[19]0.638	[26]0.522	[24]0.017	[24]0.008			[19]0.159	[21]0.125	
45	DAHUA-003	[26]0.025	[32]0.014	[24]0.054	[27]0.041	[26]0.024	[16]0.579	[20]0.447	[19]0.013	[17]0.006	[11]0.081	[12]0.043	[14]0.134	[13]0.109	
46	DEEPGLINT-001	[11]0.010	[12]0.003	[7]0.018	[7]0.014	[5]0.010	[138]1.000	[22]0.503	[7]0.006	[10]0.004			[18]0.159	[10]0.097	

Table 24: **Threshold-based accuracy**. *Values are FNIR(N, T, L) with N = 1.6 million with thresholds set to produce FPIR = 0.0003, 0.001, and 0.01 in non-mate searches. Throughout blue superscripts indicate the rank of the algorithm for that column. Caution: The Power-low models are mostly intended to draw attention to the kind of behavior, not as a model to be used for prediction.*

2021/08/05 02:00:58

FNIR(N, R, T) = False neg. identification rate
FPIR(N, T) = False pos. identification rate
N = Num. enrolled subjects
R = Num. candidates examined
T = Threshold
T = 0 → Investigation
T > 0 → Identification

MISSES BELOW THRESHOLD, T		ENROL RECENT MUGSHOT, N = 1.6M									ENROL APPLICATION PORTRAIT, N = 1.6M				
ENROL		DATASET: MUGSHOT			DATASET: MUGSHOT			DATASET: MUGSHOT			DATASET: VISA		DATASET: BORDER		DATASET: VISA
PROBE		DATASET: MUGSHOT			DATASET: WEBCAM			DATASET: PROFILE			DATASET: BORDER		DATASET: BORDER 10+YR		DATASET: KIOSK
#	ALGORITHM	FPIR=0.0003	FPIR=0.001	FPIR=0.0003	FPIR=0.001	FPIR=0.001	FPIR=0.01	FPIR=0.001	FPIR=0.01	FPIR=0.001	FPIR=0.01	FPIR=0.001	FPIR=0.01		
47	DEEPSEA-001	[75] 0.073	[90] 0.046	[80] 0.129	[86] 0.101	[80] 0.059	[71] 0.985	[90] 0.973	[79] 0.077	[80] 0.041			[56] 0.326	[64] 0.251	
48	DERMALOG-003	[189] 0.550	[202] 0.482	[190] 0.715	[198] 0.655	[202] 0.526			[133] 0.677	[132] 0.554			[111] 0.870	[126] 0.791	
49	DERMALOG-004	[191] 0.554	[201] 0.480	[189] 0.711	[199] 0.657	[200] 0.526	[100] 0.995	[118] 0.991	[123] 0.603	[131] 0.458			[110] 0.856	[125] 0.751	
50	DERMALOG-005	[141] 0.189	[136] 0.088	[119] 0.201	[123] 0.154	[125] 0.096	[79] 0.990	[76] 0.950	[115] 0.300	[119] 0.267			[90] 0.614	[98] 0.459	
51	DERMALOG-006	[89] 0.098	[97] 0.052	[87] 0.137	[88] 0.105	[90] 0.067	[65] 0.981	[68] 0.933	[68] 0.059	[69] 0.031			[55] 0.318	[59] 0.230	
52	DERMALOG-007	[138] 0.188	[134] 0.086	[118] 0.200	[121] 0.152	[122] 0.093	[80] 0.990	[75] 0.950	[85] 0.099	[87] 0.052			[86] 0.557	[80] 0.299	
53	DERMALOG-008	[161] 0.268	[89] 0.045	[128] 0.231	[75] 0.094	[72] 0.054	[169] 1.000	[164] 1.000	[65] 0.057	[62] 0.025	[40] 0.382	[38] 0.158	[119] 0.940	[114] 0.678	
54	EYEDEA-003	[187] 0.509	[193] 0.388	[182] 0.625	[191] 0.543	[192] 0.404	[92] 0.994	[107] 0.990	[127] 0.570	[126] 0.392			[103] 0.792	[113] 0.658	
55	F8-001	[181] 0.458	[166] 0.166				[118] 0.998	[135] 0.995							
56	GLORY-000	[178] 0.441	[192] 0.367	[178] 0.586	[192] 0.547	[196] 0.470	[94] 0.995	[122] 0.993	[124] 0.453	[125] 0.381			[109] 0.839	[127] 0.795	
57	GLORY-001	[170] 0.355	[185] 0.305	[177] 0.582	[190] 0.537	[194] 0.448	[84] 0.993	[112] 0.991	[121] 0.408	[122] 0.336			[107] 0.819	[123] 0.753	
58	GORILLA-001	[201] 0.747	[197] 0.406	[179] 0.590	[185] 0.453	[186] 0.314	[158] 1.000	[172] 1.000	[125] 0.468	[121] 0.299			[140] 1.000	[117] 0.710	
59	GORILLA-002	[160] 0.266	[173] 0.188	[152] 0.342	[163] 0.268	[163] 0.170	[164] 1.000	[123] 0.993	[111] 0.250	[114] 0.137			[135] 1.000	[99] 0.466	
60	GORILLA-003	[190] 0.694	[187] 0.318	[183] 0.684	[184] 0.434	[182] 0.247	[193] 1.000	[167] 1.000	[120] 0.407	[117] 0.213			[156] 1.000	[106] 0.562	
61	GORILLA-004	[110] 0.135	[139] 0.089	[120] 0.202	[129] 0.160	[133] 0.101	[45] 0.959	[59] 0.903	[94] 0.135	[95] 0.072			[69] 0.438	[82] 0.309	
62	GORILLA-005	[84] 0.086	[112] 0.058	[107] 0.179	[116] 0.142	[116] 0.088	[22] 0.700	[27] 0.553	[83] 0.088	[79] 0.040			[54] 0.315	[56] 0.223	
63	HIK-003	[127] 0.159	[144] 0.103	[115] 0.190	[125] 0.158	[137] 0.105	[49] 0.969	[64] 0.925	[97] 0.142	[97] 0.080			[71] 0.445	[86] 0.359	
64	HIK-004	[124] 0.156	[140] 0.099	[111] 0.182	[122] 0.153	[134] 0.101	[56] 0.976	[74] 0.947	[95] 0.137	[96] 0.077			[68] 0.434	[85] 0.353	
65	HIK-005	[92] 0.102	[84] 0.044	[52] 0.098	[59] 0.077	[61] 0.048	[136] 0.999	[146] 0.998	[74] 0.068	[74] 0.036			[84] 0.541	[66] 0.258	
66	HIK-006	[116] 0.142	[92] 0.047	[61] 0.111	[67] 0.086	[67] 0.052	[154] 1.000	[159] 0.999							
67	IDEMIA-003	[190] 0.552	[93] 0.047	[227] 1.000	[131] 0.165	[109] 0.079		[219] 1.000	[91] 0.123	[89] 0.061			[101] 0.766	[110] 0.630	
68	IDEMIA-004	[60] 0.055	[80] 0.037	[90] 0.144	[99] 0.118	[108] 0.079	[55] 0.973	[82] 0.968	[90] 0.123	[90] 0.061			[100] 0.766	[109] 0.630	
69	IDEMIA-005	[73] 0.066	[86] 0.044	[110] 0.181	[120] 0.150	[136] 0.102	[60] 0.978	[88] 0.973	[92] 0.130	[94] 0.070			[112] 0.879	[120] 0.743	
70	IDEMIA-006	[71] 0.065	[83] 0.043	[138] 0.266	[148] 0.226	[156] 0.161	[67] 0.982	[98] 0.980	[98] 0.144	[101] 0.090			[96] 0.733	[105] 0.531	
71	IDEMIA-007	[37] 0.035	[42] 0.018	[36] 0.073	[39] 0.055	[38] 0.033	[209] 1.000	[218] 1.000	[61] 0.052	[59] 0.022	[24] 0.182	[27] 0.109	[203] 1.000	[137] 0.982	
72	IDEMIA-008	[3] 0.004	[5] 0.002	[6] 0.016	[5] 0.013	[3] 0.009	[3] 0.204	[4] 0.136	[3] 0.005	[2] 0.003	[4] 0.036	[5] 0.019	[7] 0.106	[7] 0.092	
73	IMAGUS-002	[211] 0.908	[210] 0.749	[197] 0.944	[203] 0.816	[205] 0.645	[168] 1.000	[169] 1.000							
74	IMAGUS-003	[210] 0.898	[211] 0.807	[202] 0.954	[205] 0.909	[207] 0.809	[153] 1.000	[165] 1.000							
75	IMAGUS-005	[35] 0.034	[45] 0.018	[43] 0.088	[47] 0.066	[46] 0.040	[32] 0.838	[35] 0.647	[36] 0.029	[41] 0.016	[23] 0.161	[26] 0.094	[34] 0.231	[46] 0.189	
76	IMAGUS-006	[42] 0.039	[47] 0.019	[47] 0.093	[50] 0.069	[53] 0.042	[39] 0.897	[30] 0.621	[35] 0.028	[37] 0.015	[22] 0.161	[25] 0.092	[41] 0.260	[43] 0.181	
77	IMPERIAL-000	[121] 0.154	[58] 0.026	[45] 0.089	[49] 0.068	[50] 0.041	[122] 0.999	[128] 0.995	[52] 0.042	[55] 0.020			[38] 0.245	[36] 0.168	
78	INCODE-000	[177] 0.423	[186] 0.310	[173] 0.486	[182] 0.420	[185] 0.304	[114] 0.998	[125] 0.994							
79	INCODE-001	[168] 0.319	[176] 0.212	[154] 0.348	[166] 0.296	[169] 0.198	[167] 1.000	[162] 1.000							
80	INCODE-002	[165] 0.285	[172] 0.184	[149] 0.333	[164] 0.269	[165] 0.176	[85] 0.993	[94] 0.976							
81	INCODE-003	[166] 0.286	[168] 0.167	[158] 0.372	[160] 0.264	[159] 0.164	[134] 0.999	[139] 0.996							
82	INCODE-004	[91] 0.099	[105] 0.054	[102] 0.167	[102] 0.120	[97] 0.070	[93] 0.995	[65] 0.929	[72] 0.063	[68] 0.031			[52] 0.313	[57] 0.226	
83	INNOVATRICS-002	[175] 0.379	[181] 0.234	[162] 0.403	[171] 0.310	[175] 0.209	[156] 1.000	[160] 0.999							
84	INNOVATRICS-003	[167] 0.297	[177] 0.221	[150] 0.351	[167] 0.297	[172] 0.203	[142] 1.000	[148] 0.998							
85	INNOVATRICS-004	[136] 0.184	[156] 0.132	[136] 0.262	[147] 0.222	[150] 0.149	[63] 0.980	[87] 0.973							
86	INNOVATRICS-005	[63] 0.057	[73] 0.034	[64] 0.114	[70] 0.089	[68] 0.052	[33] 0.846	[40] 0.723	[58] 0.047	[58] 0.022			[39] 0.251	[44] 0.182	
87	INTSYSMSU-000	[219] 0.999	[221] 0.998	[214] 1.000	[216] 1.000	[217] 0.998	[143] 1.000	[145] 0.998	[142] 0.999	[142] 0.989			[133] 0.999	[140] 0.988	
88	IREX-000	[74] 0.068	[66] 0.028	[53] 0.099	[43] 0.060	[35] 0.032	[44] 0.957	[39] 0.680	[55] 0.044	[29] 0.011	[36] 0.302	[17] 0.062	[22] 0.170	[26] 0.135	
89	ISYSTEMS-002	[123] 0.155	[127] 0.078	[98] 0.161	[106] 0.126	[111] 0.080	[107] 0.998	[121] 0.993							
90	ISYSTEMS-003	[145] 0.204	[113] 0.059	[80] 0.135	[91] 0.107	[93] 0.068	[145] 1.000	[143] 0.997							
91	KAKAO-000	[29] 0.028	[38] 0.015	[35] 0.071	[40] 0.056	[41] 0.034	[11] 0.468	[17] 0.327	[27] 0.019	[26] 0.010	[18] 0.141	[21] 0.075	[17] 0.158	[20] 0.120	
92	KEDACOM-001	[44] 0.041	[54] 0.023	[50] 0.096	[54] 0.072	[71] 0.054	[73] 0.986	[91] 0.973	[64] 0.055	[81] 0.043			[50] 0.305	[68] 0.264	

Table 25: **Threshold-based accuracy**. *Values are FNIR(N, T, L) with N = 1.6 million with thresholds set to produce FPIR = 0.0003, 0.001, and 0.01 in non-mate searches. Throughout blue superscripts indicate the rank of the algorithm for that column. Caution: The Power-low models are mostly intended to draw attention to the kind of behavior, not as a model to be used for prediction.*

MISSES BELOW THRESHOLD, T		ENROL RECENT MUGSHOT, N = 1.6M									ENROL APPLICATION PORTRAIT, N = 1.6M				
ENROL		DATASET: MUGSHOT			DATASET: MUGSHOT			DATASET: MUGSHOT			DATASET: VISA		DATASET: BORDER		DATASET: VISA
PROBE		DATASET: MUGSHOT			DATASET: WEBCAM			DATASET: PROFILE			DATASET: BORDER		DATASET: BORDER 10+YR		DATASET: KIOSK
#	ALGORITHM	FPIR=0.0003	FPIR=0.001	FPIR=0.0003	FPIR=0.001	FPIR=0.001	FPIR=0.01	FPIR=0.001	FPIR=0.01	FPIR=0.001	FPIR=0.01	FPIR=0.001	FPIR=0.01		
93	KNERON-000					[127]0.099									
94	KNERON-001														
95	LINE-000	[67]0.062	[69]0.031	[84]0.132	[79]0.095	[73]0.054		[174]1.000	[56]0.046	[56]0.021	[34]0.278	[37]0.151	[219]1.000	[69]0.268	
96	LOOKMAN-003	[72]0.066	[85]0.044	[83]0.131	[94]0.112	[112]0.082			[82]0.084	[91]0.061			[59]0.355	[81]0.304	
97	LOOKMAN-004	[76]0.074	[88]0.045	[73]0.123	[90]0.105	[103]0.075	[57]0.977	[92]0.974							
98	LOOKMAN-005	[56]0.050	[68]0.030	[54]0.102	[66]0.086	[87]0.063	[59]0.978	[89]0.973	[71]0.062	[83]0.047			[51]0.308	[71]0.273	
99	MEGVII-001	[148]0.210	[123]0.072	[69]0.119	[83]0.097	[82]0.061									
100	MEGVII-002	[159]0.258	[126]0.077	[70]0.120	[81]0.096	[79]0.059	[117]0.998	[57]0.872							
101	MICROFOCUS-003	[214]0.958	[217]0.931	[209]0.988	[215]0.979	[215]0.948			[141]0.982	[141]0.945			[129]0.991	[136]0.977	
102	MICROFOCUS-004	[221]0.999	[222]0.999	[208]0.984	[213]0.975	[214]0.940			[140]0.974	[140]0.935			[127]0.989	[135]0.976	
103	MICROFOCUS-005	[209]0.883	[215]0.835	[201]0.951	[209]0.928	[211]0.865			[138]0.935	[138]0.848			[126]0.985	[134]0.965	
104	MICROFOCUS-006	[217]0.983	[219]0.978	[200]0.950	[208]0.923	[210]0.858			[137]0.923	[136]0.843			[124]0.971	[131]0.939	
105	MICROSOFT-003	[54]0.049	[64]0.028	[65]0.117	[73]0.091	[76]0.056			[48]0.036	[53]0.019			[36]0.233	[40]0.176	
106	MICROSOFT-004	[50]0.046	[59]0.026	[62]0.111	[68]0.087	[70]0.053			[44]0.033	[49]0.018			[32]0.222	[38]0.170	
107	MICROSOFT-005	[51]0.047	[57]0.026	[46]0.090	[52]0.070	[51]0.041	[17]0.587	[18]0.354	[33]0.027	[34]0.013			[24]0.180	[25]0.134	
108	MICROSOFT-006	[25]0.025	[25]0.012	[22]0.048	[25]0.037	[27]0.024	[6]0.386	[12]0.281	[41]0.032	[38]0.015			[23]0.178	[27]0.138	
109	NEC-000	[98]0.113	[129]0.079	[103]0.171	[115]0.140	[120]0.093	[61]0.979	[84]0.969					[75]0.474	[92]0.377	
110	NEC-001	[120]0.148	[146]0.106	[129]0.238	[141]0.197	[145]0.133	[74]0.986	[86]0.972	[93]0.133	[100]0.082			[74]0.468	[93]0.378	
111	NEC-002	[17]0.018	[10]0.003	[13]0.029	[12]0.020	[11]0.013	[131]0.999	[130]0.995	[11]0.008	[14]0.005			[94]0.676	[77]0.292	
112	NEC-003	[7]0.005	[8]0.002	[11]0.021	[11]0.017	[10]0.013	[29]0.824	[32]0.628	[14]0.008	[15]0.006	[5]0.036	[6]0.023	[93]0.668	[67]0.261	
113	NEC-004	[1]0.003	[2]0.002	[3]0.015	[4]0.013	[7]0.010	[18]0.622	[28]0.575	[2]0.004	[5]0.004	[1]0.019	[1]0.012	[5]0.100	[4]0.088	
114	NEUROTECHNOLOGY-003	[220]0.999	[208]0.636	[192]0.773	[162]0.266	[158]0.164	[194]1.000	[184]1.000							
115	NEUROTECHNOLOGY-004	[100]0.120	[117]0.063	[91]0.146	[96]0.117	[99]0.073	[89]0.994	[109]0.990							
116	NEUROTECHNOLOGY-005	[99]0.117	[106]0.054	[132]0.252	[108]0.130	[102]0.074	[111]0.998	[106]0.989							
117	NEUROTECHNOLOGY-006	[218]0.987	[182]0.249	[218]1.000	[181]0.418	[174]0.206									
118	NEUROTECHNOLOGY-007	[155]0.252	[116]0.062	[212]0.996	[135]0.173	[92]0.068	[147]1.000	[142]0.997	[116]0.339	[75]0.036			[184]1.000	[141]0.989	
119	NEUROTECHNOLOGY-008	[202]0.797	[101]0.053	[60]0.110	[62]0.080	[59]0.047	[165]1.000	[175]1.000	[47]0.035	[46]0.017	[35]0.293	[36]0.149	[29]0.203	[31]0.152	
120	NEWLAND-002	[188]0.523	[199]0.438	[174]0.535	[186]0.466	[188]0.335	[125]0.999	[148]0.998							
121	NOBLIS-001	[224]1.000	[224]1.000	[217]1.000	[223]1.000	[224]1.000	[161]1.000	[170]1.000							
122	NOBLIS-002	[222]1.000	[220]0.997	[228]1.000	[224]1.000	[225]1.000	[162]1.000	[176]1.000							
123	NTECHLAB-003	[79]0.080	[104]0.054	[92]0.148	[97]0.118	[104]0.075	[31]0.837	[47]0.752							
124	NTECHLAB-004	[69]0.063	[81]0.041	[82]0.131	[89]0.105	[89]0.065	[30]0.833	[45]0.746	[63]0.053	[66]0.030			[43]0.263	[54]0.214	
125	NTECHLAB-005	[68]0.062	[82]0.042	[81]0.130	[87]0.102	[88]0.063	[25]0.771	[37]0.661	[77]0.073	[78]0.039			[48]0.294	[58]0.227	
126	NTECHLAB-006	[62]0.056	[76]0.037	[71]0.121	[76]0.094	[78]0.059	[24]0.754	[33]0.635	[66]0.057	[70]0.032			[42]0.260	[52]0.207	
127	NTECHLAB-007	[43]0.040	[56]0.026	[42]0.085	[48]0.067	[49]0.041	[23]0.750	[34]0.642	[42]0.032	[47]0.017			[33]0.223	[39]0.176	
128	NTECHLAB-008	[23]0.024	[33]0.014	[25]0.057	[29]0.045	[32]0.029	[15]0.529	[19]0.391	[45]0.033	[50]0.018			[25]0.183	[28]0.140	
129	NTECHLAB-009	[10]0.010	[17]0.005	[12]0.028	[13]0.022	[13]0.014	[8]0.430	[14]0.311	[21]0.015	[22]0.008	[15]0.109	[16]0.061	[15]0.142	[14]0.114	
130	NTECHLAB-010	[6]0.005	[9]0.003	[6]0.018	[9]0.015	[8]0.011	[5]0.252	[8]0.169	[8]0.007	[9]0.004	[9]0.059	[11]0.031	[2]0.098	[2]0.077	
131	PARAVISION-000	[164]0.278	[138]0.089	[168]0.447	[133]0.170	[130]0.100	[127]0.999	[140]0.997	[126]0.470	[129]0.443			[118]0.926	[125]0.779	
132	PARAVISION-001	[115]0.140	[94]0.049	[124]0.207	[107]0.128	[101]0.074	[120]0.999	[126]0.994	[123]0.444	[128]0.428			[97]0.739	[107]0.573	
133	PARAVISION-002	[83]0.085	[95]0.050	[96]0.152	[100]0.119	[106]0.076	[68]0.983	[46]0.748	[80]0.080	[82]0.043			[78]0.497	[70]0.268	
134	PARAVISION-003	[70]0.063	[74]0.035	[76]0.124	[80]0.096	[81]0.060	[90]0.994	[41]0.733	[67]0.058	[73]0.034			[49]0.296	[60]0.232	
135	PARAVISION-004	[24]0.025	[24]0.010	[23]0.049	[26]0.038	[25]0.024	[157]1.000	[51]0.797	[26]0.018	[28]0.011			[114]0.908	[53]0.211	
136	PARAVISION-005	[16]0.014	[14]0.004	[14]0.031	[14]0.024	[15]0.016	[62]0.980	[9]0.181	[17]0.011	[23]0.008			[12]0.132	[18]0.120	
137	PARAVISION-007	[52]0.048	[13]0.004	[175]0.560	[15]0.025	[14]0.015	[163]1.000	[177]1.000	[16]0.009	[16]0.006	[16]0.113	[8]0.024	[214]1.000	[201]1.000	
138	PIXELALL-002	[196]0.664	[145]0.105	[205]0.974	[179]0.388	[113]0.083	[155]1.000	[168]1.000	[128]0.602	[85]0.047			[183]1.000	[142]1.000	

Table 26: **Threshold-based accuracy**. *Values are FNIR(N, T, L) with N = 1.6 million with thresholds set to produce FPIR = 0.0003, 0.001, and 0.01 in non-mate searches. Throughout blue superscripts indicate the rank of the algorithm for that column. Caution: The Power-low models are mostly intended to draw attention to the kind of behavior, not as a model to be used for prediction.*

2021/08/05 02:00:58

FNIR(N, R, T) = False neg. identification rate
FPIR(N, T) = False pos. identification rate
N = Num. enrolled subjects
R = Num. candidates examined
T = Threshold
T = 0 → Investigation
T > 0 → Identification

MISSES BELOW THRESHOLD, T		ENROL RECENT MUGSHOT, N = 1.6M									ENROL APPLICATION PORTRAIT, N = 1.6M				
ENROL		DATASET: MUGSHOT			DATASET: MUGSHOT			DATASET: MUGSHOT			DATASET: VISA		DATASET: BORDER		DATASET: VISA
PROBE		DATASET: MUGSHOT			DATASET: WEBCAM			DATASET: PROFILE			DATASET: BORDER		DATASET: BORDER 10+YR		DATASET: KIOSK
#	ALGORITHM	FPIR=0.0003	FPIR=0.001	FPIR=0.0003	FPIR=0.001	FPIR=0.001	FPIR=0.01	FPIR=0.001	FPIR=0.01	FPIR=0.001	FPIR=0.01	FPIR=0.001	FPIR=0.01		
139	PIXELALL-003	[53]0.049	[51]0.022	[55]0.102	[55]0.073	[54]0.043	[141]1.000	[147]0.998	[50]0.037	[54]0.020			[85]0.554	[65]0.255	
140	PIXELALL-004	[101]0.120	[44]0.018	[193]0.783	[61]0.079	[44]0.037	[151]1.000	[154]0.999	[60]0.051	[39]0.015			[130]0.994	[132]0.942	
141	PIXELALL-005	[78]0.079	[27]0.012	[170]0.456	[32]0.050	[29]0.027	[166]1.000	[161]0.999	[34]0.027	[43]0.017	[27]0.203	[19]0.071	[134]1.000	[138]0.983	
142	PTAKURATSATU-000	[64]0.057	[75]0.037	[101]0.165	[105]0.124	[98]0.071	[41]0.924	[56]0.868	[57]0.046	[57]0.022	[29]0.206	[31]0.120	[35]0.232	[43]0.179	
143	QUANTASOFT-001	[200]0.713	[209]0.639												
144	RANKONE-002	[134]0.184	[149]0.118	[147]0.308	[158]0.261	[168]0.190									
145	RANKONE-003	[135]0.184	[150]0.118	[144]0.300	[157]0.255	[166]0.187									
146	RANKONE-004	[154]0.250	[174]0.193	[172]0.482	[183]0.426	[187]0.324									
147	RANKONE-005	[88]0.096	[114]0.059	[125]0.212	[136]0.173	[141]0.119	[112]0.998	[127]0.994							
148	RANKONE-006	[65]0.061	[77]0.037				[58]0.977	[69]0.937							
149	RANKONE-007	[34]0.034	[53]0.022	[68]0.118	[77]0.095	[83]0.061	[48]0.967	[63]0.924							
150	RANKONE-009	[31]0.031	[41]0.018	[51]0.098	[57]0.076	[56]0.045	[50]0.969	[55]0.859	[69]0.062	[65]0.029			[57]0.328	[51]0.206	
151	RANKONE-010	[20]0.023	[31]0.014	[38]0.077	[41]0.058	[43]0.036	[27]0.802	[36]0.652	[62]0.052	[63]0.027	[30]0.208	[30]0.119	[40]0.259	[48]0.194	
152	REALNETWORKS-000	[173]0.374	[179]0.234	[165]0.433	[173]0.319	[176]0.209									
153	REALNETWORKS-001	[174]0.374	[180]0.234	[166]0.433	[174]0.319	[177]0.209									
154	REALNETWORKS-002	[172]0.370	[178]0.231	[164]0.416	[172]0.315	[178]0.209									
155	REALNETWORKS-003	[162]0.273	[164]0.159	[151]0.342	[161]0.266	[164]0.172	[116]0.998	[103]0.987	[102]0.164	[105]0.103			[79]0.500	[89]0.364	
156	REALNETWORKS-004	[153]0.242	[163]0.158	[157]0.353	[159]0.263	[161]0.169	[129]0.999	[120]0.992	[103]0.170	[106]0.103			[89]0.613	[90]0.370	
157	REALNETWORKS-005	[58]0.052	[63]0.028	[49]0.094	[56]0.074	[58]0.047	[52]0.971	[58]0.896	[49]0.037	[44]0.017	[31]0.223	[33]0.123	[31]0.215	[35]0.165	
158	REMARKAI-000	[105]0.125	[107]0.055	[104]0.173	[101]0.120	[95]0.070	[126]0.999	[129]0.995	[76]0.069	[72]0.033			[95]0.717	[83]0.315	
159	REMARKAI-000	[143]0.197	[154]0.128	[137]0.263	[142]0.203	[143]0.123									
160	REMARKAI-002	[139]0.188	[153]0.124	[131]0.248	[140]0.196	[142]0.122	[82]0.991	[97]0.980							
161	RENDIP-000	[21]0.023	[26]0.012	[114]0.189	[42]0.059	[40]0.034	[38]0.894	[44]0.744	[29]0.022	[33]0.013	[25]0.185	[24]0.089	[20]0.167	[23]0.130	
162	S1-000	[111]0.137	[65]0.028	[79]0.129	[65]0.085	[60]0.048	[172]1.000	[29]0.596	[59]0.047	[51]0.018	[135]1.000	[32]0.123	[189]1.000	[112]0.632	
163	SCANOVATE-000	[93]0.103	[120]0.067	[143]0.296	[154]0.240	[151]0.150	[37]0.893	[52]0.803	[109]0.215	[112]0.118			[64]0.400	[79]0.299	
164	SCANOVATE-001	[106]0.128	[130]0.081	[142]0.281	[149]0.227	[147]0.140	[40]0.911	[53]0.834	[106]0.192	[107]0.103			[67]0.404	[75]0.290	
165	SENSETIME-000	[38]0.036	[49]0.021	[39]0.078	[45]0.063	[47]0.040	[178]1.000	[104]0.988							
166	SENSETIME-001	[39]0.036	[52]0.022	[41]0.080	[46]0.064	[52]0.041									
167	SENSETIME-002	[40]0.037	[34]0.015	[75]0.124	[19]0.028	[24]0.023	[88]0.994	[96]0.979	[40]0.032	[45]0.017			[81]0.523	[34]0.160	
168	SENSETIME-003	[4]0.004	[4]0.002	[1]0.014	[1]0.012	[2]0.009	[12]0.477	[15]0.311	[12]0.008	[13]0.005			[13]0.133	[15]0.115	
169	SENSETIME-004	[2]0.003	[1]0.002	[2]0.015	[3]0.013	[6]0.010	[4]0.229	[6]0.149	[6]0.006	[6]0.004			[10]0.113	[11]0.100	
170	SENSETIME-005	[13]0.011	[7]0.002	[10]0.018	[8]0.014	[4]0.010	[2]0.173	[3]0.103	[9]0.007	[7]0.004	[7]0.051	[7]0.023	[6]0.104	[8]0.093	
171	SENSETIME-006	[6]0.005	[3]0.002	[5]0.016	[2]0.012	[1]0.009	[115]0.998	[38]0.680	[1]0.004	[1]0.002	[3]0.034	[2]0.016	[1]0.093	[3]0.079	
172	SHAMAN-003	[186]0.506	[200]0.451	[184]0.650	[194]0.597	[197]0.472									
173	SHAMAN-004	[197]0.679	[207]0.615	[194]0.812	[201]0.754	[204]0.639									
174	SHAMAN-006	[137]0.185	[158]0.141	[140]0.278	[151]0.237	[160]0.168	[53]0.972	[80]0.960							
175	SHAMAN-007	[132]0.183	[159]0.141	[141]0.280	[153]0.240	[162]0.169									
176	SIAT-001	[109]0.132	[39]0.018	[183]0.641	[178]0.365	[189]0.348			[38]0.031	[35]0.014					
177	SIAT-002	[176]0.417	[50]0.022	[190]0.942	[187]0.478	[195]0.460			[118]0.372	[123]0.356			[117]0.923	[37]0.169	
178	SMILART-004	[216]0.970	[218]0.968	[206]0.977	[214]0.976	[216]0.973									
179	SMILART-005														
180	SYNESIS-003	[9]0.111	[118]0.065	[9]0.155	[104]0.123	[107]0.078	[46]0.960	[60]0.911	[78]0.075	[77]0.039			[53]0.314	[62]0.235	
181	SYNESIS-003	[195]0.648	[205]0.582	[188]0.708	[197]0.646	[199]0.524									
182	SYNESIS-005	[55]0.050	[55]0.025	[44]0.088	[53]0.072	[55]0.043	[69]0.984	[49]0.795	[43]0.032	[40]0.016			[30]0.214	[33]0.158	
183	TECH5-001	[204]0.807	[109]0.057	[211]0.994	[210]0.935	[75]0.055	[171]1.000	[166]1.000	[110]0.244	[64]0.028			[131]0.994	[128]0.817	
184	TECH5-002	[59]0.053	[62]0.027	[48]0.094	[51]0.070	[48]0.040	[28]0.805	[31]0.627	[51]0.039	[52]0.019	[28]0.205	[28]0.111	[70]0.440	[45]0.182	

Table 27: **Threshold-based accuracy**. *Values are FNIR(N, T, L) with N = 1.6 million with thresholds set to produce FPIR = 0.0003, 0.001, and 0.01 in non-mate searches. Throughout blue superscripts indicate the rank of the algorithm for that column. Caution: The Power-low models are mostly intended to draw attention to the kind of behavior, not as a model to be used for prediction.*

2021/08/05 02:00:58

FNIR(N, R, T) = FPIR(N, T) = False neg. identification rate / False pos. identification rate

N = Num. enrolled subjects
R = Num. candidates examined

T = Threshold

T = 0 → Investigation
T > 0 → Identification

MISSES BELOW THRESHOLD, T		ENROL RECENT MUGSHOT, N = 1.6M									ENROL APPLICATION PORTRAIT, N = 1.6M				
ENROL		DATASET: MUGSHOT			DATASET: MUGSHOT			DATASET: MUGSHOT			DATASET: VISA		DATASET: BORDER		DATASET: VISA
PROBE		DATASET: MUGSHOT			DATASET: WEBCAM			DATASET: PROFILE			DATASET: BORDER		DATASET: BORDER 10+YR		DATASET: KIOSK
#	ALGORITHM	FPIR=0.0003	FPIR=0.001	FPIR=0.0003	FPIR=0.001	FPIR=0.001	FPIR=0.01	FPIR=0.001	FPIR=0.01	FPIR=0.001	FPIR=0.01	FPIR=0.001	FPIR=0.01		
185	TEVIAN-003	[152]0.239	[171]0.177	[153]0.346	[168]0.298	[170]0.198									
186	TEVIAN-004	[129]0.170	[148]0.117	[126]0.216	[139]0.176	[140]0.115									
187	TEVIAN-005	[108]0.129	[135]0.087	[109]0.180	[117]0.144	[117]0.089	[47]0.962	[50]0.796							
188	TEVIAN-006	[22]0.024	[22]0.010	[20]0.041	[21]0.032	[21]0.021	[7]0.425	[13]0.291	[22]0.016	[25]0.009	[12]0.093	[14]0.050	[120]0.951	[16]0.117	
189	TIGER-000	[182]0.462	[195]0.390	[176]0.565	[188]0.500	[190]0.366									
190	TIGER-002	[126]0.158	[132]0.086	[121]0.202	[127]0.158	[124]0.095	[124]0.999	[93]0.975							
191	TIGER-003	[125]0.158	[131]0.086	[122]0.202	[126]0.158	[123]0.095									
192	TONGYITRANS-000	[96]0.107	[125]0.074	[89]0.141	[93]0.112	[94]0.069									
193	TONGYITRANS-001	[104]0.124	[119]0.066	[78]0.128	[85]0.101	[85]0.062									
194	TOSHIBA-000	[103]0.123	[115]0.062	[93]0.150	[98]0.118	[100]0.074	[98]0.995	[105]0.988							
195	TOSHIBA-001	[149]0.225	[111]0.058	[85]0.133	[74]0.092	[74]0.054									
196	TRUEFACE-000	[49]0.046	[43]0.018	[40]0.079	[44]0.062	[45]0.039	[34]0.882	[21]0.499	[37]0.030	[42]0.016	[26]0.194	[29]0.111	[27]0.188	[29]0.145	
197	VD-000	[213]0.950	[216]0.917	[204]0.968	[212]0.946	[212]0.871									
198	VD-001	[163]0.278	[175]0.201	[148]0.331	[165]0.281	[167]0.188									
199	VD-002	[119]0.144	[128]0.079	[113]0.188	[119]0.148	[118]0.092	[101]0.996	[102]0.987	[84]0.095	[86]0.048	[38]0.367	[40]0.220	[61]0.372	[72]0.280	
200	VERIDAS-001	[80]0.080	[79]0.037	[58]0.106	[64]0.082	[64]0.051	[76]0.987	[70]0.938	[54]0.044	[60]0.023	[32]0.266	[34]0.146	[44]0.264	[50]0.204	
201	VERIDAS-002	[81]0.080	[78]0.037	[59]0.106	[63]0.082	[63]0.051	[75]0.987	[71]0.938	[53]0.044	[61]0.023	[33]0.266	[35]0.146	[45]0.264	[49]0.204	
202	VIGILANTSOLUTIONS-003	[185]0.482	[198]0.408	[191]0.730	[200]0.660	[201]0.526	[121]0.999	[131]0.995							
203	VIGILANTSOLUTIONS-004	[194]0.624	[204]0.549	[195]0.858	[204]0.817	[206]0.709	[103]0.996	[115]0.991							
204	VIGILANTSOLUTIONS-005	[212]0.936	[194]0.388				[170]1.000	[173]1.000							
205	VIGILANTSOLUTIONS-006	[215]0.959	[189]0.353				[159]1.000	[171]1.000							
206	VIGILANTSOLUTIONS-007	[77]0.076	[67]0.028	[63]0.113	[69]0.088	[69]0.053	[102]0.996	[117]0.991	[81]0.081	[84]0.047	[39]0.371	[41]0.242	[63]0.391	[78]0.295	
207	VIGILANTSOLUTIONS-008	[57]0.051	[48]0.021	[57]0.105	[58]0.077	[57]0.046	[123]0.999	[113]0.991	[87]0.104	[88]0.054	[41]0.398	[42]0.259	[80]0.511	[84]0.316	
208	VISIONLABS-004	[85]0.091	[110]0.058	[117]0.199	[128]0.159	[126]0.097	[36]0.890	[43]0.742							
209	VISIONLABS-005	[82]0.080	[96]0.050	[112]0.183	[118]0.147	[115]0.087	[35]0.888	[42]0.736							
210	VISIONLABS-006	[47]0.044	[61]0.027	[67]0.117	[72]0.090	[66]0.051	[20]0.672	[25]0.511							
211	VISIONLABS-007	[46]0.044	[60]0.027	[66]0.117	[71]0.090	[65]0.051	[21]0.672	[24]0.511	[39]0.031	[36]0.014			[26]0.185	[30]0.145	
212	VISIONLABS-008	[28]0.028	[29]0.013	[32]0.068	[35]0.051	[36]0.032	[13]0.481	[16]0.317	[23]0.017	[21]0.008			[16]0.151	[17]0.119	
213	VISIONLABS-009	[14]0.012	[15]0.005	[15]0.032	[16]0.025	[16]0.017	[26]0.799	[10]0.196	[15]0.008	[11]0.004			[9]0.113	[9]0.093	
214	VISIONLABS-010	[15]0.014	[18]0.005	[16]0.034	[18]0.027	[18]0.019		[7]0.169	[10]0.008	[8]0.004	[8]0.055	[9]0.027	[8]0.109	[6]0.089	
215	VOCORD-003	[169]0.354	[152]0.122	[116]0.195	[124]0.155	[121]0.093	[113]0.998	[111]0.991	[101]0.157	[108]0.105			[66]0.404	[74]0.289	
216	VOCORD-004	[205]0.826	[190]0.355	[161]0.401	[134]0.173	[119]0.093	[148]1.000	[153]0.999	[107]0.193	[92]0.065			[128]0.991	[124]0.776	
217	VOCORD-005	[198]0.689	[162]0.158	[99]0.161	[109]0.130	[110]0.080	[105]0.997	[83]0.968	[96]0.138	[102]0.090			[62]0.381	[73]0.287	
218	VOCORD-006	[227]1.000	[228]1.000	[224]1.000	[228]1.000	[228]1.000	[227]1.000	[207]1.000	[225]1.000	[159]1.000			[191]1.000	[221]1.000	
219	VTS-000	[192]0.605	[206]0.598	[181]0.624	[195]0.619	[203]0.613	[130]0.999	[151]0.998	[131]0.613	[133]0.609	[42]0.760	[43]0.739	[99]0.761	[121]0.749	
220	VTS-001	[36]0.035	[30]0.013	[31]0.067	[34]0.051	[33]0.031	[87]0.994	[23]0.510	[30]0.022	[31]0.012	[20]0.141	[22]0.079	[28]0.192	[22]0.126	
221	XFORWARDAI-000	[30]0.029	[37]0.015	[34]0.070	[38]0.053	[42]0.034	[9]0.440	[11]0.250	[28]0.021	[27]0.011	[21]0.159	[23]0.082	[21]0.169	[24]0.134	
222	XFORWARDAI-001	[12]0.010	[16]0.005	[18]0.036	[20]0.028	[19]0.020	[10]0.448	[5]0.143	[13]0.008	[12]0.005	[10]0.062	[10]0.030	[11]0.123	[12]0.102	
223	XFORWARDAI-002	[9]0.007	[11]0.003	[9]0.018	[10]0.016	[12]0.014	[14]0.525	[1]0.095	[5]0.005	[4]0.003	[6]0.041	[4]0.018	[3]0.099	[5]0.089	
224	YISHENG-001	[180]0.452	[188]0.346	[207]0.983	[202]0.808	[183]0.269			[132]0.666	[127]0.396			[116]0.919	[115]0.695	
225	YITU-002	[32]0.031	[40]0.018	[27]0.063	[31]0.049	[30]0.028									
226	YITU-003	[33]0.032	[46]0.019	[29]0.067	[36]0.052	[39]0.033									
227	YITU-004	[18]0.019	[21]0.010	[17]0.035	[17]0.027	[17]0.017	[42]0.936	[61]0.913							
228	YITU-005	[19]0.022	[23]0.010	[19]0.039	[22]0.032	[23]0.023									

Table 28: **Threshold-based accuracy**. *Values are FNIR(N, T, L) with N = 1.6 million with thresholds set to produce FPIR = 0.0003, 0.001, and 0.01 in non-mate searches. Throughout blue superscripts indicate the rank of the algorithm for that column. Caution: The Power-low models are mostly intended to draw attention to the kind of behavior, not as a model to be used for prediction.*

Appendices

Appendix A Accuracy on large-population FRVT 2018 mugshots

2021/08/05	FNIR(N, R, T) =	False neg. identification rate	N = Num. enrolled subjects	T = Threshold	$T = 0 \rightarrow$ Investigation
02:00:58	FPIR(N, T) =	False pos. identification rate	R = Num. candidates examined		$T > 0 \rightarrow$ Identification

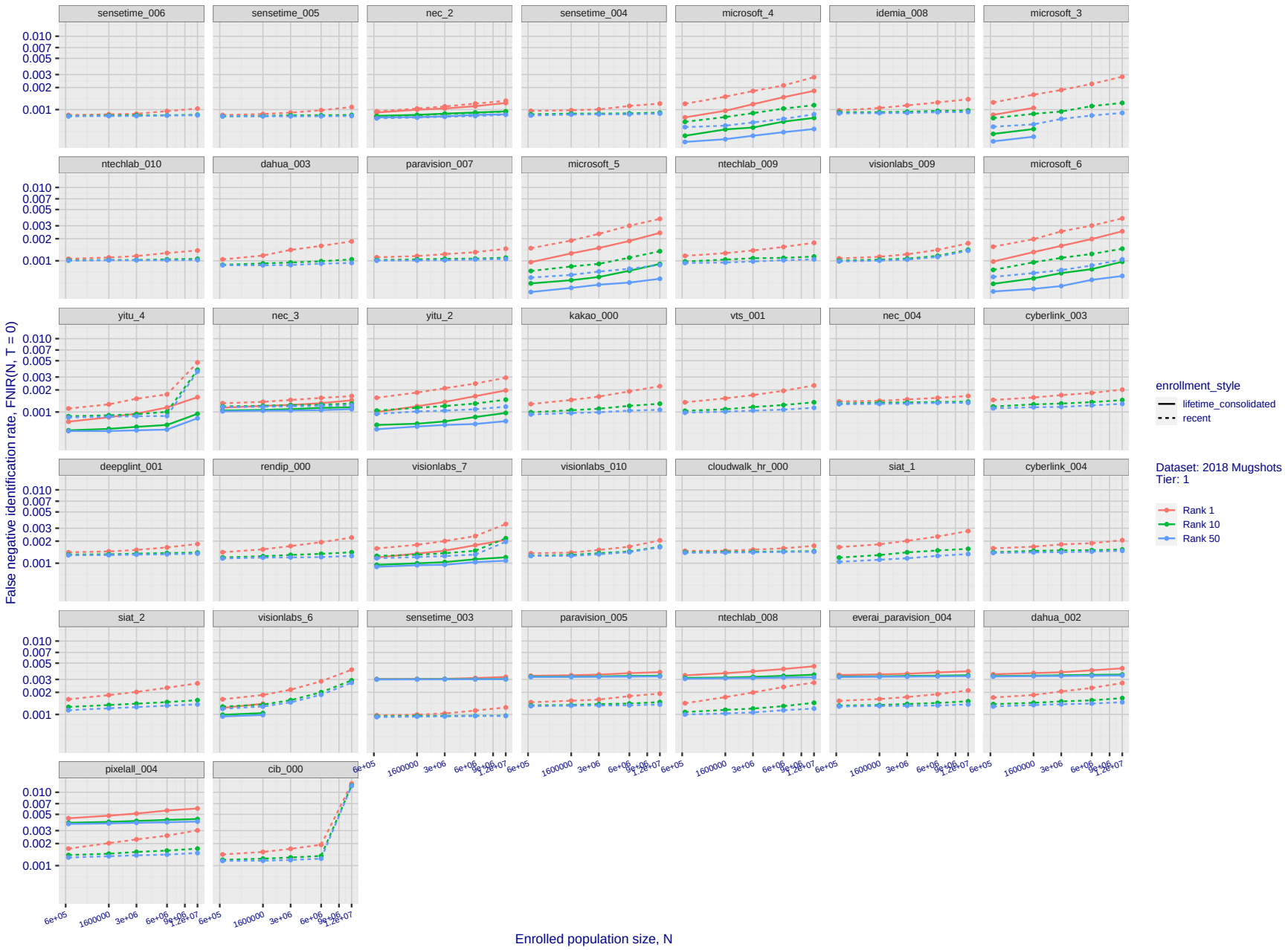

Figure 20: **[FRVT-2018 Mugshot Dataset] Rank-based identification miss rates vs. number of enrolled subjects**. *The figure shows false negative identification rates, FNIR(N, R), across various gallery sizes and ranks 1, 10 and 50. The threshold is set to zero, so this metric rewards even weak scoring rank 1 mates. This also means FPIR = 1, so any search without an enrolled mate will return non-mated candidates. For clarity, results are sorted and reported into tiers spanning multiple pages, the tiering criteria being rank 1 hit rate on a gallery size of 640 000.*

2021/08/05
02:00:58

FNIR(N, R, T) = False neg. identification rate
FPIR(N, T) = False pos. identification rate

N = Num. enrolled subjects
R = Num. candidates examined

T = Threshold

T = 0 → Investigation
T > 0 → Identification

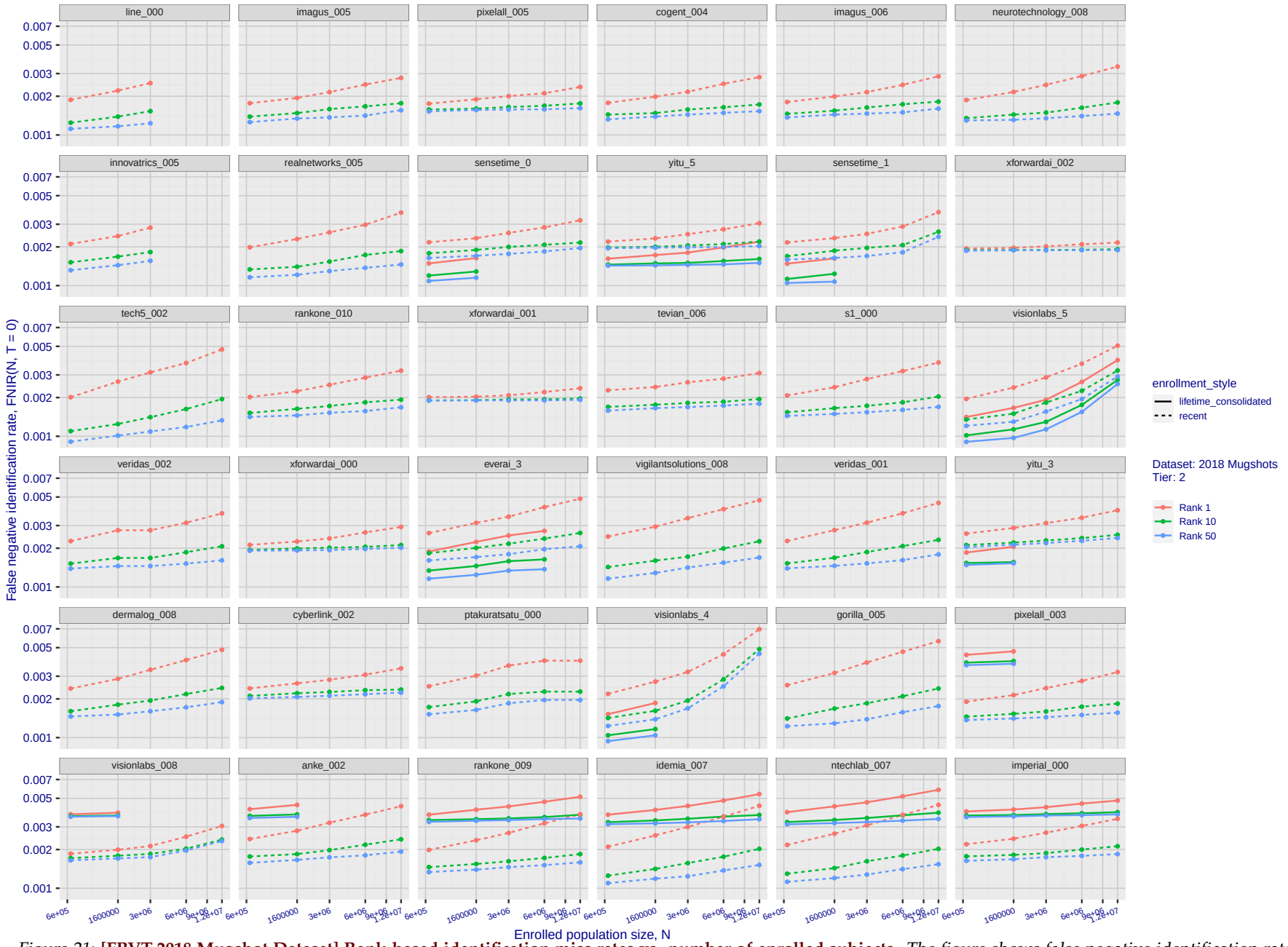

Figure 21: **[FRVT-2018 Mugshot Dataset] Rank-based identification miss rates vs. number of enrolled subjects**. *The figure shows false negative identification rates, FNIR(N, R), across various gallery sizes and ranks 1, 10 and 50. The threshold is set to zero, so this metric rewards even weak scoring rank 1 mates. This also means FPIR = 1, so any search without an enrolled mate will return non-mated candidates. For clarity, results are sorted and reported into tiers spanning multiple pages, the tiering criteria being rank 1 hit rate on a gallery size of 640 000.*

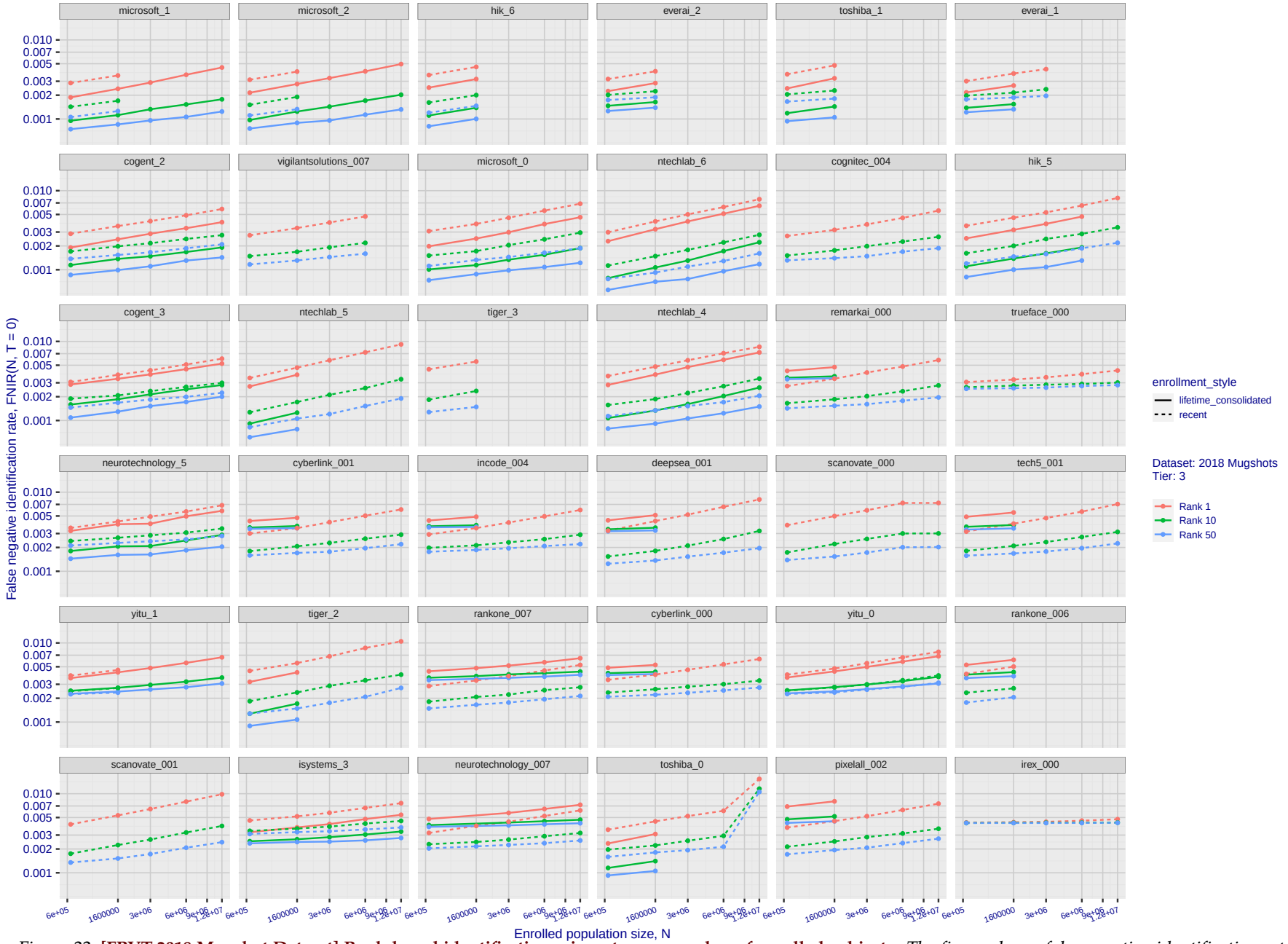

Figure 22: **[FRVT-2018 Mugshot Dataset] Rank-based identification miss rates vs. number of enrolled subjects**. *The figure shows false negative identification rates, FNIR(N, R), across various gallery sizes and ranks 1, 10 and 50. The threshold is set to zero, so this metric rewards even weak scoring rank 1 mates. This also means FPIR = 1, so any search without an enrolled mate will return non-mated candidates. For clarity, results are sorted and reported into tiers spanning multiple pages, the tiering criteria being rank 1 hit rate on a gallery size of 640 000.*

2021/08/05 02:00:58
FNIR(N, R, T) = False neg. identification rate
FPIR(N, T) = False pos. identification rate
N = Num. enrolled subjects
R = Num. candidates examined
T = Threshold
T = 0 → Investigation
T > 0 → Identification

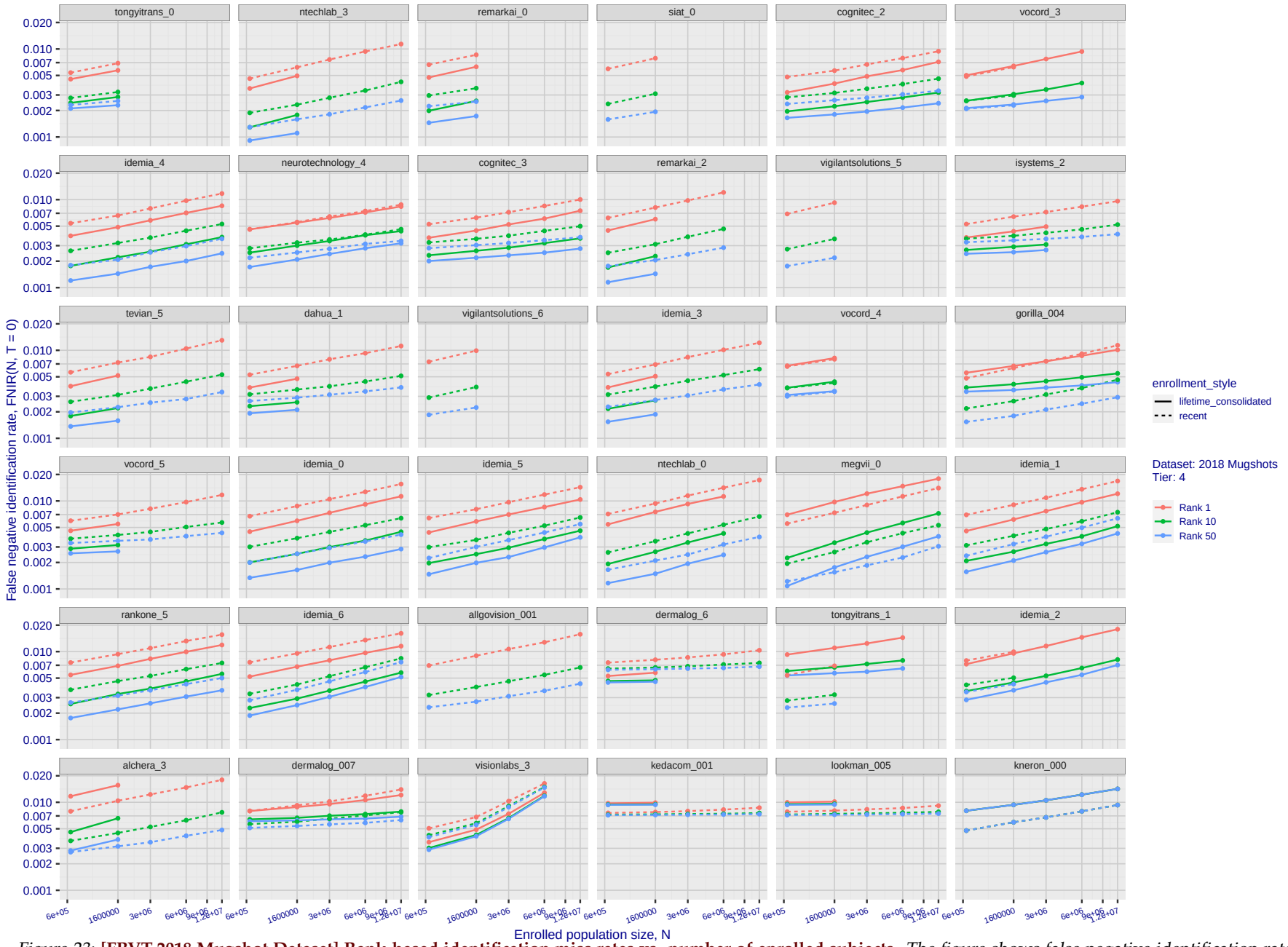

Figure 23: **[FRVT-2018 Mugshot Dataset] Rank-based identification miss rates vs. number of enrolled subjects**. *The figure shows false negative identification rates, FNIR(N, R), across various gallery sizes and ranks 1, 10 and 50. The threshold is set to zero, so this metric rewards even weak scoring rank 1 mates. This also means FPIR = 1, so any search without an enrolled mate will return non-mated candidates. For clarity, results are sorted and reported into tiers spanning multiple pages, the tiering criteria being rank 1 hit rate on a gallery size of 640 000.*

2021/08/05 02:00:58

FNIR(N, R, T) = False neg. identification rate
FPIR(N, T) = False pos. identification rate

N = Num. enrolled subjects
R = Num. candidates examined

T = Threshold

T = 0 → Investigation
T > 0 → Identification

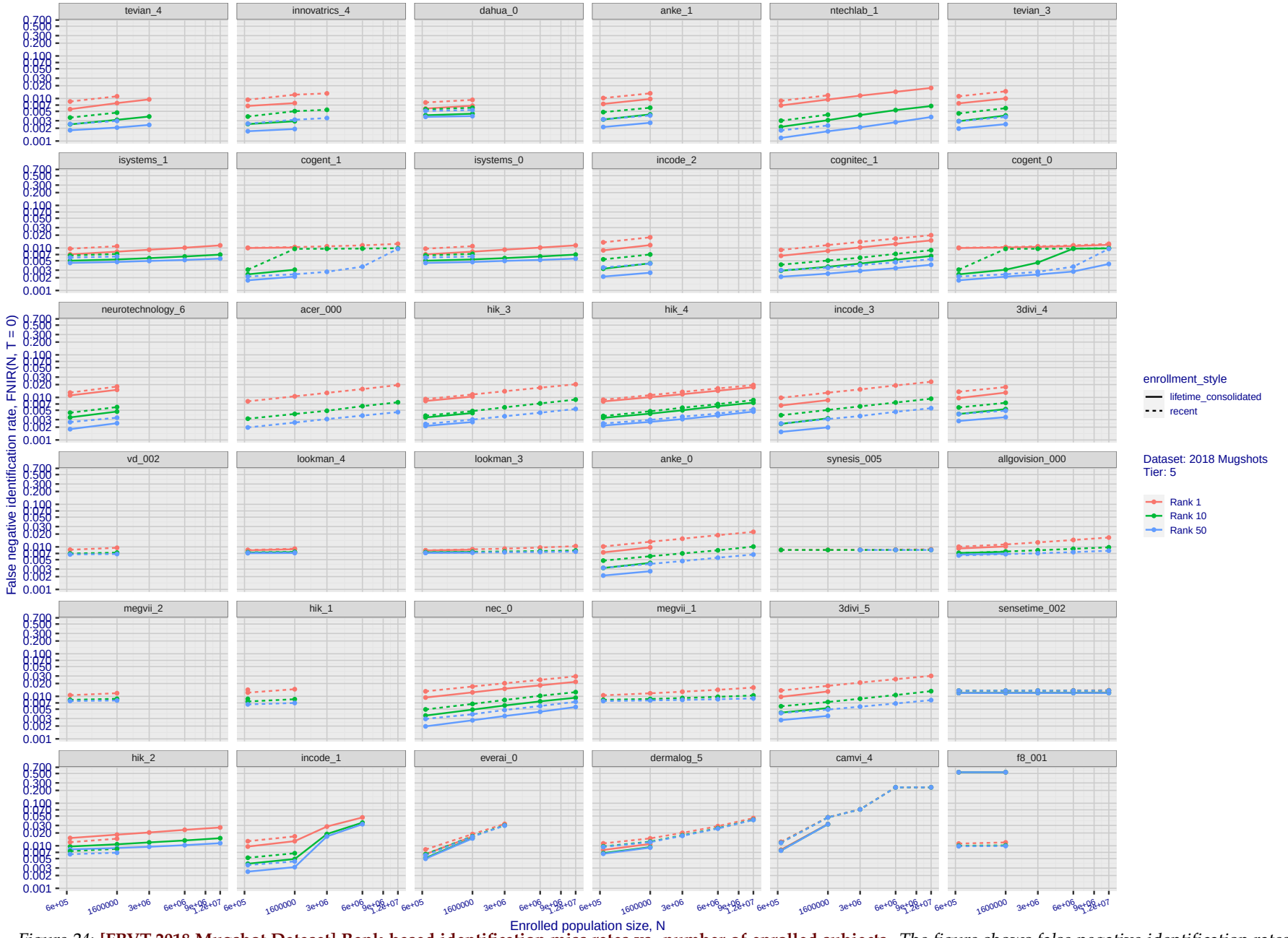

Figure 24: **[FRVT-2018 Mugshot Dataset] Rank-based identification miss rates vs. number of enrolled subjects**. *The figure shows false negative identification rates, FNIR(N, R), across various gallery sizes and ranks 1, 10 and 50. The threshold is set to zero, so this metric rewards even weak scoring rank 1 mates. This also means FPIR = 1, so any search without an enrolled mate will return non-mated candidates. For clarity, results are sorted and reported into tiers spanning multiple pages, the tiering criteria being rank 1 hit rate on a gallery size of 640 000.*

2021/08/05 02:00:58

FNIR(N, R, T) = False neg. identification rate
FPIR(N, T) = False pos. identification rate

N = Num. enrolled subjects
R = Num. candidates examined

T = Threshold

T = 0 → Investigation
T > 0 → Identification

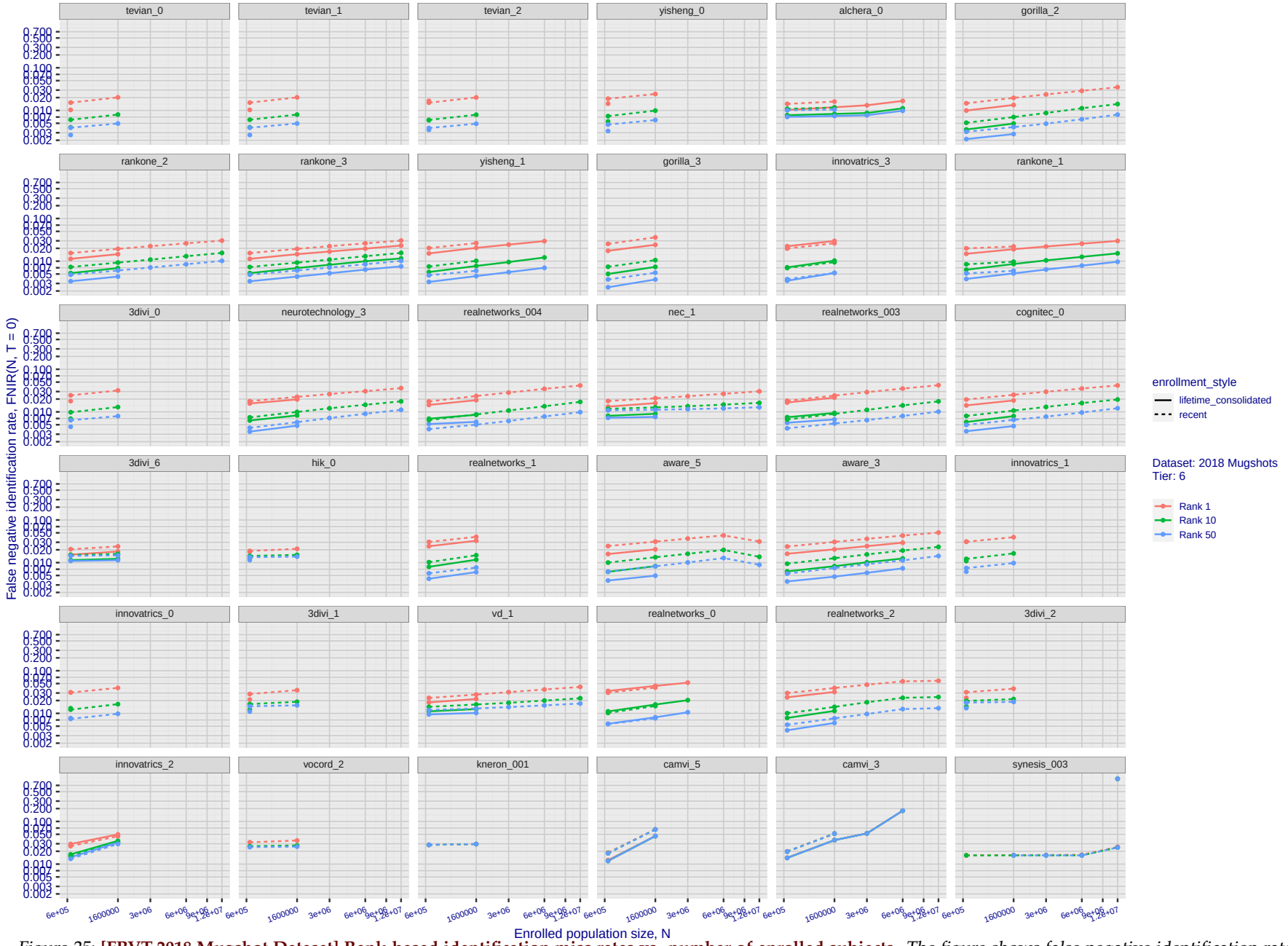

Figure 25: **[FRVT-2018 Mugshot Dataset] Rank-based identification miss rates vs. number of enrolled subjects**. *The figure shows false negative identification rates, FNIR(N, R), across various gallery sizes and ranks 1, 10 and 50. The threshold is set to zero, so this metric rewards even weak scoring rank 1 mates. This also means FPIR = 1, so any search without an enrolled mate will return non-mated candidates. For clarity, results are sorted and reported into tiers spanning multiple pages, the tiering criteria being rank 1 hit rate on a gallery size of 640 000.*

2021/08/05 02:00:58

FNIR(N, R, T) = False neg. identification rate
FPIR(N, T) = False pos. identification rate

N = Num. enrolled subjects
R = Num. candidates examined

T = Threshold

T = 0 → Investigation
T > 0 → Identification

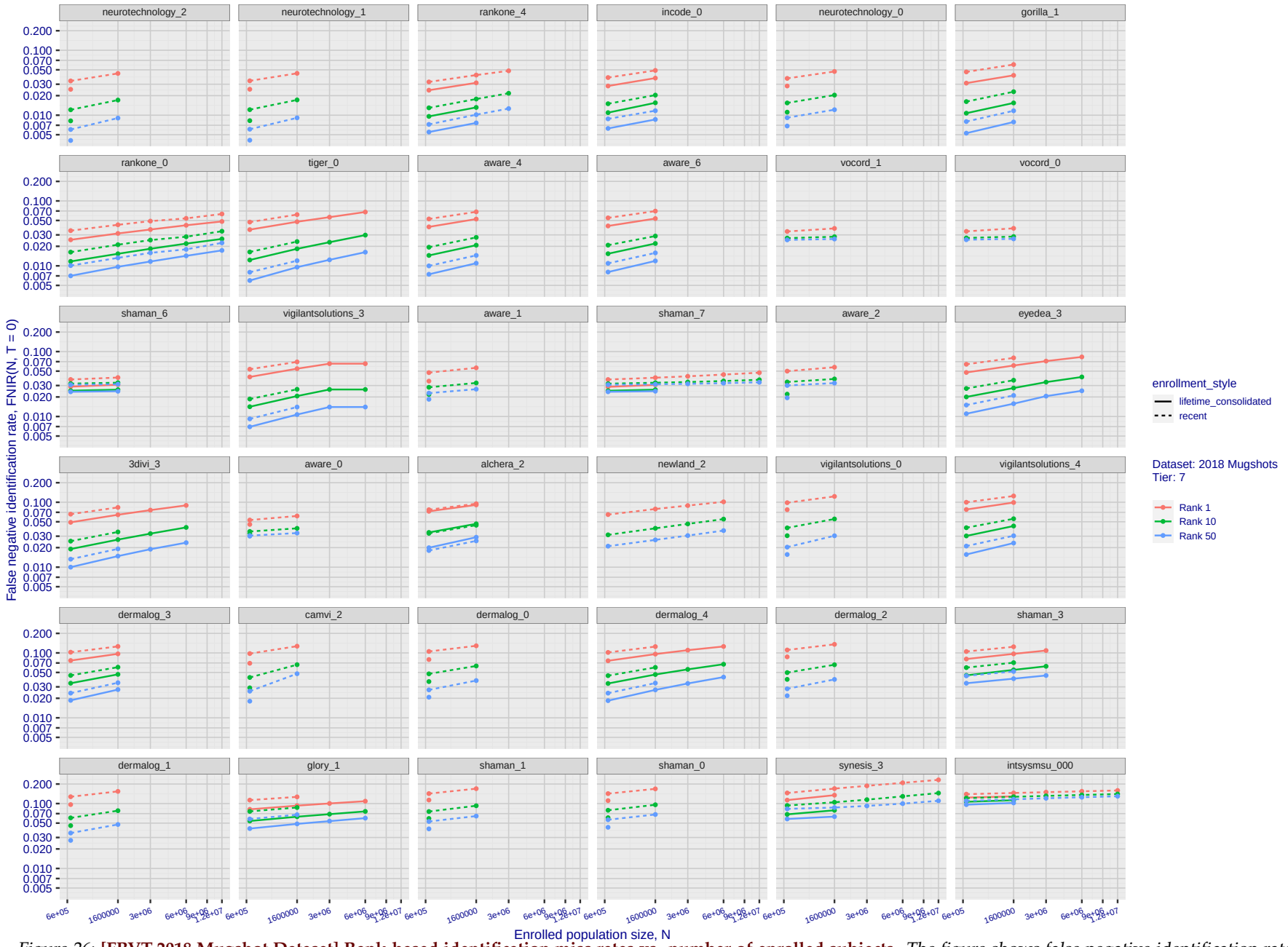

Figure 26: **[FRVT-2018 Mugshot Dataset] Rank-based identification miss rates vs. number of enrolled subjects**. *The figure shows false negative identification rates, FNIR(N, R), across various gallery sizes and ranks 1, 10 and 50. The threshold is set to zero, so this metric rewards even weak scoring rank 1 mates. This also means FPIR = 1, so any search without an enrolled mate will return non-mated candidates. For clarity, results are sorted and reported into tiers spanning multiple pages, the tiering criteria being rank 1 hit rate on a gallery size of 640 000.*

2021/08/05 02:00:58
FNIR(N, R, T) = False neg. identification rate
FPIR(N, T) = False pos. identification rate
N = Num. enrolled subjects
R = Num. candidates examined
T = Threshold
T = 0 → Investigation
T > 0 → Identification

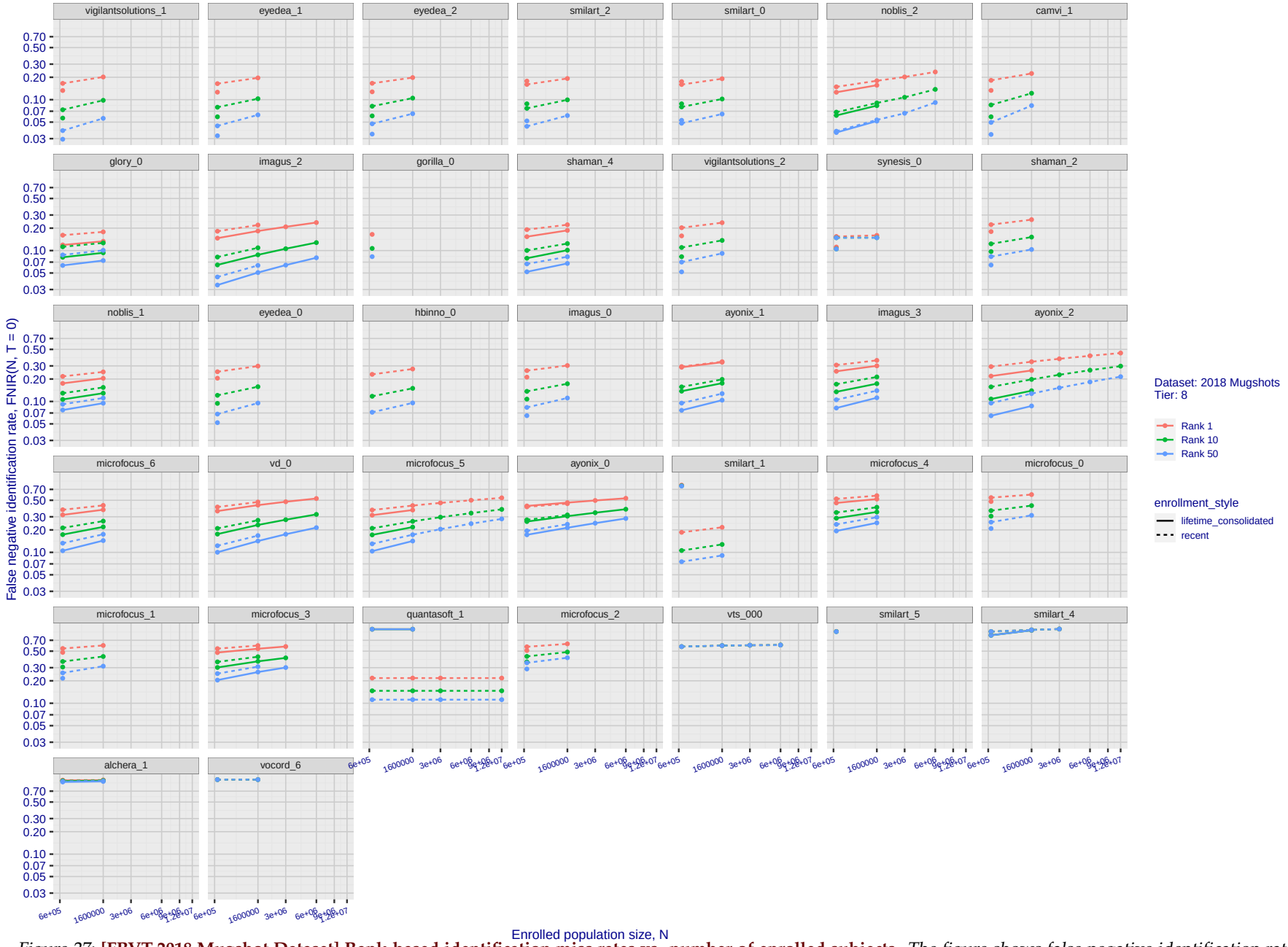

Figure 27: **[FRVT-2018 Mugshot Dataset] Rank-based identification miss rates vs. number of enrolled subjects**. *The figure shows false negative identification rates, FNIR(N, R), across various gallery sizes and ranks 1, 10 and 50. The threshold is set to zero, so this metric rewards even weak scoring rank 1 mates. This also means FPIR = 1, so any search without an enrolled mate will return non-mated candidates. For clarity, results are sorted and reported into tiers spanning multiple pages, the tiering criteria being rank 1 hit rate on a gallery size of 640 000.*

2021/08/05	FNIR(N, R, T) =	False neg. identification rate	N = Num. enrolled subjects	T = Threshold	$T = 0 \rightarrow$ Investigation
02:00:58	FPIR(N, T) =	False pos. identification rate	R = Num. candidates examined		$T > 0 \rightarrow$ Identification

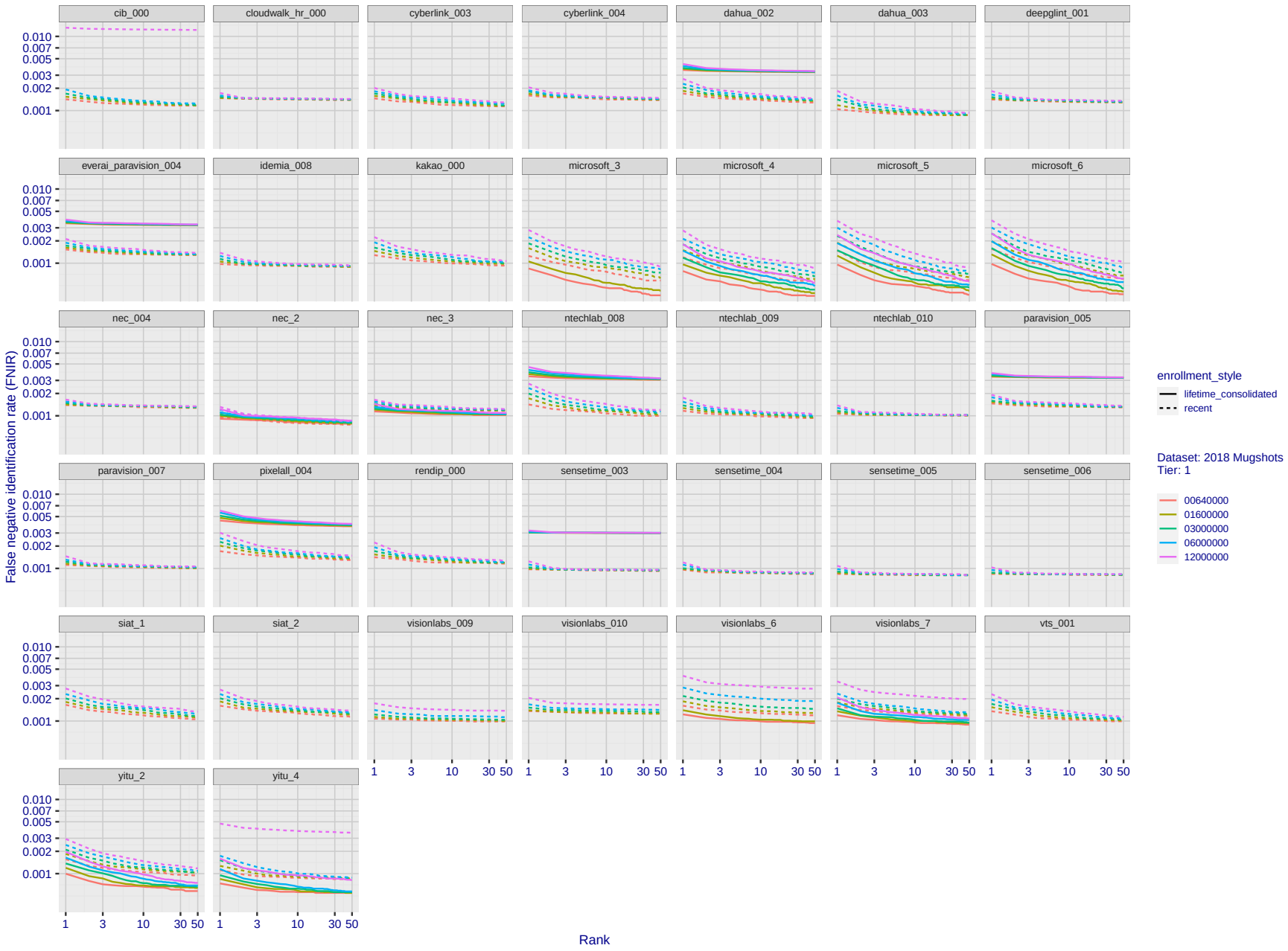

Figure 28: **[FRVT-2018 Mugshot Dataset] Rank-based identification miss rates vs. rank**. *The figure shows false negative identification rates (FNIR) for ranks up to 50. This metric is appropriate to investigational applications where human reviewers will adjudicate sorted candidate lists. Note that with threshold set to zero, FPIR = 1, i.e. any search without an enrolled mate will return non-mated candidates. Results are sorted and reported into tiers for clarity, with the tiering criteria being rank 1 hit rate on a gallery size of N = 640 000 subjects.*

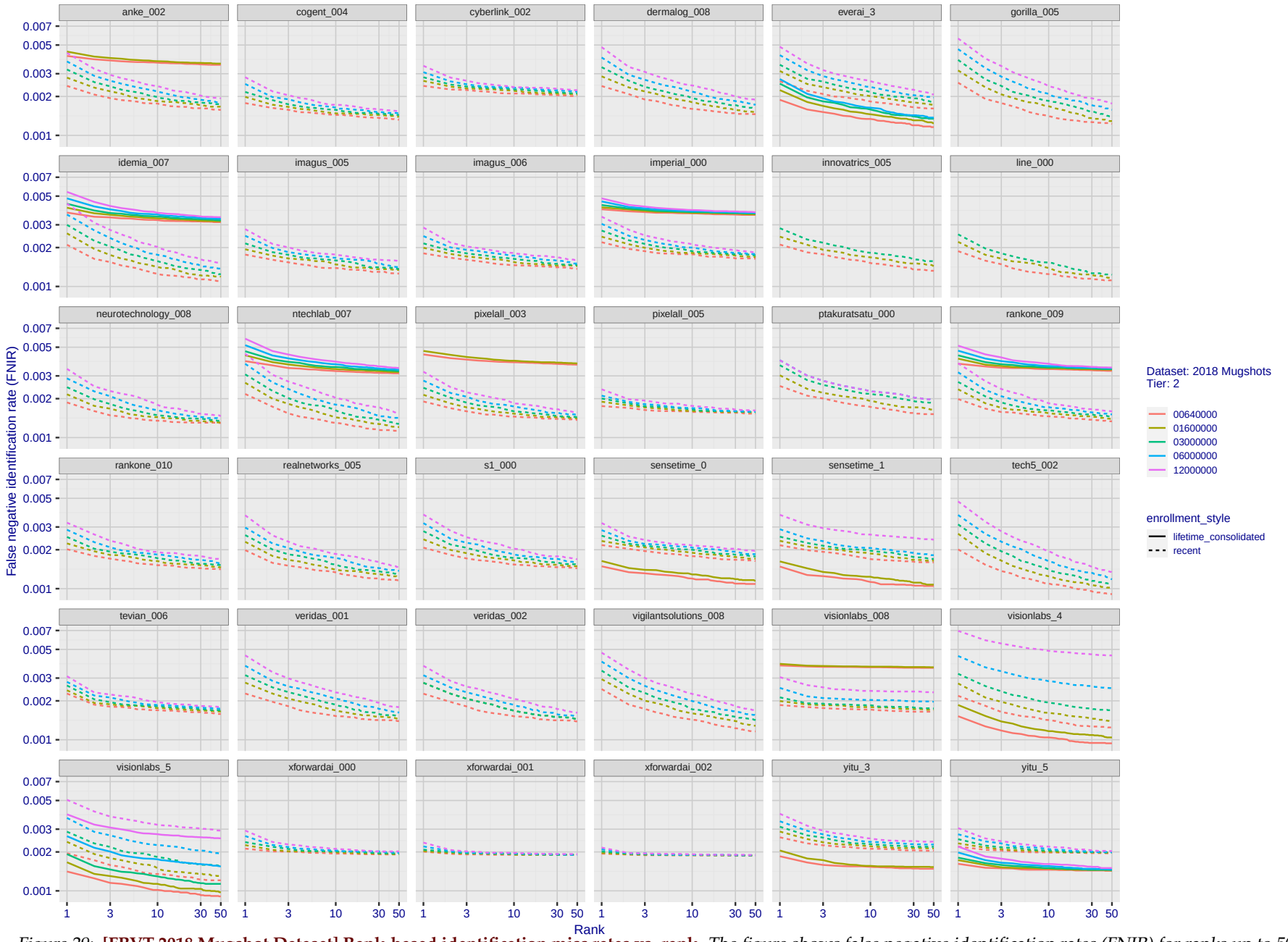

Figure 29: **[FRVT-2018 Mugshot Dataset] Rank-based identification miss rates vs. rank**. *The figure shows false negative identification rates (FNIR) for ranks up to 50. This metric is appropriate to investigational applications where human reviewers will adjudicate sorted candidate lists. Note that with threshold set to zero, FPIR = 1, i.e. any search without an enrolled mate will return non-mated candidates. Results are sorted and reported into tiers for clarity, with the tiering criteria being rank 1 hit rate on a gallery size of N = 640 000 subjects.*

2021/08/05 02:00:58
FNIR(N, R, T) = False neg. identification rate
FPIR(N, T) = False pos. identification rate
N = Num. enrolled subjects
R = Num. candidates examined
T = Threshold
T = 0 → Investigation
T > 0 → Identification

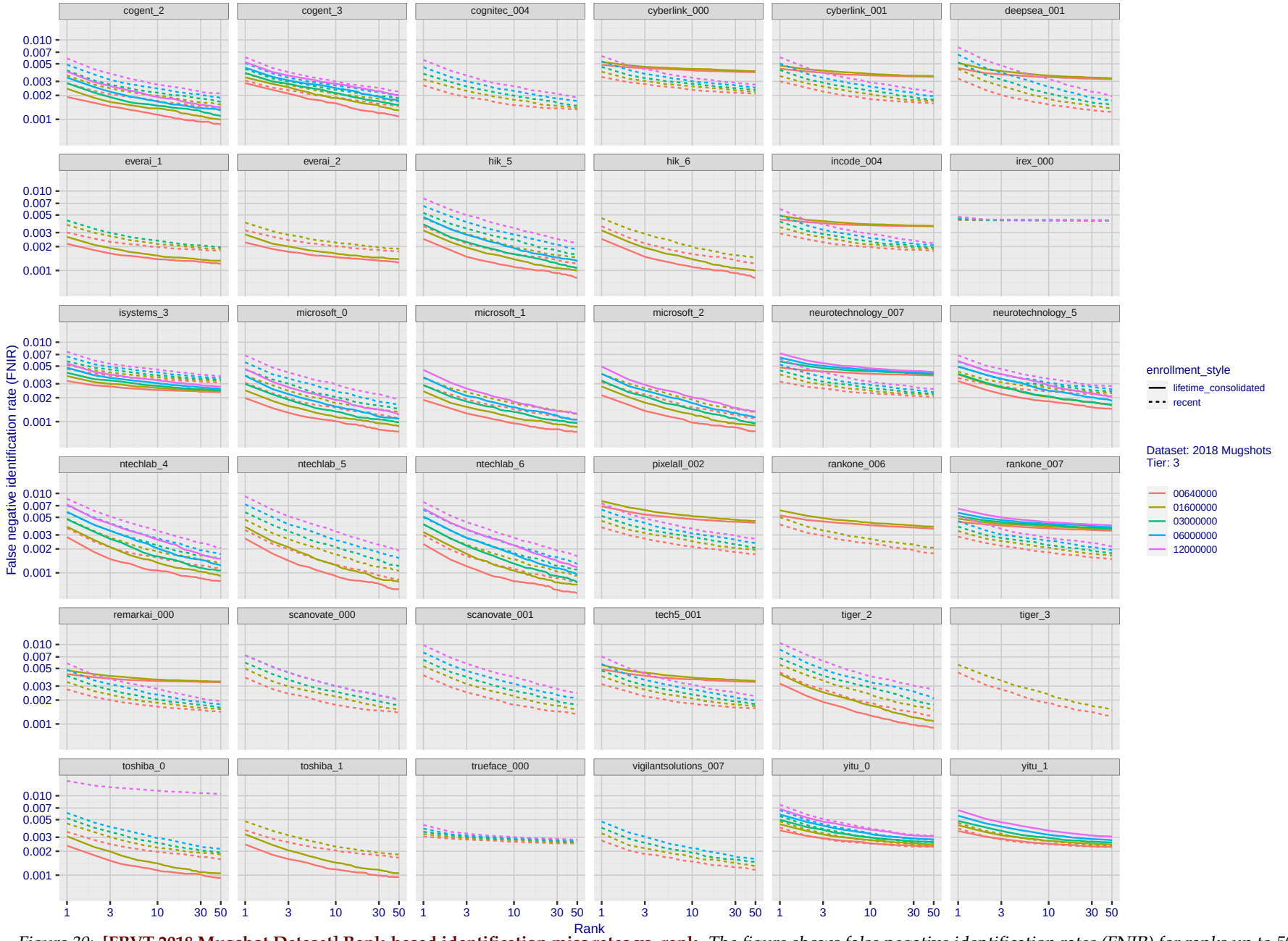

Figure 30: **[FRVT-2018 Mugshot Dataset] Rank-based identification miss rates vs. rank**. *The figure shows false negative identification rates (FNIR) for ranks up to 50. This metric is appropriate to investigational applications where human reviewers will adjudicate sorted candidate lists. Note that with threshold set to zero, FPIR = 1, i.e. any search without an enrolled mate will return non-mated candidates. Results are sorted and reported into tiers for clarity, with the tiering criteria being rank 1 hit rate on a gallery size of N = 640 000 subjects.*

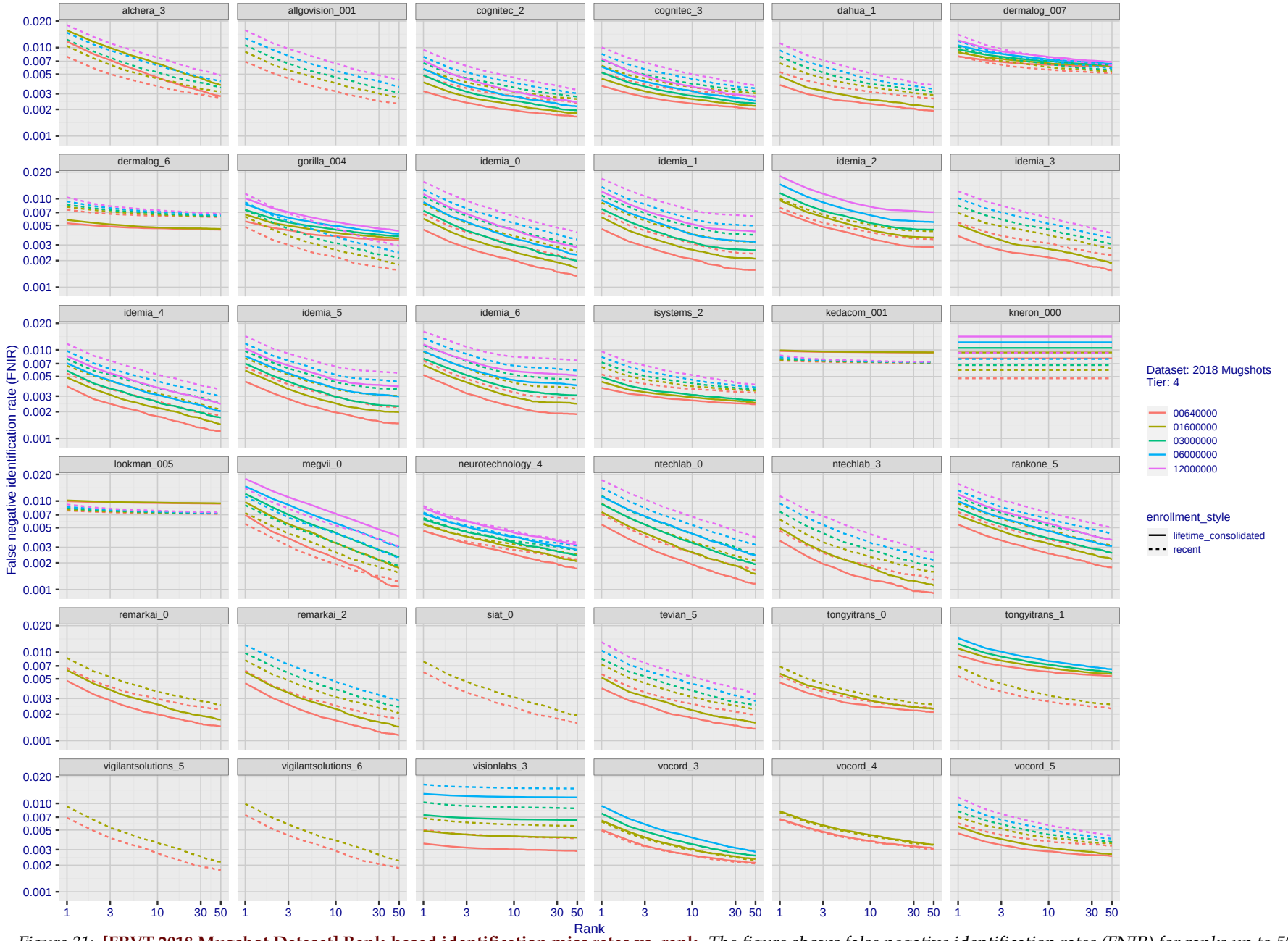

Figure 31: **[FRVT-2018 Mugshot Dataset] Rank-based identification miss rates vs. rank**. *The figure shows false negative identification rates (FNIR) for ranks up to 50. This metric is appropriate to investigational applications where human reviewers will adjudicate sorted candidate lists. Note that with threshold set to zero, FPIR = 1, i.e. any search without an enrolled mate will return non-mated candidates. Results are sorted and reported into tiers for clarity, with the tiering criteria being rank 1 hit rate on a gallery size of N = 640 000 subjects.*

2021/08/05 02:00:58

FNIR(N, R, T) = False neg. identification rate
FPIR(N, T) = False pos. identification rate

N = Num. enrolled subjects
R = Num. candidates examined

T = Threshold

T = 0 → Investigation
T > 0 → Identification

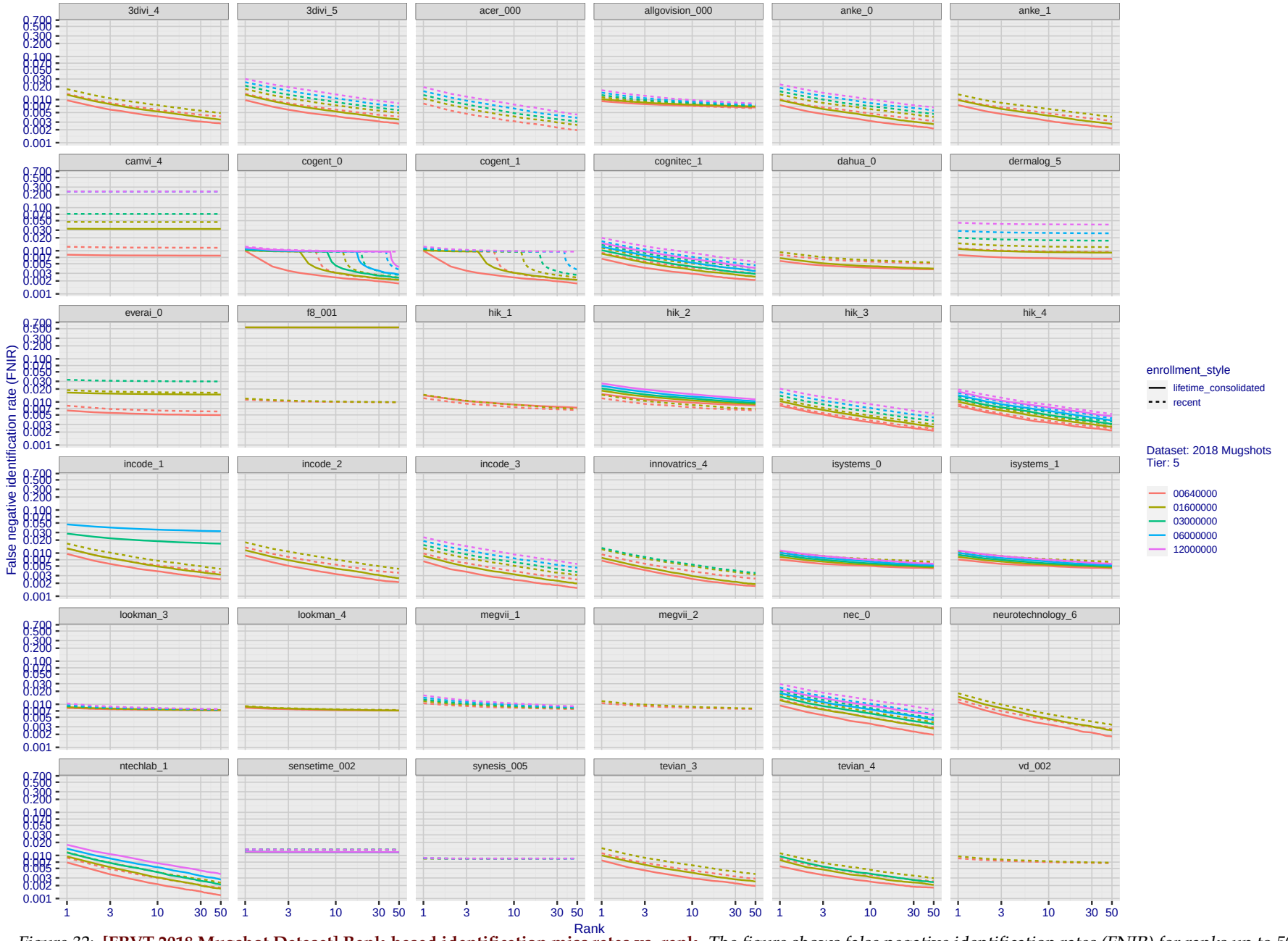

Figure 32: **[FRVT-2018 Mugshot Dataset] Rank-based identification miss rates vs. rank**. *The figure shows false negative identification rates (FNIR) for ranks up to 50. This metric is appropriate to investigational applications where human reviewers will adjudicate sorted candidate lists. Note that with threshold set to zero, FPIR = 1, i.e. any search without an enrolled mate will return non-mated candidates. Results are sorted and reported into tiers for clarity, with the tiering criteria being rank 1 hit rate on a gallery size of N = 640 000 subjects.*

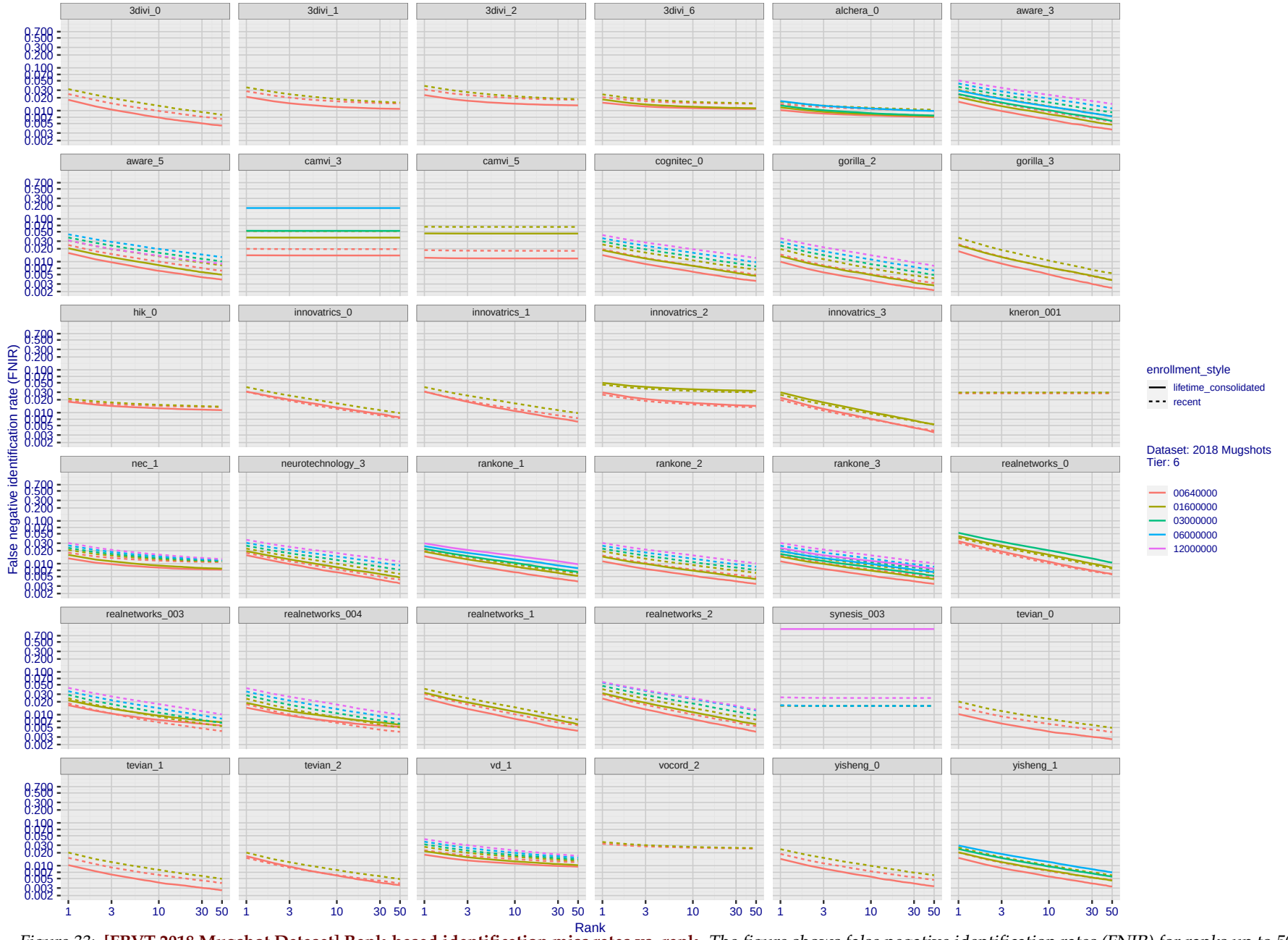

Figure 33: **[FRVT-2018 Mugshot Dataset] Rank-based identification miss rates vs. rank**. *The figure shows false negative identification rates (FNIR) for ranks up to 50. This metric is appropriate to investigational applications where human reviewers will adjudicate sorted candidate lists. Note that with threshold set to zero, FPIR = 1, i.e. any search without an enrolled mate will return non-mated candidates. Results are sorted and reported into tiers for clarity, with the tiering criteria being rank 1 hit rate on a gallery size of N = 640 000 subjects.*

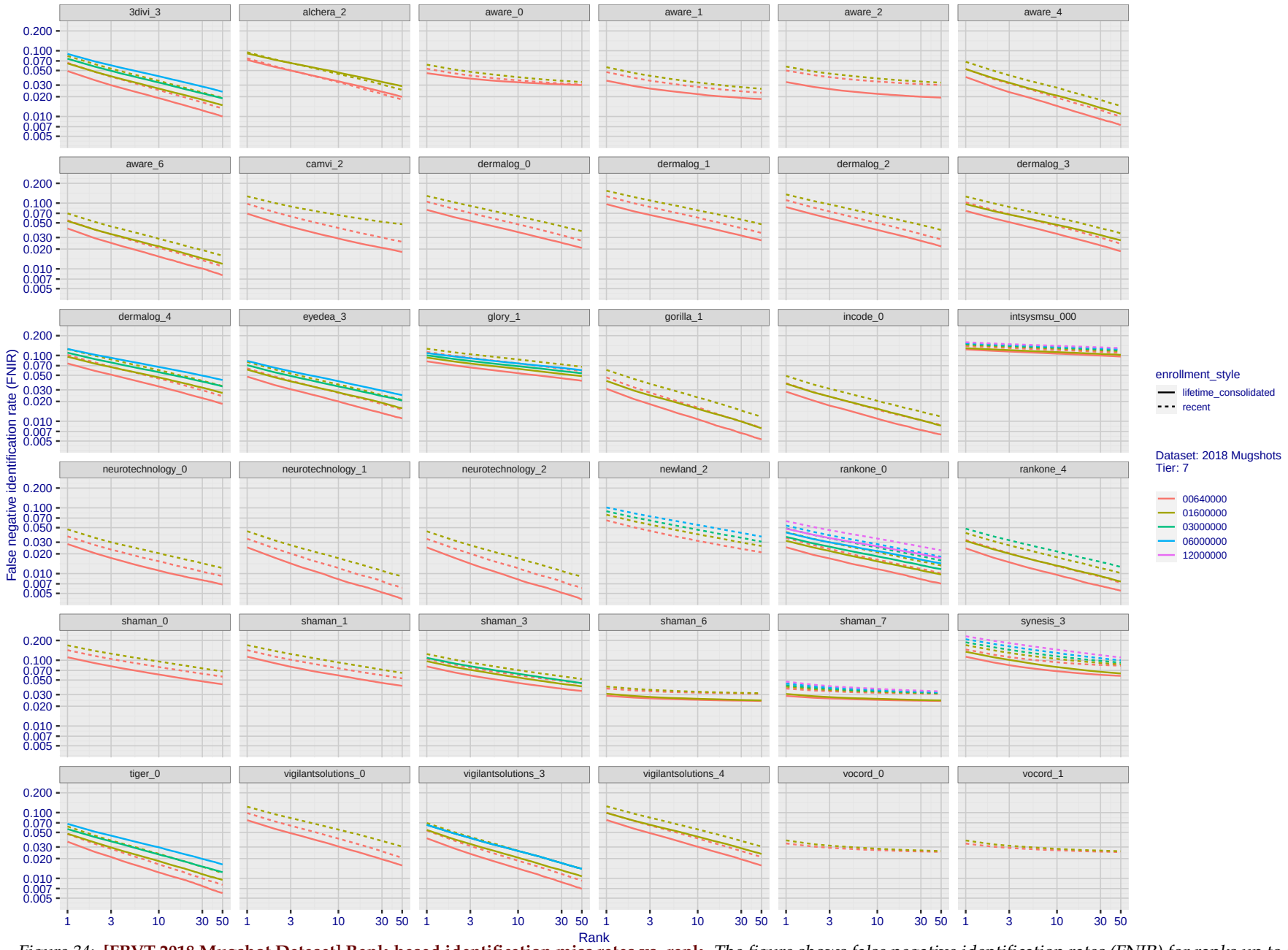

Figure 34: **[FRVT-2018 Mugshot Dataset] Rank-based identification miss rates vs. rank**. *The figure shows false negative identification rates (FNIR) for ranks up to 50. This metric is appropriate to investigational applications where human reviewers will adjudicate sorted candidate lists. Note that with threshold set to zero, FPIR = 1, i.e. any search without an enrolled mate will return non-mated candidates. Results are sorted and reported into tiers for clarity, with the tiering criteria being rank 1 hit rate on a gallery size of N = 640 000 subjects.*

2021/08/05 02:00:58

FNIR(N, R, T) = False neg. identification rate
FPIR(N, T) = False pos. identification rate

N = Num. enrolled subjects
R = Num. candidates examined

T = Threshold

T = 0 → Investigation
T > 0 → Identification

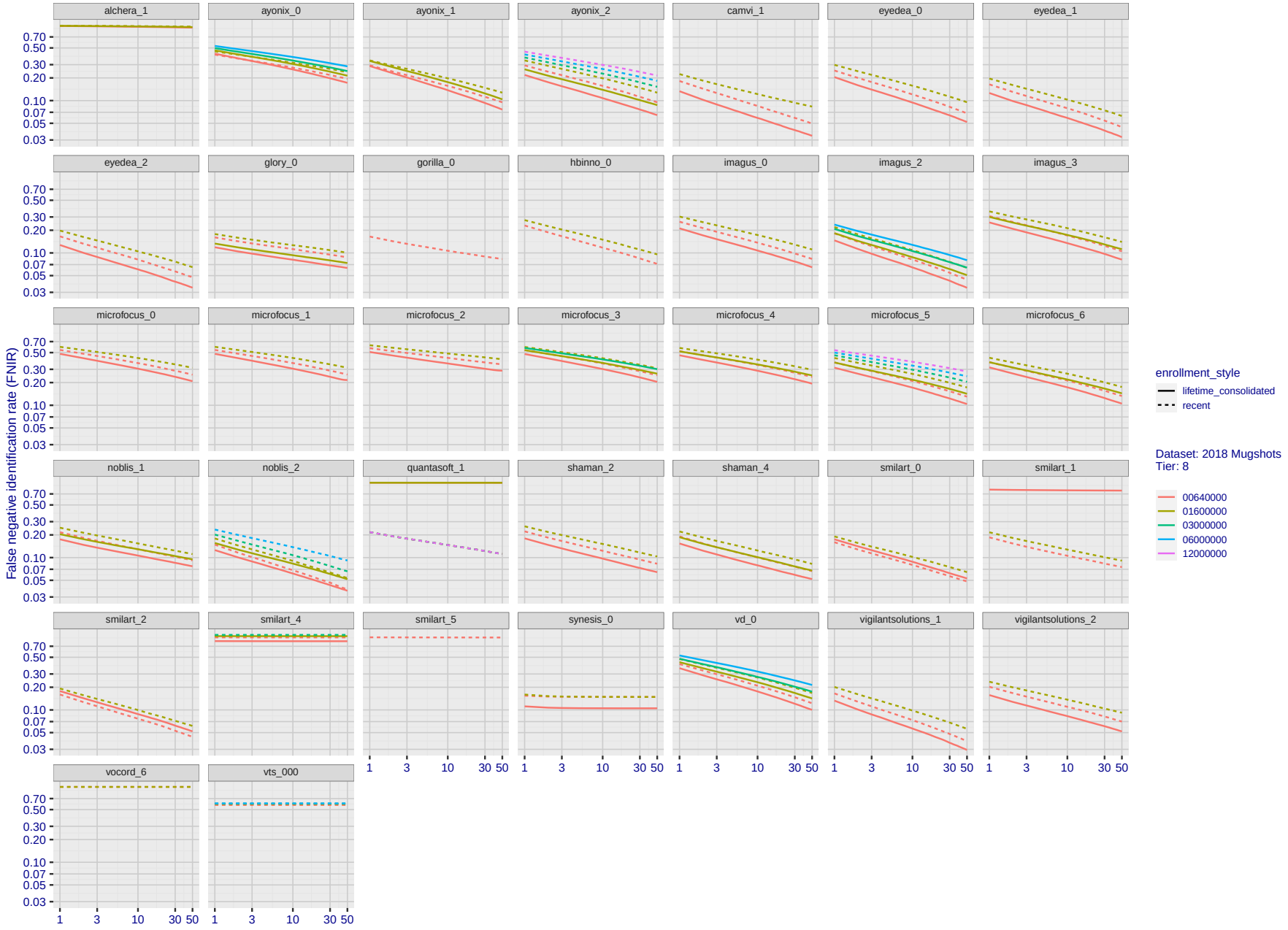

Figure 35: **[FRVT-2018 Mugshot Dataset] Rank-based identification miss rates vs. rank**. *The figure shows false negative identification rates (FNIR) for ranks up to 50. This metric is appropriate to investigational applications where human reviewers will adjudicate sorted candidate lists. Note that with threshold set to zero, FPIR = 1, i.e. any search without an enrolled mate will return non-mated candidates. Results are sorted and reported into tiers for clarity, with the tiering criteria being rank 1 hit rate on a gallery size of N = 640 000 subjects.*

2021/08/05	FNIR(N, R, T) =	False neg. identification rate	N = Num. enrolled subjects	T = Threshold	$T = 0 \rightarrow$ Investigation
02:00:58	FPIR(N, T) =	False pos. identification rate	R = Num. candidates examined		$T > 0 \rightarrow$ Identification

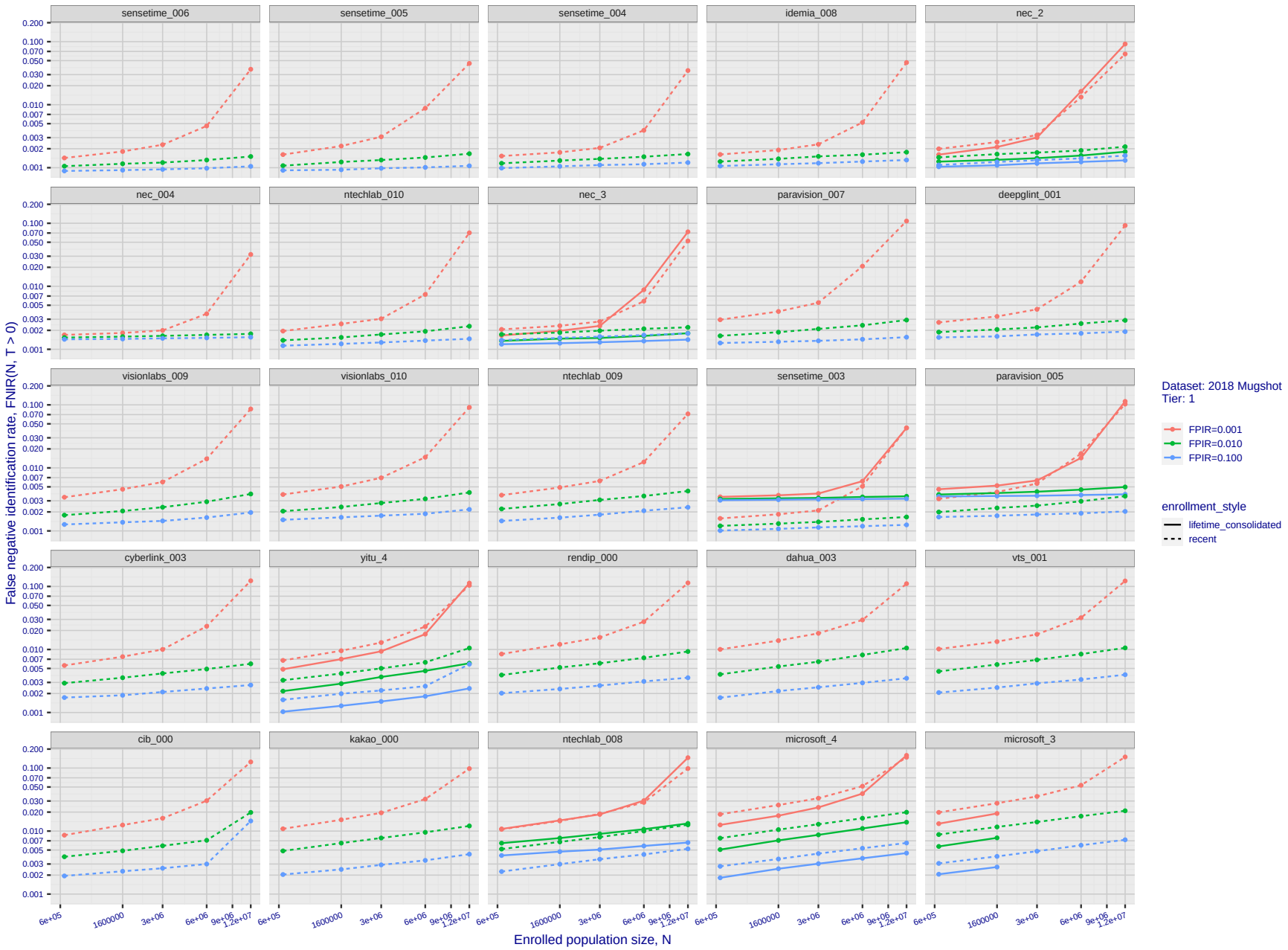

Figure 36: **[FRVT-2018 Mugshot Dataset] Threshold-based identification miss rates vs. number of enrolled subjects**. *The figure shows FNIR(N, T) across various gallery sizes when the threshold is set to achieve the given FPIRs. The rank criterion is irrelevant at high thresholds as mates are always at rank 1. The results are computed from the trials listed in rows 1-10 of Table 1. Less accurate algorithms were not run on large N, so results are missing. For clarity, results are sorted and reported into tiers spanning multiple pages. The tiering criteria is complicated: First paging by FNIR(N_b, 1, 0), then sorting by median FNIR(N_b, T), N_b = 640 000.*

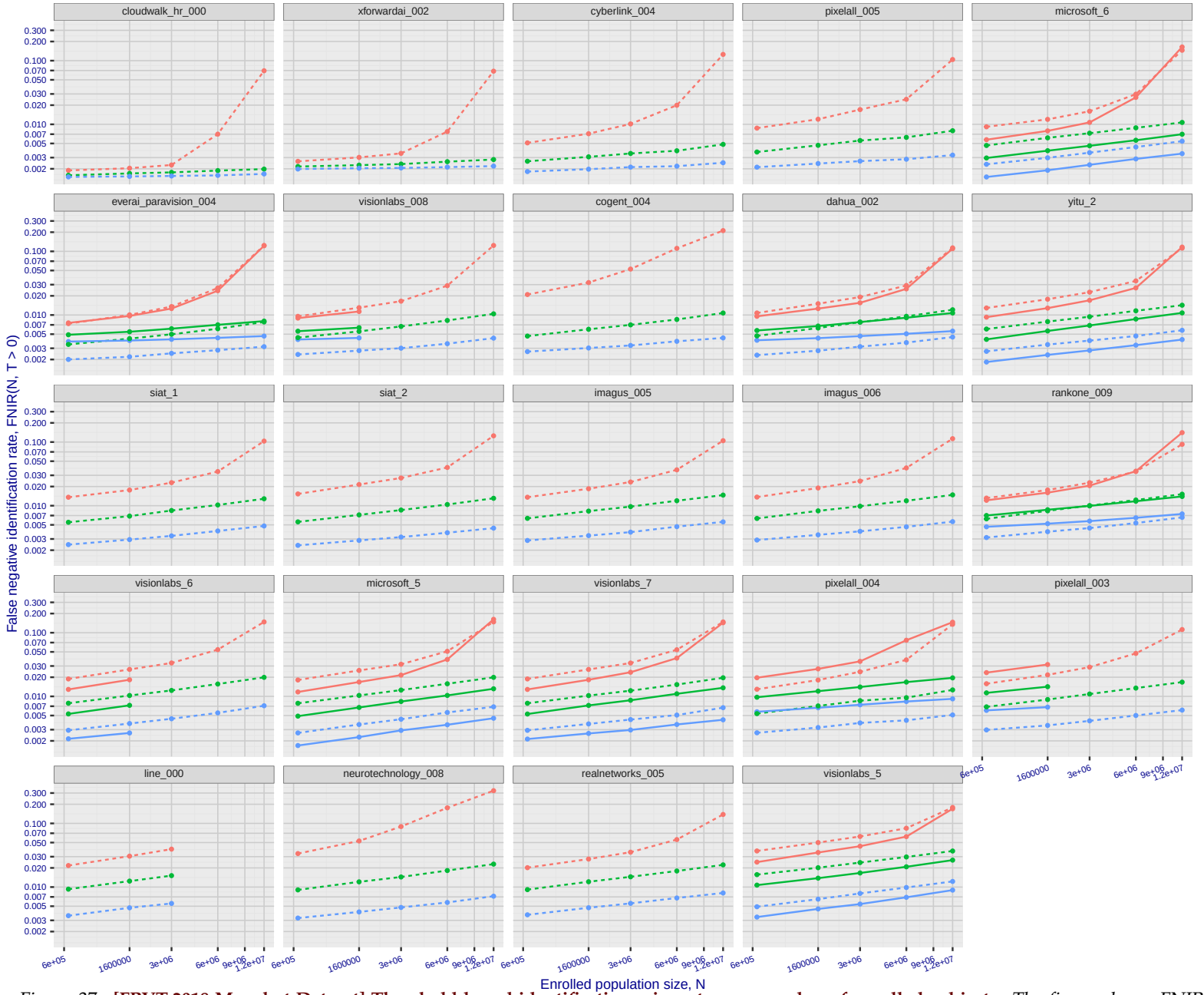

Figure 37: **[FRVT-2018 Mugshot Dataset] Threshold-based identification miss rates vs. number of enrolled subjects**. *The figure shows FNIR(N, T) across various gallery sizes when the threshold is set to achieve the given FPIRs. The rank criterion is irrelevant at high thresholds as mates are always at rank 1. The results are computed from the trials listed in rows 1-10 of Table 1. Less accurate algorithms were not run on large N, so results are missing. For clarity, results are sorted and reported into tiers spanning multiple pages. The tiering criteria is complicated: First paging by FNIR(N_b, 1, 0), then sorting by median FNIR(N_b, T), N_b = 640 000.*

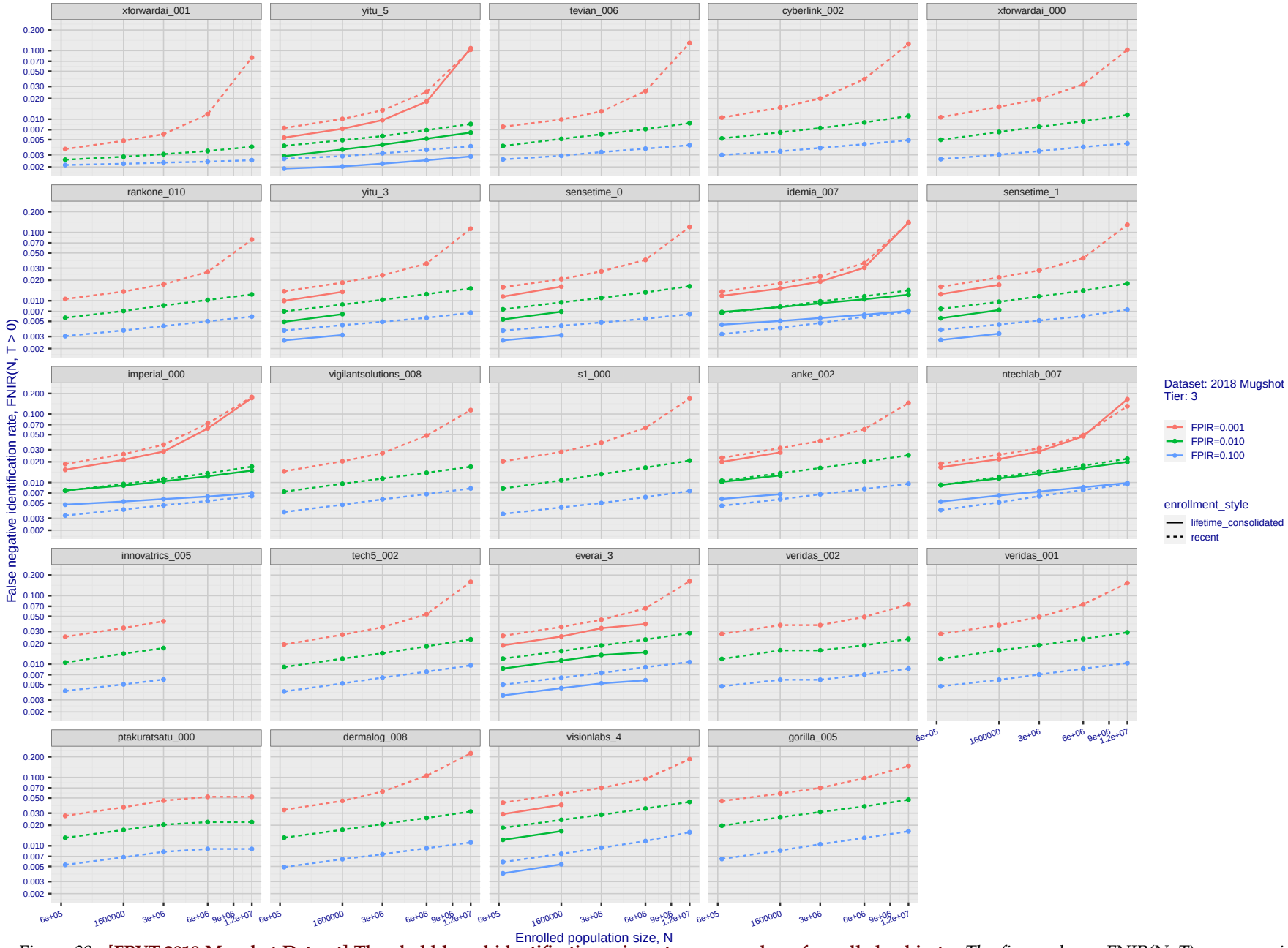

Figure 38: **[FRVT-2018 Mugshot Dataset] Threshold-based identification miss rates vs. number of enrolled subjects**. *The figure shows FNIR(N, T) across various gallery sizes when the threshold is set to achieve the given FPIRs. The rank criterion is irrelevant at high thresholds as mates are always at rank 1. The results are computed from the trials listed in rows 1-10 of Table 1. Less accurate algorithms were not run on large N, so results are missing. For clarity, results are sorted and reported into tiers spanning multiple pages. The tiering criteria is complicated: First paging by FNIR(N_b, 1, 0), then sorting by median FNIR(N_b, T), N_b = 640 000.*

2021/08/05 02:00:58

FNIR(N, R, T) = False neg. identification rate
FPIR(N, T) = False pos. identification rate

N = Num. enrolled subjects
R = Num. candidates examined

T = Threshold

T = 0 → Investigation
T > 0 → Identification

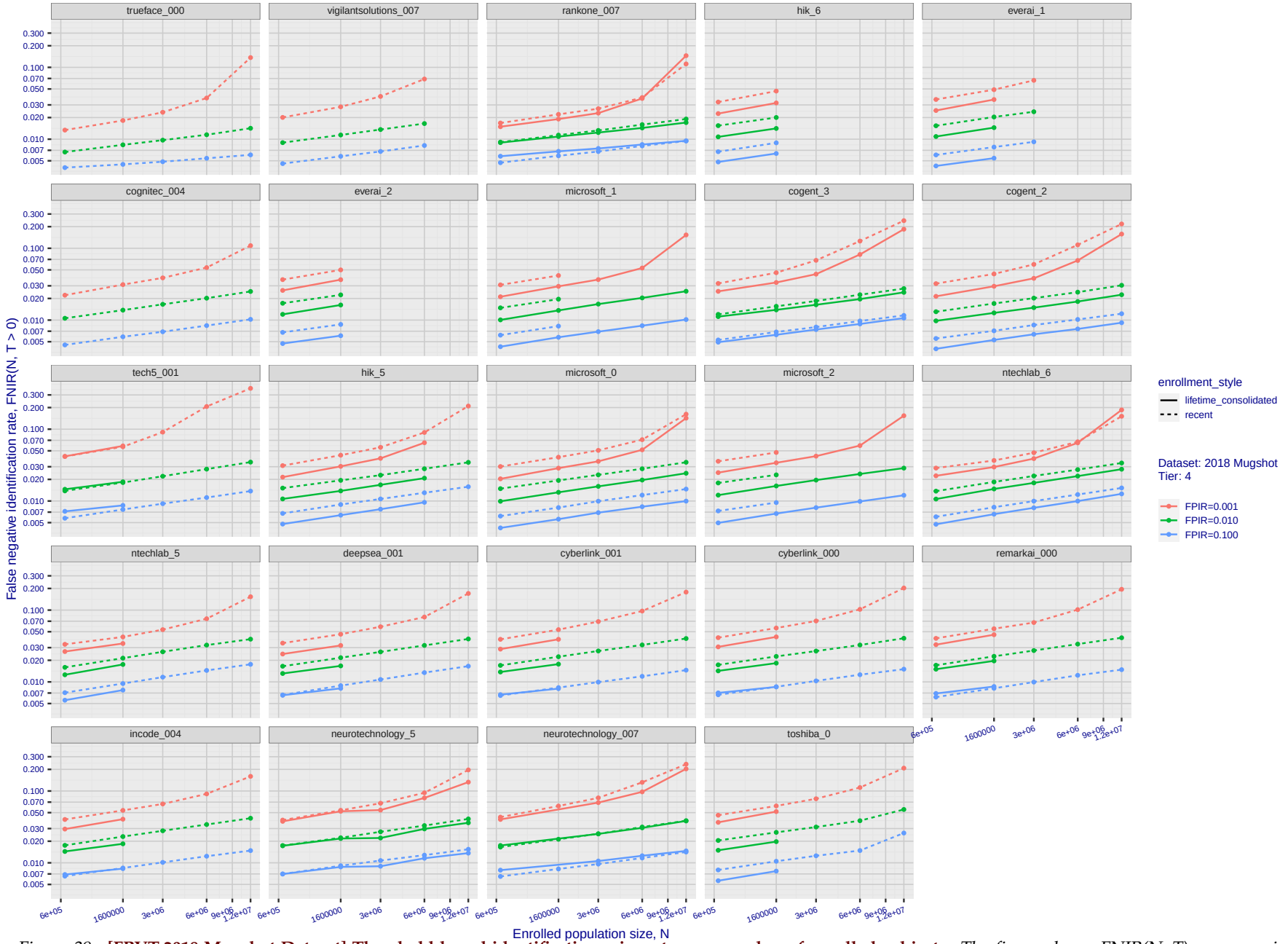

Figure 39: **[FRVT-2018 Mugshot Dataset] Threshold-based identification miss rates vs. number of enrolled subjects**. *The figure shows FNIR(N, T) across various gallery sizes when the threshold is set to achieve the given FPIRs. The rank criterion is irrelevant at high thresholds as mates are always at rank 1. The results are computed from the trials listed in rows 1-10 of Table 1. Less accurate algorithms were not run on large N, so results are missing. For clarity, results are sorted and reported into tiers spanning multiple pages. The tiering criteria is complicated: First paging by FNIR(N_b, 1, 0), then sorting by median FNIR(N_b, T), N_b = 640 000.*

2021/08/05 02:00:58
FNIR(N, R, T) = False neg. identification rate
FPIR(N, T) = False pos. identification rate
N = Num. enrolled subjects
R = Num. candidates examined
T = Threshold
T = 0 → Investigation
T > 0 → Identification

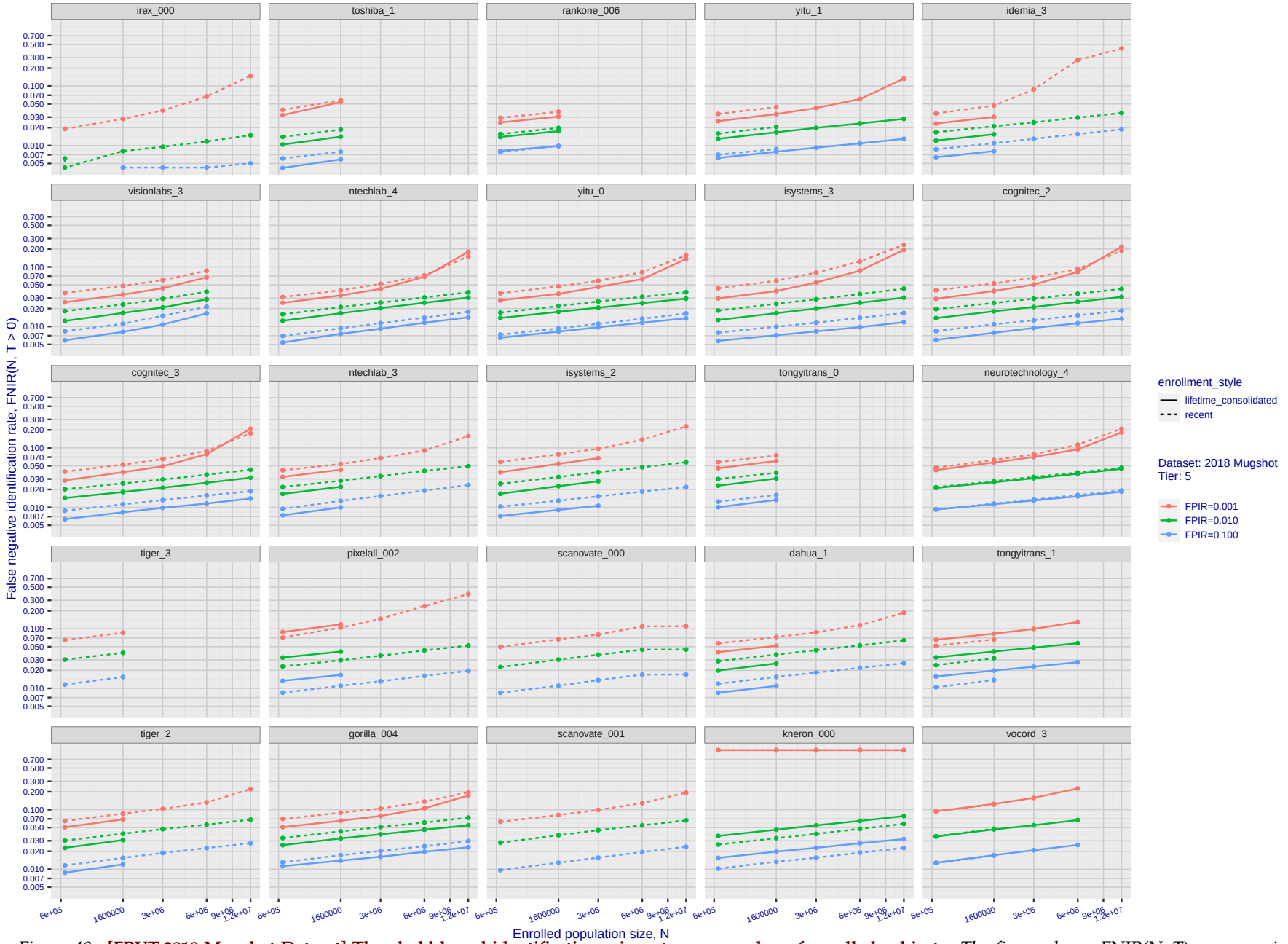

Figure 40: **[FRVT-2018 Mugshot Dataset] Threshold-based identification miss rates vs. number of enrolled subjects**. *The figure shows FNIR(N, T) across various gallery sizes when the threshold is set to achieve the given FPIRs. The rank criterion is irrelevant at high thresholds as mates are always at rank 1. The results are computed from the trials listed in rows 1-10 of Table 1. Less accurate algorithms were not run on large N, so results are missing. For clarity, results are sorted and reported into tiers spanning multiple pages. The tiering criteria is complicated: First paging by FNIR(N_b, 1, 0), then sorting by median FNIR(N_b, T), N_b = 640 000.*

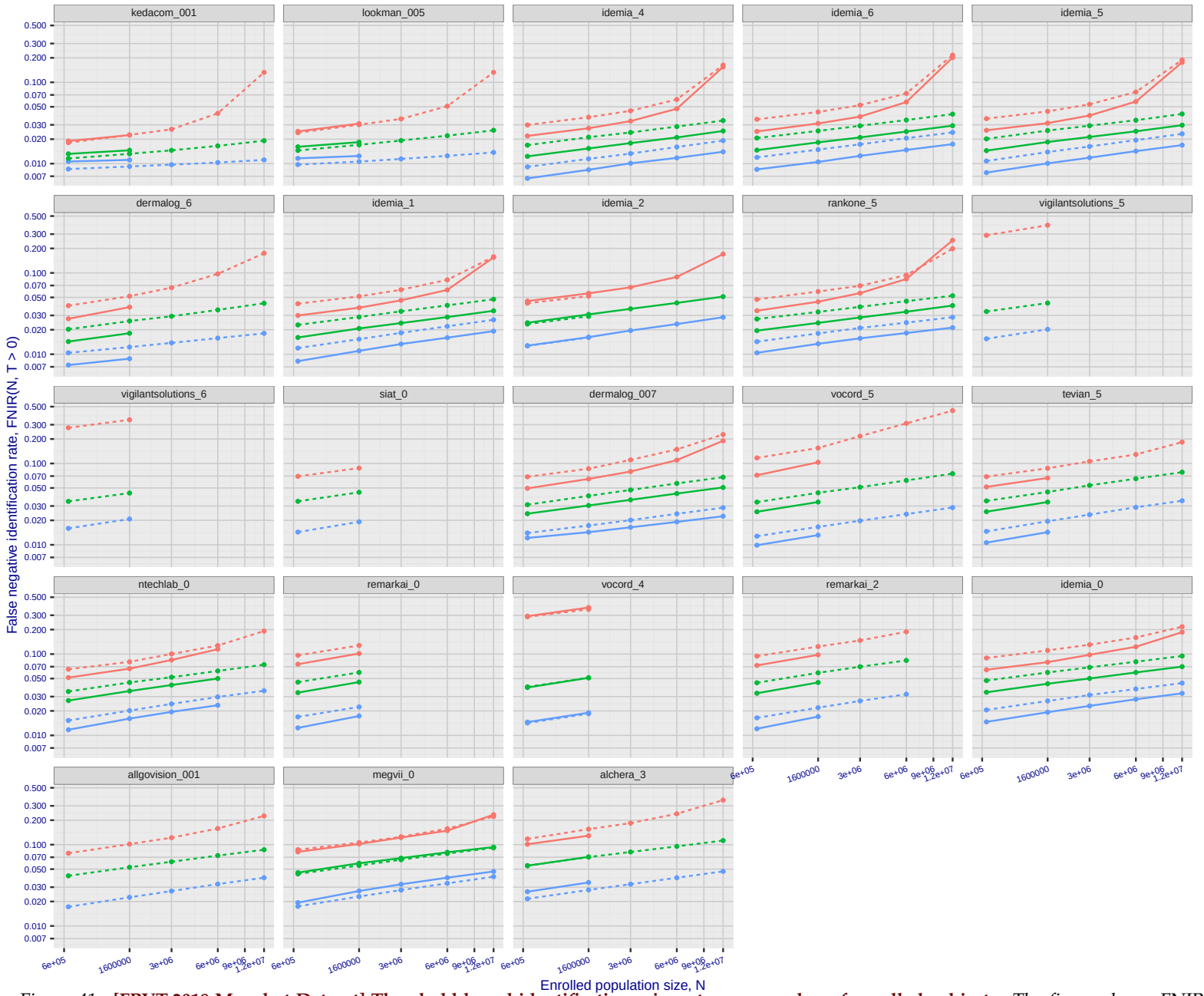

Figure 41: **[FRVT-2018 Mugshot Dataset] Threshold-based identification miss rates vs. number of enrolled subjects**. *The figure shows FNIR(N, T) across various gallery sizes when the threshold is set to achieve the given FPIRs. The rank criterion is irrelevant at high thresholds as mates are always at rank 1. The results are computed from the trials listed in rows 1-10 of Table 1. Less accurate algorithms were not run on large N, so results are missing. For clarity, results are sorted and reported into tiers spanning multiple pages. The tiering criteria is complicated: First paging by FNIR(N_b, 1, 0), then sorting by median FNIR(N_b, T), N_b = 640 000.*

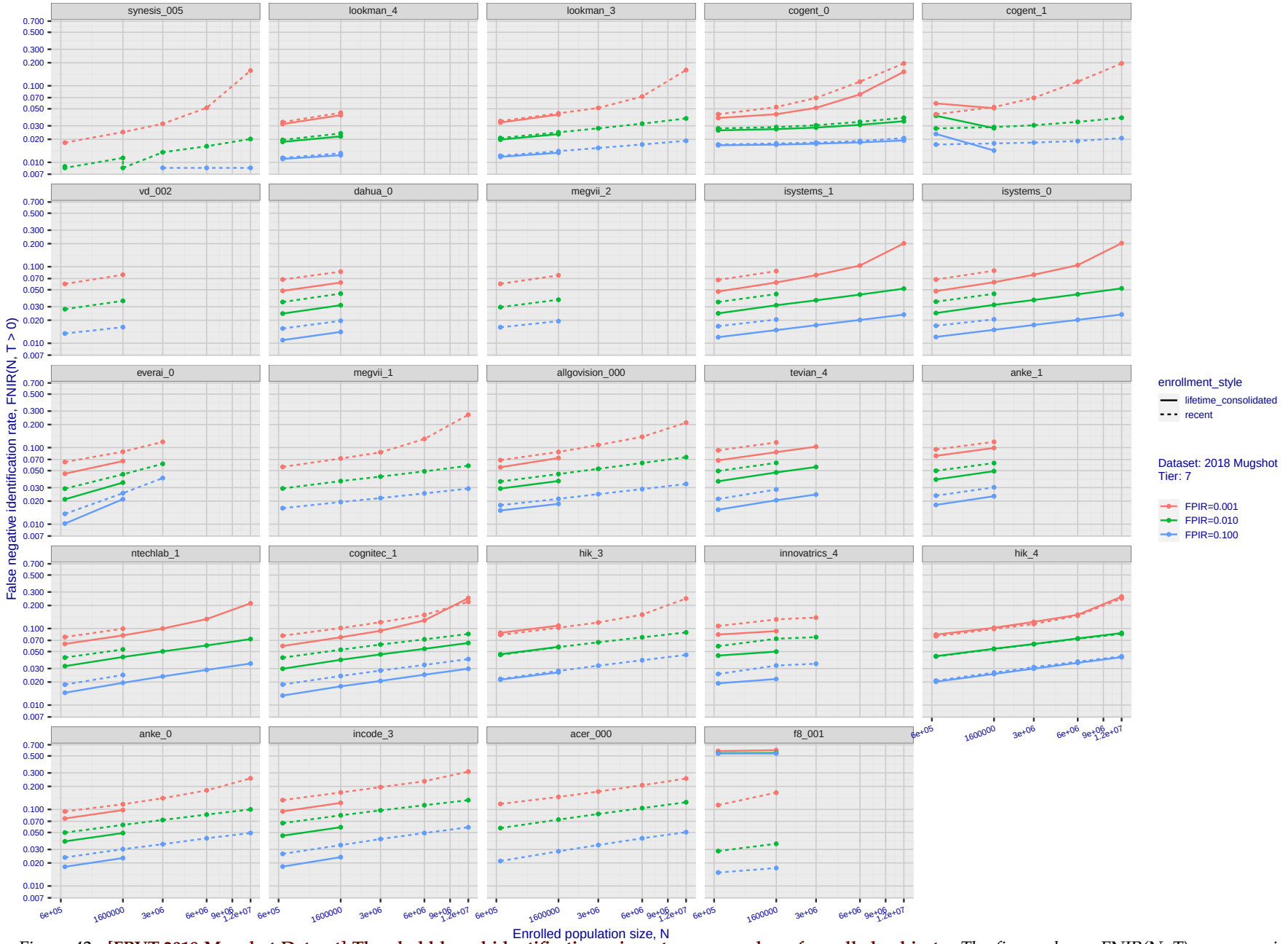

Figure 42: **[FRVT-2018 Mugshot Dataset] Threshold-based identification miss rates vs. number of enrolled subjects**. *The figure shows FNIR(N, T) across various gallery sizes when the threshold is set to achieve the given FPIRs. The rank criterion is irrelevant at high thresholds as mates are always at rank 1. The results are computed from the trials listed in rows 1-10 of Table 1. Less accurate algorithms were not run on large N, so results are missing. For clarity, results are sorted and reported into tiers spanning multiple pages. The tiering criteria is complicated: First paging by FNIR(N_b, 1, 0), then sorting by median FNIR(N_b, T), N_b = 640 000.*

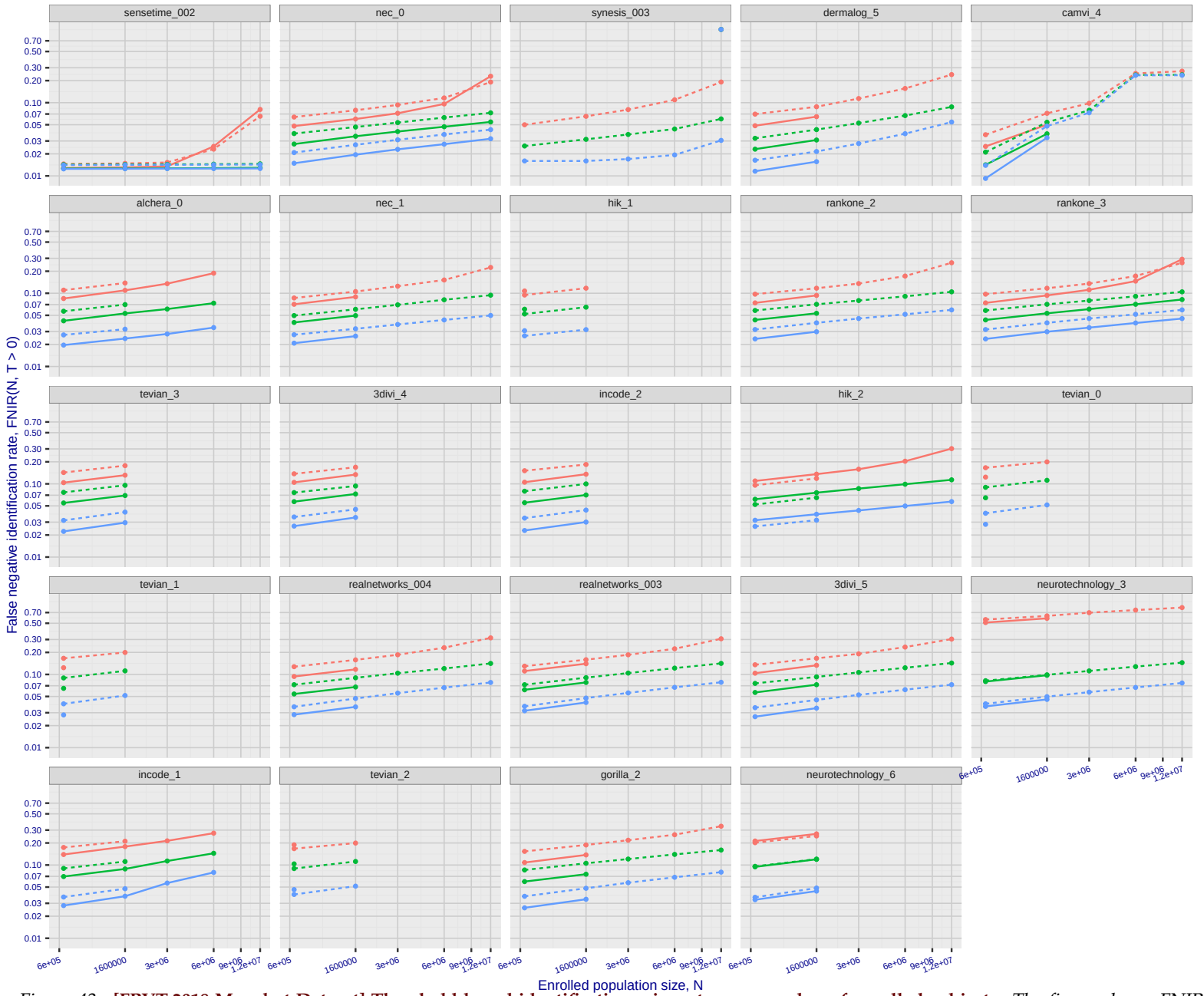

Figure 43: **[FRVT-2018 Mugshot Dataset] Threshold-based identification miss rates vs. number of enrolled subjects**. *The figure shows FNIR(N, T) across various gallery sizes when the threshold is set to achieve the given FPIRs. The rank criterion is irrelevant at high thresholds as mates are always at rank 1. The results are computed from the trials listed in rows 1-10 of Table 1. Less accurate algorithms were not run on large N, so results are missing. For clarity, results are sorted and reported into tiers spanning multiple pages. The tiering criteria is complicated: First paging by FNIR(N_b, 1, 0), then sorting by median FNIR(N_b, T), N_b = 640 000.*

2021/08/05 02:00:58

FNIR(N, R, T) = False neg. identification rate
FPIR(N, T) = False pos. identification rate

N = Num. enrolled subjects
R = Num. candidates examined

T = Threshold

T = 0 → Investigation
T > 0 → Identification

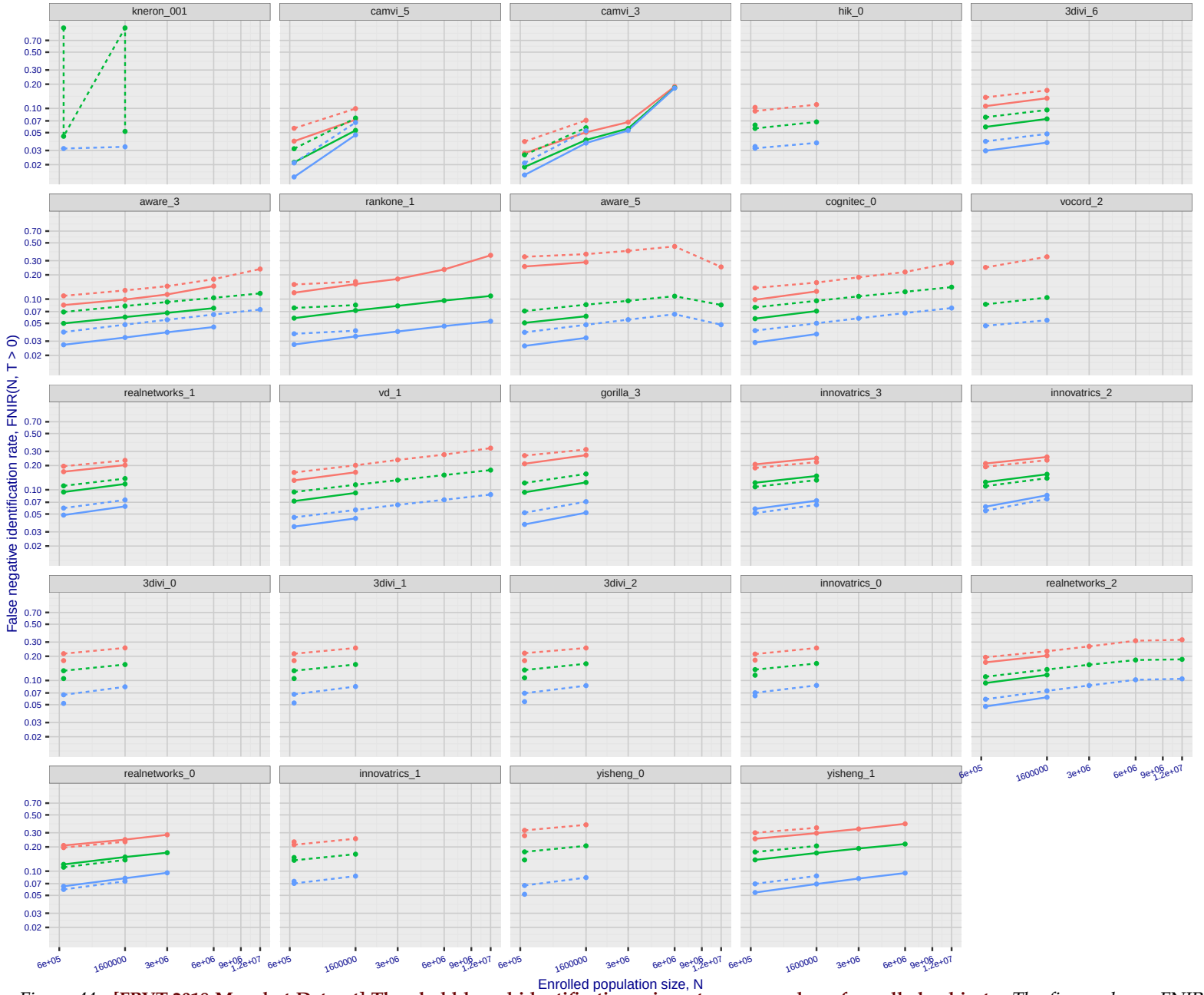

Figure 44: **[FRVT-2018 Mugshot Dataset] Threshold-based identification miss rates vs. number of enrolled subjects**. *The figure shows FNIR(N, T) across various gallery sizes when the threshold is set to achieve the given FPIRs. The rank criterion is irrelevant at high thresholds as mates are always at rank 1. The results are computed from the trials listed in rows 1-10 of Table 1. Less accurate algorithms were not run on large N, so results are missing. For clarity, results are sorted and reported into tiers spanning multiple pages. The tiering criteria is complicated: First paging by FNIR(N_b, 1, 0), then sorting by median FNIR(N_b, T), N_b = 640 000.*

2021/08/05 02:00:58

FNIR(N, R, T) = False neg. identification rate
FPIR(N, T) = False pos. identification rate

N = Num. enrolled subjects
R = Num. candidates examined

T = Threshold

T = 0 → Investigation
T > 0 → Identification

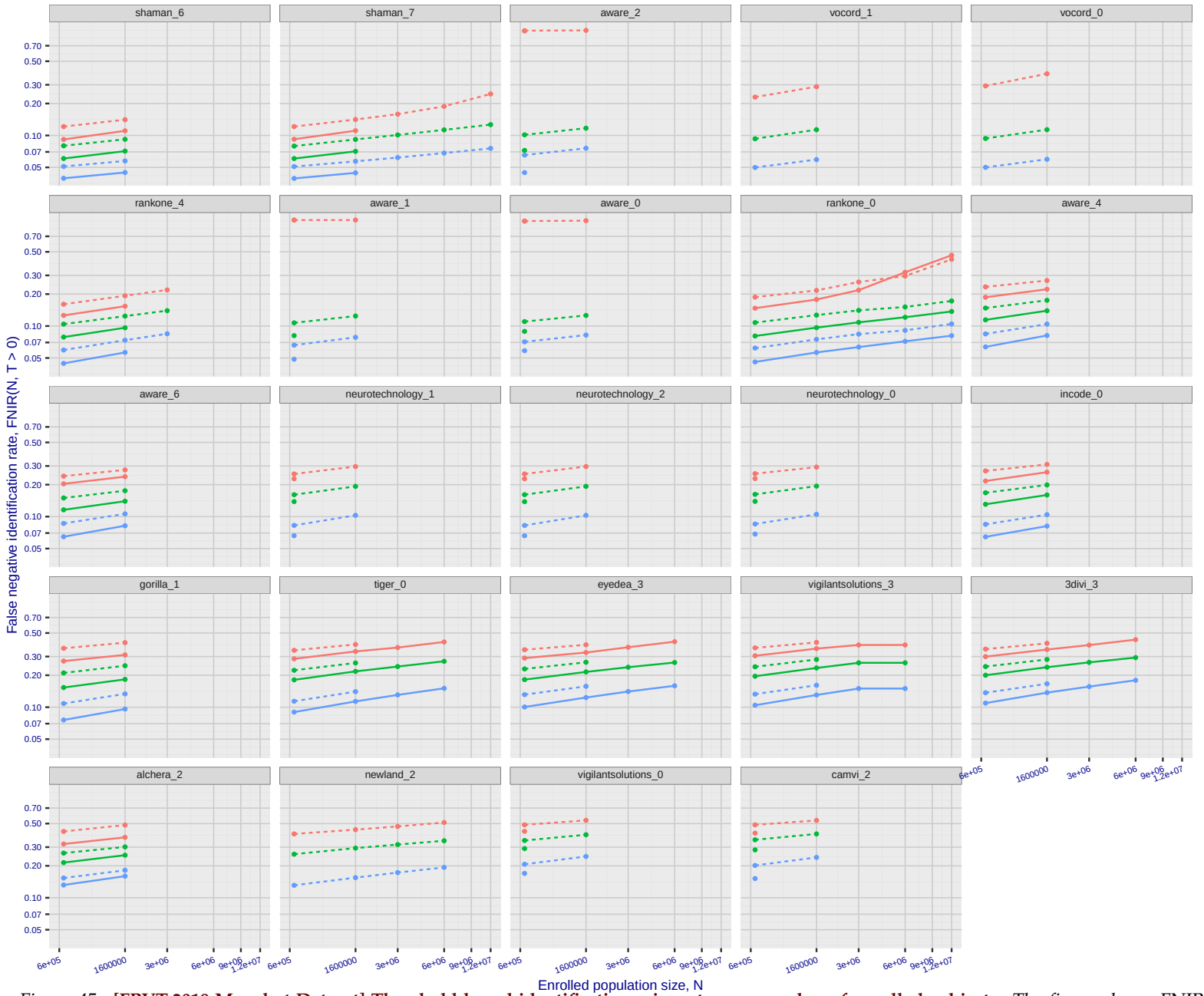

Figure 45: **[FRVT-2018 Mugshot Dataset] Threshold-based identification miss rates vs. number of enrolled subjects**. *The figure shows FNIR(N, T) across various gallery sizes when the threshold is set to achieve the given FPIRs. The rank criterion is irrelevant at high thresholds as mates are always at rank 1. The results are computed from the trials listed in rows 1-10 of Table 1. Less accurate algorithms were not run on large N, so results are missing. For clarity, results are sorted and reported into tiers spanning multiple pages. The tiering criteria is complicated: First paging by FNIR(N_b, 1, 0), then sorting by median FNIR(N_b, T), N_b = 640 000.*

2021/08/05 02:00:58
FNIR(N, R, T) = False neg. identification rate
FPIR(N, T) = False pos. identification rate
N = Num. enrolled subjects
R = Num. candidates examined
T = Threshold
T = 0 → Investigation
T > 0 → Identification

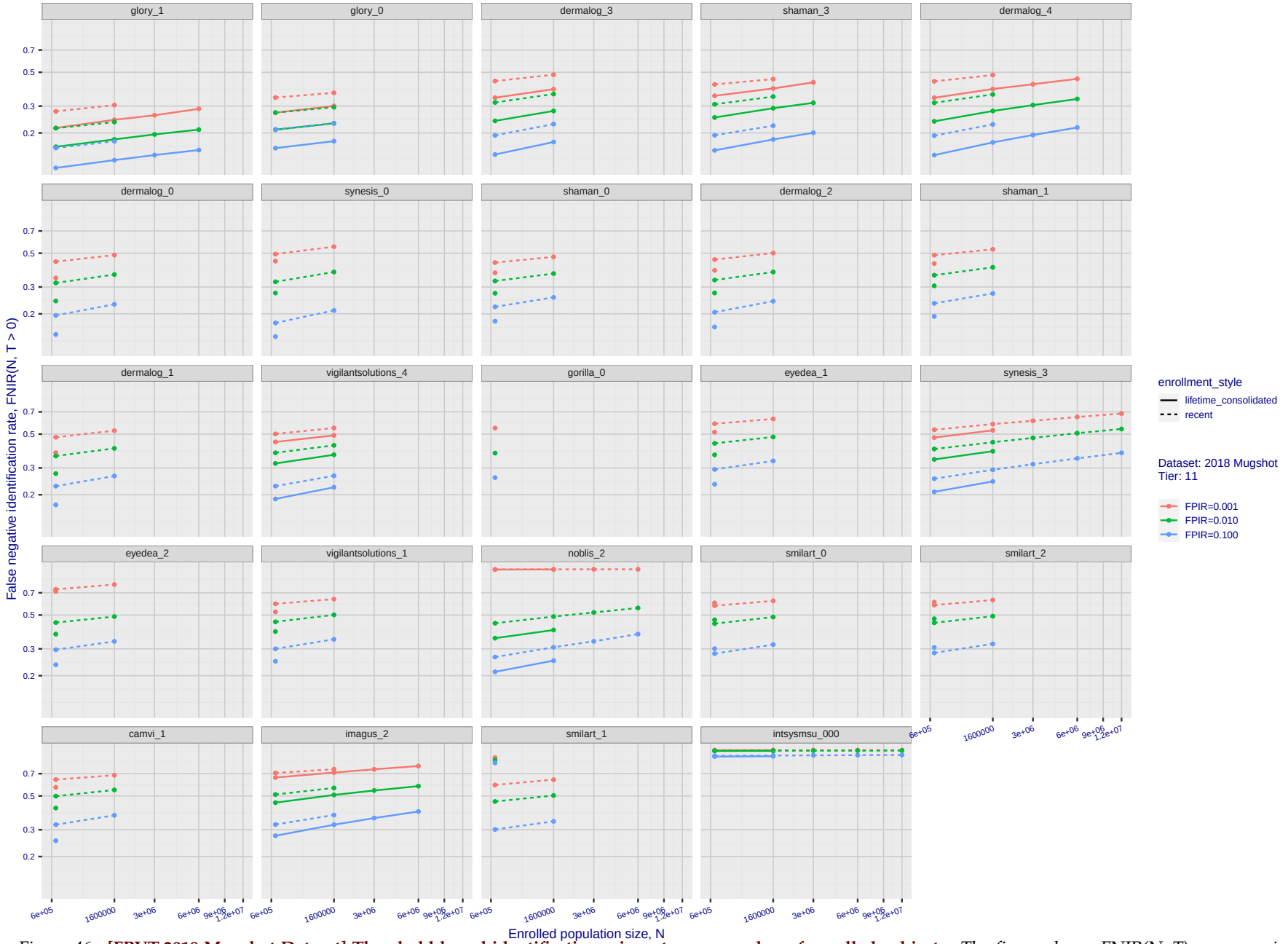

Figure 46: **[FRVT-2018 Mugshot Dataset] Threshold-based identification miss rates vs. number of enrolled subjects**. *The figure shows FNIR(N, T) across various gallery sizes when the threshold is set to achieve the given FPIRs. The rank criterion is irrelevant at high thresholds as mates are always at rank 1. The results are computed from the trials listed in rows 1-10 of Table 1. Less accurate algorithms were not run on large N, so results are missing. For clarity, results are sorted and reported into tiers spanning multiple pages. The tiering criteria is complicated: First paging by FNIR(N_b, 1, 0), then sorting by median FNIR(N_b, T), N_b = 640 000.*

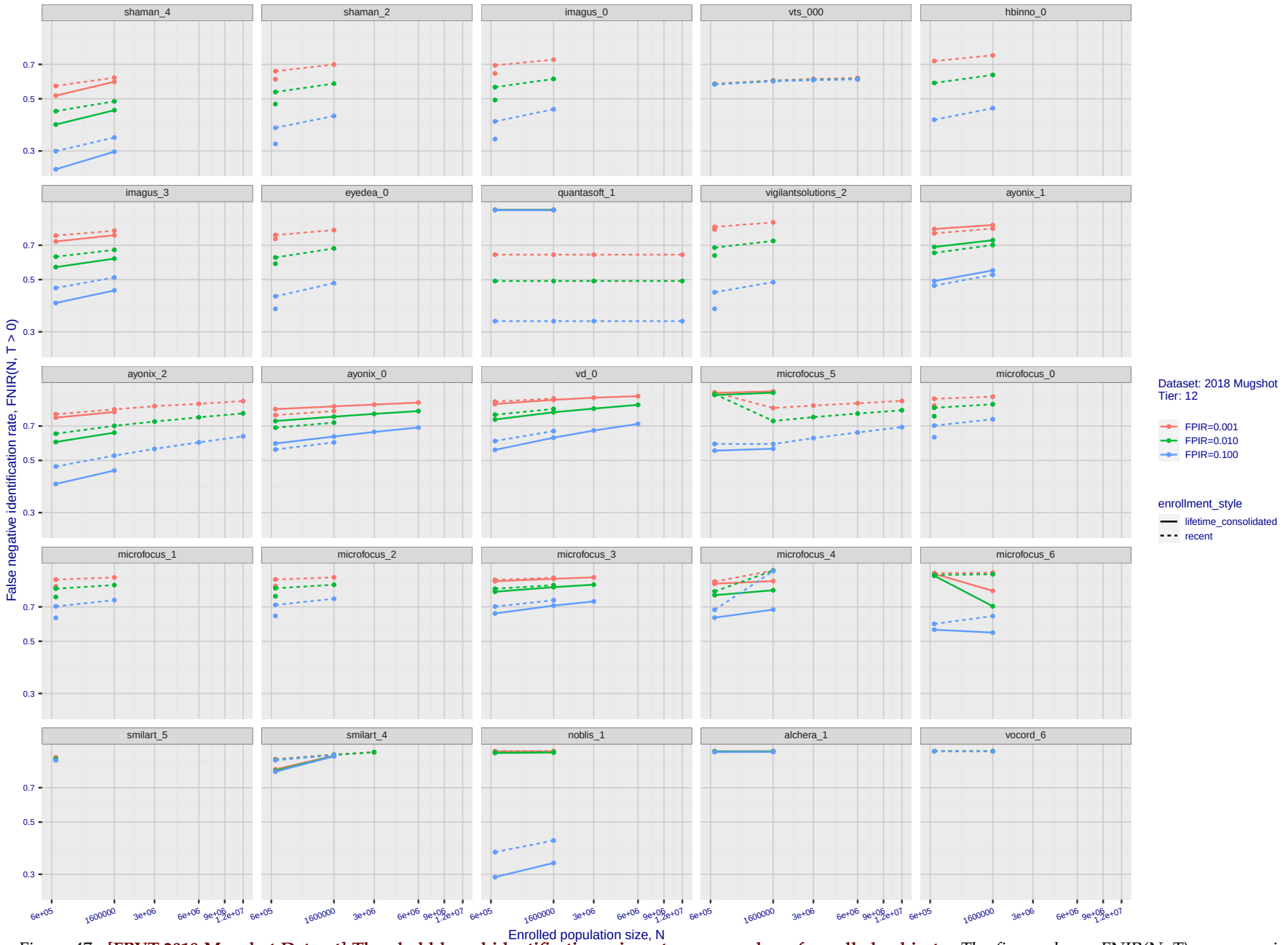

Figure 47: **[FRVT-2018 Mugshot Dataset] Threshold-based identification miss rates vs. number of enrolled subjects**. *The figure shows FNIR(N, T) across various gallery sizes when the threshold is set to achieve the given FPIRs. The rank criterion is irrelevant at high thresholds as mates are always at rank 1. The results are computed from the trials listed in rows 1-10 of Table 1. Less accurate algorithms were not run on large N, so results are missing. For clarity, results are sorted and reported into tiers spanning multiple pages. The tiering criteria is complicated: First paging by FNIR(N_b, 1, 0), then sorting by median FNIR(N_b, T), N_b = 640 000.*

2021/08/05	FNIR(N, R, T) =	False neg. identification rate	N = Num. enrolled subjects	T = Threshold	$T = 0 \rightarrow$ Investigation
02:00:58	FPIR(N, T) =	False pos. identification rate	R = Num. candidates examined		$T > 0 \rightarrow$ Identification

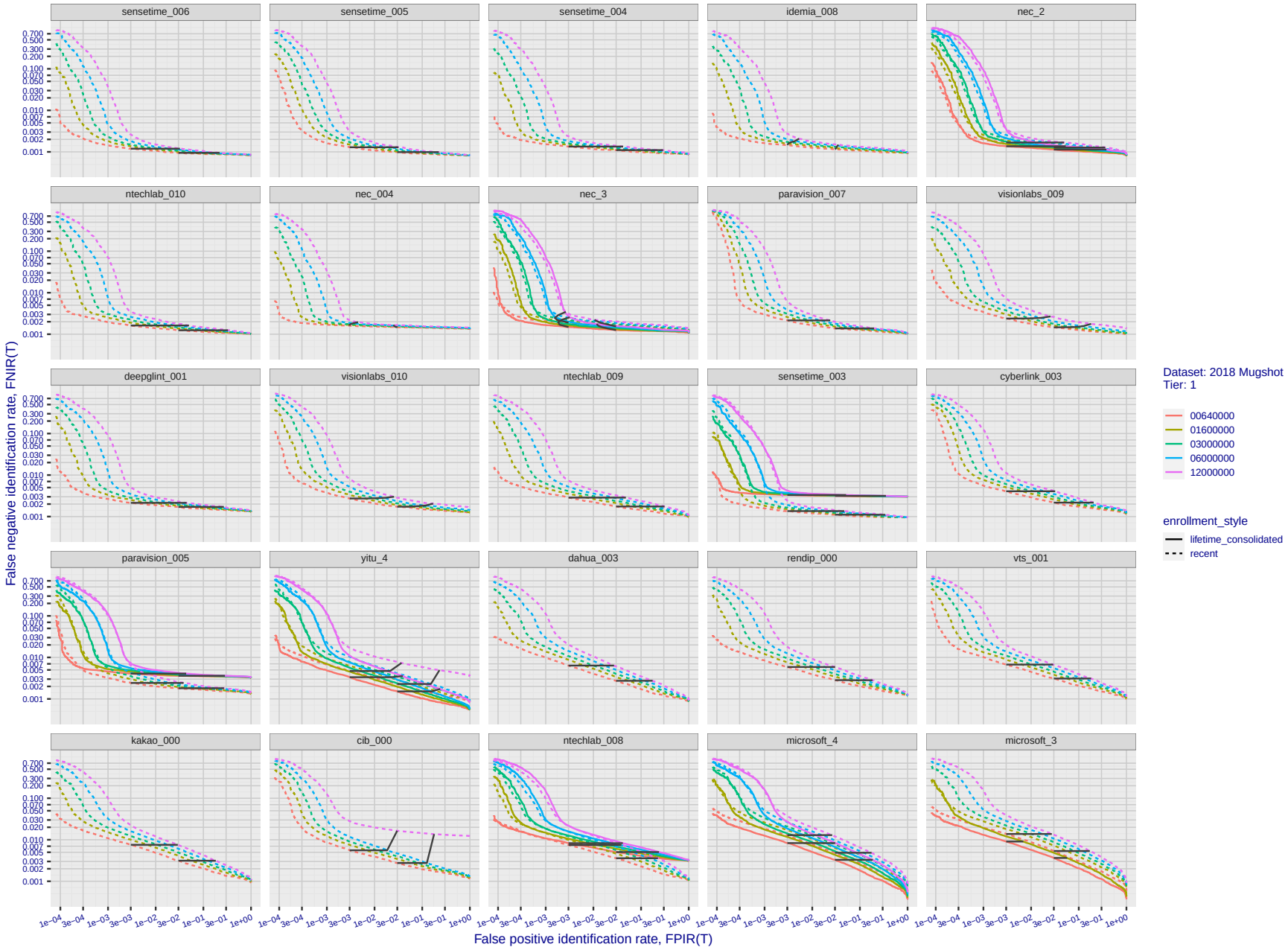

2021/08/05 02:00:58

FNIR(N, R, T) = False neg. identification rate
FPIR(N, T) = False pos. identification rate

N = Num. enrolled subjects
R = Num. candidates examined

T = Threshold

T = 0 → Investigation
T > 0 → Identification

Figure 48: **[FRVT-2018 Mugshot Dataset] Identification miss rates vs. false positive rates**. *The figure shows miss rates FNIR(N, L, T) as a function of FPIR(N, T), with N ranging from 640 000 to 12 000 000 as noted in rows 1-10 of Table 1. These error tradeoff characteristics are useful for applications where a threshold must be elevated to limit false positives, such as when human reviewer labor is not matched to the volume of searches. Dark lines join points of equal threshold: If horizontal, FPIR(T) rises with N, and mate scores are independent of N. Other algorithms adjust scores in an attempt to make FPIR independent of N.*

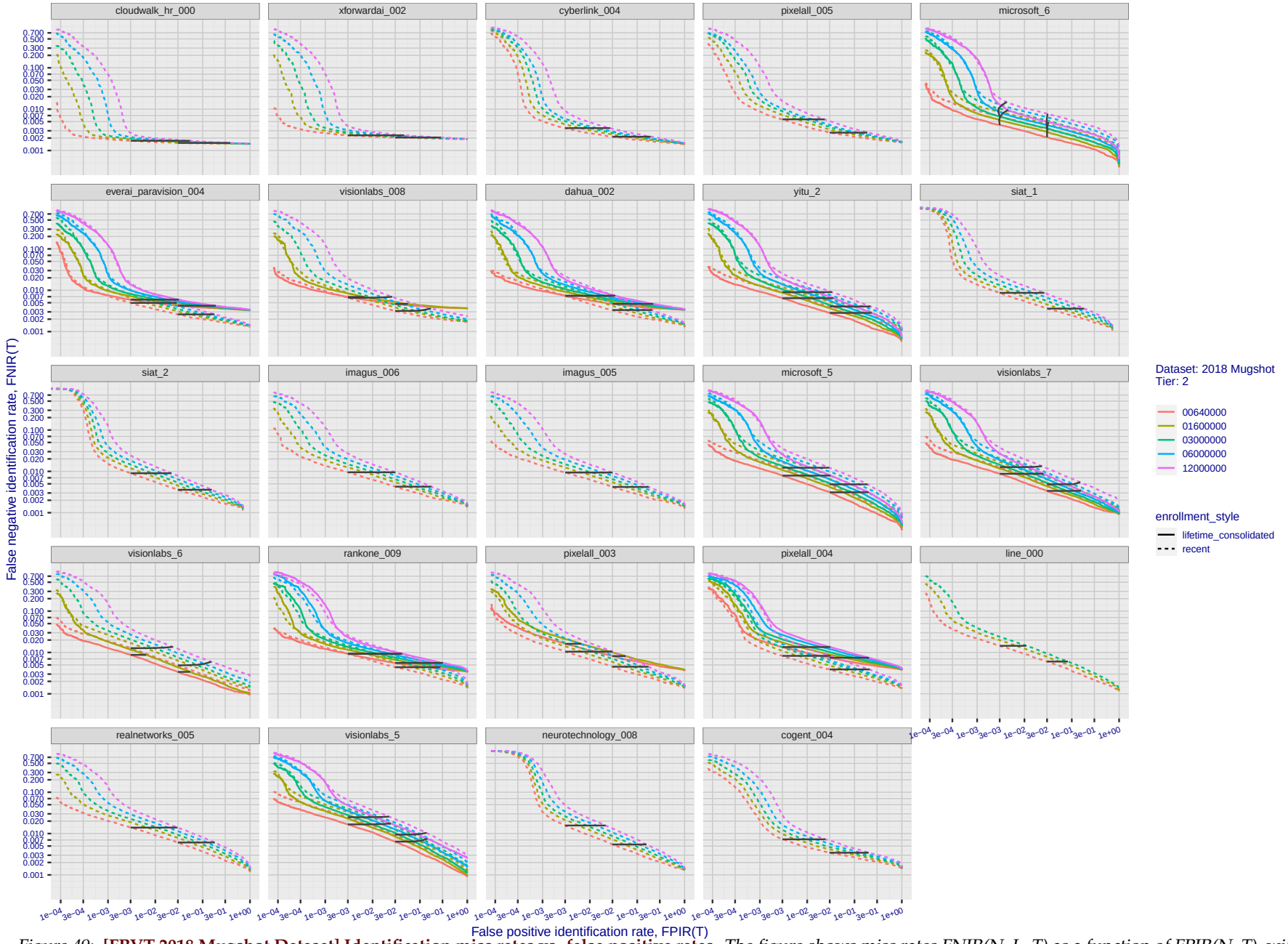

Figure 49: **[FRVT-2018 Mugshot Dataset] Identification miss rates vs. false positive rates**. *The figure shows miss rates FNIR(N, L, T) as a function of FPIR(N, T), with N ranging from 640 000 to 12 000 000 as noted in rows 1-10 of Table 1. These error tradeoff characteristics are useful for applications where a threshold must be elevated to limit false positives, such as when human reviewer labor is not matched to the volume of searches. Dark lines join points of equal threshold: If horizontal, FPIR(T) rises with N, and mate scores are independent of N. Other algorithms adjust scores in an attempt to make FPIR independent of N.*

2021/08/05 02:00:58

FNIR(N, R, T) = False neg. identification rate
FPIR(N, T) = False pos. identification rate

N = Num. enrolled subjects
R = Num. candidates examined

T = Threshold

T = 0 → Investigation
T > 0 → Identification

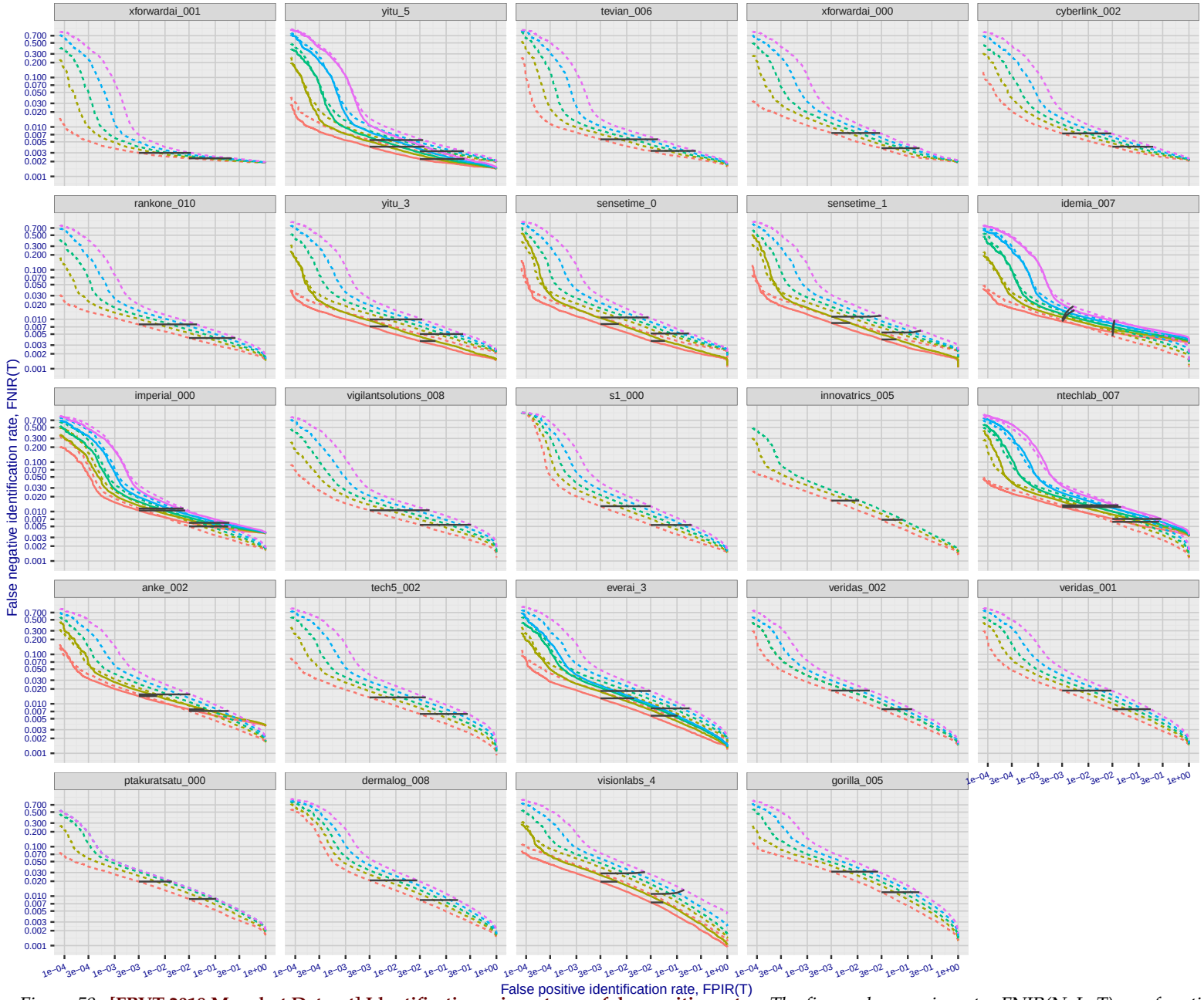

Figure 50: **[FRVT-2018 Mugshot Dataset] Identification miss rates vs. false positive rates**. *The figure shows miss rates FNIR(N, L, T) as a function of FPIR(N, T), with N ranging from 640 000 to 12 000 000 as noted in rows 1-10 of Table 1. These error tradeoff characteristics are useful for applications where a threshold must be elevated to limit false positives, such as when human reviewer labor is not matched to the volume of searches. Dark lines join points of equal threshold: If horizontal, FPIR(T) rises with N, and mate scores are independent of N. Other algorithms adjust scores in an attempt to make FPIR independent of N.*

2021/08/05 02:00:58
FNIR(N, R, T) = False neg. identification rate
FPIR(N, T) = False pos. identification rate
N = Num. enrolled subjects
R = Num. candidates examined
T = Threshold
T = 0 → Investigation
T > 0 → Identification

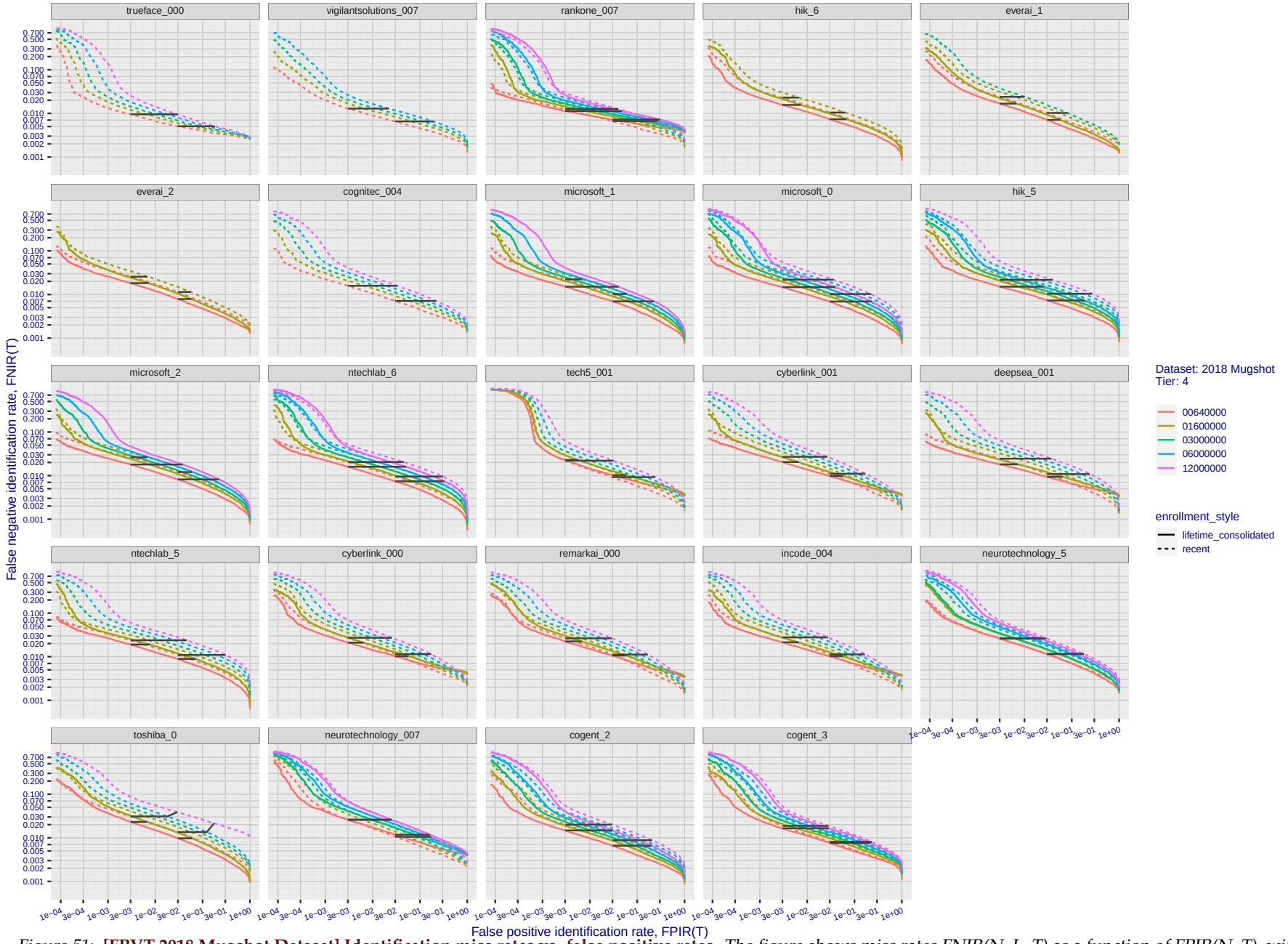

Figure 51: **[FRVT-2018 Mugshot Dataset] Identification miss rates vs. false positive rates**. *The figure shows miss rates FNIR(N, L, T) as a function of FPIR(N, T), with N ranging from 640 000 to 12 000 000 as noted in rows 1-10 of Table 1. These error tradeoff characteristics are useful for applications where a threshold must be elevated to limit false positives, such as when human reviewer labor is not matched to the volume of searches. Dark lines join points of equal threshold: If horizontal, FPIR(T) rises with N, and mate scores are independent of N. Other algorithms adjust scores in an attempt to make FPIR independent of N.*

2021/08/05 02:00:58

FNIR(N, R, T) = False neg. identification rate
FPIR(N, T) = False pos. identification rate

N = Num. enrolled subjects
R = Num. candidates examined

T = Threshold

T = 0 → Investigation
T > 0 → Identification

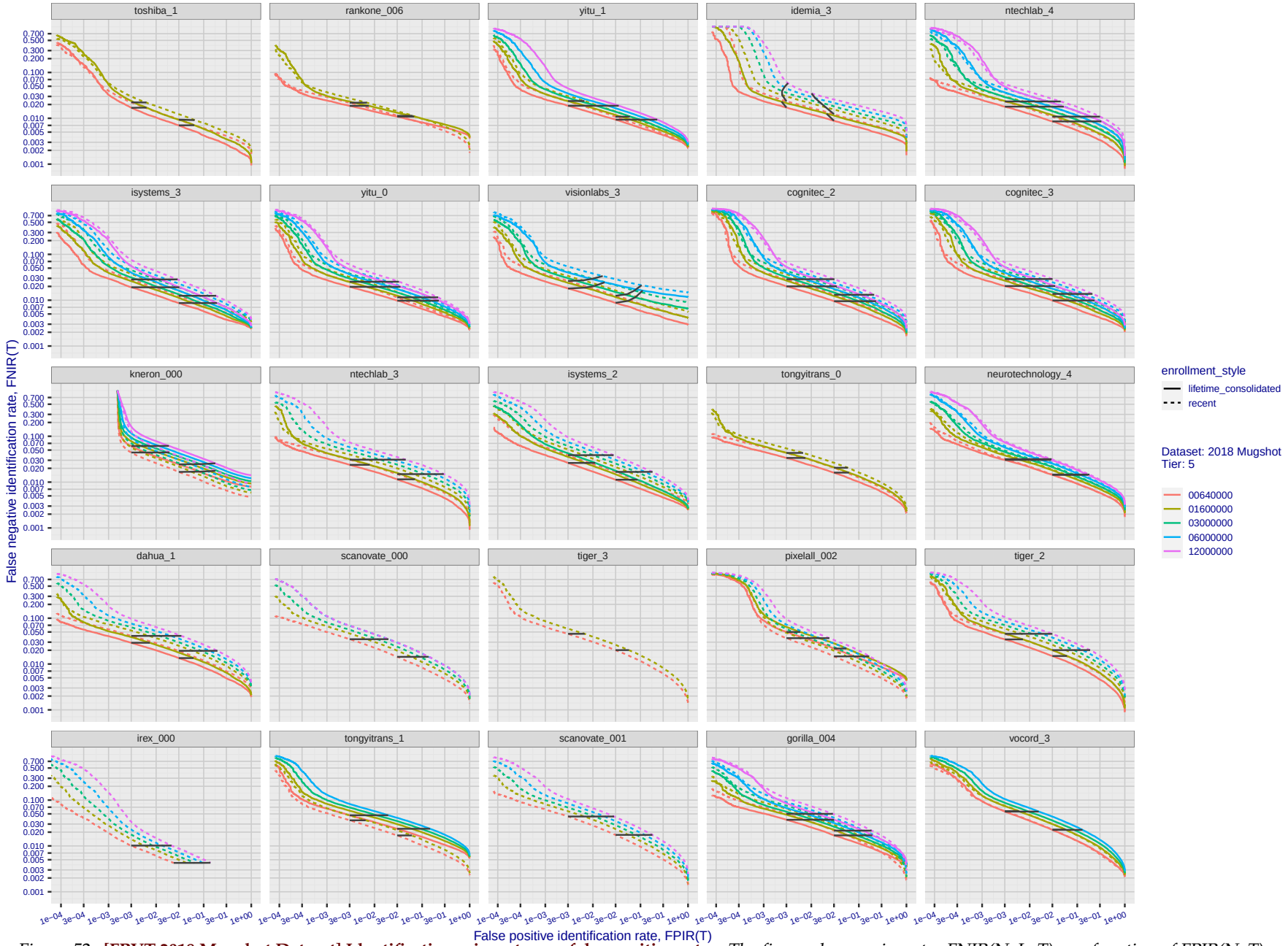

Figure 52: **[FRVT-2018 Mugshot Dataset] Identification miss rates vs. false positive rates**. *The figure shows miss rates FNIR(N, L, T) as a function of FPIR(N, T), with N ranging from 640 000 to 12 000 000 as noted in rows 1-10 of Table 1. These error tradeoff characteristics are useful for applications where a threshold must be elevated to limit false positives, such as when human reviewer labor is not matched to the volume of searches. Dark lines join points of equal threshold: If horizontal, FPIR(T) rises with N, and mate scores are independent of N. Other algorithms adjust scores in an attempt to make FPIR independent of N.*

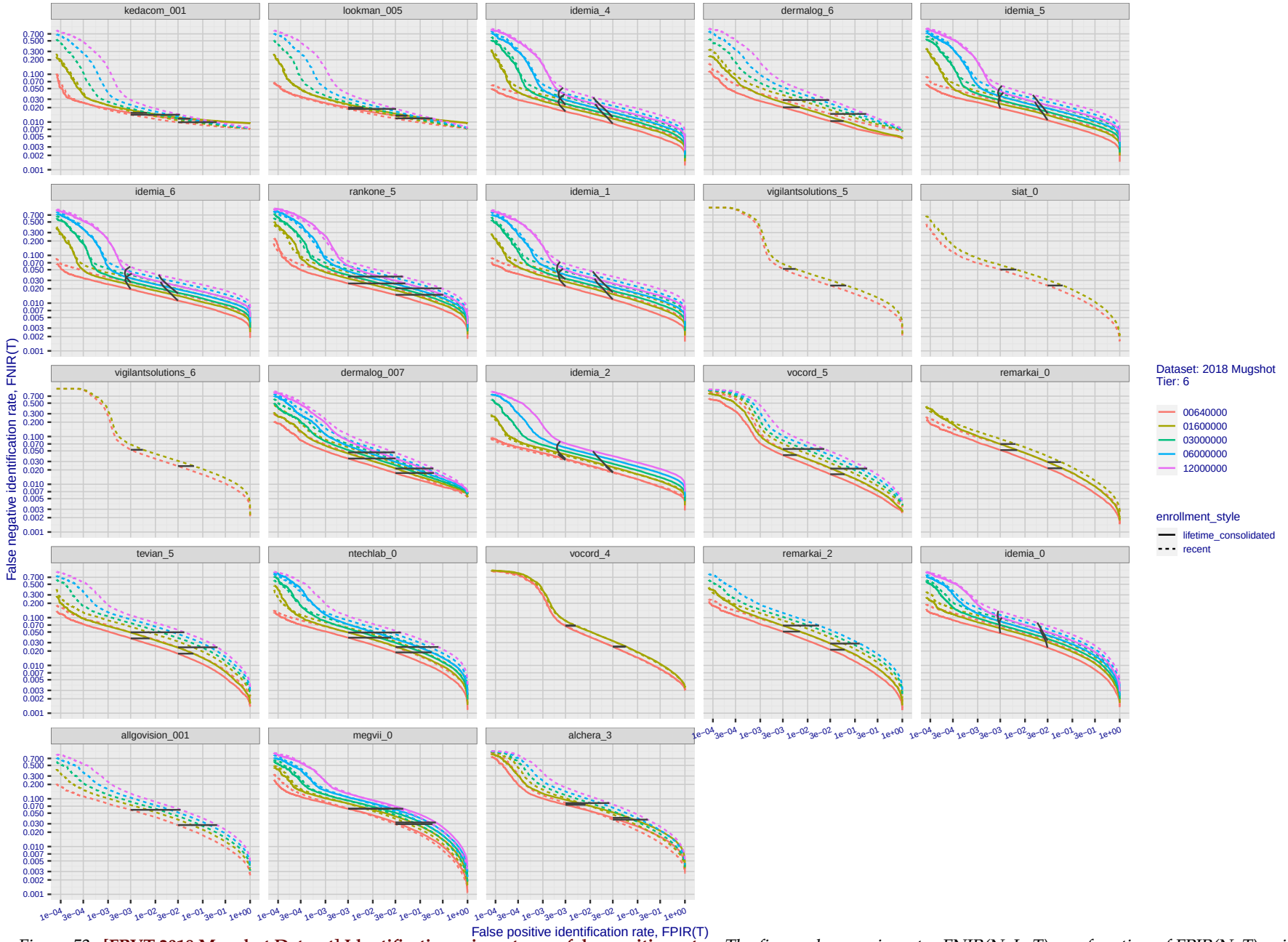

Figure 53: **[FRVT-2018 Mugshot Dataset] Identification miss rates vs. false positive rates**. *The figure shows miss rates FNIR(N, L, T) as a function of FPIR(N, T), with N ranging from 640 000 to 12 000 000 as noted in rows 1-10 of Table 1. These error tradeoff characteristics are useful for applications where a threshold must be elevated to limit false positives, such as when human reviewer labor is not matched to the volume of searches. Dark lines join points of equal threshold: If horizontal, FPIR(T) rises with N, and mate scores are independent of N. Other algorithms adjust scores in an attempt to make FPIR independent of N.*

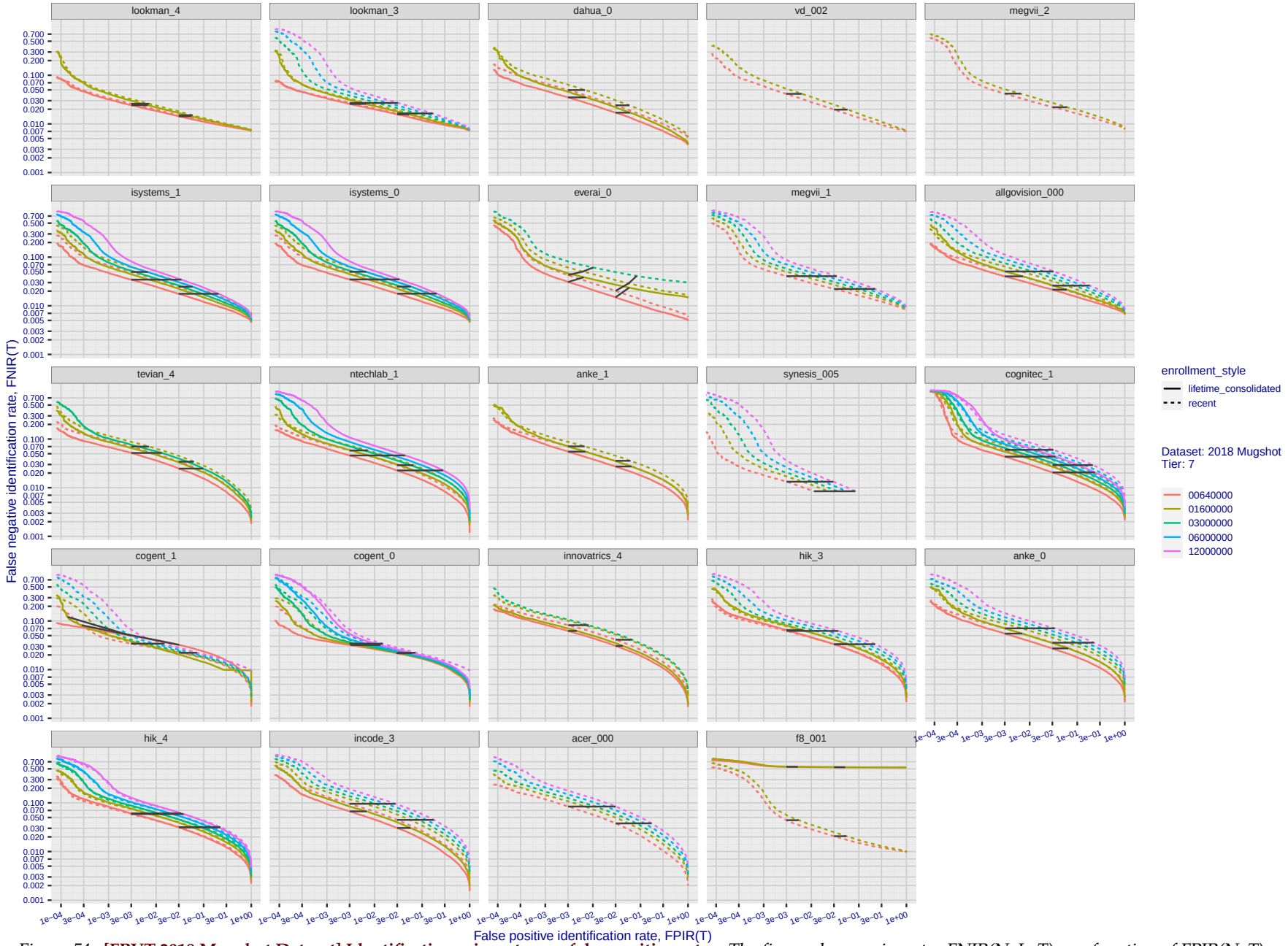

Figure 54: **[FRVT-2018 Mugshot Dataset] Identification miss rates vs. false positive rates**. *The figure shows miss rates FNIR(N, L, T) as a function of FPIR(N, T), with N ranging from 640 000 to 12 000 000 as noted in rows 1-10 of Table 1. These error tradeoff characteristics are useful for applications where a threshold must be elevated to limit false positives, such as when human reviewer labor is not matched to the volume of searches. Dark lines join points of equal threshold: If horizontal, FPIR(T) rises with N, and mate scores are independent of N. Other algorithms adjust scores in an attempt to make FPIR independent of N.*

2021/08/05 02:00:58

FNIR(N, R, T) = False neg. identification rate
FPIR(N, T) = False pos. identification rate

N = Num. enrolled subjects
R = Num. candidates examined

T = Threshold

T = 0 → Investigation
T > 0 → Identification

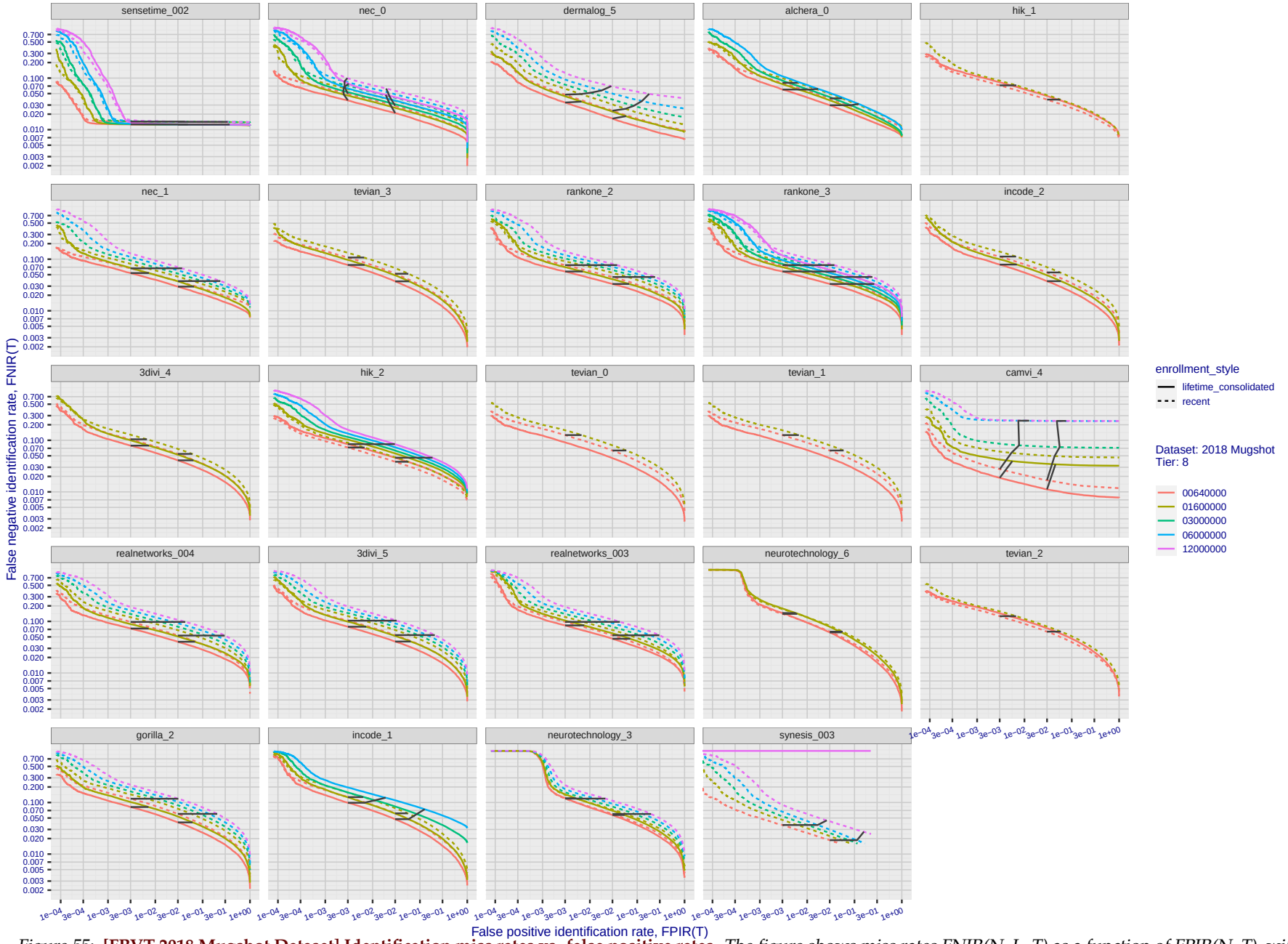

Figure 55: **[FRVT-2018 Mugshot Dataset] Identification miss rates vs. false positive rates**. *The figure shows miss rates FNIR(N, L, T) as a function of FPIR(N, T), with N ranging from 640 000 to 12 000 000 as noted in rows 1-10 of Table 1. These error tradeoff characteristics are useful for applications where a threshold must be elevated to limit false positives, such as when human reviewer labor is not matched to the volume of searches. Dark lines join points of equal threshold: If horizontal, FPIR(T) rises with N, and mate scores are independent of N. Other algorithms adjust scores in an attempt to make FPIR independent of N.*

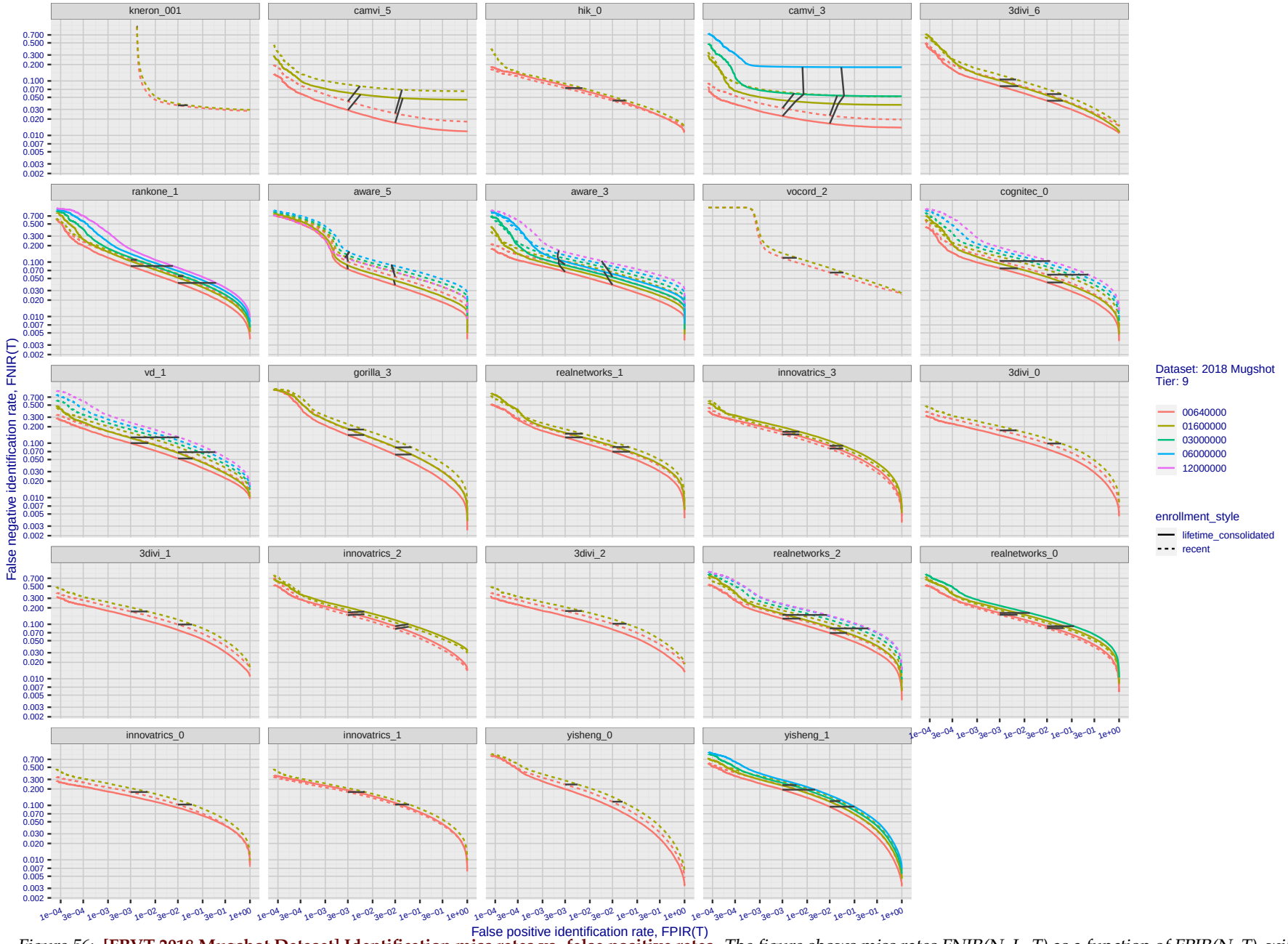

Figure 56: **[FRVT-2018 Mugshot Dataset] Identification miss rates vs. false positive rates**. *The figure shows miss rates FNIR(N, L, T) as a function of FPIR(N, T), with N ranging from 640 000 to 12 000 000 as noted in rows 1-10 of Table 1. These error tradeoff characteristics are useful for applications where a threshold must be elevated to limit false positives, such as when human reviewer labor is not matched to the volume of searches. Dark lines join points of equal threshold: If horizontal, FPIR(T) rises with N, and mate scores are independent of N. Other algorithms adjust scores in an attempt to make FPIR independent of N.*

2021/08/05 02:00:58
FNIR(N, R, T) = False neg. identification rate
FPIR(N, T) = False pos. identification rate
N = Num. enrolled subjects
R = Num. candidates examined
T = Threshold
T = 0 → Investigation
T > 0 → Identification

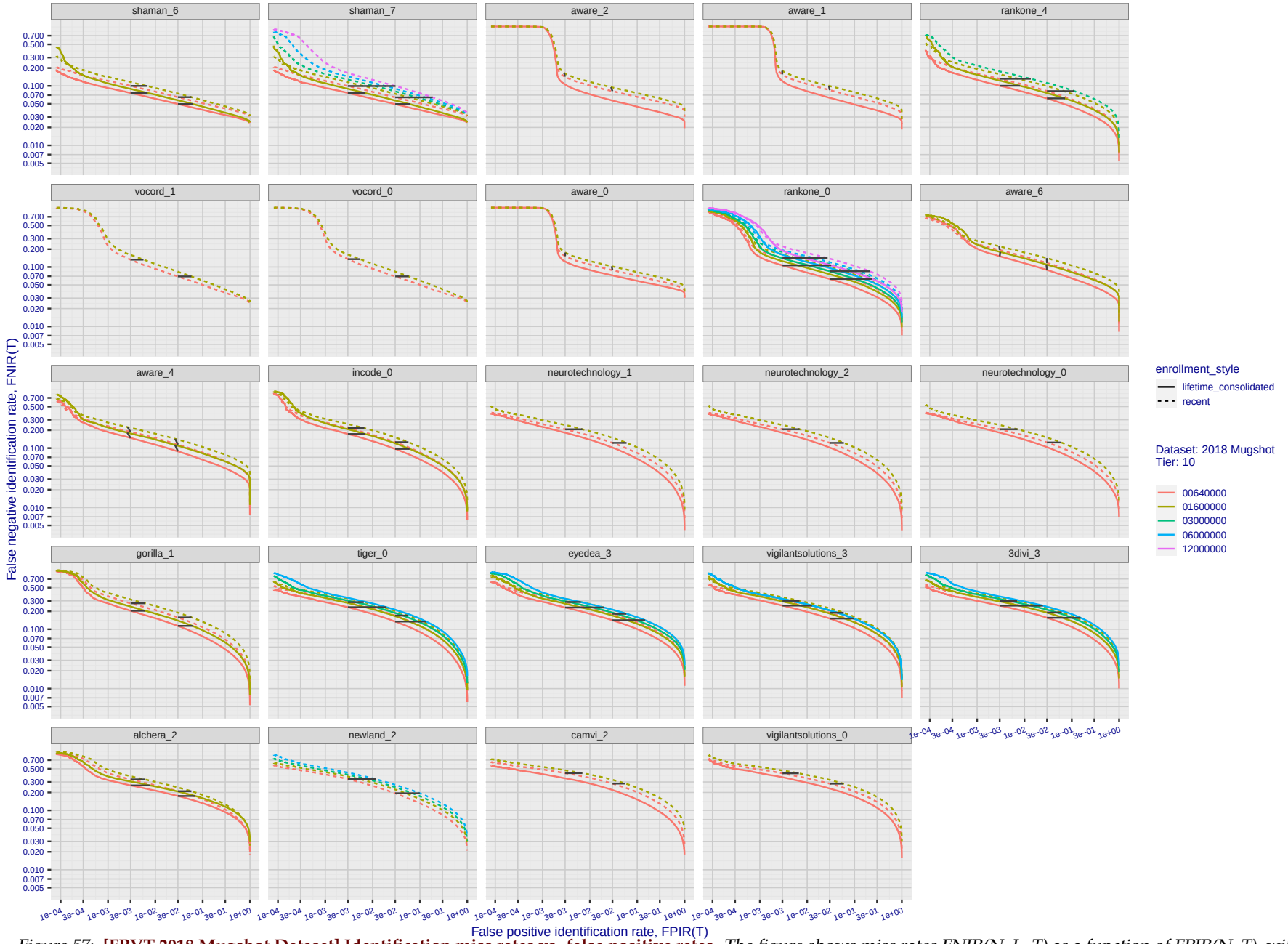

Figure 57: **[FRVT-2018 Mugshot Dataset] Identification miss rates vs. false positive rates**. *The figure shows miss rates FNIR(N, L, T) as a function of FPIR(N, T), with N ranging from 640 000 to 12 000 000 as noted in rows 1-10 of Table 1. These error tradeoff characteristics are useful for applications where a threshold must be elevated to limit false positives, such as when human reviewer labor is not matched to the volume of searches. Dark lines join points of equal threshold: If horizontal, FPIR(T) rises with N, and mate scores are independent of N. Other algorithms adjust scores in an attempt to make FPIR independent of N.*

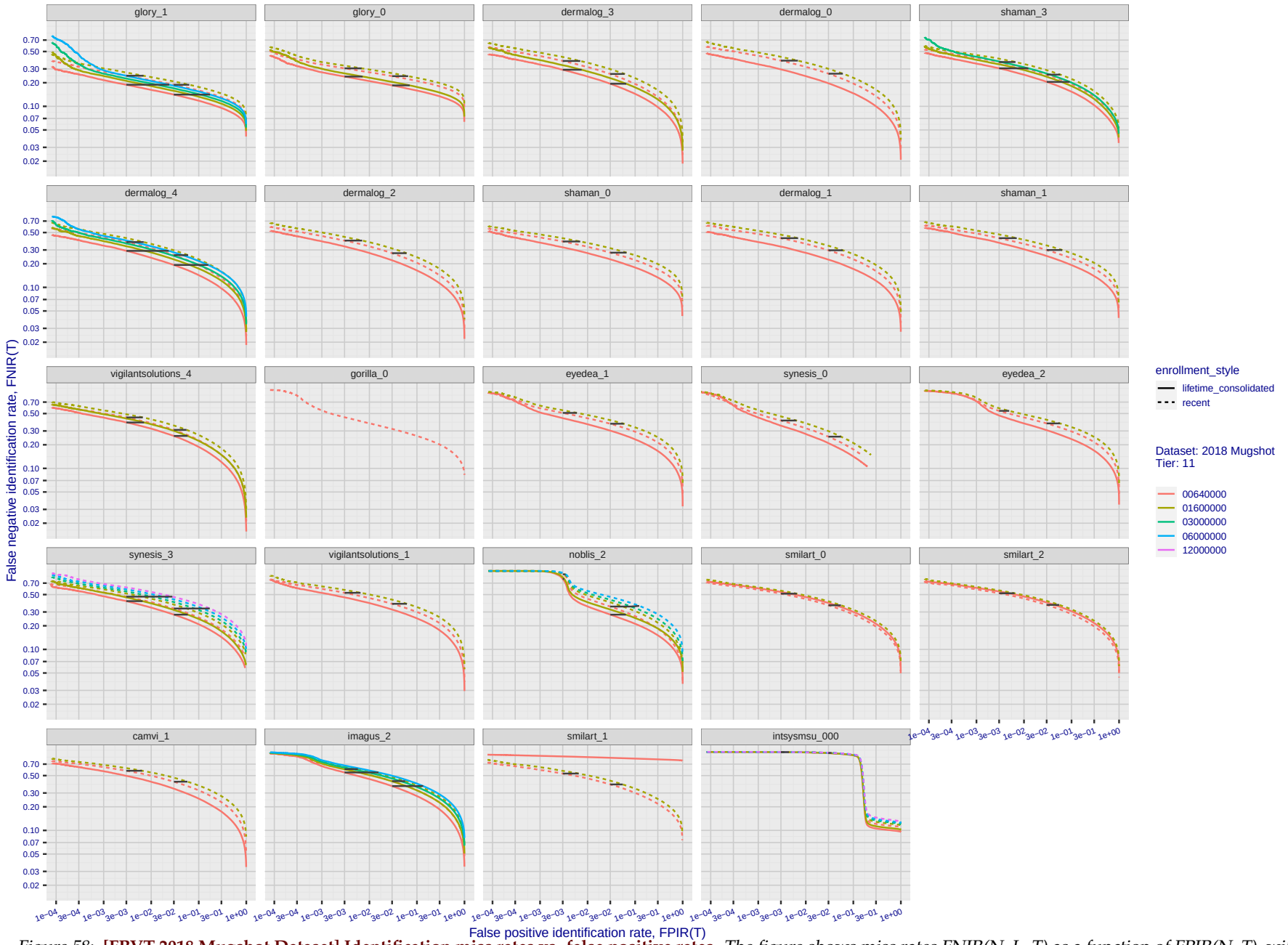

Figure 58: **[FRVT-2018 Mugshot Dataset] Identification miss rates vs. false positive rates**. *The figure shows miss rates FNIR(N, L, T) as a function of FPIR(N, T), with N ranging from 640 000 to 12 000 000 as noted in rows 1-10 of Table 1. These error tradeoff characteristics are useful for applications where a threshold must be elevated to limit false positives, such as when human reviewer labor is not matched to the volume of searches. Dark lines join points of equal threshold: If horizontal, FPIR(T) rises with N, and mate scores are independent of N. Other algorithms adjust scores in an attempt to make FPIR independent of N.*

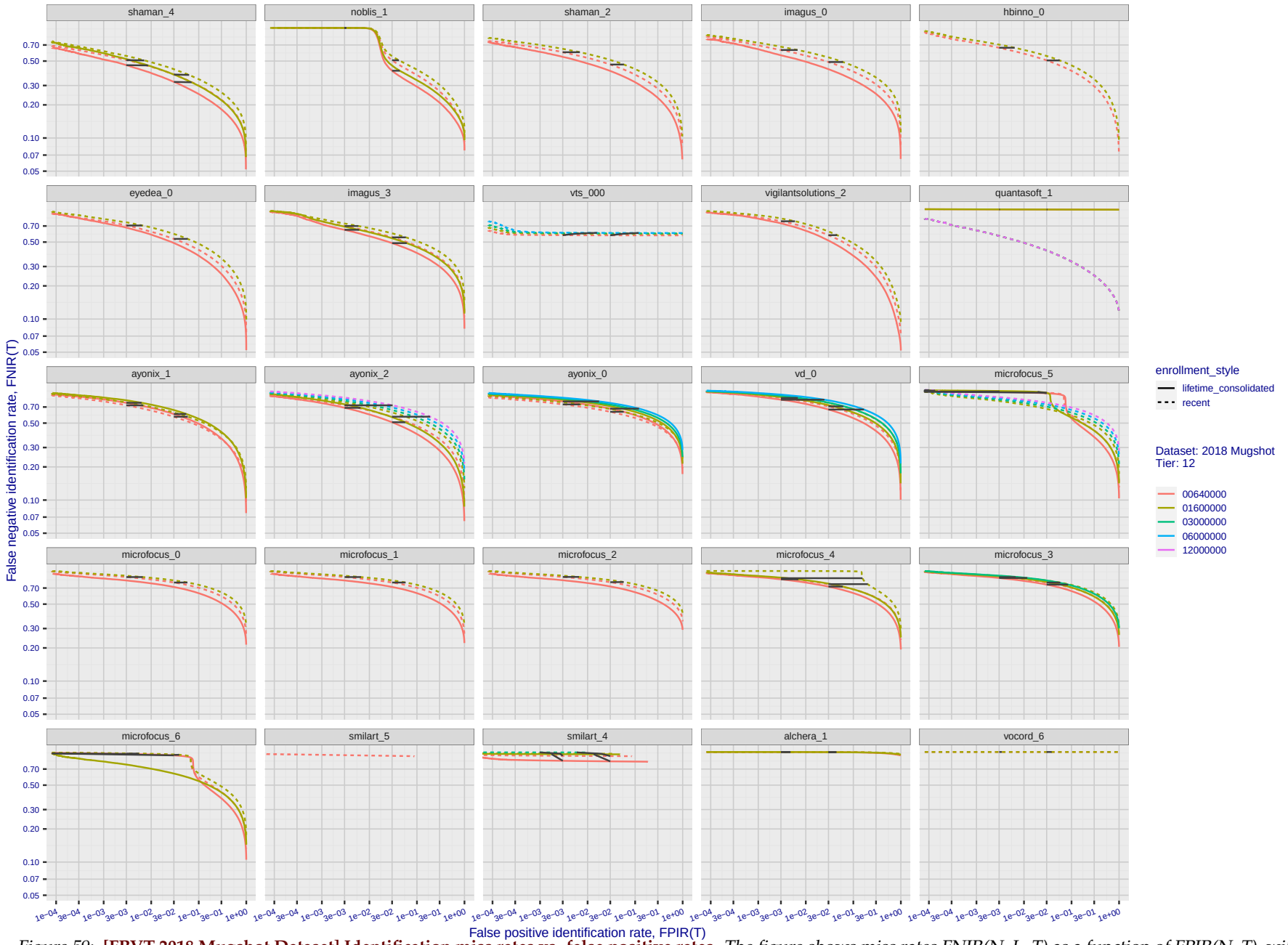

Figure 59: **[FRVT-2018 Mugshot Dataset] Identification miss rates vs. false positive rates**. *The figure shows miss rates FNIR(N, L, T) as a function of FPIR(N, T), with N ranging from 640 000 to 12 000 000 as noted in rows 1-10 of Table 1. These error tradeoff characteristics are useful for applications where a threshold must be elevated to limit false positives, such as when human reviewer labor is not matched to the volume of searches. Dark lines join points of equal threshold: If horizontal, FPIR(T) rises with N, and mate scores are independent of N. Other algorithms adjust scores in an attempt to make FPIR independent of N.*

Appendix B Effect of time-lapse: Accuracy after face ageing

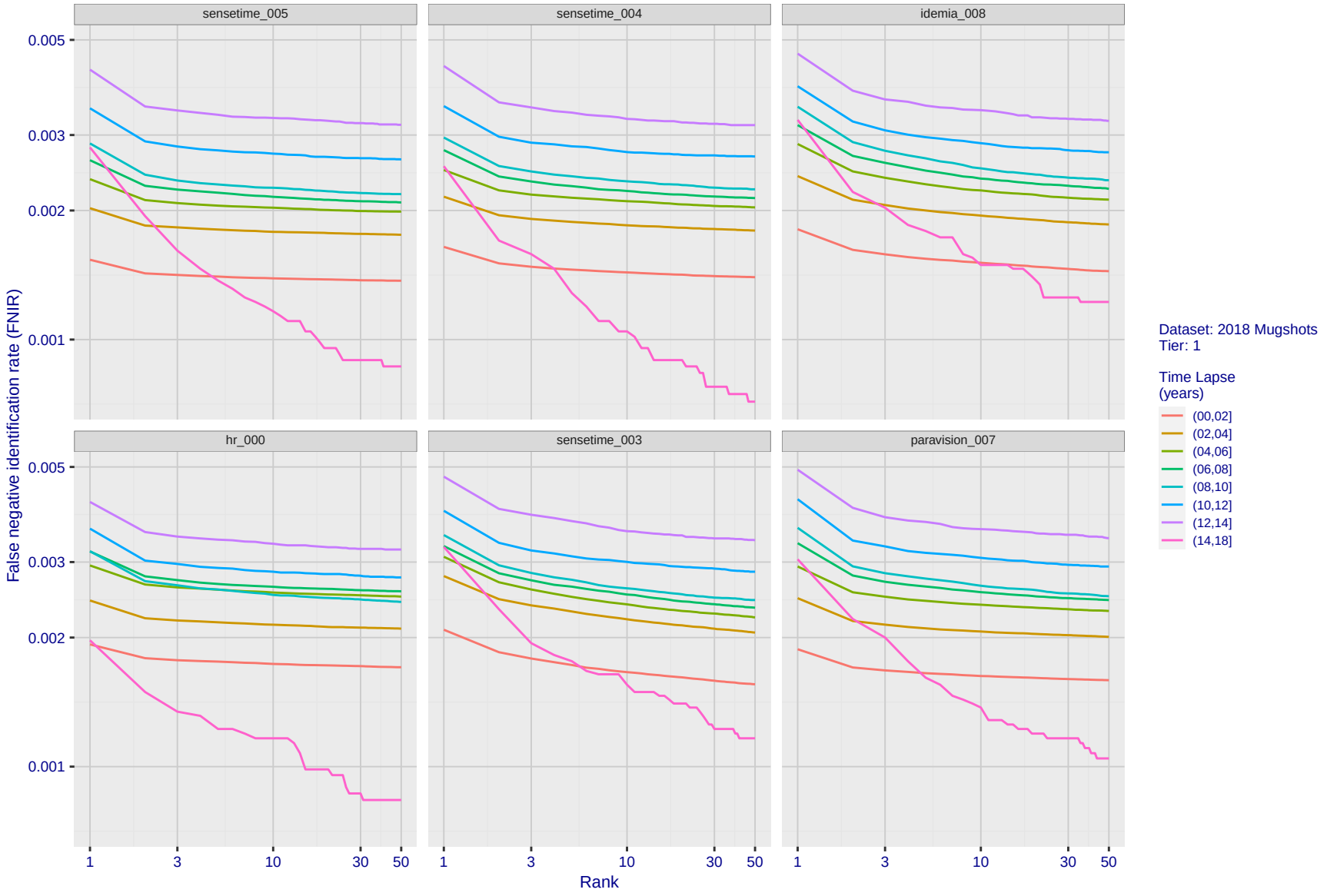

Figure 60: **[FRVT-2018 Mugshot Ageing Dataset] Identification miss rates vs. rank by time-elapsed**. *The oldest image of each individual is enrolled. Thereafter, all more recent images are searched. Miss rates are computed over all searches noted in row 17 of Table 1 and binned by number of years between search and initial enrollment.*

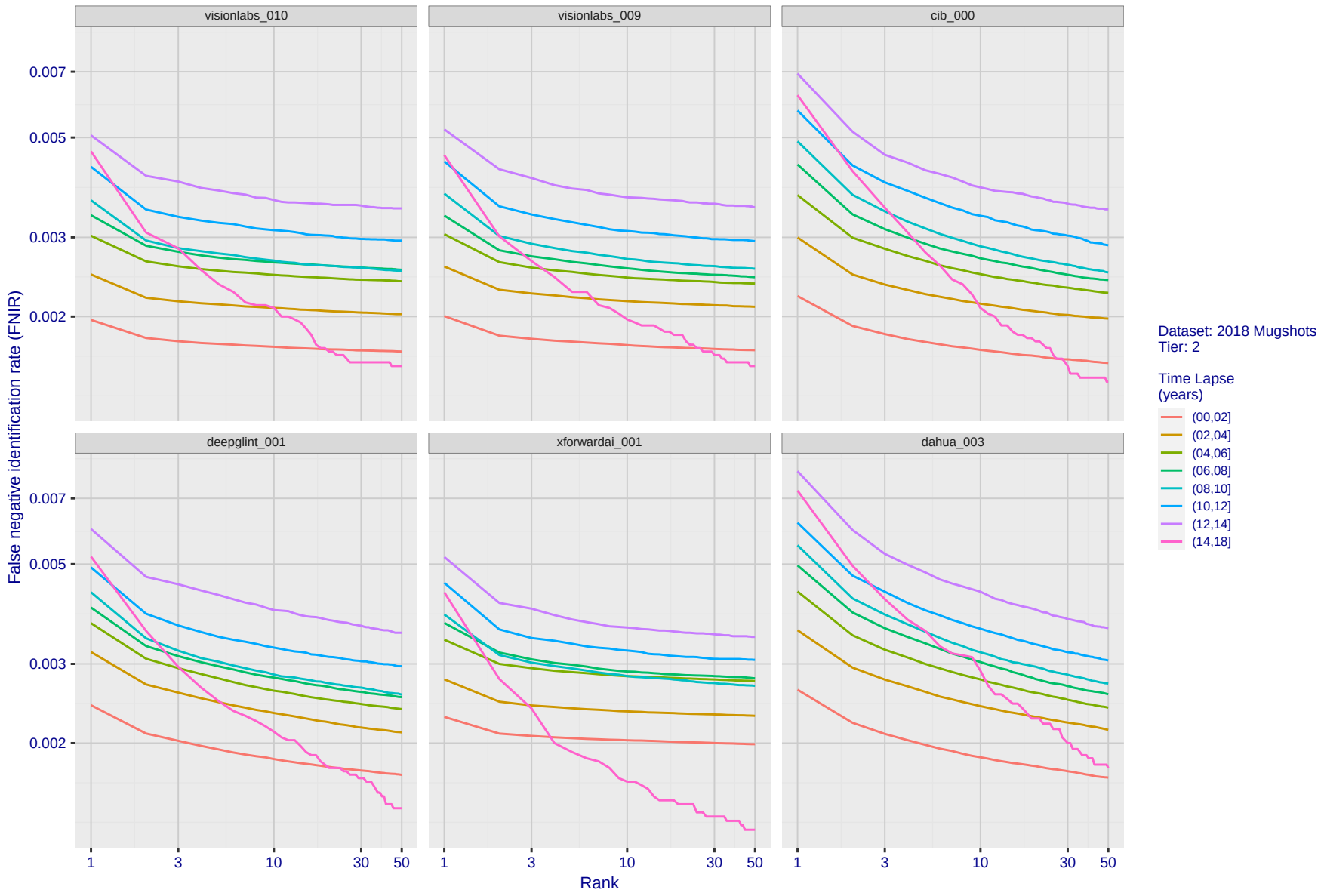

Figure 61: **[FRVT-2018 Mugshot Ageing Dataset] Identification miss rates vs. rank by time-elapsed**. *The oldest image of each individual is enrolled. Thereafter, all more recent images are searched. Miss rates are computed over all searches noted in row 17 of Table 1 and binned by number of years between search and initial enrollment.*

2021/08/05 02:00:58
FNIR(N, R, T) = False neg. identification rate
FPIR(N, T) = False pos. identification rate
N = Num. enrolled subjects
R = Num. candidates examined
T = Threshold
T = 0 → Investigation
T > 0 → Identification

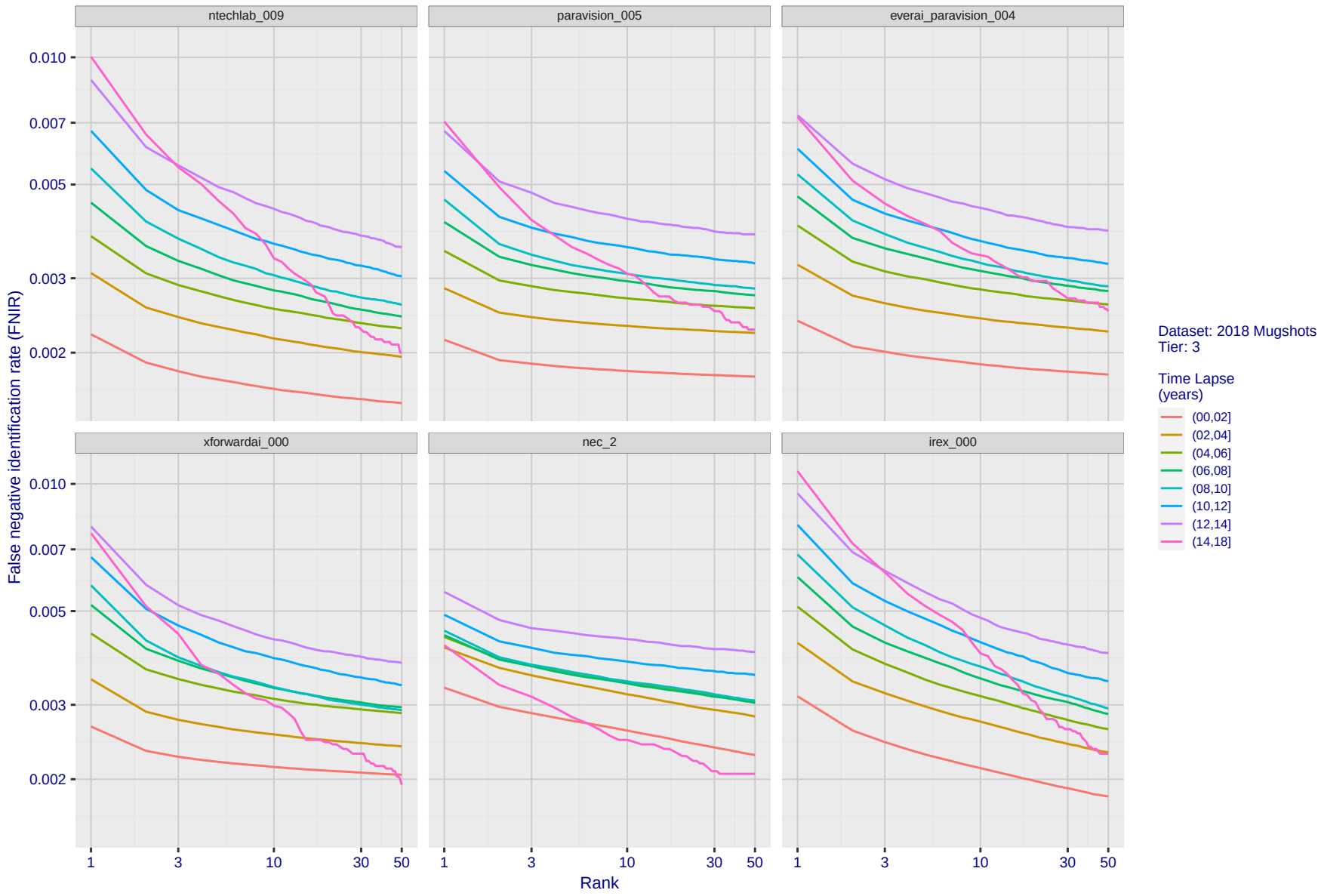

Figure 62: **[FRVT-2018 Mugshot Ageing Dataset] Identification miss rates vs. rank by time-elapsed**. *The oldest image of each individual is enrolled. Thereafter, all more recent images are searched. Miss rates are computed over all searches noted in row 17 of Table 1 and binned by number of years between search and initial enrollment.*

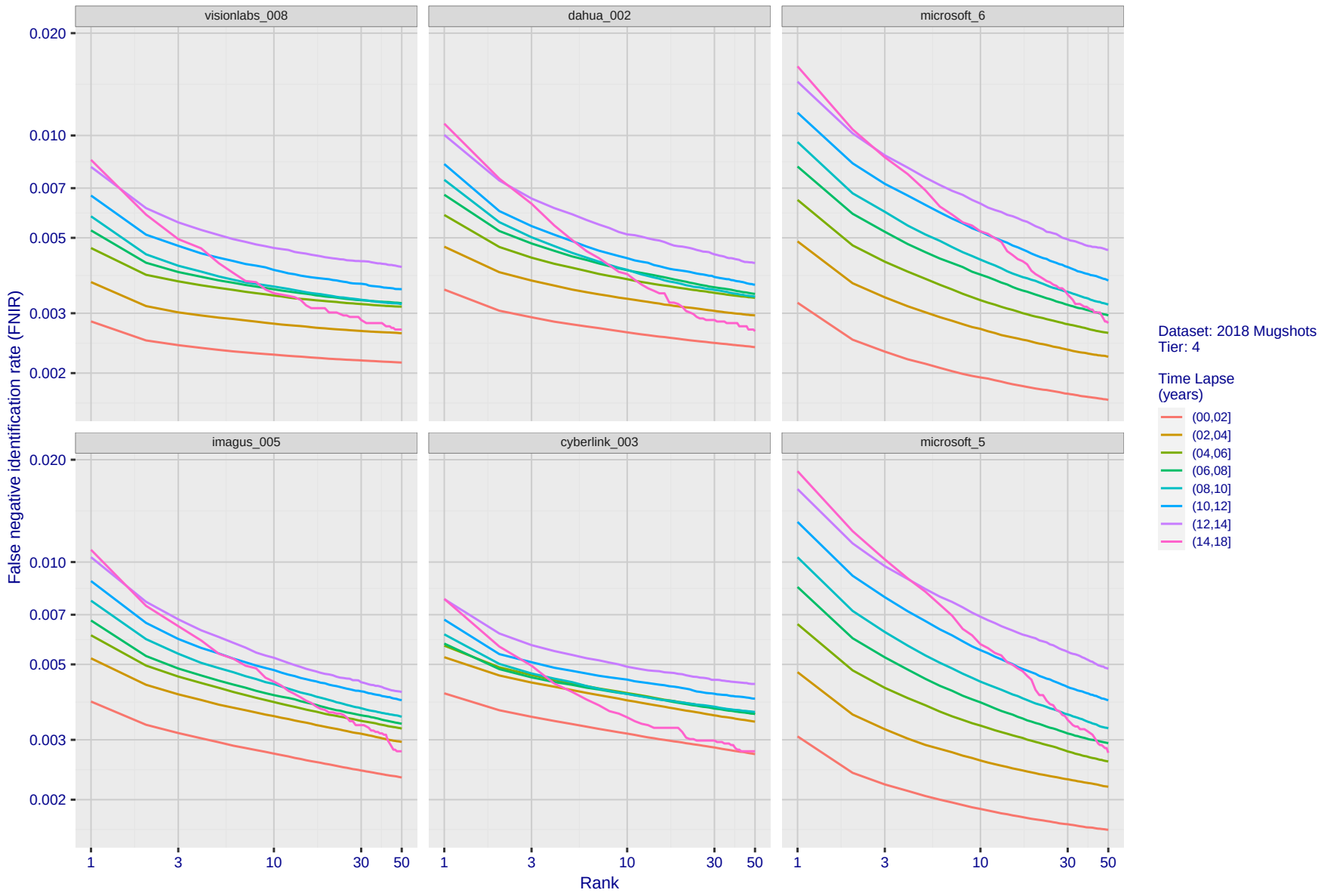

Figure 63: **[FRVT-2018 Mugshot Ageing Dataset] Identification miss rates vs. rank by time-elapsed**. *The oldest image of each individual is enrolled. Thereafter, all more recent images are searched. Miss rates are computed over all searches noted in row 17 of Table 1 and binned by number of years between search and initial enrollment.*

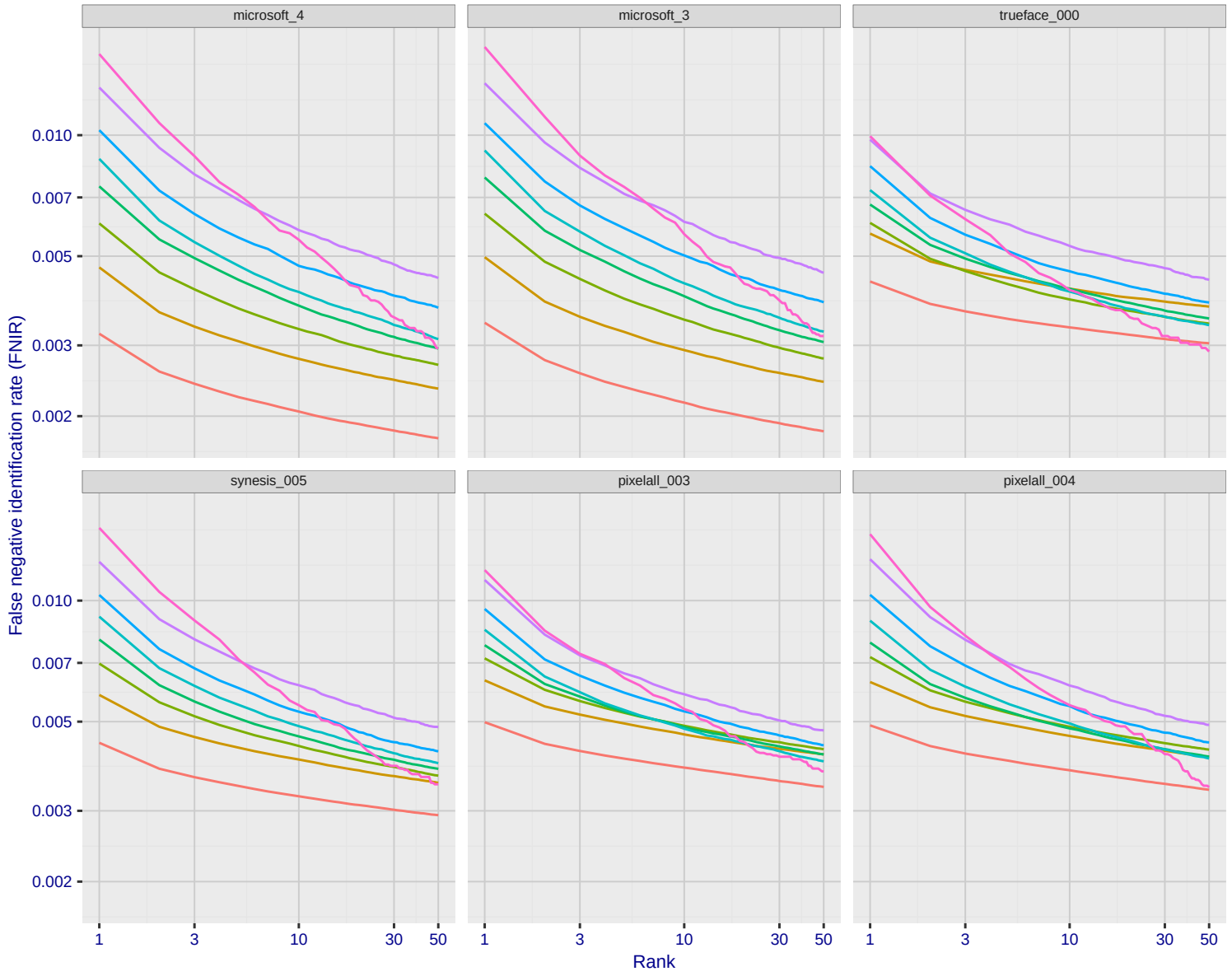

Figure 64: **[FRVT-2018 Mugshot Ageing Dataset] Identification miss rates vs. rank by time-elapsed**. *The oldest image of each individual is enrolled. Thereafter, all more recent images are searched. Miss rates are computed over all searches noted in row 17 of Table 1 and binned by number of years between search and initial enrollment.*

2021/08/05 02:00:58
FNIR(N, R, T) = False neg. identification rate
FPIR(N, T) = False pos. identification rate
N = Num. enrolled subjects
R = Num. candidates examined
T = Threshold
T = 0 → Investigation
T > 0 → Identification

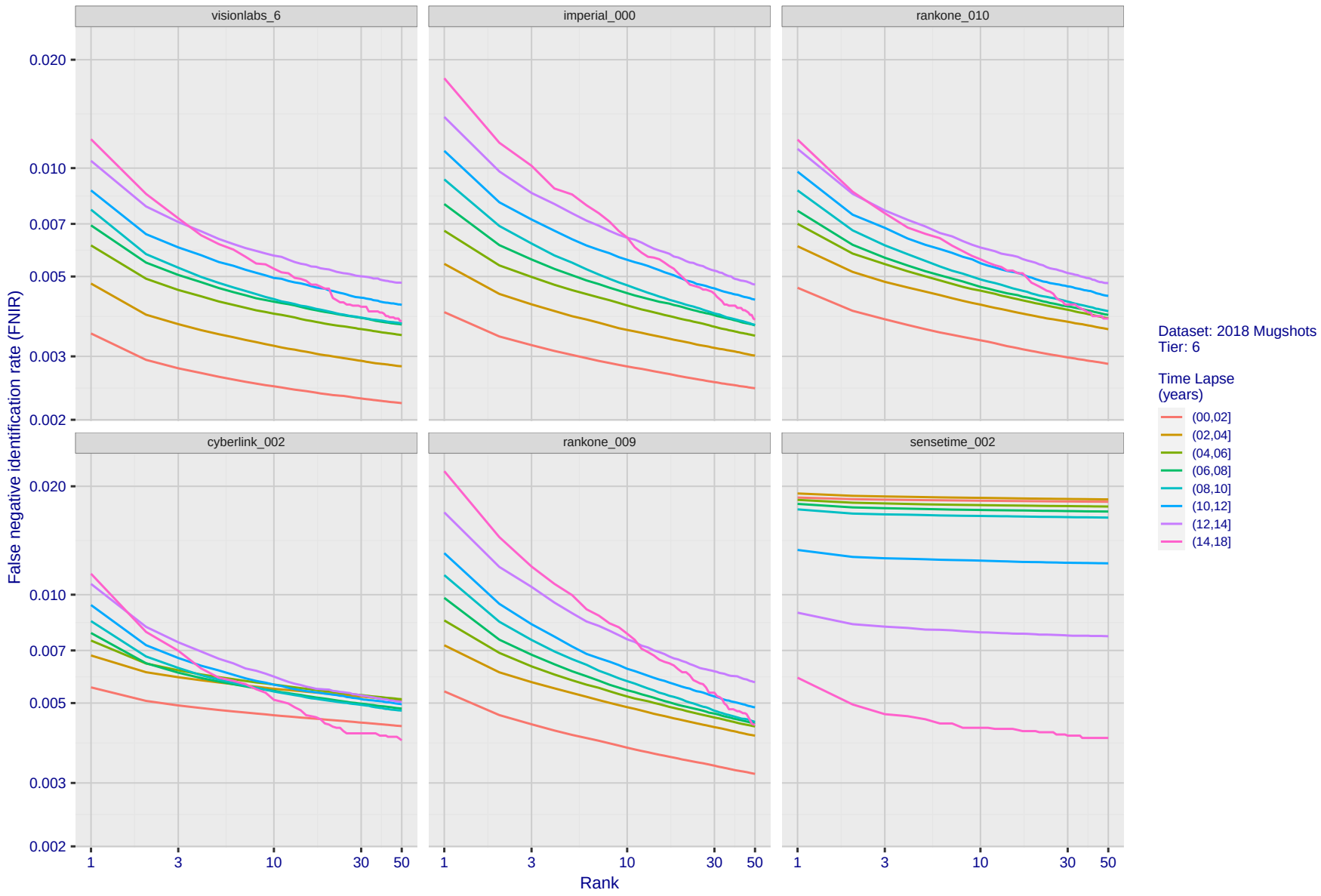

Figure 65: **[FRVT-2018 Mugshot Ageing Dataset] Identification miss rates vs. rank by time-elapsed**. *The oldest image of each individual is enrolled. Thereafter, all more recent images are searched. Miss rates are computed over all searches noted in row 17 of Table 1 and binned by number of years between search and initial enrollment.*

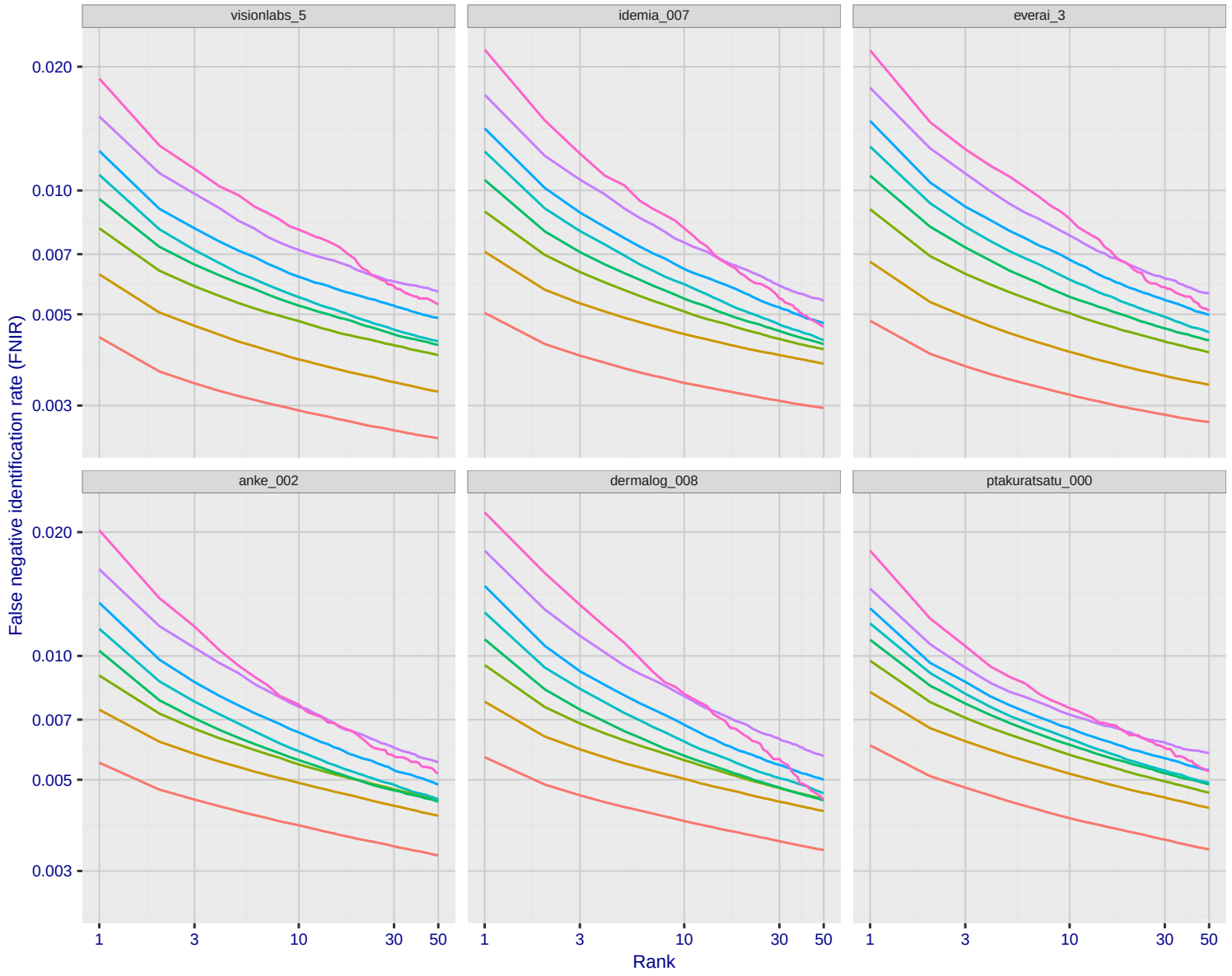

Figure 66: **[FRVT-2018 Mugshot Ageing Dataset] Identification miss rates vs. rank by time-elapsed**. *The oldest image of each individual is enrolled. Thereafter, all more recent images are searched. Miss rates are computed over all searches noted in row 17 of Table 1 and binned by number of years between search and initial enrollment.*

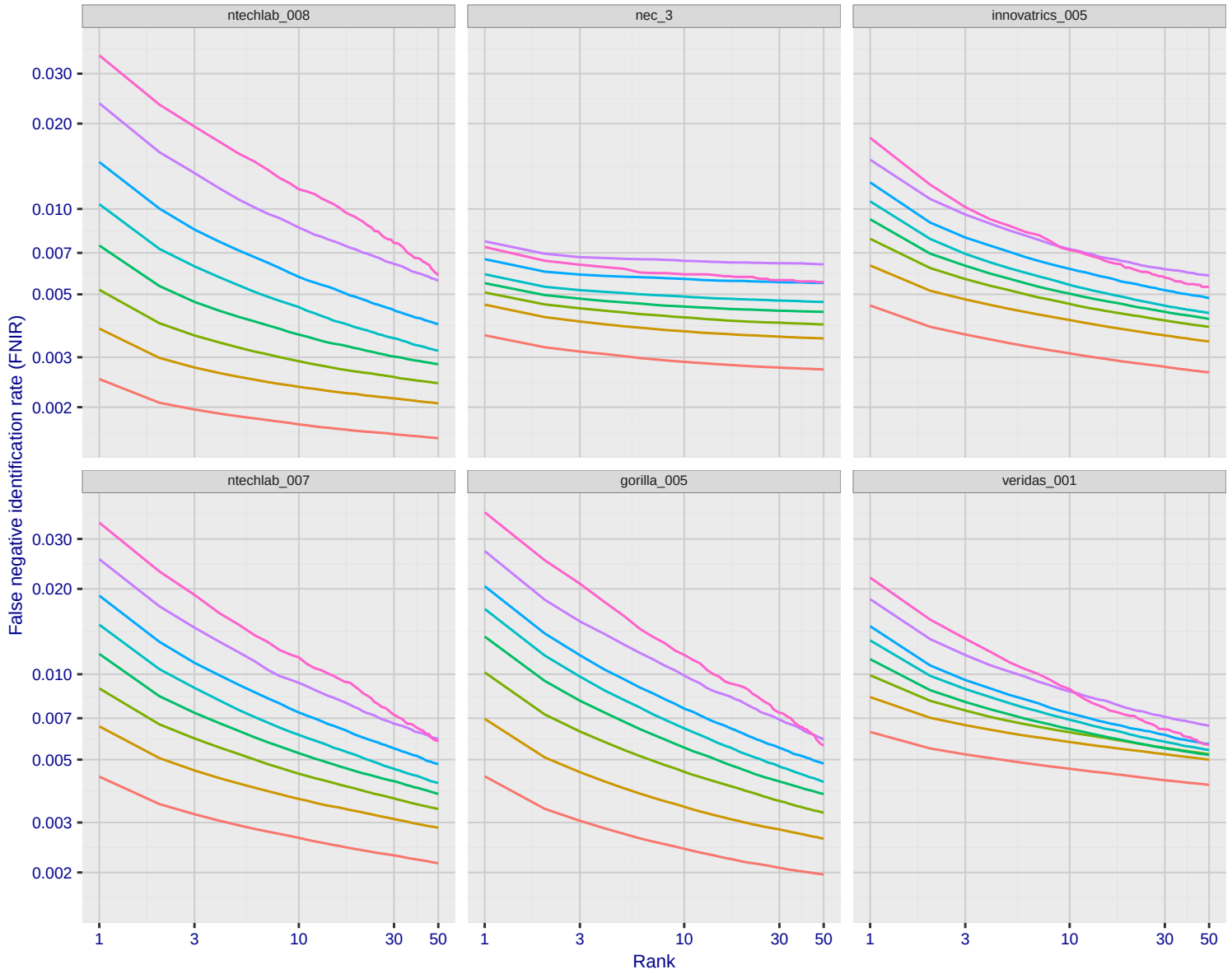

Figure 67: **[FRVT-2018 Mugshot Ageing Dataset] Identification miss rates vs. rank by time-elapsed**. *The oldest image of each individual is enrolled. Thereafter, all more recent images are searched. Miss rates are computed over all searches noted in row 17 of Table 1 and binned by number of years between search and initial enrollment.*

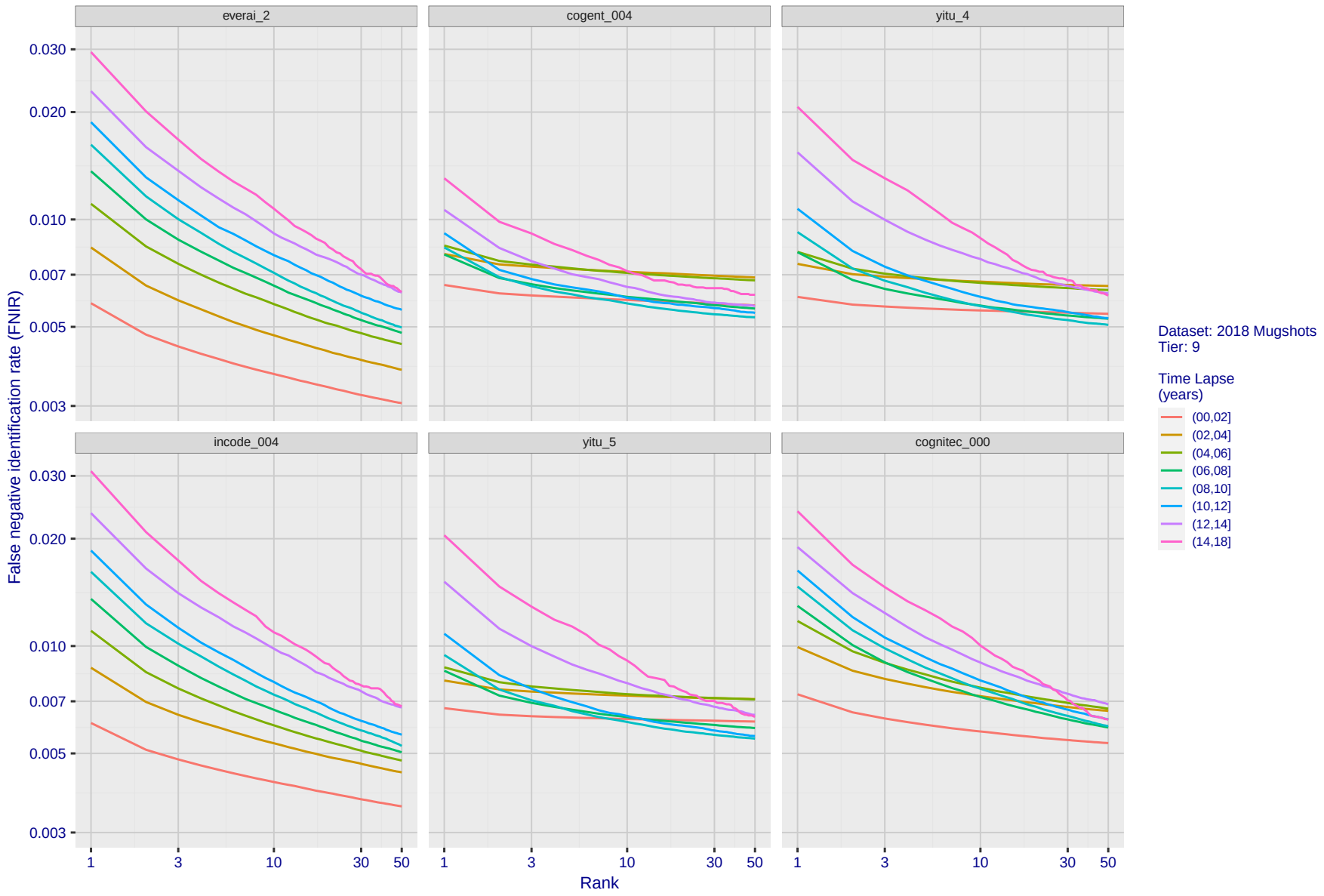

Figure 68: **[FRVT-2018 Mugshot Ageing Dataset] Identification miss rates vs. rank by time-elapsed**. *The oldest image of each individual is enrolled. Thereafter, all more recent images are searched. Miss rates are computed over all searches noted in row 17 of Table 1 and binned by number of years between search and initial enrollment.*

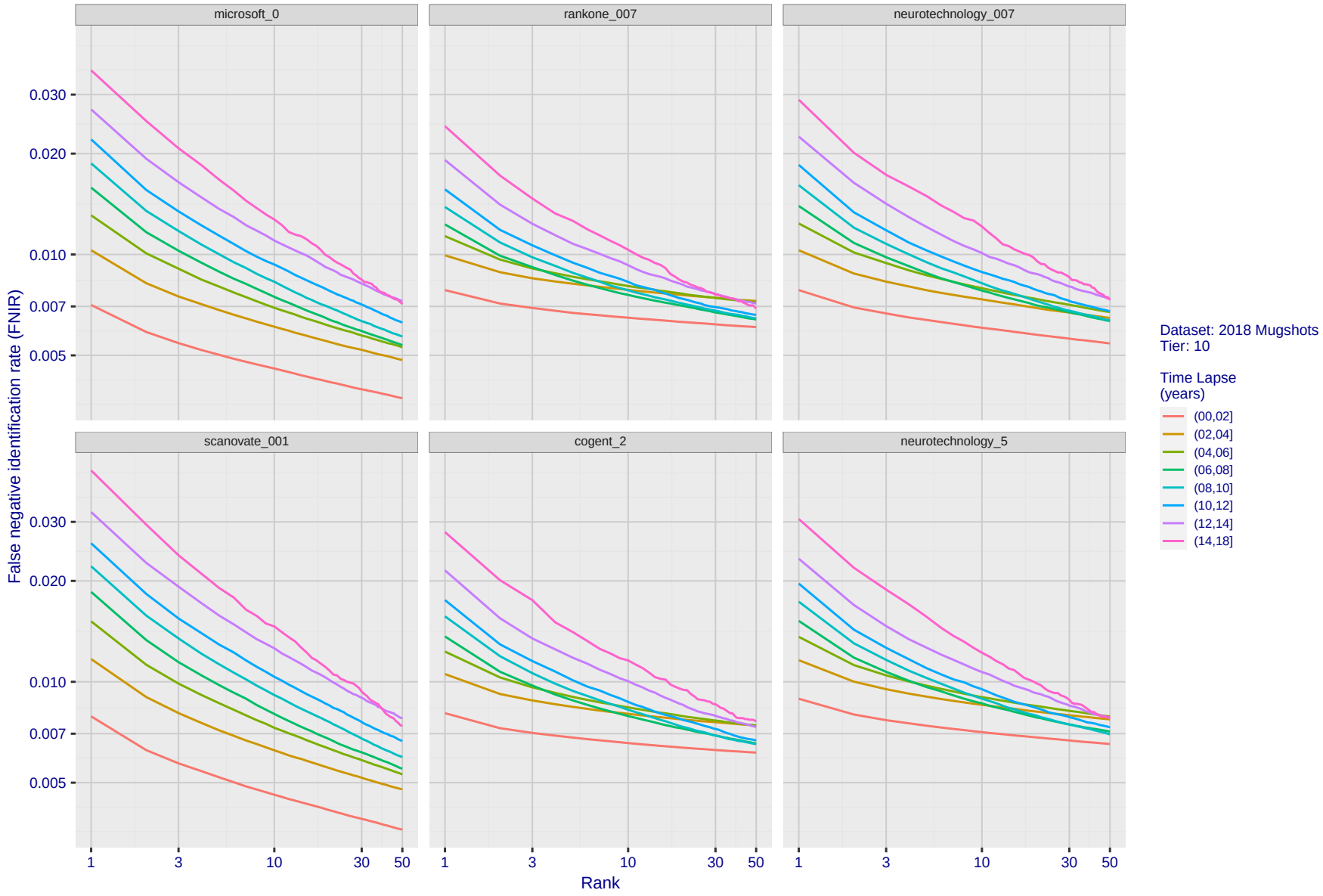

Figure 69: **[FRVT-2018 Mugshot Ageing Dataset] Identification miss rates vs. rank by time-elapsed**. *The oldest image of each individual is enrolled. Thereafter, all more recent images are searched. Miss rates are computed over all searches noted in row 17 of Table 1 and binned by number of years between search and initial enrollment.*

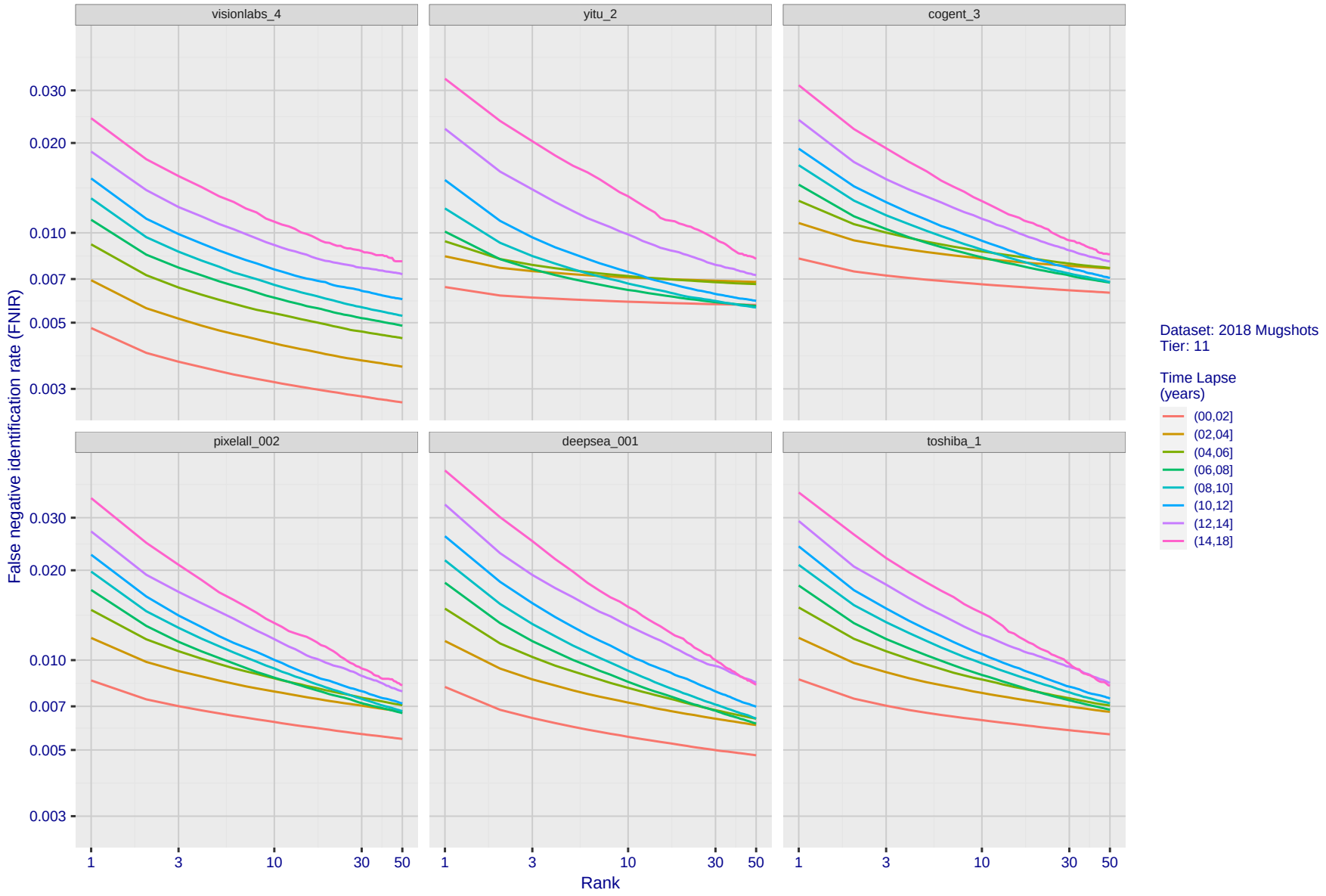

Figure 70: **[FRVT-2018 Mugshot Ageing Dataset] Identification miss rates vs. rank by time-elapsed**. *The oldest image of each individual is enrolled. Thereafter, all more recent images are searched. Miss rates are computed over all searches noted in row 17 of Table 1 and binned by number of years between search and initial enrollment.*

2021/08/05
02:00:58

FNIR(N, R, T) = False neg. identification rate
FPIR(N, T) = False pos. identification rate

N = Num. enrolled subjects
R = Num. candidates examined

T = Threshold

T = 0 → Investigation
T > 0 → Identification

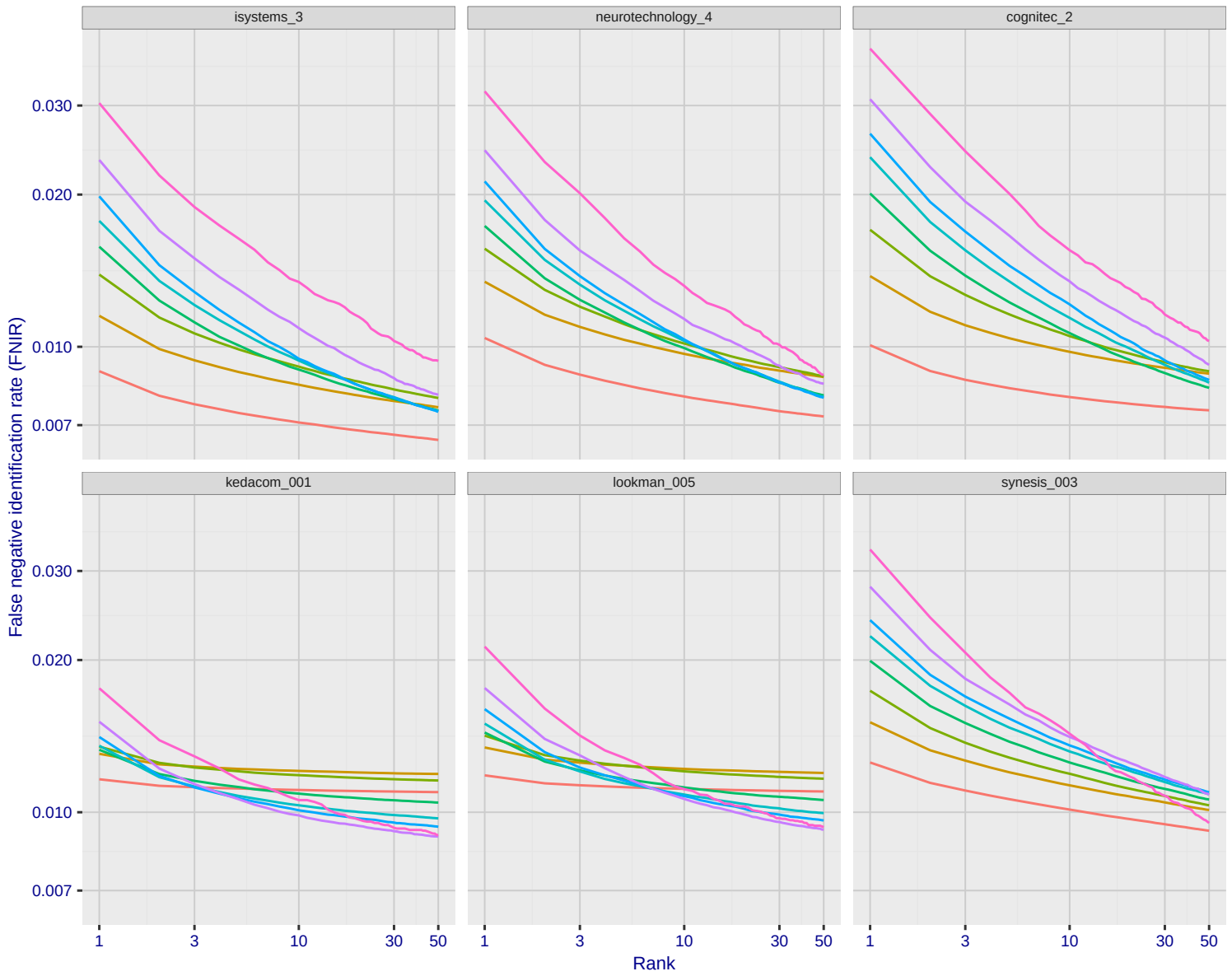

Figure 71: **[FRVT-2018 Mugshot Ageing Dataset] Identification miss rates vs. rank by time-elapsed**. *The oldest image of each individual is enrolled. Thereafter, all more recent images are searched. Miss rates are computed over all searches noted in row 17 of Table 1 and binned by number of years between search and initial enrollment.*

2021/08/05 02:00:58
FNIR(N, R, T) = False neg. identification rate
FPIR(N, T) = False pos. identification rate
N = Num. enrolled subjects
R = Num. candidates examined
T = Threshold
T = 0 → Investigation
T > 0 → Identification

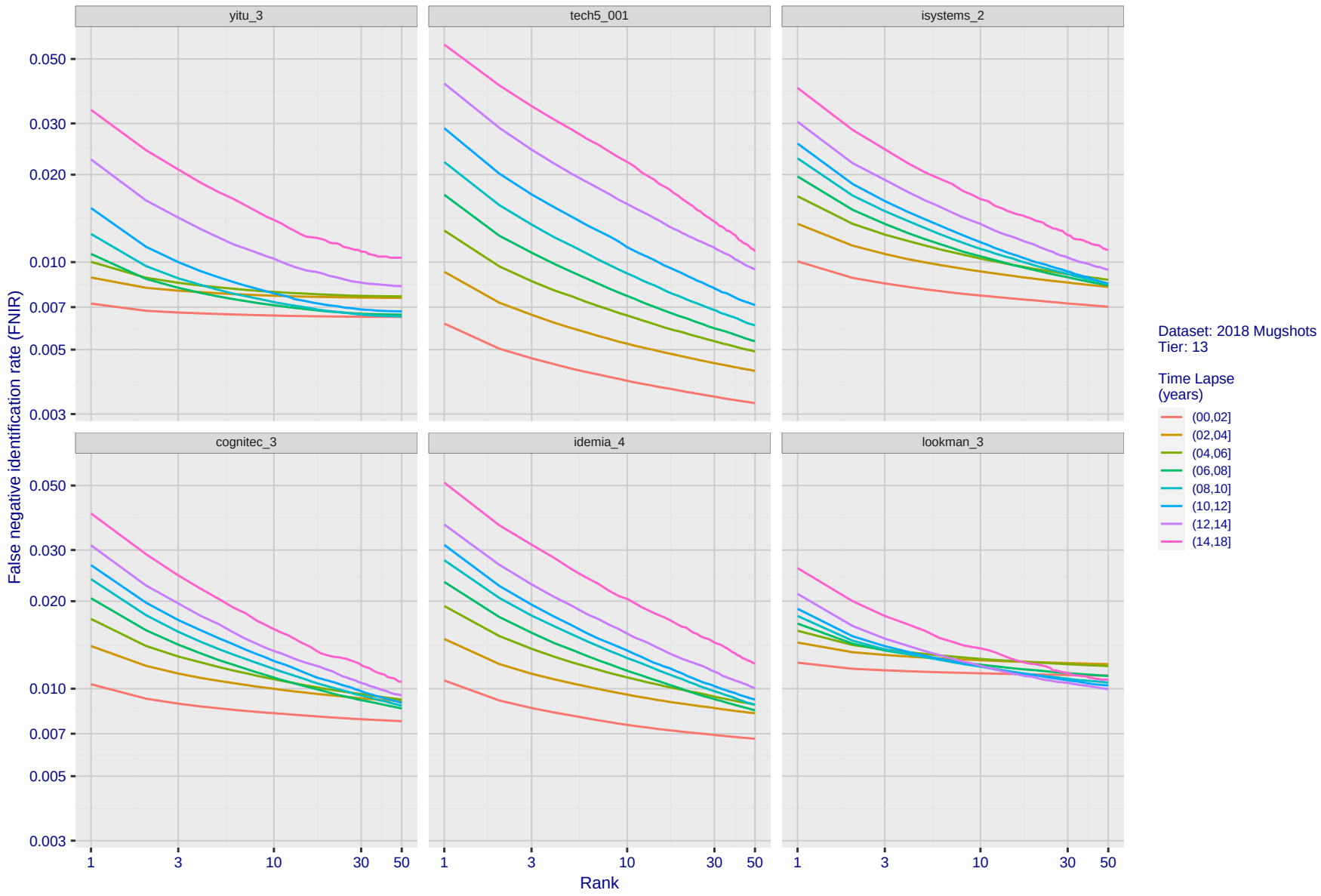

Figure 72: **[FRVT-2018 Mugshot Ageing Dataset] Identification miss rates vs. rank by time-elapsed**. *The oldest image of each individual is enrolled. Thereafter, all more recent images are searched. Miss rates are computed over all searches noted in row 17 of Table 1 and binned by number of years between search and initial enrollment.*

2021/08/05 02:00:58
FNIR(N, R, T) = False neg. identification rate
FPIR(N, T) = False pos. identification rate
N = Num. enrolled subjects
R = Num. candidates examined
T = Threshold
T = 0 → Investigation
T > 0 → Identification

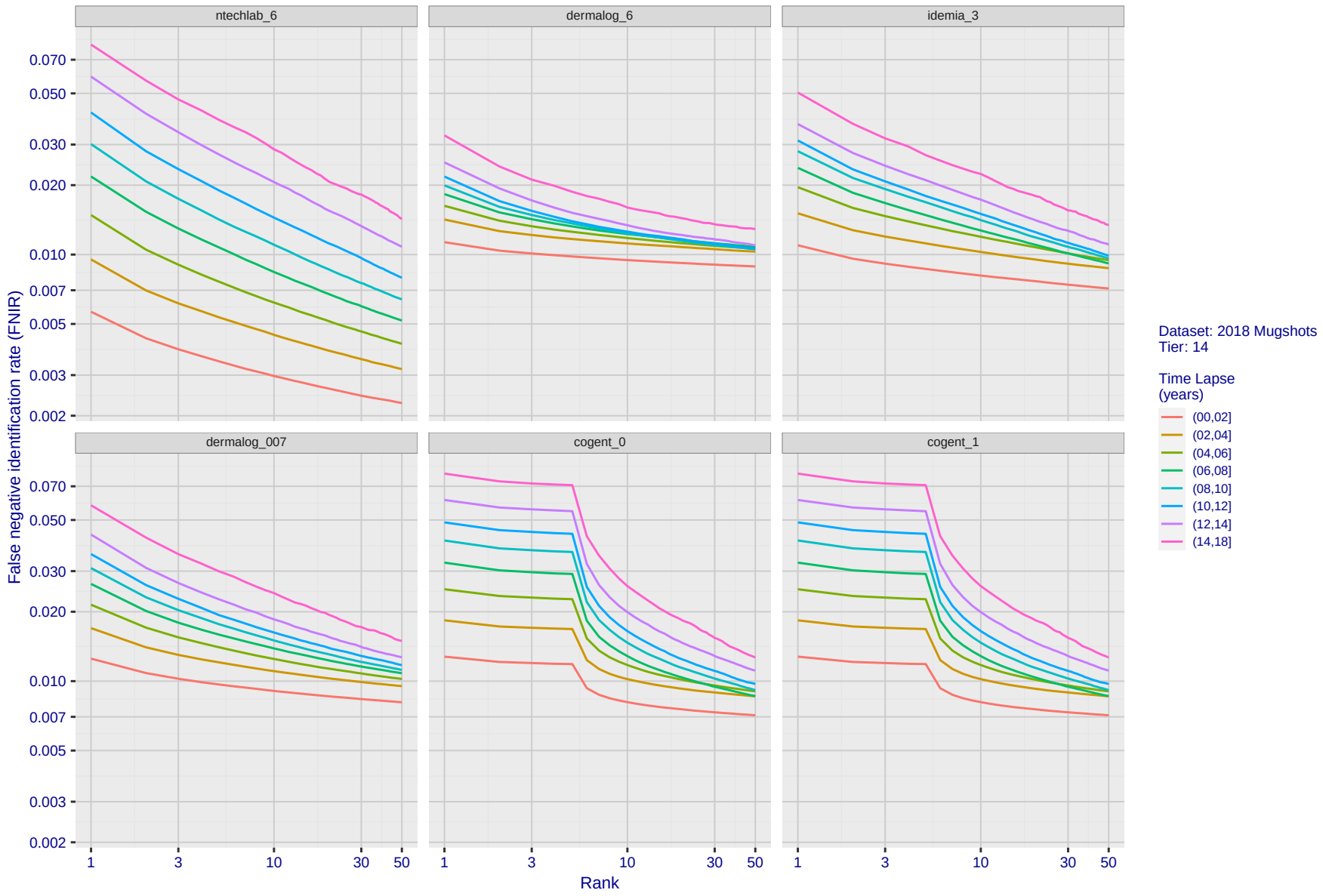

Figure 73: **[FRVT-2018 Mugshot Ageing Dataset] Identification miss rates vs. rank by time-elapsed**. *The oldest image of each individual is enrolled. Thereafter, all more recent images are searched. Miss rates are computed over all searches noted in row 17 of Table 1 and binned by number of years between search and initial enrollment.*

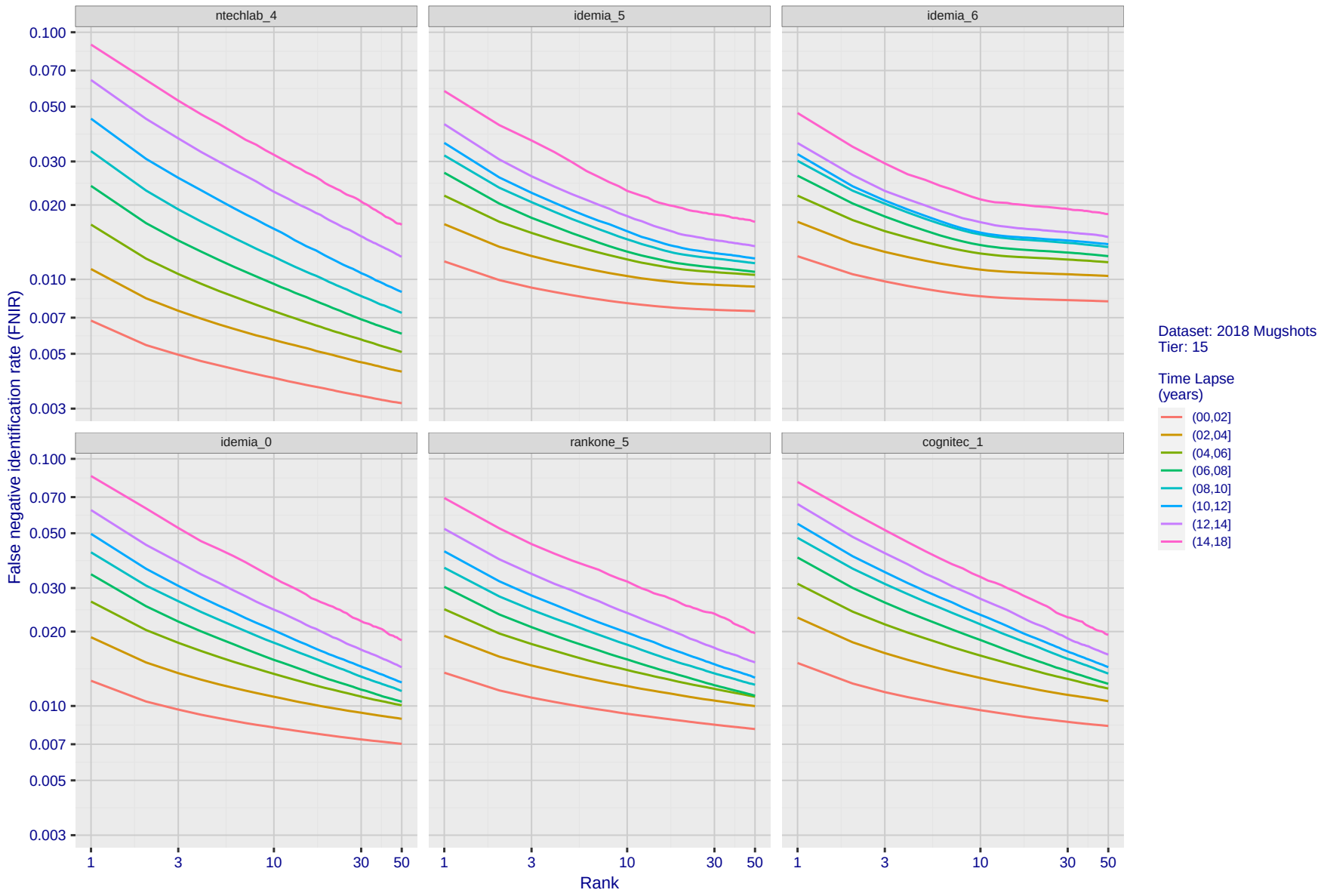

Figure 74: **[FRVT-2018 Mugshot Ageing Dataset] Identification miss rates vs. rank by time-elapsed**. *The oldest image of each individual is enrolled. Thereafter, all more recent images are searched. Miss rates are computed over all searches noted in row 17 of Table 1 and binned by number of years between search and initial enrollment.*

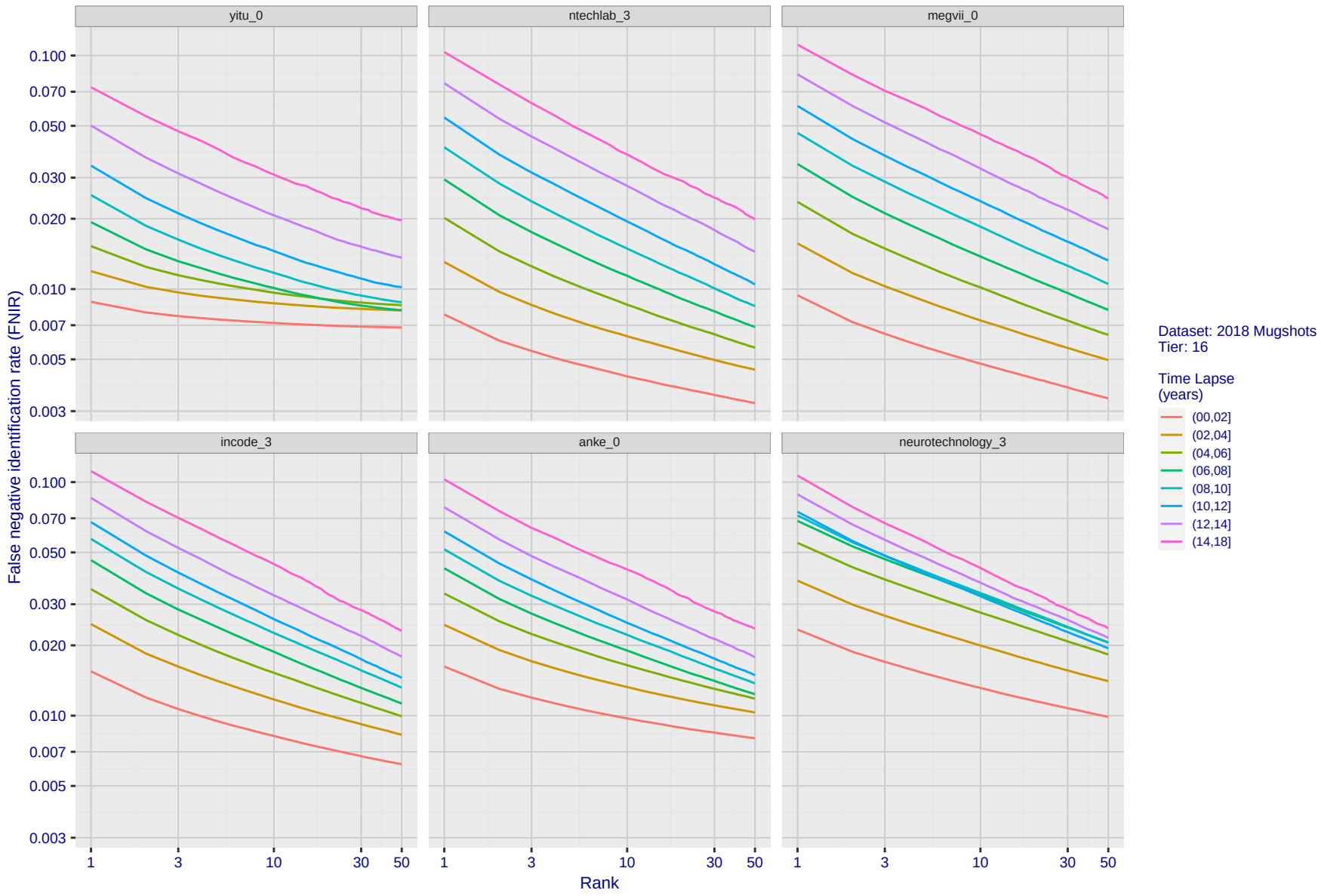

Figure 75: **[FRVT-2018 Mugshot Ageing Dataset] Identification miss rates vs. rank by time-elapsed**. *The oldest image of each individual is enrolled. Thereafter, all more recent images are searched. Miss rates are computed over all searches noted in row 17 of Table 1 and binned by number of years between search and initial enrollment.*

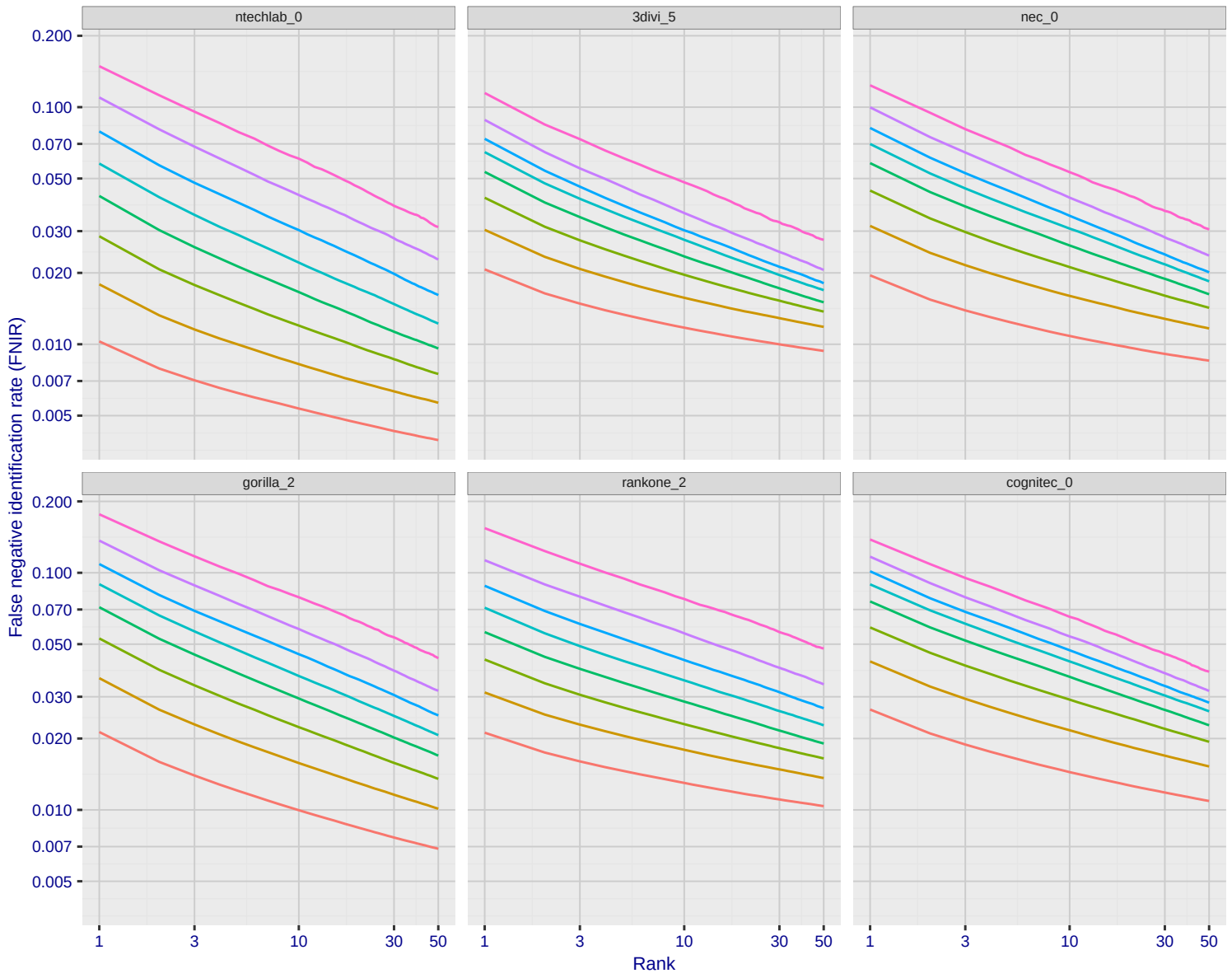

Figure 76: **[FRVT-2018 Mugshot Ageing Dataset] Identification miss rates vs. rank by time-elapsed**. *The oldest image of each individual is enrolled. Thereafter, all more recent images are searched. Miss rates are computed over all searches noted in row 17 of Table 1 and binned by number of years between search and initial enrollment.*

2021/08/05 02:00:58
FNIR(N, R, T) = False neg. identification rate
FPIR(N, T) = False pos. identification rate
N = Num. enrolled subjects
R = Num. candidates examined
T = Threshold
T = 0 → Investigation
T > 0 → Identification

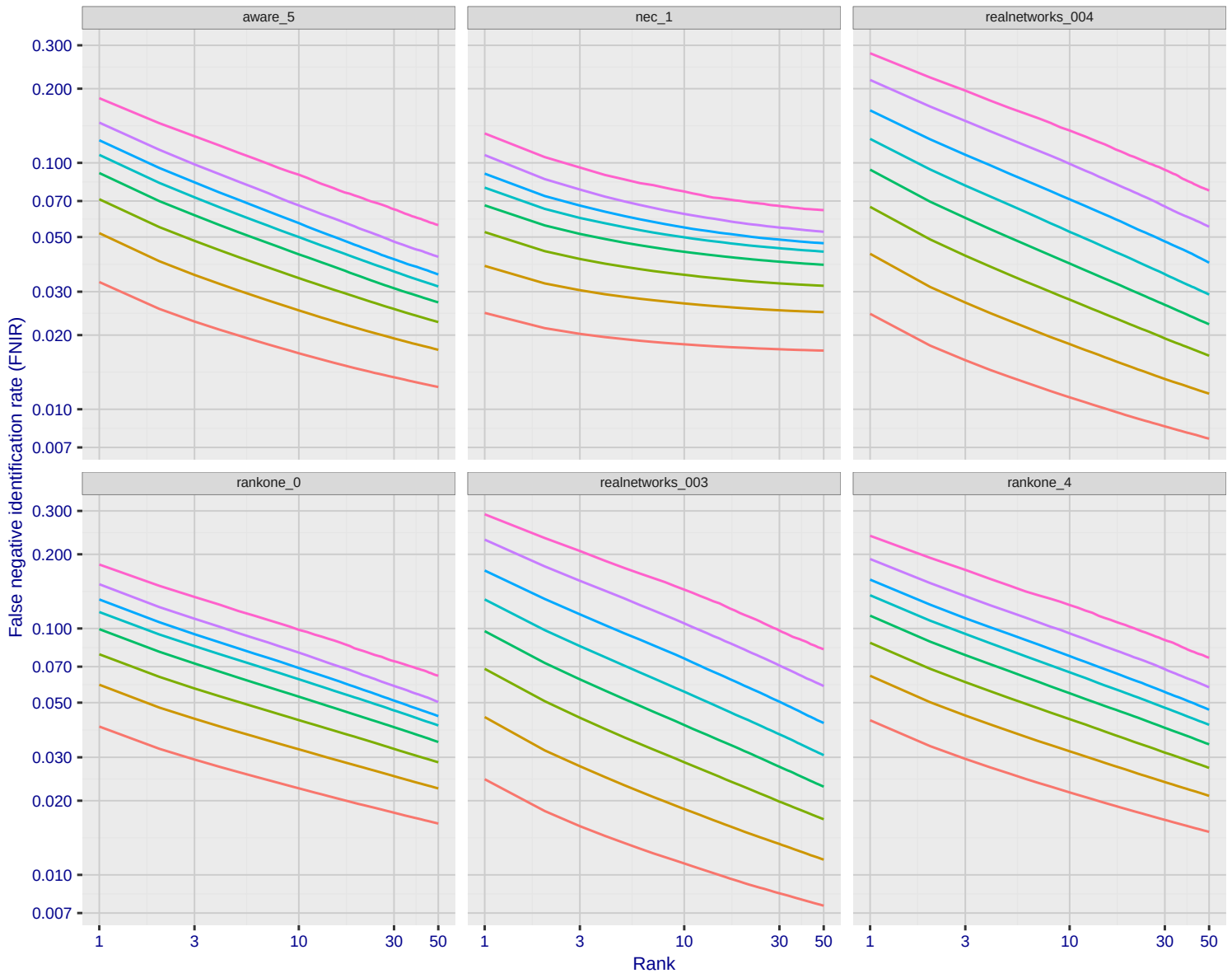

Figure 77: **[FRVT-2018 Mugshot Ageing Dataset] Identification miss rates vs. rank by time-elapsed**. *The oldest image of each individual is enrolled. Thereafter, all more recent images are searched. Miss rates are computed over all searches noted in row 17 of Table 1 and binned by number of years between search and initial enrollment.*

2021/08/05 02:00:58
FNIR(N, R, T) = False neg. identification rate
FPIR(N, T) = False pos. identification rate
N = Num. enrolled subjects
R = Num. candidates examined
T = Threshold
T = 0 → Investigation
T > 0 → Identification

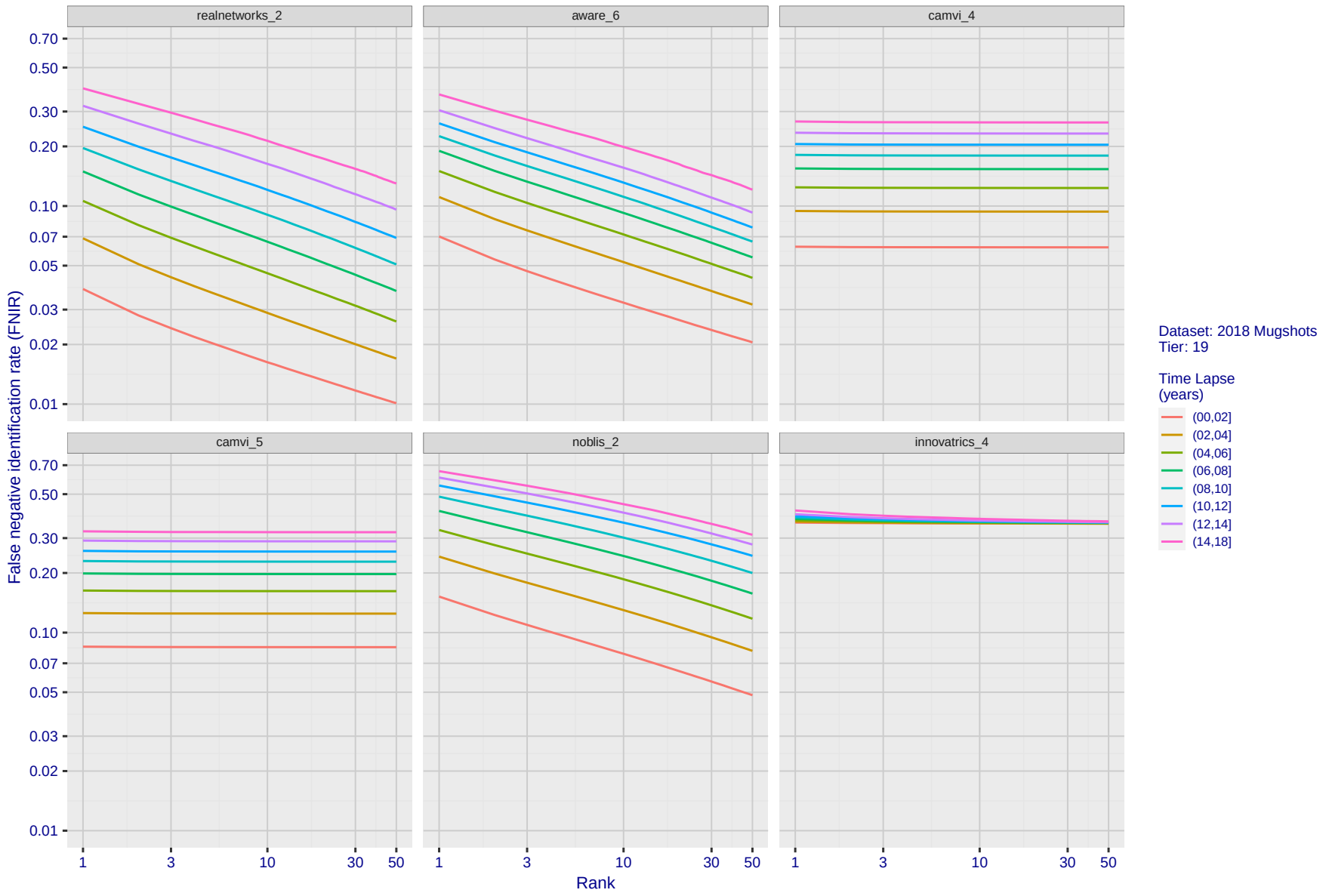

Figure 78: **[FRVT-2018 Mugshot Ageing Dataset] Identification miss rates vs. rank by time-elapsed**. *The oldest image of each individual is enrolled. Thereafter, all more recent images are searched. Miss rates are computed over all searches noted in row 17 of Table 1 and binned by number of years between search and initial enrollment.*

2021/08/05 02:00:58
FNIR(N, R, T) = False neg. identification rate
FPIR(N, T) = False pos. identification rate
N = Num. enrolled subjects
R = Num. candidates examined
T = Threshold
T = 0 → Investigation
T > 0 → Identification

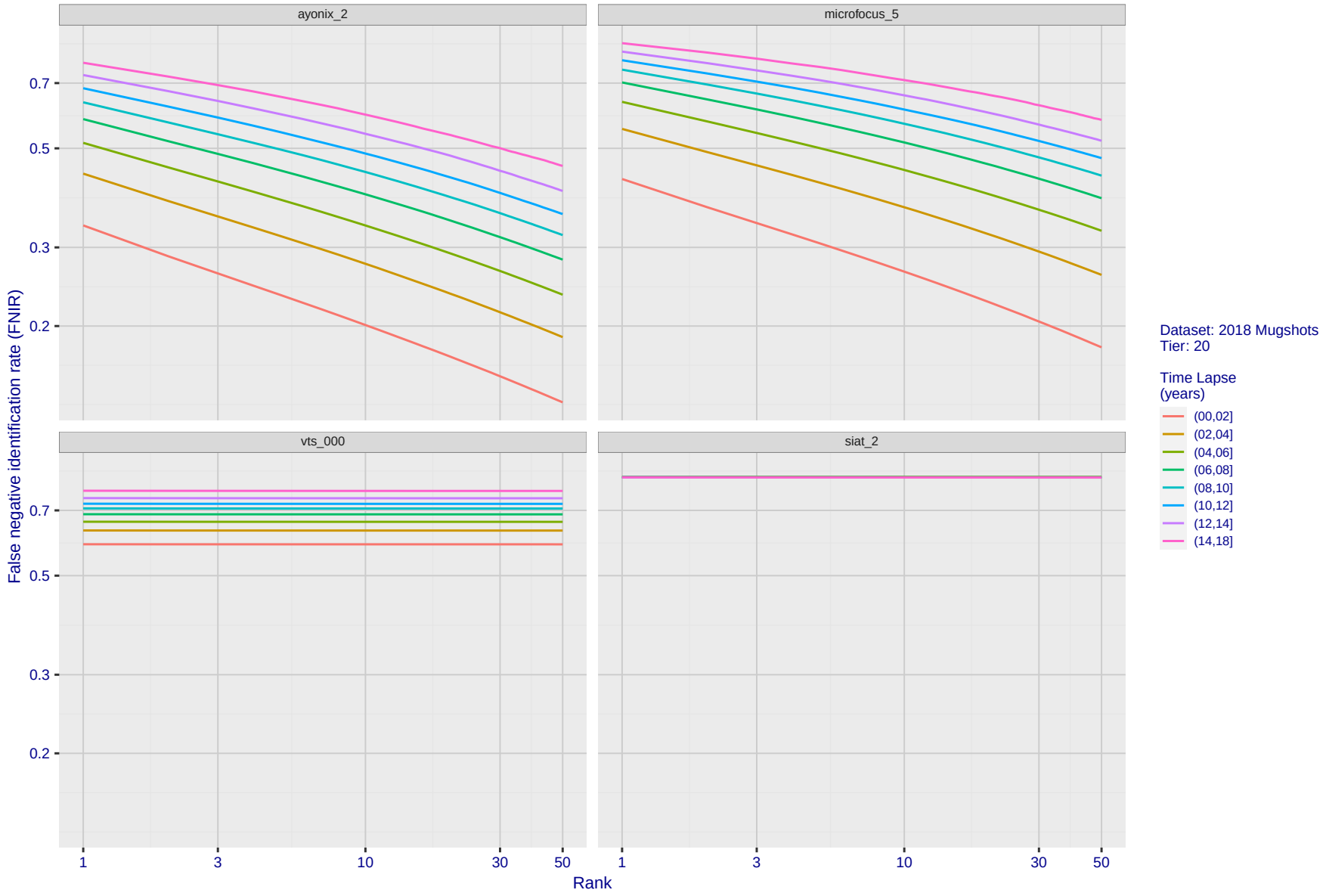

Figure 79: **[FRVT-2018 Mugshot Ageing Dataset] Identification miss rates vs. rank by time-elapsed**. *The oldest image of each individual is enrolled. Thereafter, all more recent images are searched. Miss rates are computed over all searches noted in row 17 of Table 1 and binned by number of years between search and initial enrollment.*

2021/08/05 02:00:58

FNIR(N, R, T) = False neg. identification rate
FPIR(N, T) = False pos. identification rate

N = Num. enrolled subjects
R = Num. candidates examined

T = Threshold

T = 0 → Investigation
T > 0 → Identification

2021/08/05	FNIR(N, R, T) =	False neg. identification rate	N = Num. enrolled subjects	T = Threshold	$T = 0 \rightarrow$ Investigation
02:00:58	FPIR(N, T) =	False pos. identification rate	R = Num. candidates examined		$T > 0 \rightarrow$ Identification

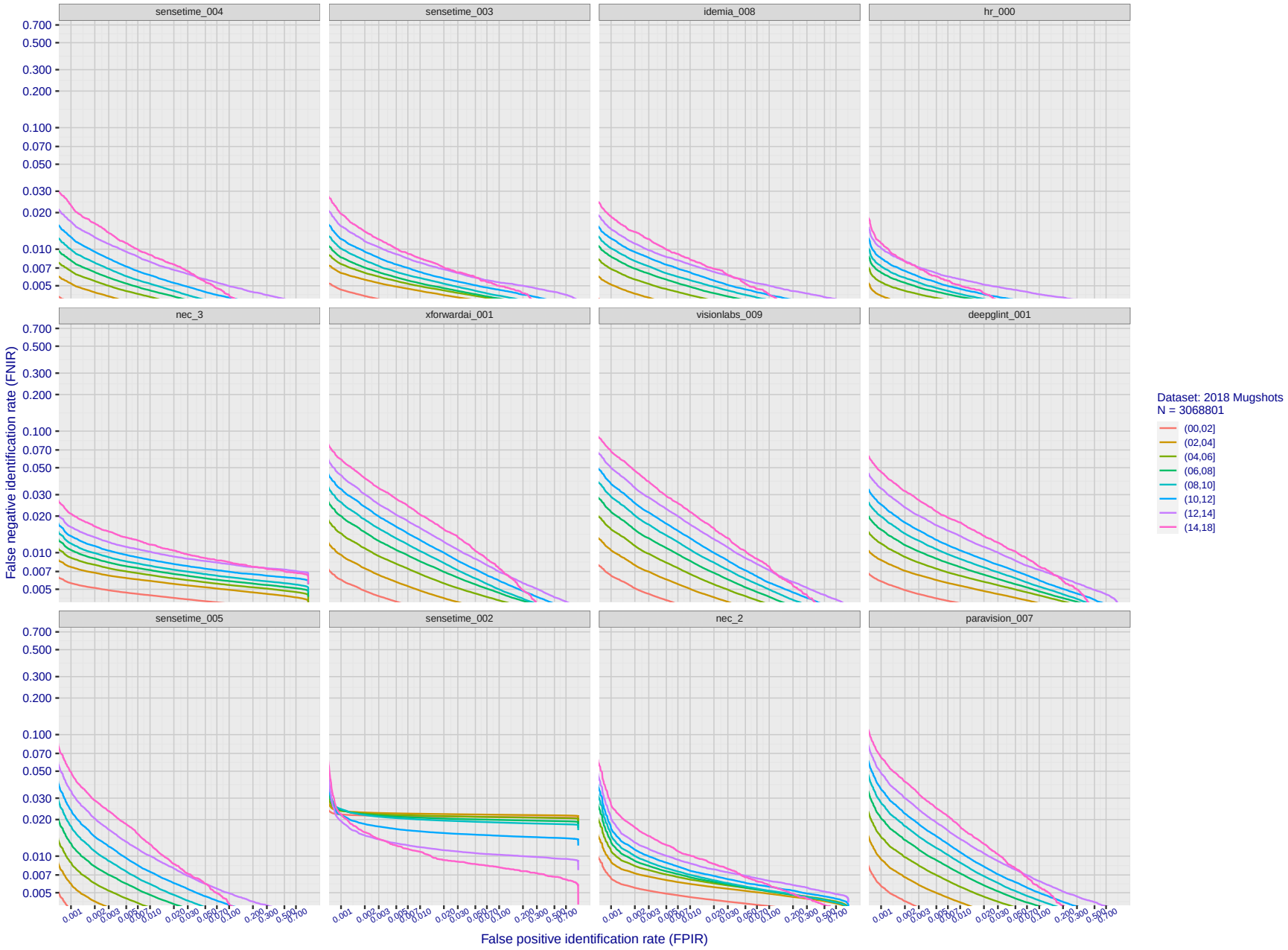

Figure 80: **[FRVT-2018 Mugshot Ageing Dataset] Identification miss rates vs. FPIR by time-elapsed**. *The oldest image of each individual is enrolled. Thereafter, all more recent images are searched. Miss rates are computed over all searches noted in row 17 of Table 1 and binned by number of years between search and initial enrollment. FPIR is computed from the same FRVT 2018 non-mates noted in row 3 of Table 1 with N = 3 000 000.*

2021/08/05 02:00:58
FNIR(N, R, T) = False neg. identification rate
FPIR(N, T) = False pos. identification rate
N = Num. enrolled subjects
R = Num. candidates examined
T = Threshold
T = 0 → Investigation
T > 0 → Identification

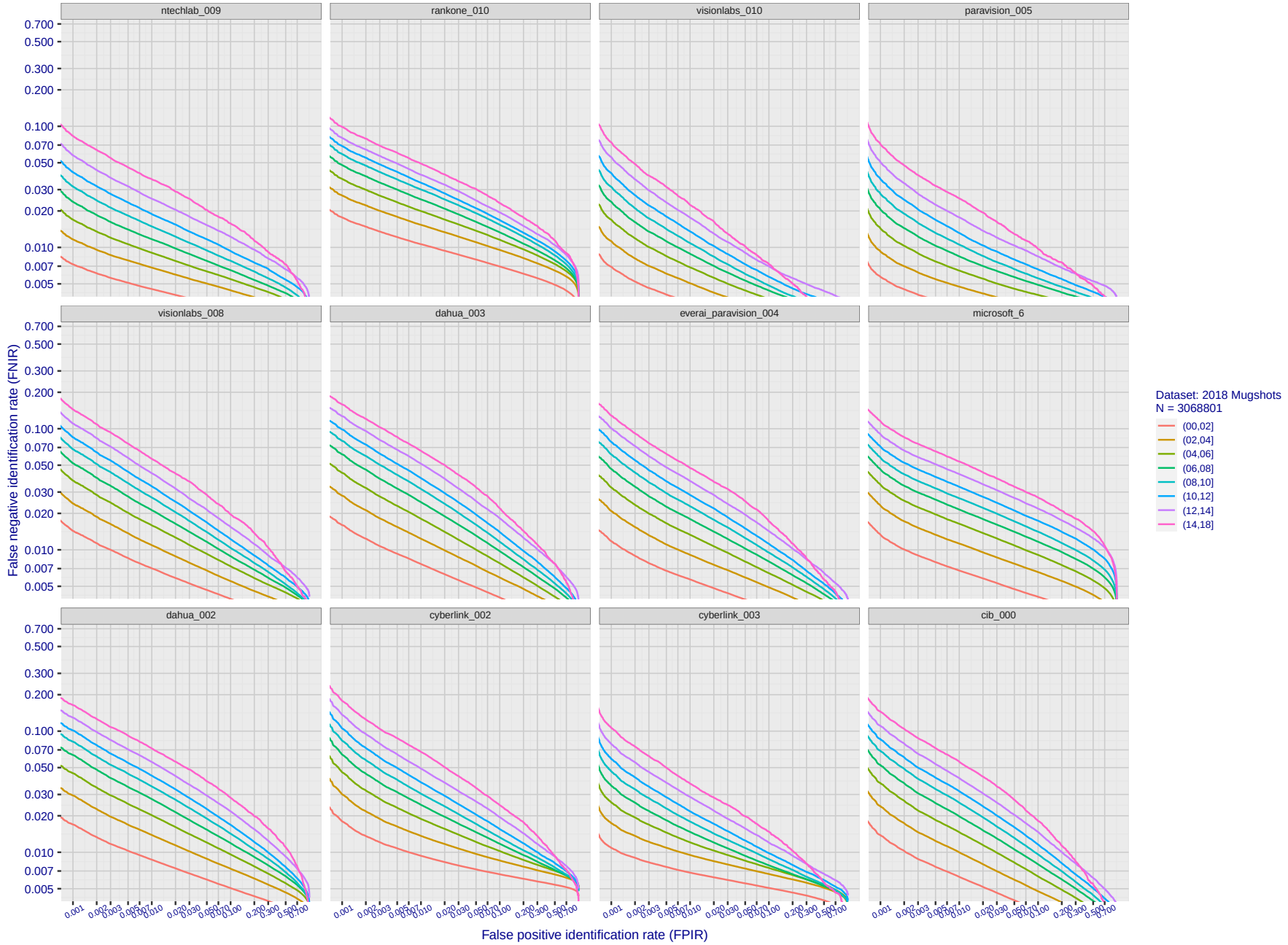

Figure 81: **[FRVT-2018 Mugshot Ageing Dataset] Identification miss rates vs. FPIR by time-elapsed**. *The oldest image of each individual is enrolled. Thereafter, all more recent images are searched. Miss rates are computed over all searches noted in row 17 of Table 1 and binned by number of years between search and initial enrollment. FPIR is computed from the same FRVT 2018 non-mates noted in row 3 of Table 1 with N = 3 000 000.*

2021/08/05 02:00:58
FNIR(N, R, T) = False neg. identification rate
FPIR(N, T) = False pos. identification rate
N = Num. enrolled subjects
R = Num. candidates examined
T = Threshold
T = 0 → Investigation
T > 0 → Identification

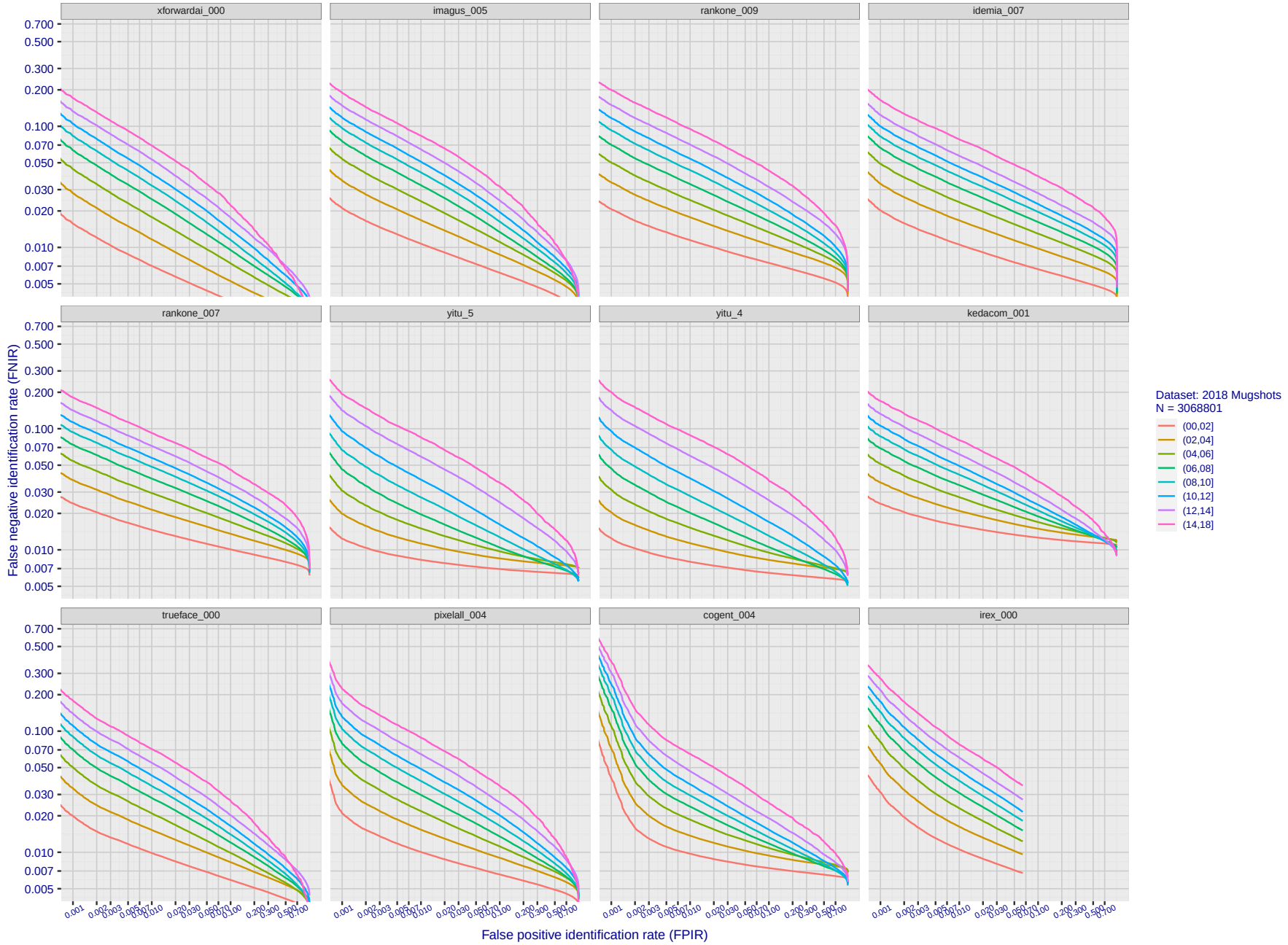

Figure 82: **[FRVT-2018 Mugshot Ageing Dataset] Identification miss rates vs. FPIR by time-elapsed**. *The oldest image of each individual is enrolled. Thereafter, all more recent images are searched. Miss rates are computed over all searches noted in row 17 of Table 1 and binned by number of years between search and initial enrollment. FPIR is computed from the same FRVT 2018 non-mates noted in row 3 of Table 1 with N = 3 000 000.*

2021/08/05 02:00:58
FNIR(N, R, T) = False neg. identification rate
FPIR(N, T) = False pos. identification rate
N = Num. enrolled subjects
R = Num. candidates examined
T = Threshold
T = 0 → Investigation
T > 0 → Identification

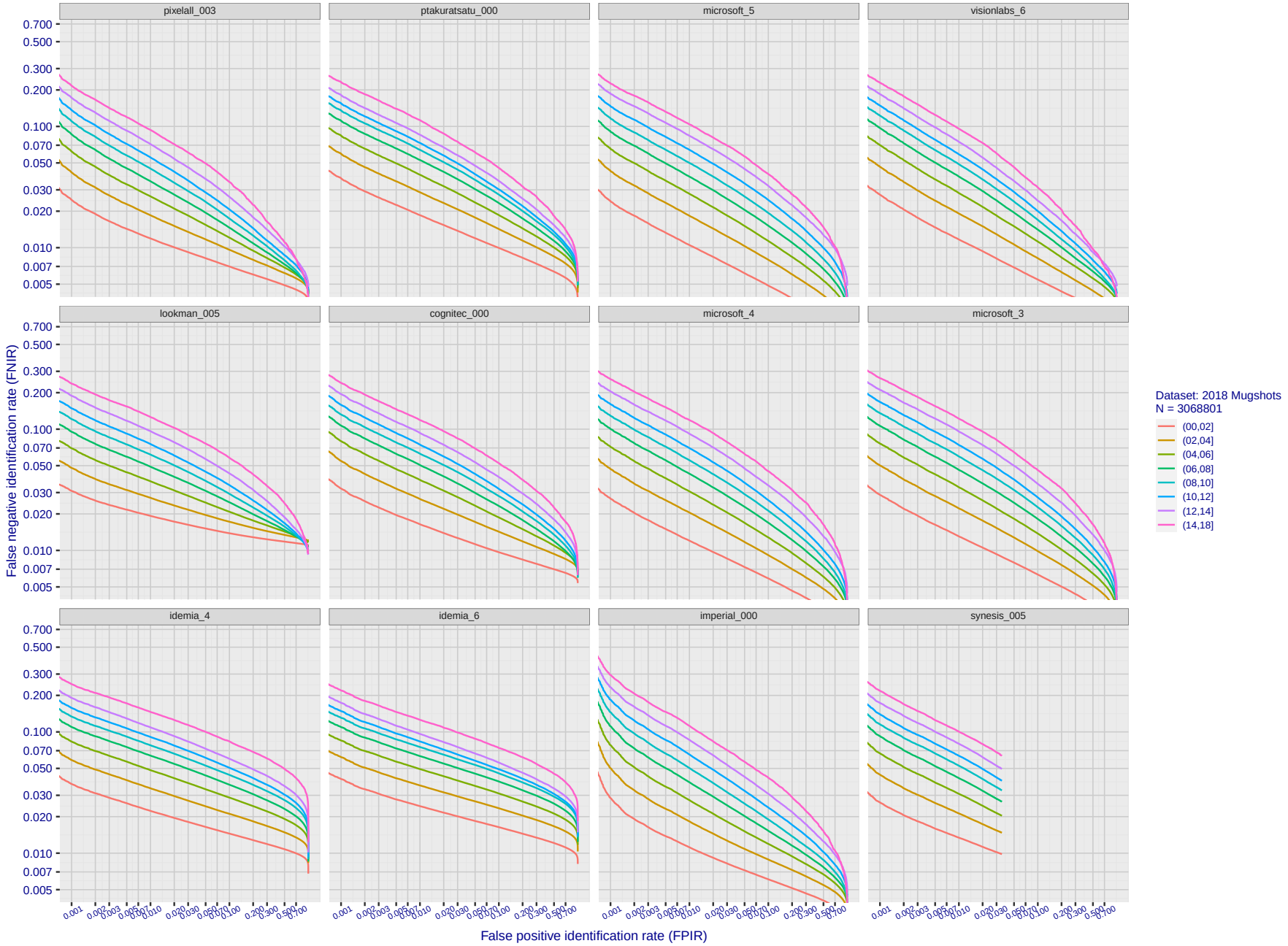

Figure 83: **[FRVT-2018 Mugshot Ageing Dataset] Identification miss rates vs. FPIR by time-elapsed**. *The oldest image of each individual is enrolled. Thereafter, all more recent images are searched. Miss rates are computed over all searches noted in row 17 of Table 1 and binned by number of years between search and initial enrollment. FPIR is computed from the same FRVT 2018 non-mates noted in row 3 of Table 1 with N = 3 000 000.*

2021/08/05 02:00:58

FNIR(N, R, T) = False neg. identification rate
FPIR(N, T) = False pos. identification rate

N = Num. enrolled subjects
R = Num. candidates examined

T = Threshold

T = 0 → Investigation
T > 0 → Identification

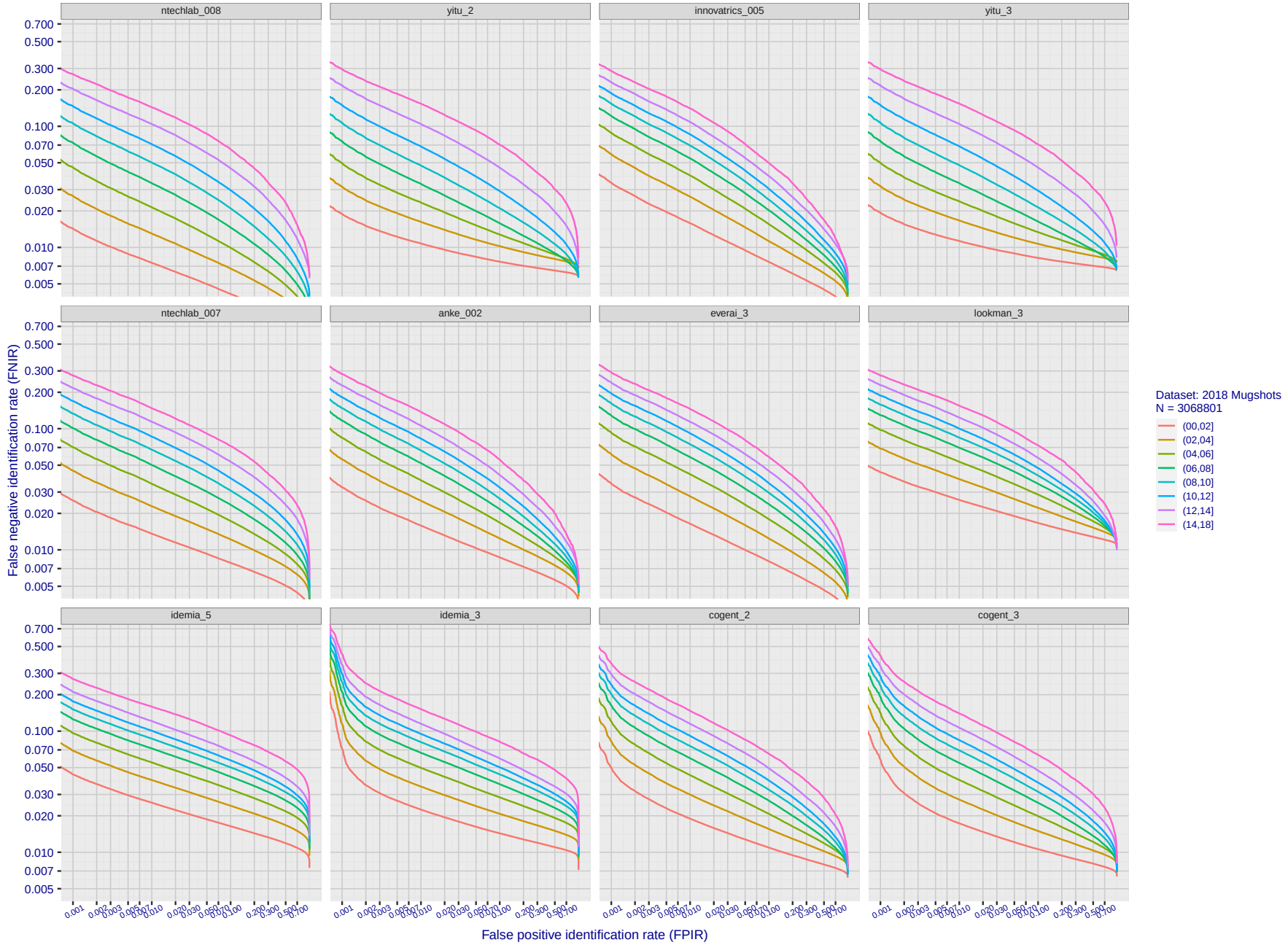

Figure 84: **[FRVT-2018 Mugshot Ageing Dataset] Identification miss rates vs. FPIR by time-elapsed**. *The oldest image of each individual is enrolled. Thereafter, all more recent images are searched. Miss rates are computed over all searches noted in row 17 of Table 1 and binned by number of years between search and initial enrollment. FPIR is computed from the same FRVT 2018 non-mates noted in row 3 of Table 1 with N = 3 000 000.*

2021/08/05
02:00:58

FNIR(N, R, T) = False neg. identification rate
FPIR(N, T) = False pos. identification rate

N = Num. enrolled subjects
R = Num. candidates examined

T = Threshold

T = 0 → Investigation
T > 0 → Identification

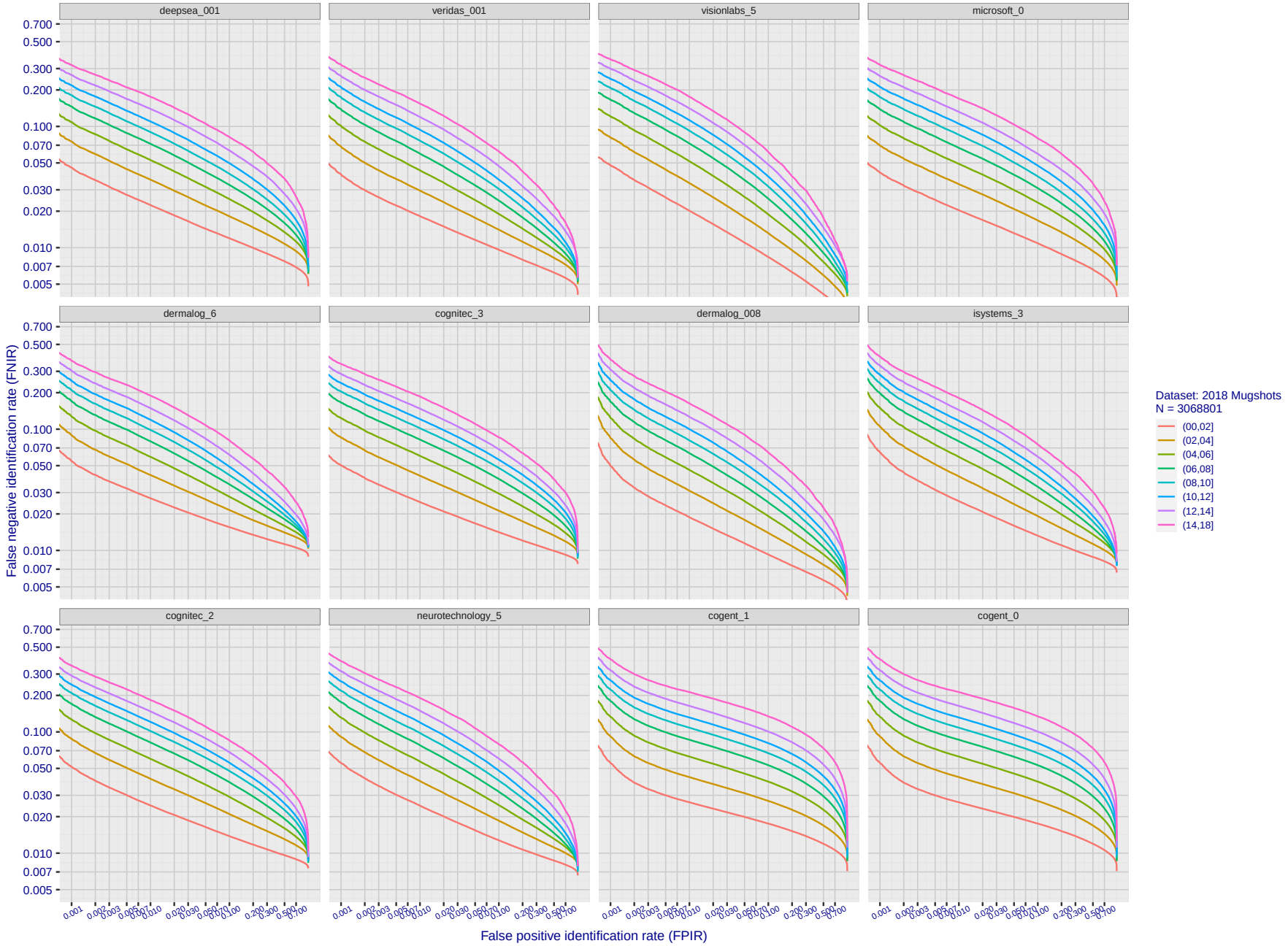

Figure 85: **[FRVT-2018 Mugshot Ageing Dataset] Identification miss rates vs. FPIR by time-elapsed**. *The oldest image of each individual is enrolled. Thereafter, all more recent images are searched. Miss rates are computed over all searches noted in row 17 of Table 1 and binned by number of years between search and initial enrollment. FPIR is computed from the same FRVT 2018 non-mates noted in row 3 of Table 1 with N = 3 000 000.*

2021/08/05 02:00:58
FNIR(N, R, T) = False neg. identification rate
FPIR(N, T) = False pos. identification rate
N = Num. enrolled subjects
R = Num. candidates examined
T = Threshold
T = 0 → Investigation
T > 0 → Identification

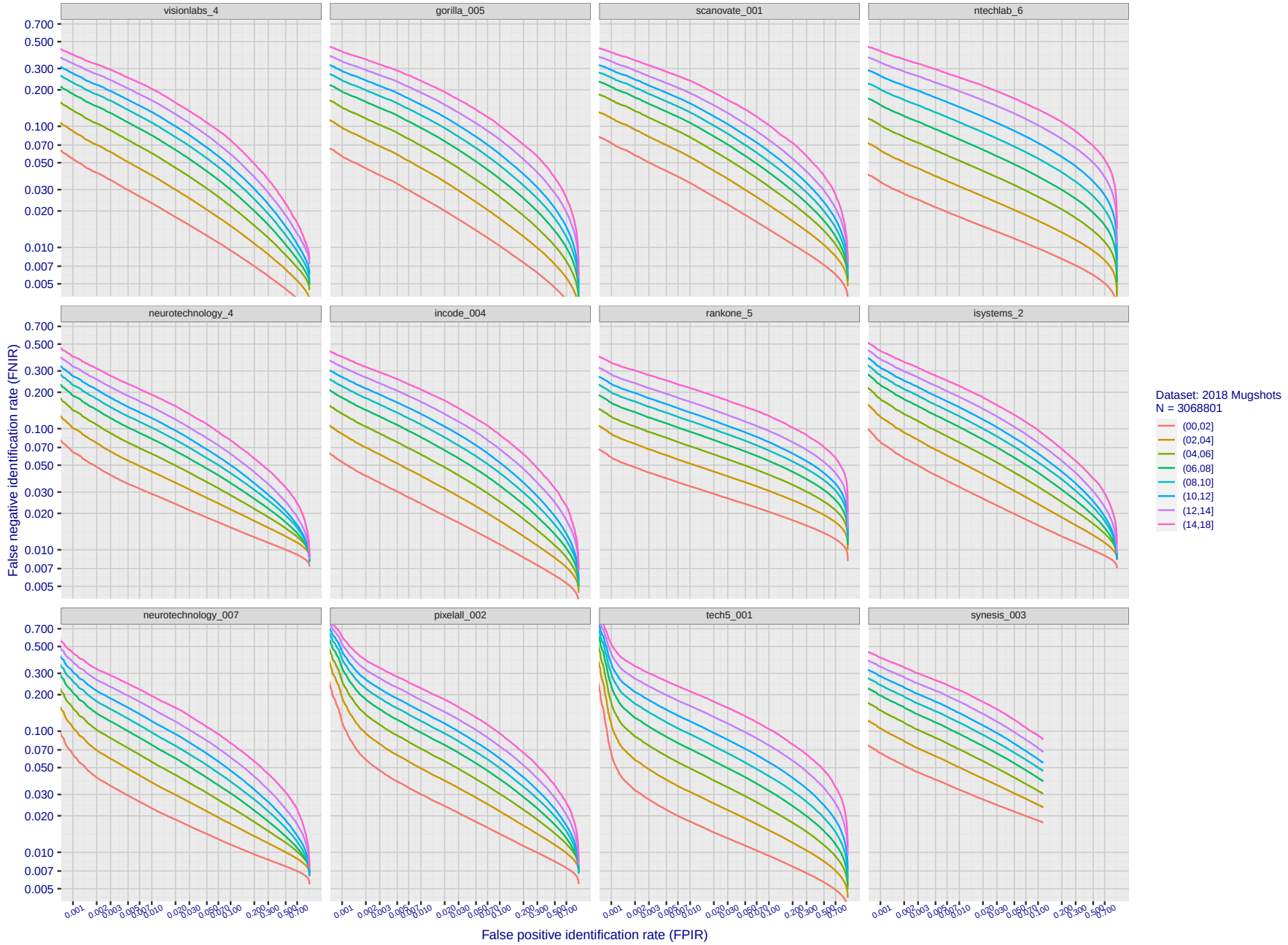

Figure 86: **[FRVT-2018 Mugshot Ageing Dataset] Identification miss rates vs. FPIR by time-elapsed**. *The oldest image of each individual is enrolled. Thereafter, all more recent images are searched. Miss rates are computed over all searches noted in row 17 of Table 1 and binned by number of years between search and initial enrollment. FPIR is computed from the same FRVT 2018 non-mates noted in row 3 of Table 1 with N = 3 000 000.*

2021/08/05 02:00:58
FNIR(N, R, T) = False neg. identification rate
FPIR(N, T) = False pos. identification rate
N = Num. enrolled subjects
R = Num. candidates examined
T = Threshold
T = 0 → Investigation
T > 0 → Identification

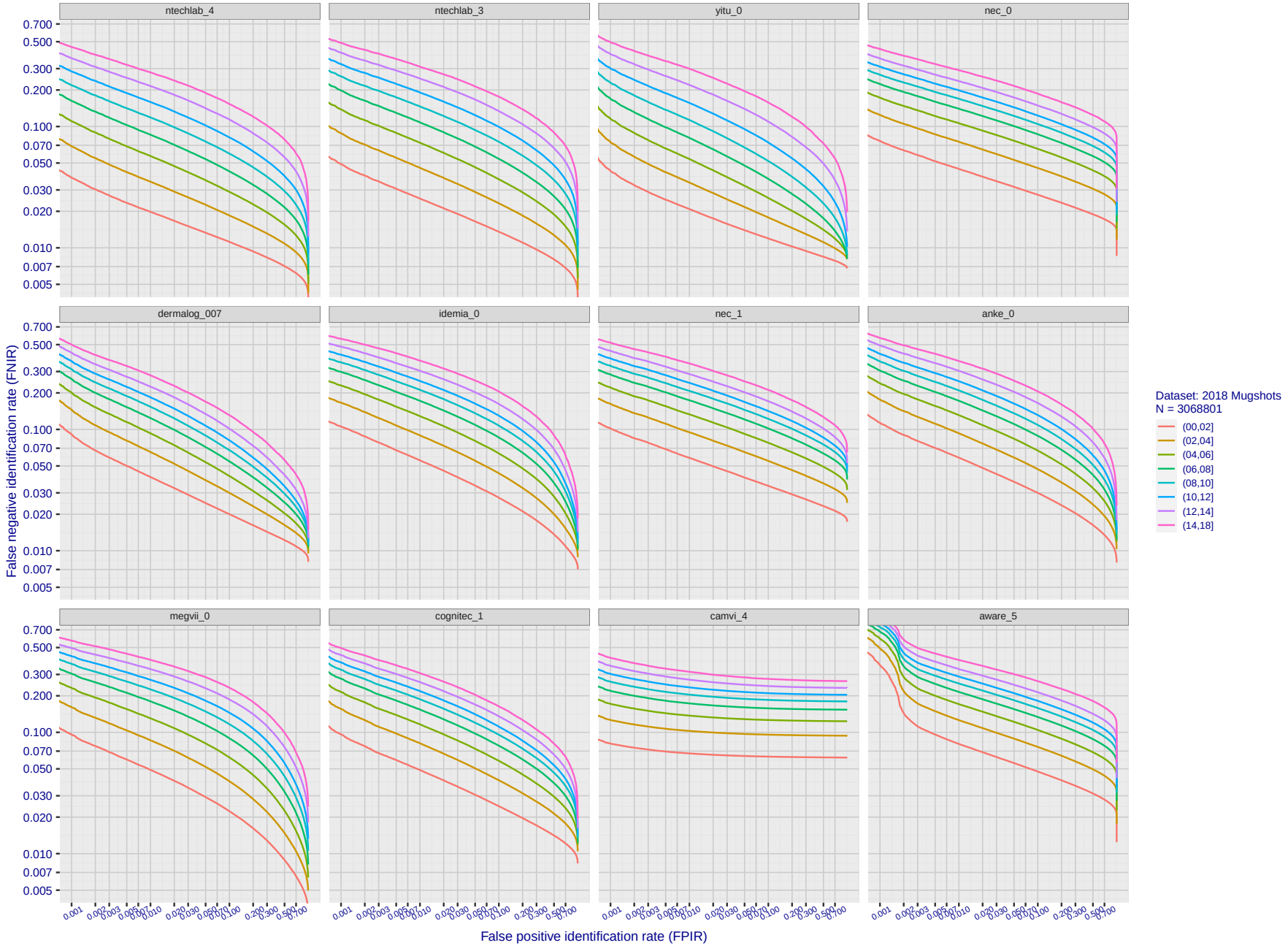

Figure 87: **[FRVT-2018 Mugshot Ageing Dataset] Identification miss rates vs. FPIR by time-elapsed**. *The oldest image of each individual is enrolled. Thereafter, all more recent images are searched. Miss rates are computed over all searches noted in row 17 of Table 1 and binned by number of years between search and initial enrollment. FPIR is computed from the same FRVT 2018 non-mates noted in row 3 of Table 1 with N = 3 000 000.*

2021/08/05 02:00:58
FNIR(N, R, T) = False neg. identification rate
FPIR(N, T) = False pos. identification rate
N = Num. enrolled subjects
R = Num. candidates examined
T = Threshold
T = 0 → Investigation
T > 0 → Identification

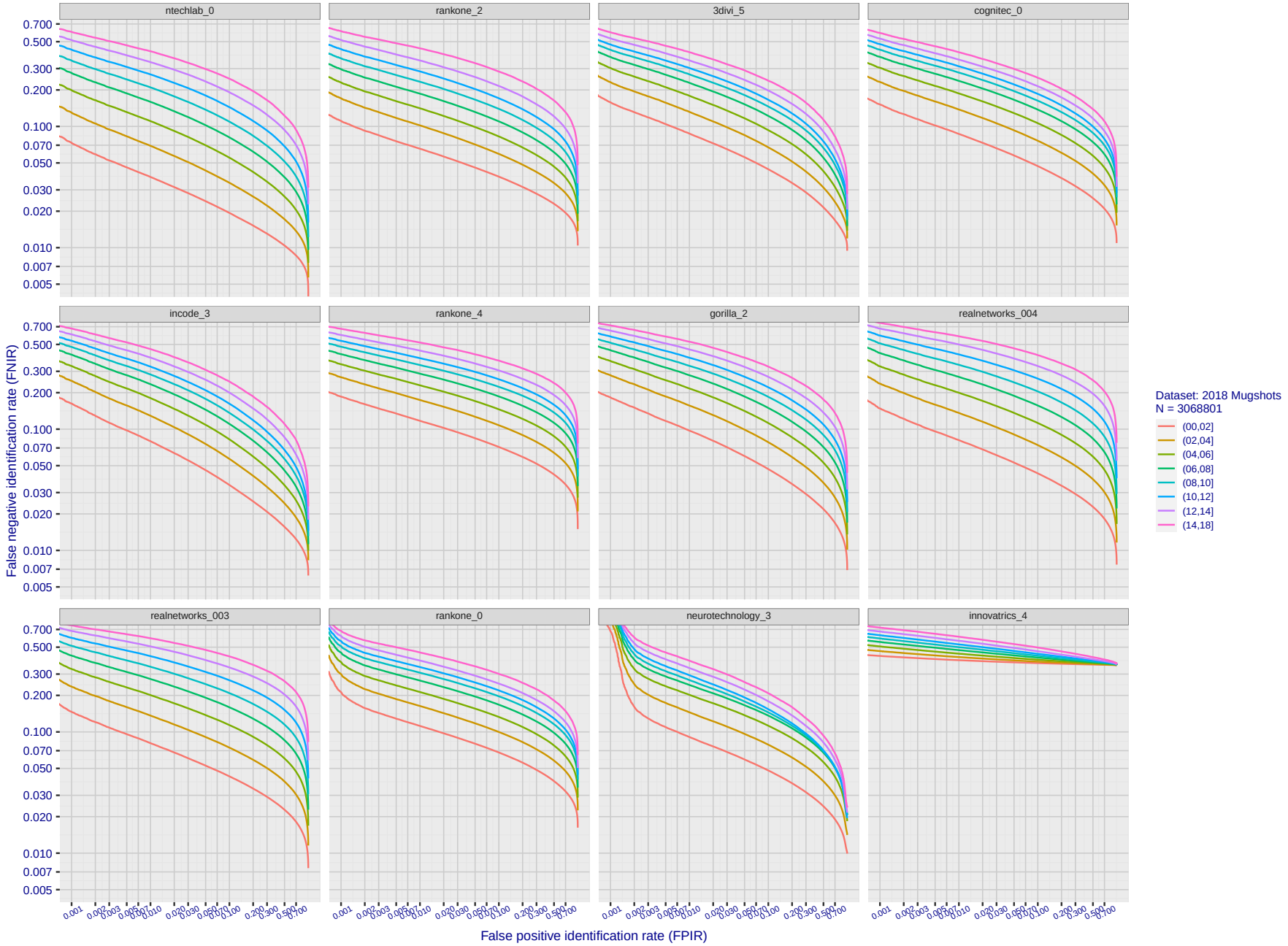

Figure 88: **[FRVT-2018 Mugshot Ageing Dataset] Identification miss rates vs. FPIR by time-elapsed**. *The oldest image of each individual is enrolled. Thereafter, all more recent images are searched. Miss rates are computed over all searches noted in row 17 of Table 1 and binned by number of years between search and initial enrollment. FPIR is computed from the same FRVT 2018 non-mates noted in row 3 of Table 1 with N = 3 000 000.*

2021/08/05 02:00:58
FNIR(N, R, T) = False neg. identification rate
FPIR(N, T) = False pos. identification rate
N = Num. enrolled subjects
R = Num. candidates examined
T = Threshold
T = 0 → Investigation
T > 0 → Identification

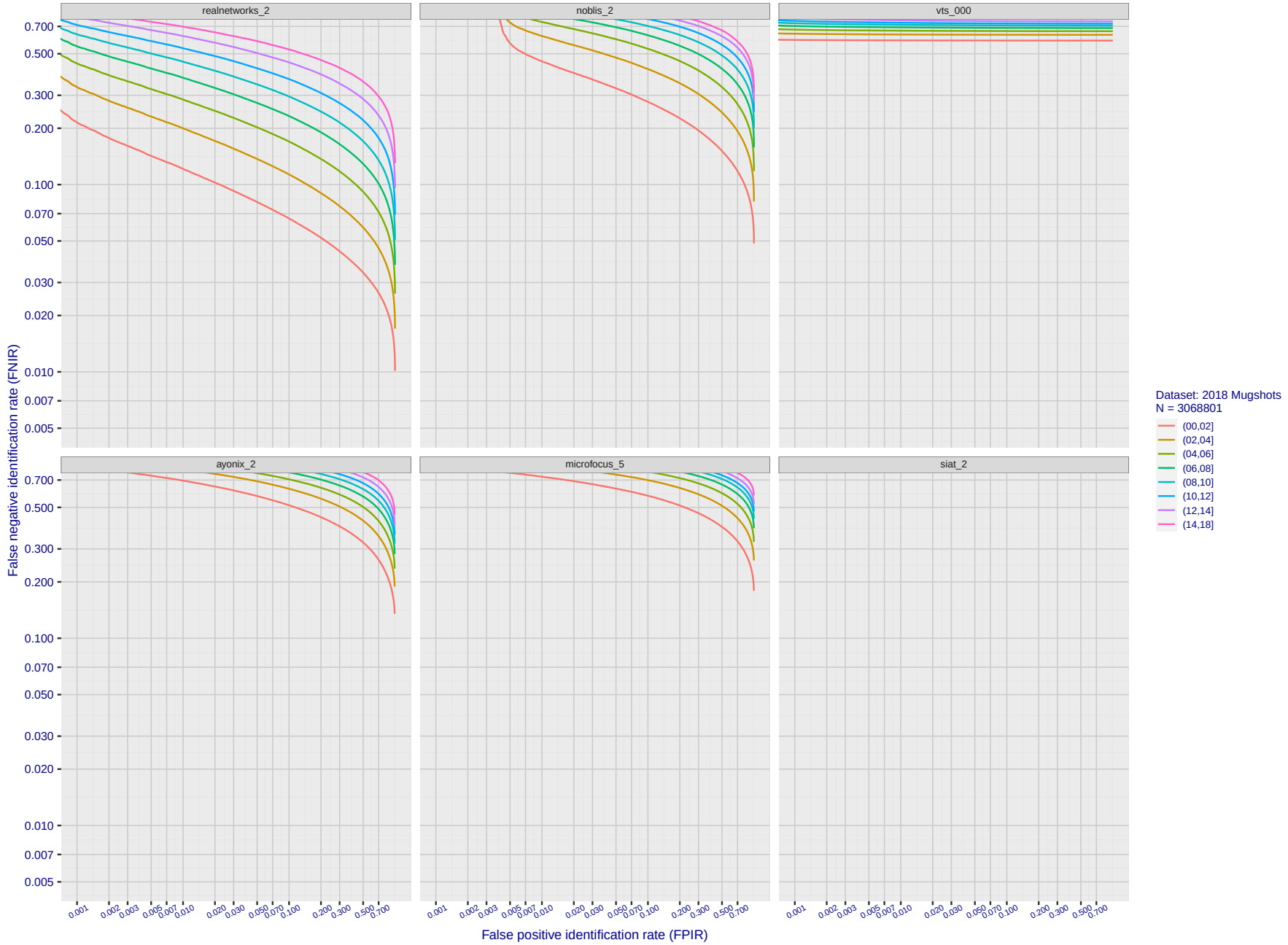

Figure 89: **[FRVT-2018 Mugshot Ageing Dataset] Identification miss rates vs. FPIR by time-elapsed**. *The oldest image of each individual is enrolled. Thereafter, all more recent images are searched. Miss rates are computed over all searches noted in row 17 of Table 1 and binned by number of years between search and initial enrollment. FPIR is computed from the same FRVT 2018 non-mates noted in row 3 of Table 1 with N = 3 000 000.*

2021/08/05 02:00:58
FNIR(N, R, T) = False neg. identification rate
FPIR(N, T) = False pos. identification rate
N = Num. enrolled subjects
R = Num. candidates examined
T = Threshold
T = 0 → Investigation
T > 0 → Identification

2021/08/05	FNIR(N, R, T) =	False neg. identification rate	N = Num. enrolled subjects	T = Threshold	$T = 0 \rightarrow$ Investigation
02:00:58	FPIR(N, T) =	False pos. identification rate	R = Num. candidates examined		$T > 0 \rightarrow$ Identification

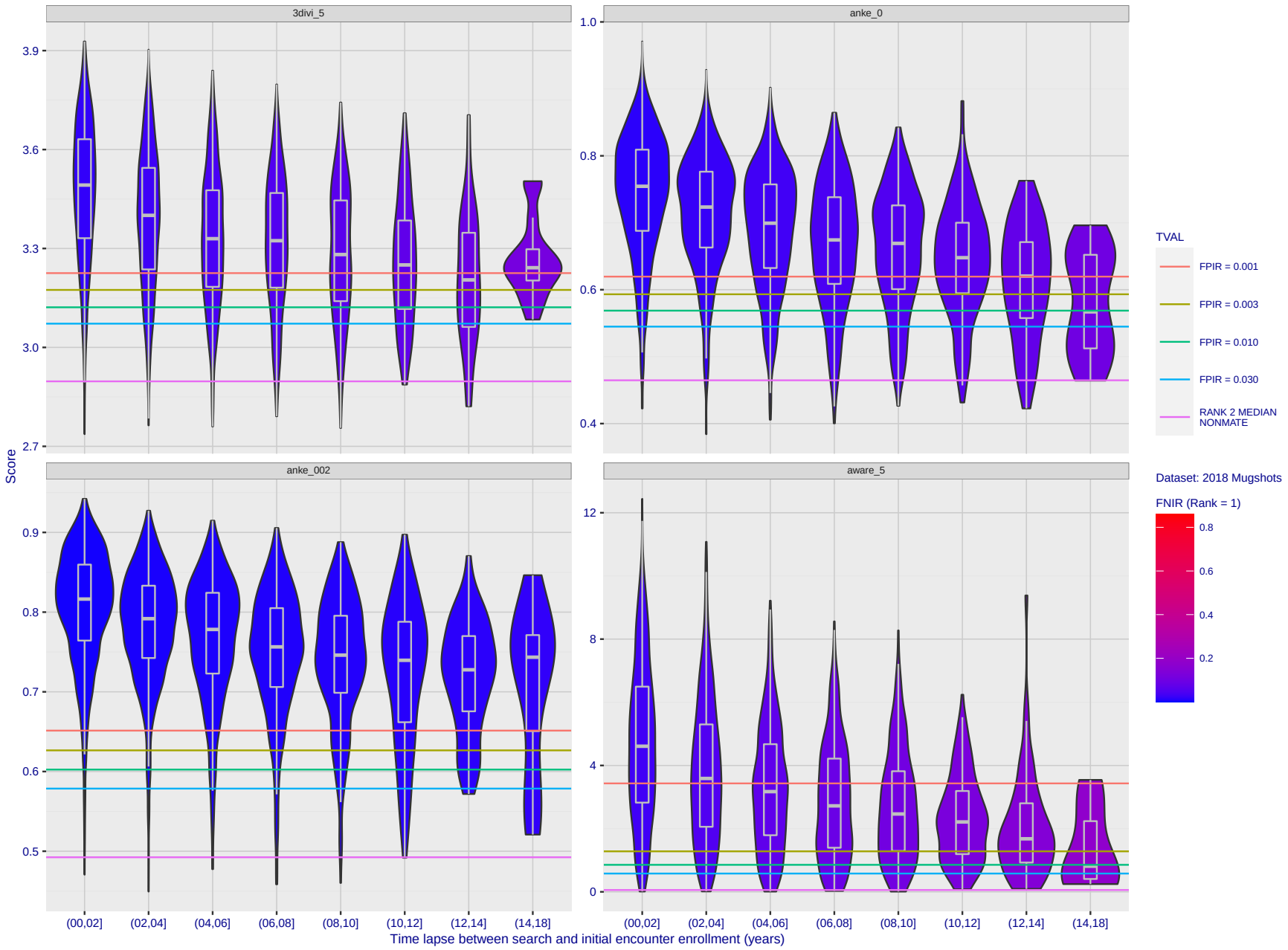

Figure 90: **[FRVT-2018 Mugshot Ageing Dataset] Native mate scores vs. time-elapsed**. *The oldest image of each individual is enrolled. Thereafter, all more recent images are searched. Mated score distributions are computed over all searches noted in row 17 of Table 1 binned by number of years between search and initial enrollment.*

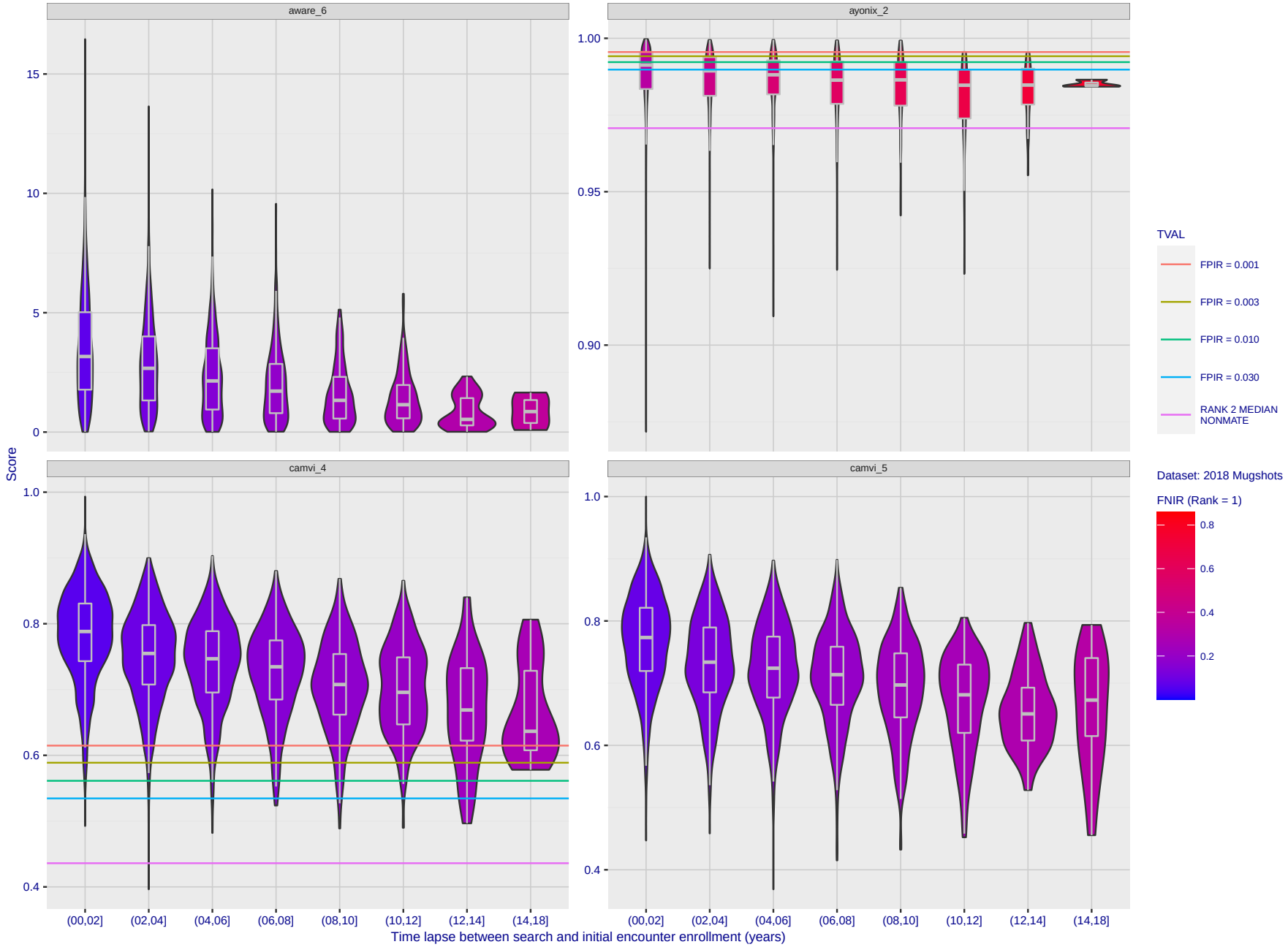

Figure 91: **[FRVT-2018 Mugshot Ageing Dataset] Native mate scores vs. time-elapsed**. *The oldest image of each individual is enrolled. Thereafter, all more recent images are searched. Mated score distributions are computed over all searches noted in row 17 of Table 1 binned by number of years between search and initial enrollment.*

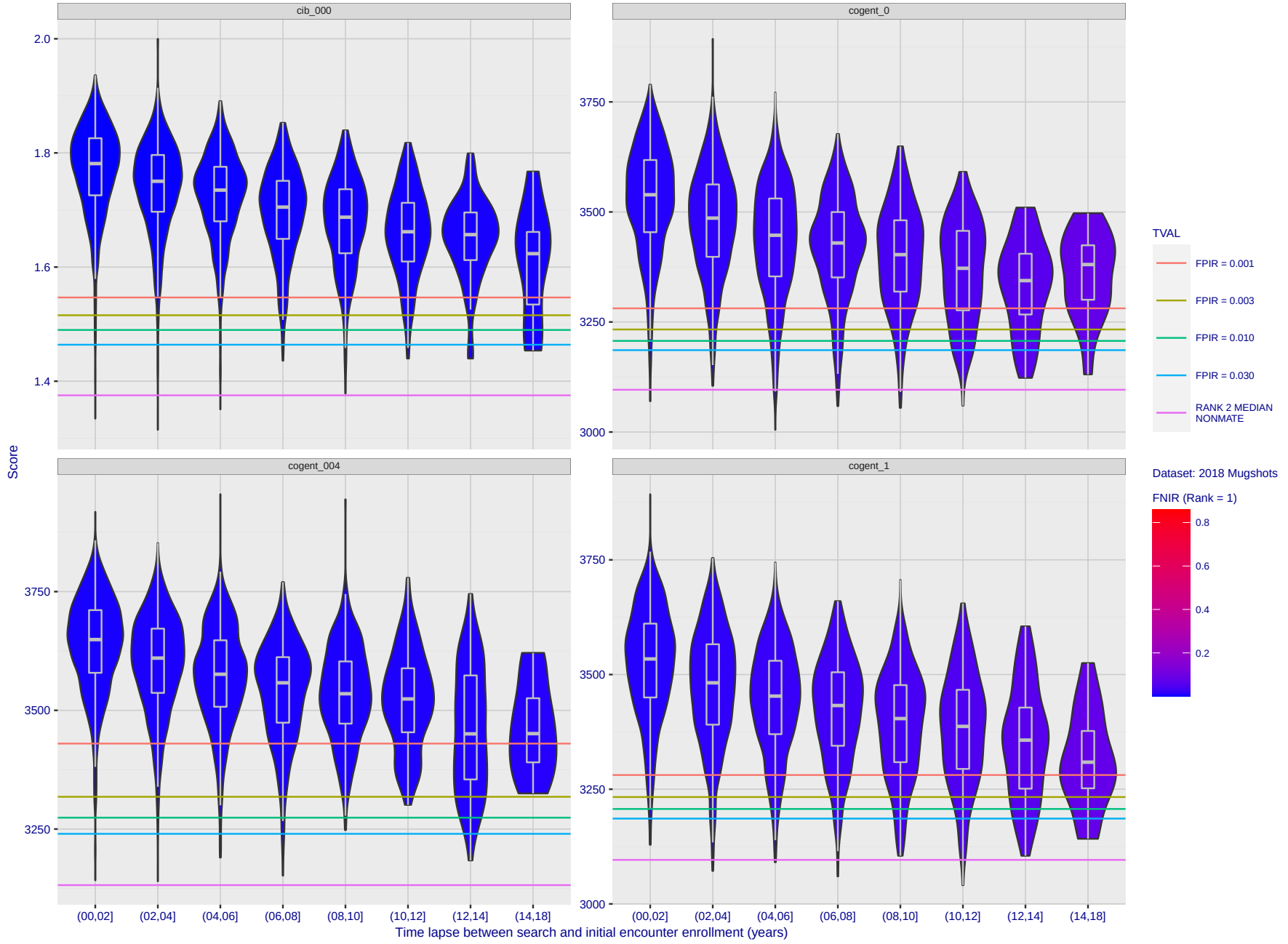

Figure 92: **[FRVT-2018 Mugshot Ageing Dataset] Native mate scores vs. time-elapsed**. *The oldest image of each individual is enrolled. Thereafter, all more recent images are searched. Mated score distributions are computed over all searches noted in row 17 of Table 1 binned by number of years between search and initial enrollment.*

2021/08/05 02:00:58
FNIR(N, R, T) = False neg. identification rate
FPIR(N, T) = False pos. identification rate
N = Num. enrolled subjects
R = Num. candidates examined
T = Threshold
T = 0 → Investigation
T > 0 → Identification

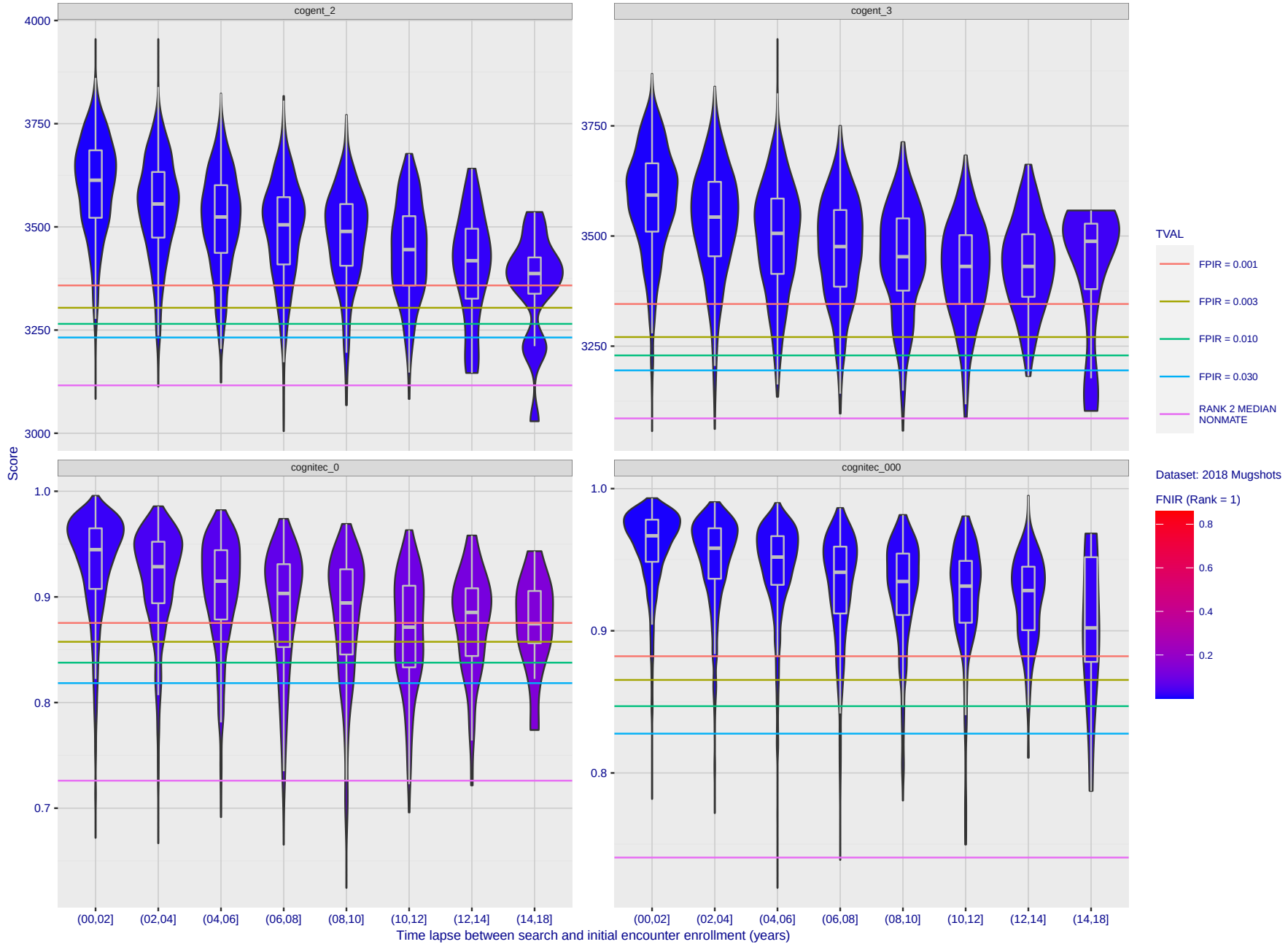

Figure 93: **[FRVT-2018 Mugshot Ageing Dataset] Native mate scores vs. time-elapsed**. *The oldest image of each individual is enrolled. Thereafter, all more recent images are searched. Mated score distributions are computed over all searches noted in row 17 of Table 1 binned by number of years between search and initial enrollment.*

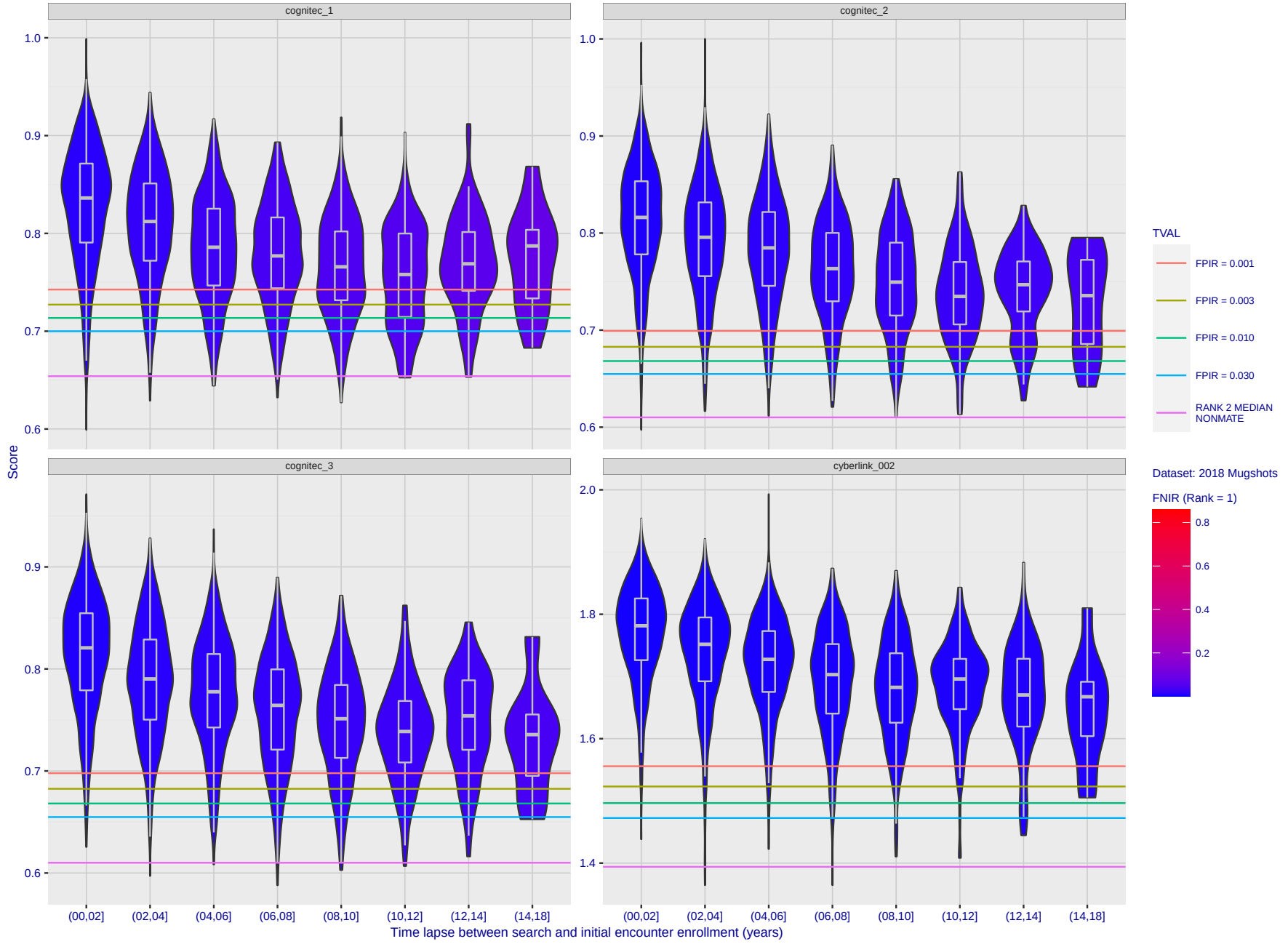

Figure 94: **[FRVT-2018 Mugshot Ageing Dataset] Native mate scores vs. time-elapsed**. *The oldest image of each individual is enrolled. Thereafter, all more recent images are searched. Mated score distributions are computed over all searches noted in row 17 of Table 1 binned by number of years between search and initial enrollment.*

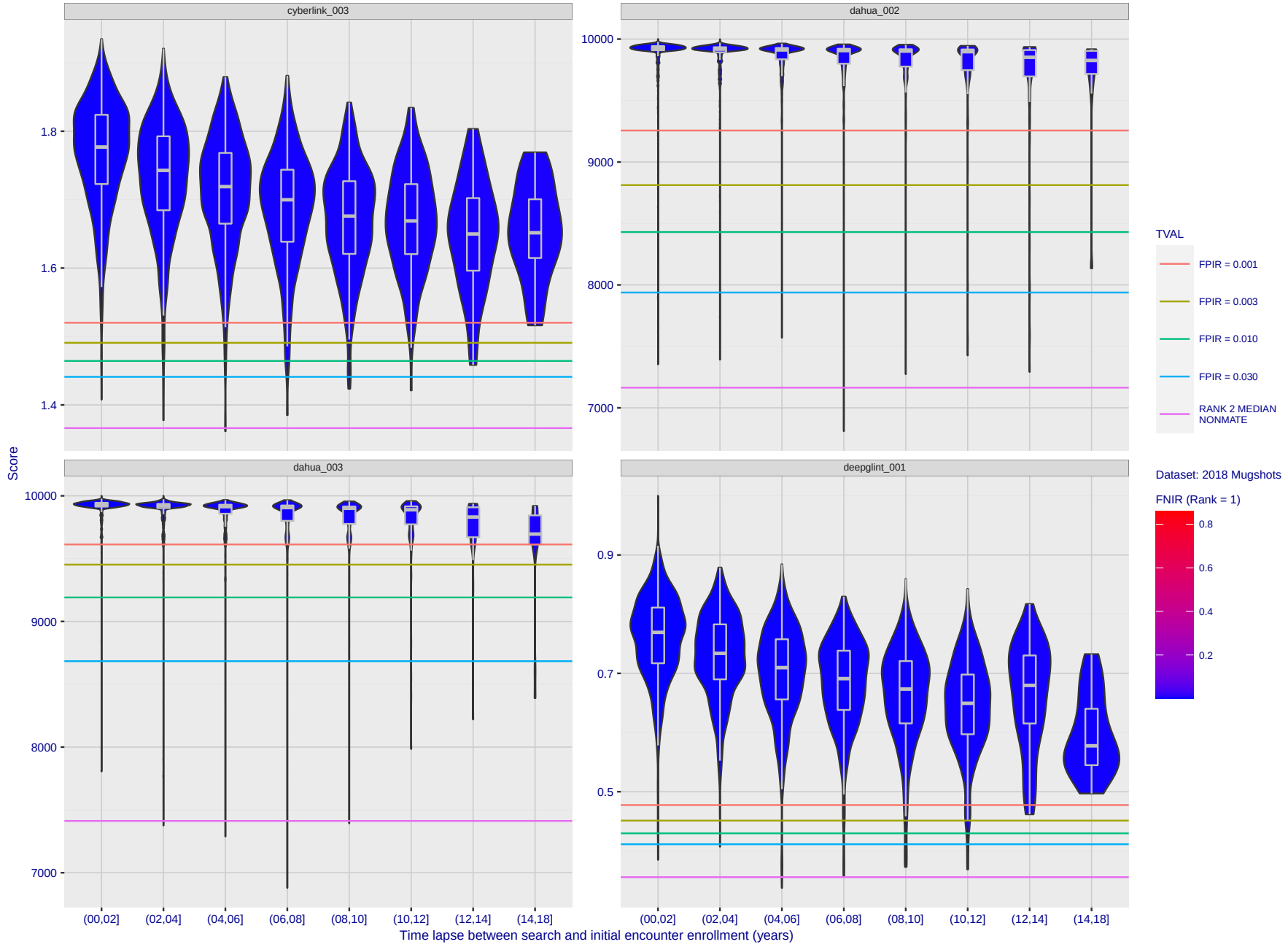

Figure 95: **[FRVT-2018 Mugshot Ageing Dataset] Native mate scores vs. time-elapsed**. *The oldest image of each individual is enrolled. Thereafter, all more recent images are searched. Mated score distributions are computed over all searches noted in row 17 of Table 1 binned by number of years between search and initial enrollment.*

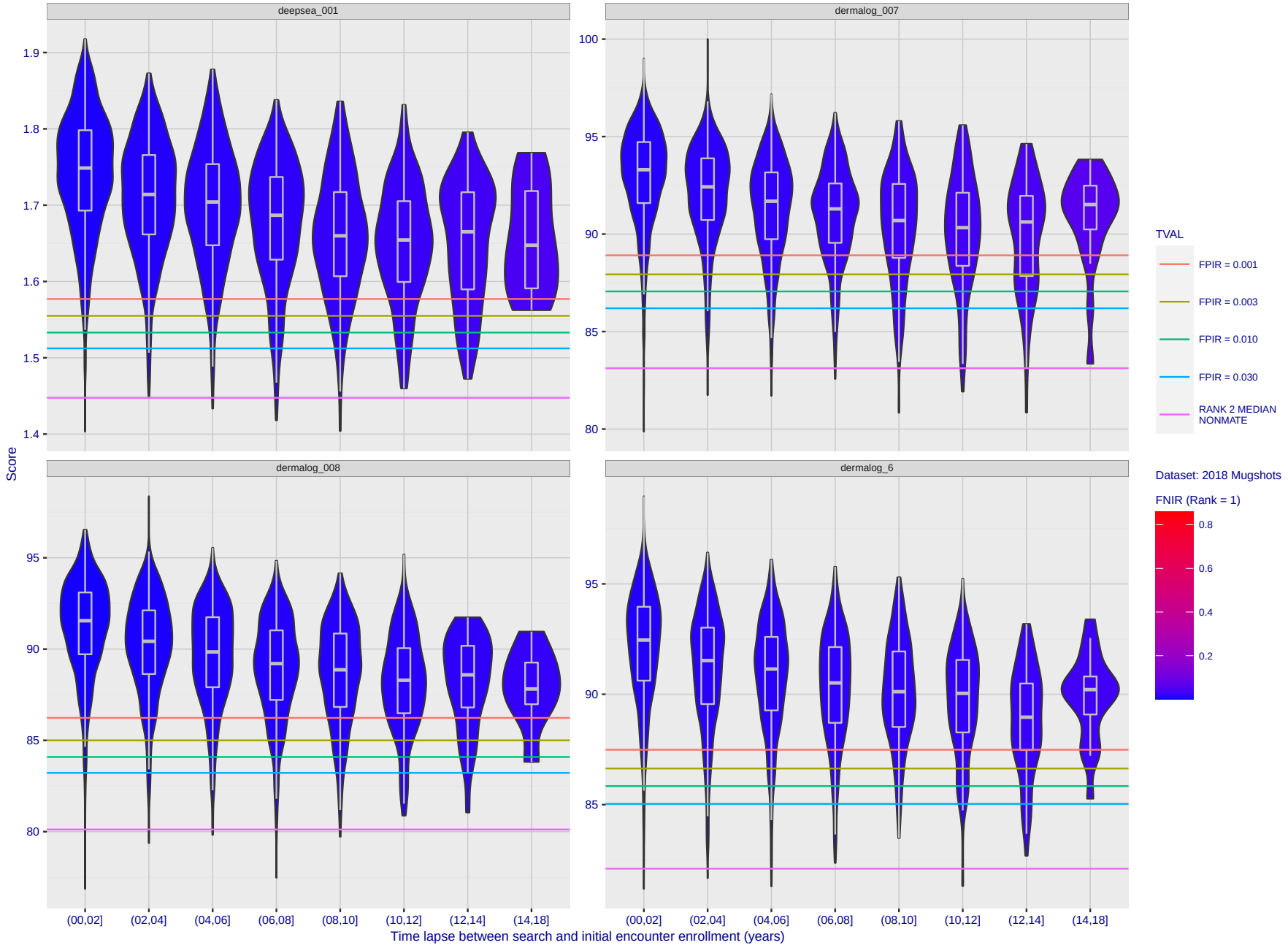

Figure 96: **[FRVT-2018 Mugshot Ageing Dataset] Native mate scores vs. time-elapsed**. *The oldest image of each individual is enrolled. Thereafter, all more recent images are searched. Mated score distributions are computed over all searches noted in row 17 of Table 1 binned by number of years between search and initial enrollment.*

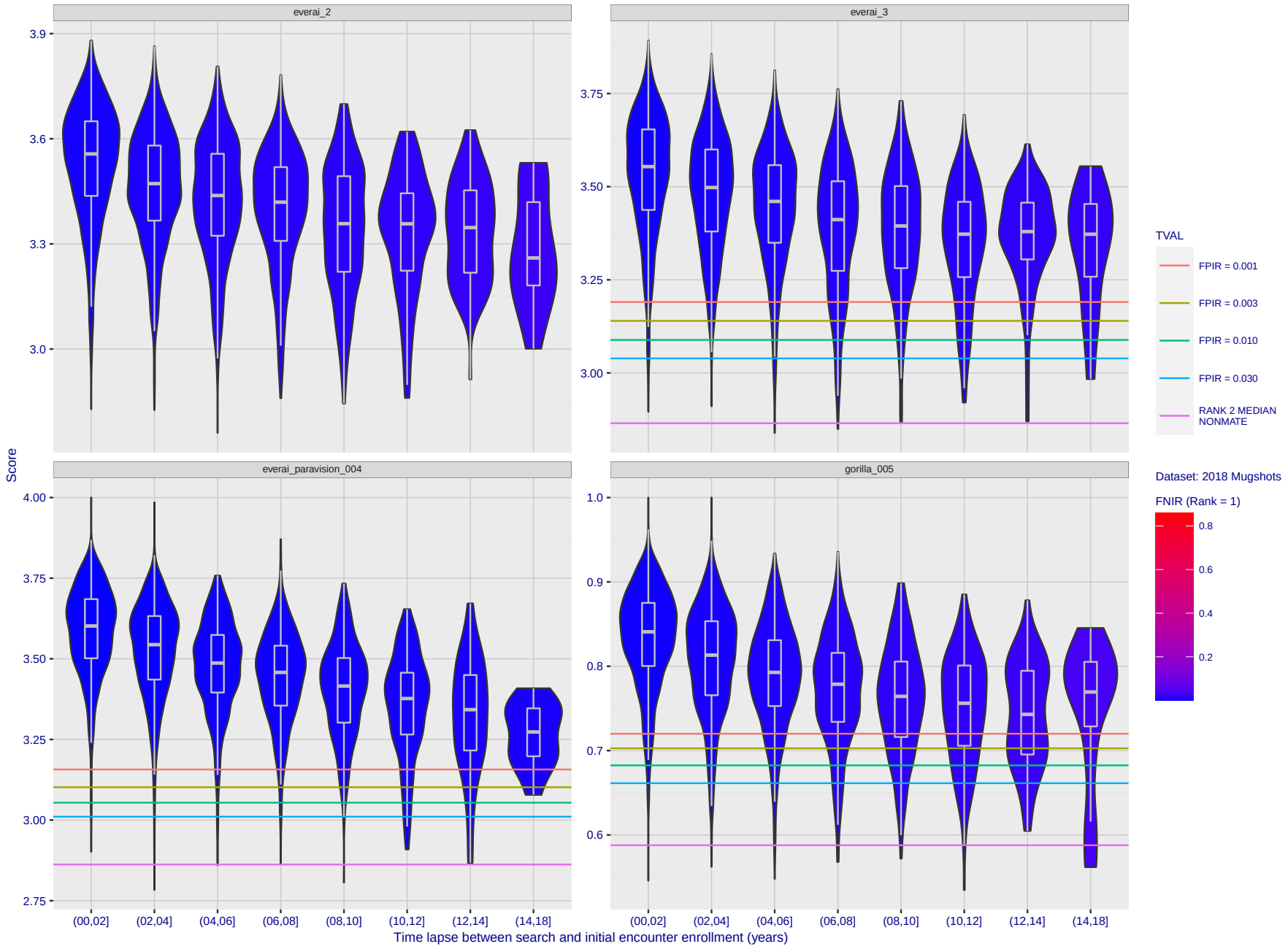

Figure 97: **[FRVT-2018 Mugshot Ageing Dataset] Native mate scores vs. time-elapsed**. *The oldest image of each individual is enrolled. Thereafter, all more recent images are searched. Mated score distributions are computed over all searches noted in row 17 of Table 1 binned by number of years between search and initial enrollment.*

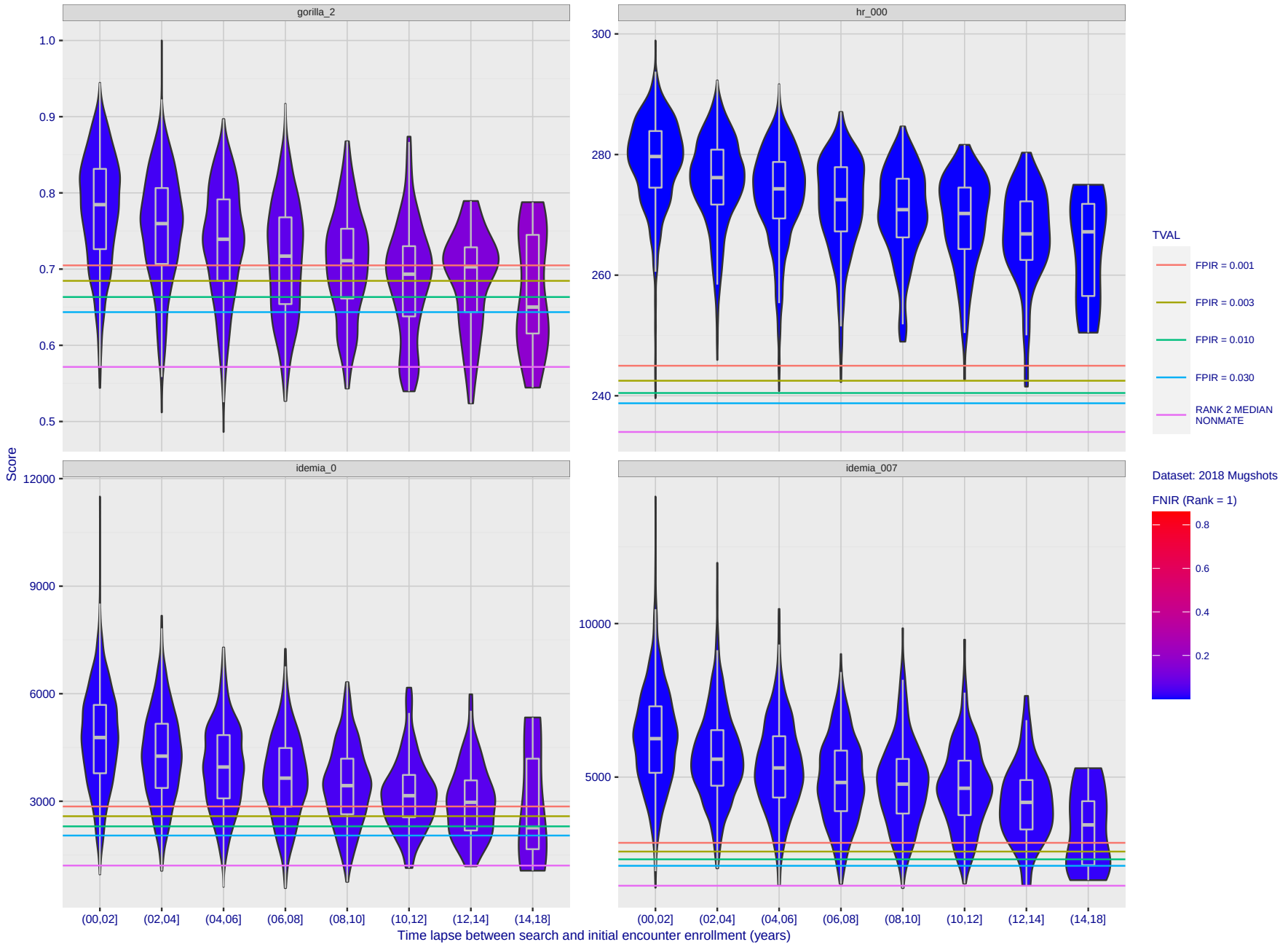

Figure 98: **[FRVT-2018 Mugshot Ageing Dataset] Native mate scores vs. time-elapsed**. *The oldest image of each individual is enrolled. Thereafter, all more recent images are searched. Mated score distributions are computed over all searches noted in row 17 of Table 1 binned by number of years between search and initial enrollment.*

2021/08/05 02:00:58
FNIR(N, R, T) = False neg. identification rate
FPIR(N, T) = False pos. identification rate
N = Num. enrolled subjects
R = Num. candidates examined
T = Threshold
T = 0 → Investigation
T > 0 → Identification

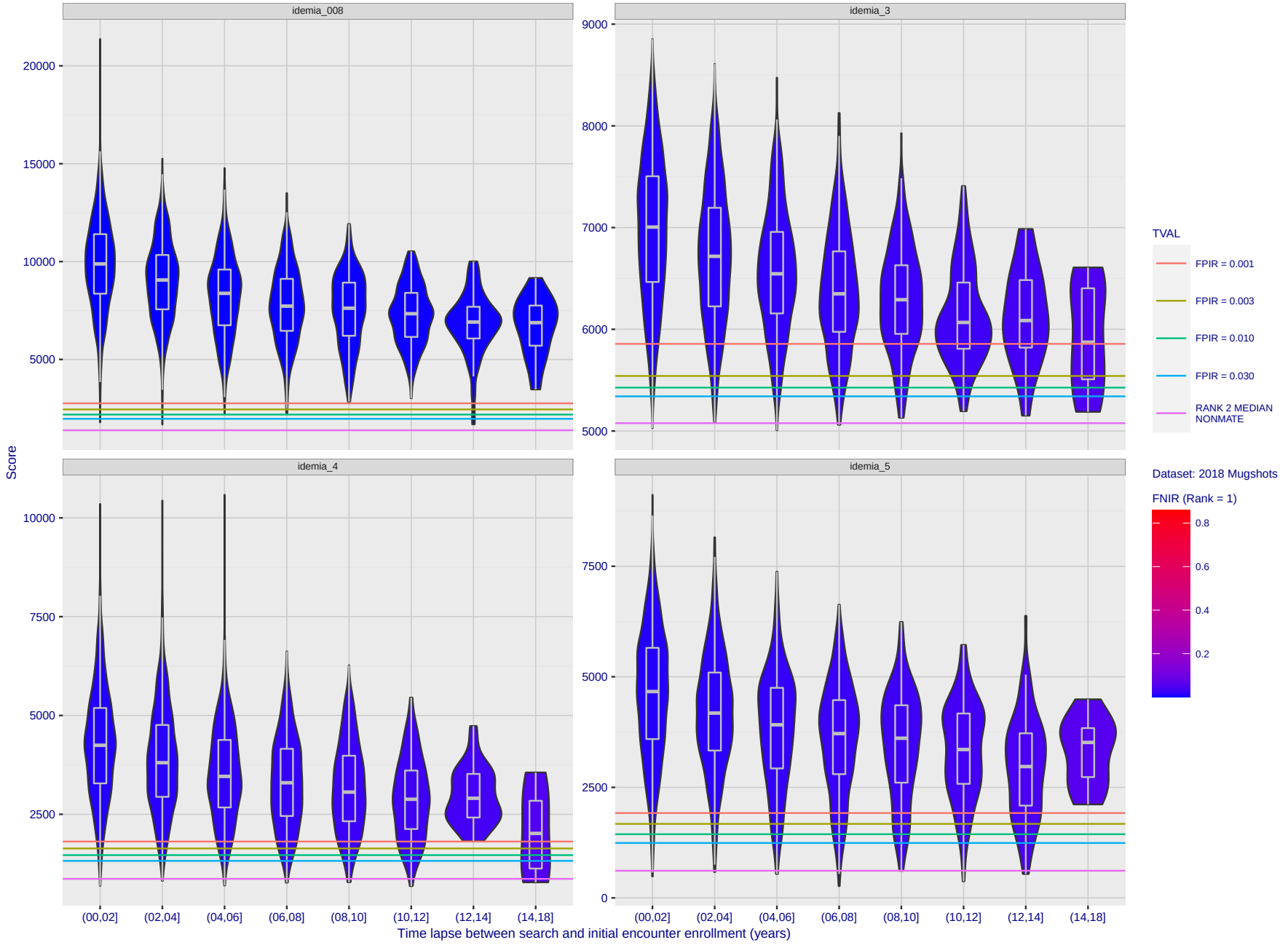

Figure 99: **[FRVT-2018 Mugshot Ageing Dataset] Native mate scores vs. time-elapsed**. *The oldest image of each individual is enrolled. Thereafter, all more recent images are searched. Mated score distributions are computed over all searches noted in row 17 of Table 1 binned by number of years between search and initial enrollment.*

2021/08/05 02:00:58
FNIR(N, R, T) = False neg. identification rate
FPIR(N, T) = False pos. identification rate
N = Num. enrolled subjects
R = Num. candidates examined
T = Threshold
T = 0 → Investigation
T > 0 → Identification

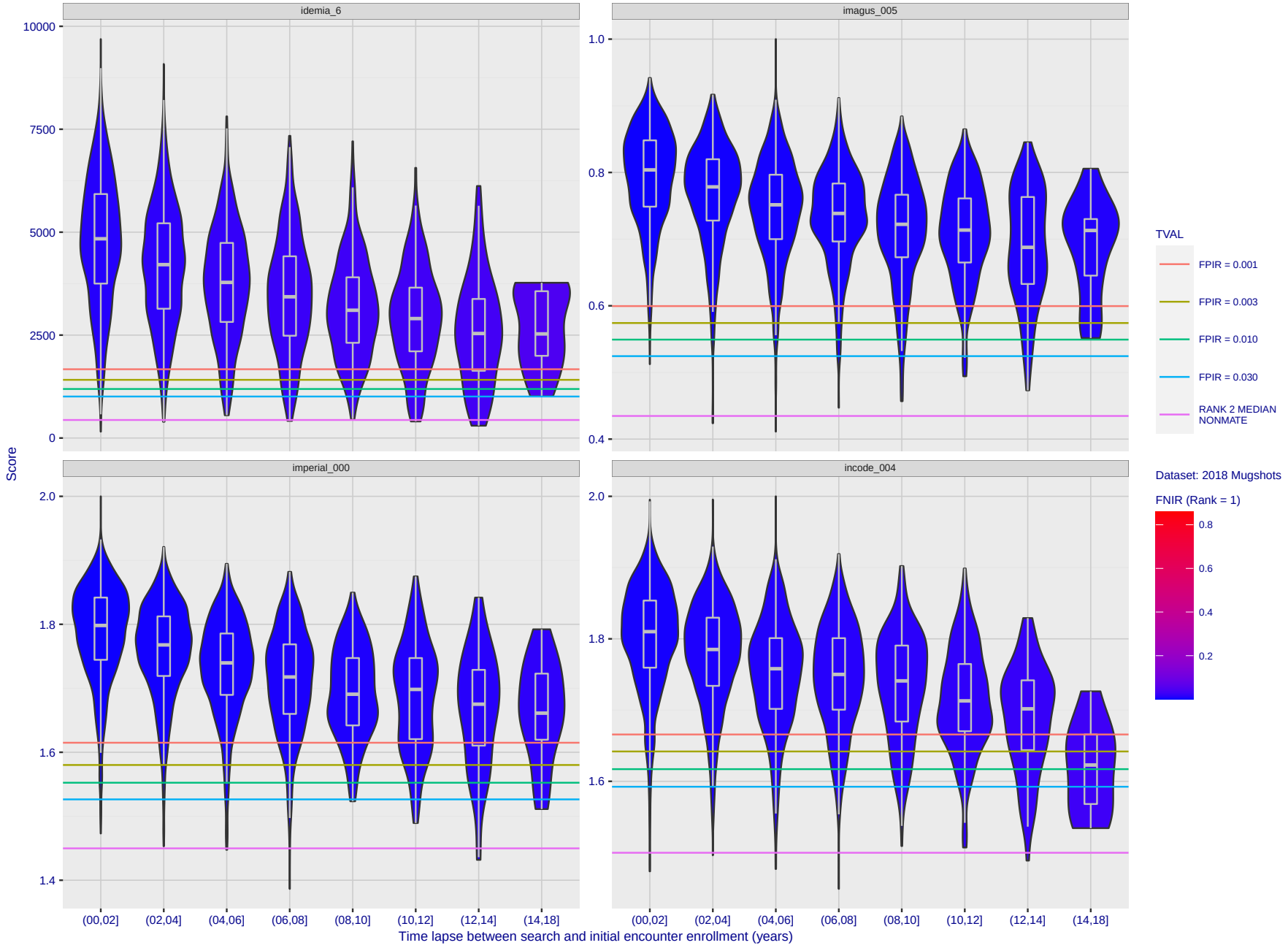

Figure 100: **[FRVT-2018 Mugshot Ageing Dataset] Native mate scores vs. time-elapsed**. *The oldest image of each individual is enrolled. Thereafter, all more recent images are searched. Mated score distributions are computed over all searches noted in row 17 of Table 1 binned by number of years between search and initial enrollment.*

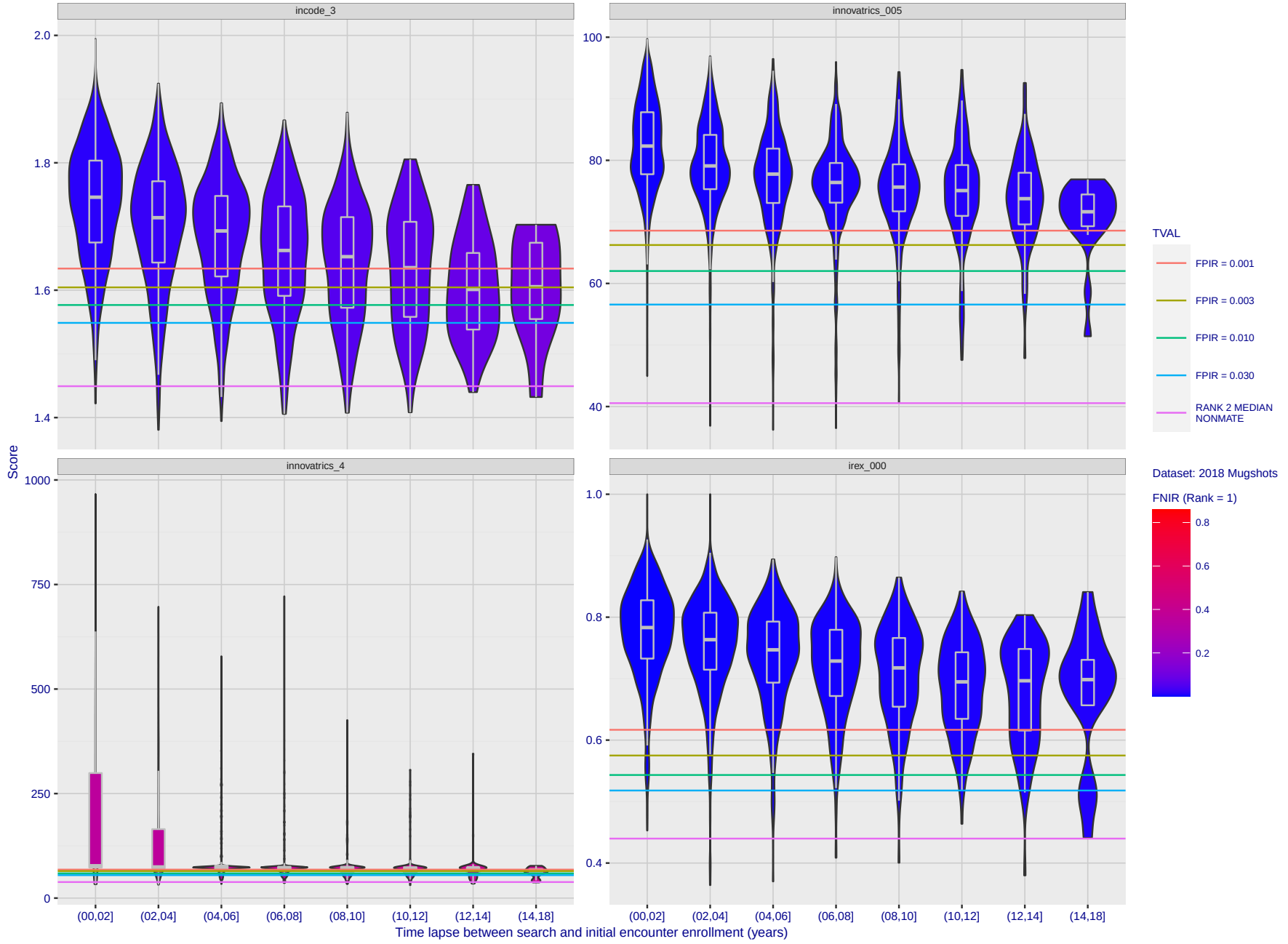

Figure 101: **[FRVT-2018 Mugshot Ageing Dataset] Native mate scores vs. time-elapsed**. *The oldest image of each individual is enrolled. Thereafter, all more recent images are searched. Mated score distributions are computed over all searches noted in row 17 of Table 1 binned by number of years between search and initial enrollment.*

2021/08/05 02:00:58
FNIR(N, R, T) = False neg. identification rate
FPIR(N, T) = False pos. identification rate
N = Num. enrolled subjects
R = Num. candidates examined
T = Threshold
T = 0 → Investigation
T > 0 → Identification

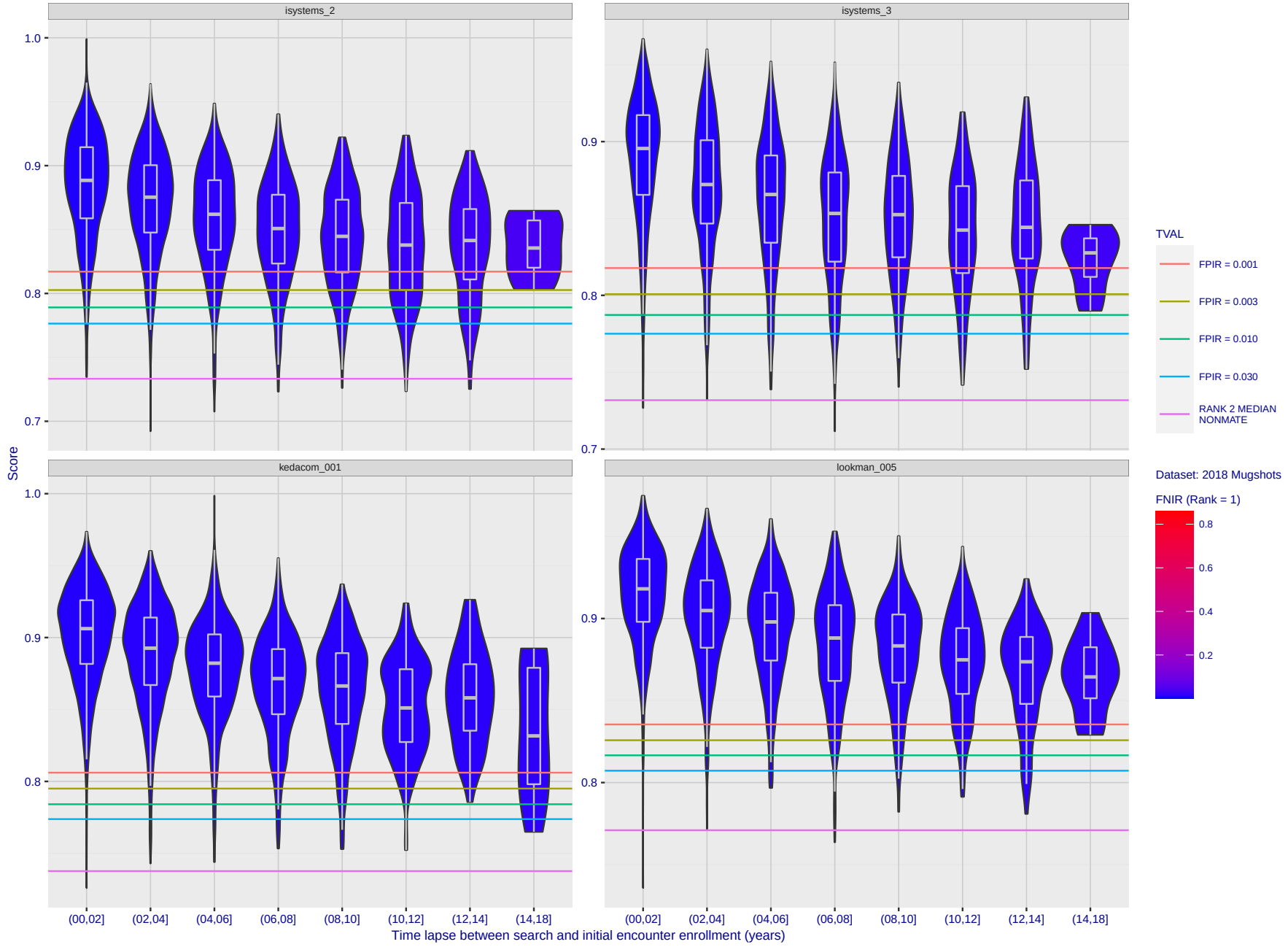

Figure 102: **[FRVT-2018 Mugshot Ageing Dataset] Native mate scores vs. time-elapsed**. *The oldest image of each individual is enrolled. Thereafter, all more recent images are searched. Mated score distributions are computed over all searches noted in row 17 of Table 1 binned by number of years between search and initial enrollment.*

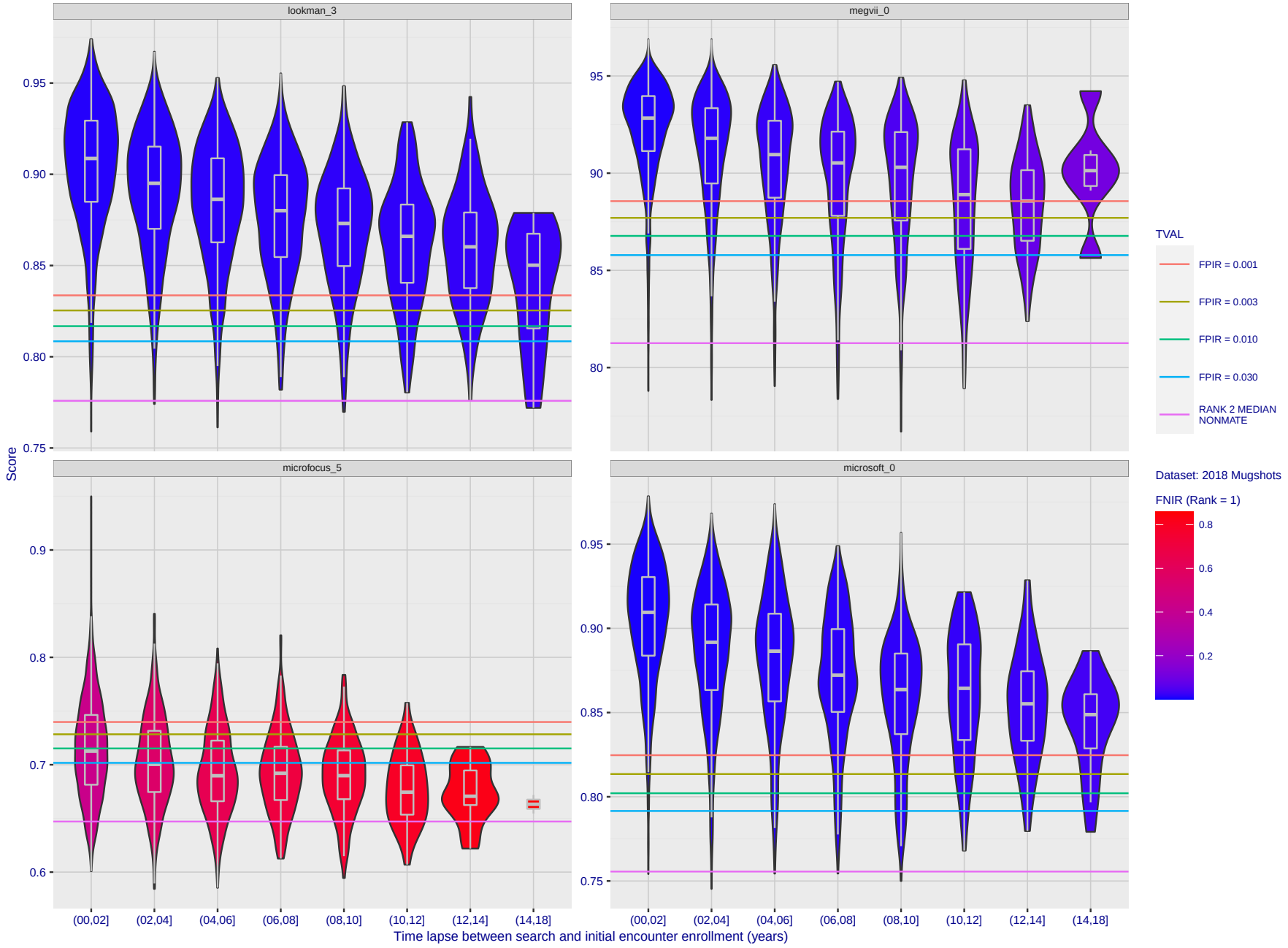

Figure 103: **[FRVT-2018 Mugshot Ageing Dataset] Native mate scores vs. time-elapsed**. *The oldest image of each individual is enrolled. Thereafter, all more recent images are searched. Mated score distributions are computed over all searches noted in row 17 of Table 1 binned by number of years between search and initial enrollment.*

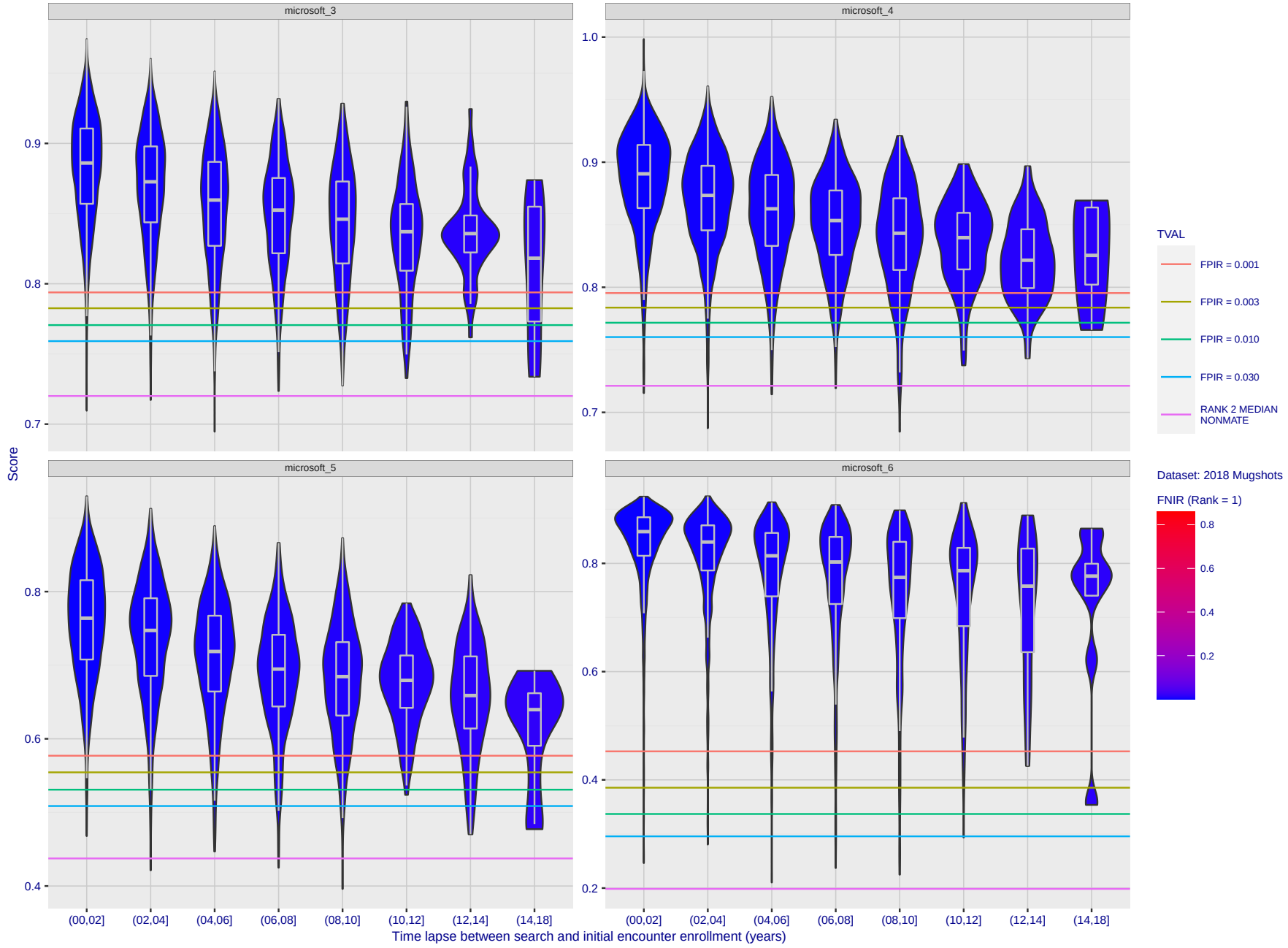

Figure 104: **[FRVT-2018 Mugshot Ageing Dataset] Native mate scores vs. time-elapsed**. *The oldest image of each individual is enrolled. Thereafter, all more recent images are searched. Mated score distributions are computed over all searches noted in row 17 of Table 1 binned by number of years between search and initial enrollment.*

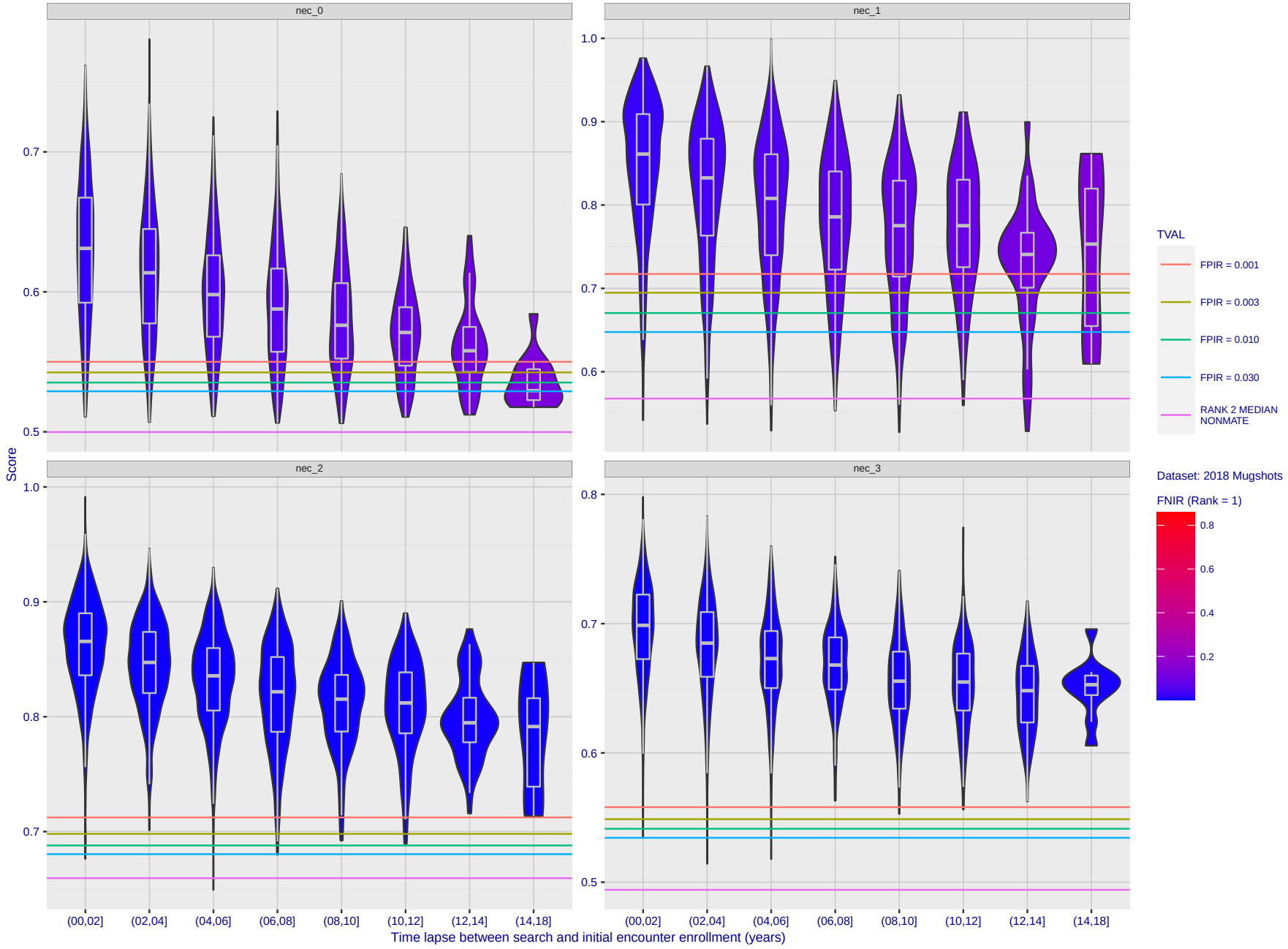

Figure 105: **[FRVT-2018 Mugshot Ageing Dataset] Native mate scores vs. time-elapsed**. *The oldest image of each individual is enrolled. Thereafter, all more recent images are searched. Mated score distributions are computed over all searches noted in row 17 of Table 1 binned by number of years between search and initial enrollment.*

2021/08/05 02:00:58
FNIR(N, R, T) = False neg. identification rate
FPIR(N, T) = False pos. identification rate
N = Num. enrolled subjects
R = Num. candidates examined
T = Threshold
T = 0 → Investigation
T > 0 → Identification

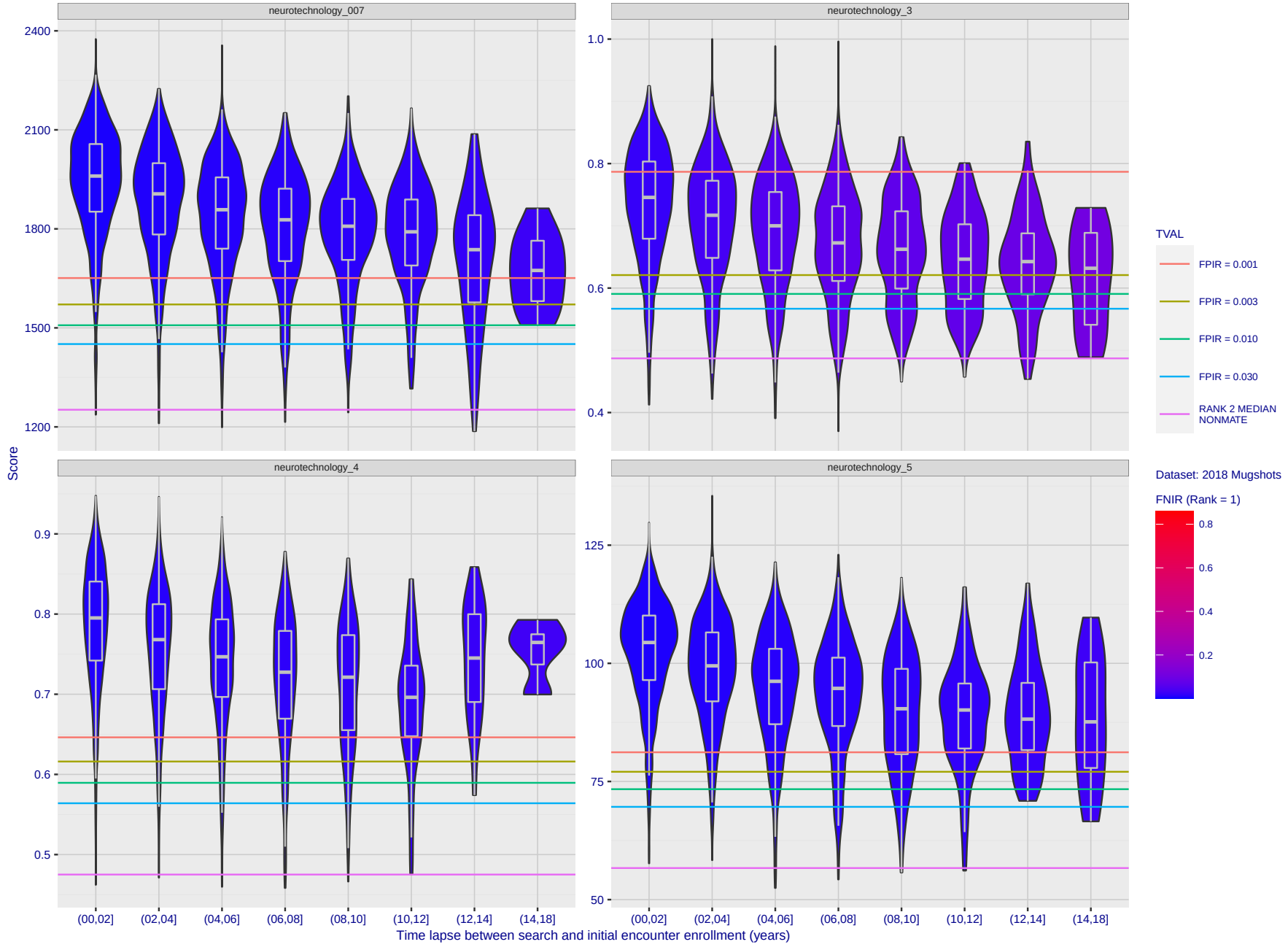

Figure 106: **[FRVT-2018 Mugshot Ageing Dataset] Native mate scores vs. time-elapsed**. *The oldest image of each individual is enrolled. Thereafter, all more recent images are searched. Mated score distributions are computed over all searches noted in row 17 of Table 1 binned by number of years between search and initial enrollment.*

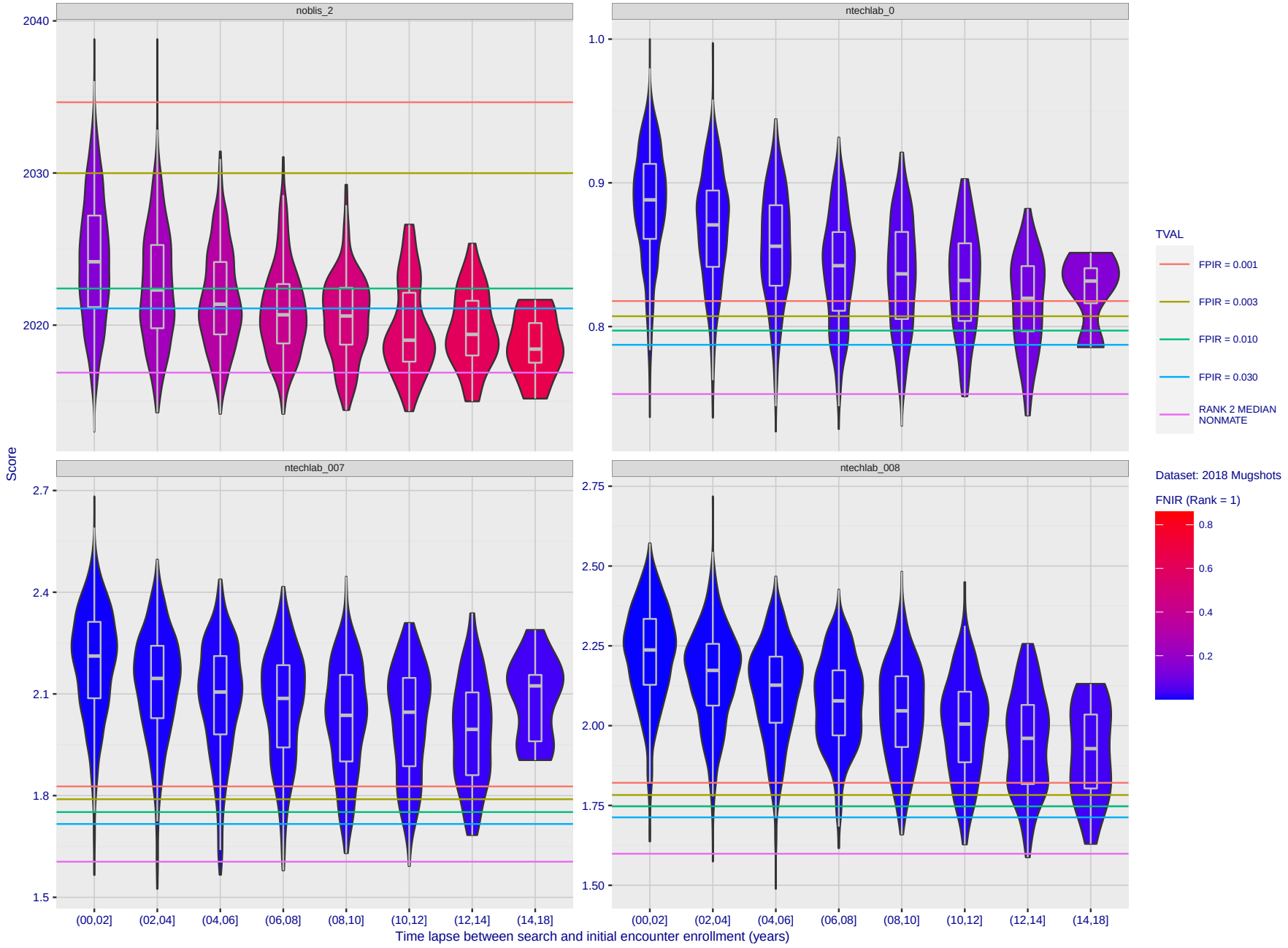

Figure 107: **[FRVT-2018 Mugshot Ageing Dataset] Native mate scores vs. time-elapsed**. *The oldest image of each individual is enrolled. Thereafter, all more recent images are searched. Mated score distributions are computed over all searches noted in row 17 of Table 1 binned by number of years between search and initial enrollment.*

2021/08/05 02:00:58
FNIR(N, R, T) = False neg. identification rate
FPIR(N, T) = False pos. identification rate
N = Num. enrolled subjects
R = Num. candidates examined
T = Threshold
T = 0 → Investigation
T > 0 → Identification

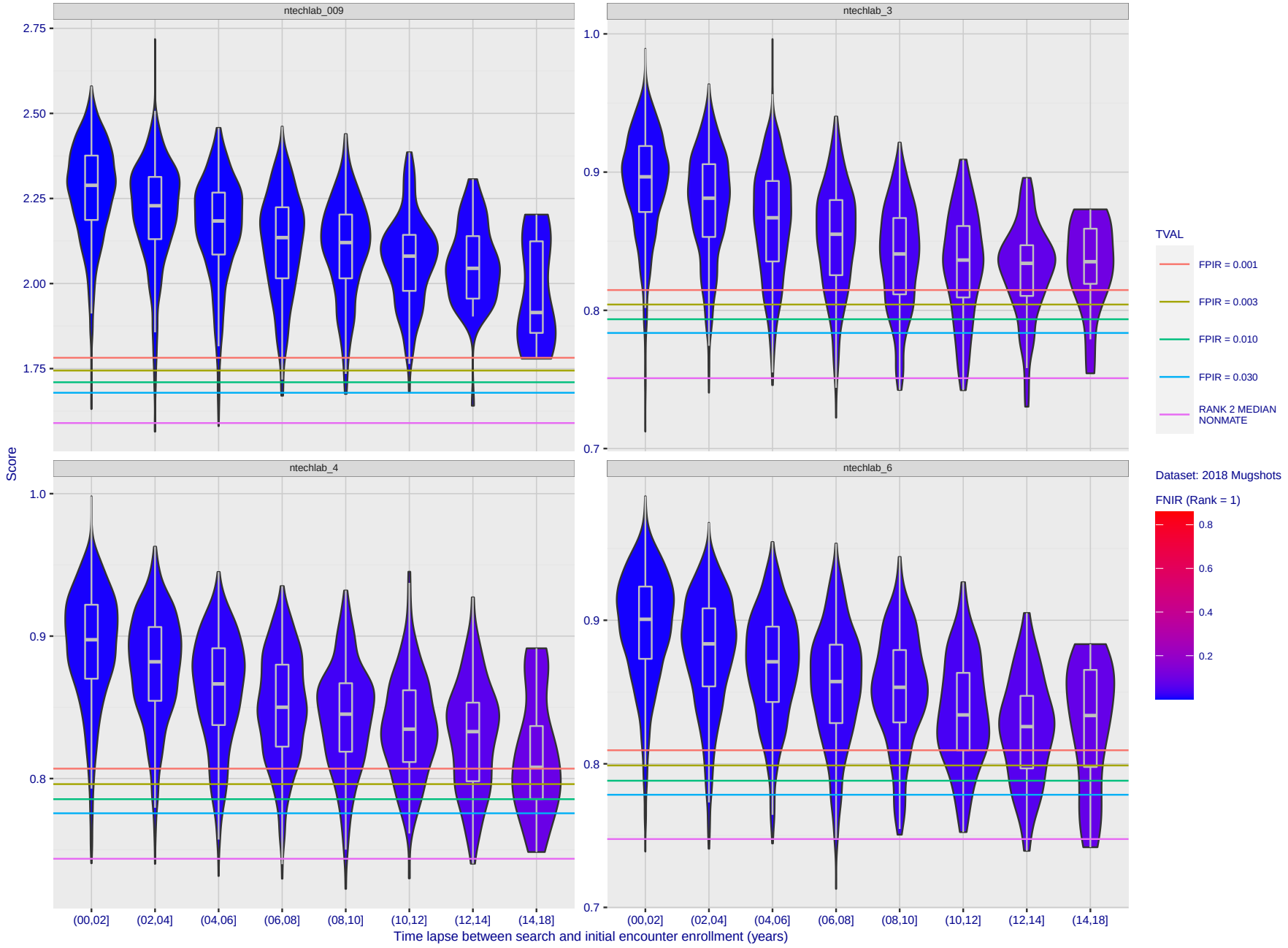

Figure 108: **[FRVT-2018 Mugshot Ageing Dataset] Native mate scores vs. time-elapsed**. *The oldest image of each individual is enrolled. Thereafter, all more recent images are searched. Mated score distributions are computed over all searches noted in row 17 of Table 1 binned by number of years between search and initial enrollment.*

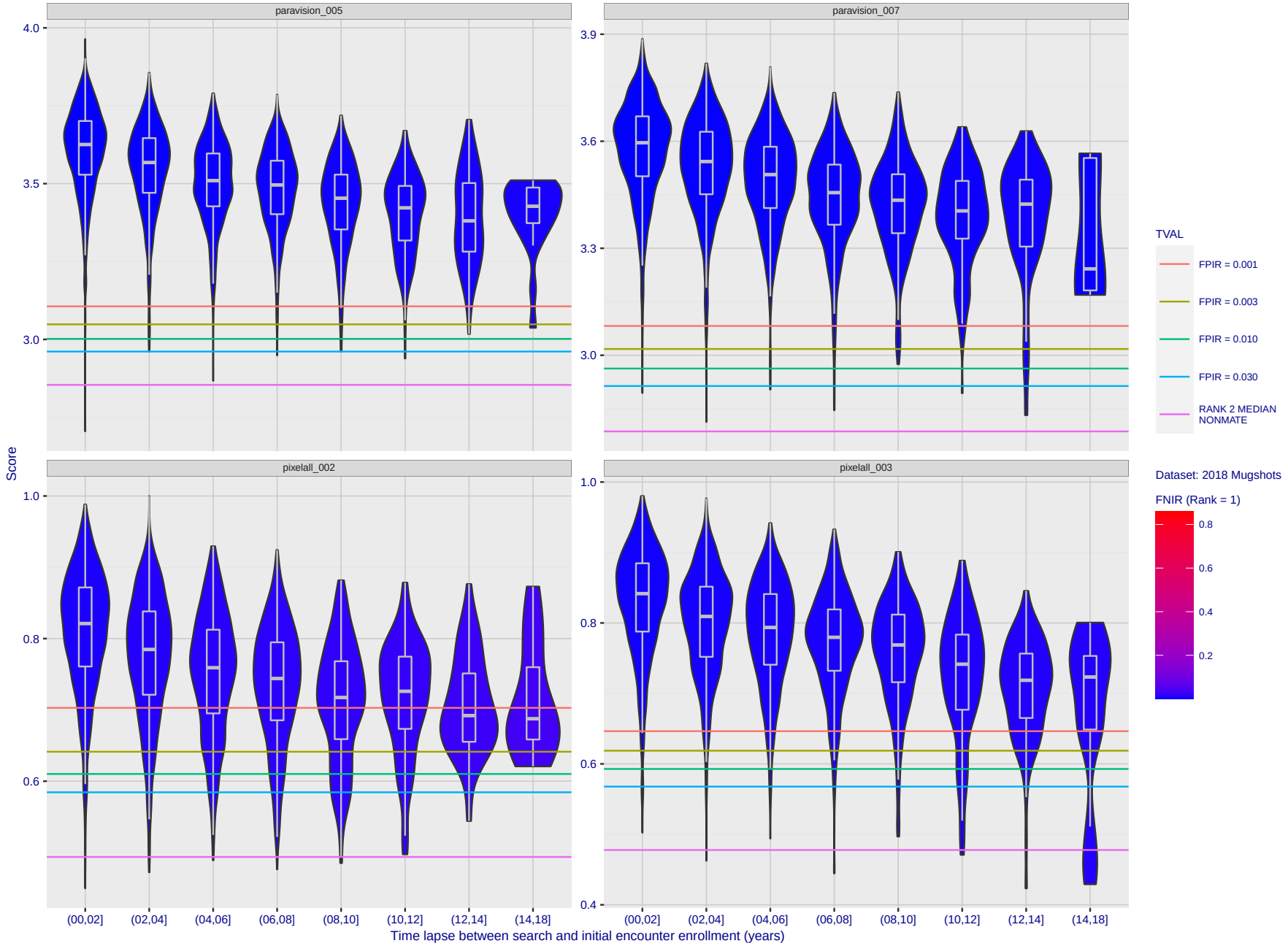

Figure 109: **[FRVT-2018 Mugshot Ageing Dataset] Native mate scores vs. time-elapsed**. *The oldest image of each individual is enrolled. Thereafter, all more recent images are searched. Mated score distributions are computed over all searches noted in row 17 of Table 1 binned by number of years between search and initial enrollment.*

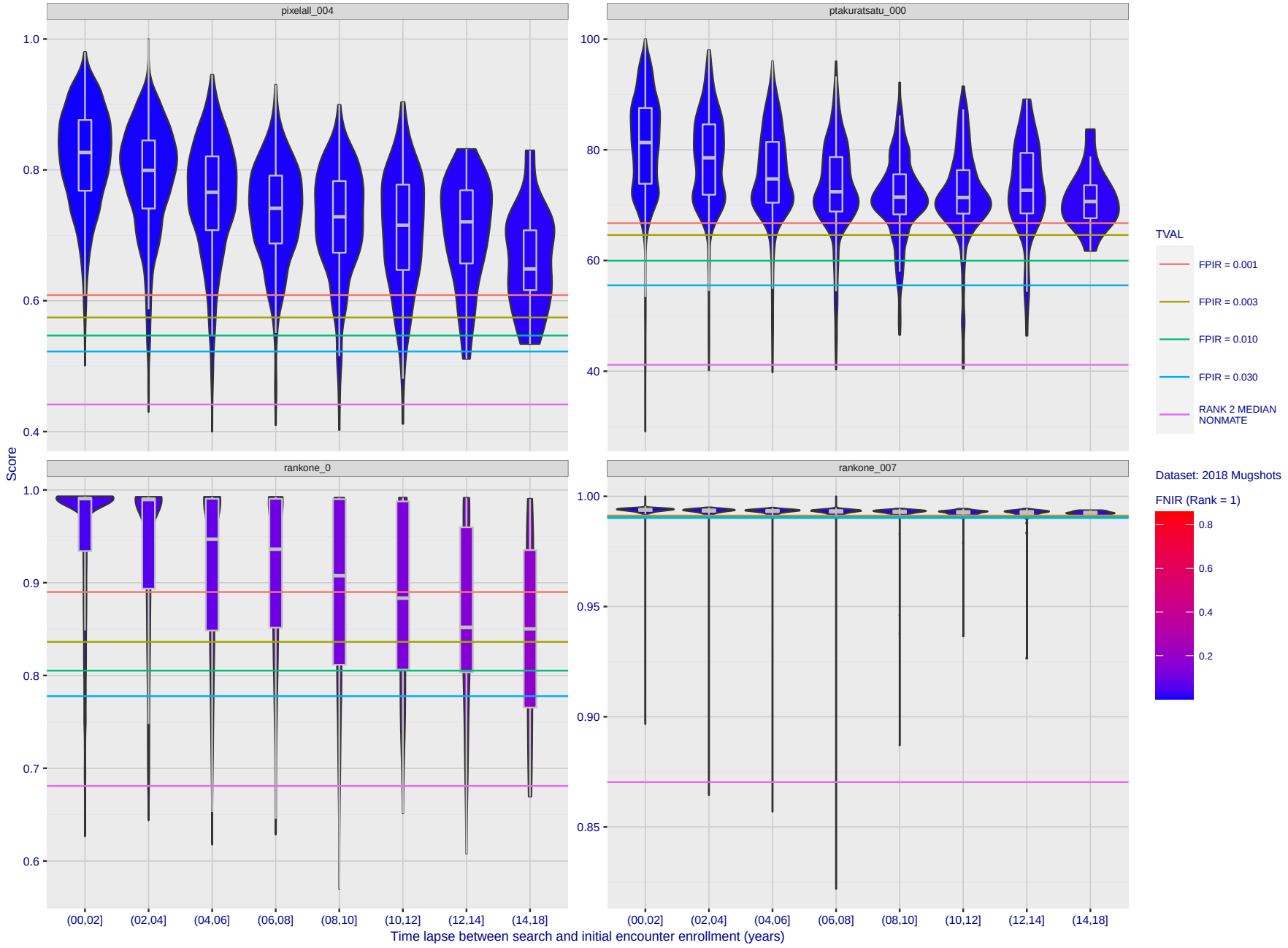

Figure 110: **[FRVT-2018 Mugshot Ageing Dataset] Native mate scores vs. time-elapsed**. *The oldest image of each individual is enrolled. Thereafter, all more recent images are searched. Mated score distributions are computed over all searches noted in row 17 of Table 1 binned by number of years between search and initial enrollment.*

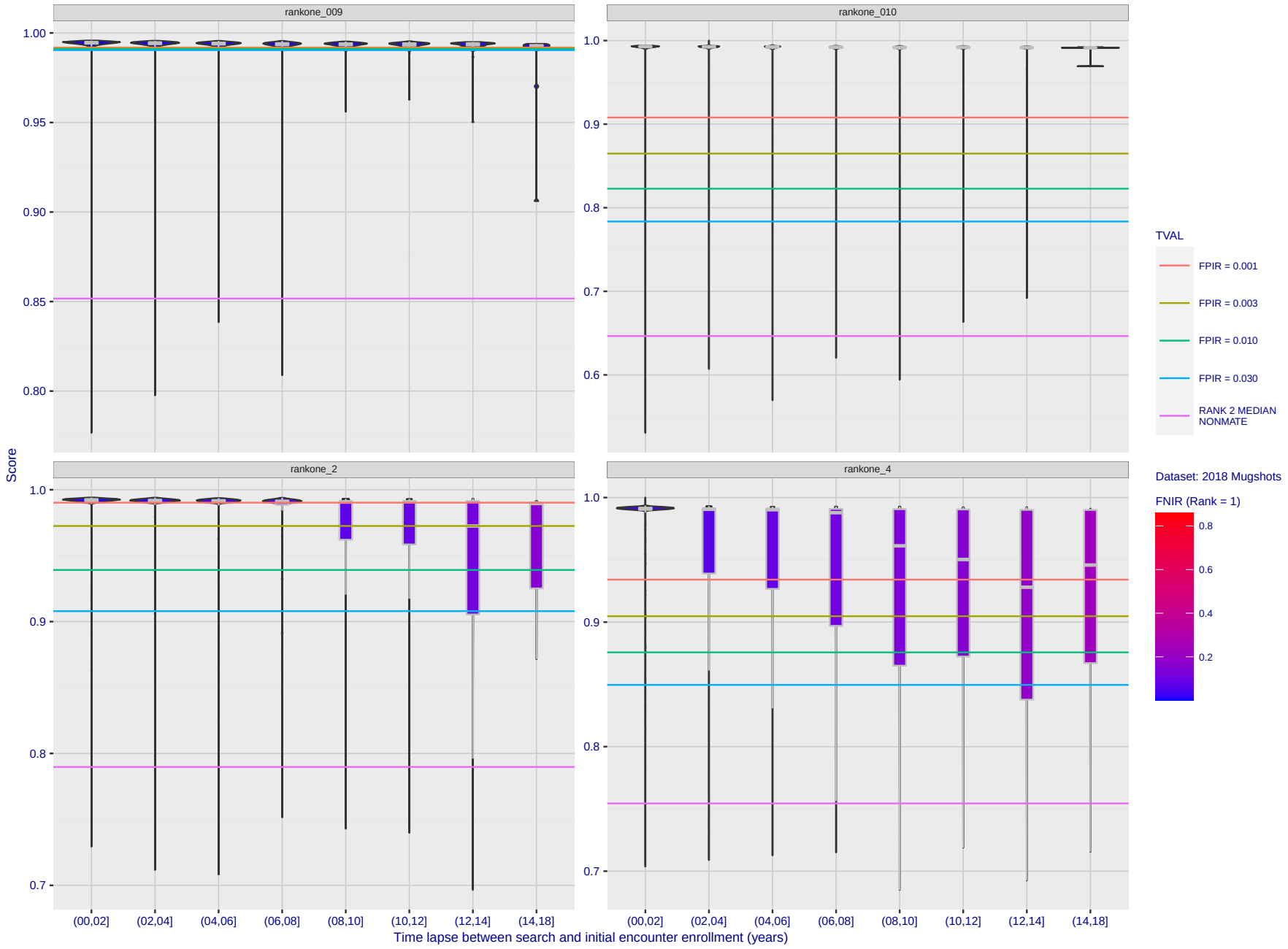

Figure 111: **[FRVT-2018 Mugshot Ageing Dataset] Native mate scores vs. time-elapsed**. *The oldest image of each individual is enrolled. Thereafter, all more recent images are searched. Mated score distributions are computed over all searches noted in row 17 of Table 1 binned by number of years between search and initial enrollment.*

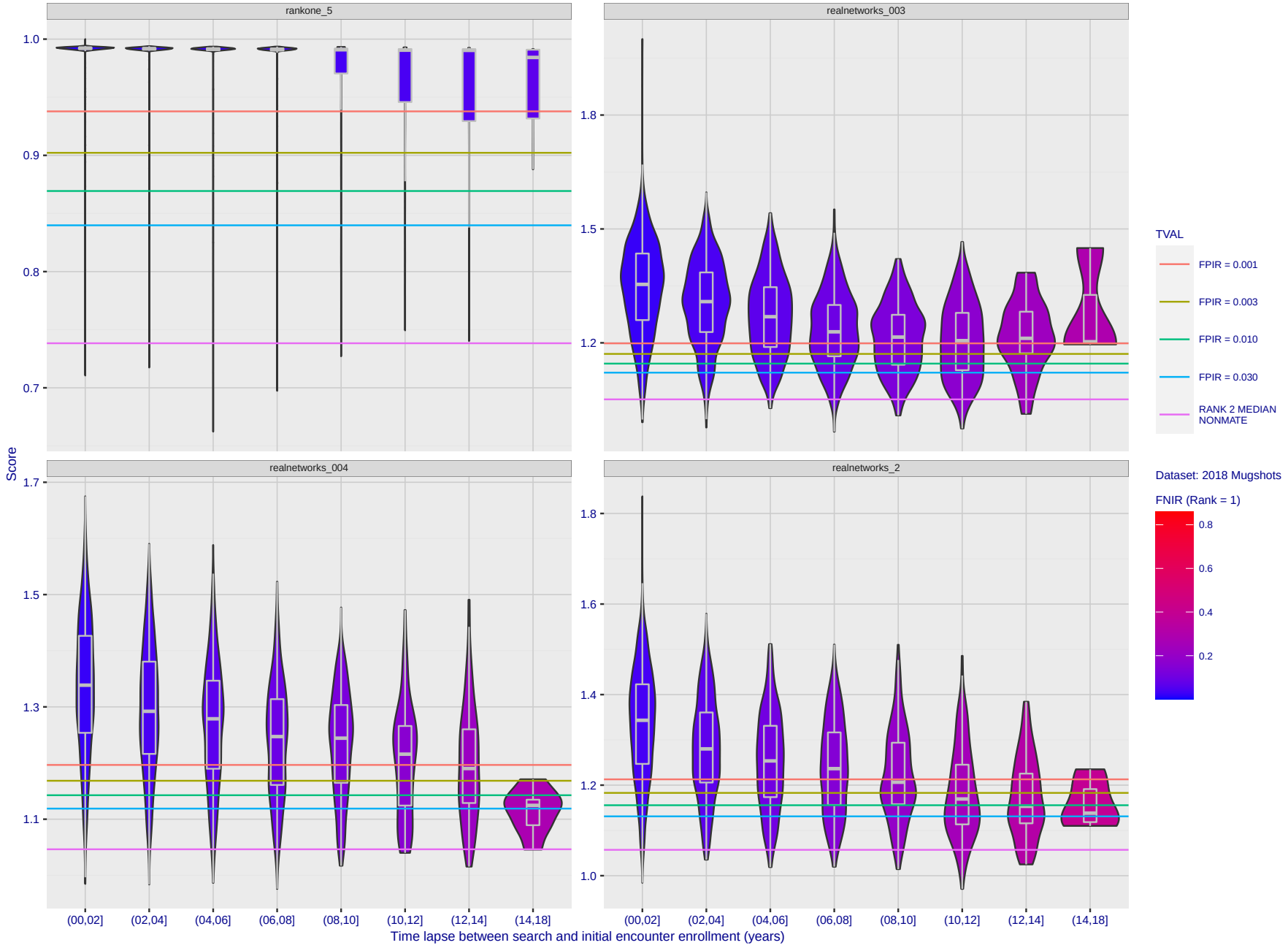

Figure 112: **[FRVT-2018 Mugshot Ageing Dataset] Native mate scores vs. time-elapsed**. *The oldest image of each individual is enrolled. Thereafter, all more recent images are searched. Mated score distributions are computed over all searches noted in row 17 of Table 1 binned by number of years between search and initial enrollment.*

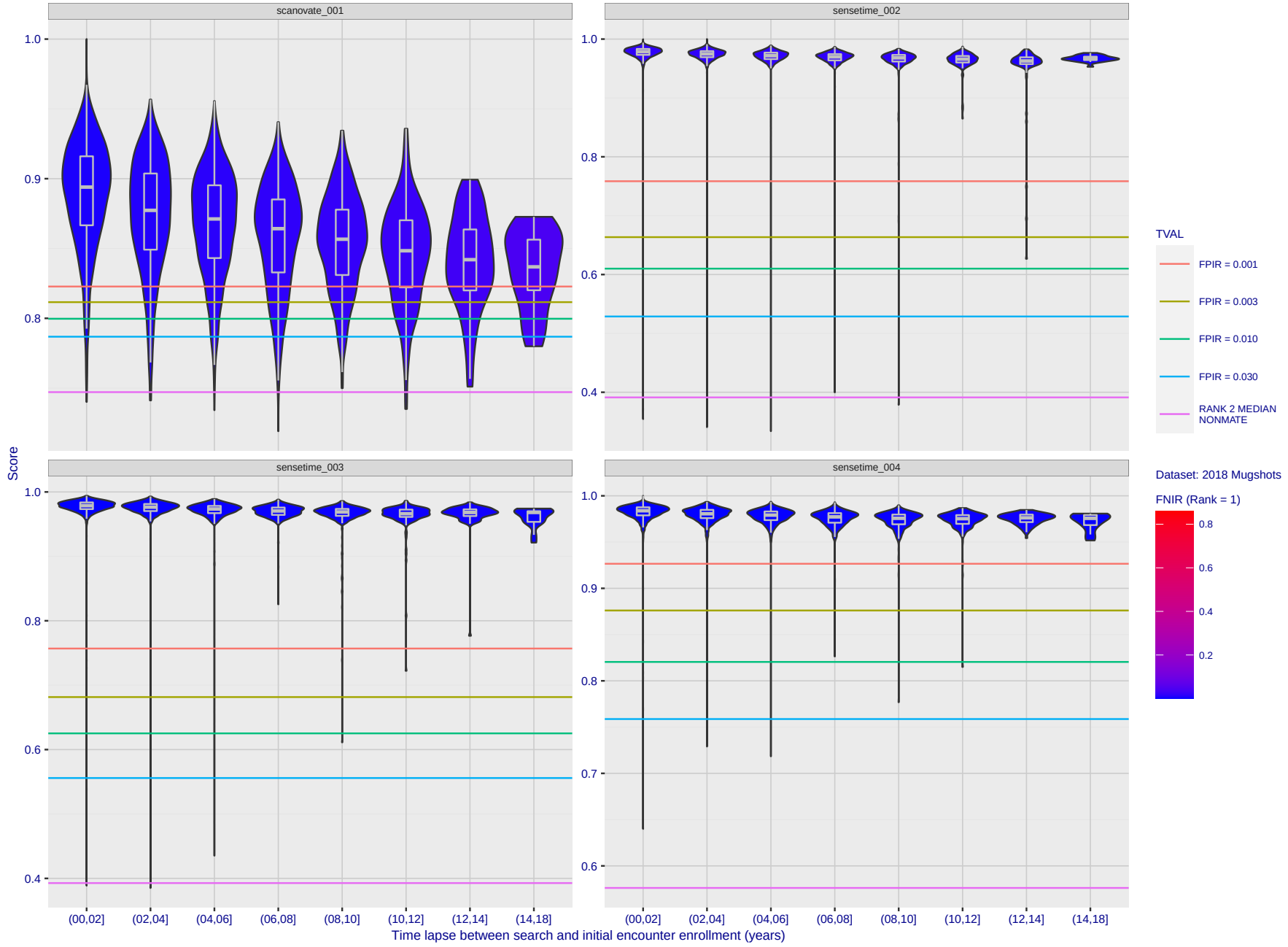

Figure 113: **[FRVT-2018 Mugshot Ageing Dataset] Native mate scores vs. time-elapsed**. *The oldest image of each individual is enrolled. Thereafter, all more recent images are searched. Mated score distributions are computed over all searches noted in row 17 of Table 1 binned by number of years between search and initial enrollment.*

2021/08/05 02:00:58

FNIR(N, R, T) = False neg. identification rate
FPIR(N, T) = False pos. identification rate

N = Num. enrolled subjects
R = Num. candidates examined

T = Threshold

T = 0 → Investigation
T > 0 → Identification

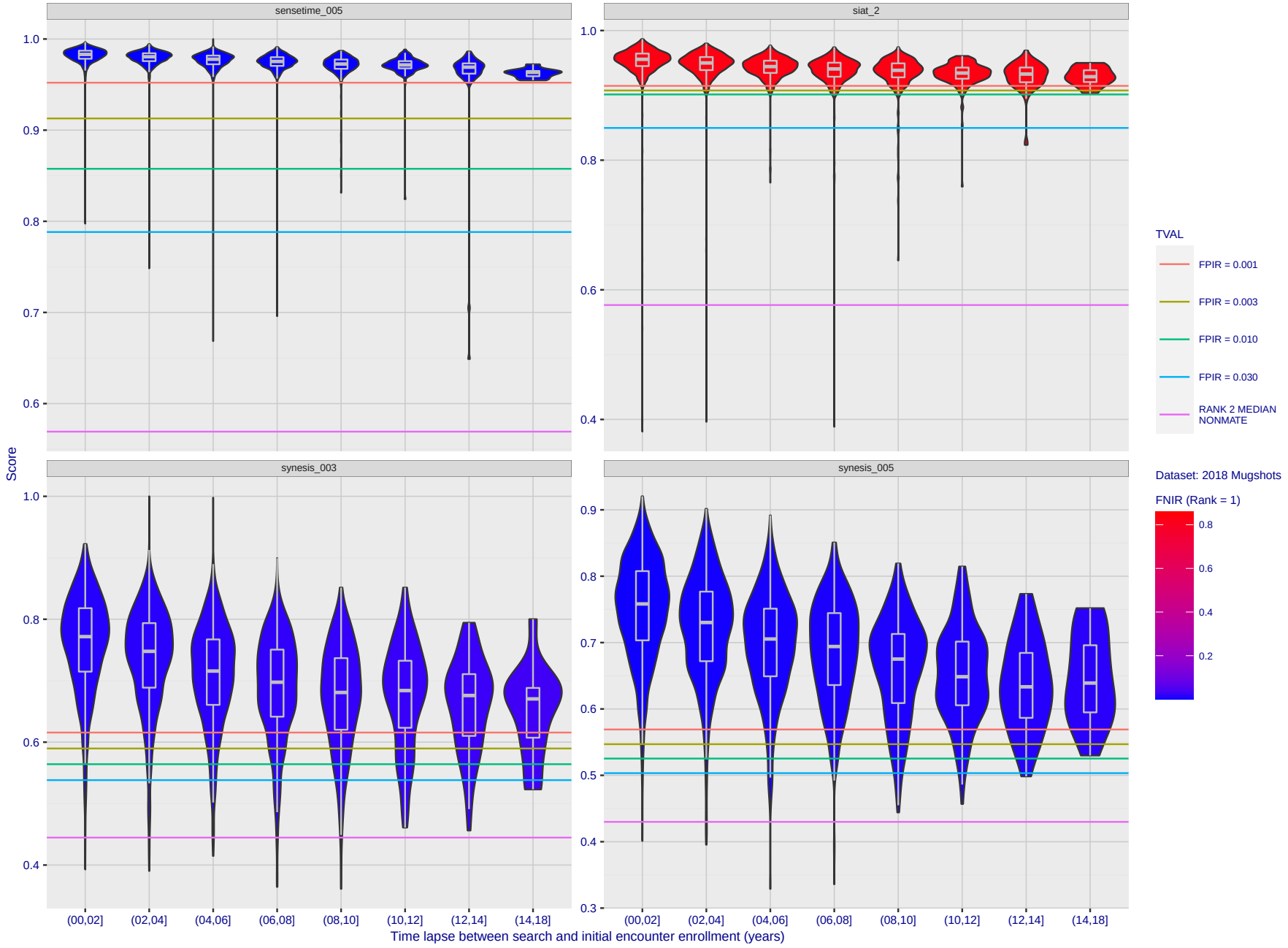

Figure 114: **[FRVT-2018 Mugshot Ageing Dataset] Native mate scores vs. time-elapsed**. *The oldest image of each individual is enrolled. Thereafter, all more recent images are searched. Mated score distributions are computed over all searches noted in row 17 of Table 1 binned by number of years between search and initial enrollment.*

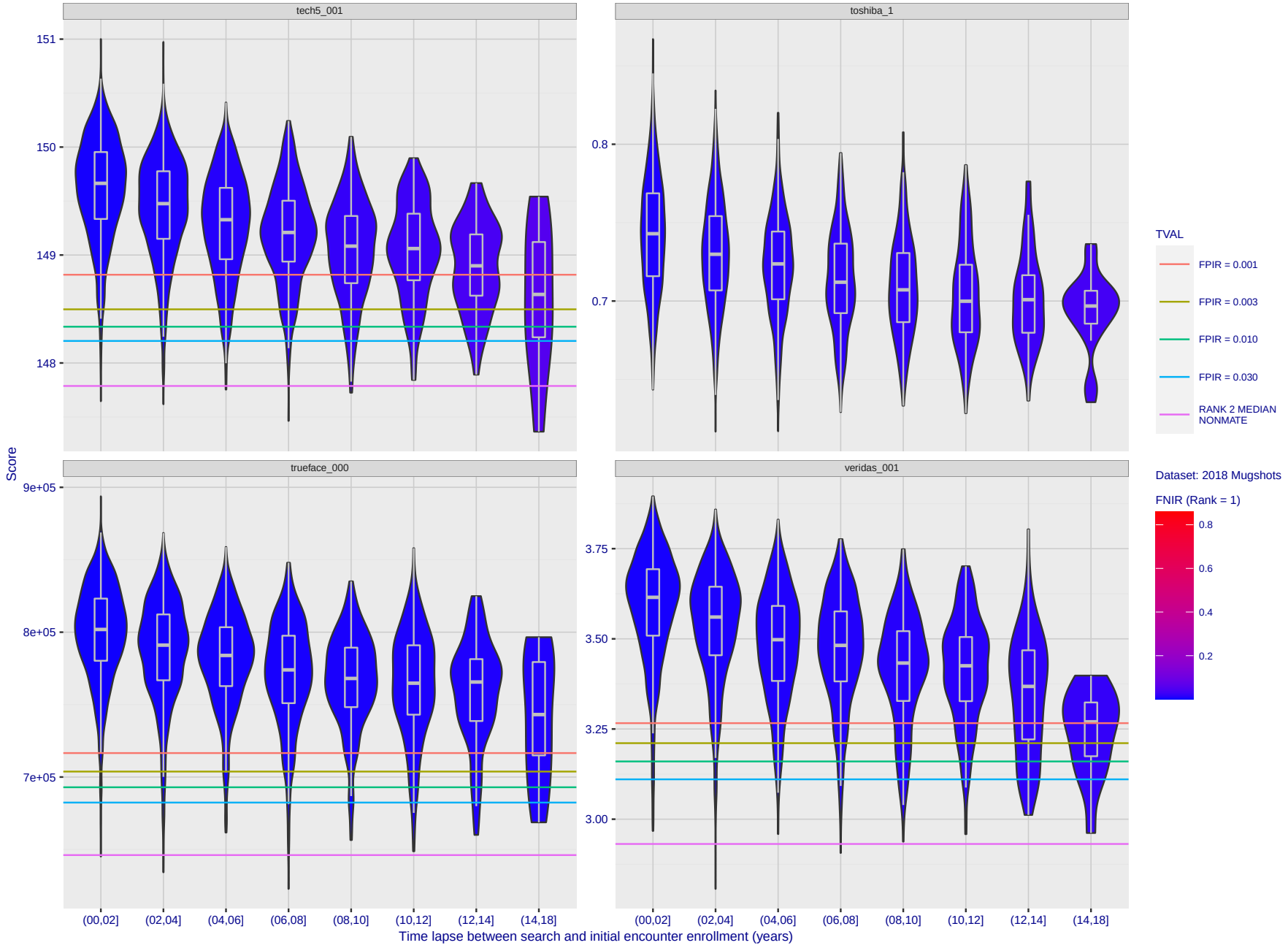

Figure 115: **[FRVT-2018 Mugshot Ageing Dataset] Native mate scores vs. time-elapsed**. *The oldest image of each individual is enrolled. Thereafter, all more recent images are searched. Mated score distributions are computed over all searches noted in row 17 of Table 1 binned by number of years between search and initial enrollment.*

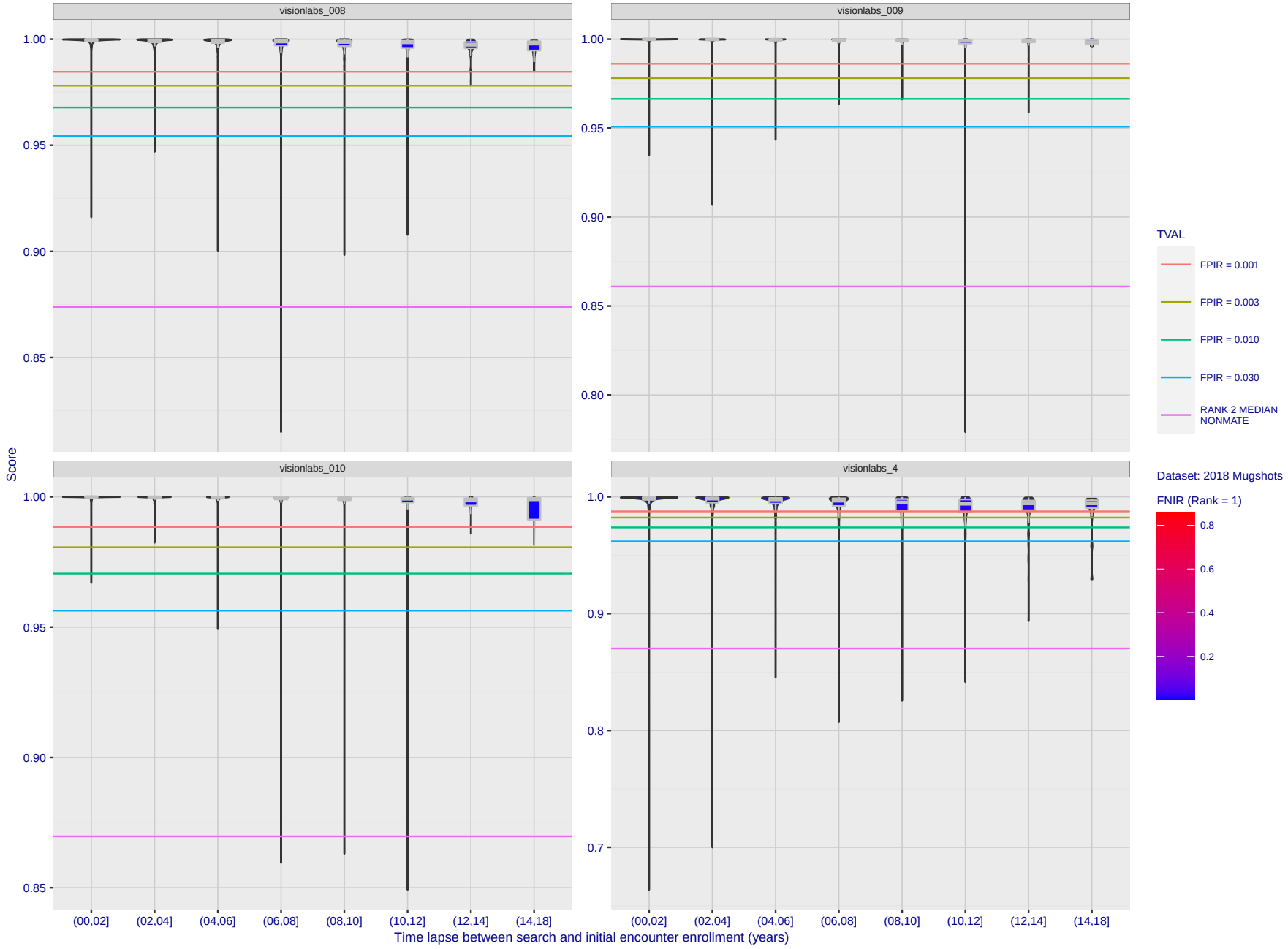

Figure 116: **[FRVT-2018 Mugshot Ageing Dataset] Native mate scores vs. time-elapsed**. *The oldest image of each individual is enrolled. Thereafter, all more recent images are searched. Mated score distributions are computed over all searches noted in row 17 of Table 1 binned by number of years between search and initial enrollment.*

2021/08/05 02:00:58

FNIR(N, R, T) = False neg. identification rate
FPIR(N, T) = False pos. identification rate

N = Num. enrolled subjects
R = Num. candidates examined

T = Threshold

T = 0 → Investigation
T > 0 → Identification

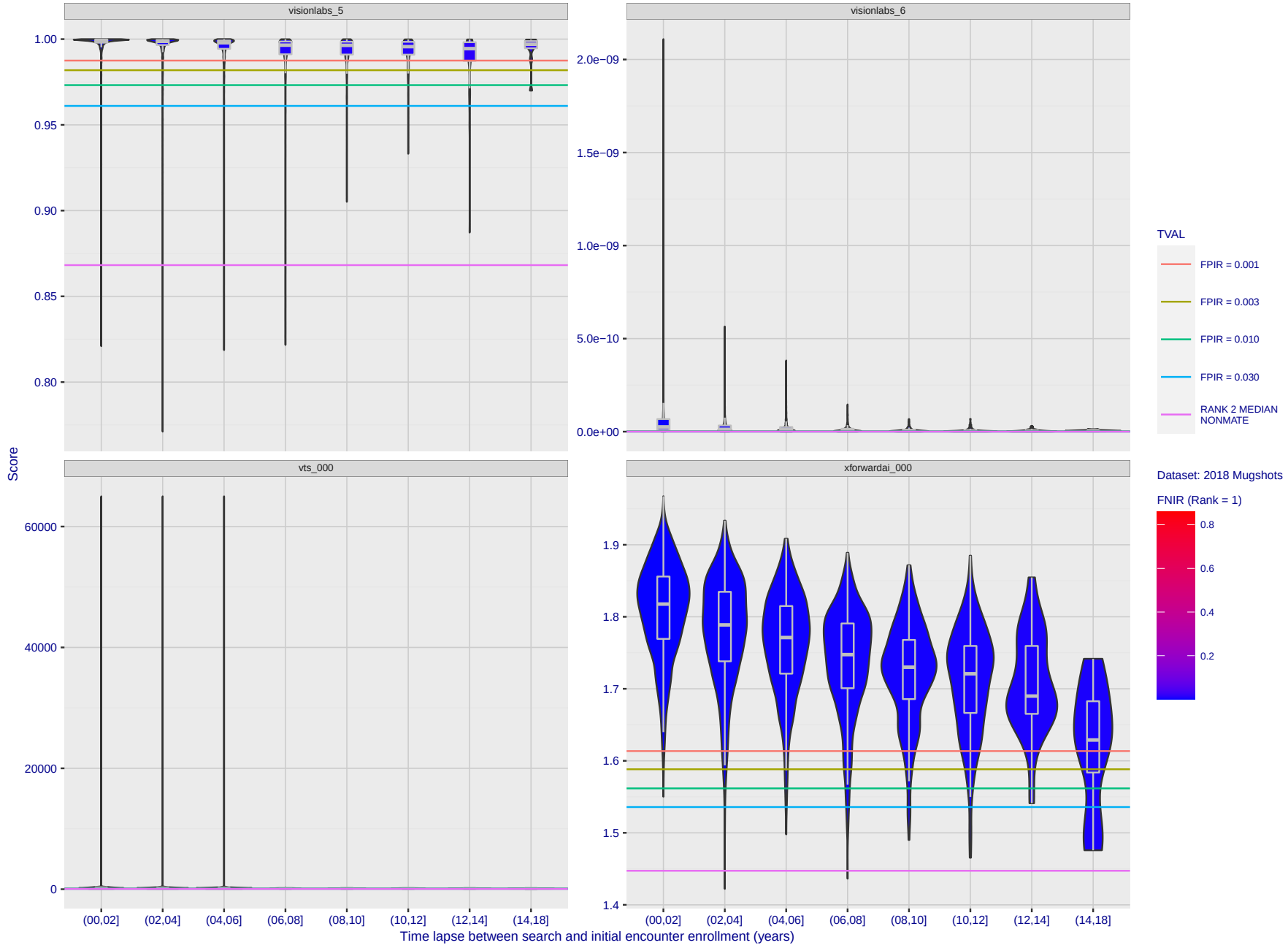

Figure 117: **[FRVT-2018 Mugshot Ageing Dataset] Native mate scores vs. time-elapsed**. *The oldest image of each individual is enrolled. Thereafter, all more recent images are searched. Mated score distributions are computed over all searches noted in row 17 of Table 1 binned by number of years between search and initial enrollment.*

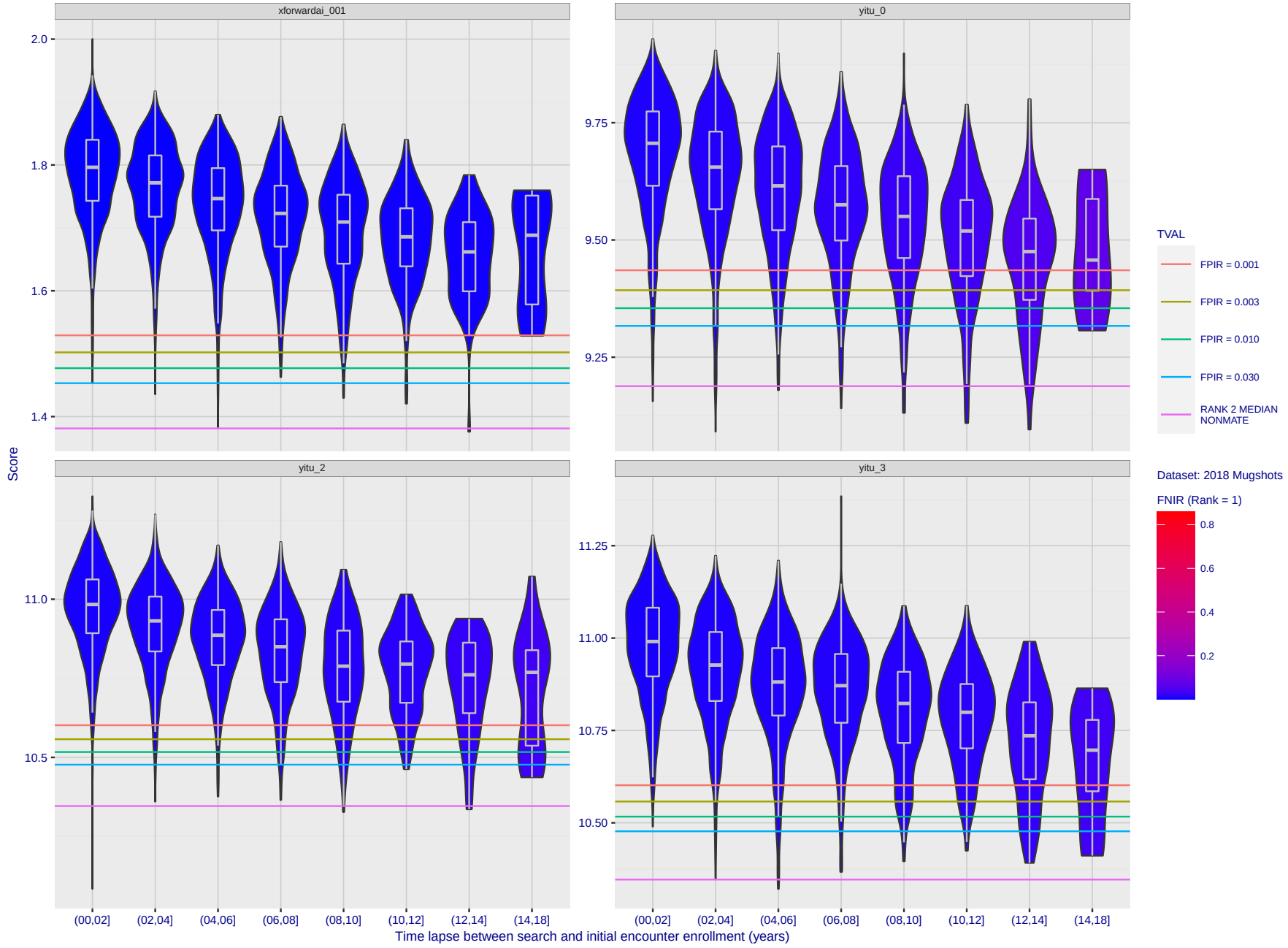

Figure 118: **[FRVT-2018 Mugshot Ageing Dataset] Native mate scores vs. time-elapsed**. *The oldest image of each individual is enrolled. Thereafter, all more recent images are searched. Mated score distributions are computed over all searches noted in row 17 of Table 1 binned by number of years between search and initial enrollment.*

2021/08/05 02:00:58
FNIR(N, R, T) = False neg. identification rate
FPIR(N, T) = False pos. identification rate
N = Num. enrolled subjects
R = Num. candidates examined
T = Threshold
T = 0 → Investigation
T > 0 → Identification

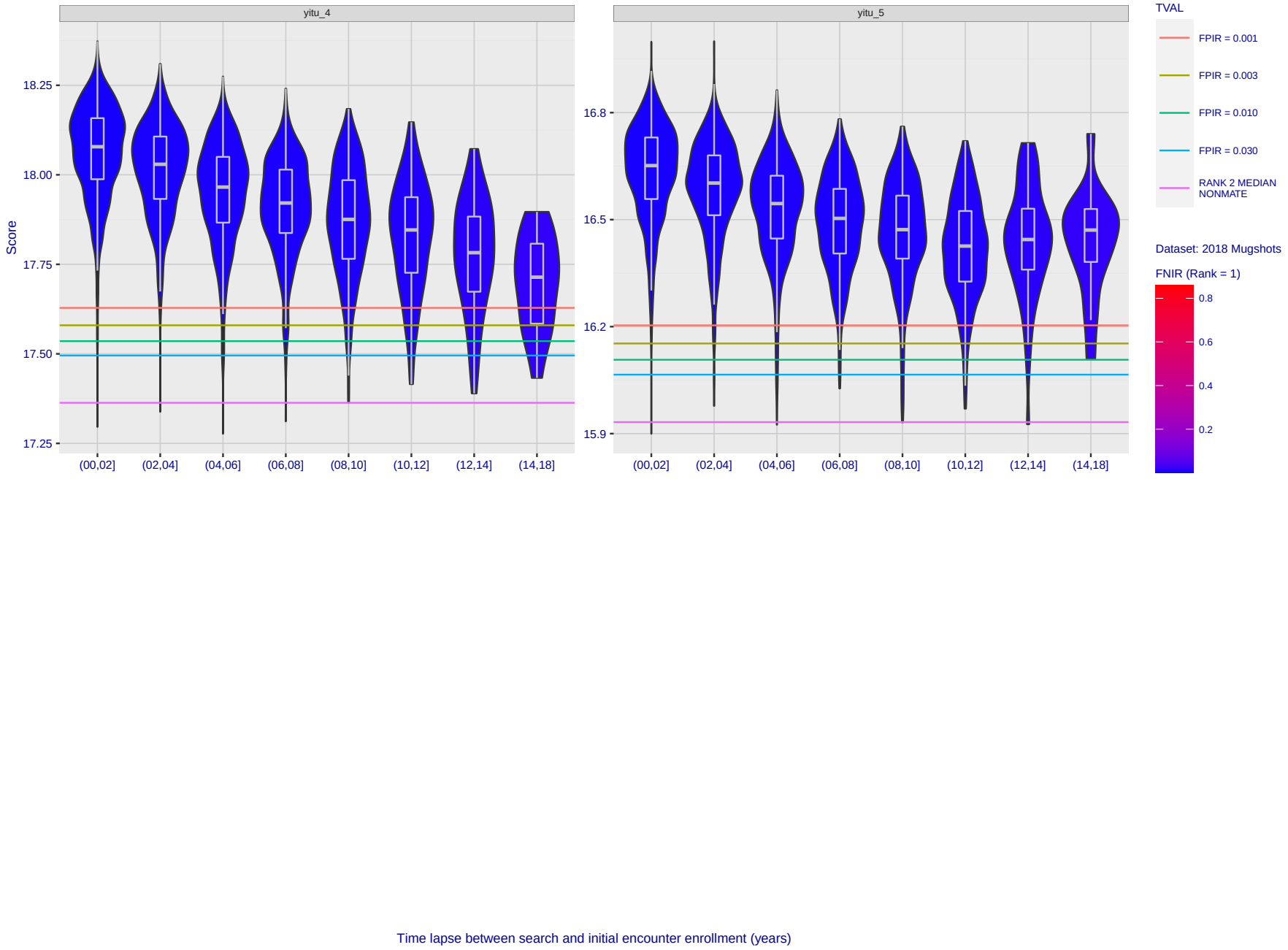

Figure 119: **[FRVT-2018 Mugshot Ageing Dataset] Native mate scores vs. time-elapsed**. *The oldest image of each individual is enrolled. Thereafter, all more recent images are searched. Mated score distributions are computed over all searches noted in row 17 of Table 1 binned by number of years between search and initial enrollment.*

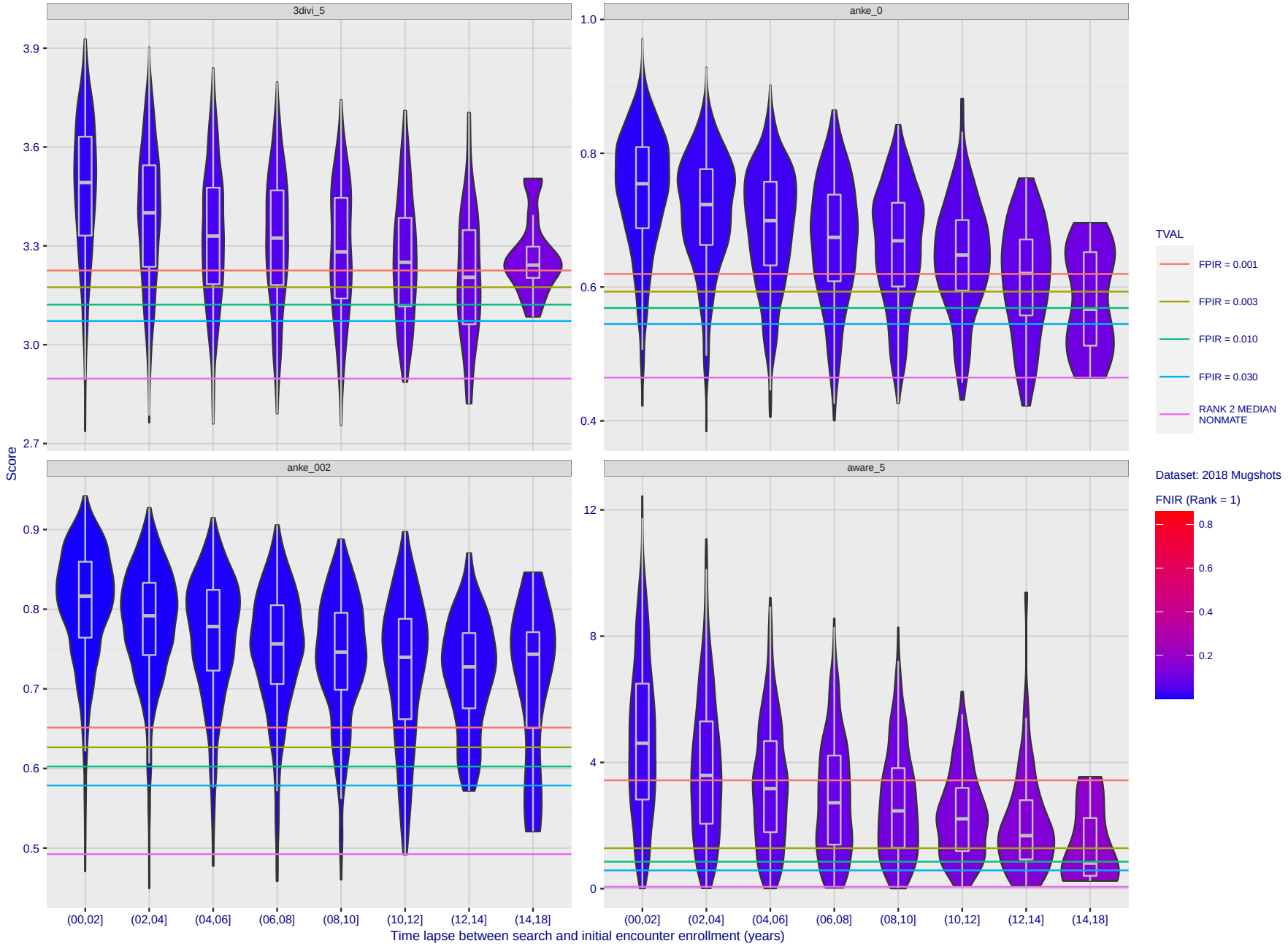

Figure 120: **[FRVT-2018 Mugshot Ageing Dataset] Native mate scores vs. time-elapsed**. *The oldest image of each individual is enrolled. Thereafter, all more recent images are searched. Mated score distributions are computed over all searches noted in row 17 of Table 1 binned by number of years between search and initial enrollment.*

2021/08/05 02:00:58
FNIR(N, R, T) = False neg. identification rate
FPIR(N, T) = False pos. identification rate
N = Num. enrolled subjects
R = Num. candidates examined
T = Threshold
T = 0 → Investigation
T > 0 → Identification

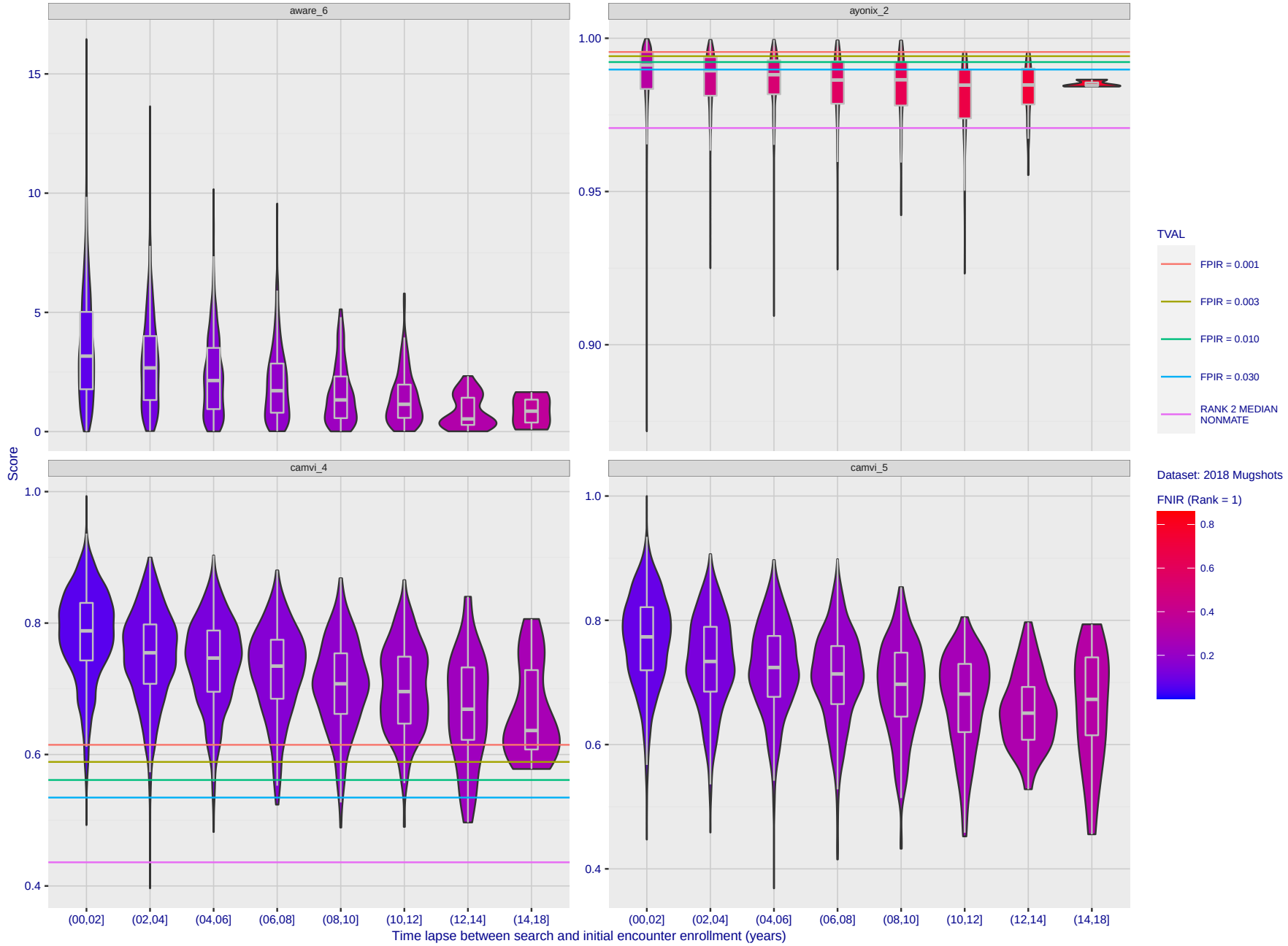

Figure 121: **[FRVT-2018 Mugshot Ageing Dataset] Native mate scores vs. time-elapsed**. *The oldest image of each individual is enrolled. Thereafter, all more recent images are searched. Mated score distributions are computed over all searches noted in row 17 of Table 1 binned by number of years between search and initial enrollment.*

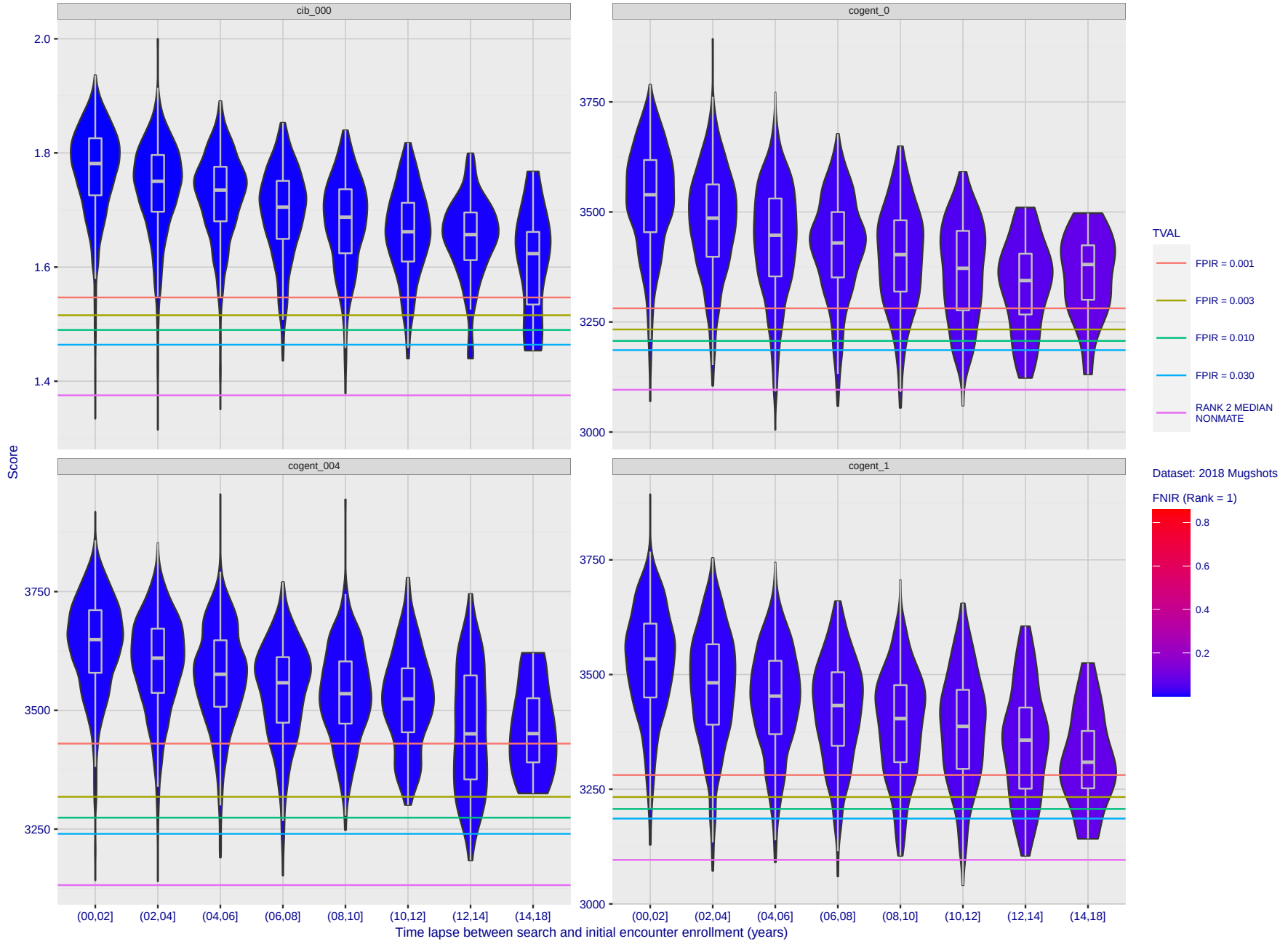

Figure 122: **[FRVT-2018 Mugshot Ageing Dataset] Native mate scores vs. time-elapsed**. *The oldest image of each individual is enrolled. Thereafter, all more recent images are searched. Mated score distributions are computed over all searches noted in row 17 of Table 1 binned by number of years between search and initial enrollment.*

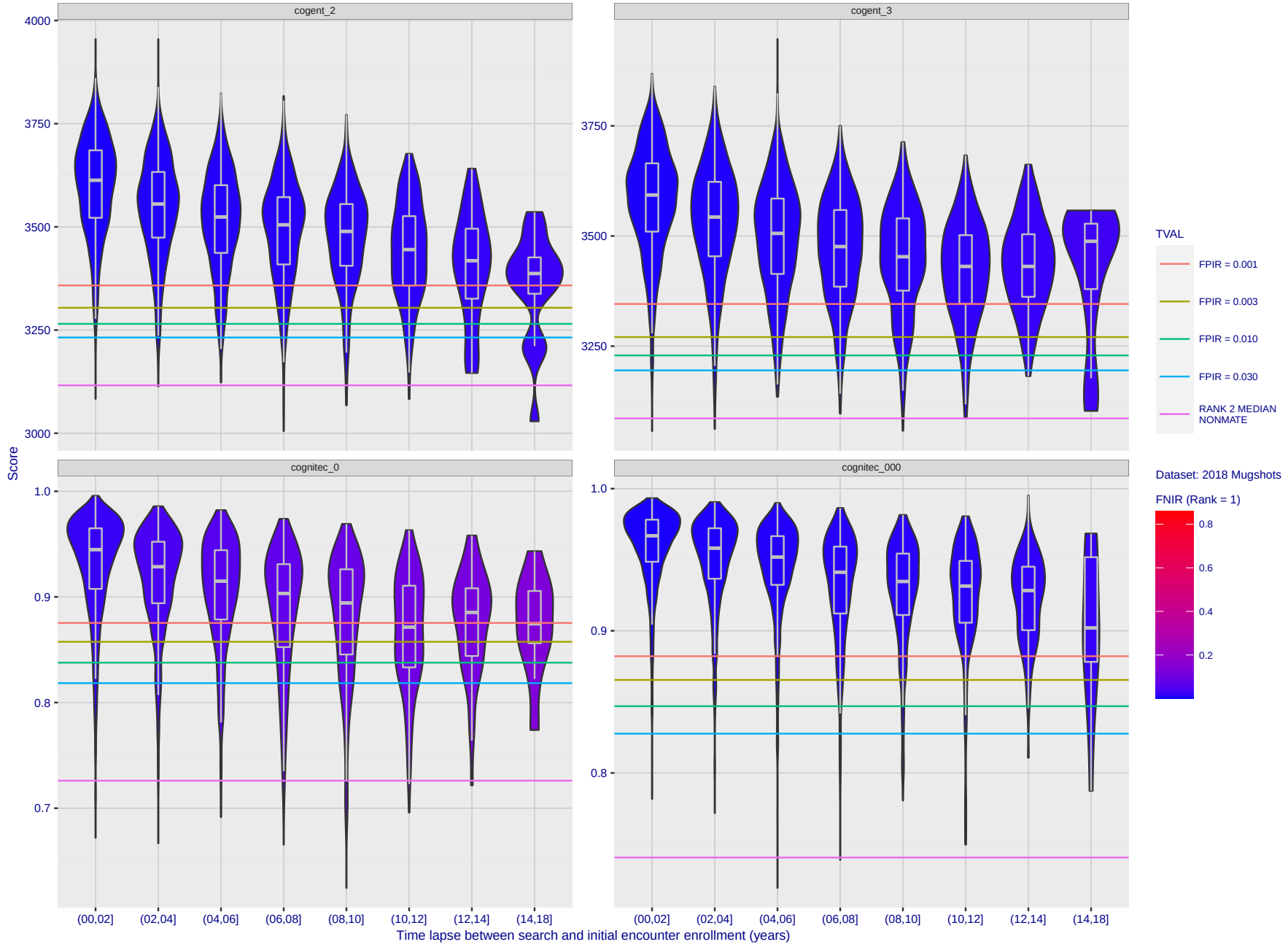

Figure 123: **[FRVT-2018 Mugshot Ageing Dataset] Native mate scores vs. time-elapsed**. *The oldest image of each individual is enrolled. Thereafter, all more recent images are searched. Mated score distributions are computed over all searches noted in row 17 of Table 1 binned by number of years between search and initial enrollment.*

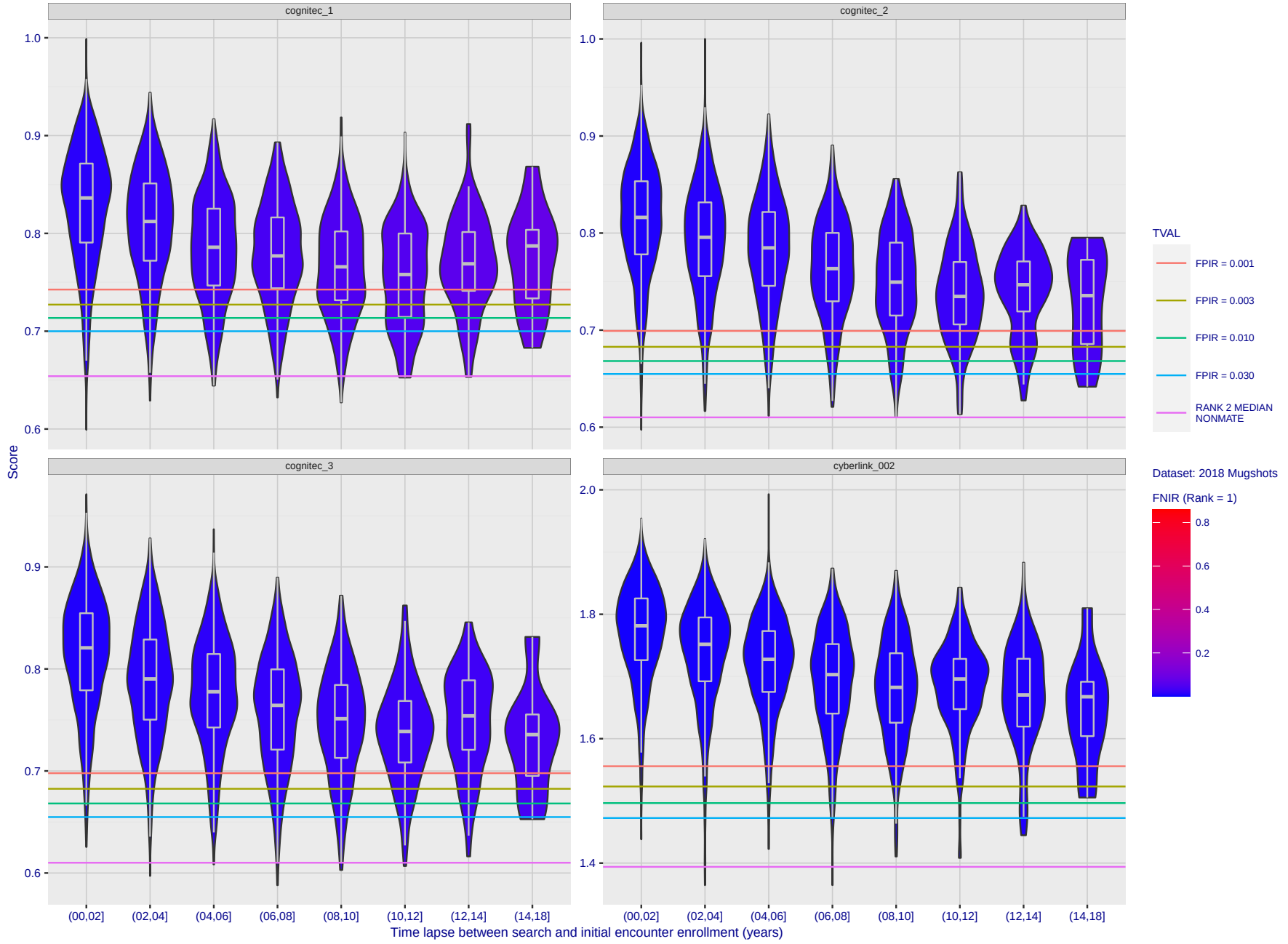

Figure 124: **[FRVT-2018 Mugshot Ageing Dataset] Native mate scores vs. time-elapsed**. *The oldest image of each individual is enrolled. Thereafter, all more recent images are searched. Mated score distributions are computed over all searches noted in row 17 of Table 1 binned by number of years between search and initial enrollment.*

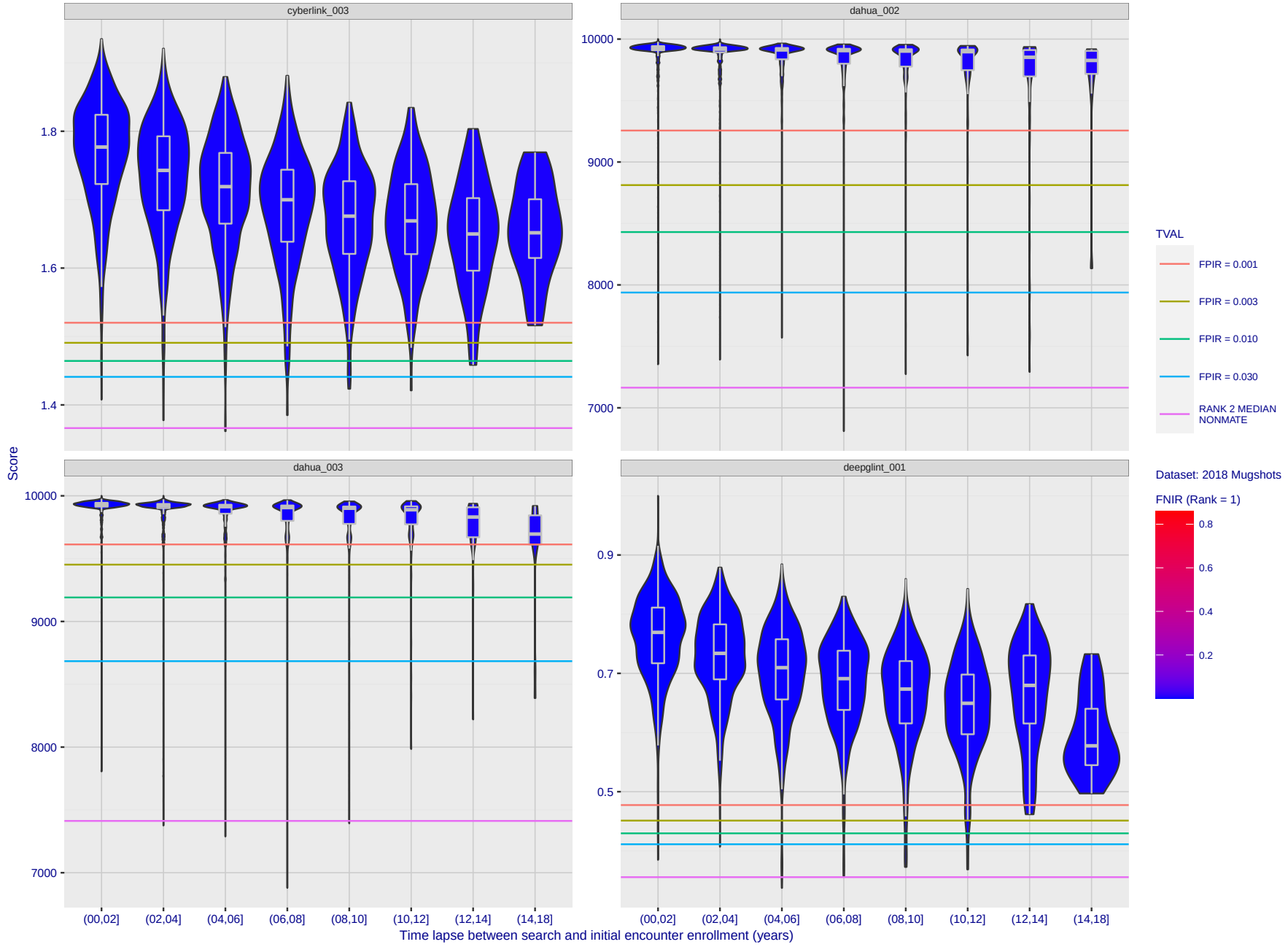

Figure 125: **[FRVT-2018 Mugshot Ageing Dataset] Native mate scores vs. time-elapsed**. *The oldest image of each individual is enrolled. Thereafter, all more recent images are searched. Mated score distributions are computed over all searches noted in row 17 of Table 1 binned by number of years between search and initial enrollment.*

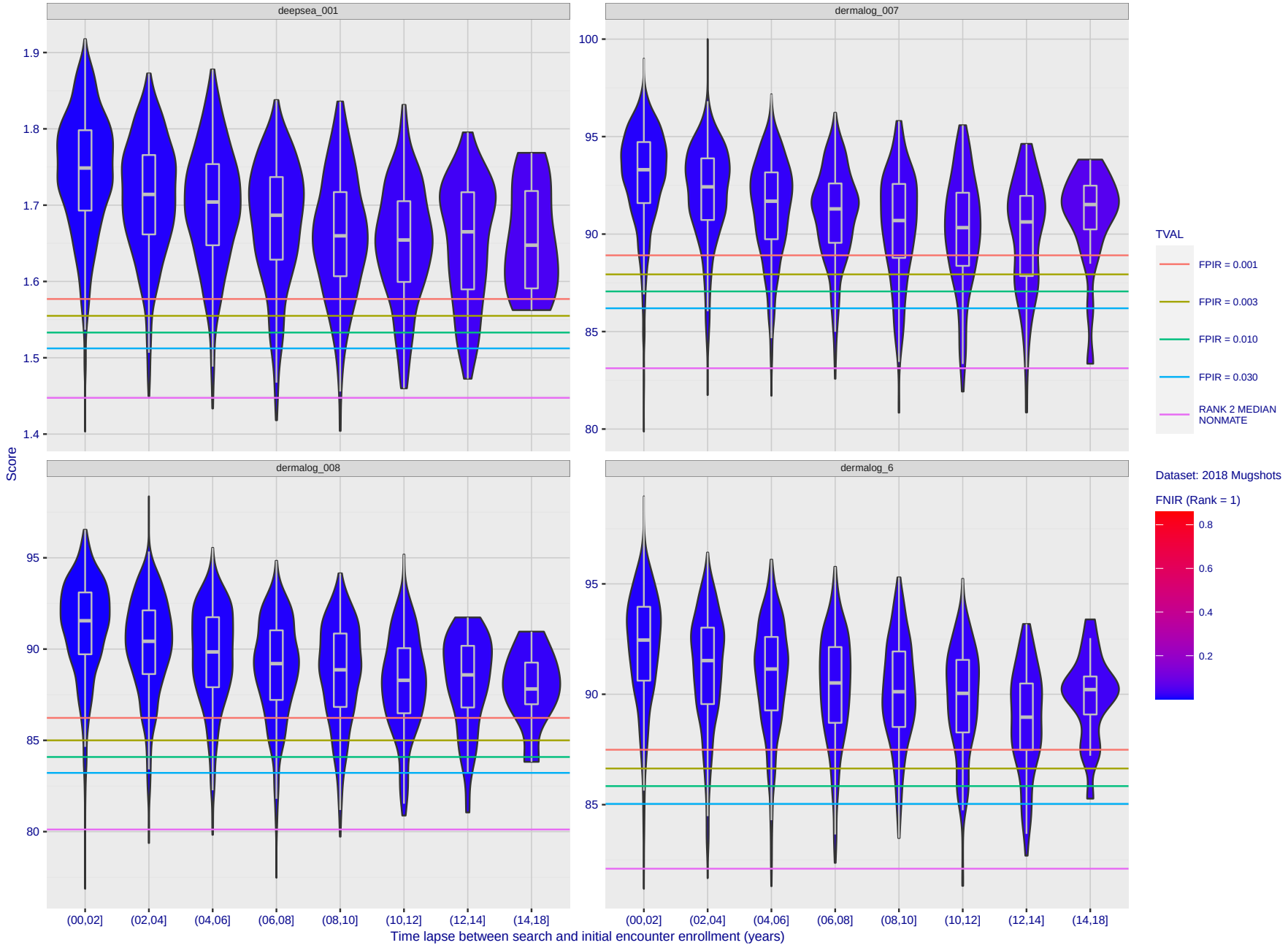

Figure 126: **[FRVT-2018 Mugshot Ageing Dataset] Native mate scores vs. time-elapsed**. *The oldest image of each individual is enrolled. Thereafter, all more recent images are searched. Mated score distributions are computed over all searches noted in row 17 of Table 1 binned by number of years between search and initial enrollment.*

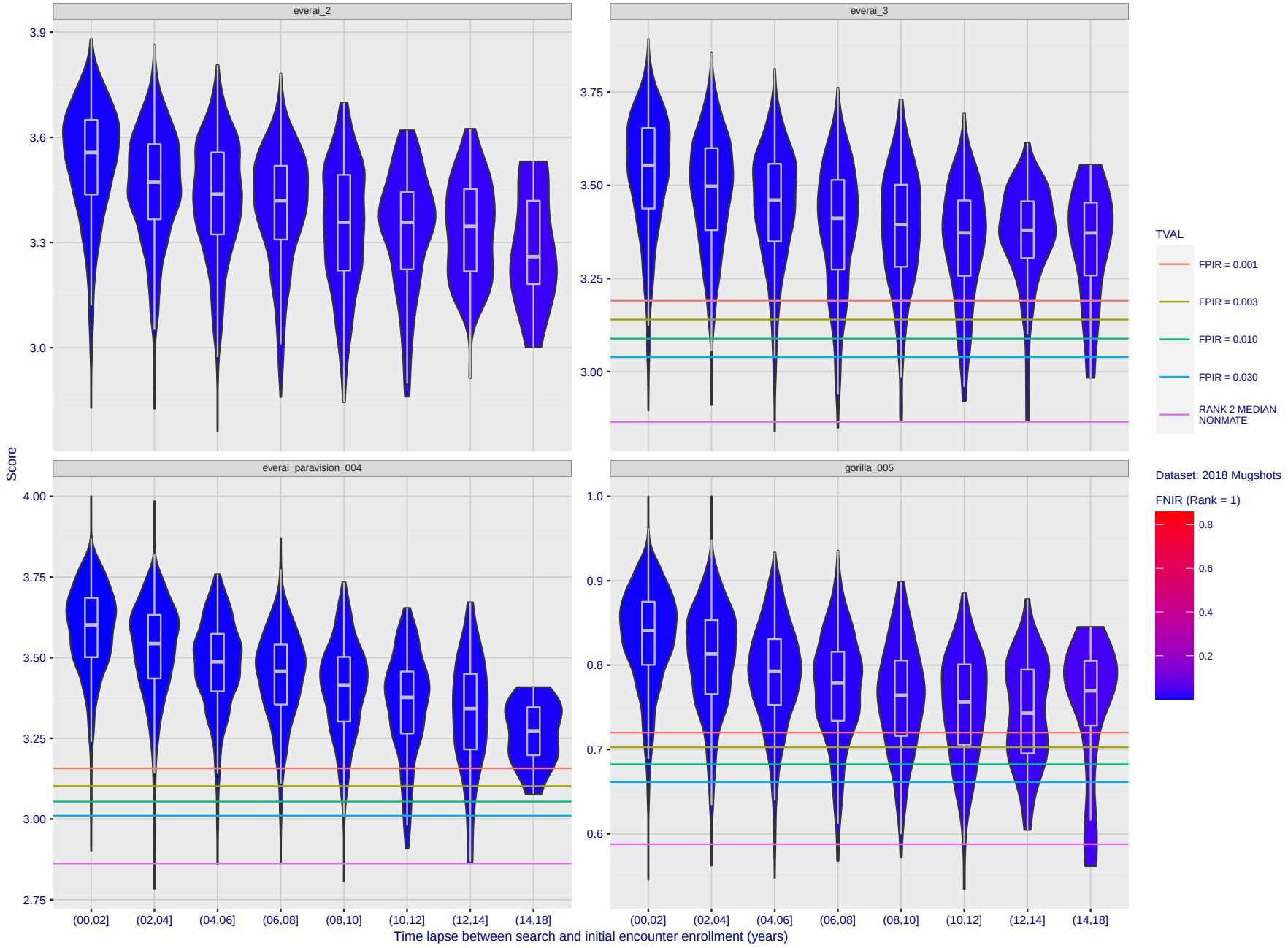

Figure 127: **[FRVT-2018 Mugshot Ageing Dataset] Native mate scores vs. time-elapsed**. *The oldest image of each individual is enrolled. Thereafter, all more recent images are searched. Mated score distributions are computed over all searches noted in row 17 of Table 1 binned by number of years between search and initial enrollment.*

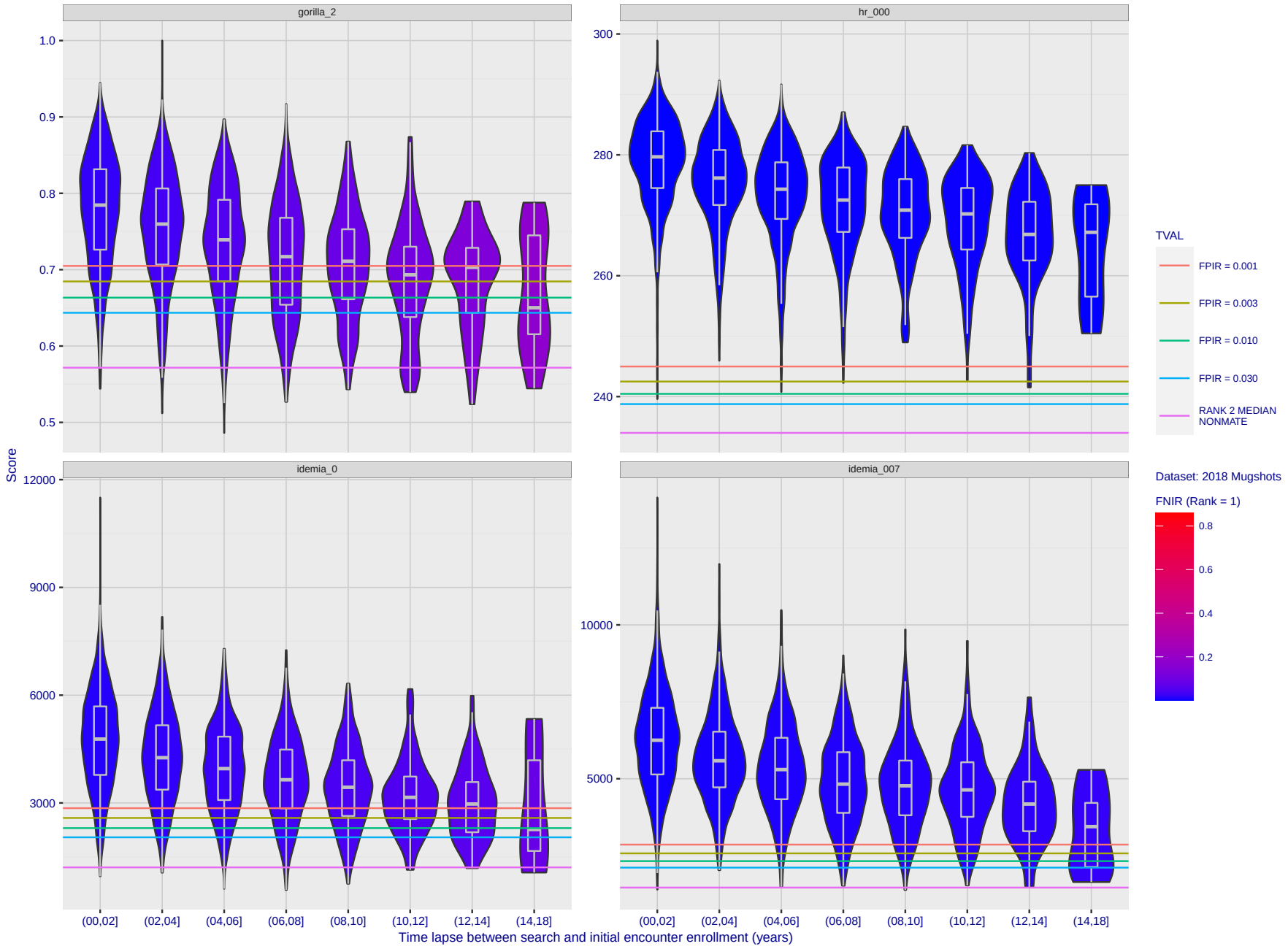

Figure 128: **[FRVT-2018 Mugshot Ageing Dataset] Native mate scores vs. time-elapsed**. *The oldest image of each individual is enrolled. Thereafter, all more recent images are searched. Mated score distributions are computed over all searches noted in row 17 of Table 1 binned by number of years between search and initial enrollment.*

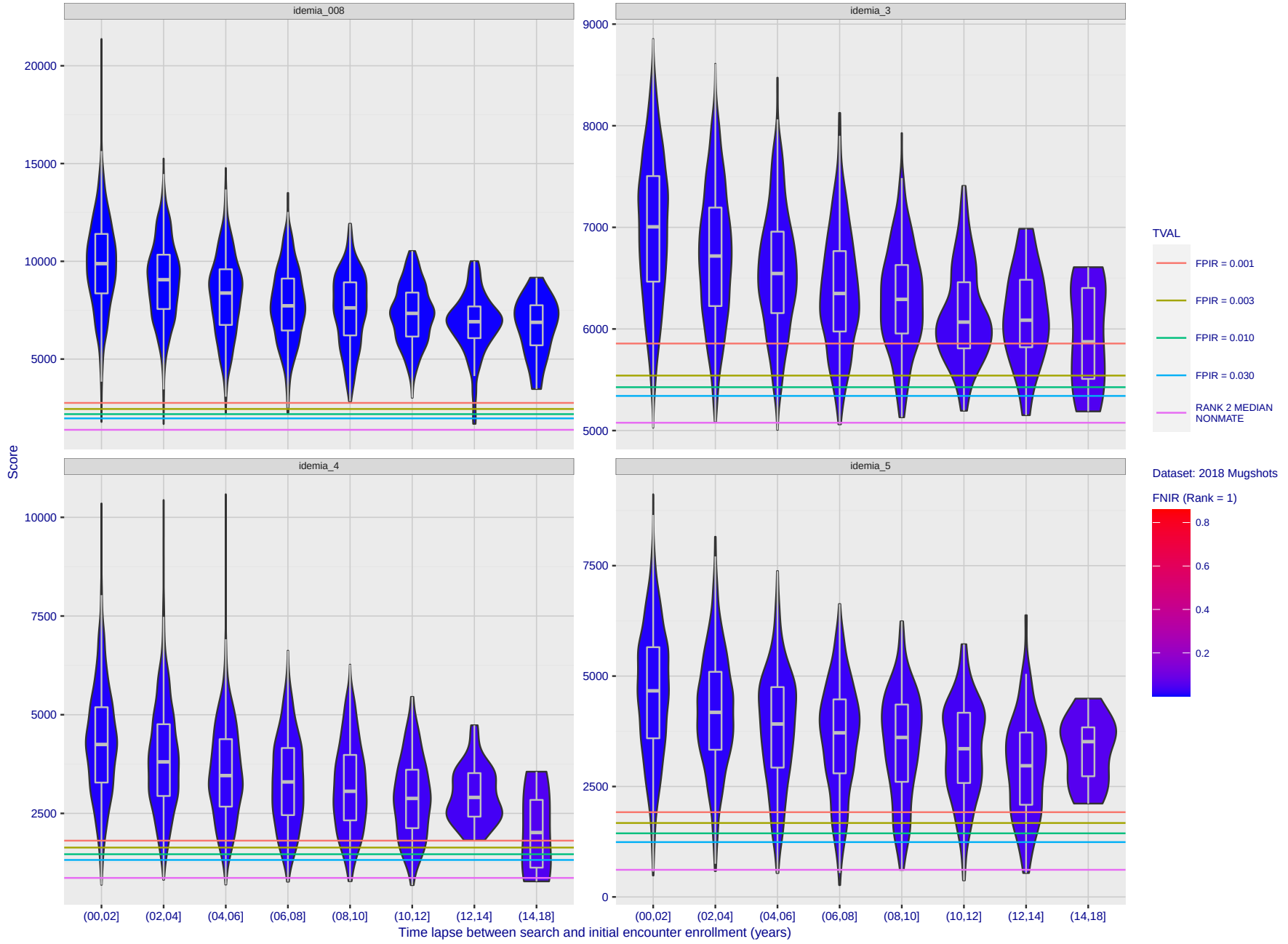

Figure 129: **[FRVT-2018 Mugshot Ageing Dataset] Native mate scores vs. time-elapsed**. *The oldest image of each individual is enrolled. Thereafter, all more recent images are searched. Mated score distributions are computed over all searches noted in row 17 of Table 1 binned by number of years between search and initial enrollment.*

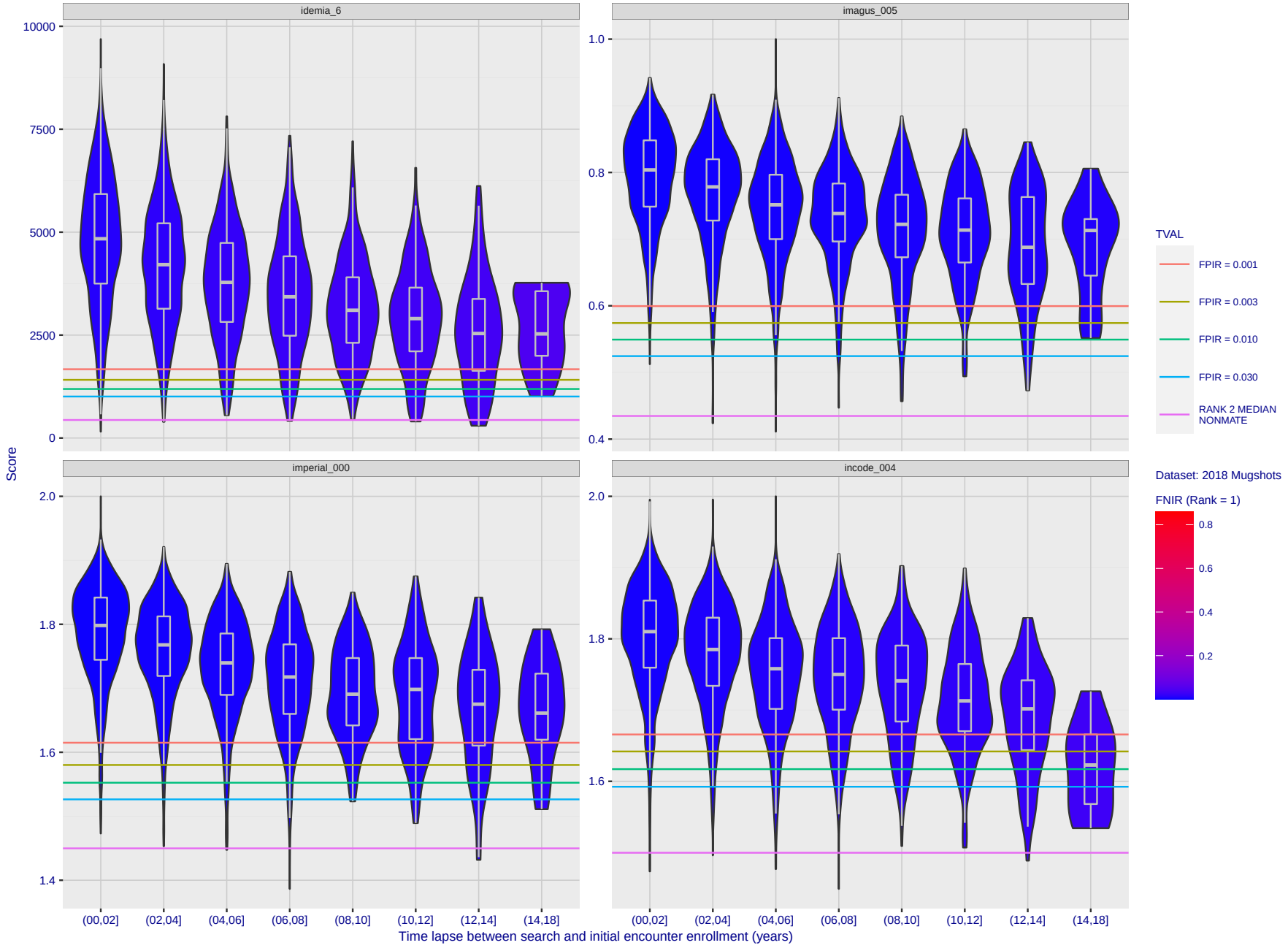

Figure 130: **[FRVT-2018 Mugshot Ageing Dataset] Native mate scores vs. time-elapsed**. *The oldest image of each individual is enrolled. Thereafter, all more recent images are searched. Mated score distributions are computed over all searches noted in row 17 of Table 1 binned by number of years between search and initial enrollment.*

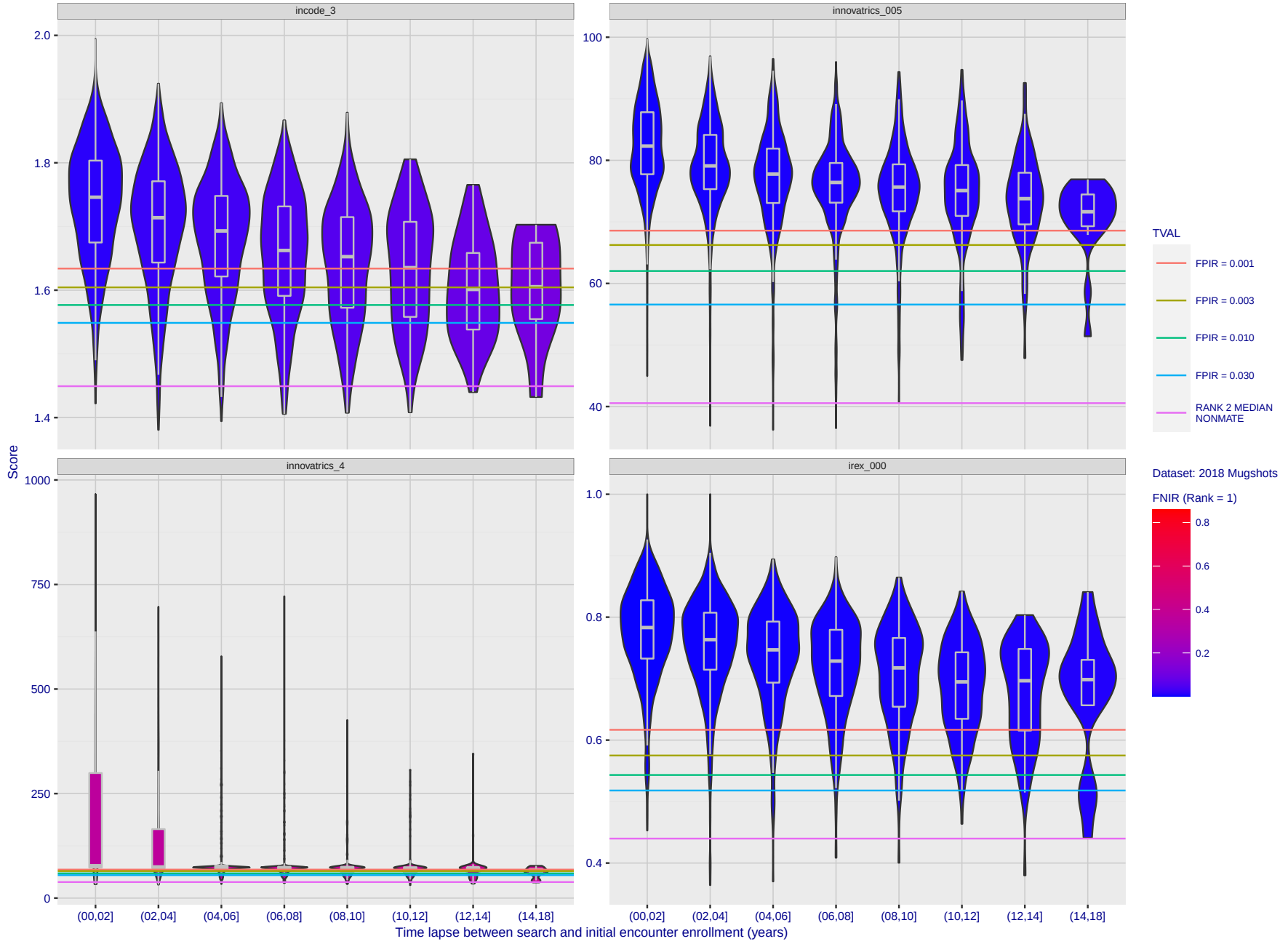

Figure 131: **[FRVT-2018 Mugshot Ageing Dataset] Native mate scores vs. time-elapsed**. *The oldest image of each individual is enrolled. Thereafter, all more recent images are searched. Mated score distributions are computed over all searches noted in row 17 of Table 1 binned by number of years between search and initial enrollment.*

2021/08/05 02:00:58
FNIR(N, R, T) = False neg. identification rate
FPIR(N, T) = False pos. identification rate
N = Num. enrolled subjects
R = Num. candidates examined
T = Threshold
T = 0 → Investigation
T > 0 → Identification

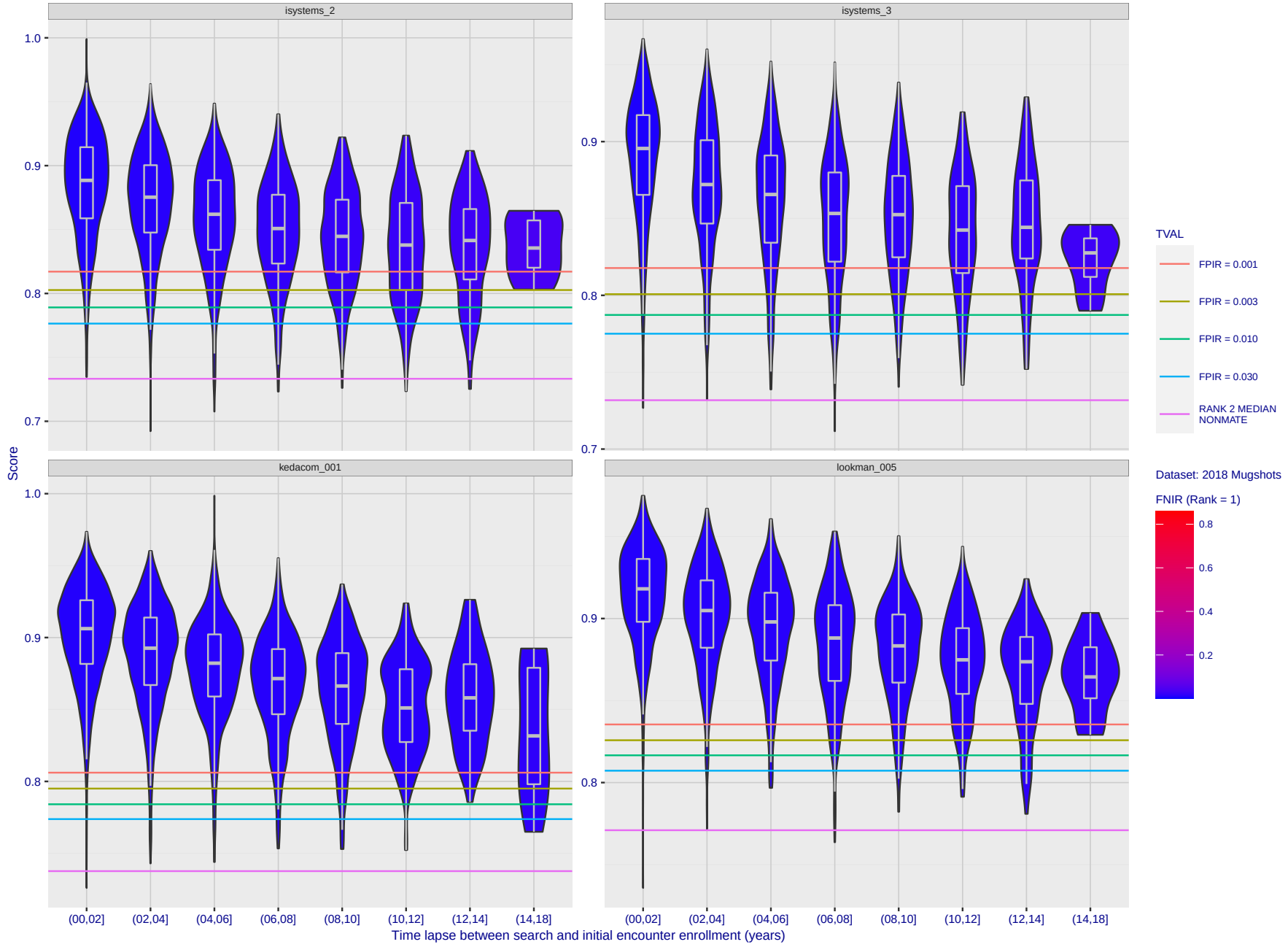

Figure 132: **[FRVT-2018 Mugshot Ageing Dataset] Native mate scores vs. time-elapsed**. *The oldest image of each individual is enrolled. Thereafter, all more recent images are searched. Mated score distributions are computed over all searches noted in row 17 of Table 1 binned by number of years between search and initial enrollment.*

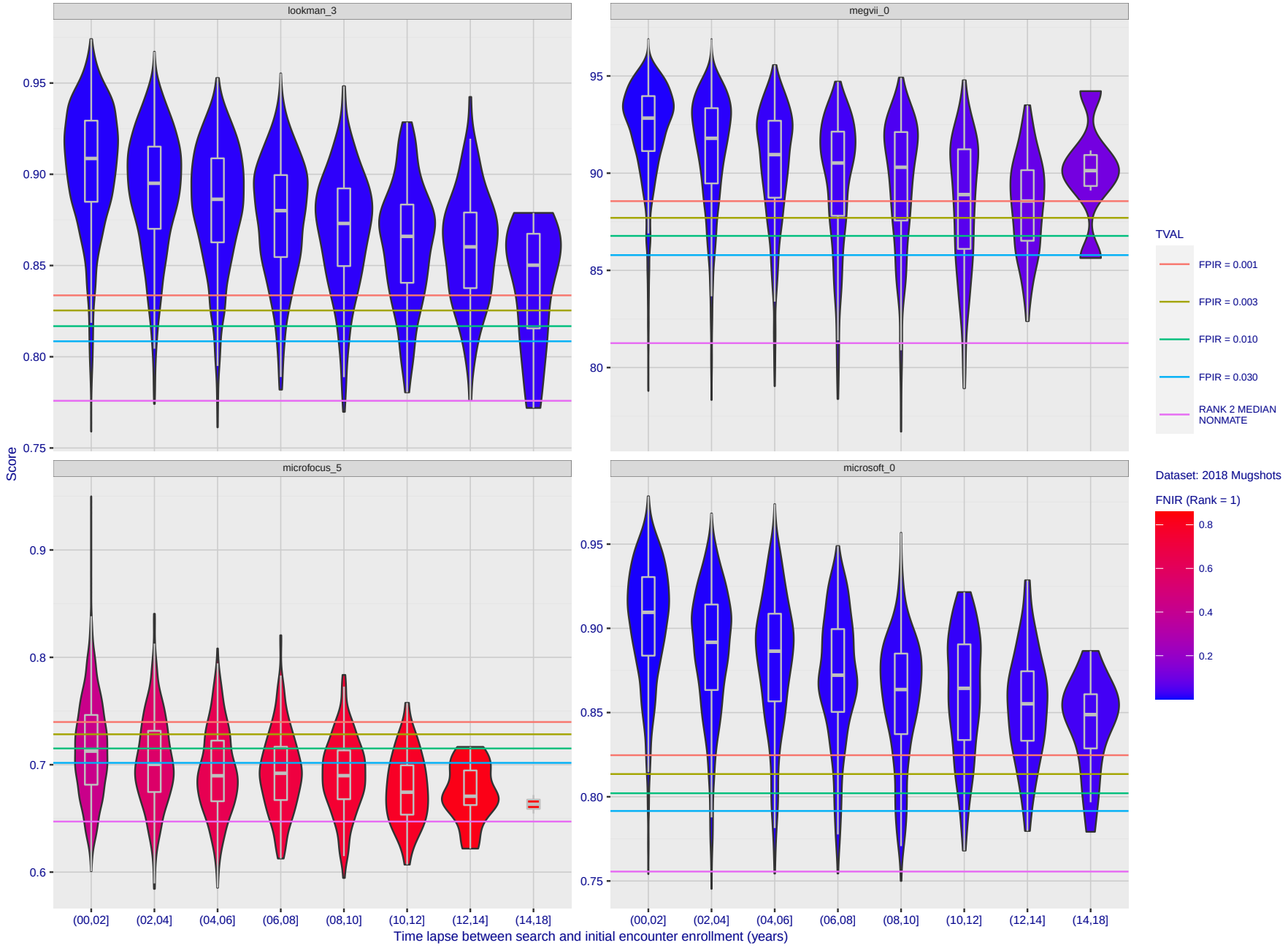

Figure 133: **[FRVT-2018 Mugshot Ageing Dataset] Native mate scores vs. time-elapsed**. *The oldest image of each individual is enrolled. Thereafter, all more recent images are searched. Mated score distributions are computed over all searches noted in row 17 of Table 1 binned by number of years between search and initial enrollment.*

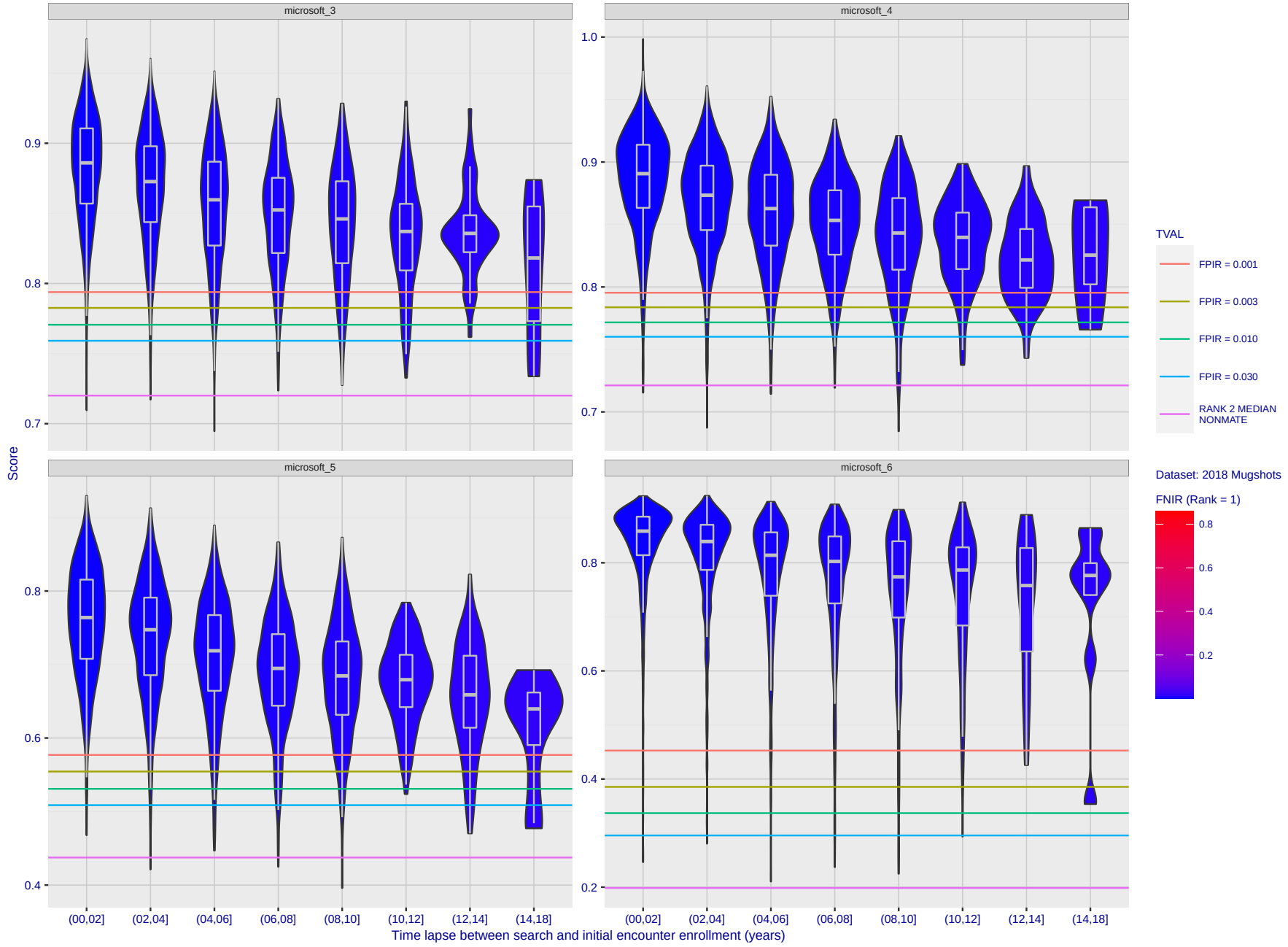

Figure 134: **[FRVT-2018 Mugshot Ageing Dataset] Native mate scores vs. time-elapsed**. *The oldest image of each individual is enrolled. Thereafter, all more recent images are searched. Mated score distributions are computed over all searches noted in row 17 of Table 1 binned by number of years between search and initial enrollment.*

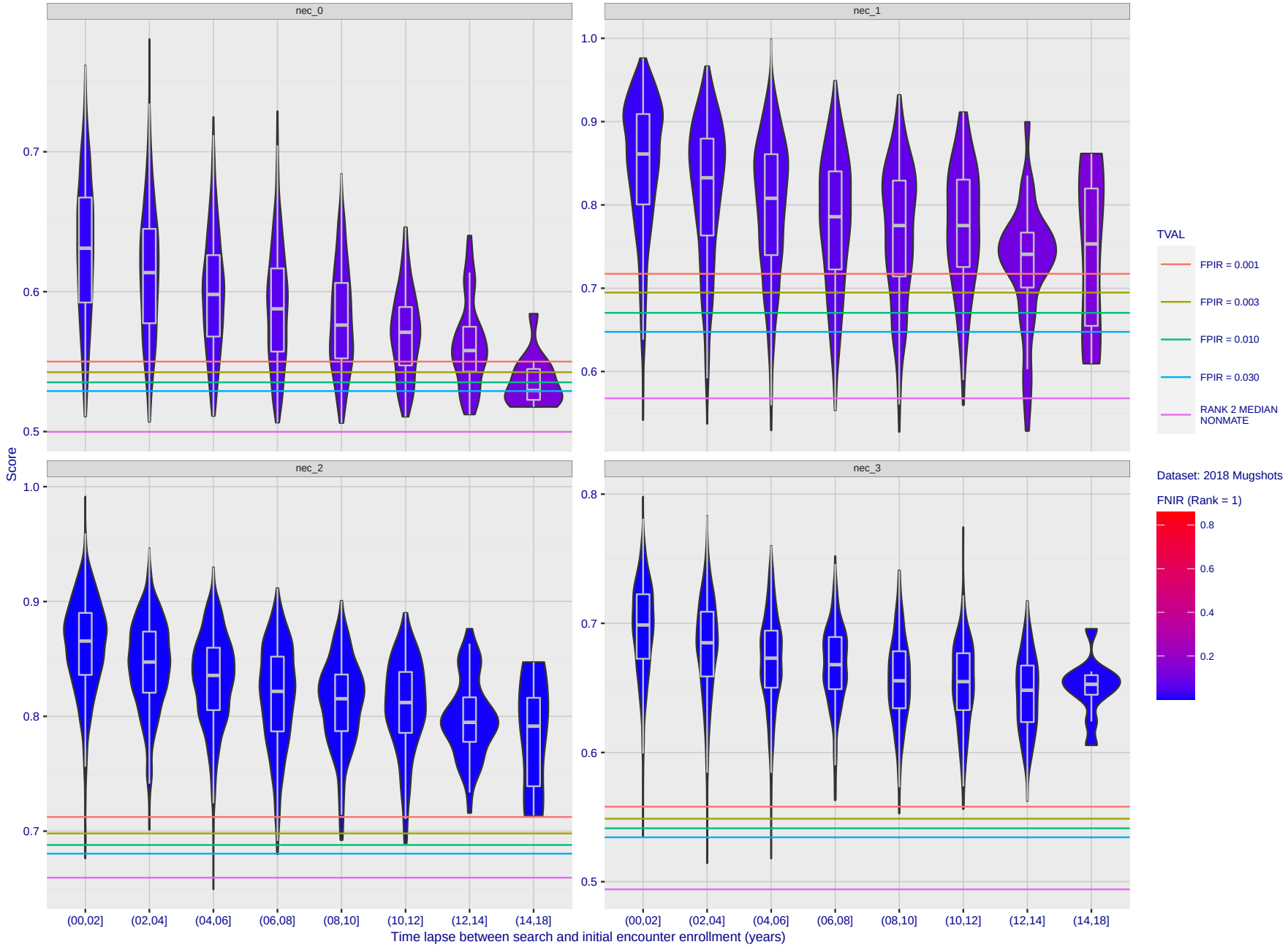

Figure 135: **[FRVT-2018 Mugshot Ageing Dataset] Native mate scores vs. time-elapsed**. *The oldest image of each individual is enrolled. Thereafter, all more recent images are searched. Mated score distributions are computed over all searches noted in row 17 of Table 1 binned by number of years between search and initial enrollment.*

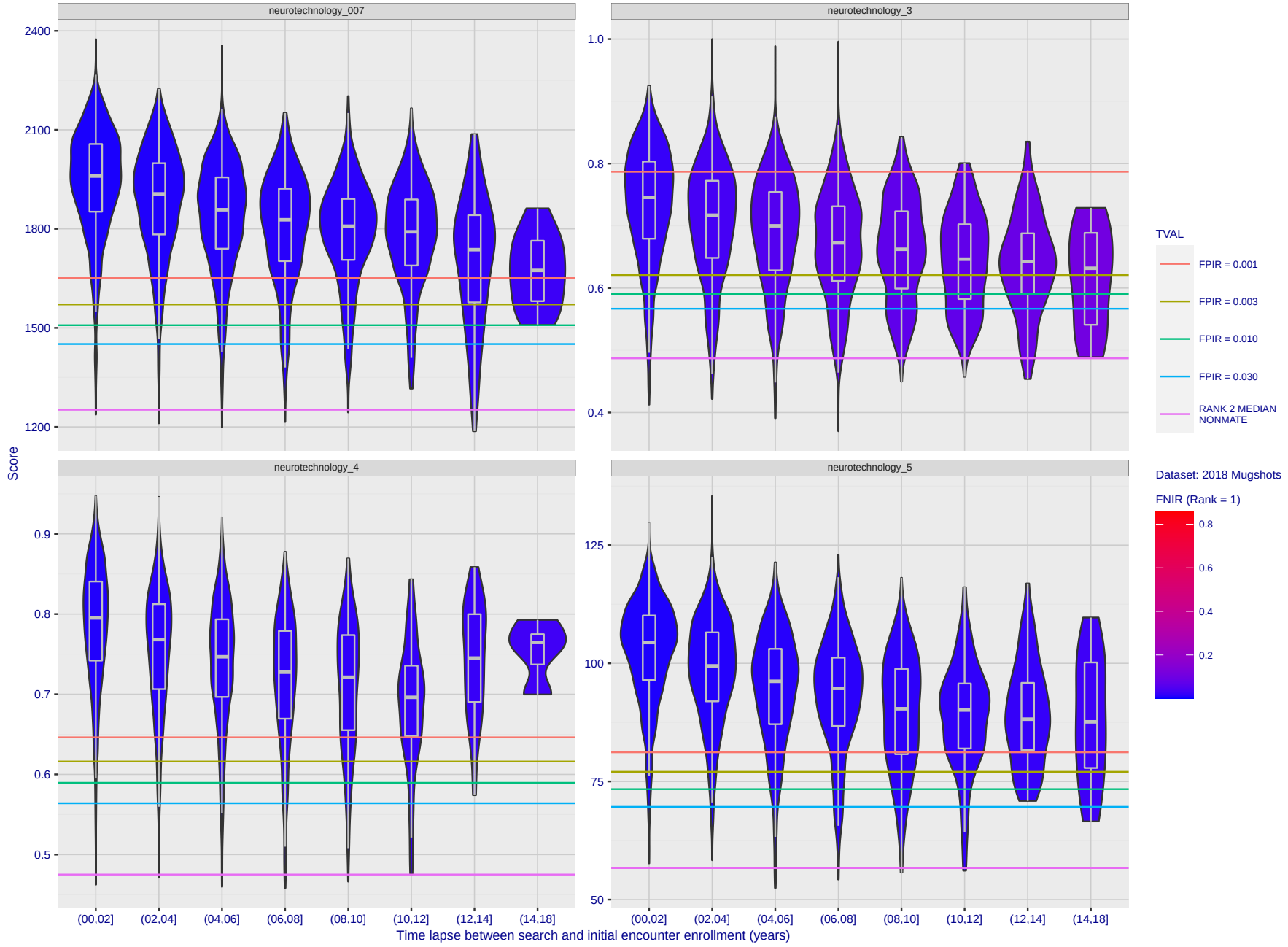

Figure 136: **[FRVT-2018 Mugshot Ageing Dataset] Native mate scores vs. time-elapsed**. *The oldest image of each individual is enrolled. Thereafter, all more recent images are searched. Mated score distributions are computed over all searches noted in row 17 of Table 1 binned by number of years between search and initial enrollment.*

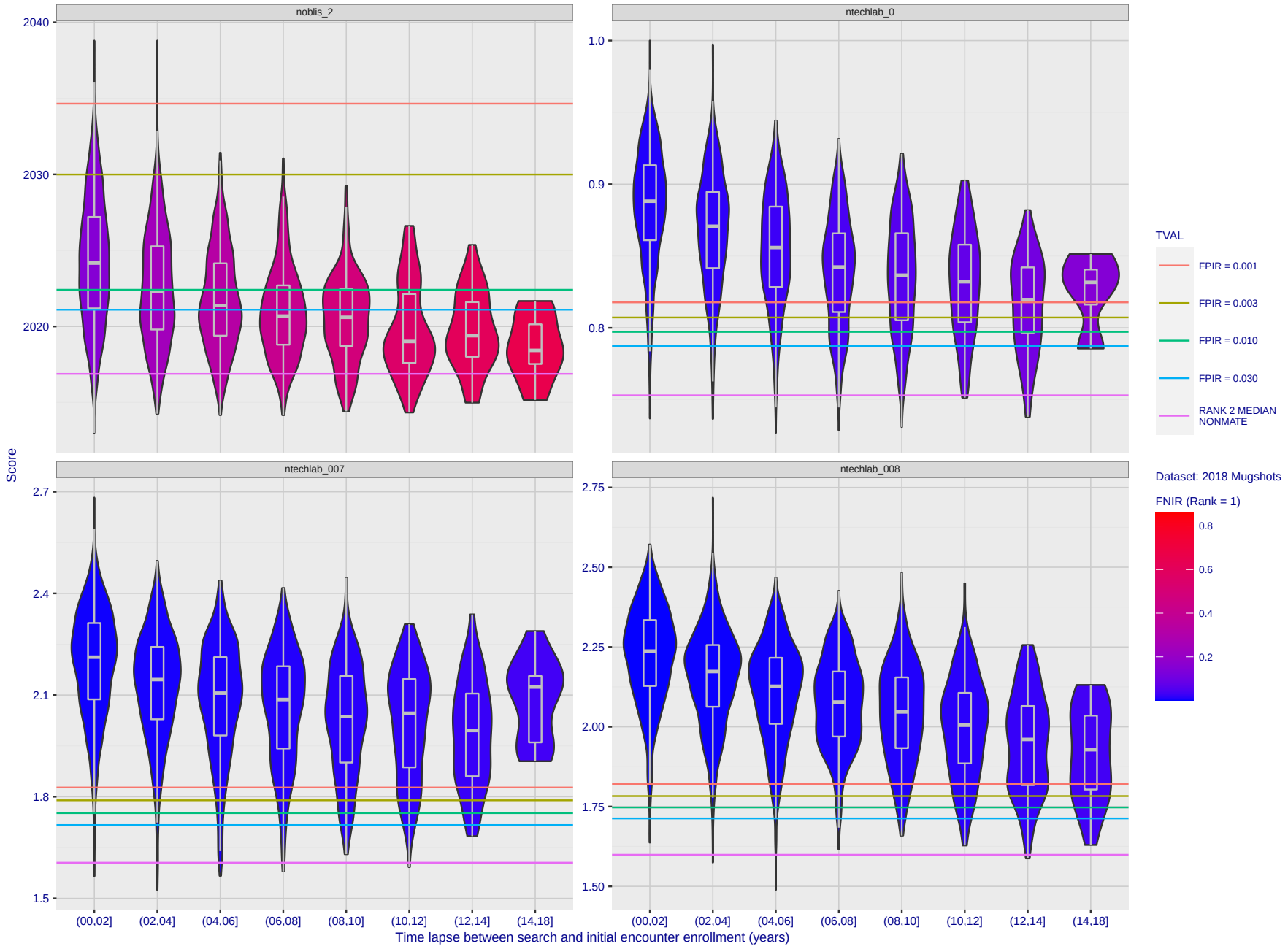

Figure 137: **[FRVT-2018 Mugshot Ageing Dataset] Native mate scores vs. time-elapsed**. *The oldest image of each individual is enrolled. Thereafter, all more recent images are searched. Mated score distributions are computed over all searches noted in row 17 of Table 1 binned by number of years between search and initial enrollment.*

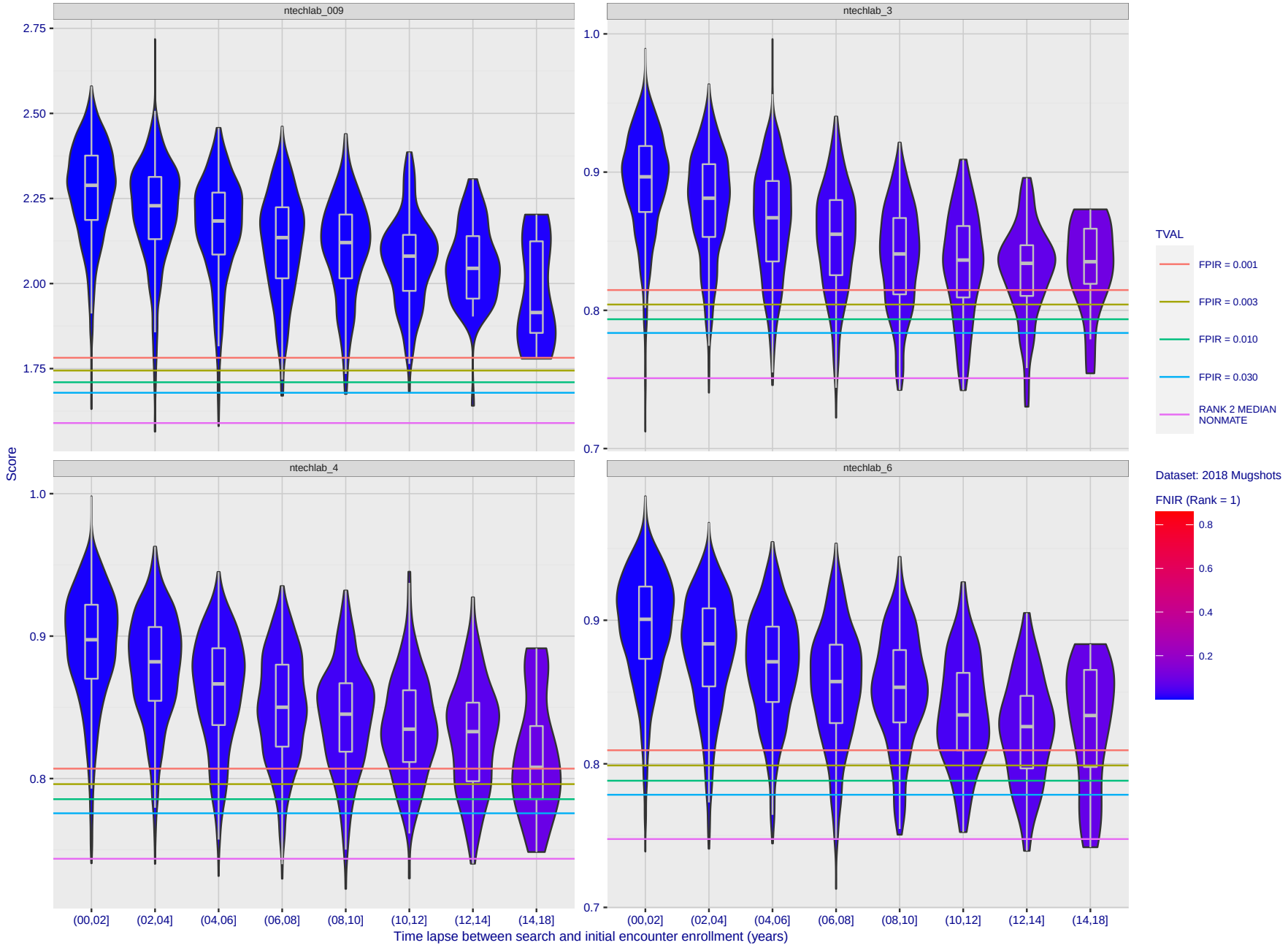

Figure 138: **[FRVT-2018 Mugshot Ageing Dataset] Native mate scores vs. time-elapsed**. *The oldest image of each individual is enrolled. Thereafter, all more recent images are searched. Mated score distributions are computed over all searches noted in row 17 of Table 1 binned by number of years between search and initial enrollment.*

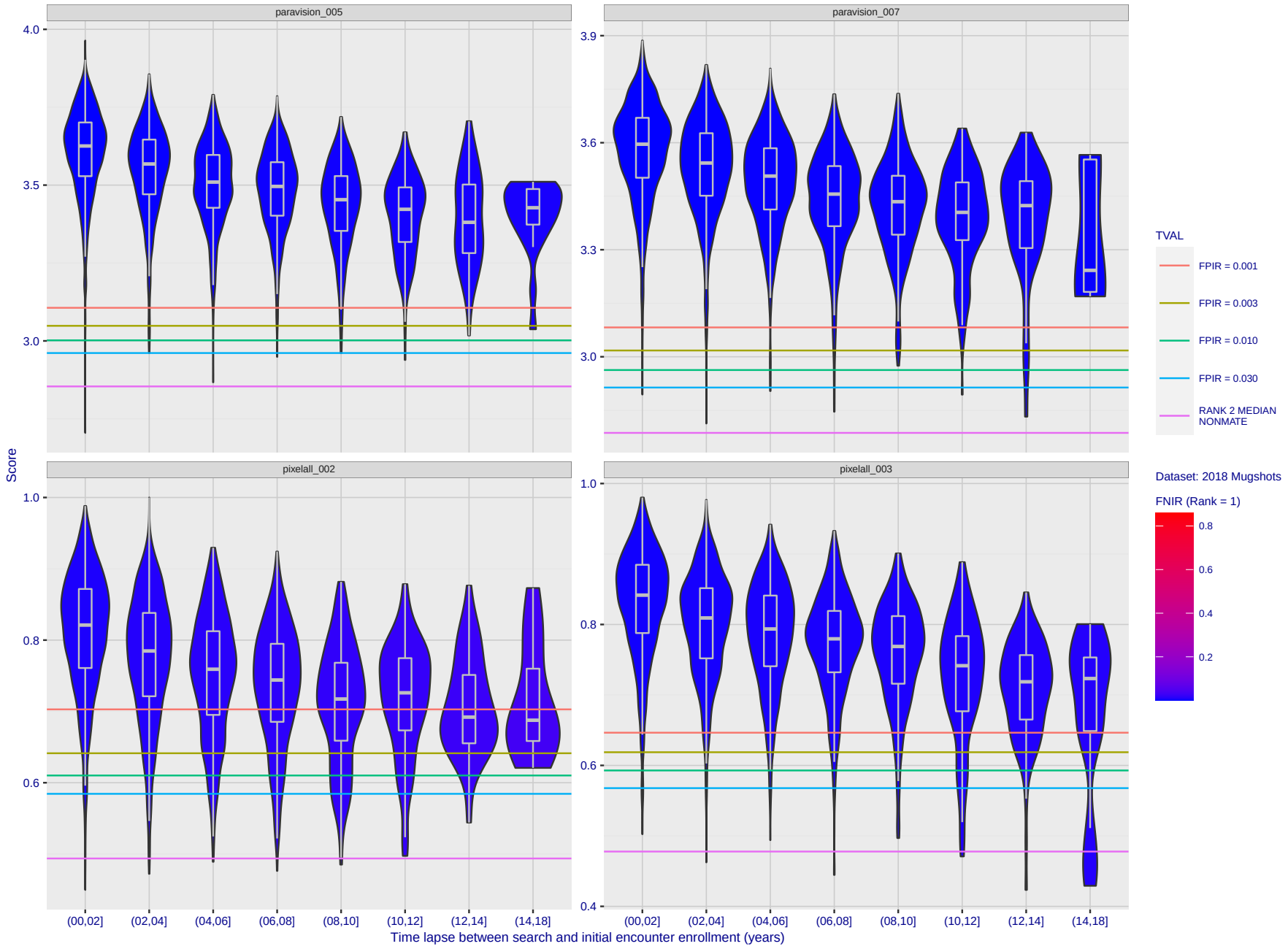

Figure 139: **[FRVT-2018 Mugshot Ageing Dataset] Native mate scores vs. time-elapsed**. *The oldest image of each individual is enrolled. Thereafter, all more recent images are searched. Mated score distributions are computed over all searches noted in row 17 of Table 1 binned by number of years between search and initial enrollment.*

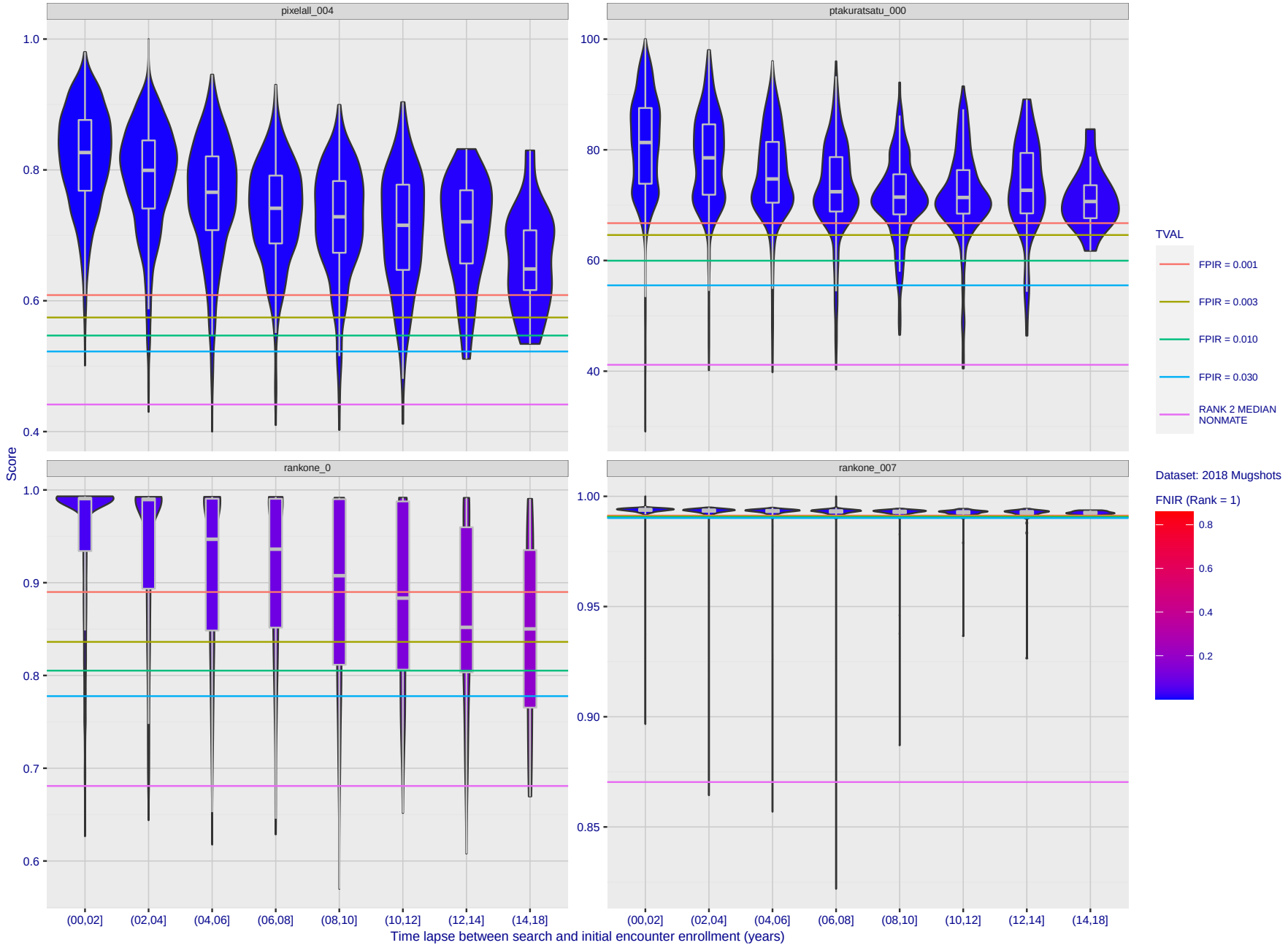

Figure 140: **[FRVT-2018 Mugshot Ageing Dataset] Native mate scores vs. time-elapsed**. *The oldest image of each individual is enrolled. Thereafter, all more recent images are searched. Mated score distributions are computed over all searches noted in row 17 of Table 1 binned by number of years between search and initial enrollment.*

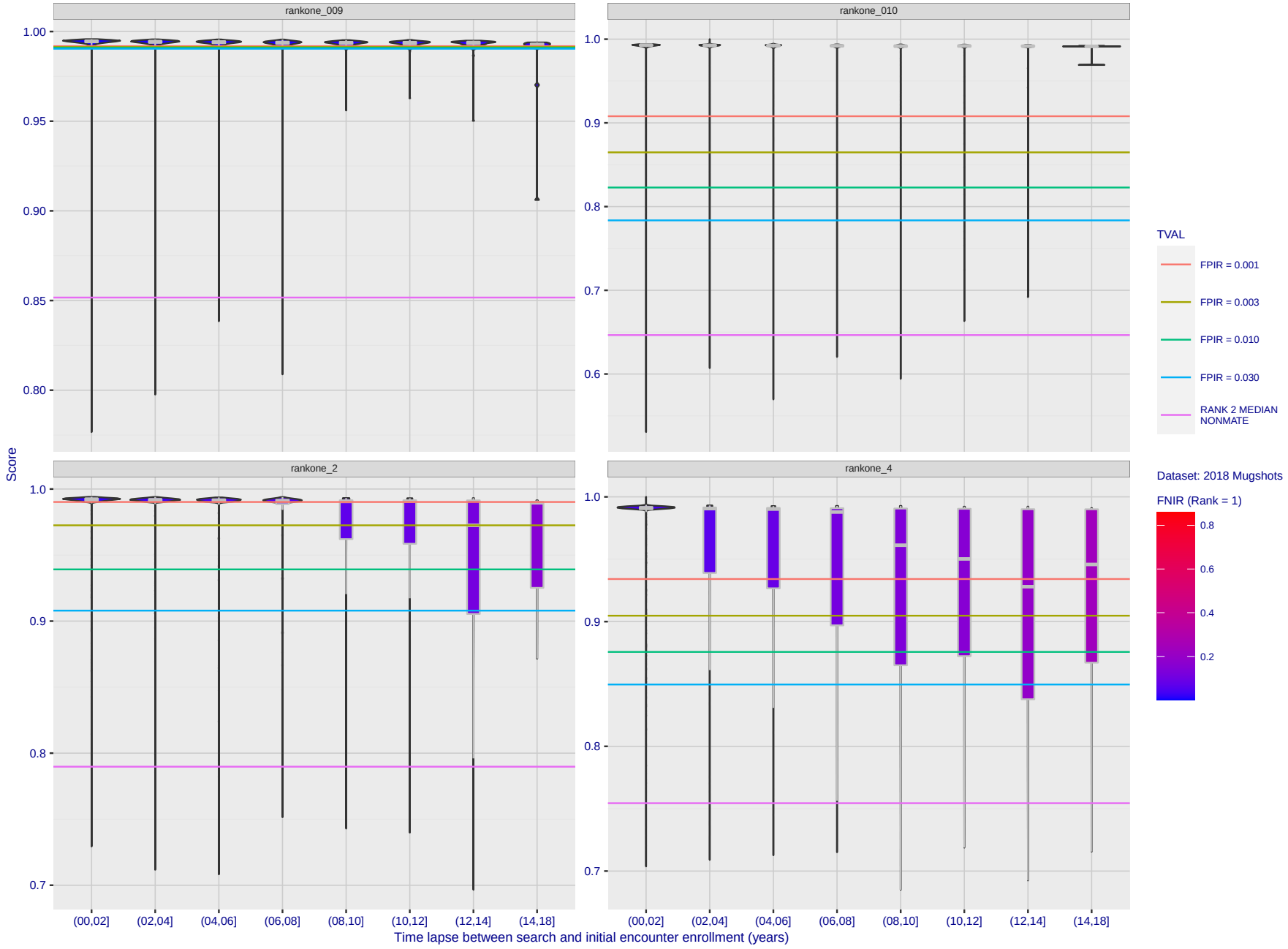

Figure 141: **[FRVT-2018 Mugshot Ageing Dataset] Native mate scores vs. time-elapsed**. *The oldest image of each individual is enrolled. Thereafter, all more recent images are searched. Mated score distributions are computed over all searches noted in row 17 of Table 1 binned by number of years between search and initial enrollment.*

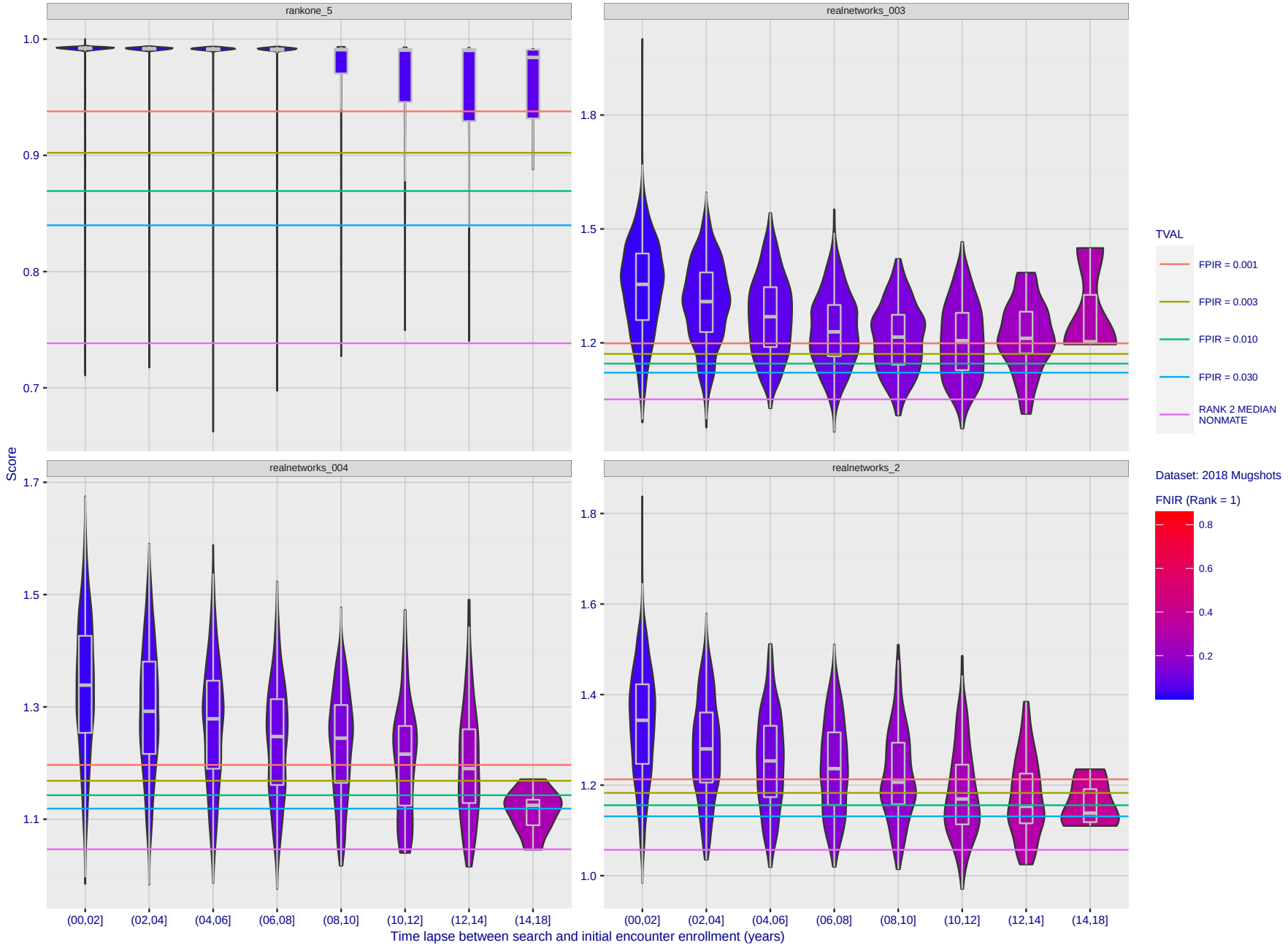

Figure 142: **[FRVT-2018 Mugshot Ageing Dataset] Native mate scores vs. time-elapsed**. *The oldest image of each individual is enrolled. Thereafter, all more recent images are searched. Mated score distributions are computed over all searches noted in row 17 of Table 1 binned by number of years between search and initial enrollment.*

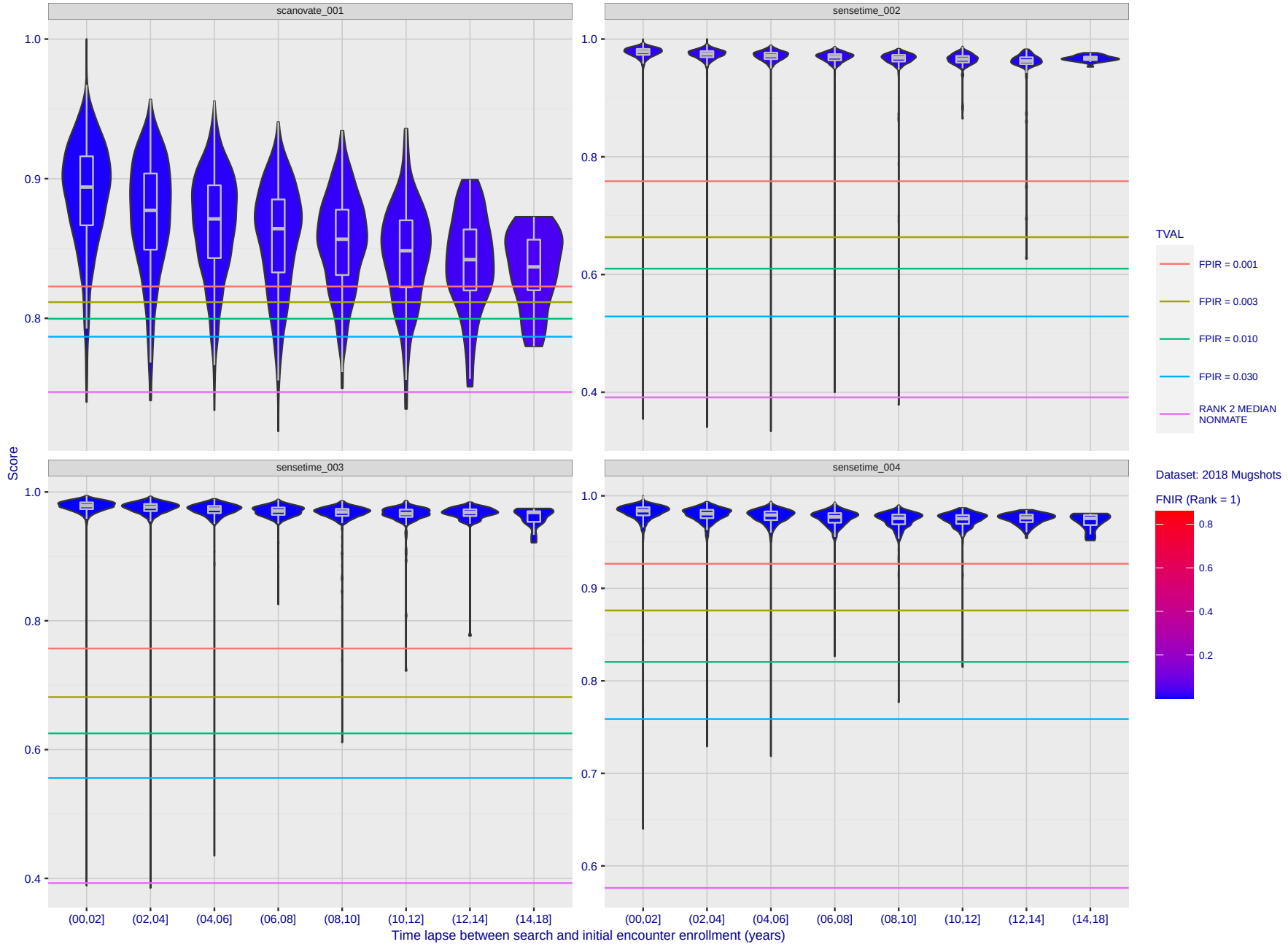

Figure 143: **[FRVT-2018 Mugshot Ageing Dataset] Native mate scores vs. time-elapsed**. *The oldest image of each individual is enrolled. Thereafter, all more recent images are searched. Mated score distributions are computed over all searches noted in row 17 of Table 1 binned by number of years between search and initial enrollment.*

2021/08/05 02:00:58

FNIR(N, R, T) = False neg. identification rate
FPIR(N, T) = False pos. identification rate

N = Num. enrolled subjects
R = Num. candidates examined

T = Threshold

T = 0 → Investigation
T > 0 → Identification

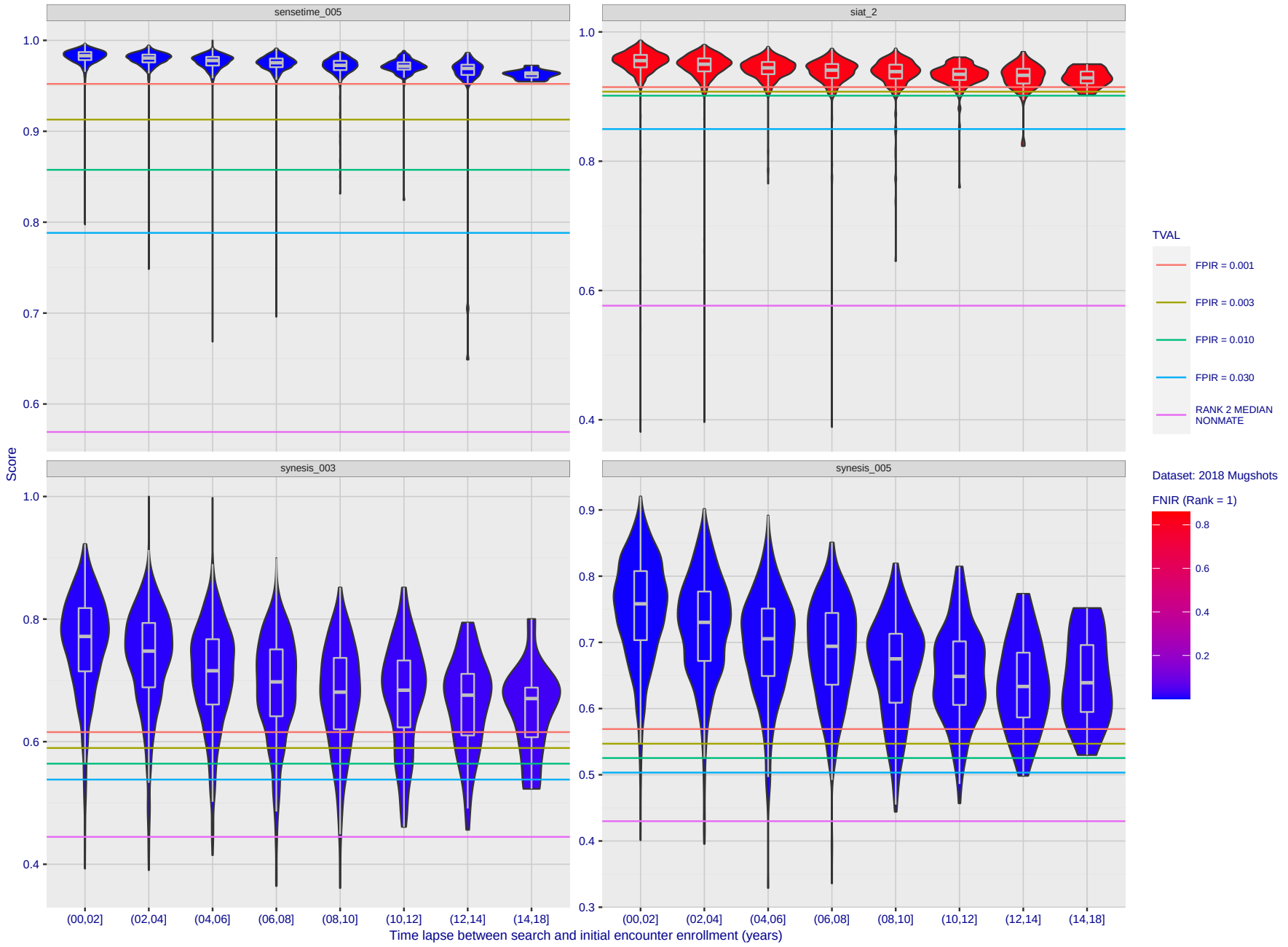

Figure 144: **[FRVT-2018 Mugshot Ageing Dataset] Native mate scores vs. time-elapsed**. *The oldest image of each individual is enrolled. Thereafter, all more recent images are searched. Mated score distributions are computed over all searches noted in row 17 of Table 1 binned by number of years between search and initial enrollment.*

2021/08/05 02:00:58

FNIR(N, R, T) = False neg. identification rate
FPIR(N, T) = False pos. identification rate

N = Num. enrolled subjects
R = Num. candidates examined

T = Threshold

T = 0 → Investigation
T > 0 → Identification

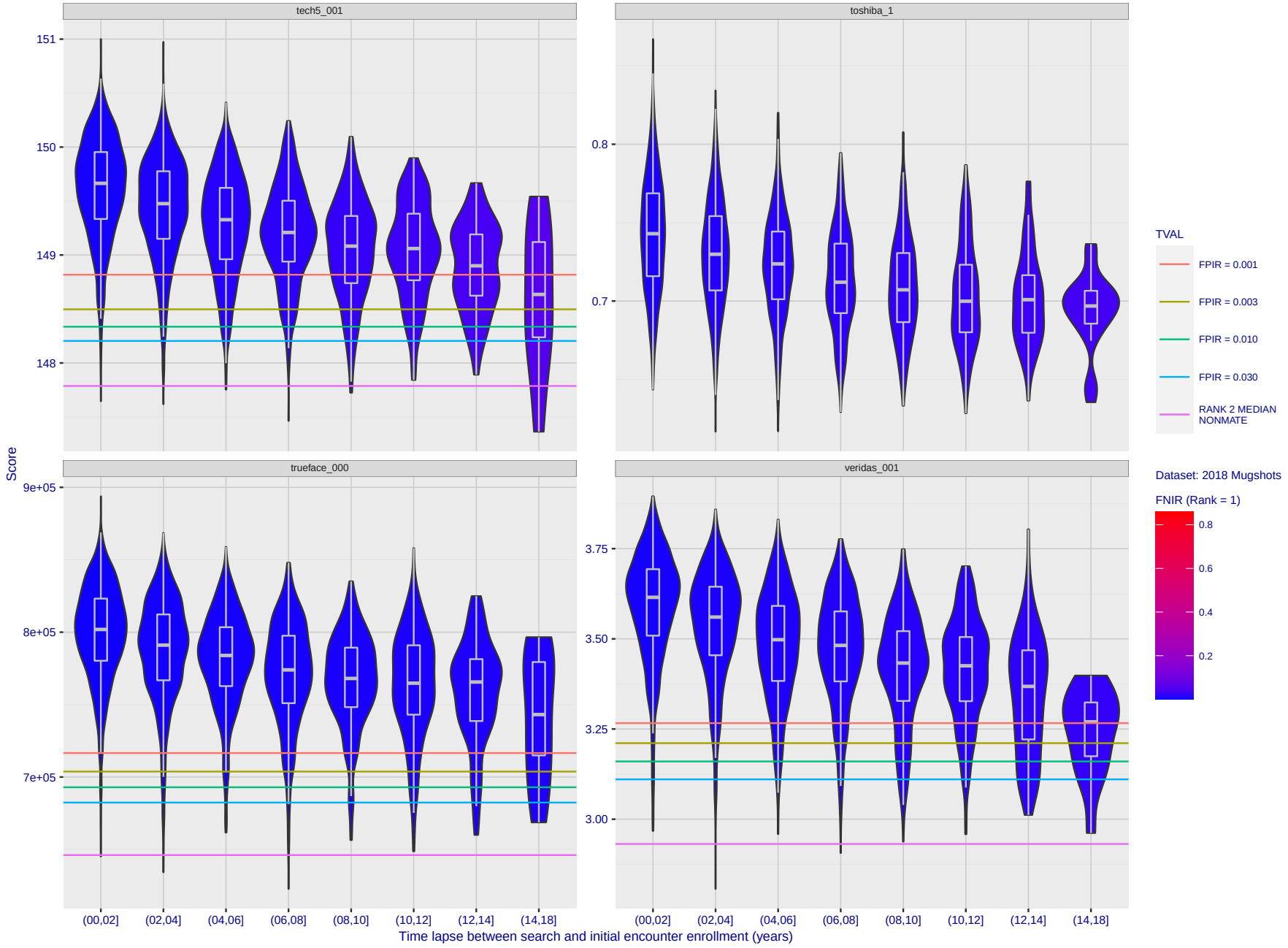

Figure 145: **[FRVT-2018 Mugshot Ageing Dataset] Native mate scores vs. time-elapsed**. *The oldest image of each individual is enrolled. Thereafter, all more recent images are searched. Mated score distributions are computed over all searches noted in row 17 of Table 1 binned by number of years between search and initial enrollment.*

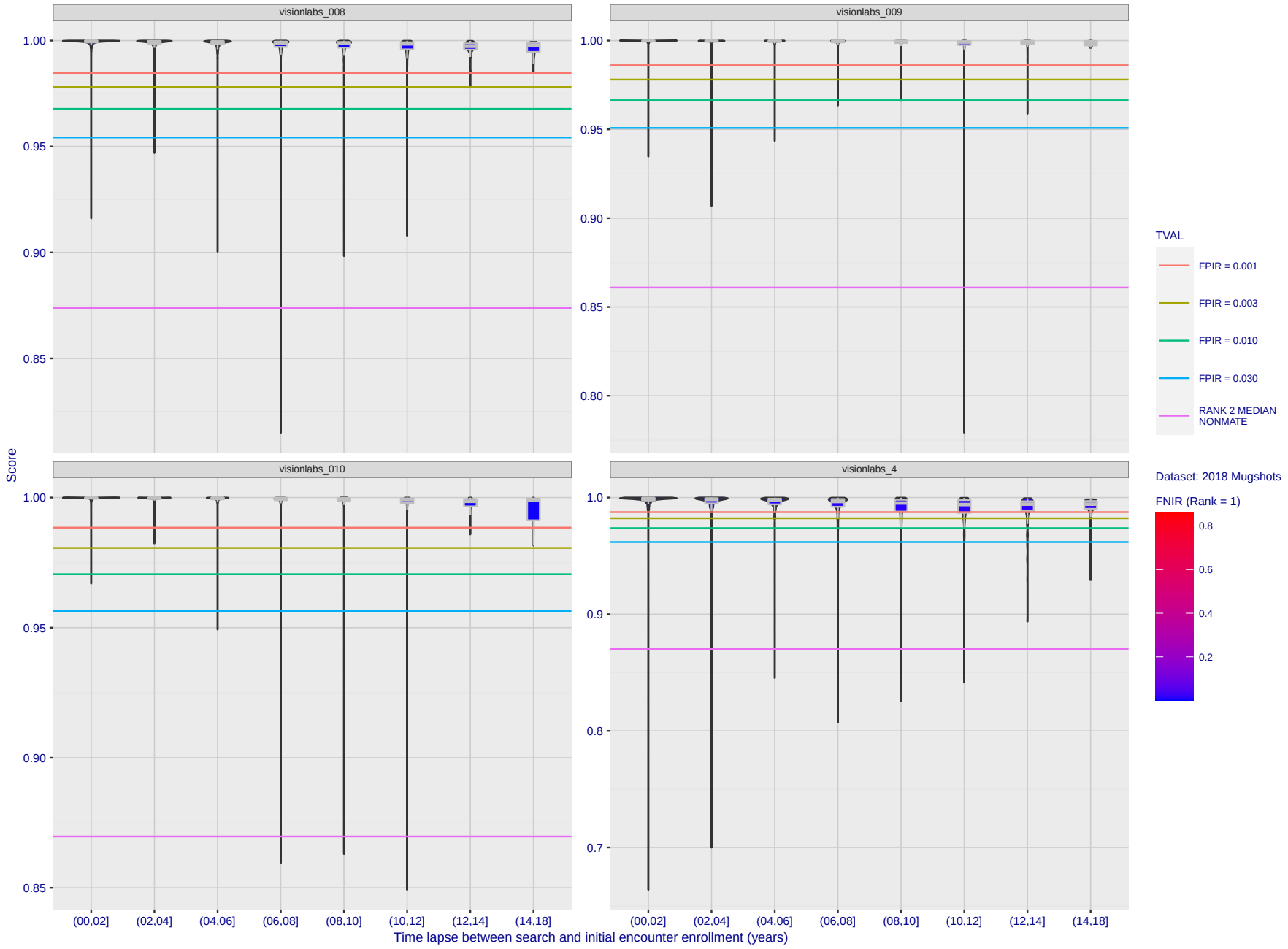

Figure 146: **[FRVT-2018 Mugshot Ageing Dataset] Native mate scores vs. time-elapsed**. *The oldest image of each individual is enrolled. Thereafter, all more recent images are searched. Mated score distributions are computed over all searches noted in row 17 of Table 1 binned by number of years between search and initial enrollment.*

2021/08/05 02:00:58

FNIR(N, R, T) = False neg. identification rate
FPIR(N, T) = False pos. identification rate

N = Num. enrolled subjects
R = Num. candidates examined

T = Threshold

T = 0 → Investigation
T > 0 → Identification

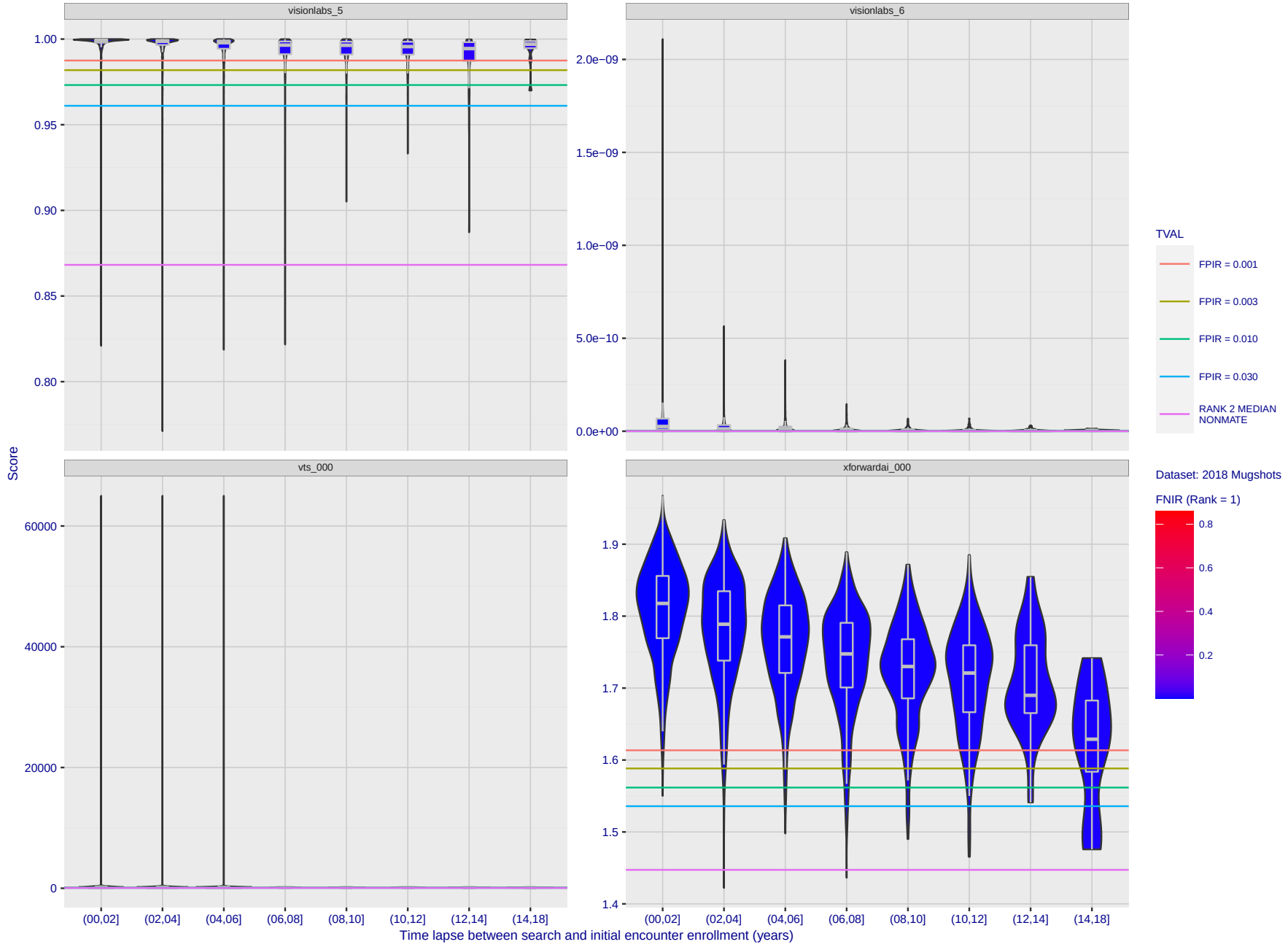

Figure 147: **[FRVT-2018 Mugshot Ageing Dataset] Native mate scores vs. time-elapsed**. *The oldest image of each individual is enrolled. Thereafter, all more recent images are searched. Mated score distributions are computed over all searches noted in row 17 of Table 1 binned by number of years between search and initial enrollment.*

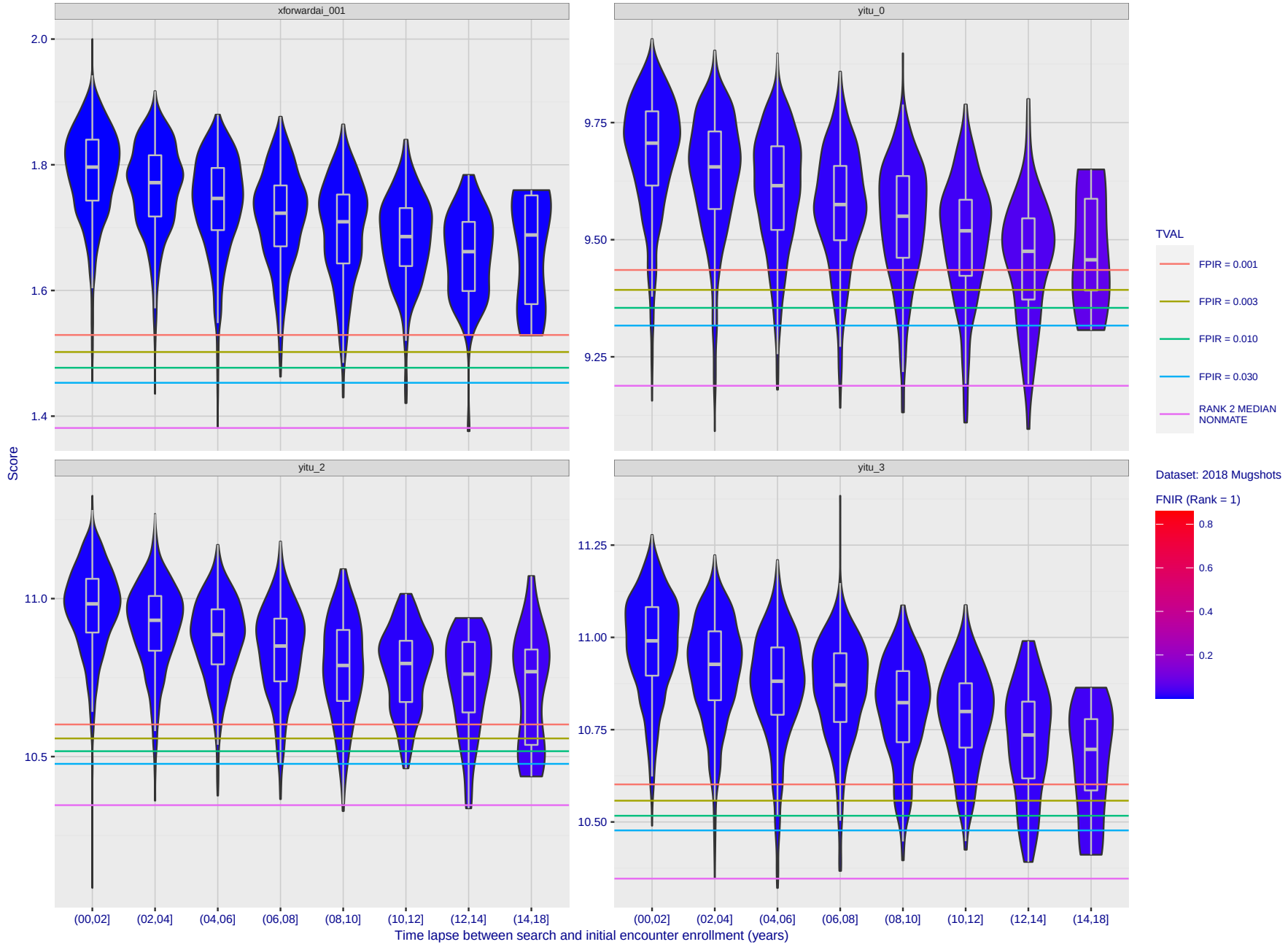

Figure 148: **[FRVT-2018 Mugshot Ageing Dataset] Native mate scores vs. time-elapsed**. *The oldest image of each individual is enrolled. Thereafter, all more recent images are searched. Mated score distributions are computed over all searches noted in row 17 of Table 1 binned by number of years between search and initial enrollment.*

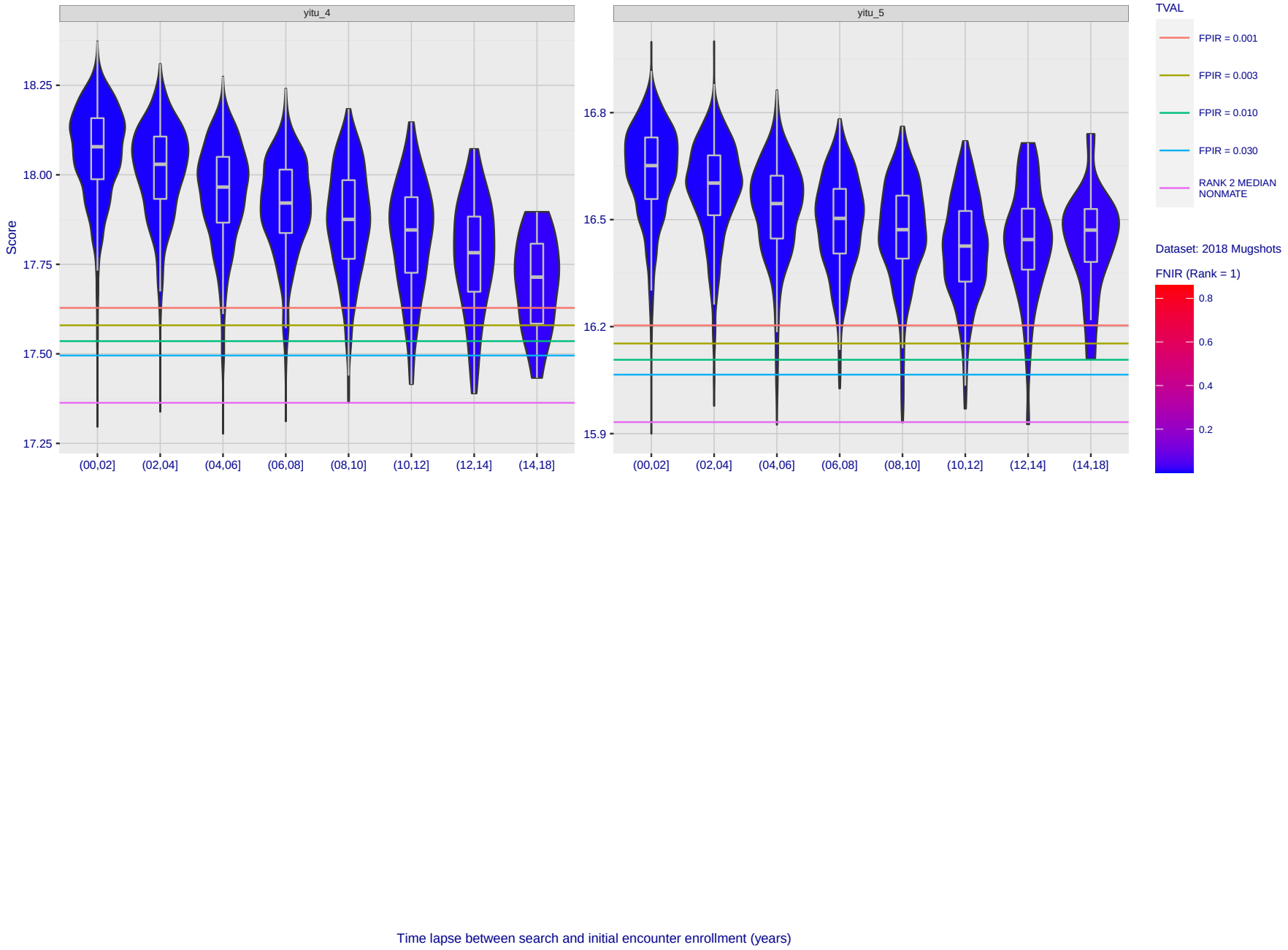

Figure 149: **[FRVT-2018 Mugshot Ageing Dataset] Native mate scores vs. time-elapsed**. *The oldest image of each individual is enrolled. Thereafter, all more recent images are searched. Mated score distributions are computed over all searches noted in row 17 of Table 1 binned by number of years between search and initial enrollment.*

Appendix C Effect of enrolling multiple images

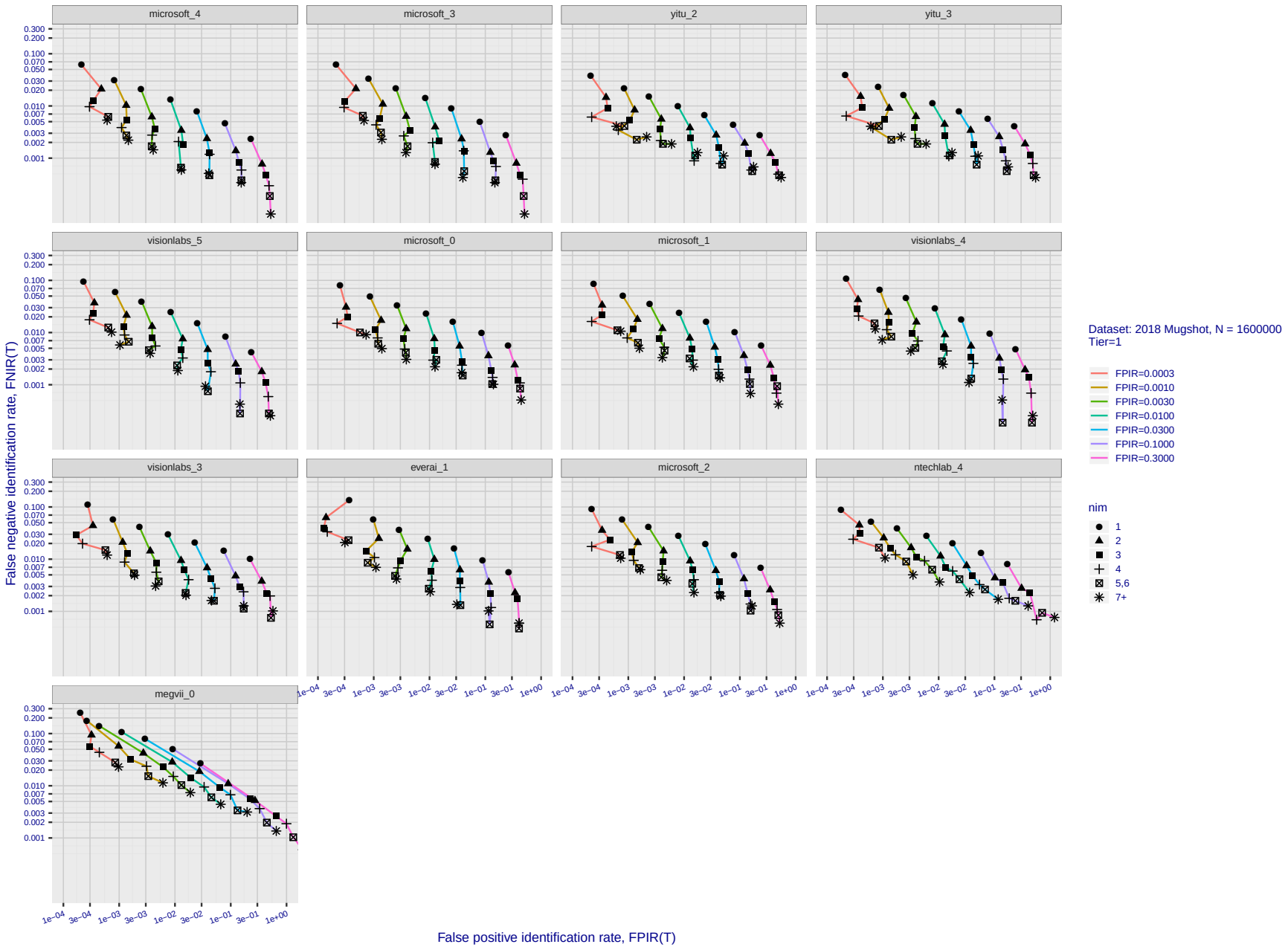

Figure 150: **[FRVT-2018 Mugshot Dataset] Effect of enrolling multiple images for each identity**. *The plot shows an identification miss rates vs. false positive rates, at seven operating thresholds. The enrolled population size is fixed. The images are enrolled with lifetime-consolidation - see section 2.3.*

2021/08/05 02:00:58

FNIR(N, R, T) = False neg. identification rate
FPIR(N, T) = False pos. identification rate

N = Num. enrolled subjects
R = Num. candidates examined

T = Threshold

T = 0 → Investigation
T > 0 → Identification

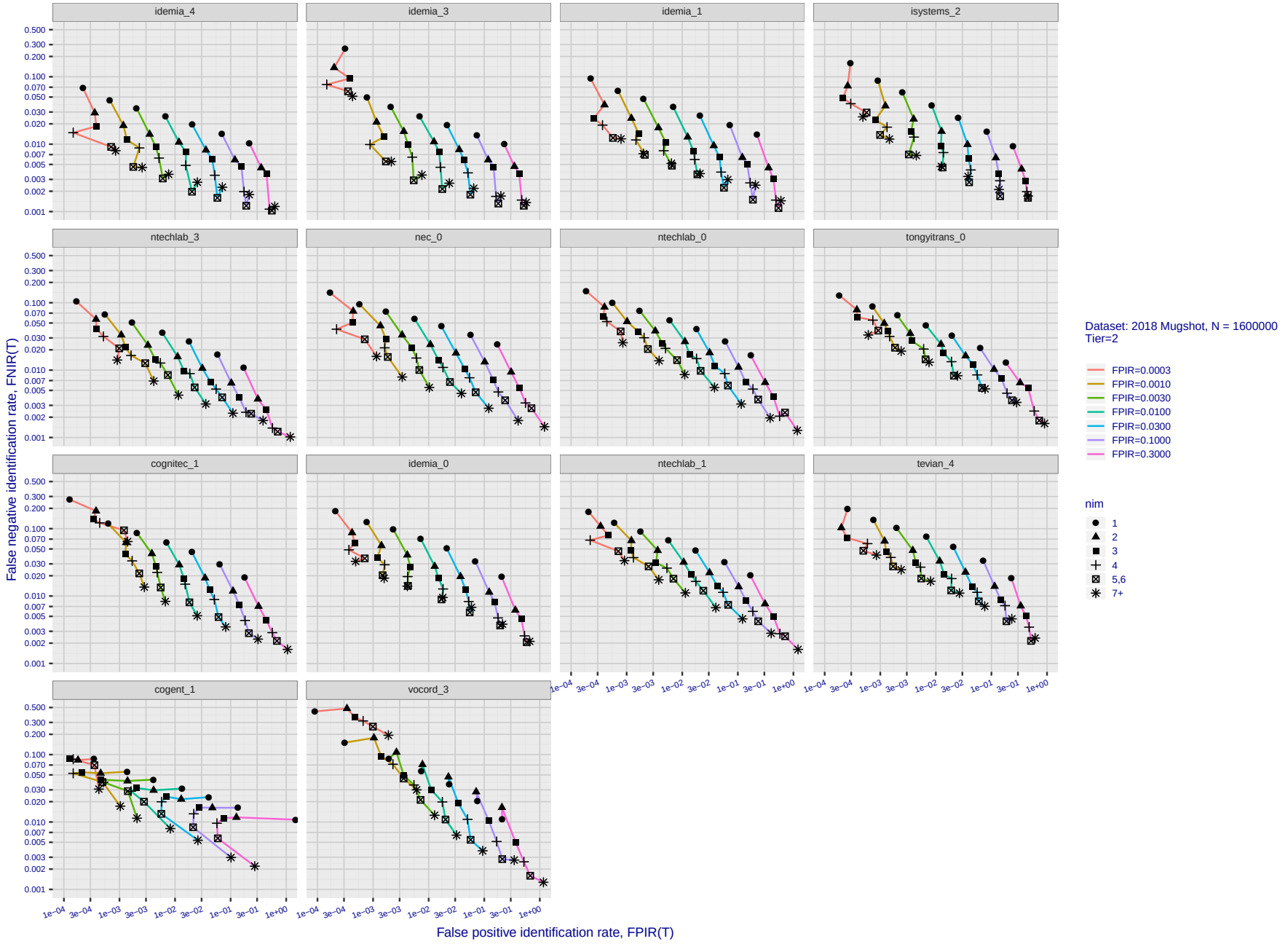

Figure 151: **[FRVT-2018 Mugshot Dataset] Effect of enrolling multiple images for each identity**. *The plot shows an identification miss rates vs. false positive rates, at seven operating thresholds. The enrolled population size is fixed. The images are enrolled with lifetime-consolidation - see section 2.3.*

2021/08/05 02:00:58

FNIR(N, R, T) = False neg. identification rate
FPIR(N, T) = False pos. identification rate

N = Num. enrolled subjects
R = Num. candidates examined

T = Threshold

T = 0 → Investigation
T > 0 → Identification

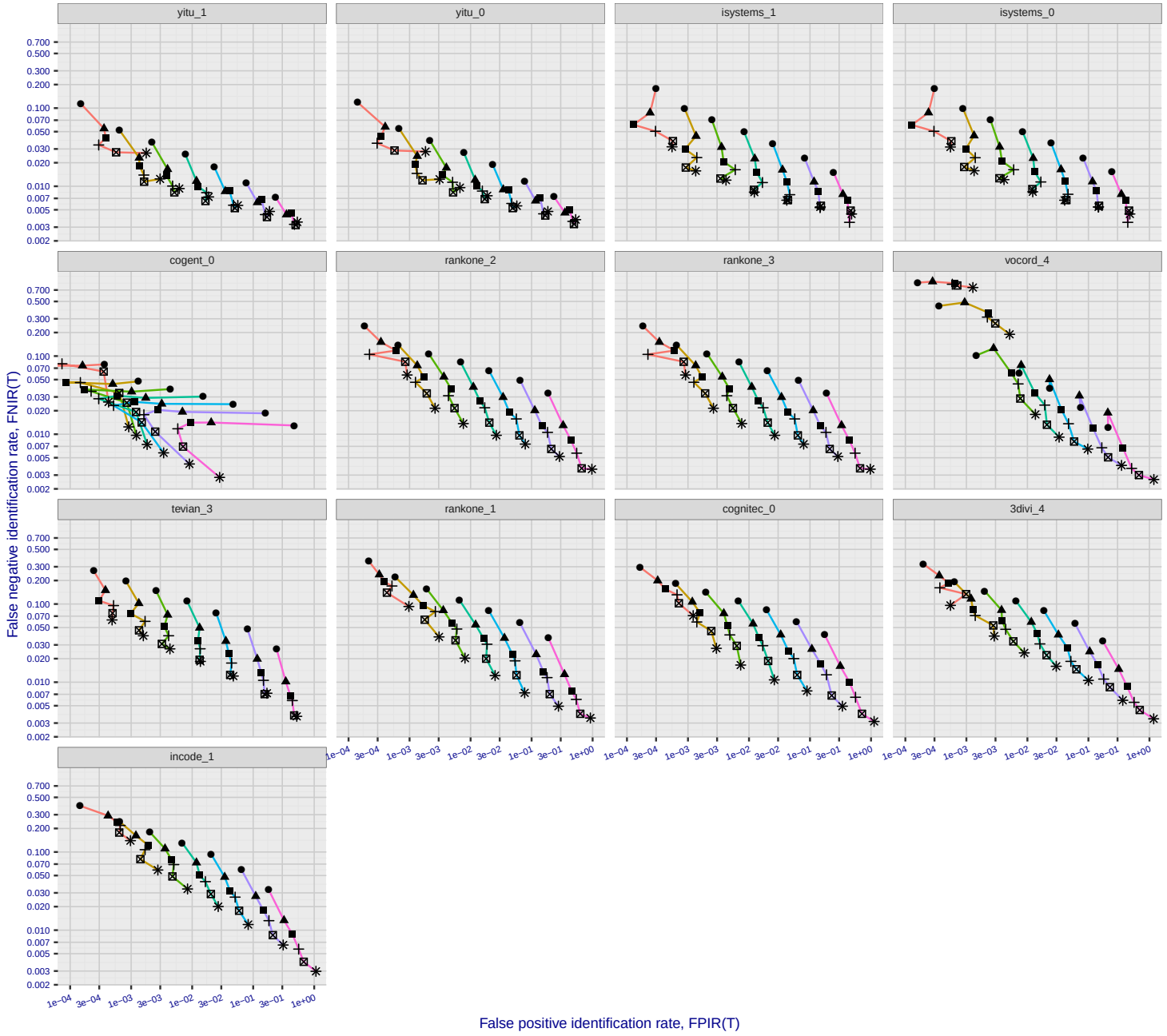

Figure 152: **[FRVT-2018 Mugshot Dataset] Effect of enrolling multiple images for each identity**. *The plot shows an identification miss rates vs. false positive rates, at seven operating thresholds. The enrolled population size is fixed. The images are enrolled with lifetime-consolidation - see section 2.3.*

2021/08/05 02:00:58
FNIR(N, R, T) = False neg. identification rate
FPIR(N, T) = False pos. identification rate
N = Num. enrolled subjects
R = Num. candidates examined
T = Threshold
T = 0 → Investigation
T > 0 → Identification

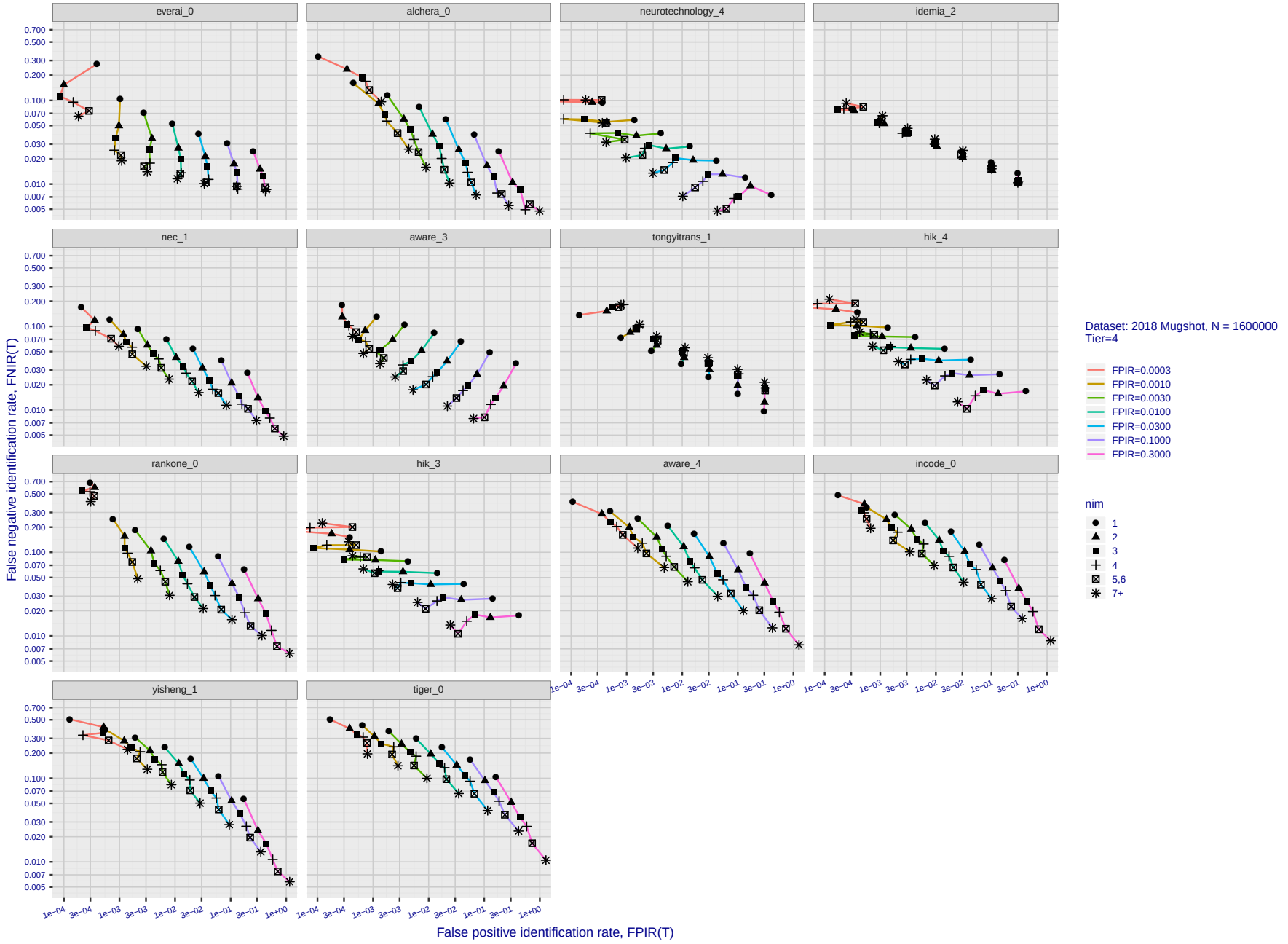

Figure 153: **[FRVT-2018 Mugshot Dataset] Effect of enrolling multiple images for each identity**. *The plot shows an identification miss rates vs. false positive rates, at seven operating thresholds. The enrolled population size is fixed. The images are enrolled with lifetime-consolidation - see section 2.3.*

2021/08/05 02:00:58

FNIR(N, R, T) = False neg. identification rate
FPIR(N, T) = False pos. identification rate

N = Num. enrolled subjects
R = Num. candidates examined

T = Threshold

T = 0 → Investigation
T > 0 → Identification

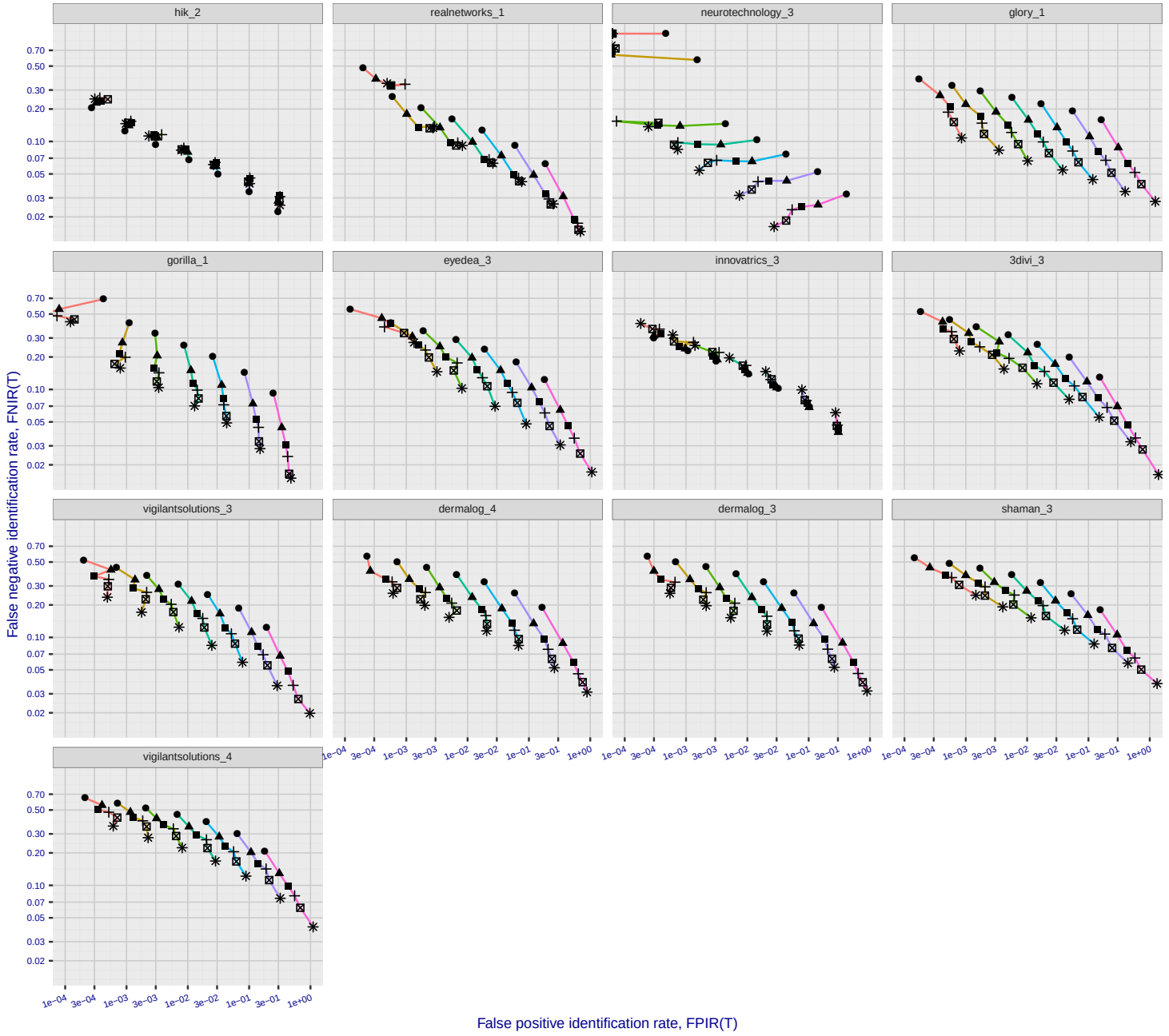

Figure 154: **[FRVT-2018 Mugshot Dataset] Effect of enrolling multiple images for each identity**. *The plot shows an identification miss rates vs. false positive rates, at seven operating thresholds. The enrolled population size is fixed. The images are enrolled with lifetime-consolidation - see section 2.3.*

2021/08/05 02:00:58

FNIR(N, R, T) = False neg. identification rate
FPIR(N, T) = False pos. identification rate
N = Num. enrolled subjects
R = Num. candidates examined
T = Threshold
T = 0 → Investigation
T > 0 → Identification

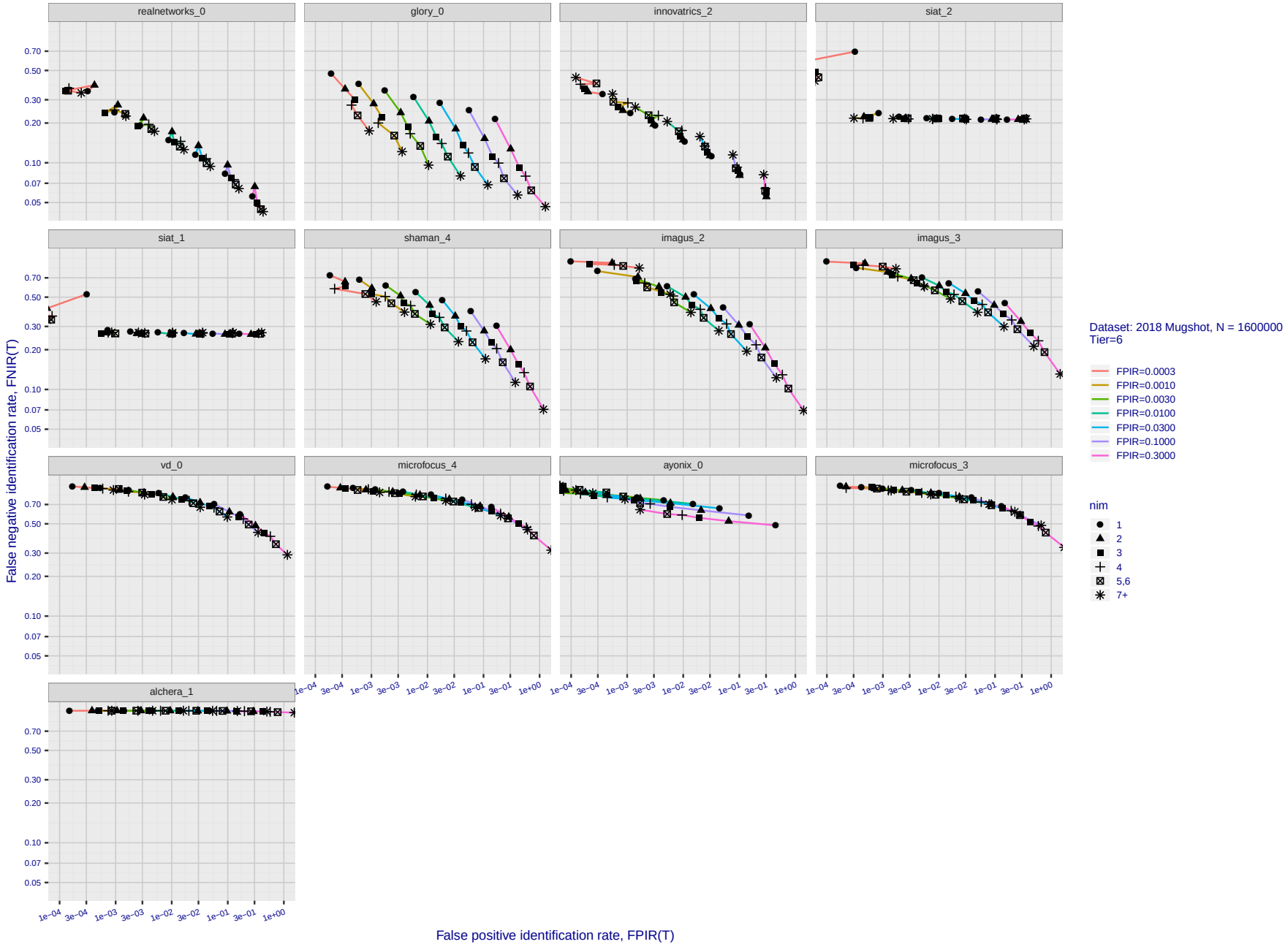

Figure 155: **[FRVT-2018 Mugshot Dataset] Effect of enrolling multiple images for each identity**. *The plot shows an identification miss rates vs. false positive rates, at seven operating thresholds. The enrolled population size is fixed. The images are enrolled with lifetime-consolidation - see section 2.3.*

2021/08/05 02:00:58

FNIR(N, R, T) = False neg. identification rate
FPIR(N, T) = False pos. identification rate
N = Num. enrolled subjects
R = Num. candidates examined
T = Threshold
T = 0 → Investigation
T > 0 → Identification

Appendix D Accuracy with poor quality webcam images

2021/08/05	FNIR(N, R, T) =	False neg. identification rate	N = Num. enrolled subjects	T = Threshold	$T = 0 \rightarrow$ Investigation
02:00:58	FPIR(N, T) =	False pos. identification rate	R = Num. candidates examined		$T > 0 \rightarrow$ Identification

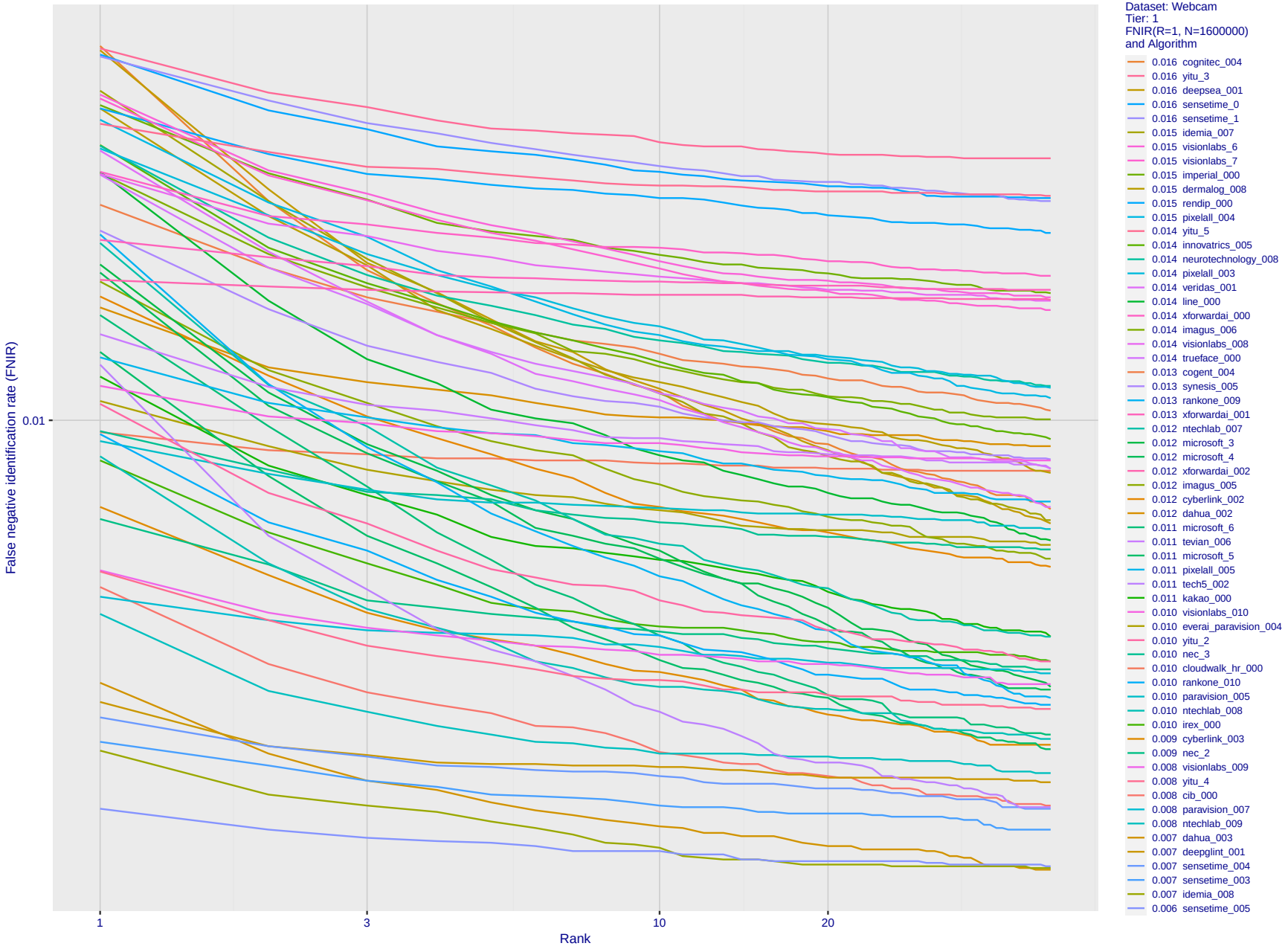

Figure 156: **[Webcam Dataset] Identification miss rates vs. rank**. *The results apply to cross-domain recognition in which webcams are searched against enrolled mugshots. The FNIR values are higher than those for mugshot-mugshot identification due to low image resolution, lighting and less constrained subject pose in webcam images - see Figure 6.*

2021/08/05 02:00:58

FNIR(N, R, T) = False neg. identification rate
FPIR(N, T) = False pos. identification rate

N = Num. enrolled subjects
R = Num. candidates examined

T = Threshold

T = 0 → Investigation
T > 0 → Identification

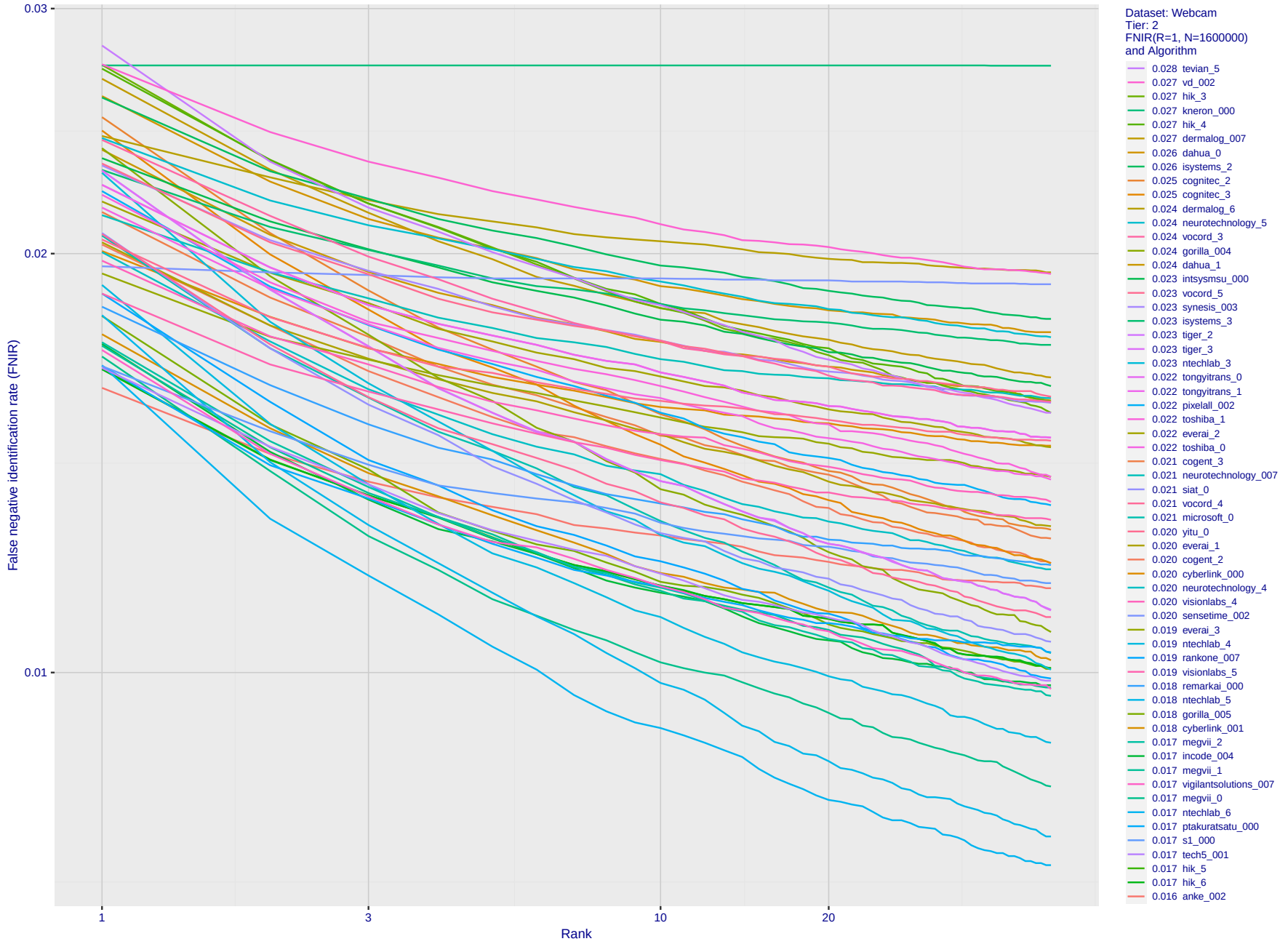

Figure 157: **[Webcam Dataset] Identification miss rates vs. rank**. *The results apply to cross-domain recognition in which webcams are searched against enrolled mugshots. The FNIR values are higher than those for mugshot-mugshot identification due to low image resolution, lighting and less constrained subject pose in webcam images - see Figure 6.*

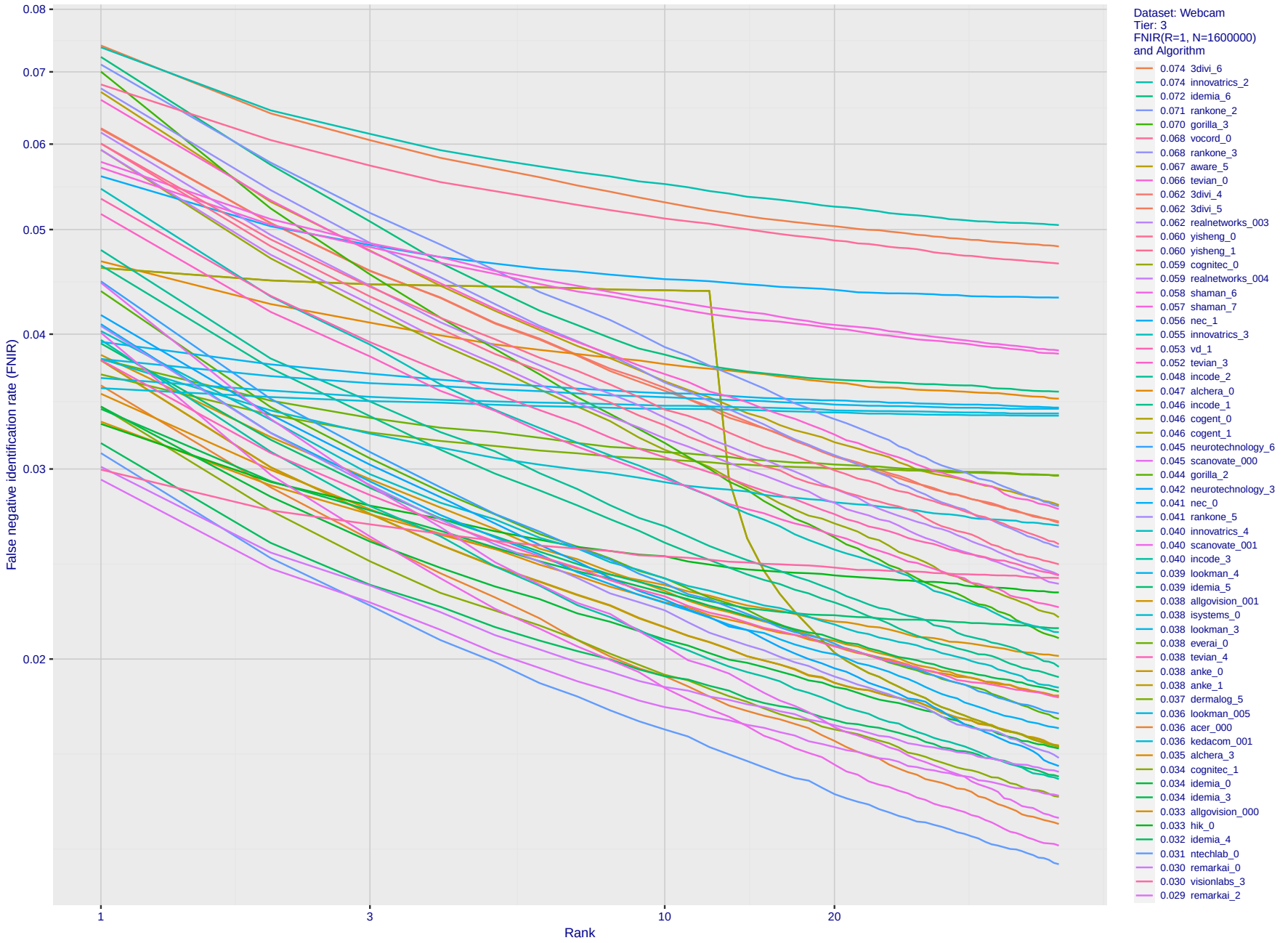

Figure 158: **[Webcam Dataset] Identification miss rates vs. rank**. *The results apply to cross-domain recognition in which webcams are searched against enrolled mugshots. The FNIR values are higher than those for mugshot-mugshot identification due to low image resolution, lighting and less constrained subject pose in webcam images - see Figure 6.*

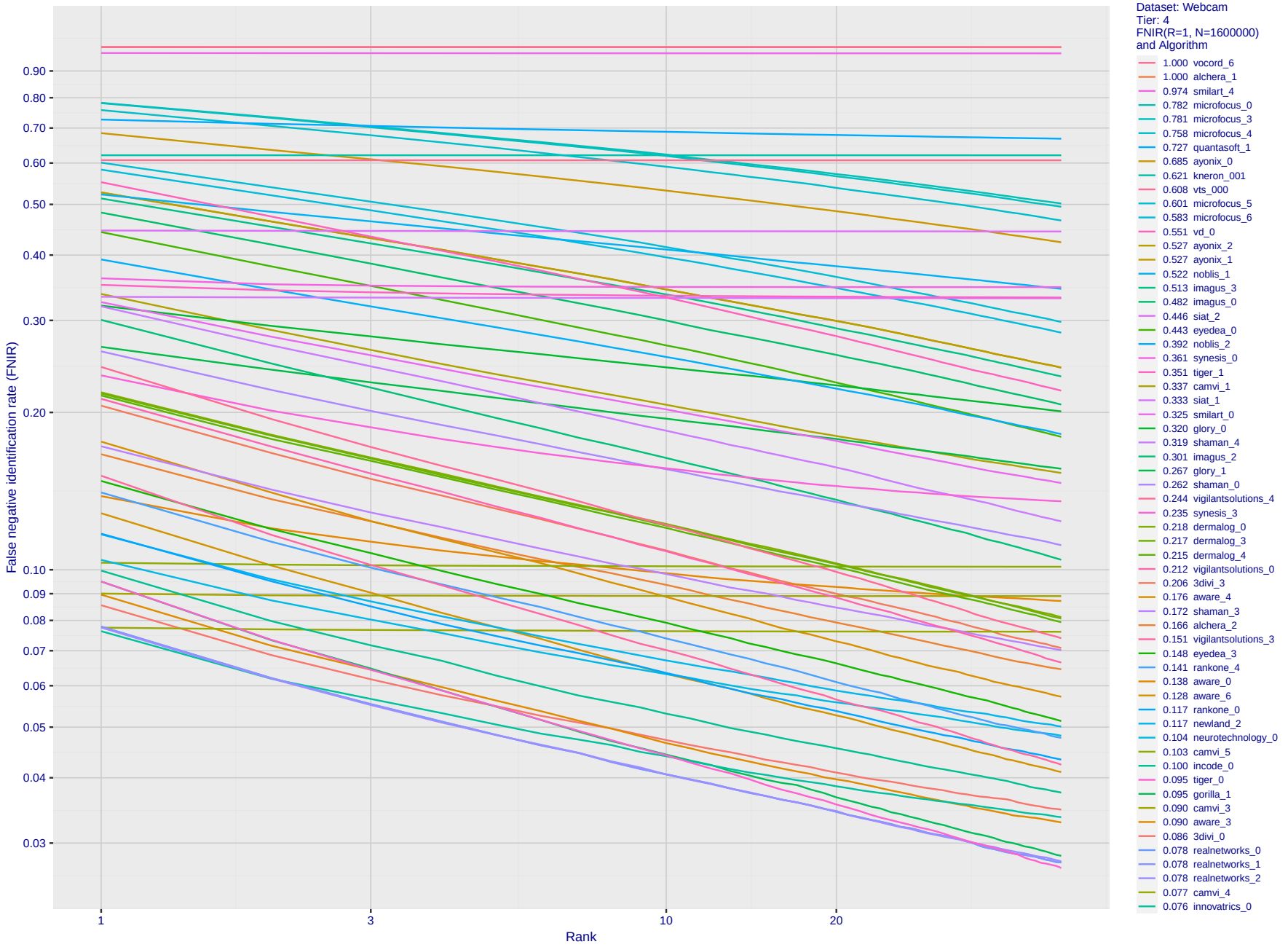

Figure 159: **[Webcam Dataset] Identification miss rates vs. rank**. *The results apply to cross-domain recognition in which webcams are searched against enrolled mugshots. The FNIR values are higher than those for mugshot-mugshot identification due to low image resolution, lighting and less constrained subject pose in webcam images - see Figure 6.*

2021/08/05 02:00:58
FNIR(N, R, T) = False neg. identification rate
FPIR(N, T) = False pos. identification rate
N = Num. enrolled subjects
R = Num. candidates examined
T = Threshold
T = 0 → Investigation
T > 0 → Identification

2021/08/05	FNIR(N, R, T) =	False neg. identification rate	N = Num. enrolled subjects	T = Threshold	$T = 0 \rightarrow$ Investigation
02:00:58	FPIR(N, T) =	False pos. identification rate	R = Num. candidates examined		$T > 0 \rightarrow$ Identification

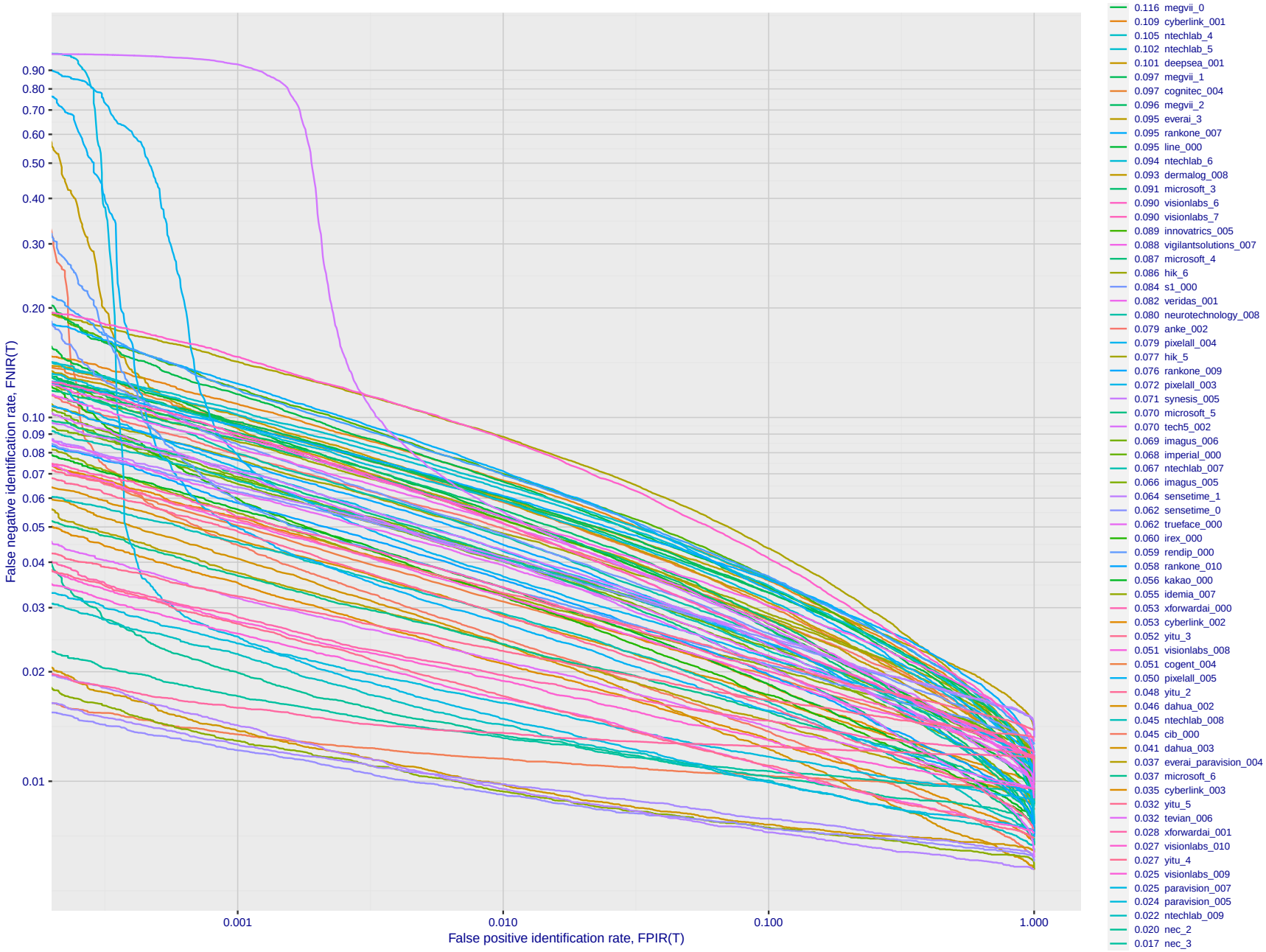

2021/08/05 02:00:58

FNIR(N, R, T) = FPIR(N, T) =

False neg. identification rate
False pos. identification rate

N = Num. enrolled subjects
R = Num. candidates examined

T = Threshold

T = 0 → Investigation
T > 0 → Identification

Figure 160: **[Webcam Dataset] Identification miss rates vs. false positive rates**. *The results apply to cross-domain recognition in which webcams are searched against enrolled mugshots. The FNIR values are higher than those for mugshot-mugshot identification due to low image resolution, lighting and less constrained subject pose in webcam images - see Figure 6.*

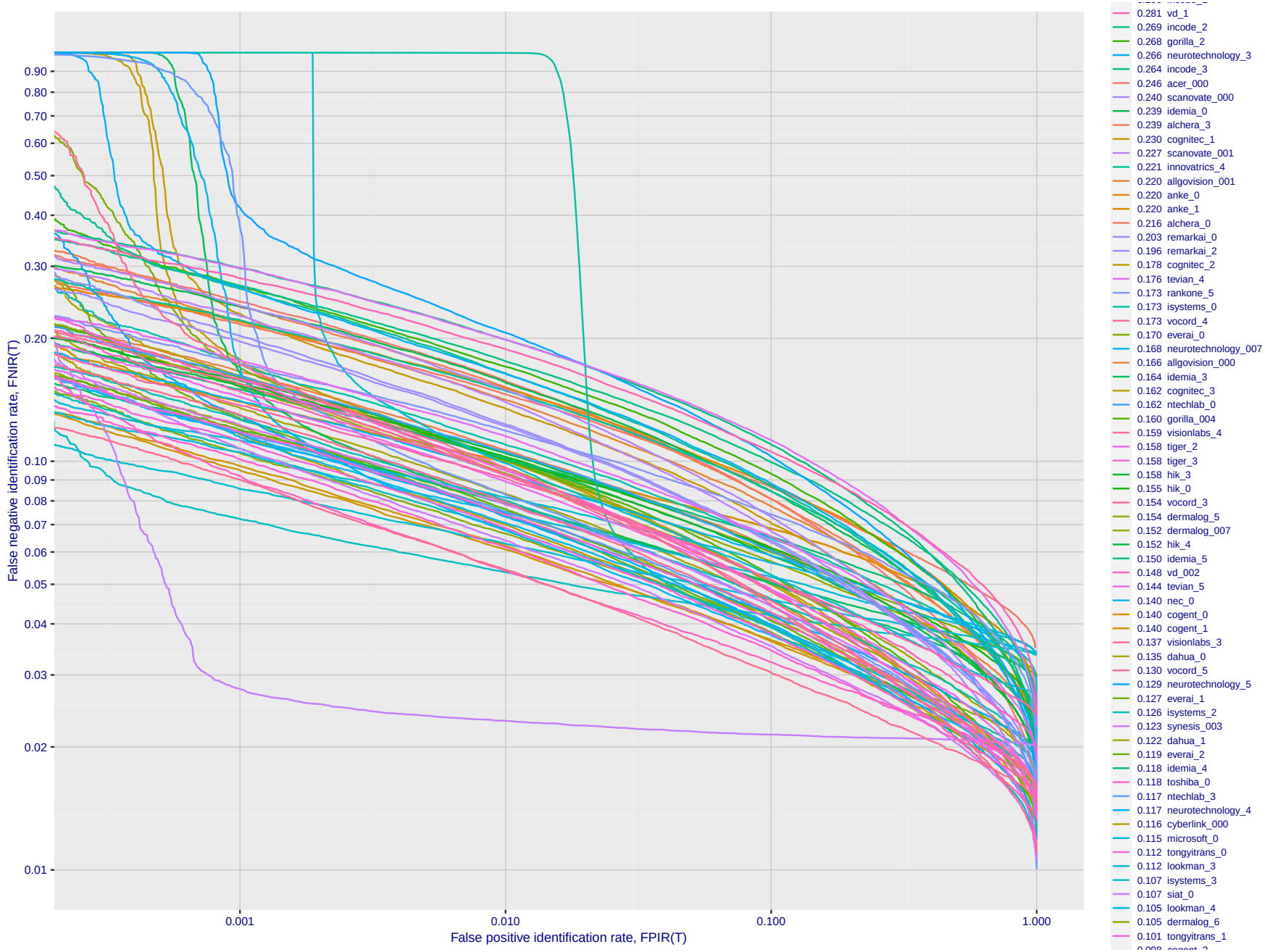

2021/08/05 02:00:58

FNIR(N, R, T) = False neg. identification rate
FPIR(N, T) = False pos. identification rate

N = Num. enrolled subjects
R = Num. candidates examined

T = Threshold

T = 0 → Investigation
T > 0 → Identification

Figure 161: **[Webcam Dataset] Identification miss rates vs. false positive rates**. *The results apply to cross-domain recognition in which webcams are searched against enrolled mugshots. The FNIR values are higher than those for mugshot-mugshot identification due to low image resolution, lighting and less constrained subject pose in webcam images - see Figure 6.*

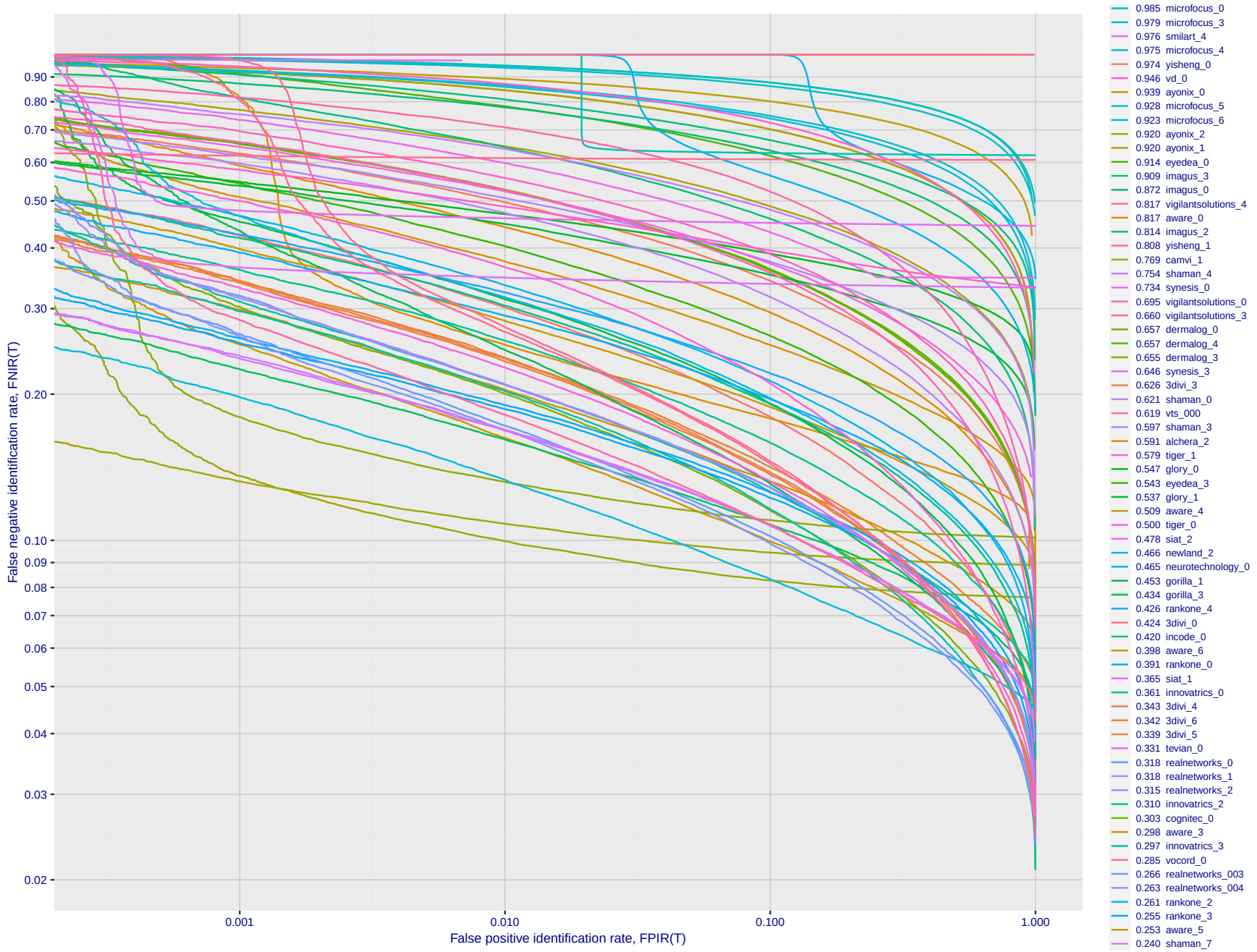

2021/08/05 02:00:58

FNIR(N, R, T) = FPIR(N, T) =

False neg. identification rate
False pos. identification rate

N = Num. enrolled subjects
R = Num. candidates examined

T = Threshold

T = 0 → Investigation
T > 0 → Identification

Figure 162: **[Webcam Dataset] Identification miss rates vs. false positive rates**. *The results apply to cross-domain recognition in which webcams are searched against enrolled mugshots. The FNIR values are higher than those for mugshot-mugshot identification due to low image resolution, lighting and less constrained subject pose in webcam images - see Figure 6.*

Appendix E Accuracy for profile-view to frontal recognition

Figures 163 - 165 gives accuracy results for searching 100 000 mated and 100 000 non-mated profile-view images against the same FRVT 2018 frontal enrollment dataset, N = 1 600 000, used in the main mugshot trials. This experiment corresponds to row-13 of Table 1. An example of profile-view image is given in Figure 7.

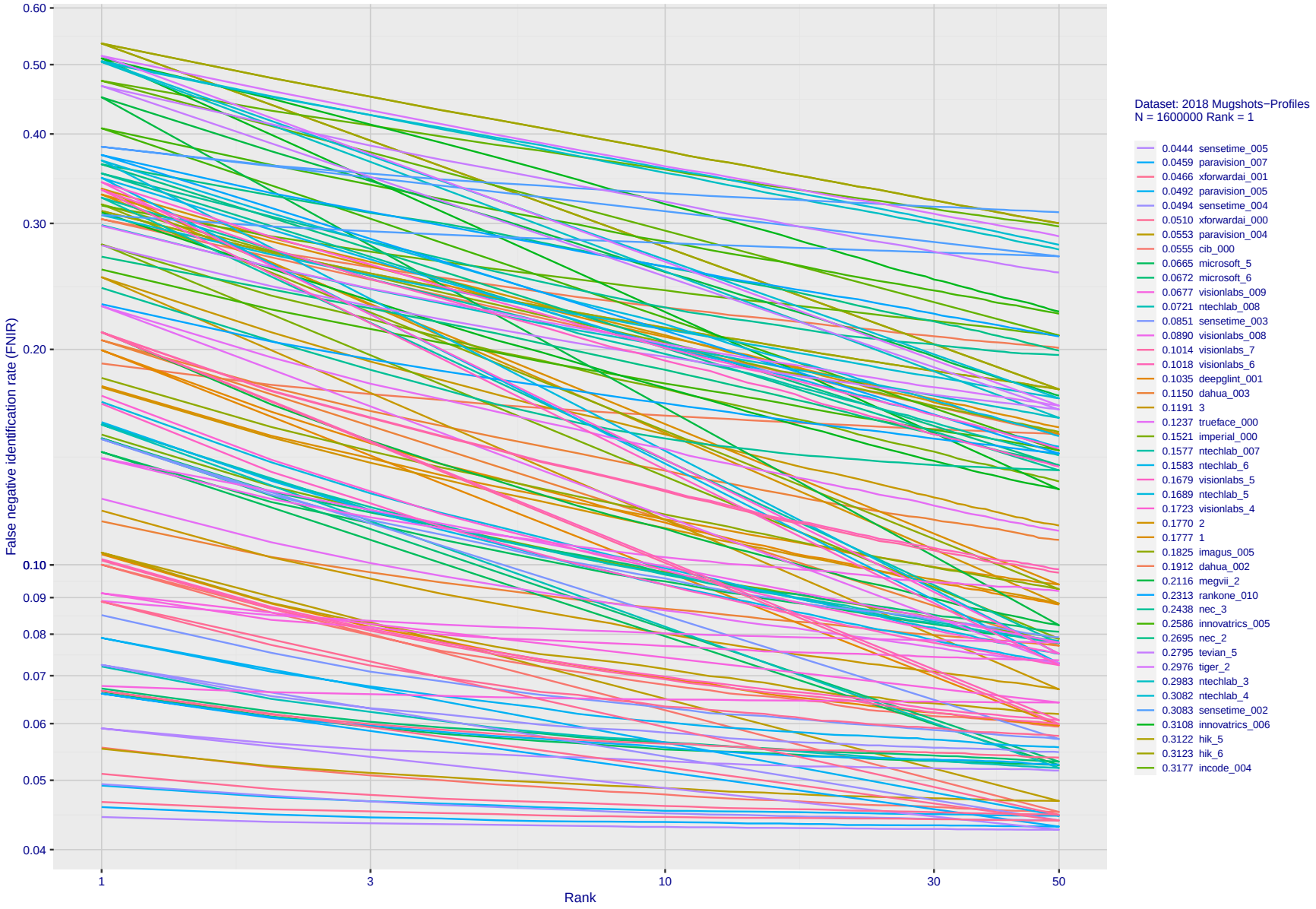

Figure 163: **[Mugshot and profile-view dataset] Rank-based accuracy**. *For some of the more accurate Phase 3 algorithms the figure plots error tradeoff characteristics for frontal and profile-view searches into an enrolled set of N = 1 600 000 frontal images. Note that some algorithms fail on profile-view images with FNIR → 1 - this evaluation did not ask developers to provide profile-view capability. Some algorithms, on the other hand, give FNIR approaching that for frontal-view searches using c. 2010 algorithms. The best result is that 91% of profile-view searches yield the correct mate at rank 1, and better than 94% in the top-50 candidates.*

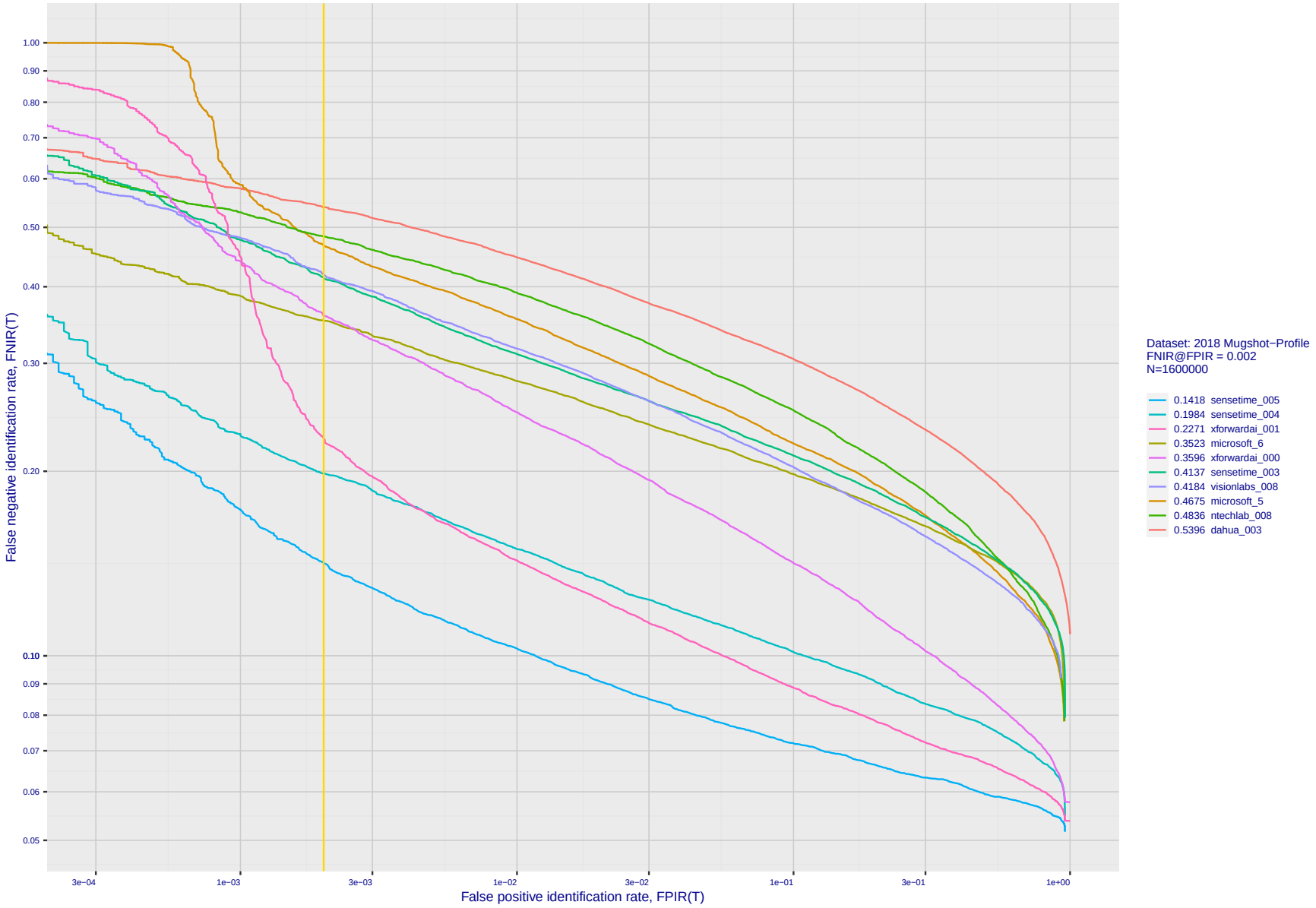

Figure 164: **[Mugshot and profile-view dataset] Threshold-based accuracy**. *For some of the more accurate Phase 3 algorithms the figure plots error tradeoff characteristics for frontal and profile-view searches into an enrolled set of N = 1 600 000 frontal images. Note that some algorithms fail on profile-view images with FNIR → 1 - this evaluation did not ask developers to provide profile-view capability. Some algorithms, on the other hand, give FNIR approaching that for frontal-view searches using c. 2010 algorithms.*

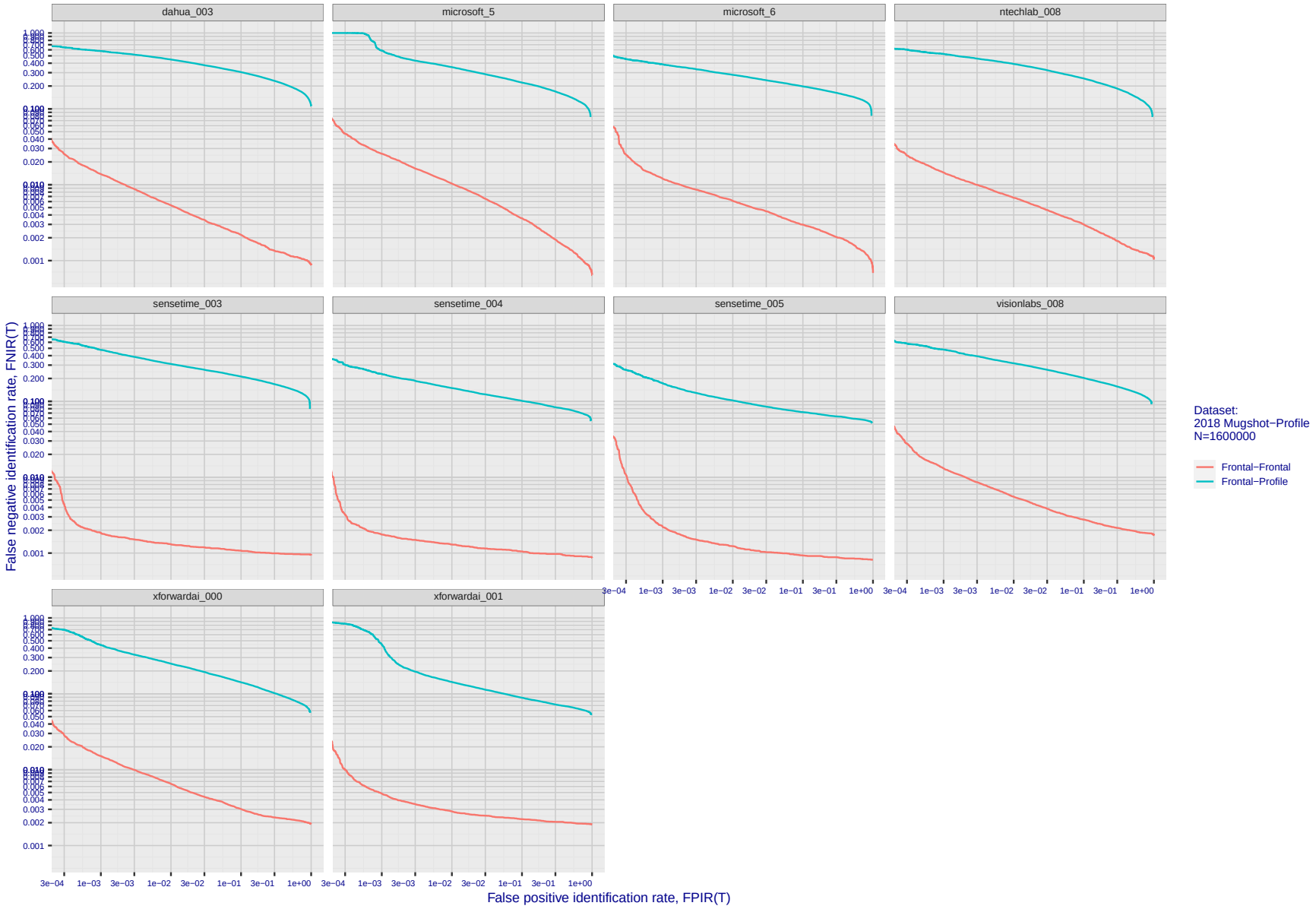

Figure 165: **[Mugshot and profile-view dataset] Speed-accuracy tradeoff**. *For some of the more accurate Phase 3 algorithms the figure plots error tradeoff characteristics for frontal and profile-view searches into an enrolled set of N = 1 600 000 frontal images. Some algorithms fail on profile-view images with FNIR → 1 - this evaluation did not ask developers to provide profile-view capability. Some algorithms, on the other hand, give FNIR approaching that for frontal-view searches using c. 2010 algorithms. Blue lines connect points of equal threshold from which it is evident that some algorithms would give markedly higher false positive outcomes if profile-view images were searched in a system configured for frontal searches. This would be a vulnerability in an access control system.*

2021/08/05 02:00:58
FNIR(N, R, T) = False neg. identification rate
FPIR(N, T) = False pos. identification rate
N = Num. enrolled subjects
R = Num. candidates examined
T = Threshold
T = 0 → Investigation
T > 0 → Identification

Appendix F Search duration

As in and prior tests, this section documents search speeds spanning three orders of magnitude. In applications where search volumes are high enough, this will have implications for hardware requirements especially for large N or when search duration is appreciably larger than the time it takes to prepare a template from the search image(s). Further, given very large (and growing) operational databases, the scalability of algorithms is important. It has been reported previously [8] that search duration can scale sublinearly with enrolled population size N. Further there has been considerable recent research on indexing, exact [13] and approximate nearest neighbor search [1,13] and fast-search [14,16].

Figure 166 charts the search duration measurements presented earlier in Tables 2 - 4.

- Most algorithms scale linearly. For those in that category, there is a wide range in speed with search durations ranging from 82 milliseconds for a 12 million gallery (for NEC-3) to more than 40 seconds (for Yitu-3, Toshiba-2) and even higher for less accurate algorithms.
- Some developers (Camvi, Dermalog, EverAI, Innovatrics, and Visionlabs) provide algorithms whose template search durations grow approimately logarithmically i.e. $T(N)\tilde{a}\log N$ with the constant a varying between implementations. In the figure this model is fit using the point $T(1) = 0$, and $T(640\,000)$. This very sublinear behaviour affords extremely fast search times in very large galleries. One caveat for the sublinear algorithms is that their fast-search data structures can require considerable computation time - on the order of hours - for N in the millions, and this scales mildy super-linearly, i.e. $O(N^b), b > 1$. There are exceptions: the Camvi algorithms take minutes; and Innvovatrics' scale sublinearly.

2021/08/05	FNIR(N, R, T) =	False neg. identification rate	N = Num. enrolled subjects	T = Threshold	$T = 0 \rightarrow$ Investigation
02:00:58	FPIR(N, T) =	False pos. identification rate	R = Num. candidates examined		$T > 0 \rightarrow$ Identification

Figure 166: **[Mugshot Dataset] Search duration vs. enrolled population size**. *In red are the actual point durations measured on a single c. 2016 core. The blue shows linear growth from $N = 640\,000$. The green line shows logathmic growth from that point to $N = 1\,600\,000$. Note the sublinear growth from algorithms from Camvi, Dermalog, EverAI, Innovatrics, and Visionlabs. The tiger_1 algorithm is also sublinear, but inaccurate and inoperable at $N \geq 3000000$. This capability sometimes comes at the additional expense of converting a linear gallery data structure into whatever fast-search data structure is used. Note that search times are sometimes dominated by the template generation times shown in Table 20.*

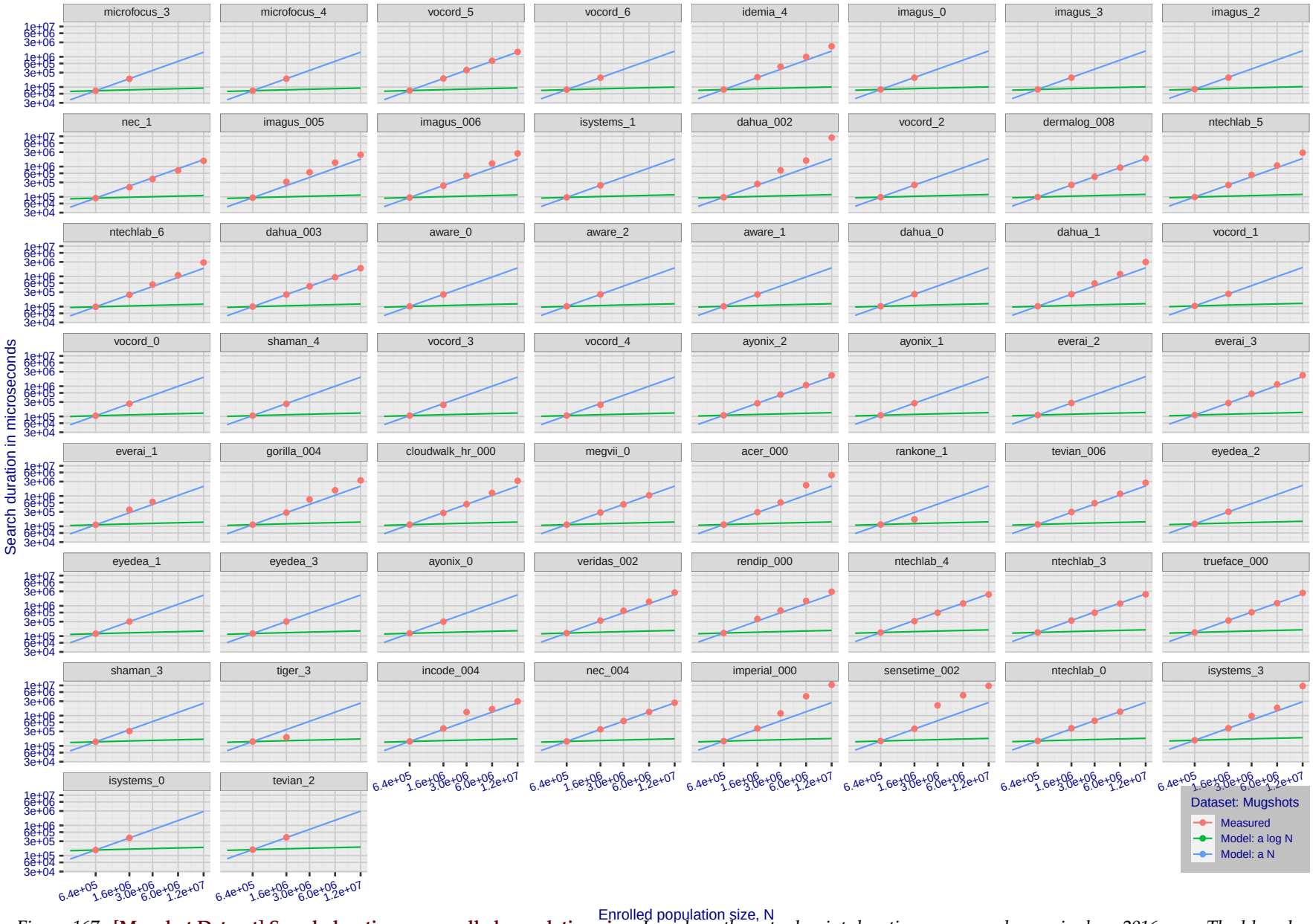

Figure 167: **[Mugshot Dataset] Search duration vs. enrolled population size**. *In red are the actual point durations measured on a single c. 2016 core. The blue shows linear growth from $N = 640\,000$. The green line shows logathmic growth from that point to $N = 1\,600\,000$. Note the sublinear growth from algorithms from Camvi, Dermalog, EverAI, Innovatrics, and Visionlabs. The tiger_1 algorithm is also sublinear, but inaccurate and inoperable at $N \geq 3000000$. This capability sometimes comes at the additional expense of converting a linear gallery data structure into whatever fast-search data structure is used. Note that search times are sometimes dominated by the template generation times shown in Table 20.*

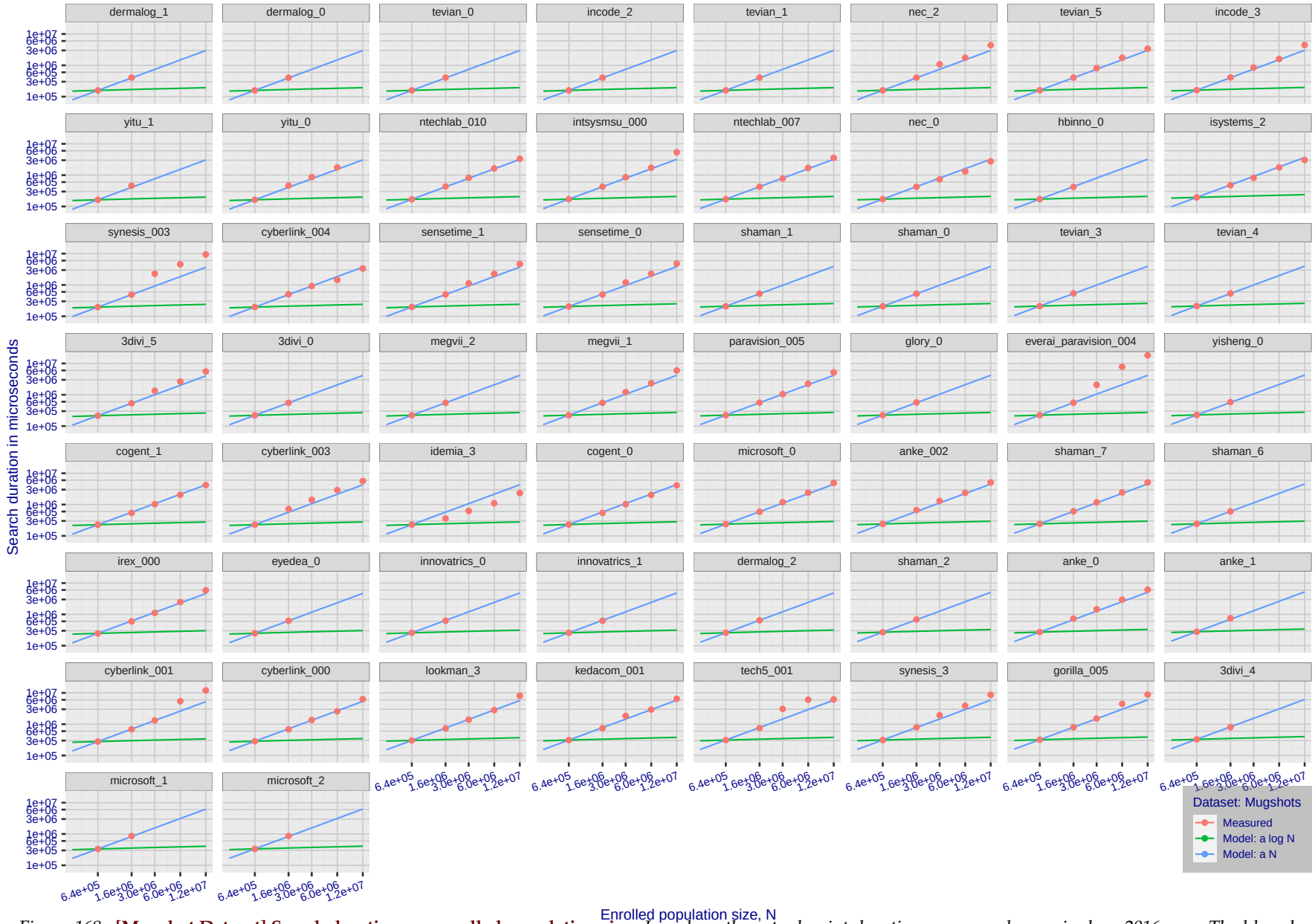

Figure 168: **[Mugshot Dataset] Search duration vs. enrolled population size**. *In red are the actual point durations measured on a single c. 2016 core. The blue shows linear growth from $N = 640\,000$. The green line shows logathmic growth from that point to $N = 1\,600\,000$. Note the sublinear growth from algorithms from Camvi, Dermalog, EverAI, Innovatrics, and Visionlabs. The tiger_1 algorithm is also sublinear, but inaccurate and inoperable at $N \geq 3000000$. This capability sometimes comes at the additional expense of converting a linear gallery data structure into whatever fast-search data structure is used. Note that search times are sometimes dominated by the template generation times shown in Table 20.*

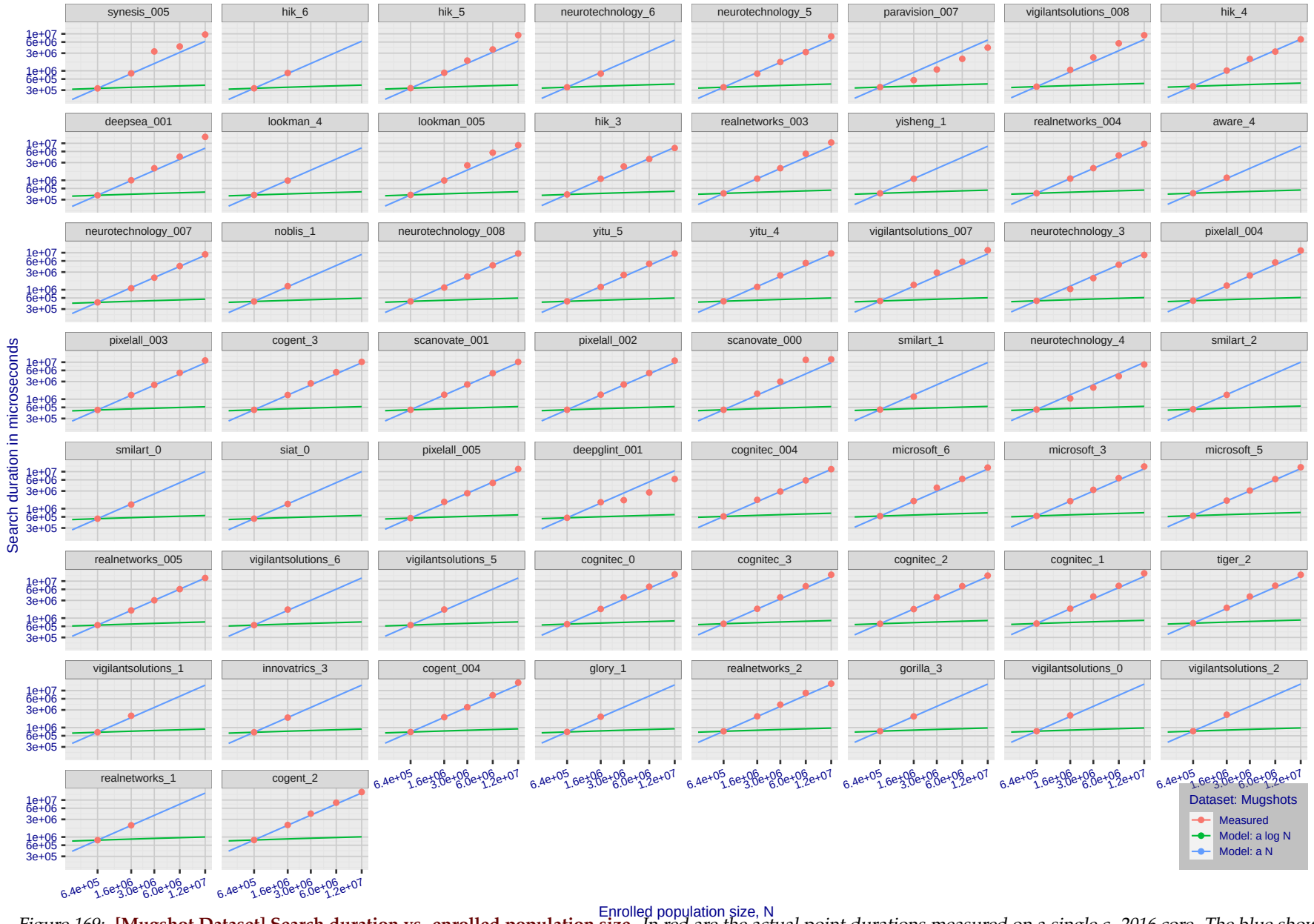

Figure 169: **[Mugshot Dataset] Search duration vs. enrolled population size**. *In red are the actual point durations measured on a single c. 2016 core. The blue shows linear growth from $N = 640\,000$. The green line shows logathmic growth from that point to $N = 1\,600\,000$. Note the sublinear growth from algorithms from Camvi, Dermalog, EverAI, Innovatrics, and Visionlabs. The tiger_1 algorithm is also sublinear, but inaccurate and inoperable at $N \geq 3000000$. This capability sometimes comes at the additional expense of converting a linear gallery data structure into whatever fast-search data structure is used. Note that search times are sometimes dominated by the template generation times shown in Table 20.*

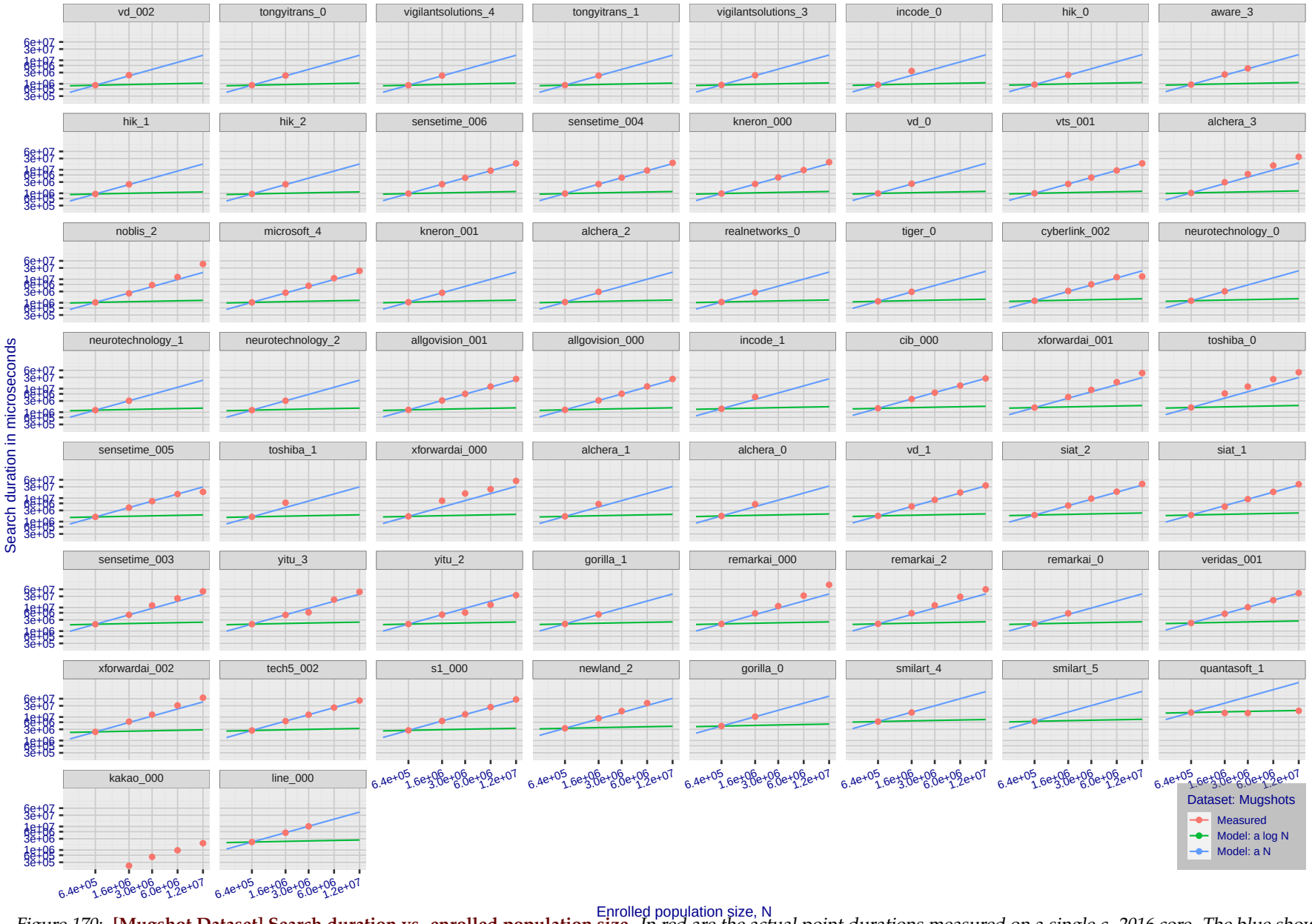

Figure 170: **[Mugshot Dataset] Search duration vs. enrolled population size**. *In red are the actual point durations measured on a single c. 2016 core. The blue shows linear growth from $N = 640\,000$. The green line shows logathmic growth from that point to $N = 1\,600\,000$. Note the sublinear growth from algorithms from Camvi, Dermalog, EverAI, Innovatrics, and Visionlabs. The tiger_1 algorithm is also sublinear, but inaccurate and inoperable at $N \geq 3000000$. This capability sometimes comes at the additional expense of converting a linear gallery data structure into whatever fast-search data structure is used. Note that search times are sometimes dominated by the template generation times shown in Table 20.*

Appendix G Gallery Insertion Timing

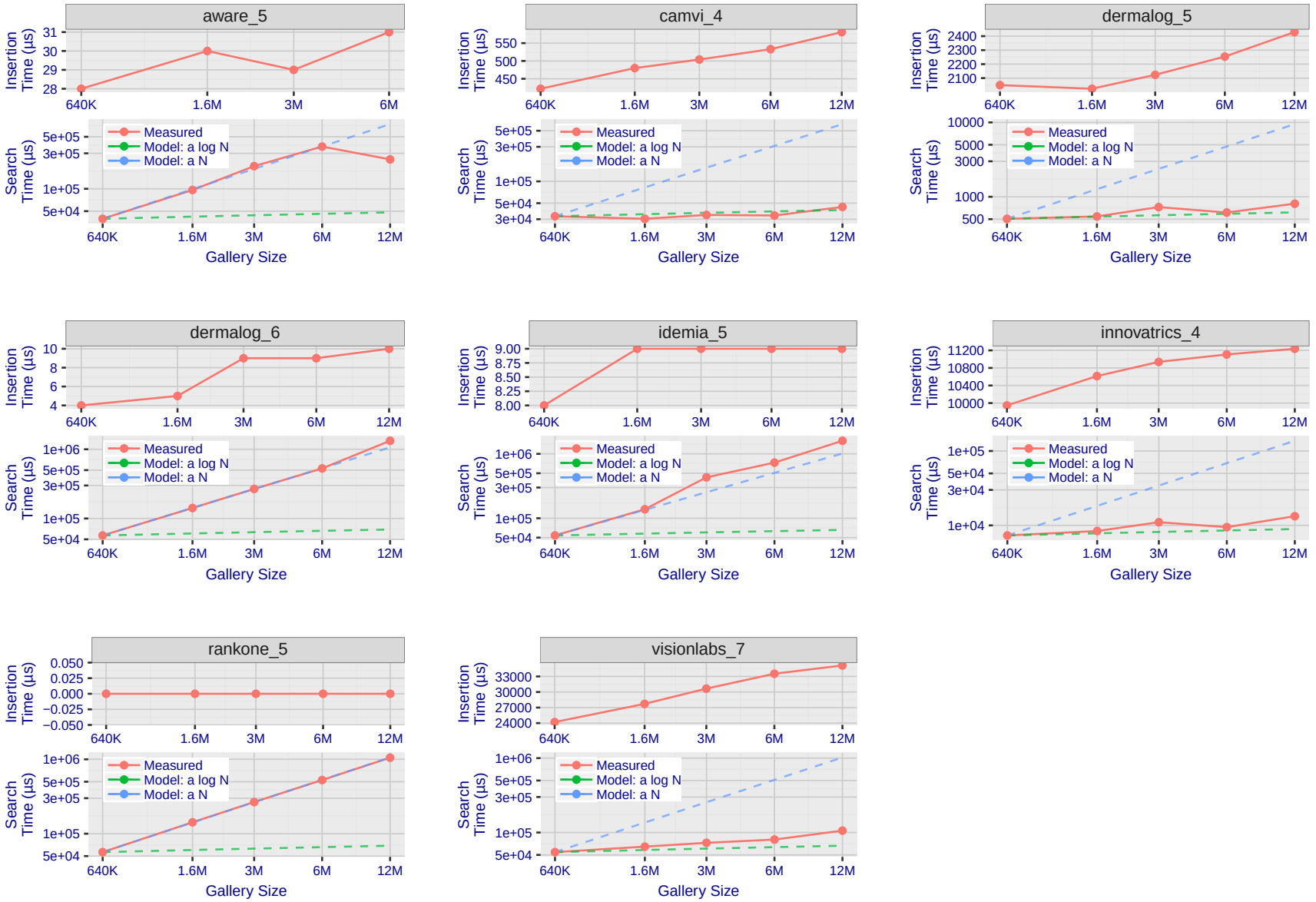

Figure 171: **[Mugshot Dataset] Gallery insertion duration vs. enrolled population size**. *This chart plots the time it takes to insert a single template into a finalized gallery, illustrated over increasing gallery sizes. For reference, search times on finalized galleries of corresponding sizes are plotted right underneath. Gallery insertion time plots were generated on algorithms that 1) successfully implemented gallery insertion with no errors and 2) that were run on galleries with N up to* 12 000 000. *Generally, only the more accurate algorithms were run on galleries with N up to* 12 000 000.

2021/08/05 02:00:58

FNIR(N, R, T) = False neg. identification rate
FPIR(N, T) = False pos. identification rate
N = Num. enrolled subjects
R = Num. candidates examined
T = Threshold
T = 0 → Investigation
T > 0 → Identification

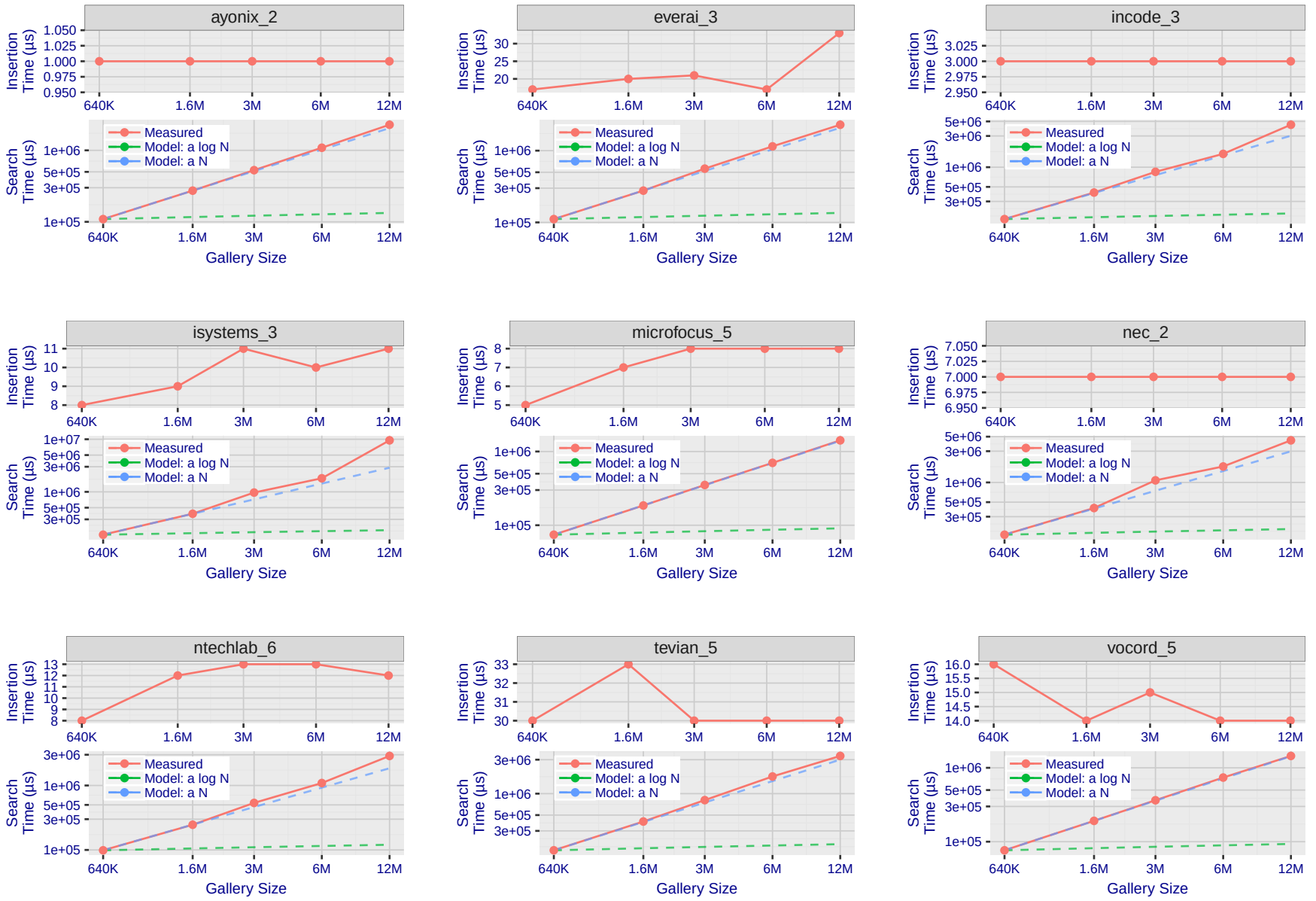

Figure 172: **[Mugshot Dataset] Gallery insertion duration vs. enrolled population size**. *This chart plots the time it takes to insert a single template into a finalized gallery, illustrated over increasing gallery sizes. For reference, search times on finalized galleries of corresponding sizes are plotted right underneath. Gallery insertion time plots were generated on algorithms that 1) successfully implemented gallery insertion with no errors and 2) that were run on galleries with N up to* 12 000 000. *Generally, only the more accurate algorithms were run on galleries with N up to* 12 000 000.

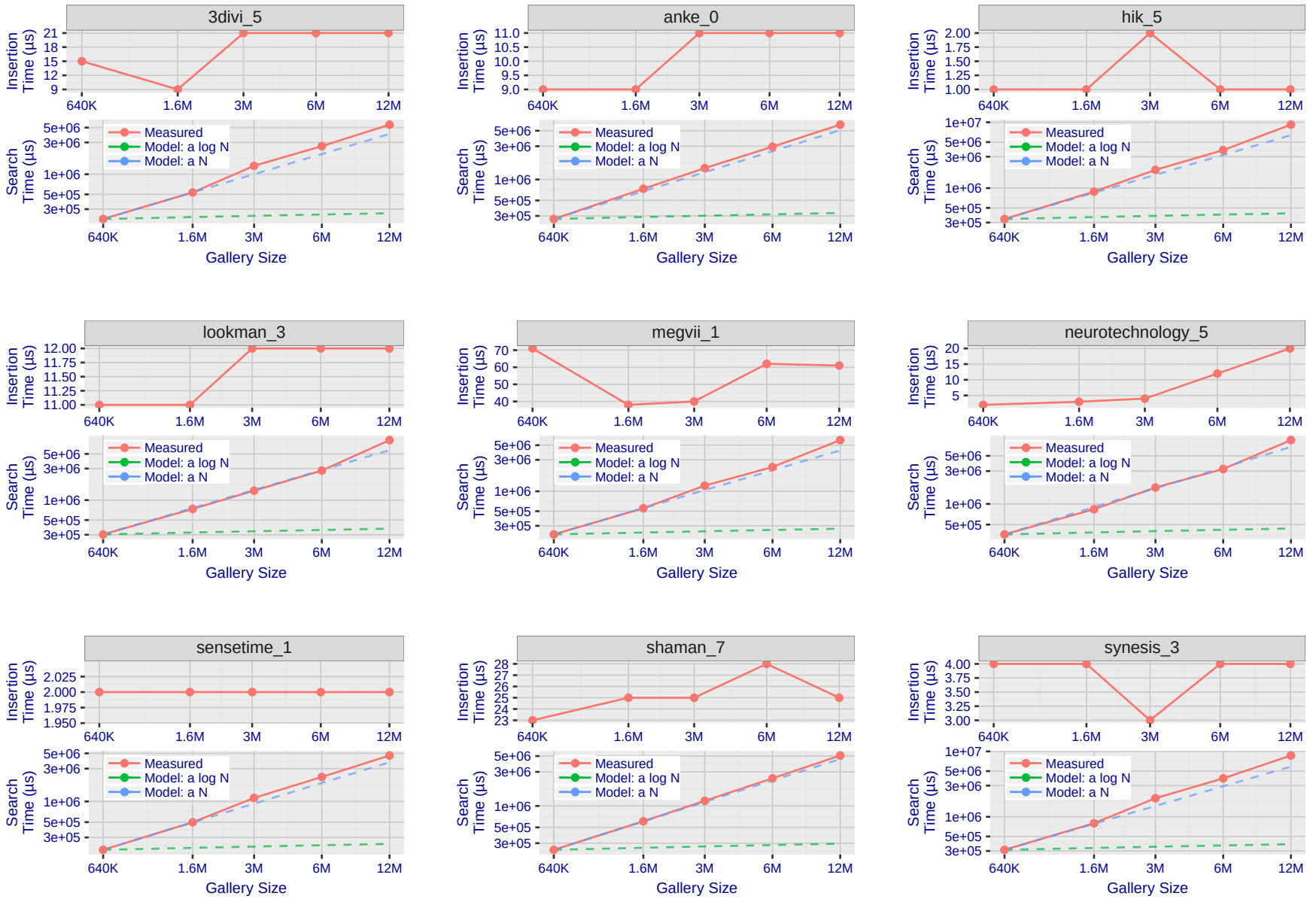

Figure 173: **[Mugshot Dataset] Gallery insertion duration vs. enrolled population size**. *This chart plots the time it takes to insert a single template into a finalized gallery, illustrated over increasing gallery sizes. For reference, search times on finalized galleries of corresponding sizes are plotted right underneath. Gallery insertion time plots were generated on algorithms that 1) successfully implemented gallery insertion with no errors and 2) that were run on galleries with N up to* 12 000 000. *Generally, only the more accurate algorithms were run on galleries with N up to* 12 000 000.

2021/08/05 02:00:58
FNIR(N, R, T) = FPIR(N, T) = False neg. identification rate / False pos. identification rate
N = Num. enrolled subjects
R = Num. candidates examined
T = Threshold
T = 0 → Investigation
T > 0 → Identification

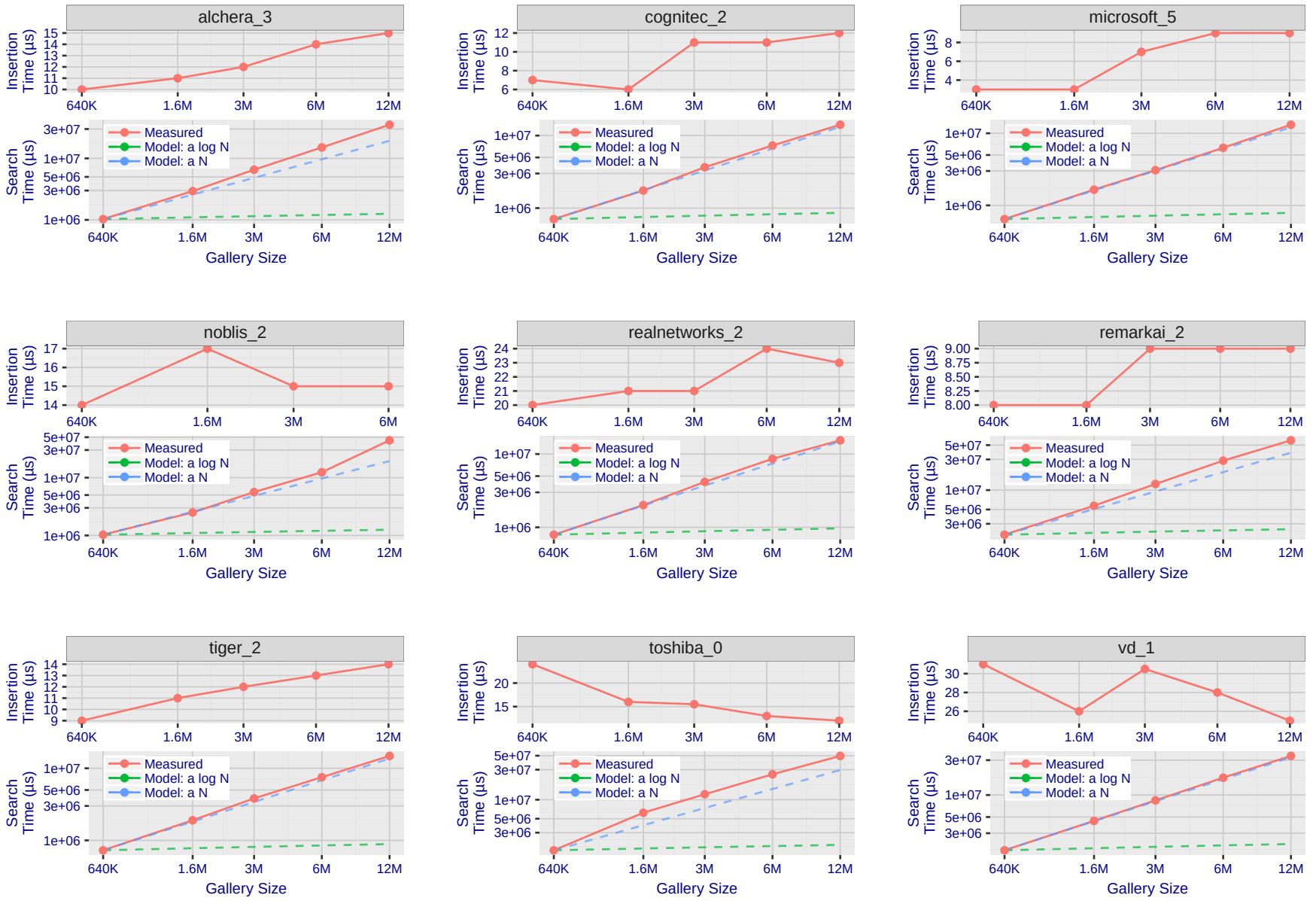

Figure 174: **[Mugshot Dataset] Gallery insertion duration vs. enrolled population size**. *This chart plots the time it takes to insert a single template into a finalized gallery, illustrated over increasing gallery sizes. For reference, search times on finalized galleries of corresponding sizes are plotted right underneath. Gallery insertion time plots were generated on algorithms that 1) successfully implemented gallery insertion with no errors and 2) that were run on galleries with N up to* 12 000 000. *Generally, only the more accurate algorithms were run on galleries with N up to* 12 000 000.

References

[1] Artem Babenko and Victor Lempitsky. Efficient indexing of billion-scale datasets of deep descriptors. In *The IEEE Conference on Computer Vision and Pattern Recognition (CVPR)*, June 2016.

[2] L. Best-Rowden and A. K. Jain. Longitudinal study of automatic face recognition. *IEEE Transactions on Pattern Analysis and Machine Intelligence*, 40(1):148–162, Jan 2018.

[3] Blumstein, Cohen, Roth, and Visher, editors. *Random parameter stochastic models of criminal careers*. National Academy of Sciences Press, 1986.

[4] Thomas P. Bonczar and Lauren E. Glaze. Probation and parole in the united statesm 2007, statistical tables. Technical report, Bureau of Justice Statistics, December 2008.

[5] White D., Kemp R. I., Jenkins R., Matheson M, and Burton A. M. Passport officers' errors in face matching. *PLoS ONE*, 9(8), 2014. e103510. doi:10.1371/journal. pone.0103510.

[6] P. Grother, G. W. Quinn, and P. J. Phillips. Evaluation of 2d still-image face recognition algorithms. NIST Interagency Report 7709, National Institute of Standards and Technology, 8 2010. http://face.nist.gov/mbe as MBE2010 FRVT2010.

[7] P. J. Grother, R. J. Micheals, and P. J. Phillips. Performance metrics for the frvt 2002 evaluation. In *Proceedings of Audio and Video Based Person Authentication Conference (AVBPA)*, June 2003.

[8] Patrick Grother and Mei Ngan. Interagency report 8009, performance of face identification algorithms. *Face Recognition Vendor Test (FRVT)*, May 2014.

[9] Patrick Grother, George Quinn, and Mei Ngan. Face in video evaluation (five) face recognition of non-cooperative subjects. Interagency Report 8173, National Institute of Standards and Technology, March 2017. https://doi.org/10.6028/NIST.IR.8173.

[10] Patrick Grother, George W. Quinn, and Mei Ngan. Face recognition vendor test - still face image and video concept, evaluation plan and api. Technical report, National Institute of Standards and Technology, 7 2013. http://biometrics.nist.gov/cs_links/face/frvt/frvt2012/NIST_FRVT2012_api_Aug15.pdf.

[11] K. He, X. Zhang, S. Ren, and J. Sun. Deep residual learning for image recognition. In *2016 IEEE Conference on Computer Vision and Pattern Recognition (CVPR)*, pages 770–778, June 2016.

[12] Gary B. Huang, Manu Ramesh, Tamara Berg, and Erik Learned-Miller. Labeled faces in the wild: A database for studying face recognition in unconstrained environments. Technical Report 07-49, University of Massachusetts, Amherst, October 2007.

[13] Masato Ishii, Hitoshi Imaoka, and Atsushi Sato. Fast k-nearest neighbor search for face identification using bounds of residual score. In *2017 12th IEEE International Conference on Automatic Face & Gesture Recognition (FG 2017)*, pages 194–199, Los Alamitos, CA, USA, May 2017. IEEE Computer Society.

[14] Jeff Johnson, Matthijs Douze, and Hervé Jégou. Billion-scale similarity search with gpus. *CoRR*, abs/1702.08734, 2017.

[15] Ira Kemelmacher-Shlizerman, Steven M. Seitz, Daniel Miller, and Evan Brossard. The megaface benchmark: 1 million faces for recognition at scale. *CoRR*, abs/1512.00596, 2015.

[16] Yury A. Malkov and D. A. Yashunin. Efficient and robust approximate nearest neighbor search using hierarchical navigable small world graphs. *CoRR*, abs/1603.09320, 2016.

[17] Joyce A. Martin, Brady E. Hamilton, Michelle J.K. Osterman, Anne K. Driscoll, , and Patrick Drake. National vital statistics reports. Technical Report 8, Centers for Disease Control and Prevention, National Center for Health Statistics, National Vital Statistics System, Division of Vital Statistics, November 2018.

[18] O. M. Parkhi, A. Vedaldi, and A. Zisserman. Deep face recognition. In *British Machine Vision Conference*, 2015.

[19] P. Jonathon Phillips, Amy N. Yates, Ying Hu, Carina A. Hahn, Eilidh Noyes, Kelsey Jackson, Jacqueline G. Cavazos, Géraldine Jeckeln, Rajeev Ranjan, Swami Sankaranarayanan, Jun-Cheng Chen, Carlos D. Castillo, Rama Chellappa, David White, and Alice J. O'Toole. Face recognition accuracy of forensic examiners, superrecognizers, and face recognition algorithms. *Proceedings of the National Academy of Sciences*, 115(24):6171–6176, 2018.

[20] Florian Schroff, Dmitry Kalenichenko, and James Philbin. Facenet: A unified embedding for face recognition and clustering. *CoRR*, abs/1503.03832, 2015.

[21] Jeroen Smits and Christiaan Monden. Twinning across the developing world. *PLOS ONE*, 6(9):1–5, 09 2011.

[22] Yaniv Taigman, Ming Yang, Marc'Aurelio Ranzato, and Lior Wolf. Deepface: Closing the gap to human-level performance in face verification. In *Proceedings of the 2014 IEEE Conference on Computer Vision and Pattern Recognition*, CVPR '14, pages 1701–1708, Washington, DC, USA, 2014. IEEE Computer Society.

[23] A. Towler, R. I. Kemp, and D White. *Unfamiliar face matching systems in applied settings*. Nova Science, 2017.

[24] Working Group 3. Ed. M. Werner. *ISO/IEC 19794-5 Information Technology - Biometric Data Interchange Formats - Part 5: Face image data*. JTC1 :: SC37, 2 edition, 2011. http://webstore.ansi.org.

[25] David White, James D. Dunn, Alexandra C. Schmid, and Richard I. Kemp. Error rates in users of automatic face recognition software. *PLoS ONE*, 10:1–14, October 2015.

[26] Bradford Wing and R. Michael McCabe. Special publication 500-271: American national standard for information systems data format for the interchange of fingerprint, facial, and other biometric information part 1. Technical report, NIST, September 2015. ANSI/NIST ITL 1-2015.

[27] Andreas Wolf. Portrait quality - (reference facial images for mrtd). Technical report, ICAO, April 2018.

[28] D. Yadav, N. Kohli, P. Pandey, R. Singh, M. Vatsa, and A. Noore. Effect of illicit drug abuse on face recognition. In *2016 IEEE Winter Conference on Applications of Computer Vision (WACV)*, pages 1–7, Los Alamitos, CA, USA, mar 2016. IEEE Computer Society.